

HANDBOOK OF EXPLORATION GEOCHEMISTRY

G.J.S. GOVETT (Editor)

1. ANALYTICAL METHODS IN GEOCHEMICAL PROSPECTING
2. STATISTICS AND DATA ANALYSIS IN GEOCHEMICAL PROSPECTING
3. ROCK GEOCHEMISTRY IN MINERAL EXPLORATION
4. REGOLITH EXPLORATION GEOCHEMISTRY IN TROPICAL AND SUBTROPICAL TERRAINS
5. REGOLITH EXPLORATION GEOCHEMISTRY IN ARCTIC AND TEMPERATE TERRAINS

Handbook of Exploration Geochemistry

VOLUME 4

Regolith Exploration Geochemistry in Tropical and Subtropical Terrains

Edited by

C.R.M. BUTT
Division of Exploration Geoscience
CSIRO
Floreat Park, WA 6014, Australia

H. ZEEGERS
Département Exploration
BRGM
F-45060 Orléans Cedex 2, France



1992

ELSEVIER

Amsterdam · London · New York · Tokyo

ELSEVIER SCIENCE PUBLISHERS B.V.
Sara Burgerhartstraat 25
P.O. Box 211
1000 AE Amsterdam, Netherlands

ISBN 0 444 89095 5

Library of Congress Cataloging-in-Publication Data

Regolith exploration geochemistry in tropical and subtropical terrains

/ edited by C.R.M. Butt, H. Zeegers.

p. cm. -- (Handbook of exploration geochemistry ; v. 4)

Includes bibliographical references and indexes.

ISBN 0-444-89095-5 (acid-free)

1. Geochemical prospecting--Tropics. I. Butt, C.R.M.

II. Zeegers, H. (Hubert), 1942- . III. Series.

TN270.R45 1992

622'.13'0913--dc20

91-34317

CIP

© 1992 Elsevier Science Publishers B.V. All rights reserved

No part of this publication may be reproduced, stored in a retrieval system, or transmitted, in any form or by any means, electronic, mechanical, photocopying, recording or otherwise, without the prior written permission of the Publisher, Elsevier Science Publishers B.V., Copyright and Permissions Department, P.O. Box 521, 1000 AM Amsterdam, Netherlands.

Special regulations for readers in the USA - this publication has been registered with the Copyright Clearance Center Inc. (CCC), Salem, Massachusetts. Information can be obtained from the CCC about conditions under which photocopies of parts of this publication may be made in the USA. All other copyright questions, including photocopying outside of the USA, should be referred to the Publisher.

No responsibility is assumed by the Publisher for any injury and/or damage to persons or property as a matter of products liability, negligence or otherwise, or from any use or operation of any methods, products, instructions or ideas contained in the material herein.

This book is printed on acid-free paper.

Printed in The Netherlands

EDITOR'S FOREWORD

The original concept for the Handbook of Exploration Geochemistry envisaged volumes on the principal sample media and procedures (e.g., analytical, data processing, drainage, soils, rocks and biogeochemistry). The explosion in knowledge and information quickly made the initial scope inadequate, and this is especially true for the soil component. A decision was made to consider soils from glaciated and temperate regions of the higher latitudes separately from those of the lower latitudes. The latter include regions that range from humid tropical rain forest to desert and are the subject of this volume. The fact that there are two volume Editors (who are also the dominant contributors) is a reflection of the diversity and complexity of the subject. Drs. C.R.M. Butt and H. Zeegers between them bring extensive experience that encompasses the whole range of conditions encountered in these terrains; Dr. Zeegers additionally provides a welcome input from the French school of Geochemistry.

The word "soil" deliberately does not appear in the title of this book, nor in the companion volume for glaciated and temperate terrain; it is replaced by the term "Regolith" that embraces all overburden material above bedrock. This is clearly a more appropriate—and accurate—description of modern exploration geochemical practice than the much more restrictive term "soil". Nevertheless, it is probable that practising exploration geologists and geochemists will continue—colloquially at least—to refer to soil surveys regardless of which part of the overburden profile they sample.

The title of this volume, "Regolith Exploration Geochemistry in Tropical and Subtropical Terrains", was the cause of much discussion between myself and the editors. The final outcome is probably still not an entirely adequate description of the contents; it does not, for example, convey the important concept that "fossil" regoliths formed under humid tropical conditions occur in some contemporary arid climatic zones. This particular situation, in fact, typifies many of the complexities of interpretation of surficial geochemical data in the ancient tectonically stable land areas of the lower latitudes.

Given the complexities of regolith development in humid and arid tropical areas (that in many cases are reflected by the superposition of multiple—and contrasting—weathering cycles) it is obviously vital to understand the processes in order to comprehend and interpret geochemical patterns in the regolith. This fundamental truism is reflected by the editors devoting Part I and the first chapter of Part II (a total of seven chapters) of the book to a thorough description and discussion of the chemical and physical processes of weathering and geochemical dispersion. In some sense these are the most important part of the book: many "failures" of exploration geochemistry in the secondary environ-

ment are directly attributable to an inadequate understanding of surface processes.

Parts II, III, and IV of the book address specific exploration practice using gossans, and applications in savannas, rainforests, semiarid and arid terrains, and dissected terrains and tropical mountains. Here, also, the geochemical response is effectively linked to processes. Part V gives a useful description of specific techniques for diamonds, gold and uranium in tropically weathered terrains, and the use of heavy mineral surveys in lateritic terrains. The final section—Summary and Conclusions by the Editors—is an admirably succinct statement of all that is important in regolith exploration geochemistry in tropical and subtropical terrains.

The central theme of the Handbook Series is ore-finding, and a particular objective is to present material in a form that is useful and can readily be understood by the practising field exploration geologist and not just the specialist exploration geochemist. This volume meets these practical objectives. It also provides a thorough discussion of the basic underlying scientific principles that is sufficiently comprehensive to be useful as a reference source for researchers and postgraduate students.

G.J.S. GOVETT
Sydney, NSW, Australia

PREFACE

This volume of the Handbook of Exploration Geochemistry has taken us several years to prepare and we wish to acknowledge the managements of CSIRO (Institute of Minerals, Energy and Construction; Division of Exploration Geoscience) and BRGM for their support and for their encouragement of this collaboration between our two organizations. We thank Professor G.J.S. Govett for giving us the opportunity to contribute to the Handbook series, and for his advice and comments during the course of its preparation. In compiling and editing the volume, we have endeavoured to present our topic as a single unit, rather than as a series of separate essays or papers. In order to do so, we have attempted to develop a unifying theme, namely to set the processes of geochemical dispersion in the context of landform and regolith development. The authors of the various chapters are thanked, therefore, for generously acceding to our requests to relate to this theme where relevant and appropriate and, in some cases, altering the scope of their contributions. We are grateful to Dr. R.R. Anand, Dr. R. Davy, Dr. D.J. Gray, Dr. I.D.M. Robertson, Dr. R.E. Smith and Mr. G.H. Sherrington for their reviews of parts of the text. We also wish to acknowledge the contributions of Mr. A.D. Vartesi (CSIRO) who drafted the majority of the figures in Chapters I.1, I.5, I.6, II.i, II.1, II.2, III.3, IV.4 and V.3 and Mme. F. Trifigny (BRGM) for her secretarial assistance in preparing the final manuscript. Finally, we wish to acknowledge the forbearance, support and assistance of our families during the period it has taken us to complete this task.

Charles BUTT
Hubert ZEEGERS

LIST OF CONTRIBUTORS

C.R.M. Butt
Leader, Weathering Processes Group
Division of Exploration Geoscience
CSIRO
Private Bag, P.O.
Wembley, Western Australia
Australia 6014

H. Zeegers
Chief
Département Exploration
BRGM
BP 6009
F-45060 Orléans Cedex 2
France

R.R. Anand
Geochemist
Division of Exploration Geoscience
CSIRO
Private Bag, P.O.
Wembley, Western Australia
Australia 6014

F. Bianconi
Senior Exploration Geologist
Uranerzbergbau-GmbH
Kölnstrasse 38-44
D-5047 Vesseling
Germany

A. Chauvel
Directeur de Recherches
ORSTOM
213, rue Lafayette
F-75480 Paris Cedex 10
France

P.M. Downes
Consultant Geologist
28 Greenock Avenue
Como, Western Australia
Australia 6152

G. Friedrich
Director
Institut für Mineralogie und Lagerstättenlehre
Technische Hochschule
D-5100 Aachen
Germany

D.J. Gray
Chemist/Geochemist
Division of Exploration Geoscience
CSIRO
Private Bag, P.O.
Wembley, Western Australia
Australia 6014

G.P. Gregory
General Manager Exploration and Development
Ashton Mining Ltd.
P.O. Box 805
West Perth, Western Australia
Australia 6005

A.J.A. Janse
Diamond Exploration Consultant
Intel Pty. Ltd.
11, Rowsley Way
Carine, Western Australia
Australia 6020

M. Kanig
Institut für Mineralogie und Lagerstättenlehre
Technische Hochschule
D-5100 Aachen
Germany

K. Kögler
Commission of the European Communities
DGXII/C-5
MO75 3/24
200, rue de la Loi
B-1040 Bruxelles
Belgium

L.M. Lawrance
Division of Exploration Geoscience
CSIRO
Private Bag, P.O.
Wembley, Western Australia
Australia 6014

P. Lecomte
Project Manager
Département Exploration,
BRGM
BP 6009
F-45060 Orléans Cedex 2
France

M.J. Lintern
Geochemist
Division of Exploration Geoscience
CSIRO
Private Bag, P.O.
Wembley, Western Australia
Australia 6014

Y. Lucas
Chargé de Recherches
ORSTOM
213, rue Lafayette
F-75480 Paris Cedex 10
France

A. Marker
Institut für Mineralogie und Lagerstättenlehre
Technische Hochschule
D-5100 Aachen
Germany

D. Nahon
Laboratoire de Géosciences des Environ-
nements Tropicaux
Université d'Aix-Marseille III
Case n° 431
F-13397 Marseille Cedex 13
France

R.E. Smith
Leader, Laterite Geochemistry Group
Division of Exploration Geoscience
CSIRO
Private Bag, P.O.
Wembley, Western Australia
Australia 6014

Y. Tardy
Directeur de Recherches
ORSTOM
213, rue Lafayette
F-75480 Paris Cedex 10
France

G.F. Taylor
Geochemist
Division of Exploration Geoscience
CSIRO
P.O. Box 136
North Ryde, New South Wales
Australia 2113

M.R. Thornber
Project Manager
Division of Mineral Products
CSIRO
Private Bag, P.O.
Wembley, Western Australia
Australia 6014

J.-J. Trescases
Laboratoire de Pétrologie de la Surface
Université de Poitiers
40, avenue du Recteur Pineau
F-86022 Poitiers Cedex
France

INTRODUCTION

BACKGROUND AND SCOPE

Soil scientists and geomorphologists have long recognized the influence of climate on soil types and landforms. Climate is an independent factor in weathering and soil formation and may become the dominant factor if it remains relatively unchanged over long periods of time. Thus, particular climatic regions appear to be characterized by certain soil types and associations, this being the basis for zonal soil classification schemes. As a result of long-term changes in climate, however, weathering and soil profiles developed during former climatic regimes are modified by the newly imposed conditions and become, in effect, the immediate parent materials of the newly formed soils. Such superimposed soils, therefore, have features inherited from past pedogenetic episodes as well as those relating to the most recent. Climate similarly determines the mode of the mainly physical processes that actively shape relief. The association of particular landforms with certain climatic zones has been the stimulus to the study of climatic geomorphology. However, the adaptation of an entire relief to a given set of morphogenetic processes may take in excess of 10^7 years (Budel, 1968), during which time further climatic change would give rise to new conditions and processes. Consequently, most landscapes contain ancient relief features being modified by processes responding to the newly prevailing conditions.

The chemical and physical processes of weathering, soil formation and landscape development are, of course, essentially the same as those involved in secondary geochemical dispersion. Thus, the determination of weathering history and the recognition of the effects of past and present climates on these processes are essential for the interpretation of geochemical data. This concept is basic to the structure of this volume. In Part I, climatic and geomorphological criteria are used to define the three regional zones into which the tropical and adjacent parts of the world may be divided—namely, the humid tropics (the equatorial and monsoonal rainforests), the seasonal, wet-dry tropics (savannas) and the warm arid zone (deserts and semi-deserts). For geochemical purposes, further subdivision in terms of relief (and altitude) is appropriate. These zones are, of course, broad and merge one with another; they represent the present situation and define the ranges of presently active dispersion processes. Nevertheless, the influence of past climatic episodes is implicit in the definition, so that the regions have a number of features in common, particularly those relevant to periods of deep chemical weathering and lateritization. The characteristic processes of weathering, lateritization, soil formation and erosion are described in succeeding chapters, discussing, where appropriate, the differences between the climatic

zones and the influence of past weathering episodes. The role of these processes in the chemical and physical dispersion of ore-related elements is then considered.

In Part II, the processes of sulphide weathering, supergene enrichment and the formation of gossans and cap rocks are described. The importance and potential of gossan search in mineral exploration is then illustrated, with examples from a wide range of environments. Parts III and IV then develop models describing geochemical dispersion in the principal climatic-geomorphological zones, illustrated by appropriate case histories. These models and case histories demonstrate the dominant dispersion mechanisms that have operated in each region and environment and indicate suitable exploration procedures. Finally, in Part V, some exploration procedures and problems specific to tropically weathered terrains are discussed in detail. The Appendices briefly describe sample media, sample preparation and analytical procedures commonly used in the exploration, and include a Glossary of terms, particularly those used to describe the regoliths of these regions.

CLIMATE, GEOMORPHOLOGICAL ENVIRONMENT AND GEOCHEMICAL DISPERSION MODELS

C.R.M. BUTT and H. ZEEGERS

CLIMATE

Climatic elements

The present climate is of fundamental importance in determining the nature of the active geochemical dispersion processes in any given area. It is the climate of the soil itself that is of most relevance but data are generally meagre. There is, of course, abundant information on atmospheric climate and although this does not always directly indicate the soil climate, which responds to very local influences (e.g. slope, drainage), it is nevertheless a good guide on a regional basis.

The principal elements of the atmospheric climate known to have most influence on the soil are temperature and moisture, which are determined by geographical factors such as the relative distribution of continents and oceans, latitude, altitude, physiography and aspect. Temperature influences the rate of chemical reactions, which increase by factors of two or three with every 10°C in temperature. Moisture has significance both for its involvement in most chemical reactions, either as a reagent itself or as the medium in which reagents and reaction products are transported, and for its role in physical erosion.

Temperature

Temperature is a function of solar radiant energy, of which less than 50% of global incidence reaches the surface of the earth, the remainder being absorbed or reflected by the atmosphere. The heating efficiency of the radiation depends upon its angle of incidence, i.e. latitude and aspect, being greatest on land surfaces that are normal to the rays. Efficiency is greatest in tropical areas, where the distance travelled through the atmosphere is the shortest. Cloudiness, humidity and dust in the atmosphere reduce the effectiveness of radiation but, conversely, reduce heat loss at night; vegetation has a similar insulating effect. The insulating properties have the result that humid, well-vegetated equatorial areas do not experience extremes of heat, but have a narrow range of diurnal and annual temperature variation, whereas the drier, less vegetated savannas and deserts of higher latitudes experience extremes of temperature.

Depending upon depth, soil temperatures show hourly (1–2 cm), diurnal (to 50 cm) and annual (to 10–20 m) variations, the maxima lagging behind the

atmospheric variation. In each soil, the mean annual soil temperature is about the same at all depths; a single reading at about 15 m, where the temperature is uniform, therefore, can yield this mean value, which is usually very similar to the mean annual air temperature.

Moisture

Soil moisture in the tropics is derived from precipitation as rain or mist, and/or by the movements of water over or within the soil. Snow contributes only at high altitude. Total annual precipitation is the most readily available measure of rainfall but it is not an accurate guide to the actual amount entering or retained by the soil. Rainfall is most effective in entering the soil when it is of moderate intensity and duration and where all horizons of the soil are porous, permeable and not already saturated. Intense rainfall may cause water to accumulate and runoff rather than infiltrate, particularly where vegetation is sparse or in dry areas where hydrophobicity or a near-surface crust have developed. Light rainfall may be held by foliage or only penetrate to shallow depths and thus evaporate rapidly.

Some of the most important effects of soil moisture are the leaching and removal of soluble components. The intensity of leaching is related to the volume of water passing through the soil. Water is lost from the soil by evapotranspiration—the combined effects of transpiration by plants and evaporation—and by drainage. Evapotranspiration is a function of the type and abundance of vegetation, and to atmospheric conditions such as radiation, temperature and humidity. One measure of the leaching effect is the excess of precipitation over potential evapotranspiration, i.e. the difference between the total precipitation and the amount that might be lost given an unlimited supply of water and a complete cover of vegetation. This measure can only be an approximation, since the effectiveness of rainfall and the actual evapotranspiration are not considered. It may, however, be useful for regional comparison, for localized effects, such as runoff from higher ground into depressions, become less significant. In areas of seasonal or erratic rainfall, excesses are commonly only temporary. The net leaching from the whole landscape then is a function of the drainage. Where this is endorheic or nearly so, as in many arid and semiarid areas, material leached from upland parts of a drainage basin may be deposited and accumulated in lower parts of the landscape.

Classification of climate

The complexity and variability of climate almost defy usable classification other than into a few, broad groups. However, such groupings are adequate for discussion of regional pedology and geomorphology. The mostly widely used classification is that of Köppen (1936), which depends on monthly and annual measures for temperature and precipitation. Other systems are also appropriate, for example that of Thornthwaite, which uses potential evapotranspiration.

TABLE I.1-1

Climatic zones of the tropics and subtropics using the Köppen (1936) classification (detailed descriptions of the classification are given by Gentilli (1958), Trewartha (1968))

	Rainfall driest month mm	Mean annual rainfall mm	Temperature coldest month °C	Temperature warmest month °C	Mean annual temperature °C	Number of frost days
<i>A: Tropical humid climates</i>						
Af	> 60	> 20 (t + 14)	> 18 (21-27)	27-29	24-27	Nil
Am	> (100 - r / 25)	> 20 (t + 14)	> 18 (21-27)	27-29	24-27	Nil
Aw	< 60	> 20 (t + 14)	> 18 (21-24)	27-32	24-27	Nil
<i>B: Tropical dry climates</i>						
BSh	< 10	< 20 (t + 14)	12-16	35-38	> 18 (21-27)	0-25
BWh	< 10	< 10 (t + 14)	12-18	35-38	21-27	0-25
<i>C: Subtropical to temperate humid climates</i>						
<i>Dry winter</i>						
Cwa:	< 30	< 20 (t + 14)	> - 3 (4-13)	> 22 (24-29)	16-21	15-65
Cwb	< 30	> 20 (t + 14)	> - 3 (4-13)	< 22		15-65
<i>Dry summer</i>						
Csa	< 30	> 20 (t + 14)	> - 3 (7-10)	> 22 (24-30)	12-20	15-65
<i>No dry season</i>						
Cfa	> 30	> 20 (t + 14)	> - 3 (4-13)	> 22 (24-29)	16-21	15-65

t = mean annual temperature; r = mean annual rainfall.

Climate symbols: a: warmest month > 22°C.

b: warmest month < 22°C.

f: rainfall, driest month > 60 mm.

h: warm, dry, all months > 0°C.

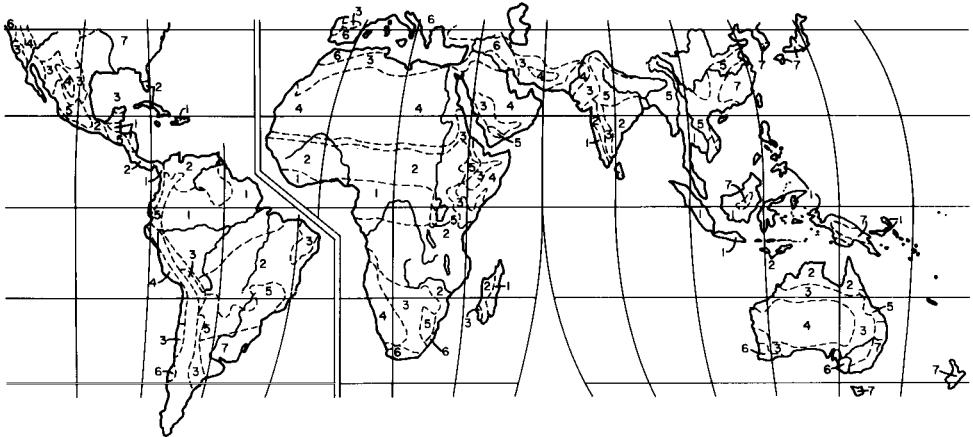
m: monsoon rain.

s: dry summer.

w: dry winter.

W: desert.

Italic type indicates diagnostic criteria.



Köppen climate (modified)

Tropical humid climates
(Coldest month $>18^{\circ}\text{C}$)

1	Af Rainforest Am Monsoon
2	An Savanna

Tropical dry climates
(<600 mm annual rainfall)

3	BSh Semi-arid (Steppe)
4	BW h Arid (Desert)

Sub-tropical-temperate humid climates
(Coldest month $>-3^{\circ}\text{C}$ to 18°C)

5	Cw Dry winter
6	Cs Dry summer (Mediterranean)
7	Cfa No dry season

Blank land areas refer to colder climates

Fig. I.1-1. Modified Köppen climate map for the tropics and subtropics.

However, difficulty in estimating potential evapotranspiration restricts the value of the scheme. All classifications use some arbitrarily defined boundaries, usually established to coincide with other readily observable features—the Köppen scheme being based on vegetation communities. Such boundaries are, of course, gradational over tens or hundreds of kilometres. The Köppen classification for the tropical and subtropical regions is given in Table I.1-1 and a modified version shown in Fig. I.1-1. The most critical boundaries are:

(1) between tropical (A) and subtropical to temperate (C) humid climates, based on temperature, and

(2) between humid (A,C) and dry (B) climates, based on a temperature–rainfall function (rainfall effectiveness). Within the A climates, subdivision is based on rainfall distribution and the presence of a dry season, defined as months having < 60 mm rain.

This effectively divides the rainforests from the seasonal wet-dry tropics or savannas—the latter term referring to the climate rather than vegetation type.

For pedological purposes, these boundaries are not always satisfactory (Young, 1976). Firstly, there seems to be no difference in soils between the Asian monsoonal rainforests (Am) and the lowland rainforests of Africa and South America, despite the more seasonal climate. Secondly, as originally discussed by

Trewartha (1968), the Köppen Aw–Cwa boundary in Central Africa reflects a change in altitude rather than a change in soil properties. Thirdly, the arid zone boundary is better placed at the 600 mm isohyet, rather than as defined at 680–780 mm for 20 and 25°C mean annual temperatures. This corresponds more closely to the transition between leached soils (pedalfers) and those in which carbonates are accumulating (pedocals). Drawing largely upon African examples, Young (1976) incorporated these considerations into a classification of the principal climatic zones of the tropics relevant to pedology and vegetation type based largely upon rainfall and seasonality. This classification, with the addition of Mediterranean climates, is summarized in Table I.1-2 and is included, in part, in Fig. I.1-1.

Altitudinal variation

Temperature declines with altitude, at a rate of about 1°C per 100–200 m, because the increase in intensity of radiation is more than offset by the reduced absorption of heat by the atmosphere. However, the effect is minimal below 500 m in the tropics. Diurnal fluctuations are greater, however, due to a similarly reduced insulation effect. Precipitation tends initially to increase with altitude, reaching a maximum and then declining again. These factors combine to produce a vertical climatic, soil and vegetation zoning that to some extent parallels that due to increasing latitude, and similarly terminates in glacial phenomena.

CLIMATIC GEOMORPHOLOGY

Variations of climate with time

Climate determines the active processes of weathering and erosion that are important in geochemical dispersion and these have expression not only as soils and weathering profiles but also as landforms. It is evident, however, that climates have changed frequently and often quite profoundly even within the last half million years, so that a number of different weathering and dispersion processes will have been operating during the course of time. These are recorded as regoliths and landforms that are not in equilibrium with present conditions. In general, only the more recent, extreme or older, longer established, climatic episodes will have left pedological or geomorphological records of significance. In the high latitudes, at present having mostly temperate climates, these records are dominated by the effects of Pleistocene glaciation and its aftermath, whereas in the subtropical and tropical middle and lower latitudes, particularly in continental areas of low relief, the regolith and landforms are an expression of the cumulative effects of subaerial weathering that may have continued for tens or hundreds of millions of years. Parts of the Precambrian Western Shield of Australia, for example, may have been exposed to subaerial conditions since the

TABLE 1.1-2
Climatic regions of pedogenetic significance in the tropics and subtropics (after Young, 1976)

Climatic region	Mean annual rainfall (mm)	Dry season months < 60 mm rain	Köppen equivalent	Natural vegetation	Biomass tonnes/hectare	Zonal soils
Rainforest	> 1800	0-2	Af, Am	Lowland tropical rainforest	300-1000	Leached ferrallitic soils; kaolinitic-gibbsitic; always moist.
Rainforest-savanna transition	1200-1800	2-6	Am	Semi-deciduous forest or forest-savanna mosaic and Asian monsoon forest;	-	Ferrisolic soils on intermediate-basic rocks, less leached than rainforest; top metre may dry out in dry season.
Moist savanna; two wet seasons	900-1200	3-5	Aw	Forest and grasslands	-	Ferrisolic soils on intermediate and basic rocks. Moderately weathered and leached
Moist savanna	900-1200	3-5	Aw, Cwa	Forest and grasslands	67-100	Ferruginous and ferrallitic soils, pH 5-6; kaolinitic some smectite. Base saturation 40-60%. Leached in wet season, dry to 1 m in dry season.
Dry savanna	600-900	6-8	Aw, Cwa	Grasslands with 5-50% tree cover	27-29	Ferruginous and ferrallitic soils, pH 6-7. Base saturation 60-90%. Less intense leaching. Dry to 2 m in dry season.
Semiarid (semi-deserts, steppes)	250-600	8-10	BSh	Xerophytic trees, perennial grasses.	6-10	Brown calcimorphic soils, sierozems, arenosols and lithosols. Carbonate accumulating in profile.
Arid (deserts)	< 250	10-12	BWh	Bare ground commonly 50%. Xerophytic shrubs, often thorny.	-	Dry most of year.
Tropical, high altitude (> 1600 m)	> 600	0-6	Cwb, Cwa	Evergreen forest, merging to grasslands and alpine at high altitudes	-	Humic latosols; podzolic at high altitudes.
Subtropical humid	> 900	0-3	Cfa	Deciduous woodlands	-	Leached ferruginous soils.
Mediterranean	400-800	2-6	Csa	Mixed forests	-	Red and brown earths; lateritic podzolics; terra rossa.

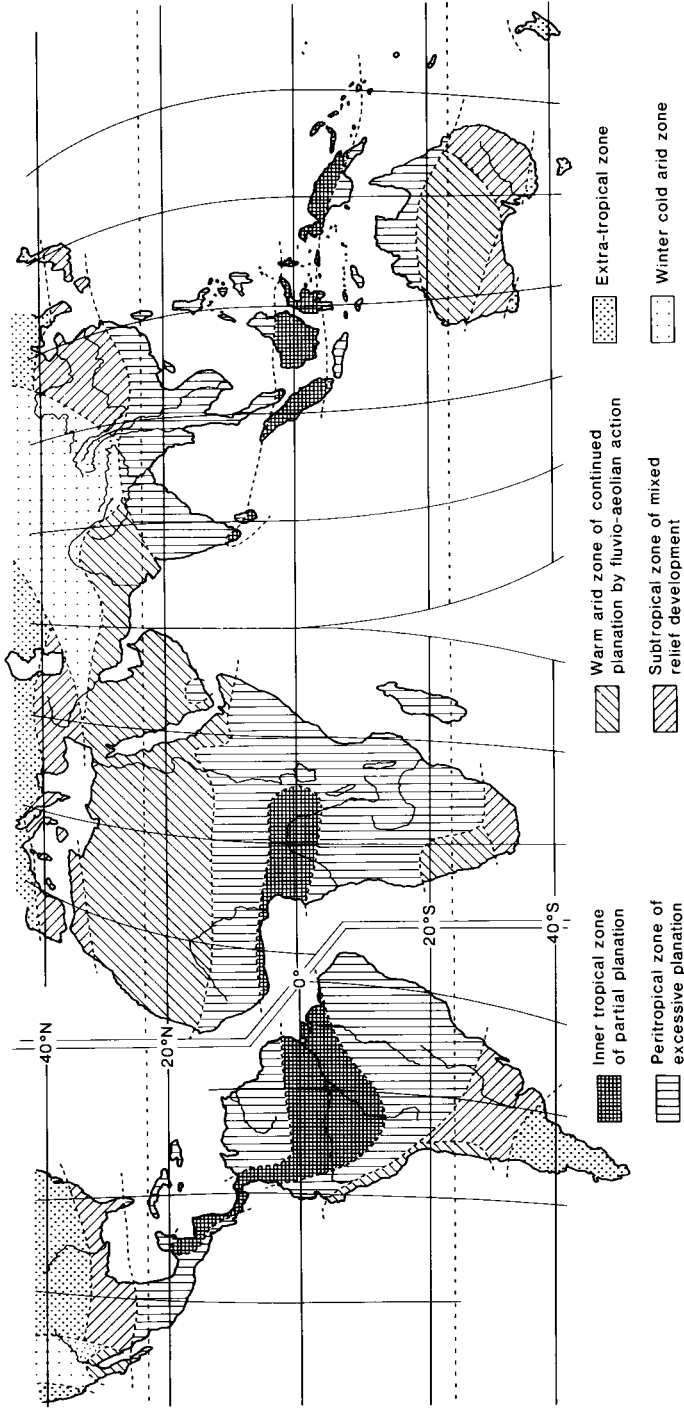


Fig. I.1-2. Present morphoclimatic zones. Redrawn from Budel (1982).

Middle or Upper Proterozoic (Daniels, 1975; Butt, 1989b), with some of the iron ores of the Hamersley region being products of deep supergene weathering about 1800 million years ago (Morris, 1980). Consequently, interpretation of weathering history is possible from geomorphological analysis of landforms and associated regoliths and this can provide a sound basis for geochemical study.

Morphoclimatic zones

Where currently active processes are depicted on soil maps at various scales or maps of pedogeochemical regimes (Pedro and Sieffermann, 1979), they can be misleading in that they refer only to the near-surface and take little account of parent materials that may range from fresh rocks to highly weathered residuum. In morphoclimatic classifications such as that of Budel (1982), however, the current processes are considered in the context of the weathering history, i.e. the effects of the processes on pre-existing regolith, and the classes are defined in these terms. The importance of relict features in landscape development has, of course, been recognized by other geomorphologists but the concepts of Budel are emphasized here. Budel identifies three principal climate-related zones, namely glacial, periglacial (the "subpolar zone of excessive valley cutting") and peritropical (the "zone of excessive planation"); the peritropical zone has an important variant, the inner tropical "zone of partial planation", approximately coextensive with the equatorial rainforests. Six other zones are recognized but these are strongly influenced by relict features from earlier periglacial and peritropical episodes.

The morphoclimatic zonation relevant to the tropics and subtropics is shown in Fig. I.1-2. The geomorphology and regoliths of these regions are dominated by the processes of the peritropical zone, that is, the processes of the present seasonal tropics or savannas. This zone is characterized by a deep (3- > 40 m) intensely weathered regolith, formed over long periods in tectonically stable

TABLE I.1-3

Summary of the chemical effects of deep weathering

-
1. Leaching of mobile constituents:
-alkalis, alkaline earths.
 2. Formation of stable secondary minerals:
-clays (principally kaolinite), Ti and Al oxides.
 3. Partial leaching of less mobile constituents:
-silica, alumina, titanium
 4. Mobilization and partial reprecipitation of redox-controlled constituents:
-iron, manganese.
 5. Retention and residual concentration of resistant minerals:
-zircon, chromite, quartz.
-

landmasses. The principal geochemical effects occurring during the evolution of this regolith, summarized in Table I.1-3, are described in Chapters I.2 to I.4. The areas now occupied by the peritropical zone have been subjected to broadly similar seasonal climates for very long periods, perhaps since the late Mesozoic, with climatic fluctuations mainly restricted to changes in humidity. Such conditions were once more widespread than at present. During the period of global warming, well-documented for the Cretaceous (Barron, 1983) and probably continuing to the mid-Tertiary, such peritropical climates extended not only to marginal areas at latitudes now occupied by the warm arid zone, but possibly to much higher latitudes.

Budel (1982) introduced the concept of relief development at dual planation surfaces, namely the ground surface, which is denudational, open to seasonal effects and subject particularly to erosion processes, and the weathering front, which has continuous warm and moist conditions that favour chemical alteration. Aleva (1983) and Millot (1983) both suggest there to be a third surface between the saprolite and the soil which may be either a second denudational surface marked by an unconformity or a second weathering front. This third surface may represent the boundary between pedochemical and geochemical weathering, or the reworking of relict material under new conditions. Certainly, in either circumstances, its identification may be important in defining exploration sample media. Planation proceeds by the lowering of the surfaces, with a thick regolith developing because the chemical processes at the weathering front are more rapid than the erosional processes at the denudation surface. Both surfaces are regionally flat, though they have some local relief and in places are punctuated by unweathered rock rising as inselbergs. The final product can be described as an etchplain, which ideally should show little stream incision although climatic, vegetational or tectonic change since the Pleistocene will have caused some to occur (Thomas, 1974). The presence of several planation levels implies that stripping of old etchplains and their renewal at lower levels has occurred repeatedly.

Hardening of aluminium and iron oxide accumulations to form cuirasses in the near-surface is significant in the development of tropical relief. They form as the result of dehydration following lowering of the water-table, induced either climatically (by seasonal or long-term change) or tectonically (by uplift). The armouring effect of the cuirasse is most important, preserving the friable and otherwise erodable regolith and producing the characteristic plateaux and mesas, which are recognizable, with other features of the etchplain-inselberg terrain, as relicts in other morphogenic zones.

Processes of the inner tropical zone are similar to those of the peritropical zone, the main differences being that, 1) weathering is more intense, usually with little obvious horizon development and, 2) erosion is less severe, due to more dense vegetation. Some relief elements, such as cuirasses, may have been inherited from past seasonal climates, or be due to dehydration and hardening following uplift. A high proportion of this zone, however, is either depositional

(e.g. Amazon and Congo basins) or tectonically active, which impose special conditions.

In the warm arid zone, the major relief features are inherited from pre-Pleistocene savanna climates, and may range from partly or completely preserved etchplains, in which the present plateau surfaces more or less correspond to the original upper denudational level (e.g. much of Australia and the Sahel) to stripped etchplains or etchsurfaces that corresponds to the weathering front (Sahara and Arabian deserts). Fluvio-aeolian processes dominate, so that striping proceeds without significant chemical weathering and the development of a new etchplain at a lower elevation.

Deeply weathered regoliths are also found at higher latitudes, for example, 35–42°S in southeast Australia (Victoria and Tasmania), 40–45°N in the USA (Oregon and Wisconsin) and 55°N in Europe (Northern Ireland, Germany) (Dury, 1971). These generally have no more than local significance, except in some areas with subtropical and Mediterranean climates where climates are cooler but not greatly dissimilar to those of the seasonal tropics. Accordingly, although pedochemical and erosional modifications may affect the near-surface horizons, deep weathering may continue. The near-surface may already have been affected by an intervening episode of aridity, as in southwest Australia, but the origins and characteristics of the landscape remain clear and often dominant.

This interpretation of the tropical origins of some landforms and regoliths of the higher latitudes is not universally accepted. The effects of temperature are kinetic, enabling reactions to occur more rapidly. Accordingly, lateritic profiles may form in cooler climates, but over a longer period of time (Paton and Williams, 1972). This discussion is of particular importance to southern Australia, which was situated at 50–75°S during the late Cretaceous and early to mid-Tertiary. A rainforest vegetation prevailed but climates may have been subtropical to temperate (Kemp, 1981), possibly with some warmer and cooler periods. However, temperature is not the only factor; the timing of any seasonality of the climate may also be significant but has not been considered in this context. If rainfall occurred in winter, rather than in summer, the kinetic effects of lower temperatures may have been partly offset by the retention and greater activity of soil moisture. This is exemplified by the strong leaching and active formation of gibbsite under the winter rainfall of the Mediterranean climate in the Darling Range, Western Australia (Anand et al., 1985), compared to lesser leaching and the formation of kaolinite in uplifted plateaux in savannas having a similar, but summer, rainfall.

Tropical mountains and areas of high relief

Areas of high relief in the tropics occur on the margins of etchplains, whether destabilized by climatic change or raised by epeirogenic uplift, around depressions and in tropical mountains. An effect of double planation is that changes in slope tend to be rather abrupt, with few intermediate gradients. Thus, the

intersection of two erosional surfaces, or of a plain and inselberg, tends to an escarpment or steep rock slope, irrespective of whether the climate is humid and able to promote continued deep weathering, or arid, supporting predominantly erosional processes. This situation broadly prevails, whether the separation between the two levels is a few tens of metres or is several hundreds of metres.

Above the forest level (2000–3500 m), tropical mountains have features similar to periglacial regions, but at lower levels they have some distinctive characteristics. Valleys tend to be narrow, steep-sided and linear, commonly following joints or other planes of weakness, dividing mountains into blocks with upper plateau surfaces of low relief surrounded by often precipitous slopes. These upper plateau surfaces are raised etchplains, on which the regolith may be retained or partly or wholly stripped. Examples are the ferruginous cuirasses, now occurring at 300 to 1500 m, overlying the nickel laterites in New Caledonia, and the high level bauxites of the Eastern and Western Ghats in India, at 1300–1550 m and 1980–2285 m respectively. Where mountains have been subject to continuous uplift or volcanic activity or are juvenile, no former planation surfaces may have been preserved or developed. Such areas are characterized by a ridge and ravine topography, with landforms strongly influenced by geological structure and lithology.

In humid, equatorial rainforests, dense vegetation continues on slopes greater than 40° and provides some stability for the development of thick soil profiles. However, the high rainfall results in erosion by solifluction and, more catastrophically, by landslide. Rivers tend to have relatively small bedloads and hence little erosive power, so that chemical weathering is an important factor in valley development. With time, flat floors form in valleys, but valley sides remain steep, dissected by tributary streams. As humidity decreases, in the seasonal and semiarid to arid regions, vegetation density also declines and soil development on slopes also declines. Rock exposures are more common and in deserts slopes may consist of bare rock surfaces or merely have a thin cover of lithosols or screes of rock or duricrust.

Landforms of the tropics and subtropics

Because of their common origin, the landforms and regoliths of the humid and arid tropics and subtropics have many similarities. The landsurface is, of course, affected by any changes from the conditions of formation, whether these are induced by tectonic, climatic, vegetational or even anthropomorphic forces. Thus, denudation by water (rain splash, rill wash, sheetwash, gullying or fluvial erosion) or by wind will take place. But although the nature and intensity of the processes depend upon the climatic zone, their effects on a cuirasse- or duricrust-armoured regolith on an etchplain produce terrains with a number of common geomorphological features. The smallest features that can conveniently be considered are slope elements or facets, which are defined in terms of their form, situation within the landscape and the materials, including profile horizon,

TABLE I.1-4

Common facets of the landforms of tropically weathered terrains (modified after Thomas, 1974)

Slope-forming materials	Usual position in landscape
<i>Residual materials</i>	
1. Topsoil on deep weathering profile	Plateau surfaces
2. Duricrust of deep weathering profile	Plateau surfaces
3. Duricrust rubble	Summits and hillslopes around 2
4. Duricrust cliffs (breakaways)	Cliffs around 1
5. Upper zones of weathering profiles	Extensive plains
6. Lower zones of weathering profiles: saprolite, rock fragments and cores	Extensive plains
7. Boulder controlled slopes	Tors as residual hills, boulders on steep hillslopes in forest and semi-desert.
8. Soils on actively weathering rock	Slopes in juvenile or rejuvenated terrain.
<i>Bedrock</i>	
9. Angular jointed rock	Steep hillslopes
10. Smooth bare rock surfaces	Domed inselbergs and rock pavements
11. Truncated rock surfaces	Piedmont footslopes
<i>Transported materials (overlie residual regolith or bedrock)</i>	
12. Hillwash (pedisediment) and scree	Valley sides and lower pediments (also 3)
13. Gravel, scree	Valley sides and lower pediments (also 3)
14. Colluvium	Hillslopes, lower pediments, plains
15. Alluvium, lacustrine deposits	Plains, valley floors/terraces
16. Aeolian deposits	Dunes and sandplains
17. Cemented deposits (some laterites, silcretes and calcretes)	Valley-side benches; deposits in drainage channels and aquifers

in which they are developed (Thomas, 1974). A list of some of the facets common to etchplain relief which can serve as a basis of comparison between different morphoclimatic zones is given in Table I.1-4. This list is not, of course, comprehensive, principal omissions being facets specific to particular lithologies, structures and climatic zones. Landforms are combinations of facets and repetitions of landforms into characteristic patterns are referred to as land or landform systems. This hierarchical classification provides a basis for the description of terrain through a range of mapping scales. The land system approach, for example, has been used to describe arid, savanna and rainforest terrains in

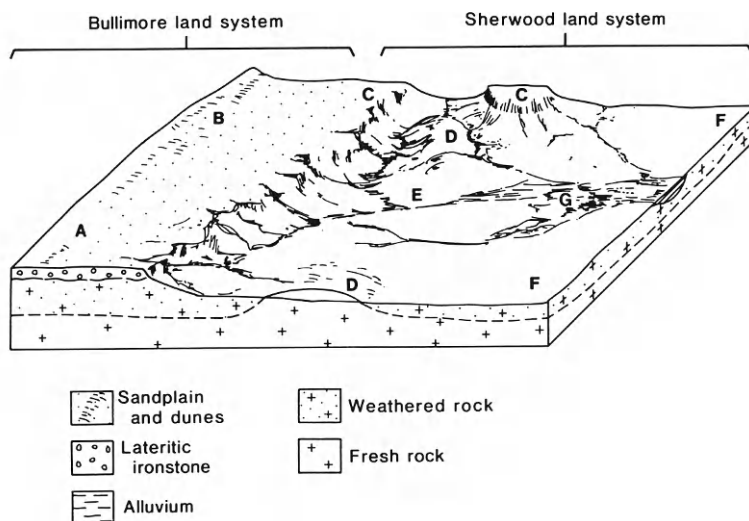


Fig. I.1-3. Examples of land systems, landforms and landform facets from a partly stripped etchplain in semiarid Western Australia. Modified after Mabbutt et al. (1963).

<i>Landform</i>	<i>Facets</i> (see Table I.1-4)	<i>Surficial materials</i>
A Sandplain	14,16	Red clayey sands on colluvium
B Dunes (mostly stable) and swales.	14,16	Red sands
C Partly stripped laterite	1,2,3,4,5,	Ironstones and saprolite
D Low rock hills, to 10 m	7,9,10	Lithosols
E Hill footslopes	7,9,10,11,12	Lithosols and colluvium
F Plains	5,6,11,13	Stony soils on weathered rock
G Drainages	15,17	Red earths on alluvium; valley calcrete.

Australia and Papua New Guinea. Typical examples are shown in Figs. I.1-3 and I.1-4.

Caution must be exercised in the identification of facets and landforms for some with apparently identical appearance may have quite different origins. Thus, erosion of chemical and cemented deposits in alluvium (facets 15 and 17, Table I.1-4) may result in topographic inversion and yield landforms very similar to those derived by erosion of residual ironstones on deep weathering profiles.

Changes from the conditions of formation also affect the regolith, but again many properties remain in common. The intense weathering involved in the formation of the regolith under peritropical conditions result in it being composed of only the most stable secondary minerals (kaolinite, gibbsite, ferric oxides) and the most resistant primary minerals (quartz and accessories such as chromite and zircon) (Table I.1-3). These minerals are largely unaffected by

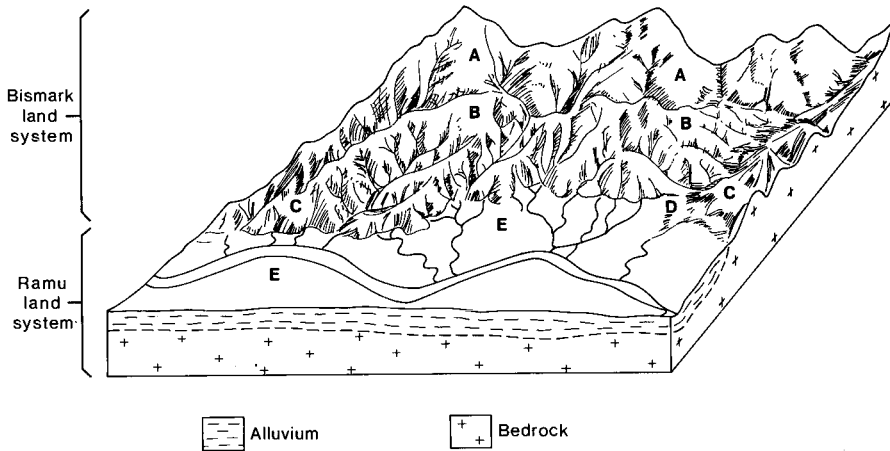


Fig. I.1-4. Examples of landsystems, landforms and landform facets from mountainous humid tropical terrain in Papua New Guinea. Modified after Robbins (1976).

<i>Landforms</i>	<i>Facets</i>	<i>Surficial materials</i>
A Lower mountain ridges, rounded crests. Relief 60–240 m; slopes 0–35°	1,7,8,11,14	Latosolic soils, lithosols, colluvium; well drained.
B Dissected lower mountain slopes. Relief 60–120 m; slopes 17–45°	7,8,11,12,14	Latosolic soils, lithosols, colluvium; well drained.
C Severely dissected foothills. Relief 60–240 m; slopes 17–35°	7,8,11,12,14	Shallow colluvial soils, lithosols; excessively drained.
D Colluvial aprons; some gullying. Relief 10 m.	14,15	Colluvium and alluvium; well drained.
E Flood plains	15	Alluvium; poorly drained.

change to less humid or less severely leaching conditions, and hence the broad chemical characteristics of the regolith are retained, except for erosional and some pedochemical modifications at the surface. In drier climates, continued weathering at the base of the profile does, however, result in rather different mineralogy, especially the development of 2:1 lattice clays (e.g. smectites) and, in semiarid and arid environments, retention and accumulation of components such as alkali and alkaline-earth elements and silica. The principal modifications of the regolith due to changes from the conditions of formation are summarized in Table I.1-5. An understanding of the geochemical significance of these modifications is essential for the correct interpretation of exploration data. Dispersion patterns associated with these later episodes are superimposed upon those inherited from the past and together give rise to the present surface expression of mineralization.

GEOCHEMICAL DISPERSION AND EXPLORATION MODELS

Objectives of geochemical dispersion models

Conceptual and methodological models that represent data and interpretations for particular generalized situations provide the most convenient method of summarizing information of relevance to geochemical exploration (Bradshaw, 1975). Although geological, geomorphological and environmental conditions are different for each location, so that the geochemical response to mineralization is always unique in some respects, many similarities in dispersion characteristics may nevertheless be present over extensive regions. Geochemical dispersion and exploration models attempt to synthesize these characteristics to illustrate the nature and origin of the surface expression of mineralization. Ideally, it should be possible to use such models predictively when planning surveys, to anticipate mechanisms of dispersion, select appropriate sample media and estimate the nature and significance of anomalies. The "landscape geochemistry" approach (Fortescue, 1975) has been adopted in all attempts to derive such models and is particularly important for tropically weathered terrains in which the models must account for relict features as well as active processes.

TABLE I.1-5

Effects on the lateritic regolith of changes from the conditions of formation

TECTONIC ACTIVITY

Uplift:

- lowering of the water-table;
- irreversible dehydration and hardening of ferruginous and siliceous horizons;
- increased leaching of upper horizons under more oxidizing conditions;
- increased erosion.

Downwarping:

- waterlogging of lower parts of the landscape and imposition of reducing conditions;
- decrease in erosion, increased sedimentation in valleys.

CLIMATIC CHANGE

To a more humid climate:

- increased leaching and deeper soil development;
- decreased erosion (due to thicker vegetation).

To a less humid climate:

- decreased leaching;
- increased erosion.

To a semiarid or arid climate:

- decreased leaching;
 - retention and precipitation of silica, alkaline earths and alkalis in silcretes, clays, calcretes, salts;
 - increased erosion.
-

Classification of geochemical dispersion models

The genetic links between the various tropical and subtropical terrains provide a framework by which geochemical dispersion may be described and a basis for comparison between regions. Indeed, the facet–landform–land system classification emphasizes geochemically important parameters—i.e. origin and nature of substrate—in its definition and is appropriate at prospect, semi-regional and regional scales. An approach of this type was used to establish geochemical exploration models in Australia (Butt and Smith, 1980). The models correspond to facets and landforms defined and classified according to the degree of stripping of an etchplain, their relationship to the deep weathering profile, the presence of (later) overburden and the relief (Fig. I.1-5). A similar, more generalized classification for all tropically weathered terrains is followed in this volume. Subdivision within each climatic/morphoclimatic zone is based on the relief, the degree of preservation of the pre-existing regolith and the effects of later physical and chemical modifications (Butt, 1987; Butt 1989a; Butt and Zeegers, 1989). The criteria upon which the classification is based are as follows:

Relief. Except in extremely arid regions, such as in the Saharan and Arabian deserts, local and regional relief control the degree of preservation of the profile. In areas of low to moderate relief, physical erosion is mostly slow and inefficient so that deep regoliths may develop and any pre-existing regolith may be preserved wholly or in part; geochemical dispersion tends to be dominated by chemical mechanisms, active now or in the past. Conversely, in areas of moderate to high relief, the rates of physical erosion exceed those of chemical weathering even in humid climates, precluding preservation or formation of thick regoliths. Where uplift and rejuvenation of drainage have led to the dissection of uplifted plateaux, any pre-existing regoliths are eroded and destroyed. Accordingly, geochemical dispersion in these areas is dominated by currently active, and mostly physical, processes. In general, therefore, due to the reduction in the importance of chemical dispersion, both past and present, the greater the relief, the greater is the similarity in geochemical expression of mineralization, in all environments. Initial subdivision is thus into models for terrains of (a) low to moderate relief and (b) moderate to high relief.

Present climate and morphoclimatic zone. These govern active weathering and dispersion processes, including the formation of soil from the exposed horizons of the pre-existing regolith. The amount and seasonality of the rainfall strongly influence the degree to which the profile is modified, e.g. by leaching or the precipitation of introduced components. However, as relief increases and active physical erosion becomes the dominant dispersion process, the influence of the present climate declines.

Degree of preservation of the regolith profile. This largely determines the importance of geochemical and mineralogical characteristics inherited from

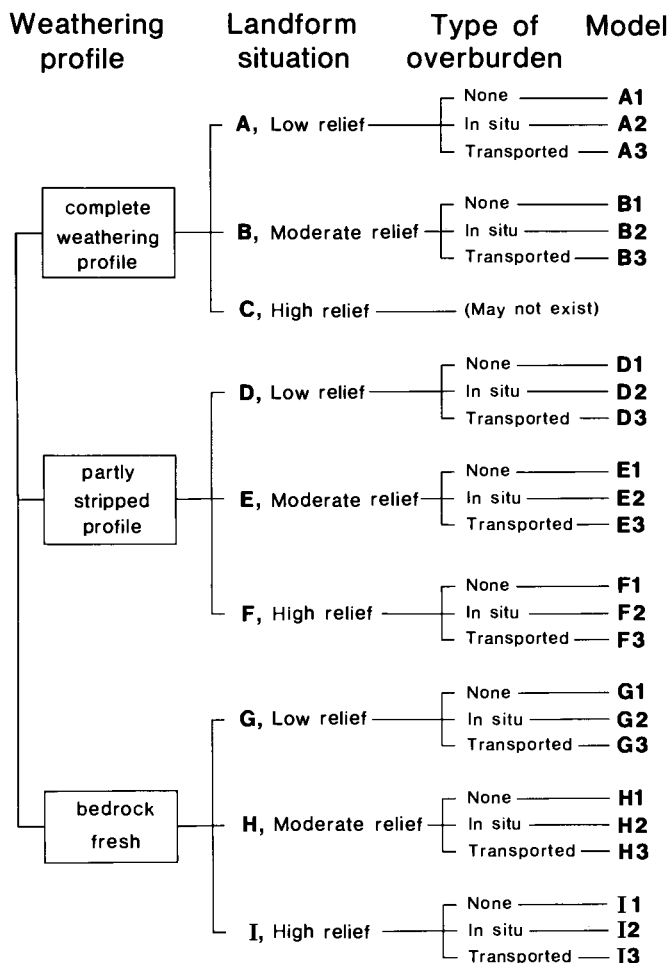


Fig. I.1-5. Hierarchical classification of geochemical dispersion models in Australia. From Butt and Smith (1980).

previous weathering episodes, for example, enrichments of Al, Fe, Ni and Au, and depletions of Na, K, Ca, Mg, Cu and Zn. It also determines the nature of the uppermost residual horizon, whether modified as soil or buried beneath transported overburden. "A" type models are those in which the profiles are fully preserved. The uppermost residual horizon is commonly the lateritic ferruginous horizon, or soils developed over or from it. "B" type models are those in which profiles are partially truncated by erosion, so that deeper saprolite horizons with quite different geochemical characteristics from the ferruginous horizon form the uppermost horizon and the parent material of residual soils. "C" type models are those in which the earlier regolith has been entirely eroded and bedrock is

either buried by transported overburden, outcrops at surface or has residual soils forming directly from it. Such models are particularly important in very arid areas in which any pre-existing profile is only preserved beneath resistant bedrock, such as basalt flows.

Recent alteration. Marked chemical alteration of the regolith may have occurred under the present climate or during an intermediate period since earlier deep weathering, induced by changes in weathering conditions due to tectonism and/or climatic change. The result is commonly either increased leaching or the neoformation or accumulation of secondary minerals (Table I.1-5). The degree of alteration is only subjectively estimated as “minor”, “low”, “moderate” or “strong”; the strongest leaching results in the formation of stone-line profiles in rainforests, whereas the strongest precipitation, in arid areas, results in replacement, e.g. by calcrete. These alterations may be cumulative and hence produce the most complex geochemical responses. For example, repeated leaching and/or the absolute accumulation of introduced components can cause strong impoverishment and/or dilution of most geochemical pathfinder elements, especially in near-surface horizons.

Neoformation or accumulation of minerals. These are consequences of changes in the degree of leaching. Increased leaching, such as in rainforests (Chapter III.1) or in winter-rainfall (Mediterranean) climates (e.g. Darling Range, Western Australia; Anand et al., 1985) may lead to allitization, the formation of gibbsite from kaolinite or directly from primary aluminosilicates (see p. 32). Conversely, in drier regions, smectites may form instead of kaolinite, and silica and alkaline earths may be retained in the soil sequence, commonly as cements (e.g. as silcrete and calcrete).

The presence and nature of overburden. The materials that form the surface layer are commonly critical in determining the most appropriate exploration sample media. There may be no overburden, so that untransformed weathered bedrock (e.g. lateritic cuirasse, saprolite) or fresh bedrock may outcrop, or the overburden may be in situ (as residual soil), transported (e.g. alluvium, aeolian sand, talus) or a semi-residual mixture (e.g. colluvium, residual soil plus aeolian silt and clay).

The classification based on these criteria is given in Table I.1-6 and can be used to summarize the characteristics of each site or prospect as a code (e.g. a prospect in an arid area of low relief, model code B 1 Ca [1], has a truncated profile slightly modified by the formation of a residual soil and the development of calcrete). The scheme is, of course, generalized and simplistic, for where there have been frequent climatic and tectonic changes, complex sequences exist. Nevertheless, it provides a framework that enables valid comparisons to be made between terrains that are now in quite different climatic zones but which have

TABLE I.1-6

Classification of geochemical dispersion models for tropically weathered terrains (see text for explanation)

Present climate	Savanna (seasonally humid; Aw, Cwa) Rainforest (humid; Af, Am, Cwb) Warm arid (BSh, BWh) (Köppen classification, Table I.1-1)
<i>Modifications to pre-existing profile within each climatic zone.</i>	
Pre-existing profile	A: Mostly preserved B: Partly truncated C: Fully truncated
Recent alteration	0: Minor 1: Low 2: Moderate 3: Strong
Recent accumulation, cementation or neof ormation	0: None Al: Al-oxides AS: Al-silicates Ca: Ca and Mg carbonates (calcrete) Gy: Gypsum Fe: Iron oxides Si: Silica (silcrete) Sm: Smectites
Overburden on pre- existing profile	0: None 1: Residual soil 2: Semi-residual 3: Transported
Examples: A 0 0 [0,1]:	lateritic cuirasse, outcropping or beneath residual soil.
B 1 Ca [3]:	truncated profile, some recent alteration with pedogenic calcrete and transported overburden.

N.B. An asterisk * can be used for generalized models for which a characteristic is not diagnostic:

B * * [3]: buried truncated profile, with any type of recent alteration, neof ormation or cementation.

important geochemical similarities. Block diagrams illustrating the classification in terms of some landform and dispersion models are shown in Figs. I.1-6 and I.1-7. Partial erosion of the pre-existing regolith as a response to uplift and/or climatic change results in similar landforms and hence a similar range of dispersion models being developed in each climatic region. The differences between equivalent models are due to modifications of the original regolith, many of which are minor and tend to have a quantitative rather than qualitative effect on dispersion patterns. In comparison with the Australian classification shown in Fig. I.1-5 (Butt and Smith, 1980), type A models correspond to

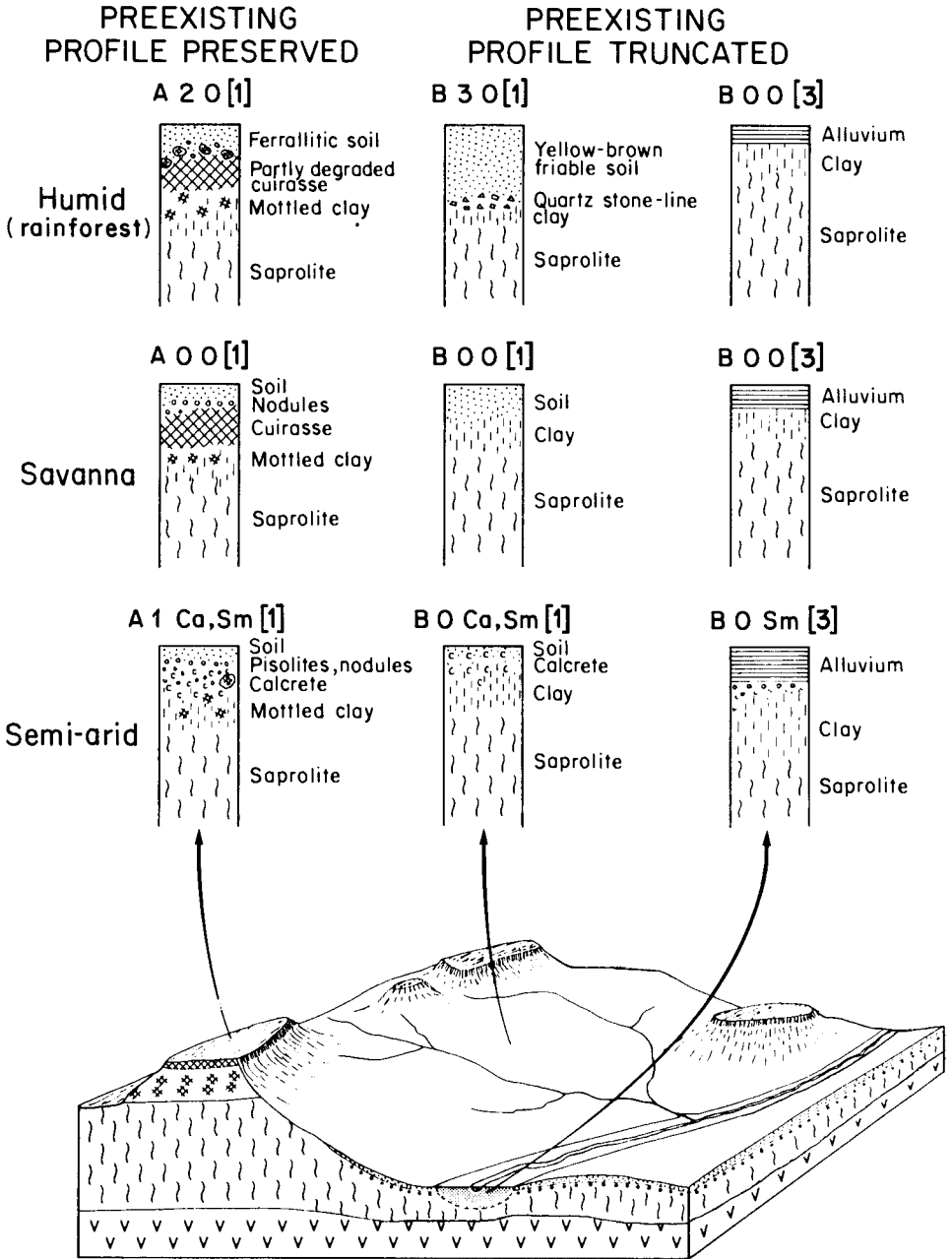


Fig. I.1-6 Comparison of some weathering profiles and models in a partly eroded, tropically weathered landscape. Equivalent models in similar landform situations in different climatic zones differ mainly through modifications to the regolith subsequent to deep weathering (from Butt and Zeegers, 1989). For explanation of model codes, see Table I.1-6.

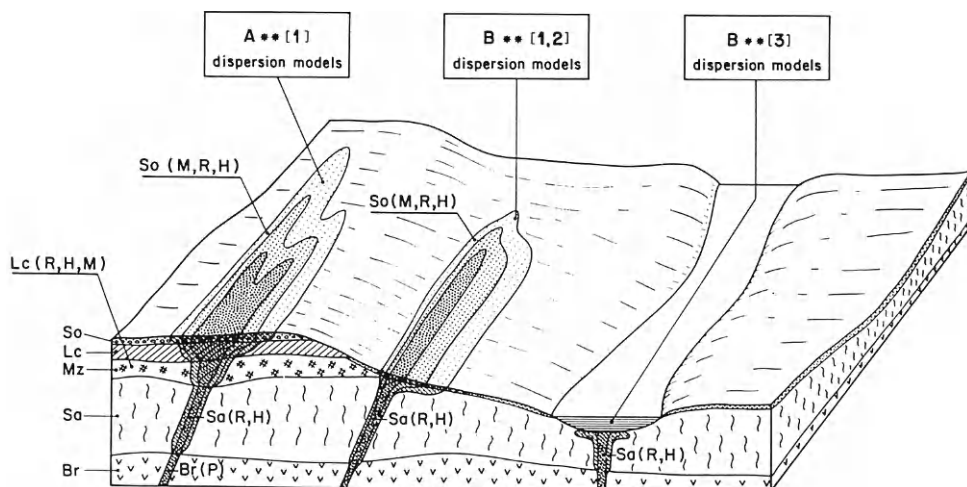


Fig. I.1-7. Typical dispersion haloes in a partly eroded, tropically weathered landscape. Stippling indicates dispersion haloes. N.B. not to scale; anomaly sizes and contrasts illustrative only. From Butt and Zeegers (1989). For abbreviations, see Fig. III.1-1, p. 204.

landform situations A, B and C, type B models to landform situations D, E and F, and type C models to landform situations G, H and I. Further subdivisions are essentially similar.

The classification, particularly of the overburden, may in effect indicate the broad land system in which the site occurs. A more specific classification can be made by using, for "overburden", terms that represent landforms or even individual facets, such as those listed in Table I.1-4. Such an approach would have particular value in a restricted region, for which landforms or facets are well defined. Although also applicable on a broader scale, such a detailed classification is not used in this volume, principally because the level of detail available for examples and case histories is inadequate.

Application of the geochemical models

The philosophy behind the model classification forms an underlying theme to this volume. The classification is the basis of the layout of Parts III and IV, in which the models are used to explain the characteristics of geochemical dispersion in each of the principal climatic zones. Each model is illustrated by appropriate case histories. Comparison of like models from different climatic zones can readily be made (e.g. by reference to the model codes) and permits the recognition and transfer of relevant experience between climatically different environments. Such comparisons should lead to better understanding of the processes involved and improvements in the interpretation of geochemical exploration data. These models apply particularly to terrains of low to moderate relief

discussed in Part III that characterize extensive regions of the continental landmasses of lower latitudes. They are less appropriate for areas of high relief. Except for remnants in uplifted plateaux, deep regoliths are neither preserved nor developed, so that differences in dispersion between different climatic zones are much less marked. Models relevant to dissected and mountainous terrain are discussed separately in Part IV.

CHEMICAL WEATHERING

Jean-Jacques TRECASSES

INTRODUCTION

Weathering of rocks

The *weathering zone* is the transitional contact between the lithosphere and the atmosphere in which the physical, mineralogical and chemical properties of fresh bedrock are progressively modified, ultimately forming soil at the surface. The thickness of the weathering zone is commonly only a few metres, but may be several tens of metres in tropical areas. It is absent only in extreme topographic environments, such as very steep slopes in young mountain areas, or in regions of extreme climatic conditions such as deserts. Weathering causes rocks that are usually coherent, dense and composed of anhydrous or weakly hydrated minerals to alter progressively to friable material with a lower bulk density composed principally of strongly hydrated phyllosilicates and hydroxides, most of which are microcrystalline.

This evolutionary change in mineralogy is the result ultimately of differences in conditions such as pressure, temperature and fO_2 between the environments in which the rocks were formed and those at the surface. The paragenesis of a rock represents, for a given chemical composition, equilibrium between the constituents under the conditions of formation. Such conditions are obviously highly variable, depending on the mechanisms that created the rock, which vary from diagenesis of sediments (low to moderate temperature and pressure) to metamorphism and magmatism (high temperature and pressure). In any case, such conditions are radically different from those prevailing at the surface, which can be defined by the following parameters: mean $T < 30^\circ\text{C}$; mean $P < 1$ bar; presence of H_2O ; availability of oxygen from the atmosphere. At the surface, the *primary* rock-forming minerals are therefore in a state of thermodynamic disequilibrium. In the presence of water, which is virtually ubiquitous as an interstitial fluid that favours exchanges of matter, the chemical constituents tend to seek a new equilibrium in the form of *secondary* minerals.

The secondary minerals are, of course, important constituents of the regolith samples collected during geochemical exploration and may host elements released and dispersed from primary mineralization by weathering. The secondary minerals may also be of direct economic interest themselves. Accordingly, determination of the mineralogy of regolith samples and a knowledge of the

reactions involved in their formation will indicate the conditions under which weathering occurred and hence lead to a more accurate interpretation of geochemical data. The principal reactions responsible for the weathering of the rock-forming minerals, the conditions under which they occur and the regolith profile that results are described in this chapter. The dispersion characteristics of the chemical elements and the weathering of sulphide minerals are discussed in Chapters I.5 and II.1 respectively.

Role of meteoric agents

Weathering is controlled by the availability of water and by the temperature. These are governed by the two fundamental factors that define the climate, namely annual average precipitation and average temperature (see Chapter I.1). This strong interaction between meteoric agents and the surficial evolution of the lithosphere is illustrated by the global distribution of the main weathering and soil types. A zone of *active* weathering is virtually absent where water is unavailable, such as in very high latitudes and in the desert belts where rainfall is insufficient. The weathered zone is relatively thin and not strongly differentiated in the temperate middle latitudes. However, it becomes very thick and chemically highly evolved in the tropics, with the formation of laterites *sensu lato*. The variations in soil types and thickness of the weathering zone with latitude are shown in Fig. I.2-1. Biological activity, principally by vegetation and microorganisms, also plays a role in soil formation but equally its significance is also governed by climate.

Within the major latitudinal climatic belts, variations in weathering development are obviously controlled by lithology. Consequently, soil maps at small scales closely resemble equivalent geological maps. At large scales, local variations play a determinant role, mainly as a function of the topographic conditions that govern drainage or the rate at which weathering solutions can be replaced.

Role of initial porosity of the bedrock

Rock weathering is the result of interactions between primary minerals and chemical agents, particularly H_2O , O_2 and CO_2 , that circulate below surface. Experimental studies on a large number of rock types and minerals, and under varying conditions, have greatly increased understanding of the reactions and mechanisms of weathering (Pedro, 1964; Wollast, 1967; Trichet, 1969; Robert, 1970; Delmas, 1979; Berner and Holdren, 1979; Berner et al., 1980; Schott et al., 1981). Thermodynamic modelling and computer simulation of the interaction between minerals and chemical agents can also explain, at least in a general sense, the mineralogical and chemical modifications caused by weathering (Garrels and Christ, 1965; Helgeson, 1968; Helgeson et al., 1969; Tardy, 1969; Michard and Fouillac, 1974; Fritz, 1975, 1980).

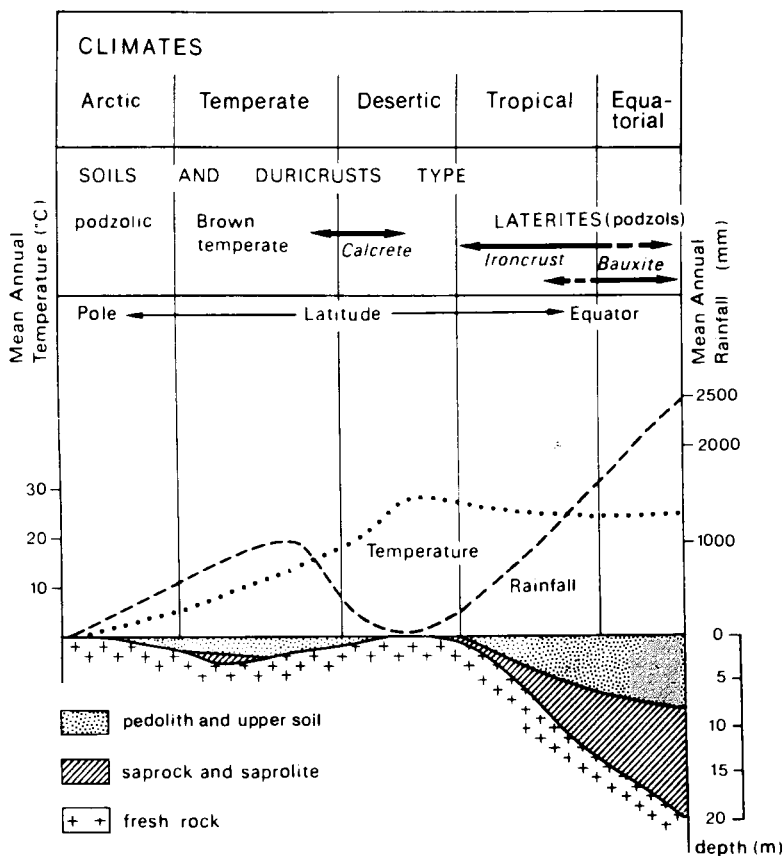


Fig. 1.2-1. Soils, types of duricrust and thickness of the weathering zone and their relationship to the principal climatic factors (mean annual temperature and mean annual rainfall). Modified after Pedro (1985).

A primary mineral only reacts with a chemical agent when they are in contact; however, this occurs at specific sites and is closely controlled by access to the solutions. For this reason, weathering usually starts at contacts between adjoining primary minerals, or along microfractures within the minerals. Because weathering causes the general removal of matter (see below), the initial porosity increases rapidly, resulting in a reduction of the bulk density of the material. As the rate of flow of percolating solutions increases, the primary minerals are progressively changed into secondary minerals. These minerals, which are usually poorly crystallized, constitute the “weathering plasma” that occupies part or all of the original volume of the rock. Initially at least, the weathering reactions can differ from site to site, so that weathering environments are thus strongly heterogeneous both spatially and geochemically (Ildefonse et al., 1979; Pedro

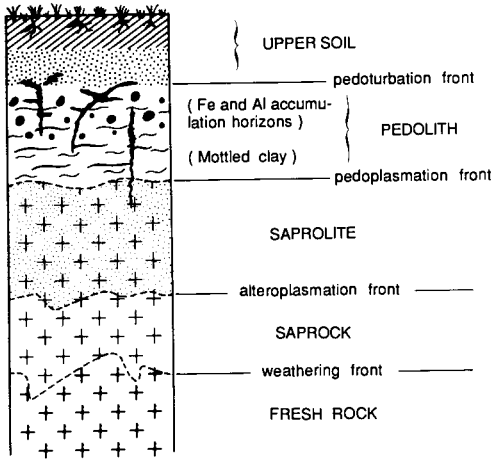


Fig. I.2-2. Schematic vertical succession of horizons in a lateritic weathering profile.

and Delmas, 1980–1981). The result is the formation of a weathering profile which consists of a vertical succession of horizons (Fig. I.2-2) or groups of horizons. In a residual profile, these are, from the base:

Saprock: compact, slightly weathered rock, with low porosity and therefore a low water content. Weathering only occurs at the contacts between minerals and intramineral fissures.

Saprolite: more-or-less friable and hydrated unit in which the primary minerals progressively decompose. The initial fabric and volume of the rock are preserved because the expansion which accompanies the transformation of some primary minerals into plasma is offset by the reduction of volume resulting from the weathering (and even dissolution) of other components.

Pedolith (mottled clay zone, nodular horizons with Fe- and Al-accumulation): the structure of the “primary” plasma is progressively modified into “secondary plasma”, which in tropical profiles includes the formation of ferruginous patches (mottled clay zone) and nodules (nodular horizons). These transformations, the main result of which is the loss of the primary lithic fabric, mark the *pedoplasma front* (see p. 60). An important characteristic of this unit, therefore, is that its formation has not been isovolumetric. Furthermore, during its development, only the base of the unit is below the water-table so that the pores in the remainder are not generally saturated with water.

Soil: the surficial unit, the development of which is closely governed by vegetation and fauna. Strong reworking of the fabric marks the *pedoturbation front*. Soil is relatively thin, even in rainforests, compared to saprolite.

N.B. Profile terminology is summarized in Appendix 3.

TYPES OF WEATHERING REACTION

Various chemical reactions take place between primary minerals and interstitial fluids, the products of which are the secondary minerals that form the weathering profile and the dissolved material that is removed from the profile by groundwater. These reactions can be classified into six main categories, depending on the type of primary mineral and the weathering conditions: dissolution, oxidation, hydrolysis, transformation, alkalinolysis and acidolysis.

Dissolution

Dissolution is the simplest weathering mechanism, but it affects only a restricted number of minerals, essentially those with a high solubility product. Minerals affected include salts (e.g. halite), sulphates (e.g. gypsum) and, to a lesser extent, carbonates (e.g. calcite and dolomite). Dissolution reactions can be represented schematically by simple dissociation into the constituent ions. For halite:



For calcite, which has a very low solubility in pure water ($[\text{Ca}^{++}] = 10^{-3.9}$ at 25°C, equivalent to about 10 mg/L CaCO_3), the principal dissolution agent is CO_2 . When CO_2 dissolves in water it yields H_2CO_3 , which partially dissociates to HCO_3^- and CO_3^{2-} . Dissolution of calcite is therefore governed by the combination of the following four equilibria:



The solubility of calcite increases with the partial pressure of CO_2 , which is $10^{-3.5}$ in the atmosphere, but can be 10–100 times higher in soils, as the result of decomposition of organic matter and root respiration. Even quartz can be dissolved, by a hydration mechanism:



The solubility of the molecule H_4SiO_4 is approximately 20 times that of quartz at 25°C and $\text{pH} < 9$ (6 mg/L SiO_2 for quartz in these conditions). Continental surface and subsurface waters usually have a silica content of more than 6 mg/L

and hence are supersaturated with respect to quartz. The dissolved silica is derived from weathering of other silicates, including amorphous silica. However, if no other silicates are present, having been weathered during an earlier phase of profile development, quartz can be dissolved by percolating waters having a composition close to that of rainwater. This may occur particularly in the uppermost horizons and is a mechanism that plays a role in the formation of lateritic profiles in the tropics.

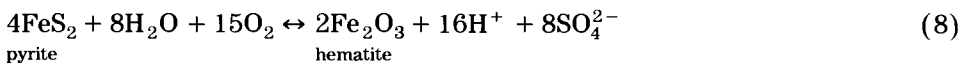
Oxidation

Some elements can be present in several oxidation states in rock-forming minerals; examples include iron (Fe^{2+} or Fe^{3+}), manganese (Mn^{2+} , Mn^{3+} , Mn^{4+}) and sulphur (S^{2-} or SO_4^{2-}). In the primary environment, the fugacity of oxygen is generally very low so that these elements are generally present in the lowest state of oxidation, i.e. Fe^{2+} , Mn^{2+} , S^{2-} . In the weathering zone, however, atmospheric oxygen is introduced by percolating solutions and oxidation may occur. For example, ferrous iron, a major rock constituent, is then oxidized to ferric iron:



Electron liberation in this half-reaction is compensated for by electron consumption by the oxygen. Dissociation of water molecule and proton (H^+) production is known as ferrollysis. According to Morris and Fletcher (1987), the solubility of quartz can be increased following the ferrous-ferric Fe-reaction. In a weathering environment, ferric iron very rapidly becomes the only stable form, forming goethite (FeOOH) or hematite (Fe_2O_3) which are responsible for the ochre or reddish colours in the profile. The respective fields of Fe^{2+} and Fe_2O_3 as a function of pH and Eh are shown in Fig. I.2-3. Similarly, oxidation of Mn^{2+} produces manganite (MnOOH) and the Mn^{4+} oxides, such as cryptomelane, pyrolusite and lithiophorite, which are responsible for the black coating in fissures and the formation of some nodules in tropical soils.

Finally, pyrite, a common accessory mineral in many rocks, is also easily weathered under oxidizing conditions:



This reaction, which corresponds to the simultaneous oxidation of Fe^{2+} and S^{2-} , contributes to strong acidification of the environment surrounding the weathered pyrite grains. The sulphate ions that are produced are generally removed in solution.

Hydrolysis

Although oxidation is the easiest mechanism to observe, because of the colour change it causes in weathered material, it only follows or accompanies reaction

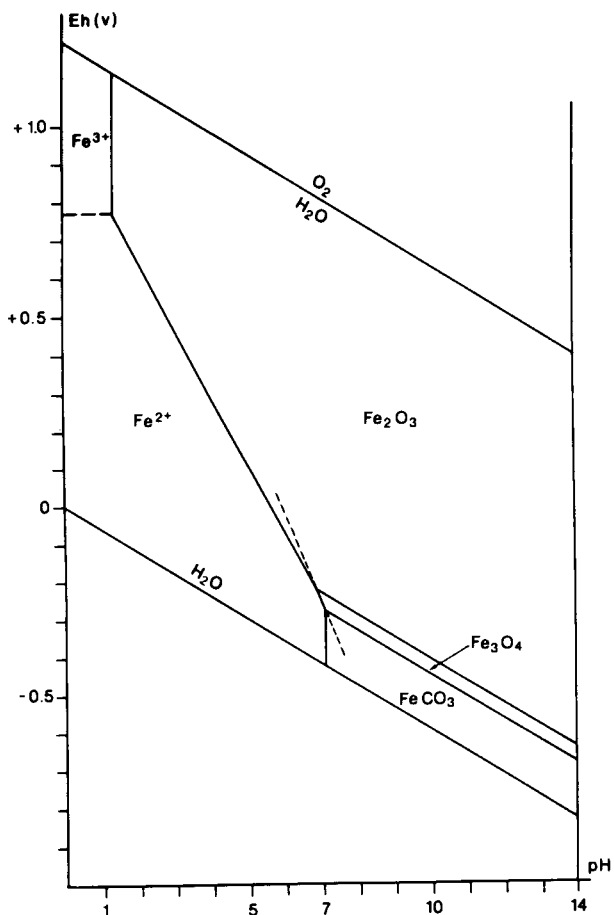
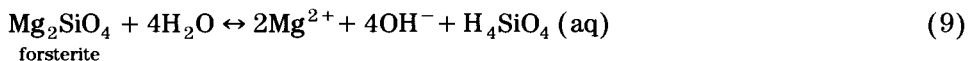


Fig. I.2-3. Phase diagram of the oxidation of Fe^{++} at 25°C and 1 atm. total pressure. Boundary between solids and ions at a total activity of dissolved species = 10^{-6} and $p\text{CO}_2 = 10^{-2}$; dashed line corresponds to $[\text{Fe}^{2+}] = [\text{Fe}^{3+}]$.

with water. The nature of this reaction is pH dependent. In most weathered environments, in which the pH is between 5 and 9, the usual reaction, particularly for the weathering of silicates, is *hydrolysis*.

The hydrolysis of silicates produces hydroxyl anions, cations, dissolved silica and, possibly, secondary minerals. The simplest system is that represented by non-aluminous minerals such as forsterite:



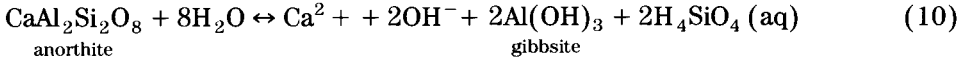
This represents true, congruent dissolution of the primary mineral (*aplasmagenic* weathering, with no solid product or residue), but unlike the dissolution of

the ionic components, the reaction involves a change in the pH. Hydrolysis causes dissociation of water molecules, consumption of H^+ ions and production of OH^- ions, in accordance with the charge balance of the reaction, but also causes the pH to rise and the solution to become alkaline.

For olivine ($(Mg,Fe)_2SiO_4$), the hydrolysis reaction is exactly the same, but has in addition the oxidation of liberated Fe^{2+} ions to form ferric hydroxide (either an orphous or as goethite), as described by equation (7). In certain cases, congruence is not perfect and some of the liberated silica precipitates as opal or microcrystalline quartz, instead of being entirely dissolved as H_4SiO_4 . If hydrolysis leaves a nonsoluble and immobile residue, it is said to be *plasmagenic*: in the case of olivine, the plasma is ferruginous or siliceous.

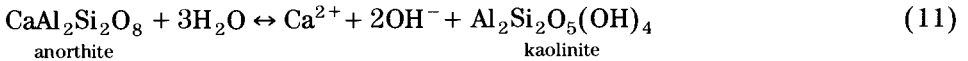
Most primary silicates are aluminous, but aluminium is least soluble in the pH range of hydrolysis and is not readily removed from the weathering profile. Three types of hydrolysis reactions involving aluminosilicate minerals are possible (Pedro, 1966), depending on the nature of the residue.

Allitization: formation of a gibbsitic residue. The liberated Al precipitates to form gibbsite:



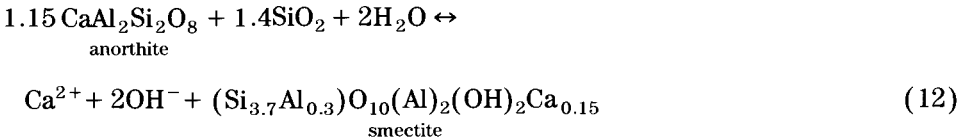
Hydrolysis is total and the gibbsitic plasma occupies part of the volume previously occupied by the anorthite. When Fe is also present, the plasma is both ferruginous and gibbsitic and the reaction can be referred to as ferrallitization: this mechanism is an important process in lateritization.

Monosiallitization: formation of a kaolinitic residue, consisting in a phyllosilicate phase with one silicic tetrahedral elemental surface (type 1/1). The liberated Al recombines with silica to form a kaolinitic plasma:

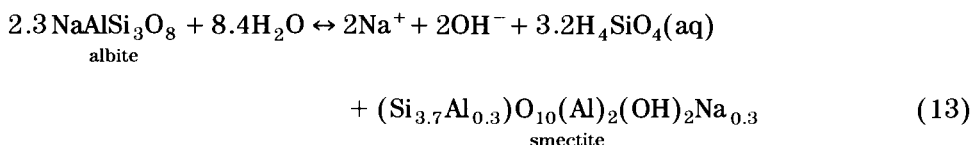


Reaction (11) uses fewer water molecules than reaction (10) and takes place in slightly less hydrated and less freely drained weathering environments. Hydrolysis is only partial, but there is still a total loss of alkaline and alkaline earth elements. However, the resultant kaolinitic plasma occupies a much greater volume than that of gibbsite formed by allitization.

Bisiallitization: formation of a smectitic residue, i.e. phyllosilicates with two tetrahedral elemental surfaces (type 2/1). The liberated Al recombines with silica, some cations and, commonly, with Fe to form a smectitic plasma:



This reaction consumes even fewer water molecules than reaction (11) and takes place in poorly drained environments from which leaching of basic cations, here Ca^{2+} , is only partial. With albite, the reaction is one of partial desilicification rather than requiring additional silica:

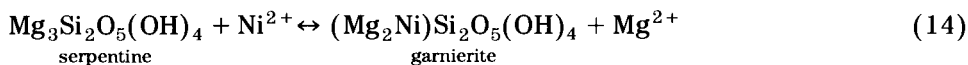


The bisiallization of ferromagnesian minerals produces smectites with an octahedral elemental surface consisting of Al and Fe^{3+} (beidellite-nontronite). With minerals that are practically devoid of Al, such as olivine or orthopyroxene, additional Al is provided by weathering of neighbouring (aluminous) minerals. In all cases, the resultant plasmic minerals are neoformed, i.e. precipitated from weathering solutions (Millot, 1964). Thermodynamic modelling of reactions (10), (11) and (12) is summarized by the phase diagram shown in Fig. I.2-4.

Transformation

In primary minerals that already have a phyllosilicate structure, weathering can be considered as a simple solid-state transformation in which the organization of oxygen and most silicon ions is retained. This mechanism, which produces a *transformation plasma*, is analogous to ion exchange. The transformation of tri-octahedral micas into vermiculite is typical (Robert, 1971, 1972; Robert and Pedro, 1972). The K of the mica is replaced by hydrated cations, but the oxidation of ferrous to ferric ions causes disequilibrium in the charge of the layer. This transformation can continue until smectite-like minerals are formed. This type of weathering is typical of humid temperate climates, but can also occur in arid environments.

A similar mechanism governs the transformation of serpentine to nickeliferous serpentine, in which Ni partially replaces Mg in the octahedral layer. This is a common process at the base of weathering profiles developed over serpentized ultrabasic rocks (Trescases, 1979):



Alkalinolysis (weathering in very alkaline environments)

In arid regions, strong evaporative concentrations can result in high alkalinity ($\text{pH} > 9.6$) in the weathering zone, so that both silica and aluminium become highly soluble:

- silica as $\text{H}_3\text{SiO}_4^- + \text{H}^+$;
- aluminium as the anion $\text{Al}(\text{OH})_4^-$.

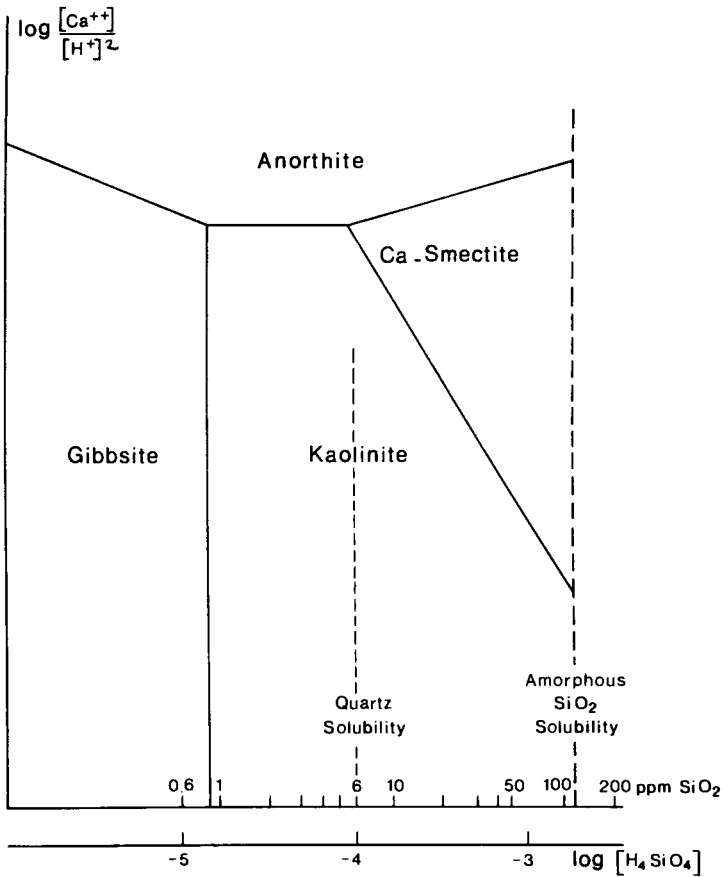
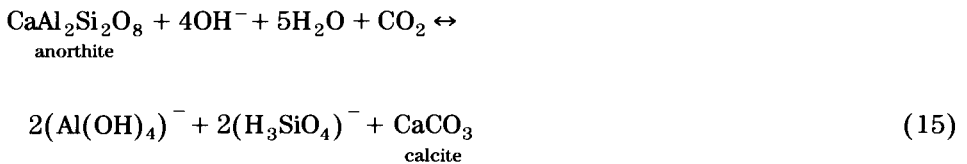


Fig. I.2-4. Phase diagram of thermodynamic modelling of the hydrolysis reactions of anorthite. Derived from Tardy (1969).

The weathering of anorthite under these conditions is:



This reaction is distinct from hydrolysis because it consumes hydroxyl anions OH^- and can be referred to as *alkalinolysis* (Pedro et al., 1969; Pedro, 1983). Calcium is no longer soluble under such alkaline conditions and precipitates as calcite in concretions or as calcretes. In hyperconcentrated environments, alka-

TABLE I.2-1

Principal geochemical mechanisms of weathering and corresponding soils and climates (modified from Pedro, 1984)

Mechanism	Secondary minerals	Soluble phase (major elements)	Soils	Climate
Acidolysis	Quartz	Al,Fe,Na,K,Ca,Mg	Podzols	Humid
Alkalinolysis	Carbonates (Ca,Mg,Na)	Al,Si	Solods	Tropical, arid
Hydrolysis				
Allitization	Gibbsite, goethite hematite	Si,Na,K,Ca,Mg	Ferrallitic soils (laterites)	Tropical, humid (rainforest)
Monosiallitization	Kaolinite, goethite hematite	Si,Na,K,Ca,Mg	Ferrallitic soils (laterites)	Tropical, short dry season (wet savanna)
Bisiallitization	Al-Fe smectites	Na,K,Ca,Mg	Vertisols	Tropical, long dry season (dry savanna)
Transformation	Vermiculite- smectite	Na,K	Brown soils	Temperate

host mineral (e.g. silicate, sulphide or carbonate) their behaviour is also governed by the laws of solution chemistry, and they can form secondary minerals, such as the nickeliferous silicates (garnierites, equation (14)). However, trace elements can also be adsorbed by secondary phases such as clay minerals, Fe and Mn oxides and organic matter (see Chapter I.5).

The preceding discussion implies a certain number of simplifying hypotheses. The use of thermodynamic reasoning, such as in the application of the law of mass action to construct the phase diagrams of Figs. I.1-3 and I.1-4, presupposes that the reactions are at equilibrium, that the solutions are dilute and that the pore size permits unhindered water circulation (water activity = 1). In reality, not all of these conditions are fulfilled in the weathering environment. Furthermore, even if the thermodynamics indicate the direction of a reaction and the conditions under which it is possible, they do not indicate its rate. The application of chemical kinetics to weathering processes is still in its infancy (Helgeson, 1971; Busemberg and Clemency, 1976; Delmas, 1979; Berner, 1981; Massard, 1982). A very approximate idea of the rate of weathering can be provided by a combined study of water geochemistry and the hydrological balance of catchments with uniform geology. The rates that have been calculated by different authors vary greatly, depending principally on lithology and climate, and range between from 5 and 50 mm per 1000 years (see Table I.3-2). The estimates all indicate, however, that weathering progresses very slowly and that the thick lateritic mantle of the tropics was mostly formed over periods of several million years. Conversely, the detailed development of a weathering profile can be defined with

precision, from examination of the mechanisms that are active at each level of the profile and result in the differentiation between the horizons.

DEVELOPMENT OF A WEATHERING PROFILE

Differential weathering of primary minerals

Most rocks are composed of assemblages of different minerals that, in general, do not begin to weather simultaneously. In relatively simple situations, exemplified by the weathering of peridotitic ultrabasic rocks, there can be a strong correlation between the differential weathering of the constituent minerals and the formation of successive horizons in the profile (Trescases, 1975, 1979, 1986). Olivine is the first mineral to be weathered. In tropical environments, its progressive hydrolysis results in the total leaching of Mg and, initially, some leaching of Si. In the basal horizon of the profile (saprock), poorly crystalline Fe^{3+} hydroxides (with Ni and Si) or, less commonly, ferruginous smectites, partially fill the cavities previously occupied by olivine. The other primary minerals remain unweathered, however, and the cohesion of the rock is preserved.

The hydrolysis of orthopyroxene, and then of serpentine, only commences after the total disappearance of olivine. The porosity increases markedly at this stage so that the solutions percolate faster and become less alkaline. As the serpentine network is gradually destroyed and replaced by goethitic pseudomorphs, the cohesion of the rock is lost and the texture of the weathered material becomes argillaceous. As long as serpentine remains, however, the fabric of the rock as a whole is not severely altered: the weathering is isovolumetric and the resulting products constitute the saprolite.

When the hydrolysis of all the primary silicates is complete, the residual ferruginous material (essentially goethite) progressively loses the original lithic fabric, initially by compaction, then by nodule formation and finally by the development of ferruginous crusts by the replacement of the goethite of the nodules by hematite. Such horizons, which are almost exclusively ferruginous (Fe_2O_3 contents are approximately 75%), form the upper part of the profiles that develop over ultrabasic rocks in the tropics.

Differential weathering can also be demonstrated in rocks that contain primary quartz. Over most lithologies, quartz is almost unaffected during the first stages of tropical weathering, provided that hydrolysis of other silicates maintains a high concentration of dissolved silica. Accordingly, weathering of quartz only occurs at the top of lateritic profiles where kaolinite is the only silicate present. However, if the rock contains no other silicates, dissolution of quartz can take place at an earlier stage. Thus, in banded iron formations, which have a hematite, magnetite and quartz assemblage, both the solution of quartz and the replacement of quartz by goethite occur during the first phases of weathering (Morris, 1980; Trescases and Melfi, 1985).

The succession of different weathering mechanisms

The weathering of peridotite described above demonstrates the selective behaviour through time for the different primary minerals with respect to only one mechanism: hydrolysis. Such rocks are Al-poor, so that only Fe (accompanied by such elements as Ni, Co and Cr) can accumulate in the corresponding lateritic weathering profile. Consequently, it is usually not possible to distinguish any subtle differences in the products of hydrolysis that are due to the differential retention of recombined Si and Al, i.e. the allitization-monosiallitization-bisiallitization reactions. In contrast, the weathering of Al-rich rocks commonly shows the successive effects of these different mechanisms vertically through the profile.

The weathering of Al-rich rocks under humid tropical climates can lead to the formation of bauxites, in which gibbsite is the major constituent (Bardossy, 1983) but the mechanism of formation depends on local conditions. Over alkaline rocks, such as nepheline syenite, allitization proceeds directly in freely drained situations (e.g. high plateaux and slopes), such as at Poços de Caldas in Brazil; however, where drainage is less active, the same rocks weather initially by monosiallitization, to develop a basal kaolinitic horizon, which is then desilicified to form the gibbsite horizon (Melfi and Carvalho, 1983).

Some lateritic profiles developed over basic rocks in West Africa have a basal smectitic horizon formed by bisiallitization, overlain by several kaolinitic horizons, including the variegated and mottled clay zones (Leprun, 1981; Ambrosi, 1984). Such a succession of horizons may have resulted from differences in weathering mechanisms due to a concentration gradient in the solutions between bottom and top of the profile. Dissolved elements are translocated to the bottom of the profile by infiltrating waters. The upper part of the profile thus becomes relatively depleted in minerals rich in silica and alkaline and alkaline earth elements, and dominated by Fe and Al hydroxides and kaolinite. At the base of the profiles, weathering is only partial and porosity is not yet fully developed, so that the weathering solutions circulate less freely and become more concentrated. *Alternatively*, the succession of weathering mechanisms could be the result of changing climatic conditions. The development of a lateritic profile is a very long process and may have occurred under different climatic conditions than those seen today (see Chapter I.1). The lower smectitic horizon of the profiles described by Leprun (1981) in Burkina Faso can relate to the present savanna climate, which is probably less humid than that responsible for the formation of the kaolinite in the overlying horizon.

TRANSFER OF ELEMENTS DURING WEATHERING

After being released from primary minerals by weathering, some elements dissolve and are leached from the profile. Such mobile elements (which, during

hydrolysis, principally include the alkalis, alkaline earths and silica) constitute the soluble phase of weathering. Other elements, such as Fe and Al, are concentrated in the weathering profile but this does not imply that they are totally inert. In fact, all elements are susceptible to mobilization because, in a chemical sense, weathering is essentially a subtractive phenomenon, although the amount transferred may be highly variable.

Transfer can be restricted to the interior of the weathered primary mineral itself. Such *intramineral* transfer, which is characteristic of the most residual elements, is evident in the centripetal alteration of feldspar to skeletal gibbsitic pseudomorphs. *Intermineral* transfer is also possible, even confined to a single horizon, and can be demonstrated by comparative analysis of secondary phases and their parent minerals. For example, plagioclase, which is Fe-poor, may weather to Fe-bearing kaolinite, the Fe being derived from other minerals. Similarly, the simultaneous weathering of adjacent pyroxenes of different compositions, such as orthopyroxenes (without Al) and clinopyroxenes (with Al) that are found in the pyroxenites of Niquelandia (Brazil) results in the formation of a single smectite (Colin et al., 1985). *Interhorizon* transfer of matter, from an upper to a lower level, is common in weathering profiles and can be demonstrated by mass balance calculations. The mobilization of certain elements, such as Mn or Ni, at the top of the profile and their concentration at the base, are essential to the genesis of the so-called lateritic deposits of these metals over manganeseiferous protore and ultrabasic rocks, respectively. Such transfers are closely controlled by changes in weathering conditions, as explained in the previous section.

TABLE I.2-2

Partition of chemical elements between the main facies of weathering residua (from Lelong et al., 1976)

Bauxite	Fe-duricrust	Mn-duricrust	Ca-duricrust	Sulphate	Carbonates and chlorides
Al-Ga-B	Fe-Ti-V Cr-Mo	Mn-Fe-Co Pb-Ba-Ni Cu	Ca-Sr-Ba Zn	Ca-Sr-Ba	Na-Rb-Li
	Kaolinite		Smectites		Zeolites Magadiite Mg-smectite
	Al-SiO ₂ -Ga-B		SiO ₂ -Al-Mg-Ti Fe-Ni-Zn-Pb-Cu		SiO ₂ -Mg-Na-Ca
increasing mobilities →					
Humid climate				Arid climate	
Upstream				Downstream	
Top of profile				Base of profile	

Finally, transfer can be lateral, with the elements moving downgradient in the landscape. The most mobile elements can cover enormous distances before being trapped in endorheic basins or being flushed into the ocean. The scale of increasing mobility of elements can be related to the increasing confinement of weathering environments, not only from the humid equatorial climate to the arid deserts in the tropics and subtropics, but also, albeit less extremely, from a well-drained area in high topographic position to a confined environment, down-slope. The chemical elements undergo the equivalent of chromatographic separation in the different weathering environments, based on the conjunction of two factors: chemical mobility and degree of confinement. The most allitizing environments only retain the most inert elements and release all others, whereas the most confined environments only concentrate the most mobile elements as the others never reach them. Between these two extremes, different conditions can lead to various degrees of accumulation or leaching. The effects of this partitioning of elements under different conditions is illustrated schematically in Table I.2-2, which indicates environments favourable for accumulation.

THE FERRUGINOUS LATERITES

D. NAHON and Y. TARDY

INTRODUCTION

Laterites are widespread in the intertropical belt. The depth of weathering ranges from a few metres to over 150 m depending on the age of the laterite, the regional tectonic activity, the climate, the climatic history and the nature of the parent rock. Although exhibiting a wide variety of colours, textures and petrographic features, laterites have markedly homogeneous mineralogical and chemical compositions and do not obviously reflect the parent rocks from which they are derived. They therefore may mask the underlying geology and are a considerable hindrance in mapping and mineral exploration. Nevertheless, many elements, including Al, Fe, Mn, Co, V, P, Cr, Ni, Cu and Au, may be concentrated to ore grade in the lateritic mantle and become significant targets for exploration.

The term "laterite" is commonly attributed to Buchanan (1807), who described naturally hardening surficial materials that were used as bricks (Latin: *later*, a brick) from Malabar, southern India. In some African dialects, red surficial materials are called brick earth (Maignien, 1966) and laterite refers to blocks used for construction (Prescott and Pendleton, 1952).

For 150 years, a considerable and controversial literature has been devoted to the definition of the term laterite and two essentially different positions have emerged. *Firstly*, many scientists have used "laterite" to designate those Fe- and Al-rich weathering products, generally formed under tropical conditions, that are either hard or become hard upon exposure to alternate wetting and drying (Pendleton, 1936; Kellogg, 1949). This definition also includes certain highly weathered material with sesquioxide-rich, humus-poor nodules, even though they may be surrounded by earthy material that does not harden (Sivarajasingham et al., 1962). Thus, from this point of view, laterites include bauxites, "ferricretes", Fe- or Al-duricrusts, "carapaces", "cuirasses", pisolith- or nodule-bearing formations and also clay-rich (kaolinite) horizons in which concretions and mottles are present. *Secondly*, Maignien (1958, 1966) and Millot (1964) have proposed that "laterite" should be extended to all weathering products that have those chemical and mineralogical characteristics specific to tropical environments, rather than be restricted to those that are hard or potentially hard. In this definition, the term includes materials commonly associated with indurated ferricretes such as red or yellow ferrallitic soils, tropical ferruginous soils, kaolinitic saprolites and lithomarges, all of which are soft and cannot harden.

In parts of Africa, India, South America, Southeast Asia and Australia, the lateritic mantle is very thick and has been forming continuously for over 100 million years, since the Jurassic (King, 1957; Michel, 1973). Although mostly old, laterites are not fossils but have been evolving and continue to evolve under various tropical climates ranging from equatorial to semiarid or arid. However, because of their long, complex history of development, the mechanisms of formation and degradation of lateritic profiles and landscapes are difficult to reconstruct.

The purpose of this chapter is to summarize results of some recent petrographic and geochemical studies of ferruginous lateritic profiles and to discuss their palaeoclimatological significance in landscape evolution.

THE LATERITE PROFILE

Laterites can develop from most sedimentary, metamorphic and igneous rocks. However, the evolution of the profiles depends upon the climatic zones in which they formed. Lateritic profiles capped by iron crusts (ferruginous duricrusts, cuirasses, ferricretes) are mostly developed in tropical climates characterized by alternating humid and dry seasons (i.e. savanna climates). Such iron crusts tend to be less abundant in both semiarid and very humid conditions—that is if either the dry or the humid seasons become long (see Chapter I.1).

In typical old and well-preserved iron-crustated lateritic profiles (Fig. I.3-1), five main horizons are commonly preserved (Leneuf, 1959; Tardy, 1969; Tardy and Nahon, 1985; Nahon, 1986, 1987). These are, from the base:

- (1) Parent rock.
- (2) Porous, coarse grained saprolite.
- (3) Fine grained saprolite.
- (4) Mottled zone.
- (5) Iron crust, comprising
 - (a) soft, nodular iron crust (“carapace nodulaire”);
 - (b) indurated, conglomeratic iron crust;
 - (c) pisolitic iron crust;
 - (d) pebbly ferruginous layer.

Horizon 1

The parent rock is essentially fresh and unweathered, although some secondary minerals such as carbonates, phyllosilicates and Fe oxides may occur in fissures and cracks down to considerable depths.

Horizon 2

The coarse grained saprolite (sometimes referred to as “gruss” or “arène” in the French literature) forms the porous, basal horizon in which some parent rock fragments, feldspars, micas and other primary minerals remain unweathered.

ALTERNATING HUMID AND
DRY TROPICAL ZONE

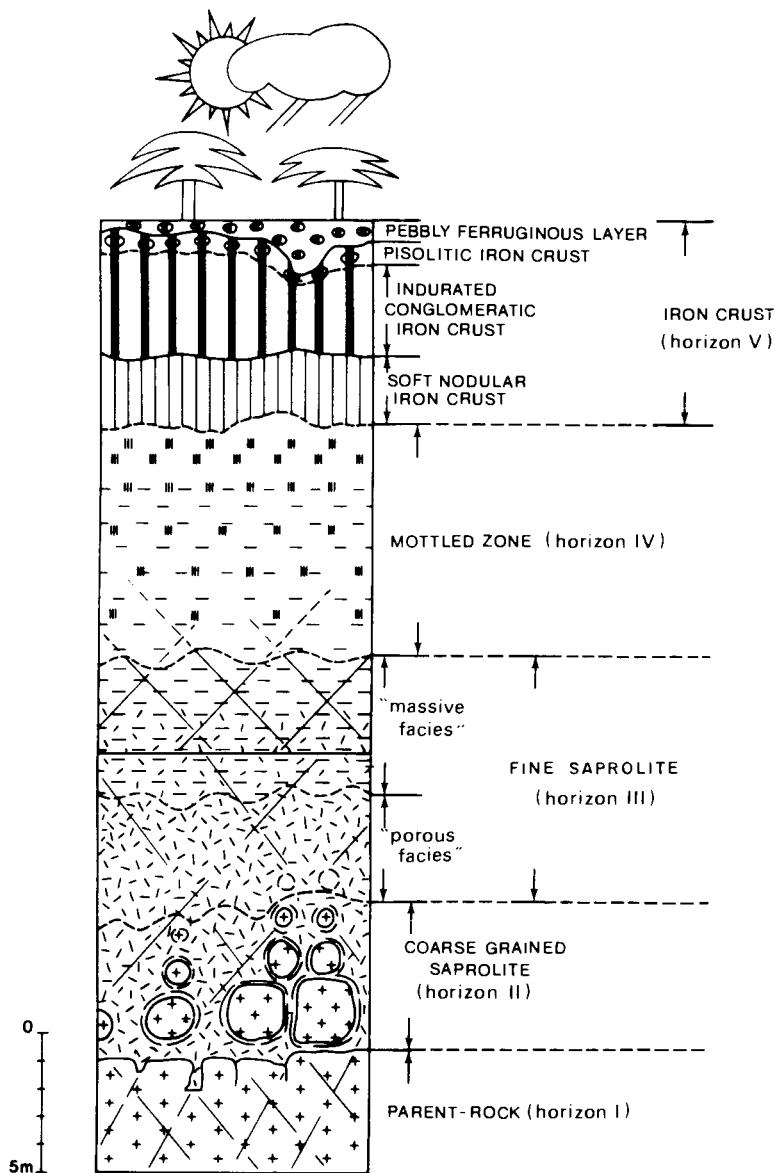


Fig. I.3-1. Sketch of a typical lateritic iron crust profile.

(The lower part of this horizon may also be referred to as “saprock”, see Chapter I.2.) Relict fragments of all sizes, from boulders to individual minerals, progressively disintegrate during weathering, without displacement of pre-existing struc-

tures or change of volume. Petrographic studies show that primary minerals are pseudomorphically replaced by weathering products which may in turn be further fragmented—yet for a single parent grain these may exhibit parallel extinction. These observations are the basis of the concept of isovolumetric weathering (Millot and Bonifas, 1955), namely the chemical replacement of a unit volume of parent rock by an equivalent volume of the weathering product.

Upwards through this horizon, the progress of weathering is expressed petrographically by (i) an increase in yellow to red colouration; (ii) partial then complete dissolution of the main primary minerals; (iii) decreasing induration of the rock and a marked increase in porosity; (iv) neoformation of authigenic smectites and kaolinite at the base of the horizon and, above, of predominantly well-crystallized Fe^{3+} -bearing kaolinite associated with amorphous or poorly crystallized Fe hydroxides. Throughout the horizon, however, Fe hydroxides are essentially restricted to the sites previously occupied by Fe-bearing primary minerals. Kaolinites derived from feldspars remain white even though they contain ferric iron.

Horizon 3

The fine grained saprolite is the horizon in which most primary minerals have been altered to secondary minerals such as kaolinite, goethite or amorphous iron oxyhydroxides. Only quartz and resistant minerals (e.g. zircon, tourmaline, chromite) remain unweathered or only partly weathered. The horizon has a considerable range in thickness, from a few metres to more than 100 m. It is a product of isovolumetric weathering, so that the original rock fabric is perfectly preserved and recognizable. There is some redistribution of Fe hydroxides but these are diffuse and no mottles are formed. The fine saprolite is also referred to as lithomarge, “argiles bariolées” and pallid zone. However, the latter term can be misleading, as the horizon may exhibit a wide variety of colours, including pale green, yellow, pink, purple, red and brown as well as white.

At the base, the fine saprolite has a fine grained, slightly porous texture, but it becomes massive at higher levels as the clay fraction increases. This increase is due essentially to the secondary precipitation and accumulation of authigenic kaolinite in pores that were created during the dissolution of primary minerals. This is evident petrographically by the presence of clays coating and filling microvoids. The kaolinite consists generally of small platy crystals ($0.5 \mu\text{m}$) together with minute crystals of goethite which impart an orange colour to the coatings and fillings. Because the clay fraction is so abundant, internal tensions due to shrinking and swelling resulting from interaction with water may rework the weathering matrix. However, kaolinite is not a highly expandable clay and in general only microstructures are affected to any degree, with macrostructures such as quartz veins preserved high in the profile. This second generation of kaolinite is an absolute accumulation within part of an isovolumetrically weathered horizon (Ambrosi and Nahon, 1986). The presence of two types of kaolinite indicates that two slightly different geochemical weathering systems are acting

simultaneously to form two different facies within the one horizon, i.e. a *porous* and a *massive* facies. Kaolinite and goethite coexist in these facies as long as they remain below the water-table. No ferruginous concretions are observed to form or develop in the permanently saturated (phreatic) zone (Nahon, 1976; Muller et al., 1980).

Horizon 4

The mottled zone overlies the fine saprolite above the water-table, in the unsaturated (vadose) zone. Here, the pre-existing macrostructure of the parent rock is progressively destroyed. Two major types of reorganization affect this horizon. Firstly, vertical and lateral percolation of water in the unsaturated zone leads to the formation of a network of channels and tubular voids of large diameter (average 10 mm). Secondly, ferruginous spots (5–150 mm) and nodules (10–30 mm) develop, becoming both more abundant and more indurated towards the top of the mottled zone. This implies that iron is mobilized from areas around large (> 1 mm) pores and reprecipitated and concentrated in clay-rich areas (Tardy and Nahon, 1985).

The channels and tubular voids act as receptacles for the secondary accumulation of kaolinite. The kaolinite occurs as coatings and fillings, and consists of minute, randomly distributed particles of detrital or authigenic origin. It has been derived from overlying horizons or upslope, either by physical translocation or dissolved in solution, and then deposited or reprecipitated lower in the profile or downslope. Because the kaolinite void fillings contain small pores, they can subsequently be ferruginized into indurated nodules.

The ferruginous segregations that accumulate in clay-rich areas commonly consist of purple-red Al-hematite. As such, they are the product of the epigenetic replacement of kaolinite by hematite (see Fig. I.3-2), that is, the simultaneous

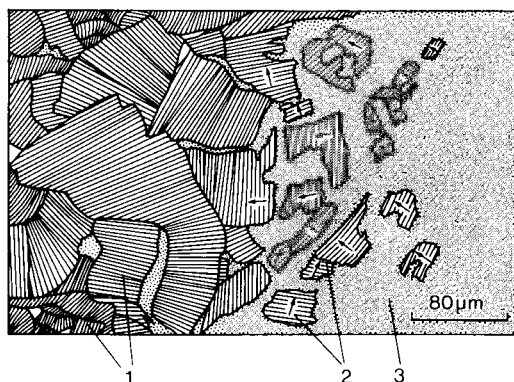


Fig. I.3-2. Sketch showing the epigenetic replacement of kaolinite "booklets" by hematite (from Ambrosi et al. (1986)). 1: kaolinite booklets; 2: relicts of the same partially replaced booklet, all retaining the same orientation (arrows); 3: purple-red hematitic plasma.

dissolution of kaolinite and precipitation of hematite (Nahon, 1976; Tardy and Nahon, 1985; Ambrosi et al., 1986). Indurated nodules become more numerous towards the top of the mottled clay horizon so that the pre-existing lithostructure is progressively obliterated and replaced by a newly formed pedostructure. However, original volumes are commonly preserved and any quartz veins that are present are strongly corroded but not displaced.

Horizon 5

The iron crust horizon overlies the mottled zone and consists of several different facies. It develops where the purple-red hematitic nodules that form in the mottled zone become more numerous, finally coalescing into an indurated cuirasse (ferricrete). Dissolution and replacement of the kaolinite is at a maximum when hematite is most abundant and most aluminous (7–15 mole % Al_2O_3).

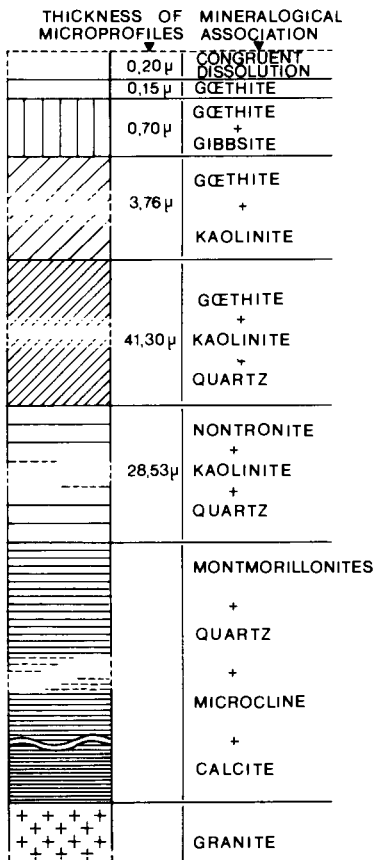


Fig. I.3-3. Profile formed by artificial weathering under conditions simulating seasonally humid climates (Fritz, 1975).

TABLE I.3-1

Element gains and losses during transformations involved in the development of some horizons of the laterite profile

Horizon formed	Leached	Accumulated
Pebbly layer	Alumina	Iron
Pisolitic cuirasse	Silica	Alumina, iron
Nodular horizon	Alumina, silica	Iron
Saprolite	Alkalis, alkaline earths, silica	

The iron crust is thus nodular, with a conglomeratic structure, but has formed by in-situ accumulation of iron oxides and is not detrital in origin.

Towards the top of the conglomeratic iron crust, a cortex develops along microcracks and microfissures through the purple-red nodules. The cortex consists of aluminous goethite containing 15–25 mole % $AlOOH$ and grows in a concentric, centripetal manner by the rehydration and replacement of Al-hematite by Al-goethite, resulting in the formation of a pisolitic structure. Initially, the pisolitic iron crust remains indurated. However, towards the periphery of the cortex, the goethite becomes progressively poorer in aluminium and at the same time the pisoliths diminish in size and become separated due to the development of cracks and dissolution features, so that the cohesion of the horizon is reduced. Finally, almost pure goethite, associated with minor kaolinite, forms in large voids between pisoliths and in cracks and fissures. Thus, the ferruginous pebbly horizon can be considered to be the result of the geochemical degradation of the indurated, cemented iron crust which it overlies.

The formation of the hematite nodules and the mineralogical succession goethite-hematite-goethite observed from the mottled zone to the cuirasse and pebbly layer is due to fluctuations in water activity in the profiles during the alternation of dry and humid seasons (Tardy and Nahon, 1985). Profiles similar to those described have been formed experimentally by simulating weathering under such seasonal conditions (Fig. I.3-3; Fritz, 1975).

The lateritic profile is the result of the progressive development of each horizon by a transformation of that immediately underlying it by the differential mobility of the elements of which it is composed (Table I.3-1). When seasonally humid climates are long established, the downward movement of the transformation fronts (Chapter I.4) leads to progressive deepening of profiles and sequences at the expense of fresh rock (Nahon, 1976).

CHEMICAL MASS BALANCES AND DIFFERENTIATION OF LATERITIC HORIZONS

The evolution of a typical lateritic profile takes place in two stages. The first stage is isovolumetric and preserves pre-existing rock structures and volumes. It

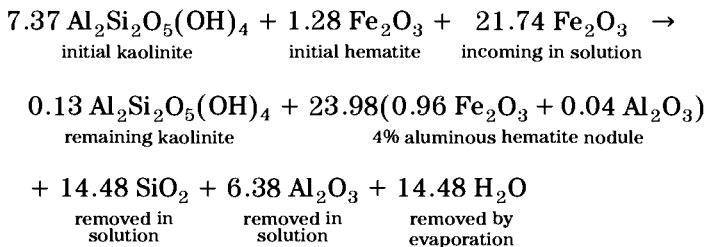
extends through the saprock and saprolite and, in some situations, to the mottled zone and even to the soft, nodular facies of the iron crust, the carapace. The second stage destroys pre-existing rock structures, commonly with some loss of volume. It affects the uppermost horizons of the profile, particularly the cuirasse.

A quantitative mass balance of the isovolumetric stage of weathering clearly displays the relative accumulation of Al and Fe as a consequence of

- (1) complete leaching of alkaline and alkaline earth elements, and
- (2) partial dissolution of silica (Lacroix, 1914).

The residual elements Si (as quartz), Al, Fe and Ti are considered immobile, but nevertheless may be partly removed (e.g. 25% reductions of both Si and Al) or weakly enriched (increases of 30% in Fe, 50% in Ti) in the fine saprolite and, particularly, the mottled zone (Tardy, 1969). Although the relative loss or concentration of Fe depends on the prevailing redox conditions, both Fe and Al are almost entirely retained in the saprolite.

In the uppermost horizons, isovolumetric mass balances can only be calculated between individual primary minerals and their pseudomorphic weathering products. The hematitic nodulation that develops at the expense of kaolinite in the mottled horizon and leads to the formation of the carapace and cuirasse is typical of the processes involved. Ambrosi and Nahon (1986) calculated mass balances from the mineralogy and porosity of specific features. Mineral compositions were established by estimating the percentage of each phase by thin section petrography and X-ray diffraction. Porosities were estimated from thin sections by optical and scanning electron microscopy and compared with values calculated from the difference between particle and bulk densities. The resultant mass balances are only approximations because they do not account for ions that have to be released into the solution to equilibrate with the newly formed minerals. The reactions are:



This mass balance corresponds to:

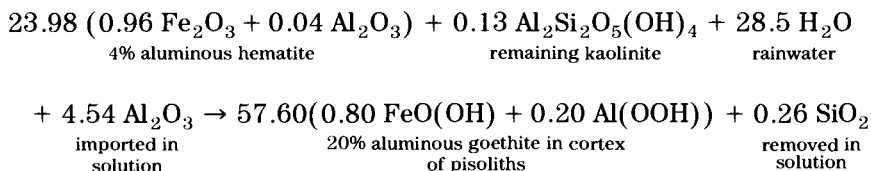
14.48/14.74 = 98% of silica released;

14.48/14.74 = 98% of water released;

21.74/23.02 = 94% of iron imported;

6.38/7.37 = 87% of aluminium released.

In the upper part of the iron crust, the Al-hematite is in turn altered to Al-goethite. The mass balance reaction of the alteration of the transformation of a nodule to a pisolith is as follows:



This corresponds to:

100% of silica removed in solution;

79% of alumina imported in solution;

99% of water imported as rain;

100% of iron conserved.

A quantitative mass balance calculation proposed by Brimhall and Dietrich (1987) for weathering and supergene enrichment relates the chemical, physical, volumetric and mechanical properties of the weathering products to those of the parent material ("protolith"). Although this is theoretically a more rigorous approach, it does not take into account the lateral flow of water which is evident in the development of profiles as old as ferruginous laterites. Because primary microfabrics may be preserved essentially undeformed high in the weathering profile, mass balances may be effectively calculated assuming isovolumetric weathering as described above.

RATES OF CHEMICAL WEATHERING AND MECHANICAL EROSION

The rate of formation of profiles and of the progress of chemical weathering as a whole can be estimated from knowledge of the hydrological regime and of overall losses of soluble elements by leaching. Mass balance calculations based on such data may be used to determine the time required to weather a given thickness of rock or to estimate the thickness of rock that can be weathered in a given period of time. Such calculations have been made for a number lithologies and regions (Table I.3-2). The data suggest an average rate of weathering of about 20 mm/1000 years, i.e. 20 m per million years. In lateritic environments, the rate appears to be about two or three times faster over basic and ultrabasic rocks, as noted by Nahon (1986).

The rate of chemical weathering is largely dependent upon, and directly proportional to, the quantity of water that percolates through the profile each

TABLE I.3-2

Rates of chemical weathering

Lithology	Location	Weathering rate mm/1000 years	Reference
Granitic rock	Ivory Coast	5-50	Leneuf (1959)
Granitic rock	Norway	12	Tardy (1969)
Granitic rock	France	10-24	Tardy (1969)
Granitic rock	Ivory Coast	15	Tardy (1969)
Granitic rock	Malagasey Rep.	25	Tardy (1969)
Granitic rock	Ivory Coast	14	Boulangé (1984)
Granitic rock	Chad	9.4	Gac (1979)
Ultramafic rock	New Caledonia	29-47	Trescases (1975)

year. This, in turn, is approximately equivalent to the difference between precipitation and evaporation. As this quantity decreases, and the length of the dry season increases, mechanical erosion becomes more significant. Thus, in the Central African Republic, the rates of mechanical erosion and chemical weathering are nearly equal, at 8.3 mm/1000 years and 9.4 mm/1000 years respectively (Gac, 1979). The region has a rainfall of 1210 mm p.a. and evaporation of 1060 mm p.a., so that only 150 mm percolates through the profile each year.

STABILITY FIELDS OF HYDRATED AND DEHYDRATED MINERALS

The most common minerals in ferruginous and bauxitic laterites are Al-goethite, Al-hematite, gibbsite, boehmite and Fe-kaolinite. Diaspore is relatively uncommon, except in karst and sedimentary bauxites, and corundum, although usually present, is rare (Valeton, 1972; Boulangé, 1984). The distribution of these minerals is a function of (i) climate, (ii) age, (iii) lithology, (iv) degree of compaction and, where appropriate (v) temperature and grade of metamorphism (Bardossy, 1982).

The principal parameters governing the stability of these minerals are water activity, temperature and grain size (Didier et al., 1983; Trolard and Tardy, 1987). In tropical climates with alternating dry and humid seasons, water activity is the crucial factor and can be defined as the relative humidity (RH%) of the air:

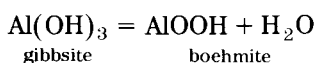
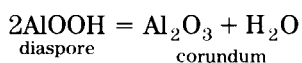
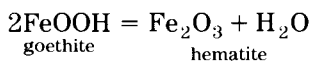
$$a_w = [\text{H}_2\text{O}] = p/p_0 = \text{RH}/100 < 1$$

where p and p_0 are the partial vapour pressures of the air and of saturated air, respectively, at temperature T . Water activity is always smaller than unity and is related to the radius of the meniscus of water trapped in capillaries of the same radius, as follows:

$$RT \ln[\text{H}_2\text{O}] = 2V \sigma/r$$

where r is the radius of the capillary, σ is the air–water surface tension, V is the molar volume of water, R is the gas constant and T the temperature.

During the wet season, the humidity of the air is close to saturation and the water-table is high in the profile, so that water activity is also high, even in the uppermost horizons. In contrast, during the dry season, the humidity is low and the water-table is deep in the profile, so that water activity in the upper horizons is also very low. In dehydration reactions, it is evident that a diminution of water activity has the same effect as an increase of temperature and tends to favour the dehydrated minerals (hematite, boehmite and corundum) over hydrated minerals (goethite, gibbsite and diaspore):



Corundum and diaspore form solid solutions with Al-hematite and Al-goethite and their occurrence in laterites is in part related to the dehydroxylation reactions of these minerals.

Equilibrium diagrams showing the conditions of formation of Al-goethite, Al-hematite, gibbsite and boehmite are presented in Figs. I.3-4, I.3-5 and I.3-6. The stability fields of the various associations are depicted in terms of water activity and temperature. From these diagrams, which allow for the substitution of Al for Fe in goethite and hematite by assuming the solid solutions to be ideal, the following conclusions may be drawn:

(1) At a given temperature, a decrease in water activity induces dehydration reactions such as:

goethite → hematite

gibbsite → boehmite → corundum.

(2) For a given water activity, an increase in temperature also induces dehydration. This is due to the increase of entropy and heat capacity as the water of hydration in hydroxides and oxyhydroxides becomes “free” water.

(3) The effects of a decrease in water activity are similar to an increase in temperature, given the same succession and parageneses of mineral phases.

For Al-poor systems:

Al-goethite → Al-goethite + Al-hematite → Al-hematite.

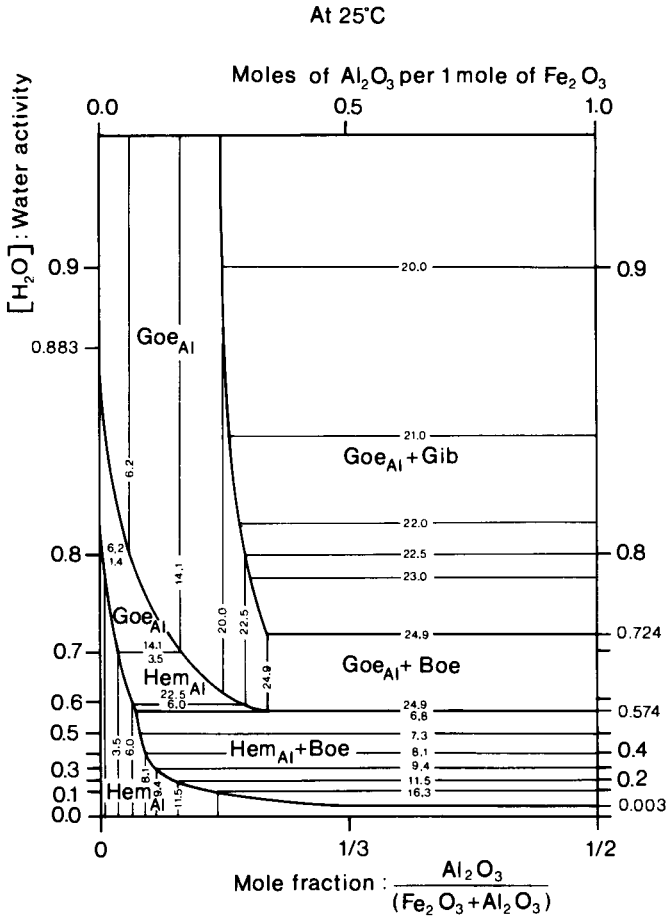


Fig. I.3-4. Equilibrium diagram for Al-goethite, Al-hematite, gibbsite and boehmite at 25°C in the system H_2O , Al_2O_3 and Fe_2O_3 .

For Al-rich systems:

Al-goethite + gibbsite \rightarrow Al-goethite + boehmite \rightarrow

Al-hematite + boehmite \rightarrow Al-hematite \rightarrow (corundum).

(4) In mineral associations such as (Al-goethite + gibbsite) and (Al-goethite + Al-hematite), the Al-goethite or Al-hematite compositions do not depend on the composition of the system but only on the water activity or temperature. The Al contents increase as water activity decreases or temperature increases.

(5) When Al-goethite and boehmite occur together, the Al-goethite composition is independent of the composition of the system, the temperature and the

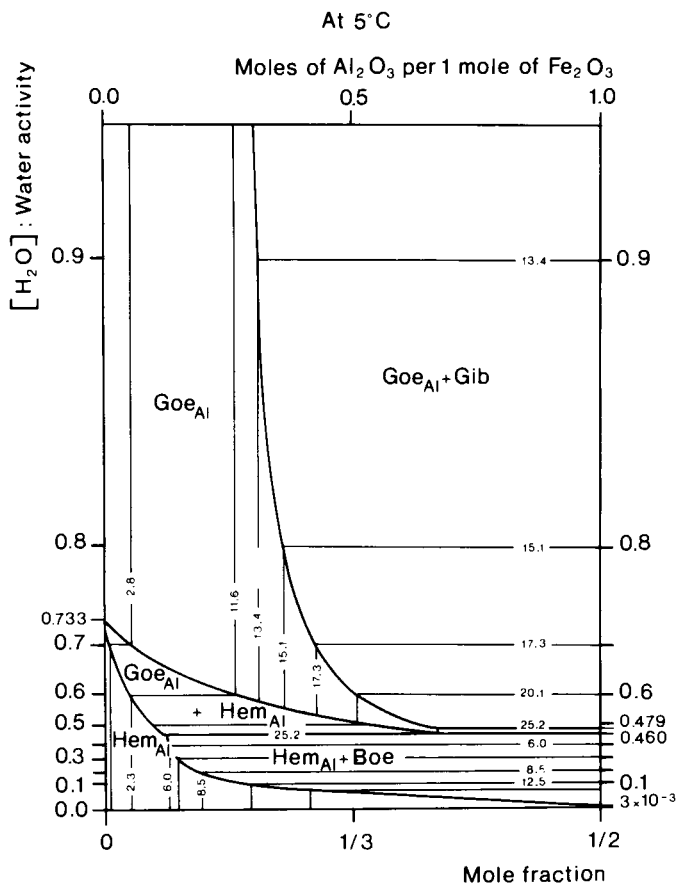


Fig. 1.3-5. Equilibrium diagram for Al-goethite, Al-hematite, gibbsite and boehmite at 5°C in the system H_2O , Al_2O_3 and Fe_2O_3 .

water activity. The Al content of goethite is almost constant at $(\text{Al}_{0.245}\text{Fe}_{0.755})\text{OOH}$ at 25°C. The Al-hematite and corundum association has a similar relationship.

(6) When only Al-goethite or Al-hematite are stable, their Al content is independent of water activity and temperature. The Al-goethite and Al-hematite compositions depend only on the $\text{Al}_2\text{O}_3/(\text{Al}_2\text{O}_3 + \text{Fe}_2\text{O}_3)$ ratio of the system.

These observations suggest that water activity and temperature are the two principal factors controlling the distribution of minerals in ferruginous laterites and bauxites. The total composition of the system is also important, particularly because goethites and hematites are Al-bearing minerals as well as Fe minerals. However, particle size may also be important because it affects the solubility products and Gibbs free energy of formation of natural iron oxides, oxyhydroxides and hydroxides such as hematite, maghemite, goethite, lepidocrocite and amorphous $\text{FeO}(\text{OH})$.

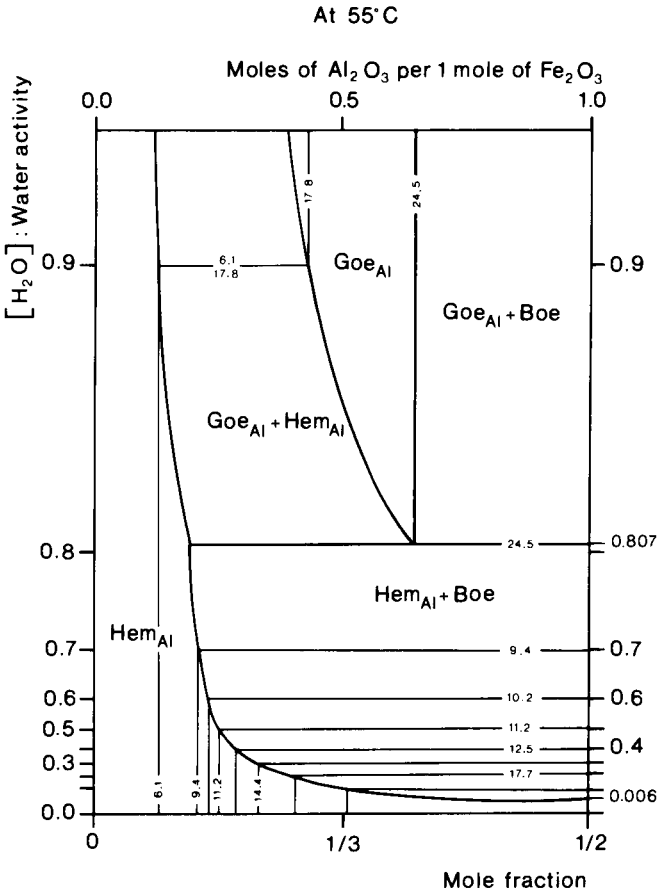


Fig. 1.3-6. Equilibrium diagram for Al-goethite, Al-hematite, gibbsite and boehmite at 55°C in the system H_2O , Al_2O_3 and Fe_2O_3 .

In conclusion, the distribution of Fe and Al minerals in ferruginous laterites and lateritic bauxites show that the hydrated minerals (goethite and gibbsite) are more abundant in humid tropical climates (rainforests) whereas dehydrated or partially hydrated minerals (boehmite and hematite) are more abundant in the seasonally humid tropics (savannas). In addition, the dehydrated minerals are more common in the drier, upper horizons than in the lower, wetter horizons close to the water-table. Within the upper mottled, nodular and pisolitic horizons, the mineral distribution is also related to the petrographic fabric, with the dehydrated forms tending to concentrate in the centre of concretions and hydrated minerals on the periphery. Thus, in ferruginous laterites, pisoliths and nodules have a core of hematite and a cortex of goethite, whereas in bauxites, boehmite forms the core and gibbsite the cortex and cement.

Sedimentary bauxites are rich in gibbsite when the deposits are young and porous but contain abundant boehmite and diasporite when they are older and compacted. The most dehydrated form of alumina, corundum, is found in very impervious materials, such as the hard, very dense nodules that occur in diagenetically-altered sedimentary bauxites in Kazakstan. It commonly occurs as very fine particles (0.1–1.0 μm) and is thought to be authigenic, formed under surface conditions; in Australia, fine corundum and maghemite are considered to have formed by the dehydration of Al-hematite and goethite by fire (Anand and Gilkes, 1987). Rather larger (0.1–2.0 mm), well-crystallized grains occur in contact or regionally metamorphosed bauxites (Bardossy, 1982) and are similarly thought to be thermal alteration products.

SOIL FORMATION IN TROPICALLY WEATHERED TERRAINS

Y. LUCAS and A. CHAUVEL

INTRODUCTION

Soils are one of the principal sample media available for geochemical exploration and the physical and chemical processes involved in their formation are the same as those responsible for geochemical dispersion. Soils thus represent tangible evidence of these processes, hence an understanding of soil genesis is essential for the correct interpretation of geochemical exploration data.

Soil formation (pedogenesis) is the result of the transformation of bedrock, pre-existing saprolite or other regolith material at the interface with the atmosphere. The nature of the transformation depends on the balance between three main processes:

- (1) alteration (weathering) of minerals;
- (2) transport in solution or as solids;
- (3) authigenesis of stable secondary minerals.

These processes result from the new thermodynamic equilibria controlled by the changed physico-chemical conditions that exist in the soil profile compared to the parent material. They act first at the base of profiles and lead to the formation of materials that have a new composition encompassing both residual and newly generated minerals and a new fabric determined by the spatial relationships of the secondary structures.

As the soil deepens, new physico-chemical conditions are imposed on the profile. Consequently, the processes of alteration, transportation and authigenesis interact with the initial soil to form another with a different composition and fabric. This pedogenetic differentiation produces layers of soil materials generally distributed as horizons that reflect the spatial variation of the soil environment. The horizons are the result of an equilibrium between soil composition, soil fabric and the physico-chemical conditions at each depth in the profile.

This chapter refers to the genesis of soil covers and their distribution within landscapes. As discussed in Chapters I.1 and I.3, the regolith is the product of processes that may have been active for millions of years: consequently, the pedogenetic processes that are active at present may be transforming a relic soil. In this chapter, a simplified model of soil development in tropical terrain is presented, followed by a discussion of the effects of climatic and other changes on the processes of pedogenesis.

DYNAMIC EQUILIBRIA IN SOILS

Physico-chemical conditions are generally more aggressive towards mineral components in the upper parts of a profile, principally because of the presence of biochemical compounds. Such compounds facilitate alteration by the action of water-soluble acids produced either directly by microorganisms or from the decomposition of organic matter. They also promote leaching of components released during weathering by the formation of soluble complexes. As pedogenesis proceeds, complete dissolution of some minerals in the upper horizons of the profile causes subsidence of the soil surface. This decrease in the profile thickness is compensated by weathering of further parent material at the base of the profile. The profile can thus be considered to represent a time sequence (Butt and Nickel, 1981), with each horizon having been derived from material similar to that now underlying it by the downward advance of a *transformation front* in which the processes of alteration, transport, authigenesis and fabric acquisition occur.

The differentiation and the evolution of a profile depend upon:

(1) The relative rates of the advance of the different transformation fronts (Fig. I.4-1). If the different horizons of a profile are maintained during profile development, they may be considered to be genetically continuous and the profile to be in *dynamic equilibrium*. However, if the fronts advance at different rates, and the vertical succession of horizons changes, then the horizons are genetically discontinuous and the profile is in *disequilibrium* (Millot, 1983).

(2) The geochemical balance of elements transported into or out of each horizon. At each front, elements may be mobile either in solution or as fine solids such as clays. Soluble components, released by weathering, may precipitate immediately as new minerals, or be transported to another horizon where physico-chemical conditions are more favourable for precipitation, or be leached from the profile entirely. Solid particles are released by the destabilization of soil fabric as fronts advance and may be transported by mechanical eluviation into underlying horizons (see p. 99).

FACTORS AND PROCESSES OF SOIL FORMATION IN THE TROPICAL ZONE

The nature and activity of pedogenetic processes depend on external factors such as climate, parent material and time, and on internal factors interdependent with the evolution of the soil such as topography, the biosphere and the hydrodynamics of the profile. In this section, the general processes of soil formation are described for the different climates of the tropical zone, then the specific effects of the others factors are discussed.

Climate

The climate of tropical environments and its influence on geochemical dispersion, including weathering, soil formation and landscape development, are con-

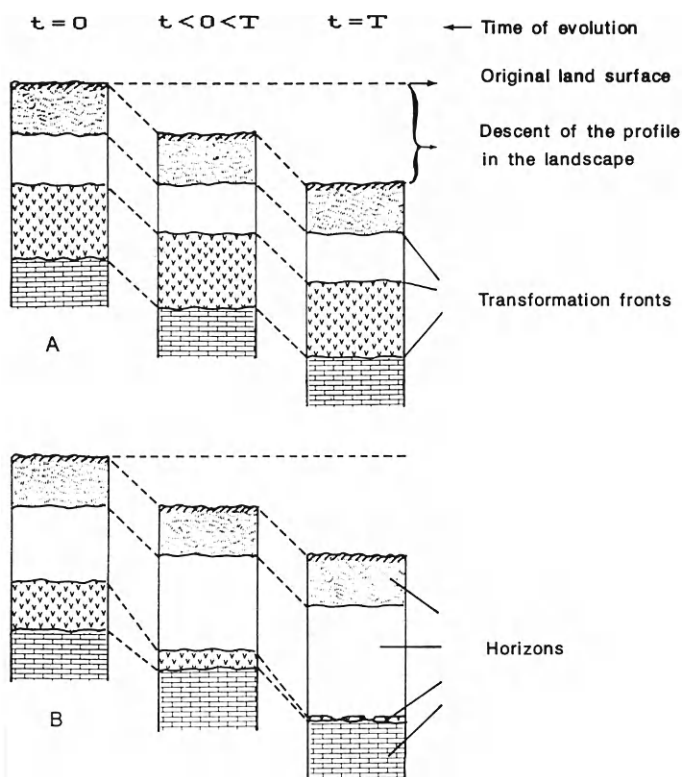


Fig. I.4-1. Dynamic equilibrium of a soil profile. (A) Profile in dynamic equilibrium. (B) Profile in disequilibrium.

sidered in Chapter I.1. The most important climatic elements are the distribution and annual averages of precipitation and temperature, summarized on the Köppen climatic map (Fig. I.1-1). These control, respectively, the amount of water percolating through the regolith in a given time, and consequently the concentration of the weathering solutions, and the rates of chemical reactions. Thus, the latitudinal variation of climatic conditions in the tropical zones north and south of the equator induces changes in the processes of soil formation.

In *humid equatorial climates* (rainfall > 2000 mm p.a., with a poorly defined dry season), the soil moisture regime is permanently humid and free draining. Soil horizons are characterized by fabrics having a good hydraulic conductivity, so that water-logging or gleying processes are only rarely developed in the landscape. The amount of water percolating through the regolith is considerable (more than 600 mm p.a.) and weathering reaches great depths.

Under these conditions, intense alteration at the weathering front at the base of the regolith affects all the weatherable minerals simultaneously. Even quartz, usually considered a stable mineral, can be highly corroded. Transport of

mobilized elements is significant and includes the loss of all the bases and some of the silica. Authigenic minerals are abundant and form most of the soil material; they include kaolinite (monosiallitization (Pedro, 1966); see Chapter I.2), oxyhydroxides of aluminium (allitization) and iron. These processes lead to the formation of saprolite in which bedrock fabrics are preserved as pseudomorphs by secondary minerals. For example, gibbsite or goethite may form septa along boundaries and cleavages of primary minerals before and during their dissolution, ultimately replacing them (Delvigne et al., 1979; Embrecht and Stoops, 1982). The saprolite is characterized by relative accumulation of Fe and Al, although absolute accumulation due to transport and deposition of material from the upper horizons may be significant (Bocquier et al., 1984). For example, granitic saprolite in the Ivory Coast may register a 250% increase in the Fe content (Boulangé, 1984).

As discussed above, the profile may be considered to be developed by the advance of different transformation fronts, named for the principal process that occurs. The *pedoplasation front* corresponds to the loss of much of the lithic fabric in the upper part of the profile. It is often associated with a *cementation front*, which corresponds to the accumulation of oxyhydroxides of iron or aluminium mainly derived by leaching from the upper horizons (Bocquier et al., 1983; Lucas et al., 1986). Iron, mainly as goethite and hematite, and aluminium, mainly as gibbsite, accumulate in pores in the saprolite, giving cemented patches that preserve the lithic fabric as relics in more or less hardened nodules or cuirasse (Eswaran et al., 1977; Chauvel et al., 1983; Bocquier et al., 1984; Didier et al., 1985). Outside these patches, solution and authigenesis of minerals and mechanical processes (such as shrink and swell) in the clay fraction cause the lithic fabric to be replaced by a new, homogeneous, plasmic fabric (pedoplasation, Flach et al., 1968). This new matrix is also characterized by the establishment and maintenance of ferric hydrate-clay bonds, and by high-chroma colours. However, oxyhydroxide nodules may also form in this kaolinitic matrix, so that relicts of both lithic and pedoplastic fabrics may coexist in the same horizon. In summary, the processes at the secondary transformation fronts may result in generally complex successions of mineral parageneses and facies and lead to the formation of horizons ranging from a soft kaolinite matrix without nodules to hardened cuirasse.

The *microaggregation front* corresponds to the appearance of a microaggregated fabric in the kaolinitic clay matrix. This fabric is produced by inorganic processes in an acid ferro-kaolinitic environment that is freely drained and constantly humid (Pedro et al., 1976; Chauvel, 1977). Where microaggregation occurs, the cemented facies start to dissolve and either disappear or remain as rounded nodules or blocks. These coarse elements, together with resistant quartz pebbles, can form a residual stone line at the base of the microaggregated horizons (see Chapter III.2).

At the top of the profile, an increase in concentration of resistant minerals, particularly quartz, corresponds to a *surface degradation front*. Under certain

conditions, for example over quartz-rich parent materials, the hydrodynamics are such that secondary podzolization processes occur, resulting in the loss of leached elements from the soil and an impoverishment in clay (Righi and Chauvel, 1987).

In the *wet savannas* (rainfall 1200–2000 mm p.a., dry season 3–6 months), alteration at the weathering front is less intense than in humid equatorial climates, so that some weatherable primary minerals can remain in the soil and quartz is only weakly corroded. Loss of material from the profiles is less significant and some of the alkaline cations are retained. Leaching of silica is only minor, and gibbsite is less stable than clay minerals; the authigenic minerals in the saprolite are dominantly kaolinite and goethite. Water-logging and gleying processes are more common in lower parts of the landscape.

The seasonal climate is responsible for contrasts in the soil moisture regime. The *pedoplasiation* and *cementation fronts*, in the upper part of the saprolite, are in a moist environment that is alternately saturated and unsaturated due to fluctuations of the water-table. The corresponding alternation in conditions from reducing to oxidizing allow the reduction and migration of iron to form enriched and depleted zones, giving a pseudo-gley facies (Vizier, 1983) or a mottled clay facies (Nahon, 1986). The loss of iron causes destabilization and eluviation of clay particles from the depleted zone, so that the horizon as a whole is relatively enriched in ferruginous components in the form of nodules or massive accumulations such as cuirasse. These processes, coupled with only relatively minor generation of gibbsite, result in the formation of major accumulations of Fe oxides in the form of laterites (Chapter I.3).

The upper soil horizons are subjected to desiccation in the dry season, corresponding to an *ultra-desiccation front* (Chauvel, 1977). One consequence is that alternately humid and dry conditions affect even the very fine pores (voids less than $0.2 \mu\text{m}$), so that the microfabric of the soil particles becomes unstable. In addition, under dry conditions, residual water molecules in thin films on the surfaces of soil particles are protonated, giving local strong acidity (Mortland, 1968; Pedro and Melfi, 1983). Clays and iron oxyhydroxides become dissociated (Brinkman, 1970; Chaussidon and Pedro, 1979) and the clays may even be dissolved. These processes promote the mechanical eluviation of clays which, together with dissolution, results in the formation of surface soil horizons impoverished in clay.

In *dry savannas and semiarid to arid regions* (rainfall less than 1200 mm p.a., dry season longer than 6 months), erosional processes increase, but weathering and pedogenetic loss of components from the profile are minor. The weathering solutions concentrate alkaline cations, the saprolite is thin and smectites are the dominant authigenic clay minerals. Because of the low rainfall, there is only weak redistribution of iron into nodules (Boulet, 1974). The fabric of the pedoplastic material reflects the swelling and shrinking properties of the smectites under alternately humid and dry conditions, such as in vertisols. The upper horizons are subjected to strong contrasts in moisture content during the

year, with saturation prevailing in the rainy season due to water-tables perched on the compact smectitic horizons, but with ultra-desiccation in the dry season. Clay impoverishment due to eluviation and dissolution leads to the formation of sandy surface horizons, especially over coarse textured lithologies. However, this process is weak when rainfall is < 700 mm p.a. Under sufficiently arid conditions (< 600 mm p.a.), the presence of weathering solutions rich in calcium and bicarbonate ions causes, in wet periods, the dissolution of quartz and clay minerals and, in the dry periods, the precipitation of calcite at a Ca-cementation front in a variety of forms of calcretes, ranging from coatings and nodules to duricrusts (Nahon, 1976; Millot et al., 1977; Halitim et al., 1983, Milnes and Hutton, 1983). The formation and exploration significance of calcretes are considered in Chapter III.3. Gypsum and other salts (Na, Mg, Cl) may also accumulate in the profile or as superficial crusts.

In summary, changes evident in the climatogenic vertical soil profile between humid equatorial, seasonally humid and arid climates are as follows:

(1) the *saprolite* becomes thinner, with the disappearance of gibbsite and the replacement of kaolinite with smectite;

(2) in the *oxyhydroxide* accumulation layer, the Fe-Al ratio increases. In sufficiently arid climates, the oxyhydroxides do not accumulate and this cemented facies disappears; however, in semiarid regions, carbonate and salt accumulations appear;

(3) *microaggregation* disappears and the upper horizons are characterized by more massive microfabrics. The amount of smectite increases progressively, giving polyhedric fabrics. Clay impoverishment in the topsoil increases, thus producing sandy horizons where quartz is abundant.

(4) physical *erosional* and *depositional* processes increase.

As described in Chapter I.1, at any latitude, high relief gives vertical climatic, vegetational and soil zoning. The increase in precipitation and the diminution of evapotranspiration result in continuously humid soil regimes, more intense leaching and accumulation of organic matter. On volcanic ash, which occurs frequently in high relief tropics, allophane accumulates, giving andosols (Tan, 1984). In the higher level of this vertical zonation, podzolization is the main pedogenetic process (Zebrowski, 1975).

Topography

Topography is both an internal and external factor in pedogenesis, either influencing or being a consequence of soil evolution. Different geochemical conditions exist upslope or downslope in the same landform unit, depending upon the influence of the topography on the drainage and the hydrology of the soil cover. For example, some Si-cementation fronts may be related to certain low topographic situations in which silica transported for several kilometres has been deposited (Milnes and Twidale, 1983). The processes of lateral surface movement of particles by water or wind action, and by mass flow on slopes,

which range from thin reworking of the topsoil to continental sedimentological processes, also depend mainly on topography and climate (see Chapter I.6). Under the dense forests of humid climates, physical erosion is less significant than leaching, even on steep slopes, but in drier areas, the steepness of slopes has a considerable bearing on the processes of erosion. Thus, an instability due to tectonism or climatic change may induce erosion of an initial regolith, so that newly developing soils will form from different parent materials according to the depth of truncation in different parts of the landscape (Stace et al., 1968). In semiarid Niger (rainfall 400–600 mm p.a.), Gavaud (1977) described an initial regolith that consists of a 30–40 m thick smectitic saprolite overlain by 40–70 m thick kaolinitic and cuirasse horizons. As a result of the truncation of this initial cover, newly formed soils have developed upslope on ferruginous and kaolinitic materials and downslope on smectitic materials. The truncated profiles may also be overlapped by new sediments, giving complex polygenetic profiles (Milnes et al., 1985). Such variations in soil parent materials have a profound effect on the surface geochemical expression of mineralization and is discussed in Part III of this volume. The interdependence of topography and soil evolution is considered further below.

Soil parent material

The foregoing description of variations in pedogenetic processes due to climate refer particularly to the weathering of common crystalline rocks such as granite, but other variations can be due to differences in lithology. Even minor differences may be significant, especially under intermediate climates. The nature and abundance of resistant minerals that become relatively enriched may influence soil fabric, drainage conditions and geochemical processes. For example, soils on a coarse-grained granite may develop a less strongly cemented facies than soils on fine-grained granite, the difference being attributed to freer drainage conditions on the former due to large residual quartz grains. The chemical composition of the bedrock can control the composition of the weathering solutions and hence of the authigenic minerals. The effect is greater when the amount of percolating water is low. On Al-poor rocks, such as dunites (and limestones), silica released at depth by weathering of primary minerals, or transferred from the degradation of topsoil, precipitates as quartz, chalcedony or opal in the absence of aluminium (Lelong et al., 1976; Nahon, 1976; Nahon et al., 1979; Leprun, 1979; Butt and Nickel, 1981). Weathering of Fe-rich parent material such as basic rocks forms, under sufficiently oxidizing conditions, a skeletal framework of Fe oxides in the saprolite that is free draining and thus prone to more intense eluviation and oxidation at depth compared to saprolite formed on acid rocks. As an example, in Niger, the saprolite on granite is 30–40 m thick and overlain by thick kaolinitic horizons, whereas on Birrimian schists the saprolite is 150–200 m thick and immediately overlain by a cuirasse (Gavaud, 1977).

Biotic factors

Biotic factors, such as vegetation, microorganisms or animals are both internal and external factors in pedogenesis, or can be a consequence of soil evolution. Organisms, whose existence and activity depend on the prevailing environment, are strongly involved in soil formation (Dommergues and Mangenot, 1970; Alexander, 1977). The presence of organic matter and the processes of biotic reworking affect the soil fabric and hence influence the soil moisture regime. Organic acids or chelating compounds produced during the decomposition of organic matter or as metabolic products of soil biota may be active in the transport of the released elements (Huang, 1986). Vegetation influences the type of soil organic matter and its presence or absence determines the effect of physical erosion processes.

Time

Time is an important factor in soil development in tropical regions, where weathering mantles have been evolving since the Tertiary or earlier. The time required to form a profile with an Fe oxide cemented horizon has been estimated by Nahon and Lappartient (1977) to be a few million years and that for intense bauxite formation to be from 1.4 to over 20 million years (Bardossy, 1983) (see Chapter 1.3). Soil formation has thus operated over very long time intervals, and any changes in the factors involved will influence the nature of the product.

The *external factors* of soil formation may have changed. Various authors have estimated the rate of descent of the weathering front to be between 30 and 290 cm per 100,000 years (Leneuf, 1959; Hervieu, 1968; Gac and Pinta, 1973; Trescases, 1975; Boulangé, 1984; see Table 1.3-2). These rates are high compared to the probable length of soil evolution in much of the tropics. Accordingly, *the soil may have descended through several lithologies*. Thus, some soil characteristics (such as trace element or heavy mineral abundances or assemblages) may not be related to the underlying saprolite, but be derived from a different parent material which has since disappeared. Climate and the chemical characteristics of the atmosphere have changed throughout pedological (and geological) time (Rognon, 1976; Frakes, 1979; Tardy, 1986) resulting in different weathering conditions. For example, Berner et al. (1983) suggest that the average temperature and CO₂ content of the atmosphere have declined from 26 to 15°C and from 2.5 to 0.055 10¹⁸ mole respectively during the last 100 million years. There are many examples of the effects of such changes on soil evolution. Thus, in Burkina Faso, Leprun (1979) demonstrated the replacement of a kaolinitic weathering front by a smectitic front, and in the Ivory Coast, Boulangé (1984) described the replacement of a gibbsitic front by a kaolinitic front. In each case, the successions are related to a change to less humid climates. In French Guiana, Boulet (1978) related the presence of a leaching front at depth in a lateritic profile to lowering of the water-table due to tectonic uplift. Numerous

examples in Australia show successive weathering and continental sedimentological processes interacting with soil formation (Mabbutt, 1980; Butt and Nickel, 1981; Milnes and Hutton, 1983; Milnes et al., 1985; Butt, 1985). All these examples indicate that the present soil represents an integration of successive variations of the external factors, as discussed later in the chapter.

The evolution of the soil cover can itself induce changes in the *internal factors of soil formation*. Landscape evolution due to pedogenesis may alter the conditions of groundwater movement. The development of horizons with different fabrics involves changes in permeability and in the rates at which minerals dissolve and are formed. These variations in the factors affecting pedogenesis induce disequilibrium in the soil; this in turn is expressed as transformation fronts that result in alteration to a profile form in equilibrium with the prevailing conditions. These fronts progress vertically, as described above, or laterally through the landscape, giving three-dimensional transformation systems (Boulet et al., 1984). The evolution of such systems is discussed and illustrated in the following section.

TRANSFORMATION SYSTEMS IN THE TROPICAL ZONE

Transformation systems represent the replacement of an initial regolith with one that is different in its mineral composition or fabric. The initial soils may either be locally preserved, or have disappeared after complete transformation. The dynamics of the systems depend on the causative factors, the location at which the transformation begins and the mode in which the fronts advance. Commencement may depend on external factors such as climatic change, base level change, or on internal factors related to the evolution of the soil itself. In both cases, all factors that control the movement of water in the soil cover interfere. When initiated, the advance of the transformation is facilitated by its own effects, as a feedback mechanism. For example, in eluvial-illuvial systems, the leaching front creates a porous soil fabric which favours transportation of material and hence further leaching; conversely, an accumulation front creates an impervious fabric which favours deposition and mineral authigenesis.

The apparent lateral advance of a transformation front (Fig. I.4-2) is the result of (a) vertical subsidence of the soil profile, and (b) lateral displacement of the transformation front. Vertical subsidence is more rapid in humid environments compared to dry environments, so that the soil material is partly renewed by advancement of the weathering front as the transformation proceeds.

The age and rates of development of systems can only be estimated indirectly. The age of the climatic change gives an upper limit to that of related transformation systems. In humid areas, assuming an average rate of descent of 1 m per 100,000 years, weathering may have advanced by 350 m since the mid-Tertiary, hence the transformation systems on the Precambrian shields may have been

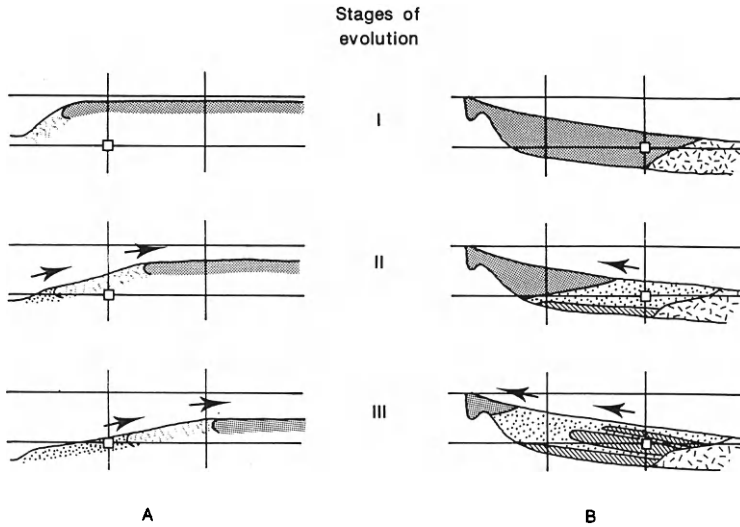


Fig. I.4-2. Dynamics of transformation systems: apparent lateral displacement of the transformation fronts. Arrows give direction of the displacement: (A) Vertical subsidence rapid compared to lateral advance of transformation fronts; (B) Vertical subsidence negligible compared to lateral advance of transformation fronts.

evolving throughout this period. However, systems developed on Pleistocene sediments are obviously much younger.

Transformation systems under humid tropical climates

All transformation systems so far recognized in humid areas demonstrate massive leaching of an initial lateritic cover, with the leached material lost to the drainage network.

Systems due to internally imposed changes in drainage conditions

In central Amazonia, the lateritic cover developed on Tertiary sandy-loam sediments is being replaced by podzols (Lucas et al., 1984, 1987). The present annual rainfall is about 2000–2500 mm, with a weak dry season. The initial soil on the plateaux is a thick clay having a microaggregated horizon consisting of more than 90% kaolinite overlying a nodular horizon consisting of a kaolinitic matrix with gibbsite and hematite nodules. On the slopes, the soils are more sandy, with giant podzols developed on the lower part of long slopes. There is a range of intermediate types between the clay-rich lateritic soils of the plateaux and the sandy podzols downslope, and most pedological features vary progressively between these two extremes. This soil differentiation is explained as follows (Fig. I.4-3). On the plateaux, elements released by the surface degradation front are transported deep into the profile. Aluminium is trapped as kaolinite

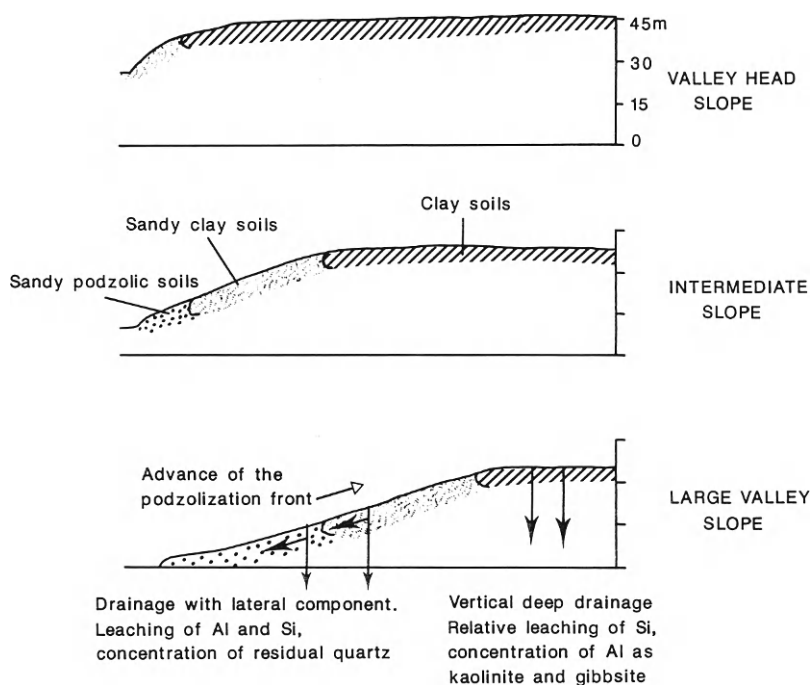


Fig. 1.4-3. Evolution of soil system on Barreiras sediments, central Amazonia.

and gibbsite, and there is a net loss of SiO_2 . This results in the formation of kaolinitic clay horizons as the soil descends through the sediment. On the slopes, lateral waterflow leaches more Al from the system so that, firstly, more material is removed than from the plateaux, emphasizing the slope and, secondly, there is a net loss of Al, giving a relative enrichment of SiO_2 as quartz. The soils are thus sandier, and podzolisation occurs on the lower slopes. As the soil descends through the sediment, these differences in vertical evolution result in the lateral advance of a leaching and podzolizing front that progresses upslope as the slope develops.

The cause of this transformation is internal, related to the flow percolating water. The transformation starts at the edges of the plateau landforms and advances towards the centre, contributing to the development of slopes.

In French Guiana, kaolinitic soils have developed over Archaean migmatites (Boulet et al., 1984). The present annual rainfall is 2500–3000 mm, with a weak dry season. The initial soil consists of the vertical superposition of a thick saptolite and an upper microaggregated sandy-clay horizon, 3–8 m thick. A thin quartz pebble stone line is commonly present between these two horizons. The quartz content increases progressively in the top metre. This cover has resulted from the partial solution of quartz and the relative accumulation of kaolinite as

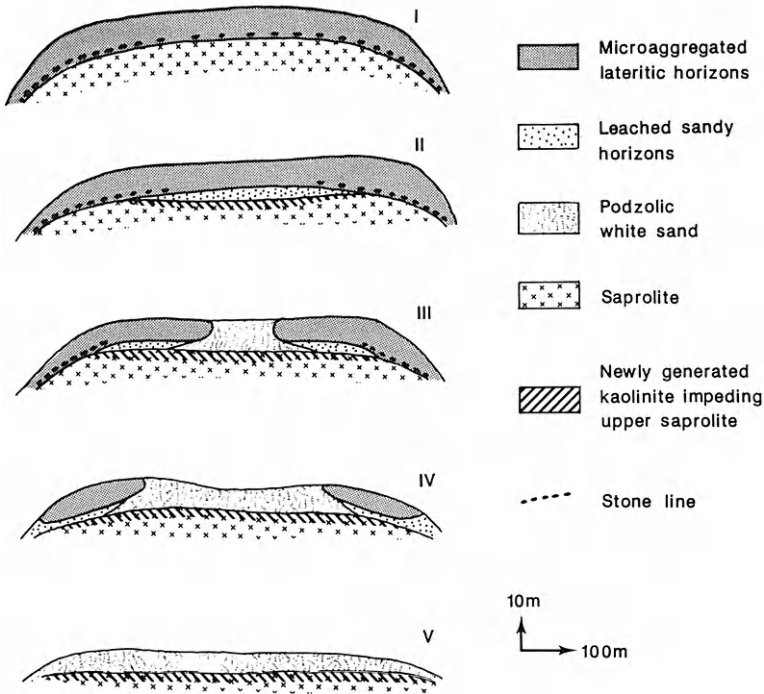


Fig. I.4-4. Evolution of the laterite-podzol system developed on migmatites, French Guiana.

the soil formed from the saprolite (Fig. I.4-4). As in the previous example, this initial cover is now being transformed into giant podzols, and the transition exhibits the same features. However, here the podzols develop at the centres of the plateaux and advance towards their margins; the kaolinitic soils, including nodules with lithic fabrics, remain on the slopes. The difference is due to the movement of percolating water, which forms a deep drainage network perched on the upper part of the saprolite, the permeability of which is impeded by newly-formed kaolinite. This transformation begins at the centre of the plateaux, where the surficial drainage is minor and the groundwater is closest to the top of the saprolite. The deep drainage allows lateral leaching of some Al from the system, so that soils become sandy and the landforms evolve towards plateaux having central depressions occupied by podzols. The more mature plateaux are entirely podzolized.

In these examples, podzolization is a secondary process that occurs after transformation has caused the initial clay or sandy-clay soil to become sandier. However, if the initial soil is already a sandy loam, podzolization may itself cause the transformation. This has been observed on Quaternary sediments in French Guiana (Fig. I.4-5), where a landscape of low flat hills with an initial cover of lateritic sandy loam, 1–3 m thick, has been transformed into a podzol with a

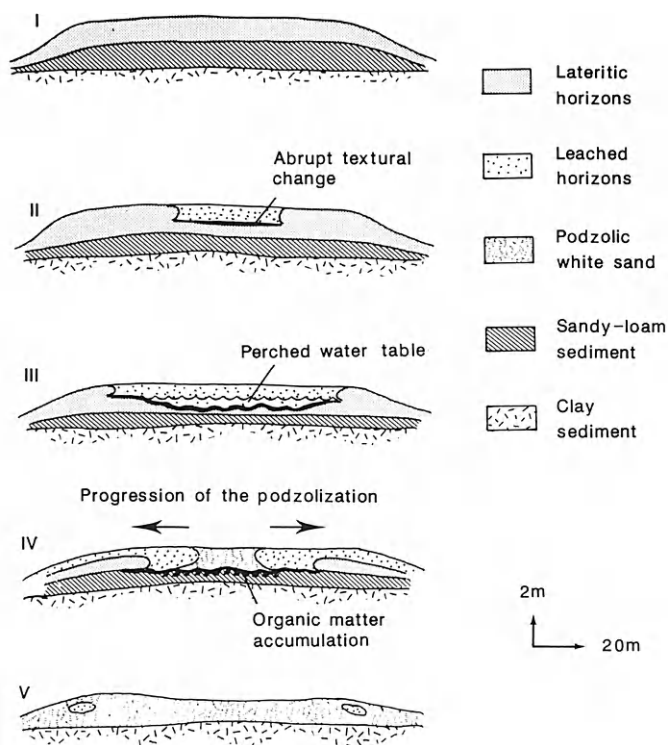


Fig. I.4-5. Evolution of the laterite-podzol system developed on coastal sediments, French Guiana. The size of landscape units is small compared to the system of Fig. I.4-3.

50–150 cm thick white sand horizon overlying a humic iron pan (Turenne, 1977; Boulet et al., 1984). In the centre of the landscape units, the external drainage is minor and the water-table is close to the surface in the rainy season. The process commences by topsoil degradation, the development of an abrupt textural change and the establishment of a temporary, shallow, perched water-table. Thereafter, alternately saturated and unsaturated conditions favour leaching of kaolinite, so that podzolization progresses both vertically and laterally. Settling of the soil material causes slight subsidence of the podzolized zones.

Systems due to external changes

Transformation may be initiated by a change in drainage conditions caused by external factors. Systems of this type are developed on Precambrian schists in French Guiana, where the water-tables have become lower following tectonic uplift during Quaternary (Boulet, 1978; Fritsch, 1984). The present climate is characterized by an annual rainfall of 2000–3000 mm and a short dry season. The landscape consists of rounded hills having an initial soil cover consisting of:

- (1) a microaggregated soil horizon, 2–4 m thick;

(2) a red pedoplastic clay horizon, 1–2 m thick, with a few ferruginous nodules with lithic fabrics;

(3) saprolite with relic muscovites.

Water percolates vertically to the water-table deep in the saprolite. The soil cover is being modified by an ascending transformation which commenced downslope (Fig. I.4-6). Morphologically, the microaggregated layer becomes thinner and is replaced by a sandy-loam horizon. At the same time, the fabric of the upper part of the pedoplastic horizon changes and becomes nearly impervious, so that lateral waterflow occurs in the surficial sandy-loam horizon. Soil creep and mechanical erosion are almost negligible. The transformation front thus corresponds to the development of a horizon permitting lateral drainage. The large volume of water percolating along the base of this horizon increases the rate at which clay dissolves and hence the quantity of soluble material lost from the system. This transformation front advances both upslope and to depth, at rates greater than that of the descent of the weathering front and is thus discordant across the initial vertical sequence of horizons, and the mean slope increases with its advance.

Cemented facies, in the form of ferruginous or gibbsitic nodules, are common in soils of the humid tropics. They are present in all stages of their genesis throughout the regolith, so that they mostly seem to be related to active cementation processes. However, in massive cemented facies such as the bauxitic formations of central Amazonia, complex successions of Fe and Al facies indicate that significant changes in weathering processes have taken place during their development (Grubb, 1979; Lucas et al., 1988). Under present conditions, they are being dissolved and replaced by a kaolinitic plasma.

Transformation systems under seasonal (savanna) climates

Eluvial–illuvial systems

In savanna climates, most of the known transformations are eluvial–illuvial systems, in which some elements are leached from the upper parts of landform units and transferred to the lower parts. The soils and upper horizons of upslope units tend to be acid and rich in kaolinite, iron oxyhydroxides and residual quartz sand, whereas deeper horizons and soils of downslope units tend to be rich in 2/1 clays and alkaline cations. As the transformation progresses, the latter become more abundant and extend upslope at the expense of the original kaolinite. Most of these systems, in Africa, South America and Australia, are attributed to the transformation of a thick, relic, lateritic cover which, because of a drier climate, is no longer in equilibrium with present pedogenetic processes (Fig. I.4-7). This is particularly obvious in the dry savannas (annual rainfall 600–1000 mm). In wet savannas (rainfall > 1000 mm p.a.), the distinction between relic soil materials and those formed under present conditions is less evident (Brabant and Gavaud, 1985). The present pedoclimate upslope is open, well drained and in equilibrium with lateritic materials, whereas downslope it is

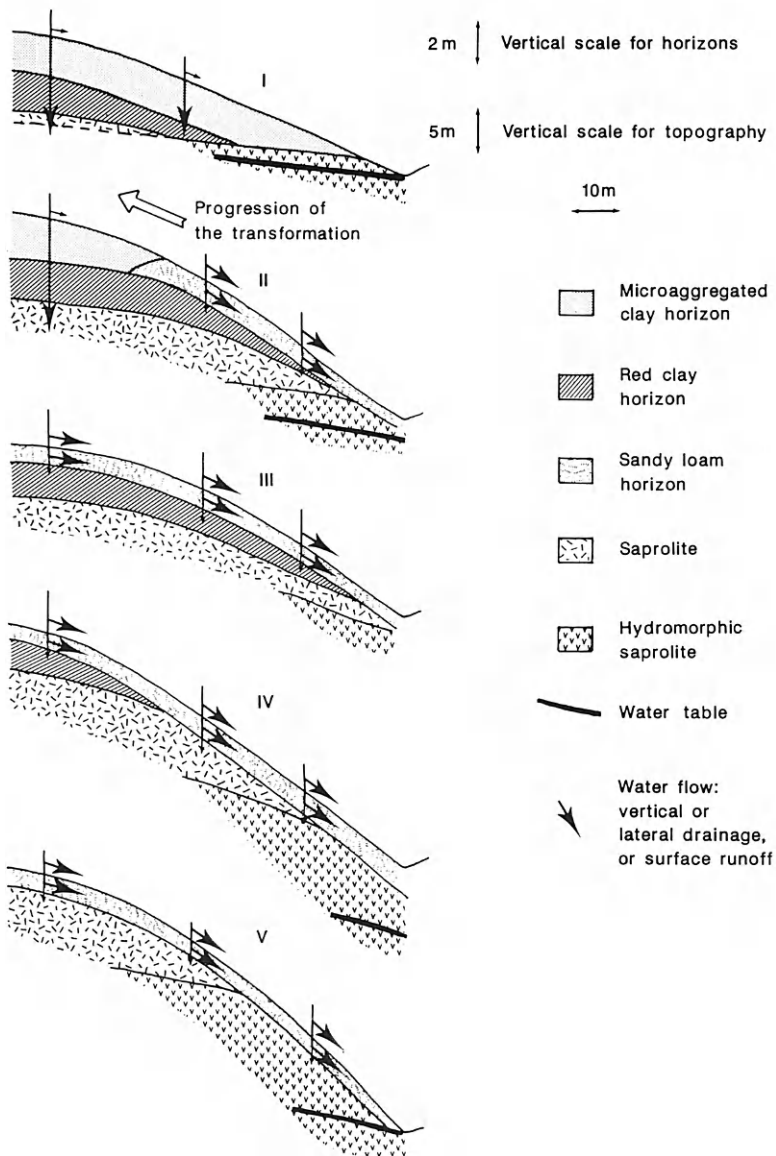


Fig. I.4-6. Evolution of a soil system developed on schists, French Guiana. Derived from Boulet (1978).

more confined and enriched with elements leached from upslope. The soils that are formed are thus organized as catenas, that is a sequence of soils.

Systems related to a climate change are developed at the base of granitic inselbergs in southern Burkina Faso (Fig. I.4-8) where the annual rainfall is

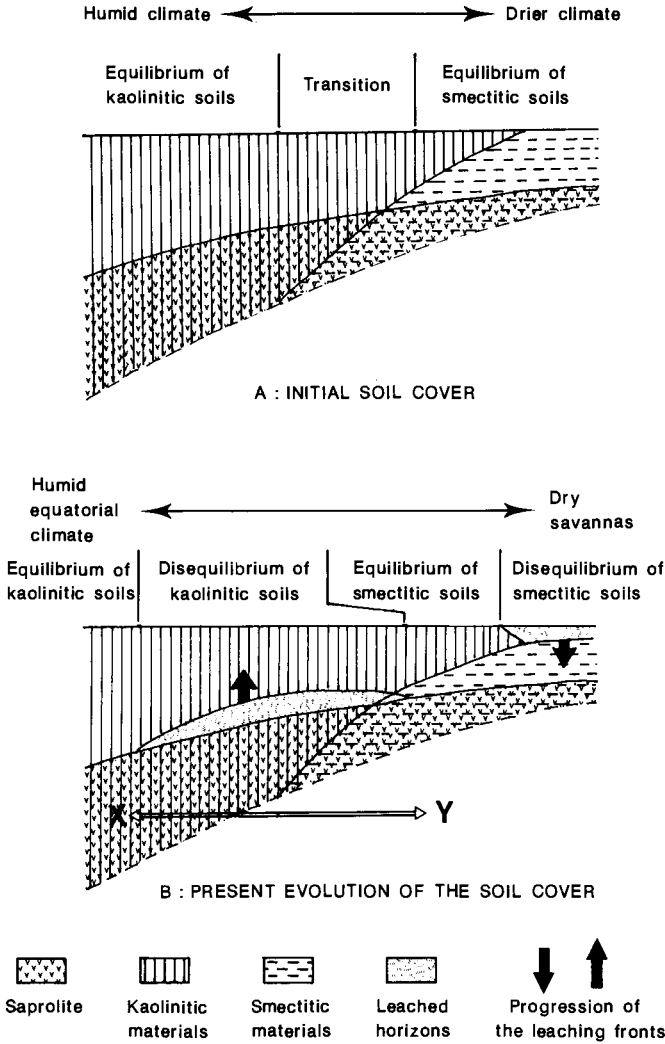


Fig. I.4-7. Disequilibrium in soil cover south of Sahara. Derived from R. Boulet, unpublished. The transformations indicated by the arrow X-Y are illustrated in Fig. I.4-8.

900 mm with a long dry season (Boulet, 1974). In the upper part of the catena, kaolinitic horizons are developed from the pre-existing saprolite, which represents the initial cover. At the centre of the catena, there is a sandy soil with features characteristic of leaching processes, such as relic kaolinitic material. This indicates that a leaching front is progressing upslope at the expense of the kaolinitic cover. The lower part of the catena has a smectitic clay soil with features characteristic of illuvial processes. Relics of leaching features at the

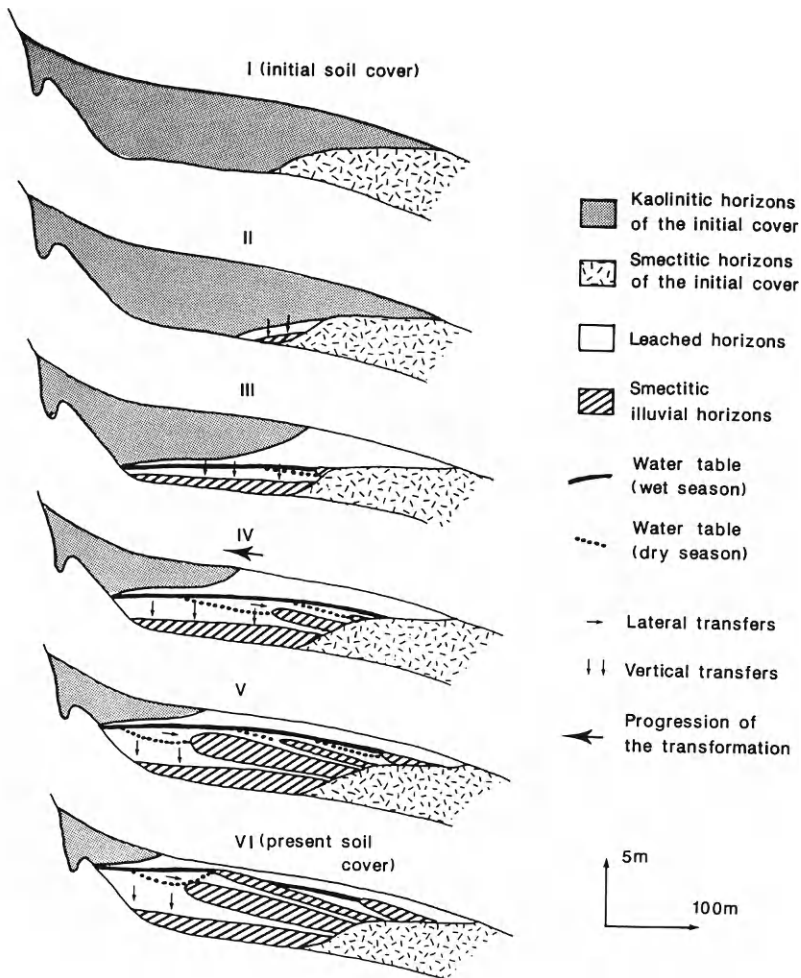


Fig. I.4-8. Soil system in Burkina Faso. Derived from Boulet (1974).

transition with the sandy soil indicate that an illuviation front is progressing upslope at the expense of the sandy soils. At the leaching front, the contrasting soil moisture regime due to the present seasonal climate facilitates the destabilization of clay particles. The released elements are transported as solids and in solution and accumulate downslope in the zone of water-table fluctuation, where the generation of massive smectite units occur. In this particular example, the presence of an inselberg increases the water input and hence the intensity of the eluvial processes during the rainy season. Similar transformation systems are present where there are no inselbergs, but where coarse granites have given rise to soils with a porous, sandy texture that facilitates water percolation.

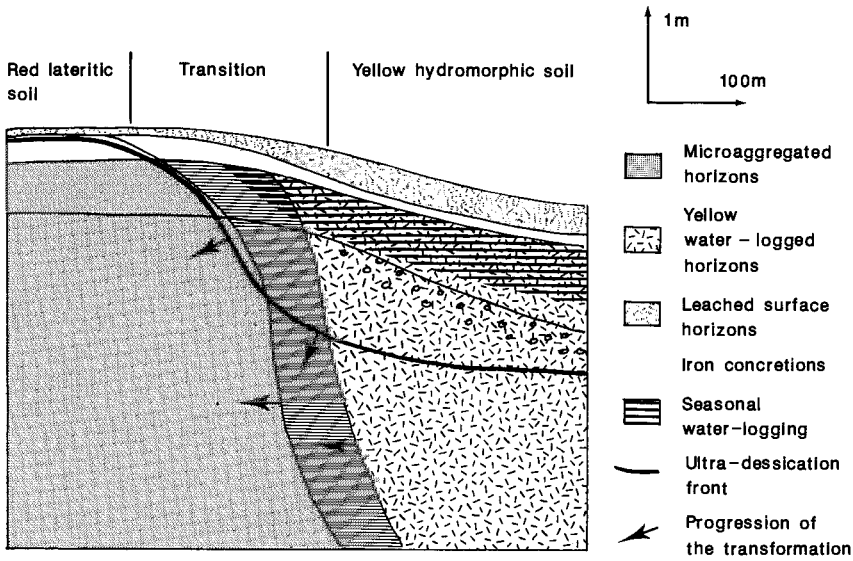


Fig. I.4-9. Sketch of the transition between red microaggregated soil and yellow hydromorphic soil, Casamance, Senegal. Derived from Chauvel (1977).

A progressive transition from systems with abundant kaolinitic soils in upper landscape units in the highlands to more transformed systems in the lowlands in which this cover has disappeared or remains only as relics have been recognized in north Cameroun (Brabant and Gavaud, 1985). Similar systems, in which the initial kaolinitic domain has already disappeared, have been described from Tchad (Bocquier, 1971).

The transformation and disintegration of cuirasse by leaching under the present climate and their replacement by kaolinitic horizons have been described from Senegal and Burkina Faso by Nahon (1976) and Leprun (1977, 1979). As the different transformation fronts have progressed upslope, Fe has been leached from both the base and the top of the crust and transported in solution to form secondary ferricretes downslope. Such processes are closely linked to the morphogenesis of the landscape.

Related systems

Changes to drier savanna climates may initiate the transformation of only the fabric or mineralogy of soil, without transport of material. Soil fabric changes are reported from Casamance, Senegal (Chauvel, 1977) where the annual rainfall ranges between 800 and 1200 mm, with a long dry season (Fig. I.4-9). The landscape is one of low plateaux having an initial lateritic cover developed on Tertiary sandstones. The profile consists of saprolite, a loamy sand horizon with soft ferruginous nodules and a red microaggregated horizon 2 m thick. The latter

remains humid during the dry season because of the “mulching” effect of the microaggregated fabric. However, with the advance of an ultra-desiccation front, the red microaggregated horizon is being replaced by a yellow horizon with a compact microfabric. This horizon has a contrasted moisture regime, being highly desiccated in the dry season and temporarily saturated in the rainy season. The initiation of this transformation is related to the onset of drier climatic conditions over the last 20,000 years, during which time the microaggregated materials have been out of equilibrium with the prevailing climate. The process commenced in the topsoil with the disintegration of the microaggregates by hydric constraints in the dry season. The transformation is more intense in the centres of the plateaux because shrinkage of the soil material causes slight subsidence. Temporary water saturation of the surface horizons in the wet season accelerates the collapse of microaggregates and the consequent modification of porosity permits even greater desiccation in the dry season.

The temporary waterlogging also results in the replacement of hematite by goethite and hence the soil colour changes from red to yellow. The ultra-desiccation front progresses both downwards and laterally and the compact yellow soil thus progressively replaces the red soil. This explains the abundance of yellow soils in the landscape. Red microaggregated soils are only observed where the annual rainfall exceeds 1200 mm. In drier climates, yellow soils appear at the centres of the plateaux. At 1000 mm annual rainfall, they occupy the most of the surface, with the red soils being restricted to the edge of the plateaux. Where rainfall is less than 1000 mm p.a., the processes have been working for a longer time and the yellow soils occupy the whole land surface. Examples of this system have been described from Brazil by Volkoff (1985), who found that an increase in aridity correlates with a *decrease* in the hematite/goethite ratio in soil material. However, in many other examples (Taylor and Graley, 1967; Lamouroux, 1972; Kampf and Schwertmann, 1983), an increase in aridity correlates with an *increase* in the hematite/goethite ratio. This ratio, which determines the yellow or red colour of the soil, is thus not only a function of climate but also of other factors such as soil texture, which controls the moisture regime, and the weathering history.

Transformation systems under arid climates

In arid areas, soil catenas in equilibrium with the present environment can be present, the accumulation of soluble salts in depressions being an example. Most of these are not transformation systems, however, because they are not progressively replacing an earlier soil cover. However, the disruptive replacement of cuirasse, saprolite or saprock by calcrete (Millot et al., 1977), known from arid and very arid climates in West Africa and Australia, can be recognized as transformation systems. In Senegal and Mauritania, for example, the pre-existing lateritic cover, which consists of saprolite overlain by a cuirasse, has been formed under past humid climates and is now in disequilibrium (Nahon, 1976).

As the climate became drier, the original kaolinitic weathering front has been replaced by a smectitic front, so that smectitic saprolite now underlies the kaolinitic saprolite. The iron cementation front has proceeded downwards at the expense of the kaolinitic saprolite and in places may directly overlie the smectitic saprolite. In a third stage of development, under the present arid climate, a calcite cementation front, corresponding to the in-situ formation of calcrete, develops downslope at the expense of the smectitic saprolite and, upslope, into the cuirasse. Consequently, the cuirasse is now progressively confined to the upper part of the landform units.

CLASSIFICATION OF TROPICAL SOILS

Consideration of the classification of tropically weathered soils is beyond the scope of this chapter. A number of classification systems have been developed

TABLE I.4-1

Main soil taxonomic units in use in the studied areas; French (CPCS, 1967) and FAO (FAO-UNESCO, 1974)

Climate	Humid	Wet savanas	Dry savanas	Arid	Humid mountains
French	Sols ferrallitiques (commonly leached or indurated)		Sols fersiallitiques	Sols minéraux bruts	Andosols
	Podzols (humic- ferruginous)	Sols ferrugineux tropicaux (commonly leached)		Sols peu évolués xériques	Sols ferrallitiques (commonly humiferous)
		Vertisols		Sols gypseux sodiques (solonetz, solods)	Podzols
		Sols hydromorphes			
FAO	Ferralsols (Haplic) (commonly Plinthic)		Cambisols (Chromic, Vertic, Calcic)	Arenosols Regosols	Andosols
		Luvisols (Plinthic, Ferric)		Yermosols	Ferralsols
	Acrisols (Ochric, Plinthic, Rhodic)		Nitosols (Dystric, Eutric)	Xerosols	Podzols
	Podzols (Ferric, Humic)	Vertisols		Solonetz Planosols	
	Gleysols and Gleyic Groups				

and for the main concepts behind them, reference should be made to the principal publications: FAO classification: FAO–UNESCO, 1974; French: CPCS, 1967; Australian: Stace et al., 1968; USA: Soil Taxonomy, Soil Survey Staff, 1975). The FAO and the French classifications, which have the most comprehensive coverage of tropical soils, are summarized in Table I.4-1. Several of the classifications are genetic and reflect the climatic zonality of the principal processes involved in soil formation, as described in this chapter. However, they do not adequately account for the weathering history of an area; for example, as discussed above, the presence of ferrallitic soils (or ferralsols) in dry savannas and arid areas commonly relates to old kaolinitic saprolites that are no longer developing under present conditions.

All existing systems of soil classification tend to refer to soil bodies in terms of vertical successions of horizons in units such as profiles, pedons and elementary soil areas. The genetic relationships between the different horizons in the classifications are, accordingly, only considered as vertical processes. However, as seen in the descriptions of transformation systems, most regoliths in tropically weathered terrains are only understandable if considered in three dimensions which, at the scale of the systems involved, is generally at least that of the landform (see Fig. I.1-4). Applying the existing soil classifications to such systems tends to subdivide the continuum and to focus attention either on typifying concepts, or on the arbitrary boundaries between types. Thus, the use of these classification schemes alone in soil surveys is inadequate for describing and understanding the geography and genesis of soils.

THE CHEMICAL MOBILITY AND TRANSPORT OF ELEMENTS IN THE WEATHERING ENVIRONMENT

M.R. THORNER

INTRODUCTION

The aqueous solution, transport and precipitation of elements is of central importance to weathering and geochemical dispersion. The hydrolysis and redox reactions discussed in Chapter I.2 are principally those that affect the major elements, being responsible for the destruction of the primary rock-forming minerals and the formation of the secondary minerals of the regolith. Of particular importance to geochemical exploration, however, are those reactions that affect the generally less abundant elements associated with mineralization. These are the reactions that are ultimately responsible for the nature of the surface expression of mineralization in the regolith, particularly its size, intensity and location. Geochemical anomalies formed as the result of chemical reactions and transport involving water are referred to as *hydromorphic* and the process as *hydromorphic dispersion*. The purpose of this chapter is to describe the chemical principles involved in hydromorphic dispersion and the manner in which individual elements or groups of elements behave in different weathering environments.

The extent to which particular elements are mobilized by groundwaters during weathering depends upon:

(1) the controls of solubility in aqueous solutions having various amounts of other dissolved species (cations, anions and organic materials), and

(2) the interaction between these solutions and the complex surfaces of primary and secondary minerals. Interactions between the two phases take place at every point on the interface, which is depicted in a schematic cross section shown in Fig. I.5-1.

The various elements may be:

(a) held within the mineral crystal lattice;

(b) loosely bound within a layer of the changing potential field at the interface;

or

(c) mobile in solution, either solvated by the water molecules or "complexed" with one or more other soluble ions. Mobility is also possible as colloidal particles; these particles will have a similar dynamic interface with the solution as depicted in Fig. I.5-1.

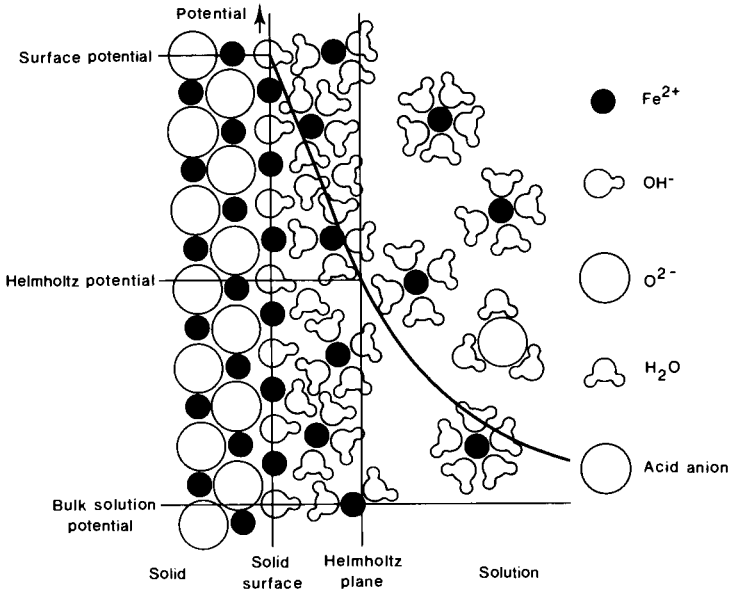


Fig. I.5-1. A schematic representation of a cross section through a solid/solution interface showing the electrical potential change. Modified from Segall et al. (1982)

During dissolution, elements move from the crystal surface through the charged layers into solution. For precipitation, the reverse is true. If other elements are adsorbed at the interface these processes tend to be hindered and, in the case of precipitation, may result in that element being coprecipitated or bound into the crystal of the precipitate. The system is thus dynamic, involving many kinetic phenomena; accordingly, the application of thermodynamic data, such as solubility product constants, which are concerned with systems in equilibrium, is not sufficient to give a full description of the likely chemical mobility of an element. Nevertheless, as an initial consideration, solubility is most important.

The aim of this chapter is to outline the major factors controlling the mobility of the chemical elements in aqueous solutions at normal weathering temperatures and to group the elements on the basis of similar behaviour. The groupings presented are recognizably derived from the Periodic Table of the elements. The classic books of Pourbaix (1963) and Baes and Mesmer (1976), and the recent compilation of Eh–pH stability field diagrams by Brookins (1988) together give an excellent basis for understanding the solubility of most elements where only water is involved. Data concerning the complexing of elements by other ions has been compiled by Sillén and Martell (1964; 1971) and Smith and Martell (1976). Langmuir (1979) has given a very useful summary of this classical approach as it relates to geochemical behaviour.

SOLUBILITY

An element may be in solution as a cation, an anion or a neutral species, depending upon the oxidation state it has been forced to adopt by the conditions of the groundwater environment. As elements become more oxidized by losing electrons, they become smaller in size and more positively charged. The solution chemistry of an element is affected profoundly by changes in oxidation state; for example, the lower +2 oxidation state of the Fe^{II} ion is far more soluble than the smaller-sized, higher +3 oxidation state of Fe^{III} (Fig. I.5-2). In Fig. I.5-2, the stippled area shows the range of pH and oxidation potential, Eh, that can be expected in groundwater environments. The range covers the conditions under which Fe solubility is strongly controlled by both Eh and pH; the other ions in solution are also affected due to co-precipitation with Fe oxides and by sec-

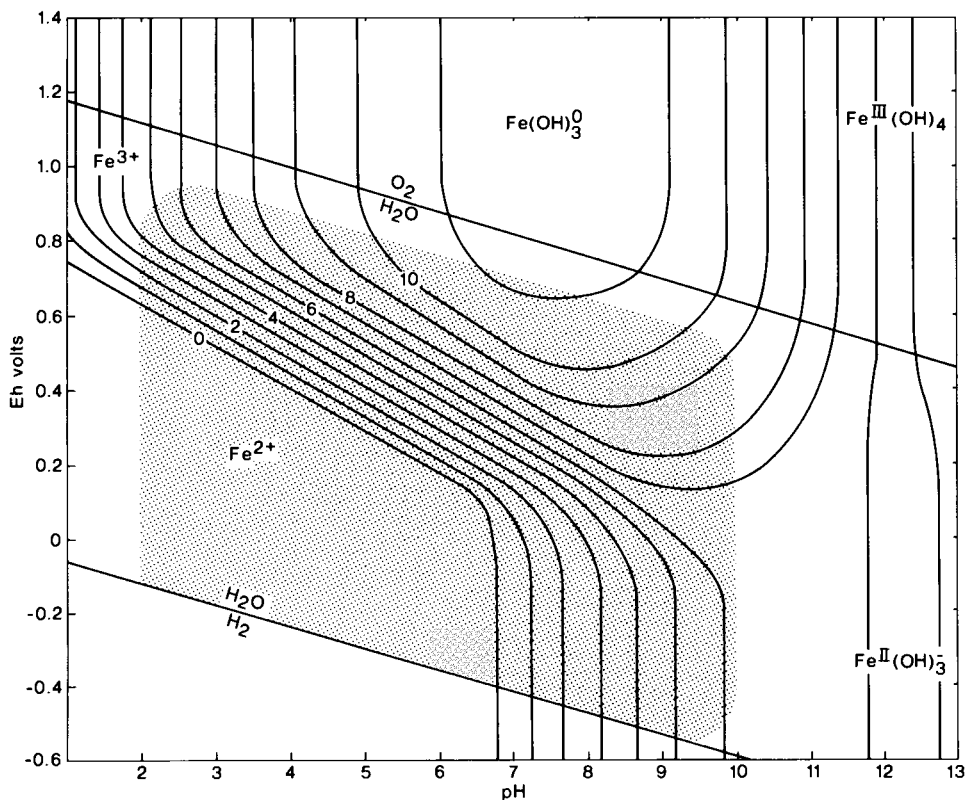


Fig. I.5-2. Solubility contours of Fe^{2+} and Fe^{3+} as a function of Eh and pH. The values on the contours are the $-\log[\text{total Fe}]$ where [total Fe] is the total activity of iron in solution in moles/litre. The stippled area represents the Eh and pH range that can be expected in natural weathering environments.

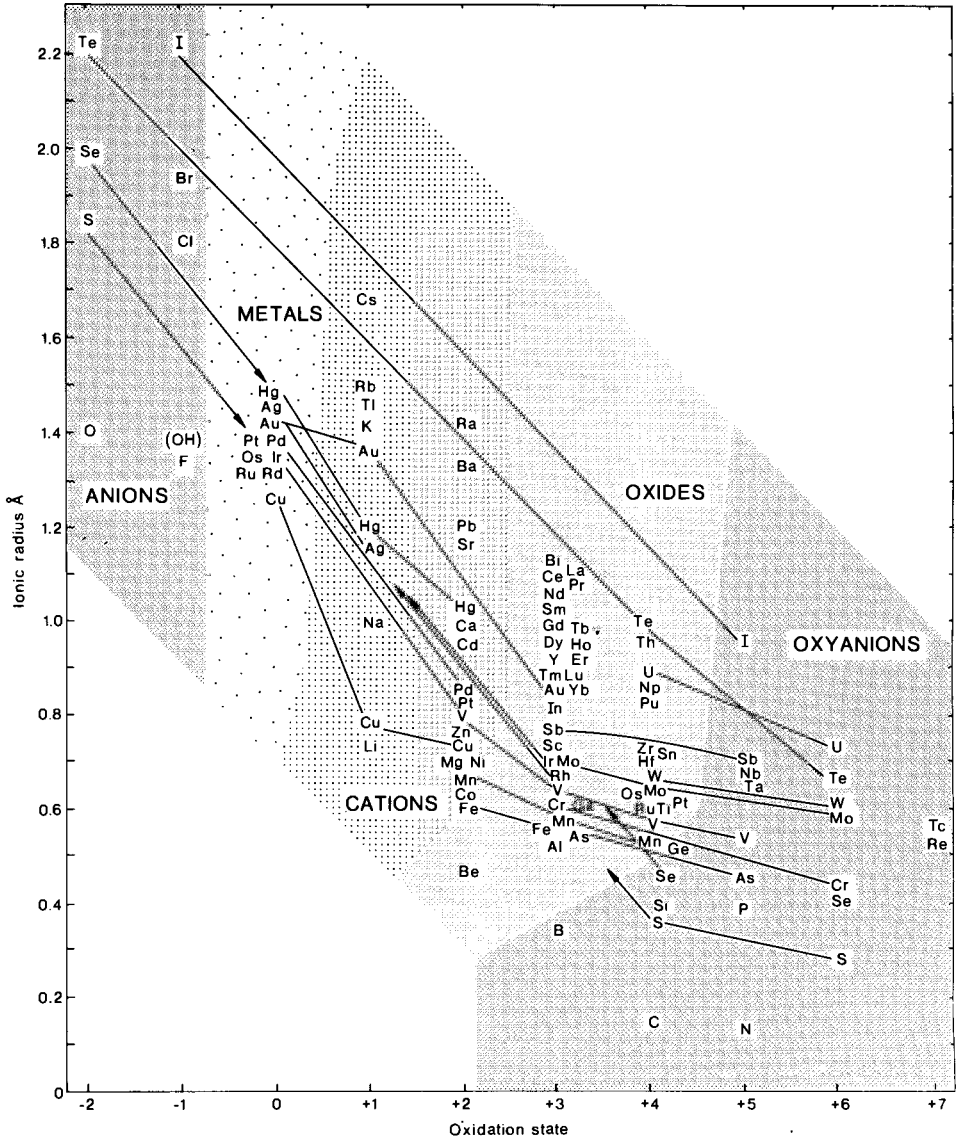


Fig. I.5-3. A plot of ionic radius, for six coordination, of the chemical elements as a function of the oxidation state possible in natural weathering conditions. Derived from Shannon (1976), and Hume-Rothery and Raynor (1958)

ondary Eh/pH control. A comparison of the six-coordinated ionic radii of all elements with their particular oxidation states that can occur within the range of Eh and pH expected during weathering is shown in Fig. I.5-3.

The elements can be divided into five groups, depending on the major factor controlling their solubility. These groups, listed in Tables I.5-1–I.5-5, are:

- (1) anions,
- (2) cations,
- (3) insoluble oxides,
- (4) variable oxidation state,
- (5) metals.

The groups are not mutually exclusive; on the listings in the tables, some elements are shown in parentheses to indicate that they also belong to other groups. Copper, for example, may occur naturally as metallic copper or in the Cu^+ or Cu^{2+} oxidation states, the latter strongly influencing its solution chemistry. Thus, Cu belongs to groups 2, 4 and 5.

These geochemical groups are dominated by the oxidation states of the elements in the Eh range of the weathering environment and consequently they can transgress the classical groupings of the Periodic Table. This is demonstrated in Fig. I.5-4 by the classical group V–A elements, where Bi is in the 3+ state and is a cation or insoluble oxide, Sb is in the 3+ state as an oxide/hydroxide or a weakly charged anion in the 5+ state, As is similar, further advanced towards being an anion, and P is fully in the 5+ state as an anion. Other classical Periodic Table groupings, such as the alkali metals, alkaline earths, the rare earth elements and most of the group III elements (Al, Ga, In, Sc and Y) have remained intact.

The solubilities of cations, hydroxide precipitates and anions of elements with respect to changes in pH have the general form of U-shaped curves depicted in Figs. I.5-5–I.5-7, respectively. These figures together demonstrate *firstly* the importance of pH and, *secondly*, the simple concept that cations are more mobile at low pH and anions more mobile at higher pH. When the insoluble elements (Fig. I.5-5) do dissolve, they form cations in acids and anions in alkalis. In effect, it appears that the U-shaped solubility curve moves, so that the minimum is at:

(1) high pH values for the cations that have low charge and large size (Figs. I.5-3 and I.5-5);

(2) mid-pH values for more oxidized and positively charged elements that have smaller sized ions, so that hydrolysis reactions (reactions with water; see Chapter I.2) form insoluble oxides and hydroxides (Figs. I.5-3 and I.5-6);

(3) low pH values for those elements with a high oxidation state that form oxyanions when hydrolyzed (Figs. I.5-3 and I.5-7).

Of the chemical elements grouped as having variable oxidation states (Table I.5-4), the most abundant and, in some respects, the most important, is iron. The change in oxidation state from Fe^{2+} , which is soluble as a cation to Fe^{3+} , which is insoluble as the oxide Fe_2O_3 , falls directly in the range of Eh and pH expected in the weathering environment (Fig. I.5-2). Thus, low oxidation potentials (Eh) and low pH values (i.e. reducing, acid conditions) produce greater Fe mobility than higher oxidation potentials and higher pH values, hence iron precipitates

Table I.5-3

Stability constants of common insoluble oxides

Oxidation state			Log of stability constants of soluble complexes			
2+	3+	4+	Cl ⁻	SO ₄ ²⁻	CH ₃ COO ⁻	C ₂ O ₄ ²⁻
BeO			-0.3	0.72	1.62	408
	Al ₂ O ₃		1.51	6.1		
	Fe ₂ O ₃		0.64	3.38	5.73	
	Mn ₂ O ₃		0.9	1.20	~ 10.0	
	Cr ₂ O ₃		-0.4	2.60	4.6	
	Ga ₂ O ₃		0.01	6.45		
	(V ₂ O ₃)		1.45			
	In ₂ O ₃		2.32	1.78	3.5	5.3
	Sc ₂ O ₃		0.04	2.59	8.74	
	Y ₂ O ₃		-0.1	1.24	1.68	5.46
	REE ₂ *O ₃		-0.4 to	1.2 to	1.8 to	4.9 to
			-0.1	2.0	2.1	5.6
	Bi ₂ O ₃		2.2	2.0		
		(SiO ₂)				
		(GeO ₂)				
		TiO ₂	2.2			
		(TiO ²⁺)				
		SnO ₂				
		HfO ₂	0.38	3.04		
		ZrO ₂	0.30	3.67		
		PuO ₂	0.14	3.66		
		NpO ₂	0.15	3.51		
		ThO ₂	0.3	3.22	3.9	8.8
		(VO ₂)	0.26	3.42		

* REE = Rare Earth Elements.

TABLE I.5-4

Elements having variable oxidation states; the change in oxidation state commonly causes a major change in solubility

Cations	Oxides		Anions	
	+3	+4	+5	+6
Fe ²⁺	Fe ₂ O ₃			
Mn ²⁺	Mn ₃ O ₄ Mn ₂ O ₃	MnO ₂		
[V ²⁺]	V ³⁺ /V ₂ O ₃	VO ²⁺ /V ₂ O ₄	VO ₄ ³⁻	
[Cr ²⁺]	Cr ³⁺ /Cr ₂ O ₃			CrO ₄ ²⁻
	Mo ³⁺	MoO ₂		MoO ₄ ²⁻
		[WO ₂]		WO ₄ ²⁻
	As(OH) ₃ ⁰ /As ₂ O ₃		AsO ₄ ³⁻	
	Sb(OH) ₃ ⁰ /Sb ₂ O ₃		SbO ₄ ³⁻	
		UO ₂		UO ₂ ²⁺
		U ₄ O ₉		(UO ₂) ₃ (OH) ₅ ⁺
				UO ₂ (CO ₃) ₃ ⁴⁻

TABLE I.5-5

Ions and ionic complexes of some metals in different oxidation states

Oxidation state								
0	+1	+2	+3	+4	+5	+6	+7	+8
Ru		RuSO ₄ ⁰	RuSO ₄ ⁺	RuO ₂				
Rh	Rh ⁺ /RhO ₂	Rh ²⁺	Rh ³⁺ Rh ₂ O ₃					
Pd		Pd ²⁺ /PdO PdCl _x ^{2-x}						
Os				Os(OH) ₄ OsO ₄ ²⁻				OsO ₄ ⁰ OsO ₄ (OH) ⁻
Ir				IrO ₂		IrO ₄ ²⁻		
Pt		Pt(OH) ₂ PtCl ₄ ⁻		Pt(OH) ₄ PtCl ₆ ²⁻				
Au	Au(S ₂ O ₃) ₂ ³⁻		Au(OH) ₃ Au(OH) ₃ Cl ⁻ AuCl ₄ ⁻					
Ag	Ag ⁺ Ag(S ₂ O ₃) ₂ ³⁻ AgSO ₄ ⁻ AgCl _x ^{1-x}							
Hg	Hg ₂ ²⁺ Hg ₂ SO ₄ ⁰ HgCH ₃ SO ₃ ⁻ HgCH ₃ S ⁻ HgCH ₃ S ₂ O ₃ ⁻ HgCH ₃ Cl	Hg ²⁺ HgSO ₄ ⁰ Hg(S ₂ O ₃) ₂ ²⁻ Hg(OH) ₂ HgCl ₂						
Cu	Cu ⁺ CuCl _x ^{1-x}	Cu ²⁺ CuSO ₄ ⁰						

when a solution comes into contact with air. Manganese behaves somewhat similarly. However, elements such as Mo, V, Cr and W that readily oxidize to +5 and +6 oxidation states all show an increased solubility with higher Eh due to the formation of oxy-anions. For U, the change in oxidation state is more complex, with oxy-cations such as U₂O₄²⁺ forming mobile species (Langmuir, 1978).

Copper, Ag and Hg can have the oxidation state of either a metal or a cation and are included with the metals group in Table I.5-5 or the cation group in Table I.5-2. All of the metals in the latter group are greatly assisted in their mobility by highly oxidative environments associated with solutions of high ionic strength in which soluble complexes with anions can form. However, in the presence of sulphides, a lower oxidation potential could help mobility by the incomplete oxidation of the sulphide allowing metastable thiosulphate and other metastable oxysulphur anions to be present and form soluble complexes. This is particularly relevant to Au, Ag and Hg mobility (see Webster and Mann, 1984 and

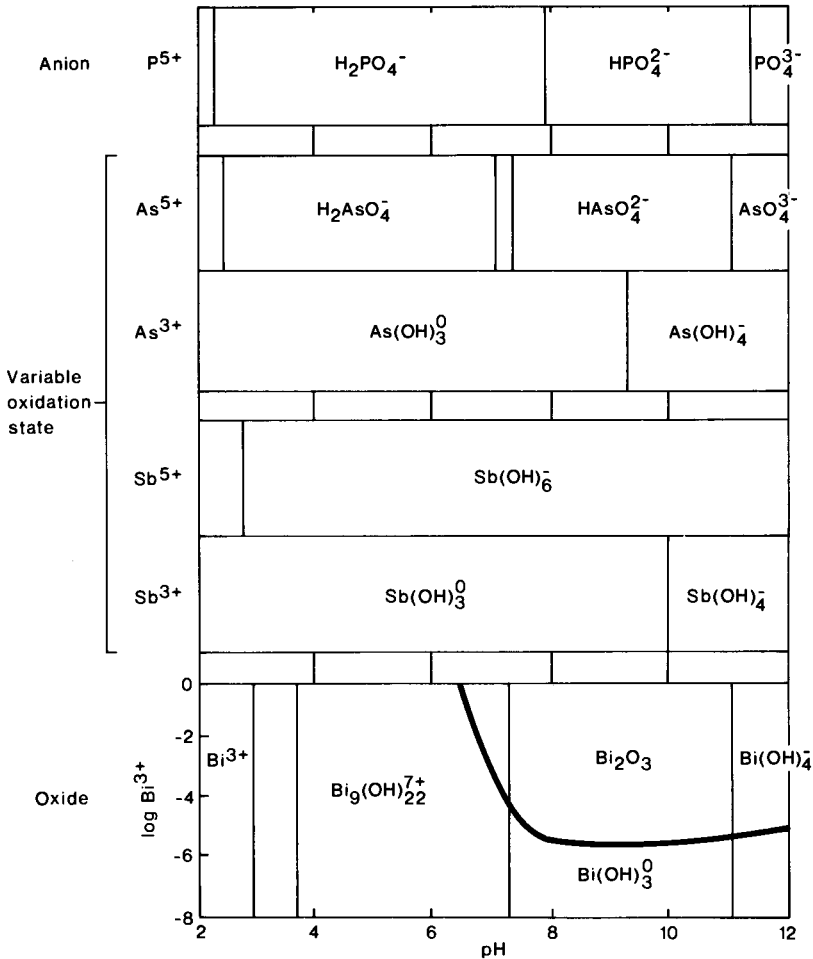


Fig. I.5-4. Variations in oxidation state of the classical group V-A elements.

Webster, 1984). The aqueous geochemistry of gold is discussed in detail in Chapter V-3.

FORMATION OF INORGANIC AND ORGANIC COMPLEXES

The solubility of most cations can be increased by bonding with anions, both organic and inorganic, to give complexes having lower overall charge. The stability constants of many of these complexes have been measured and those more important in the geochemical environment are listed in Tables I.5-2 and I.5-3. The values given are the logarithm of the stability constant of the complex,

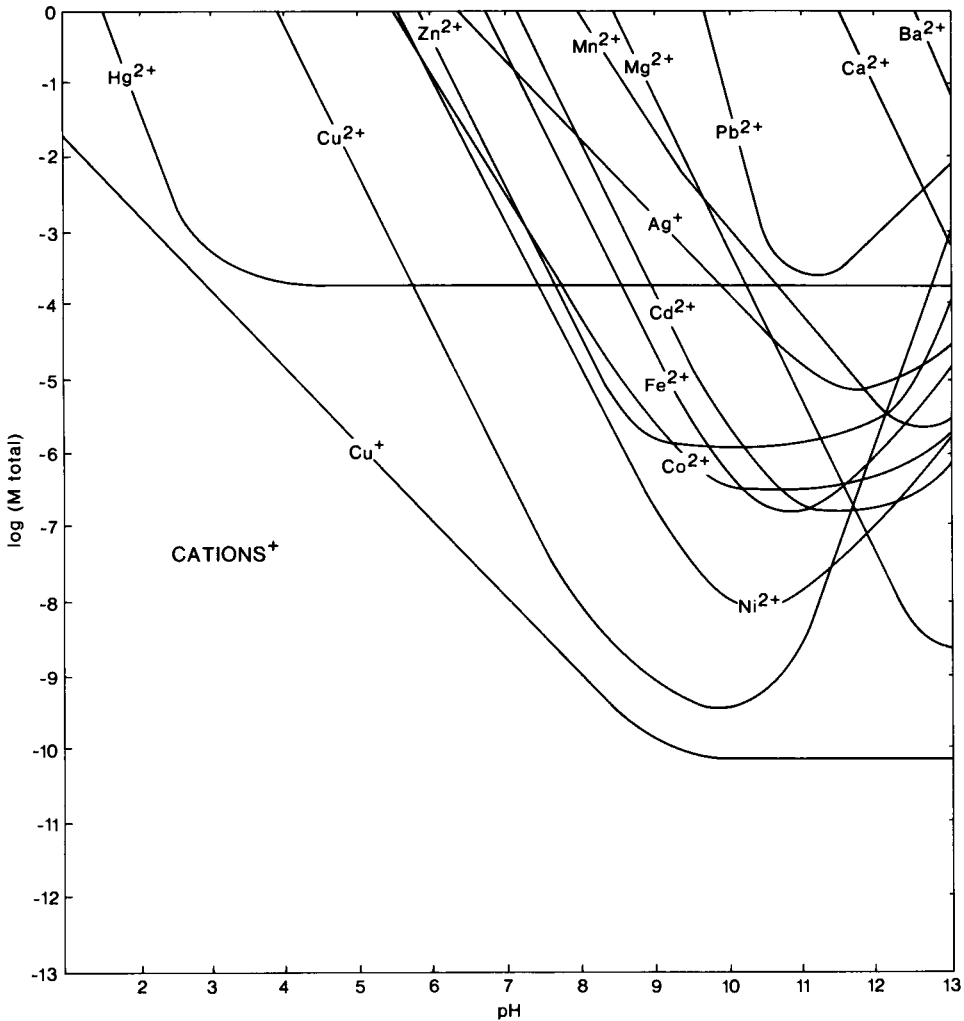


Fig. I.5-5. Solubility of cations by hydrolysis as a function of pH.

such that the larger the value the more stable is the complex. These data must, nevertheless, be used with care. For example, a comparison of the stability constants for sulphates and chlorides shows that sulphate complexes are more stable, which would suggest them to be the more significant. However, because most natural waters have higher activities of chloride than sulphate, chloride complexes are more important for geochemical mobility. The same relative stabilities of different cations are reflected by the solubility products (K_{sol}) of each complex.

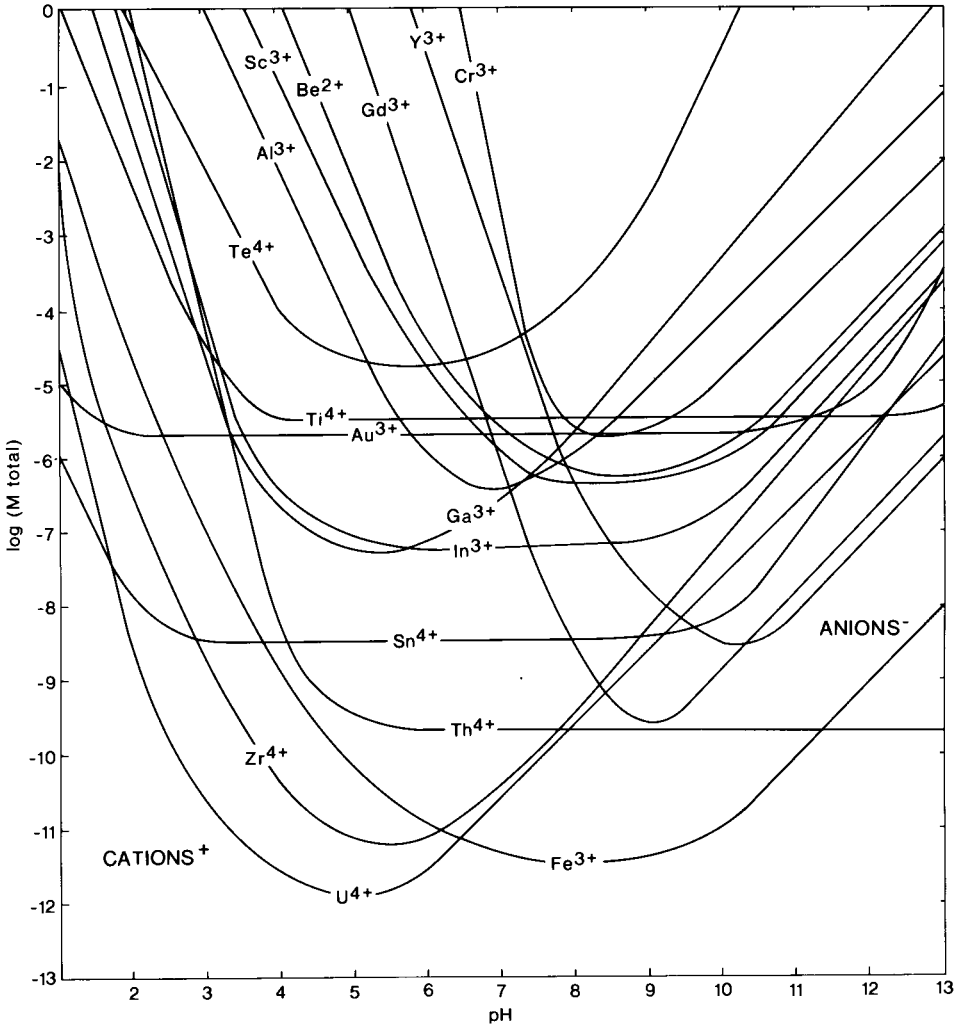


Fig. I.5-6. Solubility of various oxides by hydrolysis as a function of pH.

Organic complexing becomes important in waters in which organic materials are decaying; the stability of such complexes is illustrated by EDTA, oxalate ion ($\text{C}_2\text{O}_4^{2-}$), and humic and fulvic acids in Table I.5-2, and by oxalate and acetate (CH_3COO^-) ions in Table I.5-3. Because the dissociation of these organic anions is affected by pH, complex formation can be pH dependent. Complexation plays an important role in the processes of adsorption, co-precipitation, humic interaction and microorganism activity discussed below.

ADSORPTION

Adsorption refers to the binding of elements at the solution/mineral surface. Like solubility, adsorption is pH dependent, as illustrated by the adsorption isotherms for some cations and anions on to a goethite (FeOOH) surface (Fig. I.5-8). Many oxide surfaces, including goethite, hematite and the Al oxides change from being positively charged at low pH to negatively charged at high pH. With increasing OH^- concentration, such surfaces become increasingly negatively charged and thus more cations become adsorbed from solution. On decreasing the pH, the reverse occurs; surfaces are more positive charged, decreasing the adsorption of cations but increasing the adsorption of anions. The pH at which the change-over occurs, i.e. the point at which there is a net zero charge (pzc) can be used to give a measure of whether the surface is likely to be negatively or positively charged at a particular pH. The pzc for various common minerals are listed in Table I.5-6. In natural systems, however, the surface

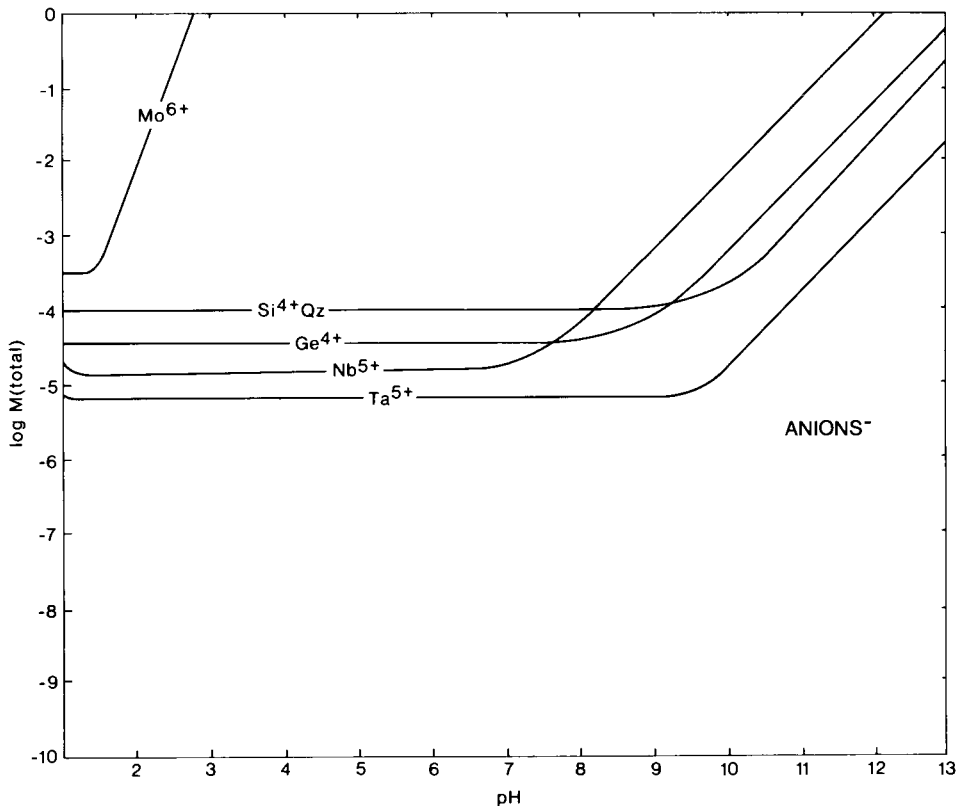


Fig. 1.5-7. Solubility of various anions by hydrolysis as a function of pH.

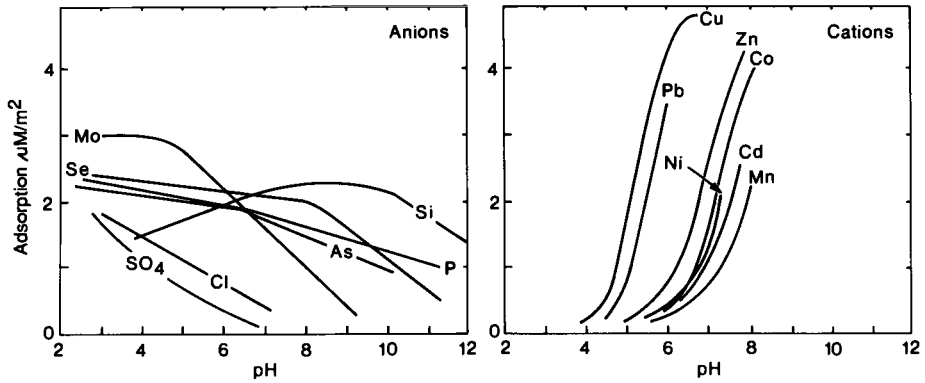


Fig. 1.5-8. Adsorption isotherms of divalent cations and anions (SO_4^{2-} , Cl^- , AsO_4^{3-} , PO_4^{3-} , SeO_3^{2-} , SiO_4^{4-} and MoO_4^{2-}) onto goethite as a function of pH.

TABLE 1.5-6

Some point of zero charge (pzc) pH values for various common minerals and soils

	pzc	Reference
Amorphous SiO_2 /quartz	1.8-3.5	1
Feldspars $(\text{NaK})\text{AlSi}_3\text{O}_8$	2.0-2.4	1
Olivine $(\text{MgFe})\text{SiO}_3$	4.1	1
Kaolinite/illite $\text{Al}_4\text{Si}_4\text{O}_{10}(\text{OH})_8$	3.3-6	1 and 2
Montmorillonite $\text{Na}_2\text{Mg}_2\text{Al}_{10}\text{Si}_{24}\text{O}_{60}(\text{OH})_{24}$	2.5-6	1 and 2
Allophanes	6-7	3
Augite $(\text{CaFeMg}(\text{AlSi})_2\text{O}_6$	4.5	1
Serpentine $(\text{FeMg})_3\text{Si}_2\text{O}_5$	9.6-11.8	1
Apatite $\text{Ca}_5(\text{PO}_4)_3\text{F}$	4-6	1
Calcite CaCO_3	8.0-9.0	1
MgO	12.5	1
CaO	12.9	1
Al_2O_3	6.8-9.5	1
Gibbsite $\text{Al}(\text{OH})_3$	9.5	3
Hematite Fe_2O_3	6.5-8.6	4
Goethite FeOOH	7.6-8.1	3
Ferrihydrite $\text{Fe}_4\text{O}_5(\text{OH})_2$	6.9	3
Andosol (young soil developed on volcanic ash)	4.4	3
Typtic Hydrandept (humic andosol)	4.25	5
Oxisol (latosol or ferrallisol of humid tropics)	4.0	3
Typtic Gibbsiumox (gibbsitic humic latosol)	4.00	5
Tropeptic Eustrtox (latosol in dry savannas)	3.75	5
Ultisol (acrisol; red yellow tropical podzol)	3.6	3
Alfisol (grey podzol of warm seasonal climates)	3.3	3
Spodosol (podzol of humid temperate climates)	4.6	3
Vertic Haplustoll (brown soil of semiarid steppes)	< 3.5	5

References: 1: Parks (1967); 2: Farrah and Pickering (1979); 3: Parfitt (1980); 4 Parks and De Bruyn (1962); 5 Stoop (1980)

properties of individual minerals are subject to interference by other components; for example, humic substances cause the surfaces of goethite to become more negatively charged (Tipping and Cooke, 1982). This problem of predicting adsorption characteristics is therefore complex, but can be partially overcome by measuring the pzc of the soils themselves (Table I.5-6). Excellent reviews of the behaviour of mineral surfaces in soils are given by Bowden et al. (1980), Parfitt (1980) and Furlong et al. (1981).

CO-PRECIPIATION

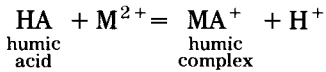
Co-precipitation is the term describing the precipitation of elements from solutions in which they would normally be soluble, as the result of the precipitation of some other, more abundant element. Co-precipitation is influenced by the same factors as solubility and adsorption, being greatest at high cation concentrations and high pH values, whether the cation be co-precipitating with Fe oxides (Thornber and Wildman, 1984) or with carbonates (Thornber and Nickel, 1976) (see Chapter II.1). The extent to which an element is co-precipitated correlates with its solubility and adsorption properties, thereby indicating that similar bonding mechanisms are involved (see Fig. II.1-9). Co-precipitation of anions is similarly influenced, with anions of low solubility and low pH favouring greater co-precipitation. This effect is demonstrated by the co-precipitation of sulphate and chloride with pyroaurite, carbonate compounds and the Fe oxyhydroxides (Thornber and Wildman 1984). At higher pH values, in which CO_3^{2-} is favoured over HCO_3^- in solution, pyroaurite-base metal compounds are formed, with CO_3^{2-} exclusively occupying the anion site; however, as the pH is lowered, other anions present, particularly SO_4^{2-} and Cl^- , occupy these sites.

CHELATION BY HUMIC MATERIALS

The strong interactions between decaying organic matter and inorganic ions may cause either enhanced solubility or complete immobility, depending on the molecular size of the humic material. Organic matter has the greatest exchange capacity (about 150 to 400 milliequivalents per 100 g) of any of the soil fractions, due to the presence of humic materials. The humic acids have adjacent carboxylic acid or phenolic -OH groups that allow the formation of chelation bonds with metal ions. The best known synthetic chelating agent, for which the most quantitative data are available, is ethylene-diamine-tetra-acetic acid (EDTA). The stability constants of the chelate compounds that EDTA forms are listed together with a compilation of stabilities for the cations with humic materials in Table I.5-2. The values are expressed as log (const) for the equation:

$$\log_{10} \text{const} = \frac{[\text{MA}^+]}{[\text{HA}]} \frac{[\text{H}^+]}{[\text{M}^{2+}]}$$

where the reaction is assumed to be



(M = divalent metal; A⁻ = humic anion)

i.e. the greater the constant the greater the stability of the complex. Humic substances are commonly subdivided into three general categories, namely humic acids, fulvic acids and humin. *Humic acids* are those fractions that can be extracted into strongly alkaline solutions but are insoluble in strong acids; *fulvic acids* are soluble in both acids and bases whereas *humic* is soluble in neither. This separation is related to molecular size, with fulvic acid < humic acid < humin, the latter possibly bound firmly to soil grains. Chelation of a cation with humic material may have three effects:

- (1) it may be rendered more soluble by chelation with a fulvate molecule;
- (2) it may chelate with two soluble humates to form a larger molecule which then precipitates; or
- (3) it could be chelated into an immobile humin.

Fulvate molecules may be important in increasing the mobility of many cations by attacking otherwise stable minerals. One very important example of this is the group of chelating agents known as hydroxamate siderophors, which are complex molecules of unknown formula produced by microorganisms within the rhizosphere. These compounds form such strong chelates with Fe^{III} that it becomes mobile even in an oxidizing environment and hence may be responsible for leaching Fe oxide minerals (Cline et al., 1983). Hydroxamate siderophors are released by plant roots and fungi and not only do they favour the mobility of Fe³⁺ even at alkaline pH, they form solutions that can keep other metals such as Al³⁺, Mn²⁺, Zn²⁺, Cu²⁺, Ca²⁺ and Mg²⁺ dissolved under conditions in which they would normally precipitate.

MICROORGANISMS

Microorganisms are ubiquitous throughout the weathering environment, particularly in association with organic matter, whether living or decaying. Their involvement with weathering reactions is generally accepted but poorly understood. They play two major roles:

- (1) they accelerate the rate at which reactions take place, making use of the energy so released. Examples include the *Thiobacillus* bacteria, especially *T. ferro-oxidans*, that accelerate oxidation of sulphur and iron compounds;
- (2) they change the conditions of the system. For example, one organism may change the pH so that another organism can then operate in a preferred environment to complete an oxidation reaction; the two organisms thus act together as a symbiotic system. Alternatively, an organism may produce special-

ized compounds that are capable of causing greatly increased solubility, as described in the previous section.

Microorganisms can also derive energy by breaking down large, immobile humic molecules into smaller, more mobile ones. Hence, metals rendered immobile within precipitated humic material may become mobilized with these smaller molecules.

Research on the humic materials accumulated on the sea floor in the north-western Pacific Ocean has indicated peroxidase enzyme activity in Pleistocene humic materials (Nissenbaum and Serban, 1987). It appears that peroxidase released during cell breakdown can form very stable humic-enzyme complexes; the enzyme is thereby able to maintain a reduced environment and aid the stability of the humic materials.

Although the potential has been recognized, there has been relatively little research into the role of microorganisms in weathering and geochemical dispersion. The scope for interdisciplinary study involving biochemistry, microbiology and geochemistry is considerable.

ENVIRONMENTAL EFFECTS

Physico-chemical environment

The two most important factors controlling the solubility of an element are oxidation potential (Eh) and hydrogen ion activity (pH). The oxidation state has the overriding control of the mobility of an element in solution. However, the Eh relationships determined for pure solutions may be distorted by the ionic strength, pH and concentration of other ions and of humic chelating molecules. For example, in chloride-rich solutions, metallic gold has an appreciable solubility in the +3 oxidation state, due to the formation of the stable AuCl_4^- mobile complex. Mobilization by solubilizing reactions including hydrolysis, inorganic complexing, and complexing with smaller organic anions such as oxalate, and immobilization by adsorption onto surfaces of minerals with variable charge, co-precipitation and ion exchange, are all pH controlled and respond to pH changes in the same way. Under high pH conditions, anions are more mobile and cations less mobile, whereas at lower pH, cations are mobilized and the anions become immobile. When humic materials are present, however, the net effect can be reversed because the strength of the chelated bond with the cation increases with increasing pH, and the complexes become more stable. At higher pH, such chelate complexes behave as anions and thus become more mobile.

Climatic environments

Regional or local climate may have a general influence on weathering mechanisms. Thus, in arid environments in which soils have low humic contents,

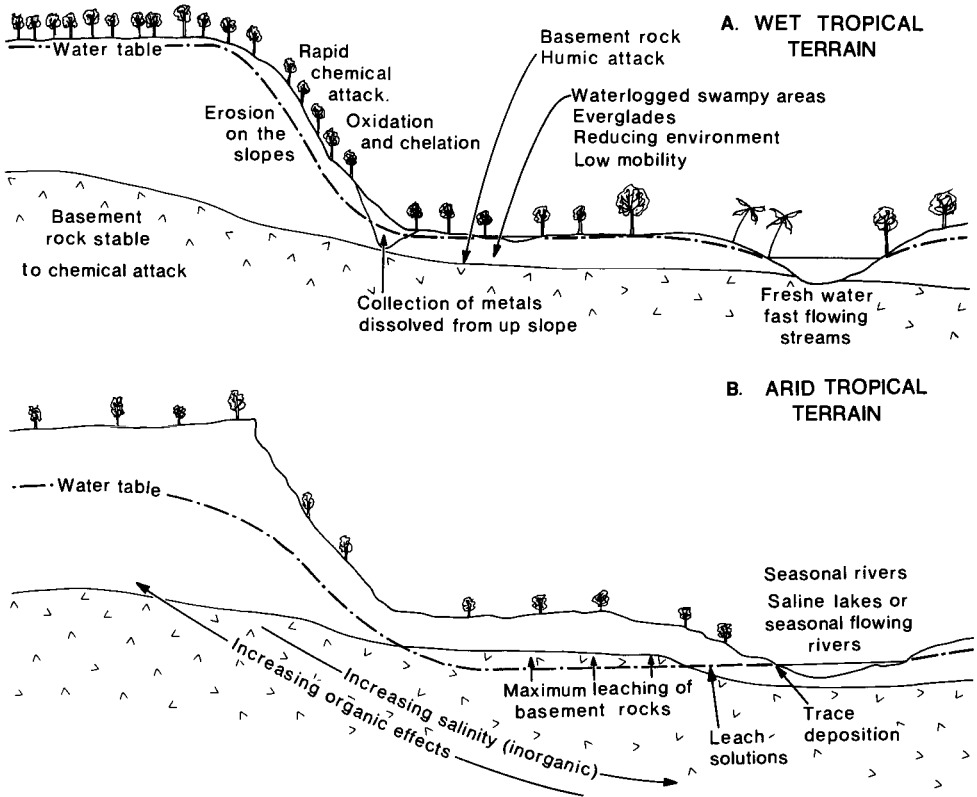


Fig. I.5-9. Schematic representations of the complex conditions that need to be considered for similar topographies in tropical terrains in (A) humid and (B) arid climates.

inorganic reactions tend to dominate. However, in humid environments, especially in the tropics, where plant growth is prolific, the mechanisms that involve humic break down and microorganisms become more dominant. Schematic representations of the many factors that must be considered in order to contrast the mobilities of chemical elements in humid tropical terrains compared to arid terrains are shown in Figs. I.5-9A and I.5-9B. The position of the water-table, the presence or absence of accumulated organic litter, the rate of waterflow, activity of microorganisms, degree of salinity, access of air to the soil, topography and many other factors need to be assessed so that the dominant chemical parameters can be considered. An understanding of these parameters indicates that the factors that influence oxidation state, pH and the formation of soluble and insoluble complexes have the greatest significance in controlling hydromorphic dispersion in the secondary environment.

PHYSICAL WEATHERING AND DISPERSION

C.R.M. BUTT

INTRODUCTION

Physical (or mechanical) processes contribute at every stage and at every scale to the evolution of landscapes, from the initiation of weathering to their destruction by erosion. The same processes are involved in geochemical dispersion and hence are important in determining the nature of the surface expression of mineralization. The principal agents are water and, to a lesser extent, wind and organisms, operating mainly under the influence of gravity and temperature gradients. Gravitational and thermal effects alone, however, have only a minor role. Many of the processes are common to all climatic zones but, nevertheless, climate, as well as relief, lithology and weathering history, determines their relative significance in any region. A few processes are essentially static, related to the disintegration of rocks and minerals—including those comprising the weathered zone—but the majority are associated with the transport of rock debris or secondary products, either within the weathering profile or across the land surface. Their nature and effects are described in this chapter, emphasizing their role in geochemical dispersion.

DISINTEGRATION OF MINERALS AND ROCKS

Physical processes that cause disintegration are important in initiating weathering or reweathering, and reducing fragments to sizes suitable for transport. There are several mechanisms, which may operate independently, together or sequentially.

Unloading

The release of confining pressure by uplift and the erosion of cover rocks has long been considered a cause of sheeting and exfoliation (Gilbert, 1904). Unloading, particularly of laterally confined rocks, leads to expansion, the development of radial stress, production of joints parallel to the surface and, ultimately, arching of the surface layer. Water entering these joints accentuates the fractures by further physical and chemical activity. The sheeting and exfoliation that results is most common on massive, poorly jointed rocks such as granite and

sandstone, and may contribute to the formation of inselbergs. Unloading may also lead to the initiation of chemical weathering because dilation of the rock allows water to penetrate fractures, grain boundaries and cleavages in minerals. The role of unloading has been questioned by Cailleux (in Birot, 1968) since, following erosion, the expansion due to pressure release must be compensated by simultaneous contraction due to cooling. However, the stresses due to previous cooling from igneous and high grade metamorphic temperatures must be considerable and unloading fractures may exploit weaknesses inherited from such stressing.

Insolation

Repeated thermal expansion and contraction due to diurnal heating by the sun and cooling at night are causes of rock fragmentation, especially in hot arid areas. In particular, rapid change, such as cooling by rain, may result in high tensile stress and, ultimately, the cracking of rocks. Similar effects are produced by fire. Differential expansion of minerals in a rock, due to a combination of differences in specific heats, coefficients of expansion and heat absorption may lead to local stress and disaggregation.

Swelling

Reversible absorption of water can give similar stresses to those of thermal expansion. Since rock porosity may increase with heating and cooling, the combined effects accelerate surface flaking. The presence of swelling clays (e.g. smectites) in soils and exposed saprolites similarly causes disaggregation and increases susceptibility to erosion.

Crystal growth

Frost shattering and salt weathering fragment and disaggregate fresh and weathered rocks, usually by exploiting existing fractures. The volume increase that occurs as water freezes is a very powerful physical process, but is of little importance in tropically weathered regions. It is, however, of significance in winter-cold deserts and at high altitudes, where frost-shattered rocks may be widespread as surface rubble and in talus. In arid areas, salt weathering has a similar disruptive effect due to the volume expansion of chemical precipitates (especially halite and gypsum) by crystal growth, thermal expansion and, for minerals such as anhydrite-gypsum, reversible hydration. When confined, these processes each may exert pressures equivalent to the tensile strength of rocks, in the range 2–20 MPa (Cooke and Warren, 1973; Ollier, 1984), hence expansion of salts precipitated in fine cracks can prise rocks apart. In porous rocks, saprolites and soils, capillary migration and evaporation of solutions result in precipitation at or below the surface. Volume increases, especially crystal growth,

give rise to exfoliation and granular disaggregation—particularly evident on the faces of cliffs and erosion scarps. The precipitation of carbonates as calcretes tends to cause cementation as well as disaggregation. In some lateritic profiles (e.g. in Mauritania (Nahon et al., 1977) and southern Western Australia) the precipitation and growth of pedogenic calcretes leads to the replacement, disruption and erosion of pisolitic ironstones in an environment in which they are usually highly resistant. In places, however, such pedogenic calcrete may itself become a resistant duricrust. Similarly, where carbonates precipitate as massive groundwater calcretes, upward growth leads to the displacement and erosion of overlying sediments, so that the calcretes form mounds in valley axes (Mann and Horwitz, 1979). Because of this uplift and exposure, where such calcretes are uraniferous (see Chapter III.3), they are detectable by ground and airborne radiometric surveys, and this has been the principal exploration technique for such uranium deposits (e.g. Yeelirrie, Western Australia (Cameron, 1984)).

PHYSICAL TRANSLOCATION WITHIN WEATHERING PROFILES

Most compositional variations within residual profiles, expressed as soil horizons and weathering zones, are chemical in origin, but a number of physical processes are also involved. Recognition of the effects of these processes can be of significance in the selection of sample media and the interpretation of geochemical data.

Physical eluviation

The downward percolation of water through the regolith causes, in addition to chemical leaching, the movement of fine particles in suspension—i.e. physical eluviation. Colloids, clays, iron oxides and organic matter are the most affected. Since these are commonly hosts to metals dispersed from mineralization, the *illuvial* horizons in which they accumulate are usually better for sampling than the *eluvial* horizon from which they are derived. Illuvial horizons include both chemically and physically translocated materials and the predominant mechanism may be difficult to identify. Examples of physical eluviation, however, include the accumulation of organic matter in podzolic B horizons, and the formation of clay skins (argillans) on void walls. In arid regions, fine aeolian dust may accumulate in the illuvial horizon, where it become protected from deflation (Barbier, 1987). Because the coarse fraction commonly gives a better response, sampling of the eluvial horizon may be preferred (e.g. lag sampling, see p. 346). If the illuvial horizon is selected, the effectiveness of sieving is reduced by dilution caused by aggregated dust and precipitated salts.

Although most physical eluviation is vertical, lateral movement within the profile may occur on slopes. Such movement increases as the illuvial horizon becomes choked with clay, perhaps forming a perched water-table, and encour-

aging lateral drainage and the selective erosion of fine particles by groundwater. Eluviation may be strongest along the stone line. This process is particularly evident in shallow, sandy soils in the seasonal tropics and, where it occurs, soils high in the landscape tend to become clay-poor and those on lower slopes, clay-rich (Ruxton, 1958; Thomas, 1974; Duchaufour, 1982). Physical illuviation may also be partially responsible for the formation of "soil karst" by the removal of clays from the mottled zone and the subsequent collapse of the lateritic duricrust (see below). Near erosion scarps, such collapse, accompanied by slumping and flow of unconsolidated material, contributes to the destruction of the duricrust and the profile as a whole (Thomas, 1974).

Even supposedly immobile phases are subject to eluvial movement if present as fine particles. The effects are rarely of direct significance in exploration, although in saprolites at Dorlin, French Guiana, high contents of B, a pathfinder element for Au, may be due to illuvial concentration of tourmaline (Taylor et al., 1989; see p. 272). Zircons up to 3 μm are physically mobile in silcrete formation (Butt, 1985), hence their use in weathering mass balance calculations may be misleading. Calculations based on the high Zr contents (200–400 ppm) in the ferruginous B horizon of the Liberdade Ni laterite, Brazil, suggest that the present 11 m thick profile has been derived from weathering 200 m of serpentinite (Esson, 1983). Similar concentrations of Zr, however, are found in both pisolitic and partly saprolitic ironstones over the Mount Keith serpentinitized dunite, Western Australia (Butt and Nickel, 1981; see p. 324), where the profile is overlain by 35 m of transported overburden. The Zr/Ti ratios (Fig. I.6-1) plot in the fields characteristic of fresh and weathered basaltic and intermediate rocks (Hallberg, 1984), and geological and mineralogical data suggest the overburden to be of mixed intermediate, basic and ultrabasic origin. It is concluded that the Zr and Ti in the ironstones were derived by illuviation as zircon and anatase from the overburden, rather than being residually concentrated during weathering. A similar sedimentary origin is at least as plausible as residual concentration in profiles such as that at Liberdade, hence the calculation of wasting due to chemical weathering may be questioned.

Profile homogenization

Smectite-rich soils in savannas and semiarid areas with a strongly seasonal climate have self-churning properties that result in profile homogenization. Such soils, *vertisols*, are very widespread, occupying over 230 million hectares between 30°N and 30°S, mainly in the Indian Deccan, Sudan, Ethiopia, Chad and eastern Australia (Young, 1976). Vertisols are commonly, but not always, dark in colour, due mainly to dispersed organic matter, a property reflected in local names such as black earths, black cracking clays and Regur (India). Parent materials are usually basic rocks, shales and limestones, transported materials derived from these rocks and from smectite-rich alluvium and lacustrine sedi-

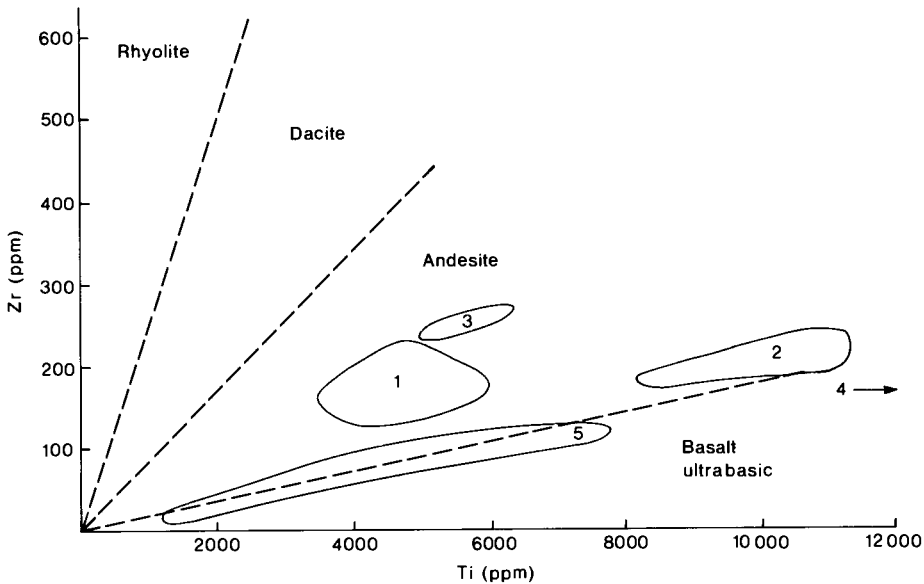


Fig. I.6-1. Zirconium and titanium in transported and residual overburden at Mount Keith, Western Australia, plotted on the rock discrimination diagram of Hallberg (1984). Saprolitic and fresh dunite contains < 5 ppm Zr and < 100 ppm Ti. Residual ironstones have been enriched in these elements by illuviation from the transported overburden. 1: Colluvium, 0–4.5 m. 2: Colluvium with pisoliths and clay, 4.5–14.6 m. 3: Mottled and bleached clay, 14.6–25.3 m. 4: Transported ironstones of ultramafic origin, 25.3–33.0 m. 5: Transported and residual ironstones, ultrabasic origin, 33.0–44.0 m.

ments. The soils develop on gentle slopes (usually $< 3^\circ$), where impeded drainage and a near-neutral pH restrict leaching and favour smectite formation.

During the dry season, contraction of the clays causes the soil to shrink by 25–50%, so that hollows and desiccation cracks are formed, to depths of 1 m or more. Material from the walls or the surface falls in, so that when the soil becomes wet and expands, pressures develop and can only be relieved by upward movement (Fig. I.6-2). Slickensides on crack walls and the formation of wedge structures are evidence for such movement. Annual repetition of this cycle results in the mixing and churning of the soil down to the depth of cracking, with no horizon development. Where such soils are essentially residual, they may be expected to give good geochemical responses. Although vertisols are usually fine grained, the churning process causes larger fragments to be brought to the surface; the presence of occasional “floaters” of fresh or recognizable weathered rock is of great benefit in mapping such areas. Fragments larger than the cracks tend to be concentrated upwards and, particularly in more arid climates, they may form a complete layer at the surface. Broadly similar mechanisms may operate in any soil in arid regions and may contribute to the surface concentration of gravel “lags” suitable for geochemical sampling (see p. 346).

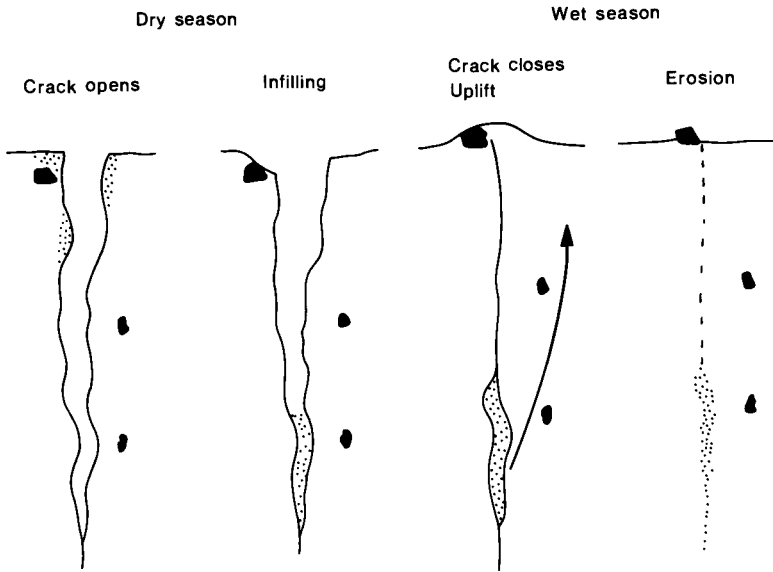


Fig. I.6-2. Profile homogenization by churning in vertisols, caused by seasonal contraction and expansion of smectites. Modified after Duchaufour (1982).

Consolidation

The dissolution of primary or secondary minerals without pseudomorphic replacement leads to downward settling and consolidation of the profile. The consolidation causes the destruction of original rock fabrics and their replacement by some apparently sedimentary features, more or less conformable with the present surface, giving the impression that upper horizons are transported. Grain-supported sandstones, for example, may develop from granite saprolite by settling following kaolinite solution, but the residual nature is indicated by persistent quartz veins (Butt, 1985). The settling may also alter the apparent dip of quartz veins and other resistant units (Fig. I.6-3); where these are mineralized, the effect is to broaden the anomaly. These features are most easily seen in partly stripped and reweathered terrain, or where lateritic ironstones have not developed. The formation of some stone lines is an extension of this process.

Soil karst

Closed depressions have been described from lateritic terrains in Africa, South America and Australia (Thomas, 1974; Budel, 1982; Busche and Erbe, 1987; McFarlane and Twidale, 1987). Such features were originally described as occurring close to erosion escarpments; they were considered to be largely due to the lateral physical eluviation of clays from the mottled zone, the formation of

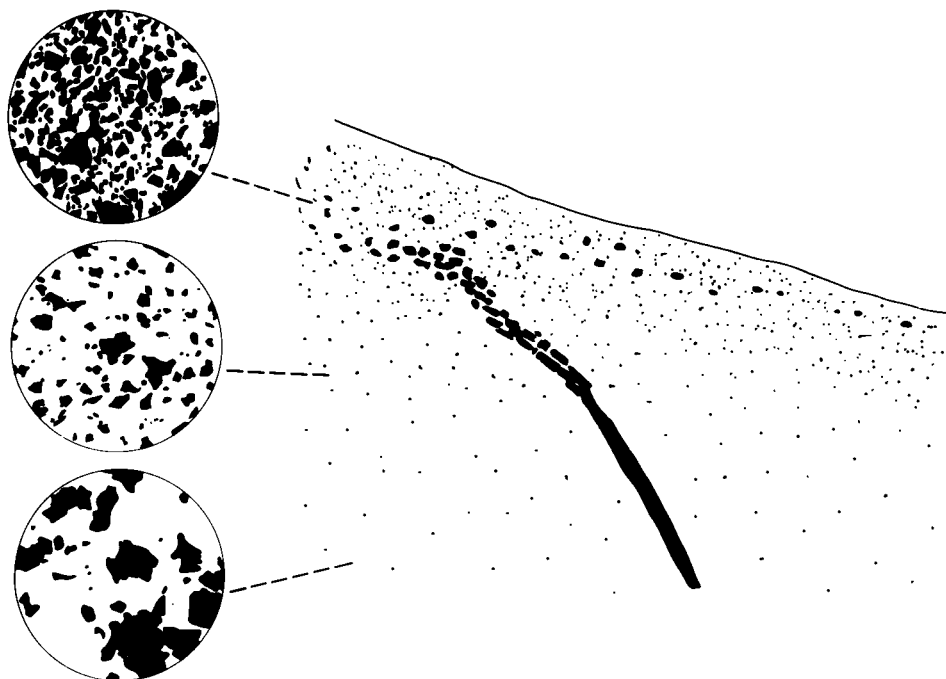


Fig. I.6-3. Flattening of dip and disintegration of quartz vein by profile consolidation and dispersion by soil creep. Solution and eluviation of clays causes settling of quartz grains and destroys granitic fabric of saprolite. Micrograph field width 12 mm. Derived from Butt (1985).

cavities and the eventual collapse of the lateritic duricrust. Similar features, however, have been recognized as being widespread in lateritic plains and it is probable that solution processes contribute to the development of the cavities. In rainforests, surface wash is directed towards these depressions, which drain via underground “subrosion” channels (Budel, 1982).

Stone lines

Many deep weathering profiles have stone lines at depths of 0.5 to 2 m or more which, in rainforests and humid savannas, more or less follow the present topography. The stones themselves may be quartz, lithorelicts and degraded lateritic ironstone (cuirasse). In some localities, the stone line and overlying horizon contain dateable artefacts in an age sequence, with the oldest at the base (e.g. Stoops, 1967; Lecomte, 1983, 1988). Numerous theories for the origin of stone lines have been suggested, including aeolian accession of the upper horizon, erosion and deposition by hill wash, and reworking by termites (Ruhe, 1959; Webster, 1965; Thomas, 1974). However, some of these are not in accord with the known climatic histories of the present humid tropics, nor with the

conformity of the profiles with the present landforms. Although some stone lines are clearly sedimentary, with cross-bedding, scour structures or exotic pebbles, the majority appear residual, with stones related to the underlying lithologies. Lecomte (1983, 1988) has suggested that in rainforests such stone lines formed as follows:

(1) chemical reweathering by aggressive leaching of pre-existing lateritic profiles destroys the cuirasse and saprolite to produce the unconsolidated clay-sand surface horizon;

(2) gravitational settling of coarse fragments, predominantly quartz but including cuirasse close to the old surface, with accumulation as a stone line near the base of the chemically reweathered, unconsolidated horizon.

Stone-line profiles in the present savannas (e.g. in eastern Africa) may have formed similarly, either under the current climate or during more humid periods in the Pleistocene. Here, the accumulation and homogenization of the fine grained near-surface horizon has been attributed to the activities of termites in the past 50,000 years (Webster, 1965; Watson, 1970) and they may indeed have an role in promoting gravitational settling.

This origin has considerable exploration significance, for it implies that stone-line profiles are essentially residual and that near-surface sampling procedures can be used effectively. The residual nature of such stone lines, which was first recognized in the Zambian Copperbelt (Tooms and Webb, 1961) and Zimbabwe (Webster, 1965), is the basis for the relevant dispersion model described in Chapter III.2 (p. 275).

Biogenic processes

Surface materials, including soils and pisoliths, are commonly observed at many metres depth in otherwise residual profiles as illuvial infillings of root channels, illustrating the role of plants, albeit passive, in physical translocation. Infillings of root channels and other fissures are observed to occupy about 5% of the volume in saprolite at 15 m in some profiles near Kalgoorlie, Western Australia. Termite burrows deep in saprolite may also be infilled, e.g. in the Zambian Copperbelt (Cloud et al., 1980) and at 20 m or more at Coober Pedy, South Australia (R.S. Robertson, written communication, 1985), perhaps partly by the termites themselves.

Bioturbation by soil mesofauna (e.g. worms, insects and other small animals) plays a significant, *active* role in the aeration of soils and the mixing of soil components in near-surface horizons. Of these, the role of termites has received the most attention from exploration geochemists. In the drier savannas and semiarid regions of Africa, India and Australia, termite mounds 0.5 to 3.0 m or more high are features of the landscape. Termites burrow to great depths in search of water—for example, they have been observed at 70 m at Jwaneng, Botswana (Lock, 1985) and at 45–55 m in the Sahel (see Cloud et al., 1980). Termites use soil materials to build their mounds and in so doing transport

minerals from deep horizons to the surface. Williams (1968) calculated that erosion of termite mounds in northern Australia contributes 30 mm to the topsoil every 1000 years, a rate comparable with that of the mean rate of chemical weathering (see Table I.3-2). Webster (1965) attributed the development of essentially residual horizons 2 m thick above stone lines to be due to the transport of fine particles by termites (see above and p. 224 and p. 275). Similarly, they may contribute to the development of soils above lateritic cuirasse. Termite activity can thus be considered to be a significant factor in soil formation.

The location and composition of termitaria have been used for over 2400 years in exploration for groundwater and minerals, especially gold (see Gleeson and Poulin (1989), for a recent review). Termite activity has also been credited with transporting metal-enriched clays (d'Orey, 1975) and diamond indicator minerals (Lock, 1985; see Chapter V.1) to give surface expression to otherwise concealed targets. As a result of erosion, however, enrichments related to mineralization are generally passed to the soil as a whole, rather than being restricted to the mounds. In most instances (e.g. Fig. I.6-4), there is no significant difference between metal contents of mounds and the appropriate horizon of the surface soils (Tooms and Webb, 1961; Prasad et al., 1987; Gleeson and Poulin, 1989). Enrichments of Cr (1740 ppm) and V (110 ppm) in termitaria compared to surface ("A1" horizon) soils (640 ppm Cr and 70 ppm V) were reported at Khondapalli, southern India, by Prasad and Vijaysaradhi (1986), but it is uncertain whether this is due to preferential concentration or is an artefact of sampling an inappropriate horizon. In general, termitaria offer no advantages other than as a readily accessible, apparently homogeneous, friable sample medium—but with the disadvantage of erratic distribution.

Even in areas of transported overburden, broadly similar dispersion patterns are commonly shown by soil and termitaria sampling. For example, Watson (1970, 1972) demonstrated that in Zimbabwe (then Rhodesia), Au and Zn anomalies were similar in termitaria and soils in areas where transported Kalahari Sands were 3 m and 8 m thick. The similarity was attributed to erosion of the mounds and homogenization of the Sand and soils within the past 50,000 years. For Zn, concentrations were higher in subsoils (65 ppm, 60–274 cm) than in the mounds (55 ppm) and topsoils (52 ppm, 0–60 cm), due to hydromorphic effects. However, where surface transport is recent or still active so that there is little or no cumulative enrichment of the soil, termitaria may be a better surface sampling medium. Gleeson and Poulin (1989) found that mound sampling in the Koma Bangou gold field, Niger, gave rather higher values and more continuous anomalies than soils in areas where there is a cover of 3–7 m of aeolian and alluvial sands. Similarly, in Mozambique, d'Orey (1975) reported that on steep slopes with up to 15 m of scree and colluvium, termite mounds above mineralization had anomalous Cu (435–610 ppm) and Ni (1380–2620) contents, whereas soils contained only background values (e.g. < 100 ppm Cu). There was also good discrimination between different lithological units (Table I.6-1).

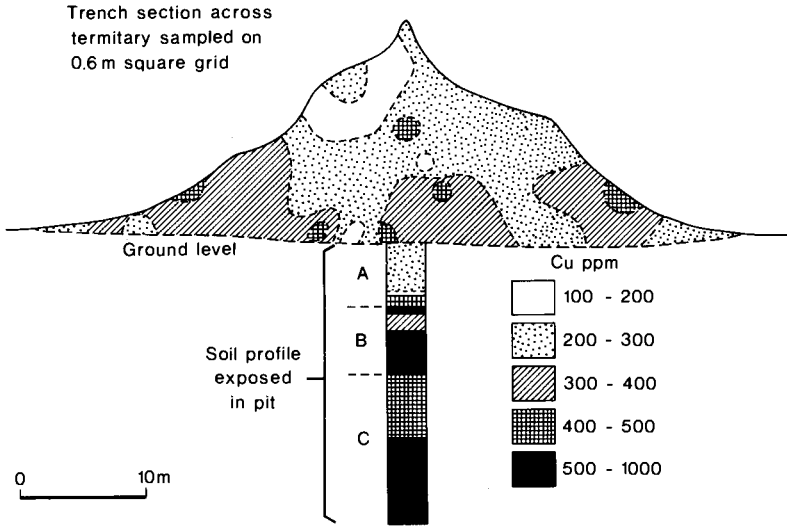


Fig. I.6-4. Distribution of copper in a termite mound and underlying soil, Baluba, Zambia. Modified after Tooms and Webb (1961).

PHYSICAL TRANSPORT ON SLOPES

The physical transport of materials across slopes by water is the principal mode of erosion of landscapes in low latitudes, although rivalled by wind erosion in very arid climates. In regions of low relief especially, fluvial erosion, whether lateral, vertical or headward, is of little significance. Drainage in arid zones is mostly subsurface and in the humid tropics, rivers are relatively passive, carrying weathering and erosion products in solution or as a suspended load. They have no coarse bedload capable of erosion, hence the common occurrence of rock bars in tropical rivers. The nature and intensity of slope erosion depends upon the relief, rainfall and vegetation. On gentle slopes, erosion affects particles

TABLE I.6-1

Copper and nickel contents of termite mounds over various rock types, Edmondian mine region, Mozambique (d'Orey, 1975)

Bedrock	Number of samples	Range Cu ppm	Range Ni ppm
Mineralization	7	435-610	1380-2620
Suspected mineralization	5	315-495	955-2750
Barren serpentinite	8	90-150	540-995
Basic rocks	9	44-100	120-675
Granites and sediments	6	10-39	50-205

individually, whereas on steeper slopes, mass movement also occurs. The erosional capacity of water increases with slope and amount of rainfall; the combined effect, however, is lessened by a concomitant increase in vegetation, which stabilizes the surface and encourages infiltration rather than runoff. In humid regions, slopes $> 65^\circ$ may be thickly forested. Seasonal rainfall distribution is also important; in savannas and arid zones, erosion is greatest at the beginning of the wet season, when runoff is not impeded by vegetation.

Rainsplash

The impact of falling raindrops is an important aspect of surface erosion. Rainsplash during intense storms erodes directly by dislodgement and indirectly by breaking down surface layers (Mabbutt, 1977). Single impacts may carry soil particles equal to the mass of the raindrop for up to one metre (Ghadiri and Payne, 1988) or move 4 mm pebbles by 20 cm. Rainsplash has most effect on bare or poorly vegetated sloping surfaces, hence it is of most significance in arid regions and at the beginning of the wet season in savannas. Even in rainforests, however, temporary breaks in the canopy expose soils unprotected by an understorey or humus and erosion ensues (Thomas, 1974). A converse effect of rainfall is to compact the surface layer, which slows infiltration and increases runoff; in arid areas, a thin (3 mm) clay-rich carapace forms and protects the soil from erosion by wash and wind (Cooke and Warren, 1973).

Sheetwash

When precipitation exceeds infiltration, excess water runs off as a fairly continuous film, or sheet, washing across the surface. Sheetwash is a dominant process of erosion on surfaces of low relief in all but thickly vegetated regions. The process is able to mobilize clays, silt and fine sand even in rainforests, but in arid areas, during rare heavy rainstorms, gravel and small pebbles may be moved across slopes of less than 1° . Fine particles are carried in suspension and coarser fractions as a traction load. In arid and seasonally dry climates, runoff is immediate where soils are water repellent (hydrophobic), but erosion will be significant only when the surface layers become wetted. Infiltration of rainwater is rapid once wetting occurs and until desiccation cracks are closed by clay expansion or infilling from above. When the uppermost horizons are saturated and soft, runoff increases and becomes erosive. Water-flow is discontinuous, changing with surface irregularities and rainfall intensity. Networks of braided rills and wash channels can develop and, depending upon the local topography, may converge into larger washes or diverge across flatter depositional areas. Such networks are only temporary and, from season to season, the whole surface is affected.

Sheetwash is an important geochemical dispersion mechanism but, since the fine particles tend to be preferentially transported, anomalies are best shown by

immobilized elements in coarse fractions, retained either in resistant primary minerals or in secondary minerals in structures such as pisoliths. However, element concentrations, already low due to leaching, may be greatly diluted, so that the detectable dispersion halo is restricted in size. Thus, in Botswana, Coope (1958) found Cu dispersion by sheetwash was only 15–20 m on a 1–3° slope. In considering the downslope asymmetry of anomalies on similarly very gentle slopes in the Zambian Copperbelt, Tooms and Webb (1961) concluded that although mechanical dispersion by sheetwash was a factor, hydromorphic dispersion, perhaps including a biogenic component, was the principal mechanism. These studies, however, only encompassed mobile elements (Cu, Co, Ni). When resistant phases are included, the contribution of mechanical processes is evident. Thus, at the Scuddles prospect in semiarid Western Australia, Smith and Perdrix (1983) found that dispersion haloes of chemically immobile elements such as Bi and Sn in pisoliths extended for up to 1.5 km across a 1–2° slope (Fig. I.6-5). In the more humid Greenbushes area, Sn anomalies defined by the 3 ppm contour, extend for over 10 km downslope. These haloes are the cumulative result of wash and possibly profile consolidation over very long periods, before, during and after pisolith formation. The transport may thus have been of free resistant minerals and gossan fragments, and subsequently of pisoliths containing them (see p. 309 et seq.).

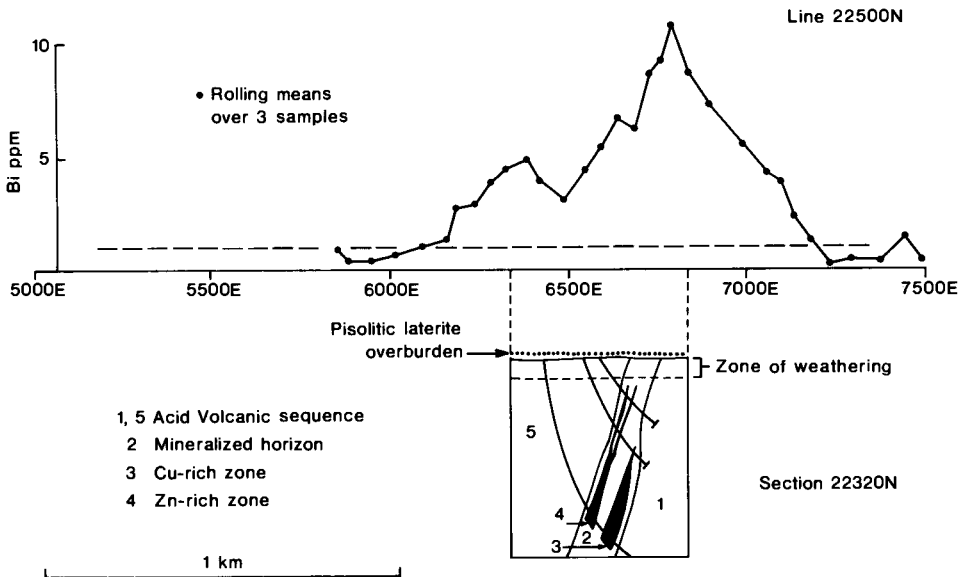


Fig. I.6-5. Dispersion of bismuth by sheetwash across a 1–2° slope shown by pisolith sampling, Scuddles, Western Australia. Redrawn from Smith and Perdrix (1983).

Nevertheless, use of the coarse fraction may not always be appropriate, even for immobilized elements. This is the case where the resistant minerals may themselves be fine grained and potential host structures such as pisoliths have not developed. For example, in the very arid pediplain of Saudi Arabia, Salpeteur and Sabir (1989) noted that heavy minerals may be enriched in the fine (minus 160 μm) fraction of the reg, concentrated by the combined effects of sheetwash and wind removing clays and low density silt particles. Use of the coarse fractions may selectively discard those elements held in heavy minerals. Conflicting recommendations as to the most appropriate fraction for these regions have been made (cf. Salpeteur, 1985 and Salpeteur and Sabir, 1989) and selection depends upon the relative importance of such enrichment and the dilution by aeolian material deposited by dust storms (see p. 369).

Soil creep (solifluction)

With increasing slope, mass movement of saturated soil occurs in the form of soil creep. This is particularly important in smectite-rich soils in which the through-flow of water is restricted. The movement may extend to several metres depth, even under forest, and is a significant mechanism of downslope dispersion (Fig. I.6-3). The displacement of quartz veins by soil creep to produce stone lines has led to the widespread but erroneous assumption that all stone lines are produced by lateral transport.

The combination of soil creep and sheetwash on moderate slopes is most important in geochemical dispersion, considerably extending anomalies to colluvial sheets at the base of slopes and into stream sediments. At Dorlin (French Guiana, see p. 272), soil creep has extended the Au and B anomaly for about 200 m downslope. Dispersion can be quite rapid, even in rainforests; in Papua New Guinea, for example, sulphides survive unweathered in soils and stream sediments (Jones, 1973). On very steep gradients, however, barren material from upslope may dilute or cover traces of mineralization. This situation was reported by d'Orey (1975), who found that soils over mineralization had background metal contents and that the only anomalies (hydromorphic and mechanical) were in colluvium at the base of the slope. The termite mounds provided a means of sampling through the barren cover (see p. 106).

Slumping and landslides

Mass movement by slumping and landslide is a significant erosional force in humid terrains on slopes of 30–60°. Clay-rich regoliths over 60 cm thick with a sharp contact to fresh rock are particularly prone to slipping. Above 60°, little regolith can form or remain. Movements generally occur after heavy rainfall in which the regolith becomes saturated and pore water pressure rises to a point when failure occurs (Thomas, 1974). Landslides are commonly triggered by exceptional rain or by earthquake activity, hence they are largely restricted to

humid, tectonically active areas, though even on drier shields, dissection of smectite-rich regolith can produce slopes prone to slumping. Salpeteur and Sabir (1989) report that gravity flow may occur on moderate to steep slopes in very arid regions of Saudi Arabia as a result of water saturation of clay-rich soil horizons if rainfall is of sufficient duration (more than 1 hour).

Landslides occur principally in regions where relatively direct geochemical responses in stream sediments, colluvium or soils may be expected. Thus, their main effects are negative, disrupting and displacing anomalies in soils and perhaps concealing mineralization beneath barren material from upslope. Mostly, however, landslips are of small dimension and unlikely to obscure mineralization entirely. For example, Leggo (1977) reported that landslips covered part of the Waivaka porphyry Cu deposit, Fiji, but that sampling of residual exposures was possible in pits and creeks.

Talus and boulder slopes

Talus is derived from the disintegration of rocks—e.g. by frost-shattering—and the accumulation of the fragments at the foot of steep slopes as talus cones. It is most abundant in dissected arid terrain, principally at high altitudes and in winter-cold deserts. Although the talus may obscure mineralization, the comminution that occurs by abrasion during the fall and settling of rock fragments produces a fine fraction that is a most effective sampling medium (Maranzana, 1972; Hoffman, 1977; see Chapter IV.1).

Boulders may also cover gentle slopes in arid areas. The boulders are derived from exfoliation, the fragmentation of resistant rocks and duricrusts (sandstone, cuirasse, silcrete) by sapping of underlying soft material (shales, saprolite) or the accumulation of core stones after the removal of alteration rims of sphaeroidally weathered basic rocks. Lateral movement of such boulders is usually minimal.

Wind

Dispersion by wind is most effective in arid regions, where there is little or no vegetation to protect the surface. Transport by wind is analogous to that by water; fine fractions (< 0.15 mm) are carried in suspension, sand (0.15–0.5 mm) is transported by saltation and coarser fractions (to 2 mm) may roll. Although surface compaction by rainfall may give some protection, wind action is capable of removing soil and saprolite to expose the etchplain base (the weathering front) and thereafter corrasion by wind-borne particles may erode unweathered basement rocks. Deflation of playas permits the recycling of soluble salts, carbonates and gypsum in the landscape, cumulatively increasing groundwater salinity and contributing to the development of alkaline soils. Subsequent solution and reprecipitation of these compounds may result in salt weathering, i.e. physical

disintegration caused by crystal growth (see p. 98). Deflation also maintains playa surfaces as erosional base levels. In southwest Australia, deflation causes playas to migrate against the prevailing westerly wind; clay, salts, gypsum and sand removed from the surface of the playa accumulate as dunes on the eastern shores, whereas western shores are commonly formed by erosion scarps where the deeply weathered regolith is undercut by salt weathering and occasional wave action and eroded by sheetwash and gullying (Jutson, 1950).

Wind-borne material forms the familiar aeolian deposits (e.g. sand dunes, loess sheets) of arid and once arid regions. Such deposits may form a complete, commonly alkaline, cover so that there can be no surface geochemical expression of underlying mineralization. In areas with residual soils, windblown material acts as a dilutant, depressing the geochemical response. However, much of this material is in the size range 0.08–0.5 mm, so that sieving to concentrate either the coarse or very fine fraction can reduce the effect of dilution. The movement of coarser particles (> 0.5–1.0 mm) is often not great; heavy mineral suites may correspond to underlying bedrock and sandplains of granitic origin rarely spill far onto basic rocks. Conversely, very fine fractions (< 80 μm), including clays, are very widely dispersed.

The use of the coarse (> 0.5 or 1.0 mm) fraction for chemical or heavy mineral analysis assumes that stable ore-related primary or secondary minerals are either of this size or are retained in coarse resistant grains of, for example, quartz gangue. However, abrasion of otherwise resistant minerals (e.g. mica, wolframite) occurs during aeolian transport, so that any dispersion haloes of these minerals are attenuated by dilution in the fine fraction (Salpeteur, 1985). The most appropriate size fraction, which should ideally be determined by local orientation surveys, may vary according to geomorphological unit. Thus, Barbier (1987) reported that in plains environments in Saudi Arabia, appreciable anomalies were only evident in the plus 1.0 mm fraction due to excessive dilution by fine sand. In hilly areas, dilution by sand is hindered and intermediate fractions (0.03–0.05 mm or 0.03–1.0 mm) are preferred. Barbier concluded that in all areas, the fine fractions (minus 0.03 mm) are quite ineffective as sample media and, indeed, are remarkably uniform in composition over wide areas. He suggested that, in some instances, these fine materials can be related to particular source rocks, indicating transport of 10 km or more, whereas in others they are polygenetic and no source can be specified (Zeegers et al., 1985). These conclusions, however, have been disputed by Salpeteur and Sabir (1989); these authors found that in areas where there has been no contamination from past mining, elements, including gold, hosted by resistant minerals are concentrated in the minus 160 μm and especially the minus 80 μm fractions, because these are least diluted by windblown dust. These are therefore the best fractions for sampling (see p. 369), although disaggregation may be necessary to offset cementation by salts and clays.

ENVIRONMENTAL INFLUENCES ON PHYSICAL DISPERSION

The processes of physical dispersion are influenced by the local environment, principally as determined by climate, vegetation, relief and, to a lesser extent, lithology. The relative importance of the various dispersion mechanisms in different climatic zones, discussed briefly in the previous sections, is summarized in Table I.6-2. Of the static processes, unloading is universal, whereas the remainder are most effective in arid areas. Nevertheless, even in rainforests, the bare rock surfaces of inselbergs provide some of the environmental extremes of humidity and temperature driving these processes. Physical movement of material within profiles occurs mainly in humid environments, where there is an abundant through-flow of water. However, seasonal aridity is necessary for the profile homogenization brought about by shrinking and swelling of smectites in vertisols and related soils.

The effectiveness of different mechanisms of dispersion across surfaces depends upon both climate and relief. Thus, particulate dispersion by sheetwash is greatest in poorly vegetated and hence more arid areas; although it occurs across almost flat surfaces, it is enhanced where slopes increase. Mass movement, however, requires lubrication by excessive water and only takes place on moderate to steep slopes.

Lithology tends not to exert a great influence on erosional processes, although certain rock types, such as quartzites, banded iron formations and some duri-

TABLE I.6-2

The activity of individual dispersion mechanisms in different climatic zones (1: little or none; 2: moderate; 3: strong)

Mechanism	Rainforest	Savanna		Arid zone		Comments
		Wet	Dry	Semiarid	Arid	
Unloading	3	3	3	3	3	
Insolation	1	1	2	2	3	Granite, sandstone
Swelling	1	1	3	3	2	
Crystal growth	1	1	2	3	3	
Eluviation	3	3	2	2	1	Granite, sandstone Basic rocks
Churning	1	1	3	3	1	
Consolidation	3	3	2	2	1	
Stone-line formation	3	3	1	1	1	
Bioturbation	2	2	3	3	1	
Rainsplash	1	1	2	3	3	↓ Increasing relief
Sheetwash	1	1	2	3	3	
Soil creep	3	3	2	1	1	
Landslide	3	3	2	1	1	
Talus	1	1	1	2	3	
Wind	1	1	2	2	3	

crusts are resistant to both chemical and physical weathering. Other examples of lithological control are

- (1) massive rocks (granite, sandstone) are most affected by insolation;
- (2) fractured, cleaved or porous rocks and regolith are most readily disrupted by crystal growth;
- (3) rocks that weather to form free draining, porous soils promote eluviation;
- (4) basic rocks give rise to self-churning soils by weathering to smectites.

Environmental change, over short or long terms, also affects the processes of physical erosion and dispersion. Climatic factors are the most significant; short-term variations in humidity and temperature (diurnal, seasonal or simply a change in the weather) drive many processes, and major, long-term climatic changes fundamentally alter the weathering and dispersion processes (both chemical and physical) operating in a terrain. A general trend from a humid savanna to semiarid climate, for example, results initially in a change of hydrological regime, and the reduction in vegetation cover makes slopes unstable and subject to erosion by sheetwash and gullyng. However, simultaneous formation of duricrusts by irreversible dehydration and hardening slows the rate of erosion, resulting in the development of the partially stripped etchplain landscapes characteristic of lateritic terrains. Environmental change may also be initiated by tectonism and by human activity. The latter may have effects similar to a change to aridity by reducing vegetation and altering the hydrological regime. Irreversible formation of duricrusts, increased erosion by sheetwash, gullyng and landslide, and salinization of groundwater are all consequences of agricultural activity influencing present dispersion mechanisms.

INTRODUCTION

G.F. TAYLOR and M.R. THORNBUR

The presence of colourful secondary minerals attracted early man to conspicuous gossanous outcrops from which he extracted gold, silver and copper. Evidence suggests that secondary copper minerals were processed at Rio Tinto in Spain during the third or fourth millennium BC and jarosites were processed to recover metallic silver as early as 1200 BC (Dutrizac et al., 1983). Throughout the Arabian Shield, there is substantial evidence of gold and copper being extracted from gossans long before the advent of Mohammed in 570 AD. The ferruginous outcrops of Cornwall yielded copper and tin twenty-four centuries ago (Pryce, 1778) and led to the term "gossan" to describe "a kind of imperfect iron ore, commonly of a tender rotten substance, and red or rusty iron in colour". Thus, for many centuries, gossans have been sought for their intrinsic value and some of the great deposits of the world were first exploited by mining of the gossan and particularly of the supergene enrichment zone.

With improvements to metallurgical processes and mine dewatering techniques, the underlying sulphides became more significant and gossans were sought as indicators of underlying mineralization. Techniques were sought to distinguish gossans associated with potentially economic mineralization from other forms of ferruginous outcrop. Considerable work in the USA at the beginning of the 20th century resulted in the description of diagnostic colours, textures and mineralogy by, amongst others, Emmons (1900, 1917), Locke (1926) and Blanchard (1939). However, not all gossans exhibited these diagnostic macroscopic features and moreover their interpretation was by no means unequivocal. The search for new techniques was largely initiated in Australia during the period 1968–1972 when microtextural evaluation was applied to ironstones in the deeply weathered Archaean Yilgarn Block of Western Australia.

The first recorded chemical analysis of gossans is that of Blanchard (1944), which lists major and minor elements in 20 gossans and limonites. As geochemical techniques of exploration became more widely accepted, Zimmerman (1964) analysed gossans from the Mount Isa region of northwest Queensland for 19 elements and concluded that such evaluation was less subjective than other techniques. This work pioneered a considerable effort during the early 1970's to determine the chemical composition of gossans associated with Ni–Cu and Pb–Zn–Ag mineralization throughout Australia and to understand the mechanisms of gossan formation. Geochemical evaluation of gossans is now universally

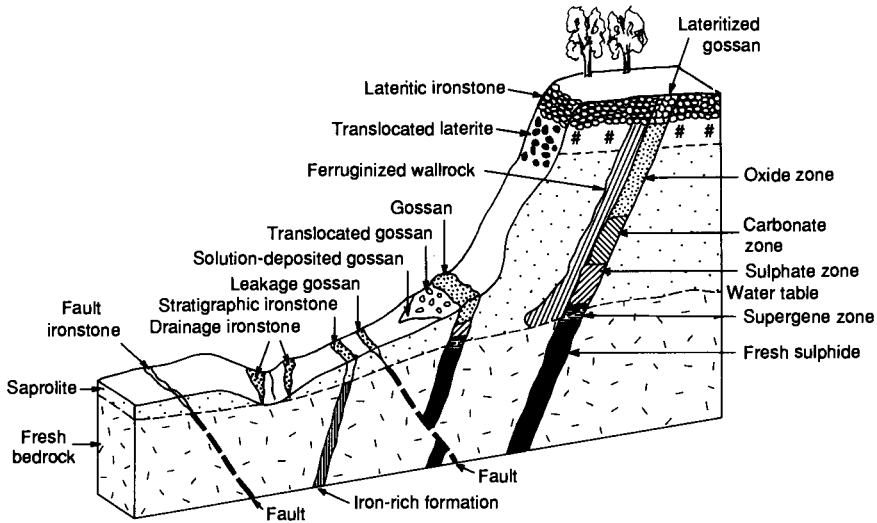


Fig. II.i-1. Types of ironstones and gossans.

accepted as a cost-effective technique in the exploration for outcropping and near-surface mineralization, particularly in deeply weathered terrain.

Despite their long and common utilization by the mineral industry, an extensive literature review and discussion by Kosakevitch (1979) showed there to be no universally accepted classification system for Fe-rich outcrops (French: *chapeaux de fer*). The terminology used herein is based upon that of Taylor et al. (1980) and is illustrated in Figs. II.i-1 and II.i-2. Because it is similar to that proposed by Wilmshurst and Fisher (1983) and used by Nickel and Daniels (1985) and Taylor (1987), it is hoped the terms will become more commonly accepted. In particular, a distinction must be drawn between an *ironstone* and a *gossan*. The occurrence of many types of ironstones and gossans is illustrated in Fig. II.i-1, the terms being defined in the glossary (Appendix 3).

The main thrust of Part II is directed towards the recognition of gossans as distinct from other ironstones, and the evaluation of the significance of the main features of gossans, particularly their chemical compositions. Chapter II.1 deals mainly with the chemical principles that control the mechanisms by which gossans form from the parent sulphides. Thus, it is concerned with the chemical weathering of some economically significant minerals and draws on the discussions of chemical weathering and element mobility given in Chapters I.2 and I.5. It is demonstrated that an understanding of the processes and conditions that can change a particular sulphide assemblage into a gossan is basic to the evaluation of a gossan.

Chapter II.2, which discusses gossan and ironstone evaluation, is based on their origin, with the mineralogy and geochemistry being described in terms of climate, topographic relief, type of mineralization, nature of wall rocks, nature of

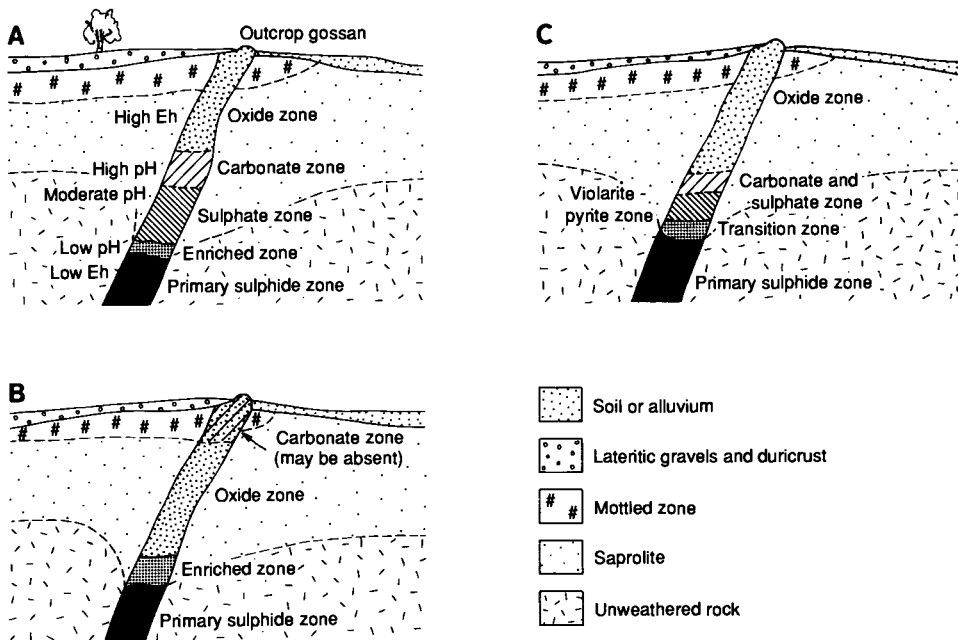


Fig. II.i-2. Generalized mature oxidation profiles for (A) volcanogenic massive sulphide deposits, (B) Cu-rich massive sulphides, and (C) Ni-Cu massive sulphides.

groundwaters, weathering history and intrinsic properties, together with data acquisition and evaluation. Although the mineralogy (and fabric) of gossans is fully described by Nickel and Daniels (1985), it is not possible to evaluate the geochemistry without reference to mineralogy.

ACKNOWLEDGEMENTS

Only some of the data and ideas within these chapters are our own. We have been privileged to work with members of the former CSIRO Division of Mineralogy who have made significant contributions to the understanding of gossan formation, mineralogy, geochemistry, fabric (texture) and evaluation. They include Anita Andrew, Charles Butt, Graham Carr, Brian Gulson, Alan Mann, Ernie Nickel, Bill Ryall, Keith Scott, Ray Smith, John Wildman, John Wilmshurst and the highly skilled and dedicated members of the North Ryde and Floreat Park laboratories who prepared and analysed the gossan and ironstone samples. To each and every one of these colleagues, we wish to express our sincere appreciation.

None of this work would have been possible without the input and collaboration of the management and staff of many exploration companies in Australia.

Their contributions are gratefully acknowledged. Valuable discussions with Ross Andrew on the gossans and ironstones of southern Africa, the management and geologists of Riofinex Geological Mission, Jeddah, Saudi Arabia, and geoscientists from the BRGM, Orléans, France have considerably widened the scope of these chapters.

THE MECHANISMS OF SULPHIDE OXIDATION AND GOSSAN FORMATION

M.R. THORNBUR and G.F. TAYLOR

INTRODUCTION

The processes by which rocks that contain sulphides weather to form gossans are initiated by the chemical interaction of aqueous solutions with minerals. These reactions take place at solid-liquid interfaces provided by cracks, fissures and grain boundaries along which weathering solutions can penetrate. Three processes need to occur for an assemblage of sulphide minerals to alter to a gossan:

(1) Dissolution of some chemical elements from the sulphide, even though their period of retention in solution may be quite short.

(2) The oxidation of S and, usually, other elements such as Se, As, Cu, Fe and Au (N.B. for Au, see also Chapter I.4). The dominant oxidation process is that of S because not only is it present in high concentrations but it also undergoes a profound change in oxidation state. The oxidation of sulphide (S^{2-}) consumes a maximum of eight electrons per atom (see Fig. II.1-1).

(3) The precipitation, recrystallization and dehydration of minerals to an assemblage that eventually becomes that of the gossan. These reactions usually involve the initial precipitation of complex metal hydroxides and include other anions such as carbonate or sulphate.

These three processes are sufficiently well understood that a careful and detailed study of all chemical and mineralogical aspects of a gossan will give a useful understanding of the nature of the original sulphide mineral assemblage.

OXIDATIVE ELECTROCHEMICAL WEATHERING

Oxidation and reduction

Oxidative weathering usually involves minerals which are semiconductors of electricity (Fig. II.1-2) so that the reactions proceed by processes similar to the galvanic corrosion of metal alloys. These are redox reactions (Sato and Mooney, 1960), i.e. the combination of a *reduction* reaction at a cathode that consumes electrons, and an *oxidation* reaction at an anode that provides the electrons that flow within the solid from the anode to the cathode (Fig. II.1-3). In this case, the

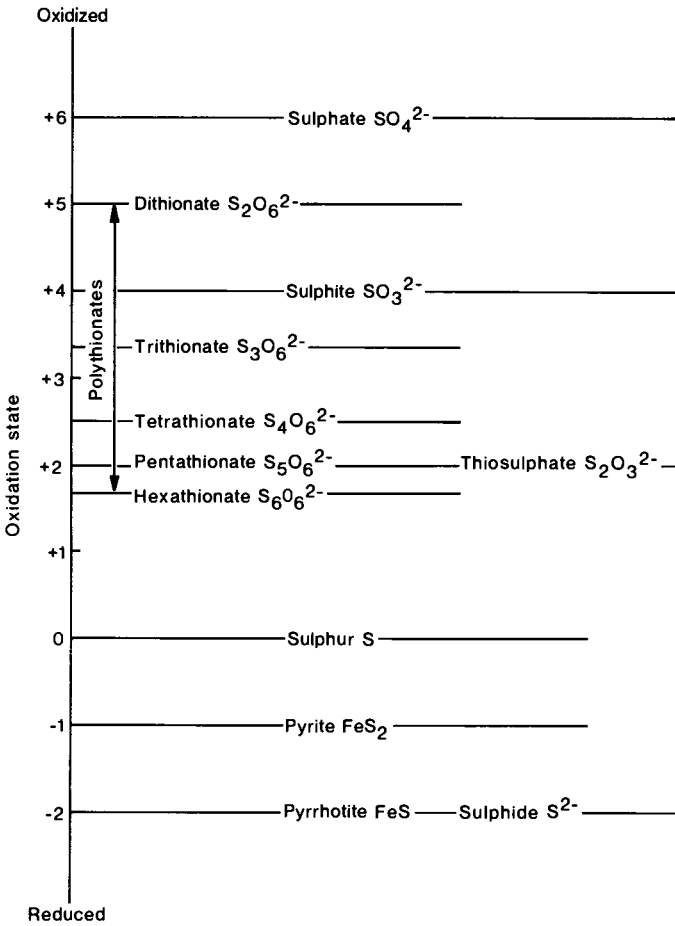
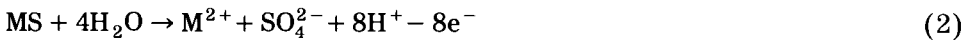


Fig. II.1-1. The average oxidation states of sulphur in various anions and Fe minerals.

cathodic reduction of dissolved oxygen which can be generalized as:



is combined with the oxidation of a mono-sulphide:



(where M is a divalent base metal)

to give the total reaction:



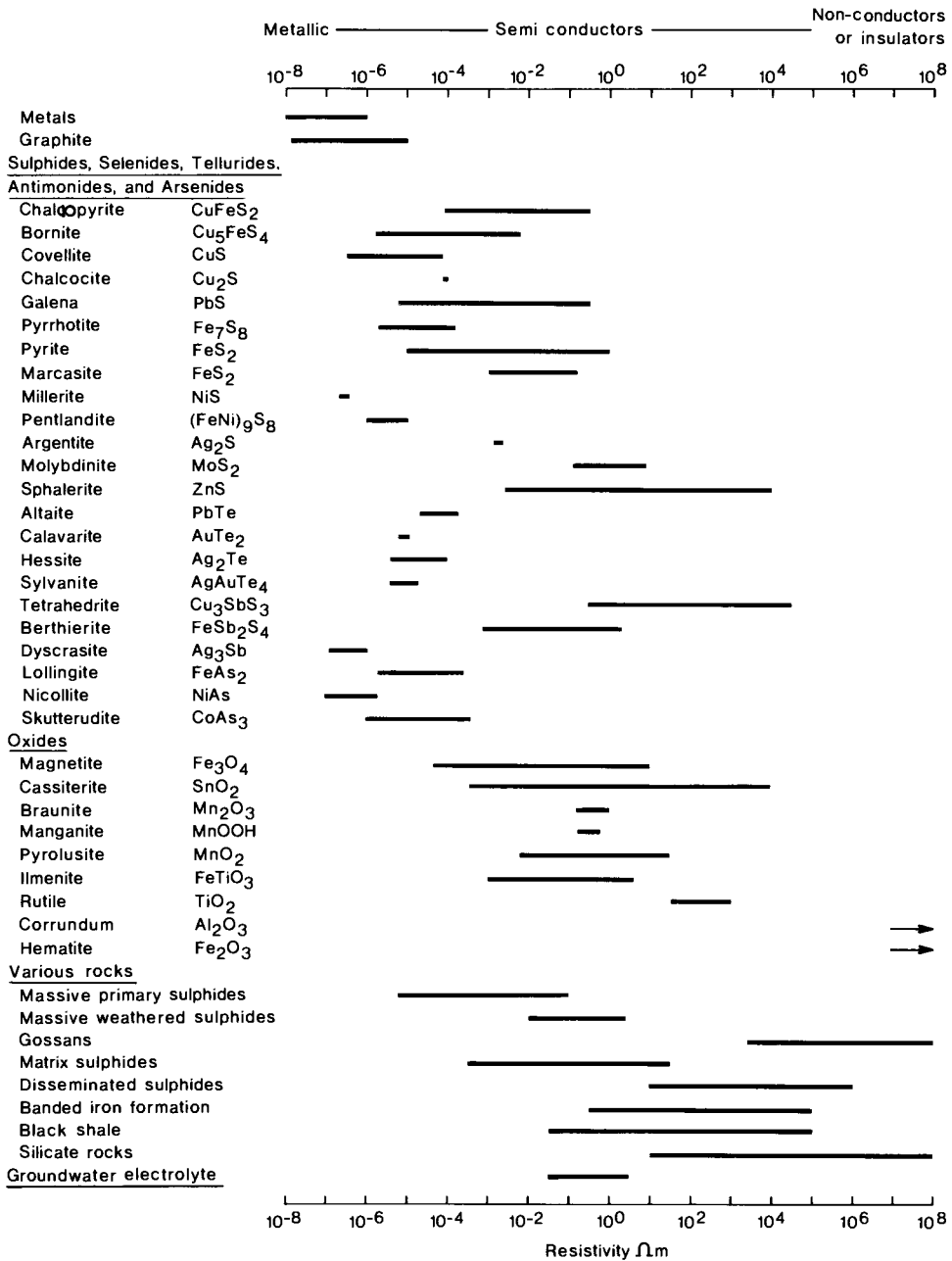


Fig. II.1-2. A comparison of the resistivities of various ore minerals and rocks.

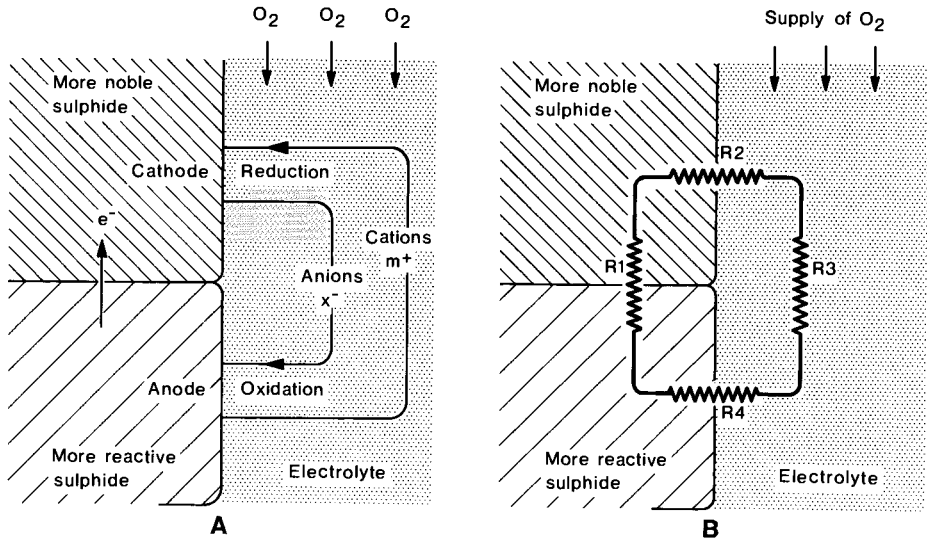


Fig. II.1-3. A diagrammatic representation of the electrochemical processes of a weathering sulphide showing (A) the flow of reactants and (B) the four resistances that slow the reactions.

The total reaction in this form is very misleading because it implies that the oxygen from dissolved air provides the oxygen in the sulphate. However, because galvanic “corrosion” allows (i) the oxygen reduction to take place at certain preferred mineral–solution interfaces which act as cathodes and (ii) dissolution or oxidation to occur at other interfaces which act as anodes (Fig. II.1-3A), the oxygen is derived from water. This has been confirmed by isotope studies (Bailey and Peters, 1976).

Cathodic reduction processes cause the associated solutions to become alkaline whereas anodic oxidation processes result in the production of acids. In addition, acid is also released when the metals that dissolve as cations at the anode hydrolyse:



and



(where M is a divalent base metal).

Acid production is most pronounced if the cation in solution is Fe^{2+} , for it can be further oxidized:



and then strongly hydrolyzed to form Fe hydroxide precipitates (Thornber, 1975b):



Rate of weathering

The rate of weathering of the sulphide may be controlled by the following five factors, each of which can be dominant and thus rate limiting (see Fig. II.1-3B):

- (1) The rate at which O_2 can be supplied to the system.
- (2) The rate at which O_2 can be reduced at the cathode-solution interface (resistance R2).
- (3) The conductivity within the electrolyte solution paths between the anode and cathode (resistance R3).
- (4) The energy barriers (polarization effects) that have to be overcome at the anode due to the anodic reaction mechanism and the build up of solution products near the interface (resistance R4).
- (5) The resistance to electron flow within the solid (resistance R1).

A major control on the nature and mineral assemblage of the resulting gossan is the separation of the cathodic oxygen-consuming, alkali-producing reactions from the anodic, oxidizing, dissolution, acid-producing reactions. In massive Ni sulphide ores, such as those at Kambalda, Western Australia (Nickel et al., 1974; Thornber 1975a,b), the anodic supergene weathering can be 100 m or more beneath the cathodic oxygen reduction at the water-table (see Fig. II.1-4). In contrast, in deposits in which the sulphide grains are disseminated and insulated from each other by silicates, cathodic oxygen reduction and anodic oxidative leaching will be within a few microns of each other.

The separation of the cathode and anode is also controlled by the electrical resistivity of the ore assemblage, a property of the ore and gangue minerals (see Fig. II.1-2) that determines factor 5 above. The lower the resistivity of an assemblage, the more rapidly will it react and the greater the distance may the cathodes and anodes develop from each other. The range of resistivities within a sulphide ore assemblage that will allow electrode separation and permit electrochemical weathering reactions can be estimated from the electrical properties of the assemblage. The Eh-pH diagram of the Fe-S-oxygen-water system (Fig. II.1-5) shows the range of oxidation potential that can be expected in an oxygen-saturated groundwater electrolyte near the water-table. This indicates that there is a potential difference of about 0.5 volts between the oxidizing environment and the reducing potential of the Fe sulphides. If it is assumed that the decline in potential from the resistances due to polarization effects at the anode and cathode surfaces plus that in the electrolyte (i.e. R2 + R3 + R4 in Fig. II.1-3) equals 0.3 volts, the potential difference between the cathode and anode within the solid is about 0.2 volts. For a rock with resistivity r ohm-metres and a

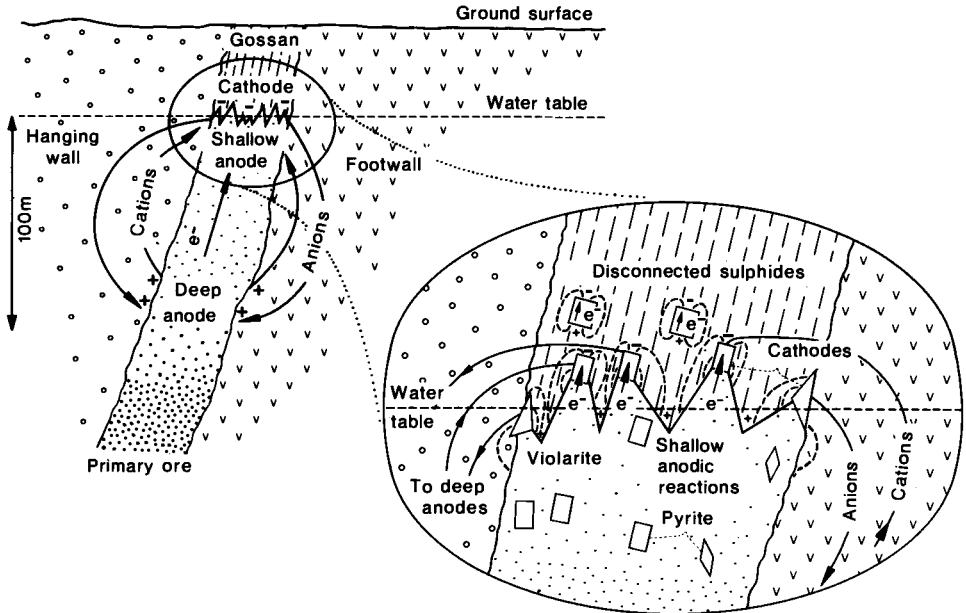
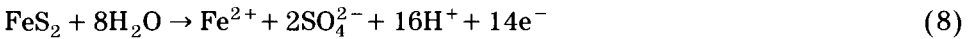


Fig. II.1-4. Cross sectional representation of the deep weathering reactions and the reactions at the water-table for Kambalda-type massive Ni sulphides.

cathode–anode separation of m metres, the current flow per square metre of rock will be $0.2/rm$ ampere, i.e. $0.2/rm$ coulombs of electricity flowing per second. Given that 96,500 coulombs = 1 Faraday and that one Faraday is the quantity of electrons equivalent to one mole, the half-reaction of anodic pyrite leaching



indicates that 14 Faradays are produced in reacting one mole (120 g) of FeS_2 . Thus, in one year (31,536,000 seconds):

$$0.2 \times 31,536,000 \times 120/rm \times 96,500 \times 14, \quad \text{i.e. } 560/rm \text{ g of pyrite}$$

are reacted per square metre of surface per year. If the resistivity, r , is 10 ohm-metre, then 56 g of pyrite per square metre could be expected to be leached per year if the cathodic and anodic reactions are 1 m apart. In geological terms, this dissolution rate is very rapid. The resistivity of most sulphides is less than 10 ohm-metres (Fig. II.1-2) so that there is even less resistance for the potential to overcome; consequently, the separation of the anodic leaching reactions from the cathode reduction of the dissolved oxygen can be considerable. Therefore, anodic leaching can take place within the cracks, fissures and open grain

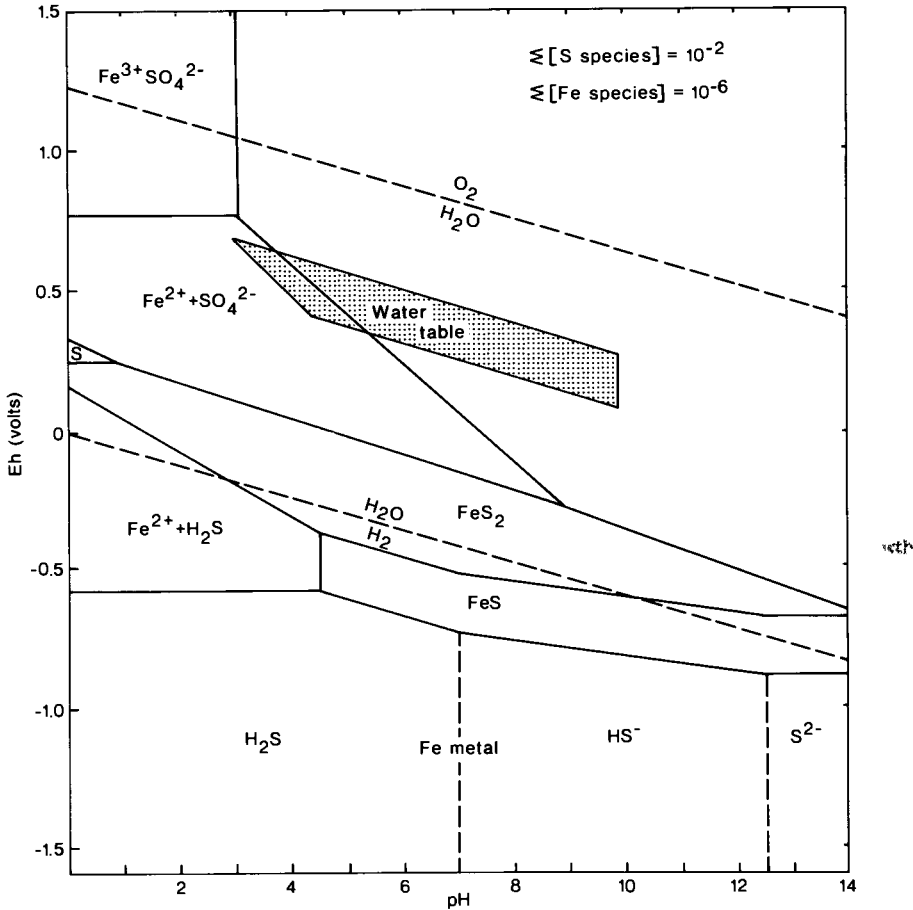


Fig. II.1-5. Eh-pH diagram for the Fe-S-O-H₂O system showing the Eh-pH domain that can be expected in an oxygen-saturated environment close to the water-table.

boundaries where the solutions have penetrated without the necessity for dissolved oxygen to be present to complete the reaction shown diagrammatically in Fig. II.1-6.

The most rapid reaction rates occur when the cathodes and anodes are close together, because the resistances in the solids and electrolytes (R1 and R3 in Fig. II.1-3B) are minimized. This situation pertains where sulphides are freshly exposed at surface by erosion. However, as the process continues, the polarization resistances from the accumulation of reaction products on the cathode and anode surfaces (R2 and R4 in Fig. II.1-3B) cause unattached anodic surfaces further from the cathodes to become relatively more reactive and the leaching spreads away from the source of oxygen. The cathodic oxygen reduction reactions will be favoured near to the oxygen supply, and this reaction will occur on

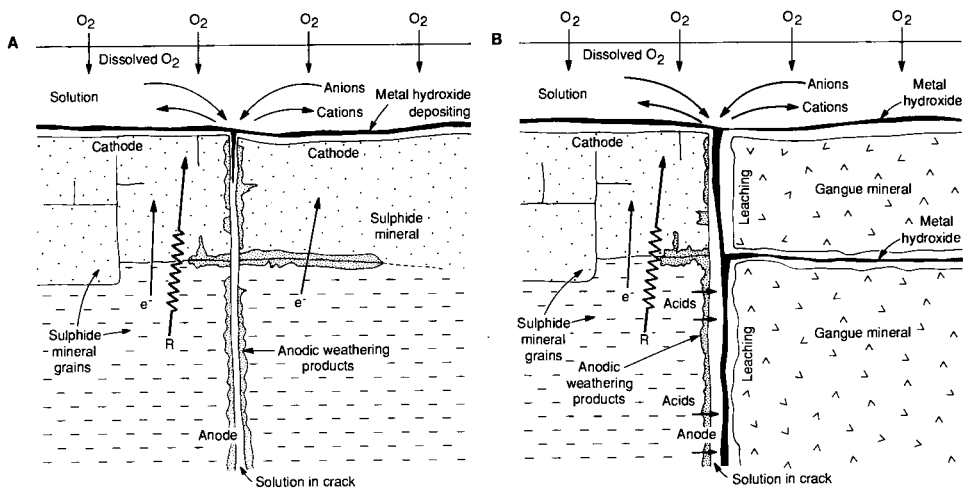


Fig. II.1-6. Representation of the anodic processes taking place in solution channels associated with weathering: (A) sulphides, (B) sulphides and gangue minerals.

those conducting mineral surfaces that are less prone to leaching, i.e. more “noble” (Fig. II.1-3). In most base metal sulphide ores, pyrite, covellite and chalcocite are more noble or less reactive than pentlandite, violarite, chalcopyrite, sphalerite and galena and consequently can remain higher in oxidized profiles (Nickel et al., 1974; Andrew, 1980). The most noble (least reactive) minerals will eventually have the other sulphides leached away from around them until they become disconnected electrically from the bulk of the weathering sulphides and at this stage they will leach away as small separate cells as depicted in Fig. II.1-4. They are then able to weather more rapidly because there are no more reactive sulphides attached to them to act as sacrificial anodes.

In those parts of the weathering profile in which the cathodic oxygen reduction dominates, the solutions become relatively more alkaline; the alkalinity spreads by the diffusion and ionic conduction of anions towards the anodes. Metal cations released simultaneously by the anodic reactions into solution-filled cracks within the sulphide assemblage can then interact with the alkaline anions to form precipitates of metal hydrolysis reactions. The precipitates develop a fabric that accentuates the solution channels and replicates the morphologies of the minerals being leached. This results in the development of the boxwork fabrics that were initially used as diagnostic features in gossan evaluation.

Gangue minerals are attacked and leached by the acids produced by both the leaching and the cation hydrolysis reactions. This results in alkaline buffering in their vicinity, favouring further metal hydrolysis in the surrounding solution channels and replication of the fabric of the gangue minerals. Silica released during the acid attack of gangue minerals is unstable in solution and is readily

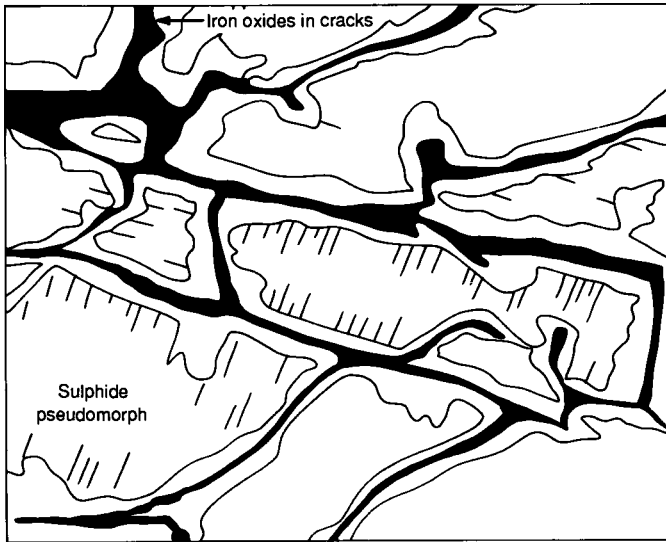


Fig. II.1-7. Gossan fabric developed by the processes represented in Fig. II.1-6.

incorporated by hydrolysis precipitates in the solution channels. The overall result is the development of boxwork fabrics that may be used as diagnostic features in gossan evaluation. Even if the hydrolysis precipitates themselves are weathered, the boxwork fabric can still be preserved by the silica. These processes are illustrated in Figs. II.1-6 and II.1-7.

The role of the water-table

Vertical changes in the level of the water-table are important controls on the development and nature of the gossan profile. With a rising water-table, the rate of gossan formation will be limited by a decline in oxygen access and weathering will cease. A static water-table will have a similar effect, for although it will assist the development of a greater separation of cathodic oxygen reduction and anodic leaching or alteration, eventually the reactions will work downwards to such a depth that they will cease due to oxygen starvation. With a falling water-table, however, oxygen access is ensured and the profile can develop. If the fall is slow, oxygen access may still control development; if the fall is rapid, control may pass to other electrochemical factors. The development of a gossan profile may therefore be considered to take place during periods of falling water-table, whether these are seasonal or due to longer term events such as climatic changes, rejuvenation by tectonic uplift or surface erosion on the side of a valley.

In a manner directly analogous to that described in Chapter I.4 for weathering and soil formation over silicate rocks, the weathering of sulphides moves downwards as a series of fronts. The cathodic, alkaline, oxygen-reducing reactions

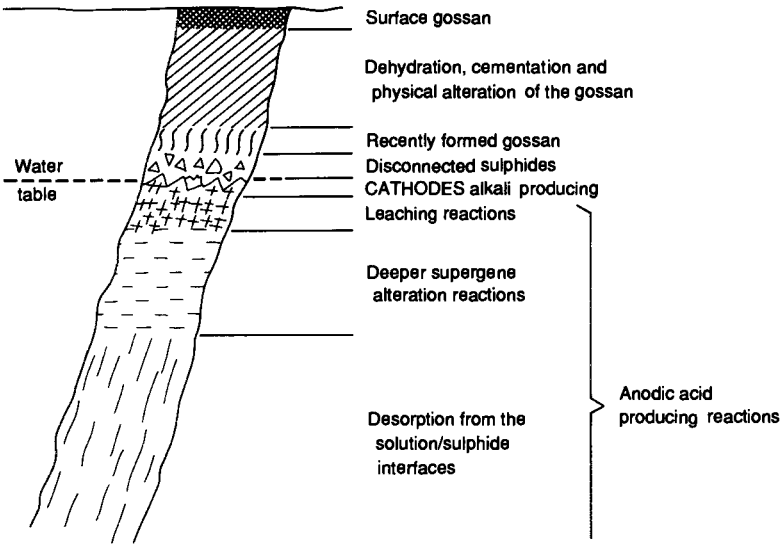


Fig. II.1-8. Representation of the various stages in gossan development.

need to be nearest the oxygen source at the top, and the anodic leaching and acid-producing reactions are developed vertically below (Fig. II.1-8). As weathering proceeds under long-term conditions of falling water-table, the environment close to the sulphide mineralization becomes increasingly leached and acid. Immediately above this, closer to the water-table, the cathodic reduction of dissolved oxygen creates a relatively more alkaline environment in which the metal hydroxide precipitates can be consolidated. Iron hydroxides are particularly abundant because the higher oxidation potential favours formation of the ferric ion. The net environment here may nevertheless remain quite acid, depending on the ore type, as discussed in the next section.

Initially, the Fe hydroxide precipitates that form are more likely to be gelatinous than in rigid crystalline forms, due to an excessive water content in their structure. Furthermore, recently-formed gossan that is found just above actively leaching sulphides commonly differs from the gossan that is exposed at the surface, because considerable reworking of the gossan minerals takes place above the water-table. Repeated wetting and drying, periodic flushing by water, changes in water chemistry and the penetration of silica-rich solutions ultimately result in the almost complete loss of the more mobile elements bound in the original precipitates and previously stable primary and secondary minerals, so that the gossan consists predominantly of Fe hydroxides and quartz.

Self potentials

The processes described in the previous sections give rise to electrical potentials in the Earth that can be measured both on the ground surface and

down boreholes as first reported by Fox (1830). Sato and Mooney (1960) correctly established these “self potentials” (SP) to the electrochemical processes associated with electric conduction in sulphidic rocks. Bolviken (1979) developed a quantitative relationship between the measured potentials and the presence of sulphides. Sivenas and Beals (1982) described the processes as “geo-batteries”, but the emphasis is more correctly placed on corrosion or weathering, for the electrical potentials that can be measured at ground level are due to the anodic dissolution and desorption reactions that take place at depth (Fig. II.1-4). These are the reactions that give the greatest separation between a cathode at surface and an anode at depth. However, they will also operate for conducting minerals that do not allow for the separation of a corroding anode from the cathode (e.g. sulphide ores containing galena and sphalerite that weather completely away and break the circuit), and on surfaces of inert minerals such as graphite. Such desorption reactions can be written:



OR



followed by the metal hydrolysis



These type of reactions have been studied for metals (Woods, 1976) and the Ni-Fe sulphides pentlandite and violarite (Thornber, 1983). The acids produced can give rise to minor alterations of the more alkaline minerals.

EFFECTS DUE TO THE MINERALOGY OF THE ORE

Most *massive sulphide ores* can be regarded as good electrical conductors. Exceptions are ores containing major amounts of sphalerite and/or significant pyrite, because these minerals have moderate resistivities, particularly when pure (Fig. II.1-2). Accordingly, a considerable separation may develop between the cathodes, near the source of oxygen at the water-table, and the anodic leaching reactions producing acids below. Furthermore, anodic acidity is enhanced because the separation isolates the leaching reactions from neutralization by oxygen reduction at the cathodes. Similarly, neutralization by minerals in wall rocks decreases as the thickness of the massive sulphides increases. This high acidity will be accentuated further in the presence of Fe sulphide minerals such as pyrrhotite and pyrite or of iron-base metal sulphides such as pentlandite and chalcopyrite. As indicated previously, the Fe is released into solution as Fe^{2+}

and it can be further oxidized to Fe^{3+} . Hydrolysis can occur even at pH values below 5 and causes the pH to fall even further as Fe hydroxide minerals precipitate. As a result of this low pH, other base metals are prevented from being bound within the Fe hydroxides (Thornber and Wildman, 1984).

Matrix sulphide ores are defined as those ores that have a significant gangue mineral content but in which the sulphides are sufficiently abundant to form a continuous matrix and so maintain electrical conductivity. These ores also allow the separation of cathodic and anodic reactions and the development of progressive weathering zones. However, because of the close proximity of sulphide and gangue minerals, the anodic acids are neutralized by reaction with the gangue minerals so that the pH is higher than in massive ore. As a result, some of the base metals originally present in the ore may be retained. The fabric of the gangue minerals is commonly preserved in the gossan by oxides infilling veins and grain boundaries.

Disseminated sulphide ores are those in which the sulphide minerals are sufficiently dispersed so as to be insulated from each other. Each sulphide grain weathers as a separate electrical cell and the only influence that one sulphide grain can have on another is via solution. Thus, access by oxygen-containing solutions will determine where leaching will occur and the chemical composition of the grains will influence the reaction rate, pH conditions and the secondary minerals that form. Generally, the sulphide grains near the water-table will be leached and those that contain Fe will produce sufficient acids to leach associated gangue minerals. The base metals will tend to move from the sulphide grains to any framework structures that develop in grain boundaries and other solution channels.

BINDING OF BASE METALS WITH GOSSAN (IRON BEARING) MINERALS

During the sulphide leaching processes, base metals such as Cu, Pb, Zn, Ni and Co are dissolved as cations, together with ferrous Fe. In many ores, Fe is dominant so that Fe hydroxides and oxyhydroxides are the main precipitates. Base metals can be bound in these precipitates either by co-precipitating with them, or subsequently being adsorbed onto their surfaces. Experimental investigations carried out with actual sulphide ore leached both electrochemically and by mixed solutions of Fe and base metals have demonstrated that the solution pH determines the type of minerals formed and the amounts of base metal co-precipitated and adsorbed (Thornber and Wildman, 1984; Thornber, 1985).

Co-precipitation and the adsorption of base metals with the Fe minerals are favoured at high pH. The mixed solubility curves of base metals and ferrous Fe sulphates in an environment being slowly oxidized by air take the form shown in Fig. II.1-9, which demonstrate the co-precipitation effects. In summary, these indicate:

(1) Co-precipitation with Fe hydroxides markedly reduces the solubility of the base metals. Although the effective change is less for Cu and Pb, they remain the

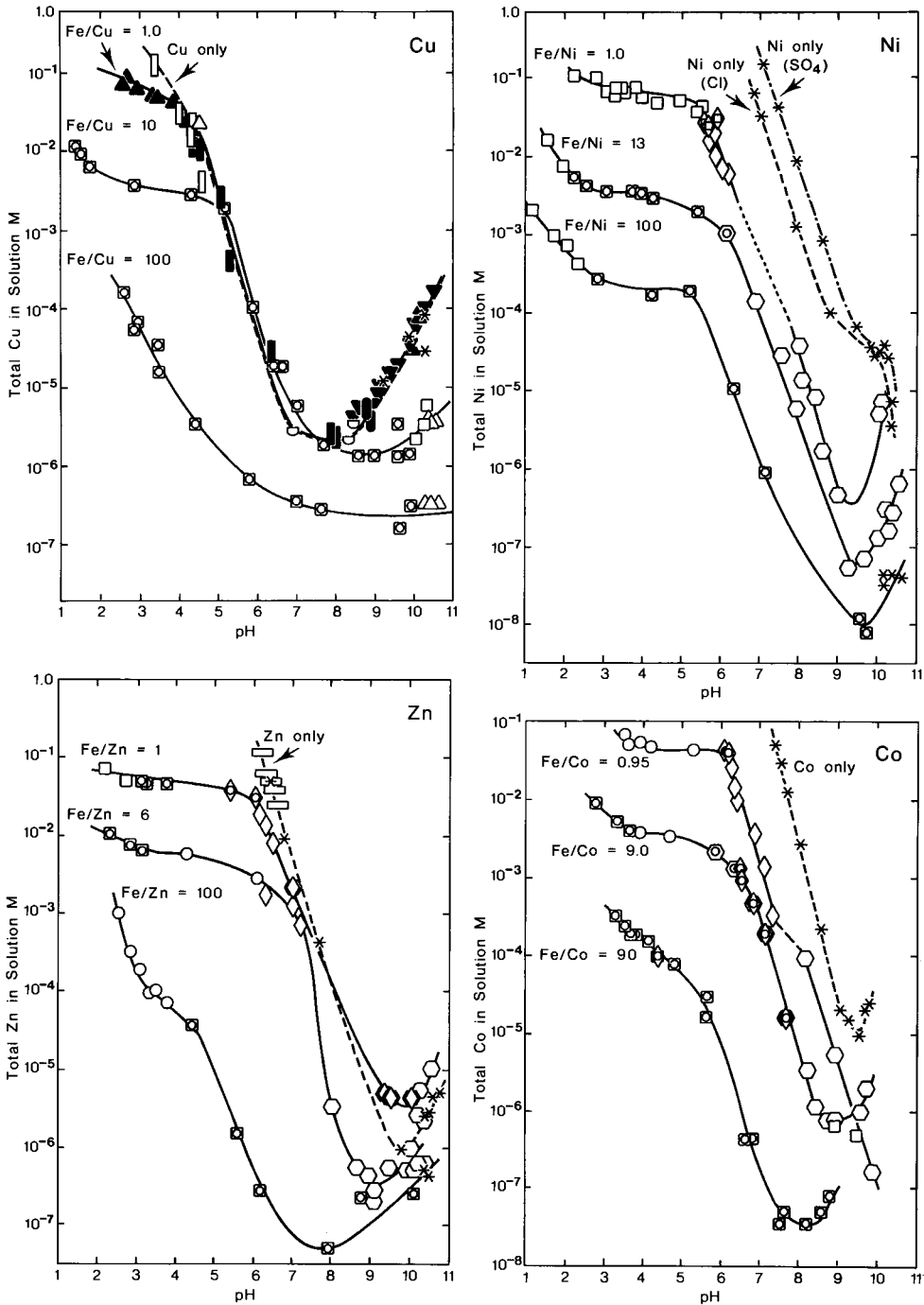


Fig. II.1-9. Results of coprecipitation experiments showing the concentration of base metals in solution as a function of pH. Each datum point is marked by a symbol representing the mineralogy of the precipitate(s) (see over, p. 132). The curves connect datum points obtained from initial solutions with the specified Fe/base metal ratio.

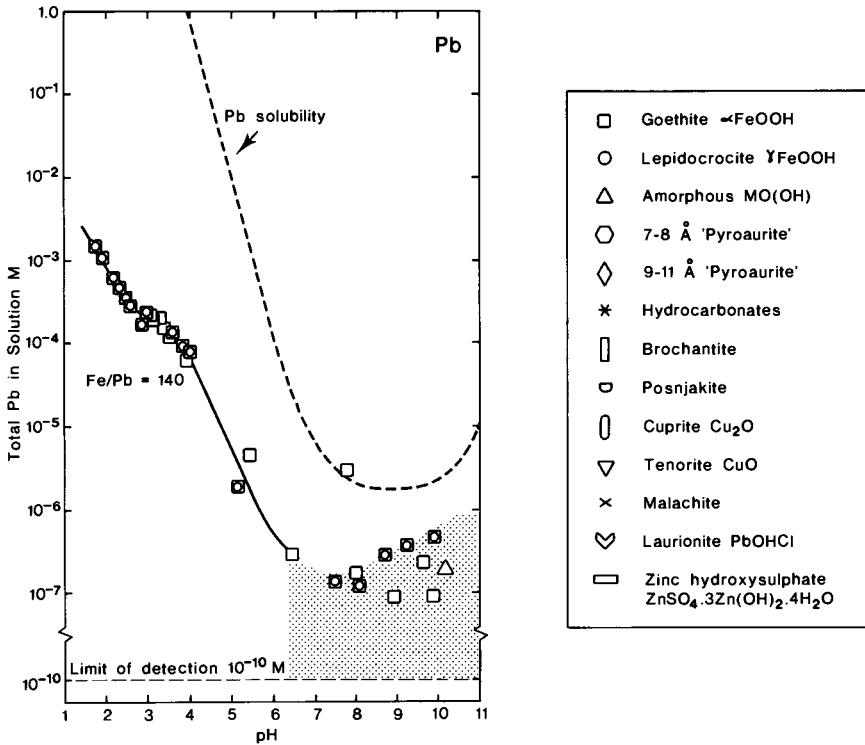


Fig. II.1-9. (continued).

least soluble and the relative co-precipitation order of the base metals is very similar to the order of adsorption onto goethite (see Fig. I.5-9).

(2) Precipitation is greater at higher pH values, and solubility increases with lower pH.

(3) The phases that form (experimentally) at lower pH values are the Fe oxyhydroxides lepidocrocite, goethite and ferrihydrite; at the pH ranges in which solubility is changing, hydroxy sulphates form and, at higher pH values at which base metals are normally insoluble, hydroxycarbonates form.

A compilation of data for adsorption onto goethite for anions and cations (see Fig. I.5-9) indicates that the pH effect for anions is the reverse of that for cations. Accordingly, anion adsorption is favoured at lower pH. The limited data available also indicate that this is true for co-precipitation with Fe oxyhydroxides.

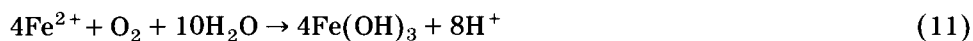
There are two distinct mechanisms of precipitating Fe oxyhydroxides:

(1) *The higher pH process*: above pH 7, only a negligible amount of Fe(II) can remain in solution as Fe^{2+} or $\text{Fe}(\text{OH})^+$; most will have precipitated as one of the so-called "green rusts". These may incorporate the base metals, with ferrous Fe precipitated as $\text{Fe}(\text{OH})_2$. Further oxidation by dissolved oxygen:



produces no further acid and the precipitate will remain stable, binding the base metals.

(2) *The lower pH process*: below pH 7, the Fe^{2+} released into solution has a significant solubility. Further oxidation of this will produce acid by the subsequent hydrolysis reaction:



This reduces the pH even further, so that only ferric oxide and oxyhydroxide form and base metals will become or remain dissolved.

CONTROL BY pH

The nature of the first gossan minerals to form, and the chemical elements that they retain, are controlled by the pH. In turn, the pH itself is determined by the nature of the initial sulphide assemblage. Consequently, the nature of the gossan is likely to reflect characteristics of the original assemblage.

Primary control; sulphide content

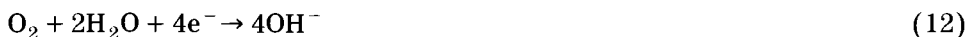
A massive sulphide assemblage with high proportions of Fe sulphide minerals will produce highly acid weathering conditions and, although it may contain substantial amounts of base metals, only a small proportion can be expected to be retained in the gossan. However, elements such as As, Sb, Se, Te, W and Mo, which form anions, may remain with the Fe minerals. If K and Al are being leached from wall rocks or gangue minerals, jarosites and alunites can be expected, and these may incorporate elements such as Pb, Ba, As, P and Sb (Scott, 1987). Of the base metals, Cu is more likely to be retained than Zn, Ni and Co as demonstrated by the gossan formed from the massive IA orebody at the Agnew (Perseverance) Ni sulphide deposit in Western Australia (Thorner et al., 1981). This gossan retained only Cu in anomalous amounts, whereas the gossan developed over the matrix-type Ni sulphide ore had anomalous concentrations of both Cu and Ni. Nevertheless, if it is suspected that a gossan had formed under acidic conditions from massive Fe sulphides, evidence for the base metals that were originally present may still remain. A careful search with an electron microprobe of minerals that are less iron-rich or appear to have been derived from gangue minerals or phases precipitated in solution channels in the wall rocks may give some indication of the composition of the primary sulphides.

Weathering assemblages that have fewer sulphides, particularly Fe sulphides, can be expected to maintain higher pH values than massive sulphide bodies. Nevertheless, the pH would still be expected to be lower close to the weathering sulphides than close to the gangue minerals.

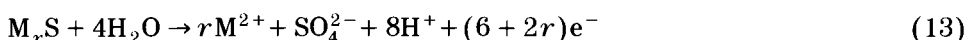
Secondary control; sulphide composition

Where the anodes and cathodes of the weathering sulphides are close together, the respective reactions can directly neutralize each other. It can be demonstrated that the composition of the primary sulphide will play a part in determining the pH. The chemical reactions at the cathodes and anodes can be written as follows, where M_rS is a base metal sulphide with the metal/sulphur ratio = r .

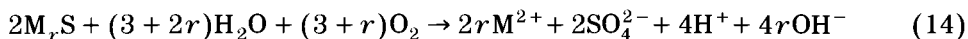
Cathode oxygen reduction:



Anode sulphide leaching:



Combining reactions (12) and (13):



These reactions demonstrate that:

(1) Sulphides with $r < 1$, such as pyrite (FeS_2), marcasite (FeS_2), monoclinic pyrrhotite (Fe_7S_8), and violarite ($(FeNi)_3S_4$), give an acid reaction.

(2) For monosulphides (MS), where $r = 1$, such as galena (PbS), sphalerite (ZnS) or chalcopyrite ($CuFeS_2$), the reaction is neutral and the overall pH will not change if there is no hydrolysis of the metals.

(3) For sulphides with $r > 1$, such as chalcocite (Cu_2S) and pentlandite ($(NiFe)_9S_8$), OH^- is in excess and may even cause alkalinity.

These processes dominate where the sulphide minerals are small and disseminated. The minerals that produce most of the acid will cause leaching of gangue minerals around them and hydrolysis of the metals will be associated with this leaching. Those minerals that produce alkalinity are more likely to have metals hydrolyzed near the original grain and leave a base metal signature in the gossan associated with remnants of the gangue minerals.

Leaching of gangue minerals

Gangue minerals such as silicates and carbonates will act as alkaline buffers to keep the pH higher in their vicinity. As indicated previously, there is a tendency for Fe and other base metals released from the weathering sulphides to diffuse towards the surfaces of gangue minerals and to precipitate by hydrolysis reactions, thereby producing acids that continue the leaching. These reactions invariably take place some distance from the leaching surface, to form precipitated shells of Fe oxyhydroxides encompassing the leached gangue mineral in

the classical "Liesegang" manner (see Clarke et al., 1985). Of the metals released from the gangue minerals, the alkalis are mostly removed, although some can be co-precipitated in the boxwork with secondary alunite/jarosite (Na, K) and silicate (Ca, Mg) minerals.

WEATHERING OF SPECIFIC MINERALS

From a combination of the observations of weathering profiles of various sulphide assemblages (see Blain and Andrew, 1977; Andrew, 1980; Nickel and Daniels, 1985) and electrochemical studies in the laboratory (Thornber, 1985), general comments can be made about the weathering reactions of the more important sulphide minerals. These are discussed in order of reactivity, commencing with those that are most reactive and therefore expected to alter deepest in the weathering profile. Detailed descriptions of the weathering of ore and gangue minerals are given by Williams (1990).

Galena (PbS) begins to oxidize before chalcopyrite and sphalerite under experimental conditions in which chloride is present. In chloride-rich groundwater, some Pb will be mobilized, but slightly alkaline or sulphate-rich waters will cause Pb carbonates and sulphates to form. In arid environments in particular, remnant galena may be preserved in the gossan due to coatings of sulphates or carbonates protecting it from further leaching. The low solubility of Pb allows it to combine with phosphate, arsenate and other anions to form a variety of complex, insoluble compounds such as plumbogummite and beudantite, which may be retained in or close to the gossans. In laboratory systems in which there is abundant electrolyte, galena reacts very rapidly with no evidence of Pb sulphate precipitation. The Pb released to solution readily replaces any Mg, Ca and Mn carbonate minerals that are within the system, to form hydrocerussite $\text{Pb}_3(\text{CO}_3)_2(\text{OH})_2$. Similar natural conditions cause weathering to gossans in which cerussite is the dominant Pb mineral. In humid environments, in which the chloride concentrations in the groundwater are very low, galena would still be expected to weather, with Pb mobility occurring in the acid environment close to the sulphide mineralization. However, the mobility even in acid solution will be limited by strong adsorption onto Fe oxyhydroxides and humic matter. Neutral-alkaline conditions (e.g. in weathering wall rocks) or sulphate-rich waters will cause carbonates and sulphates to form.

Pentlandite ($(\text{NiFe})_9\text{S}_8$) weathers pseudomorphically to the more oxidized Ni sulphide violarite $(\text{NiFe})_3\text{S}_4$ in the deeper zones of weathering sulphide bodies (Nickel et al., 1974). Although the violarite occupies a smaller volume than the pentlandite, electrical contact is retained and the classical Kambalda-type deep weathering of pentlandite (Thornber, 1975a) takes place. The blocky pentlandite texture is retained in the Fe oxide minerals that in turn replace the violarite in the gossan.

Pyrrhotite (Fe_9S_{10} , hexagonal, or Fe_7S_8 , monoclinic) has numerous crystal forms, depending on its hypogene history. All forms are highly reactive and release Fe^{2+} ions into solutions which, when hydrolyzed, give an acid reaction. Secondary pyrite or marcasite are common weathering products of pyrrhotite but, because they are entirely precipitated from solution, they usually partially fill adjacent solution channels and adopt their morphology. If Ni is present in solution, violarite forms instead of pyrite or marcasite. The violarite pseudomorphs the lamellar structure of the pyrrhotite, producing a characteristic texture that is retained in the Fe oxide minerals that in turn replace the violarite in the gossan. Thus, microscopic examination of the Fe oxides may indicate whether the primary sulphides were pyrrhotite or pentlandite, even though violarite was the intermediate supergene mineral in each case.

Chalcopyrite (CuFeS_2) is one of the last minerals to oxidize in a pyrrhotite-pentlandite-pyrite assemblage, due to the relative stabilities of the phases. However, in other assemblages, it oxidizes early, i.e. before sphalerite, pyrite and sometimes galena, giving covellite (CuS) precipitates in the solution channels or forming cubanite (CuFe_2S_3) lamellae within the weathering chalcopyrite. Similar behaviour has been observed during laboratory weathering experiments, in which chalcopyrite and galena reacted simultaneously, before sphalerite and pyrite. The Cu dissolves, leaving a ferric hydroxide gel replicating the chalcopyrite grain. On drying, this gel shrinks, leaving a cellular boxwork replicating the fabric of the original chalcopyrite crystals. In natural systems, such a process may result in the complete removal of the chalcopyrite grain or partial pseudomorphing by Fe oxides, particularly if the gossan has subsequently been silicified (Andrew, 1980).

Pyrite (FeS_2) is common as a primary mineral, but it can also form as the product of partial oxidation of minerals such as pyrrhotite and chalcopyrite, as discussed above. Marcasite may also form, especially in more acid conditions. Pyrite may be sufficiently resistant to leaching to remain in the vadose zone, where it will react as an isolated grain in an environment of high oxidation potential. The formation and subsequent hydrolysis of Fe^{III} increases the acidity, so that any Fe oxide boxworks will contain few other base metals; however, if K is available, jarosites will form.

Covellite (CuS) and *chalcocite* (Cu_2S) are more resistant to weathering than pyrite, due to the noble nature of Cu. The ultimate weathering product is usually a carbonate (malachite or azurite) if the system is sufficiently alkaline. However, under more acid conditions, an interaction between the ferrous Fe and cuprous Cu results in the formation of native Cu:



Native metals (gold, silver and platinum group elements). The Au–Ag alloy electrum is common in primary sulphide-bearing ores and when weathered in conjunction with the sulphides is likely to form complexes with any thiosulphate ion ($S_2O_3^{2-}$) present in solution as a metastable anion. Both Au and Ag will become mobile and will remain so until entering more oxidizing conditions—for example, near the water-table where Au–Ag alloys can reform (Mann, 1984a). The $Au(HS)_2^-$ complex, which is believed to be involved in Au transport in hydrothermal solutions (Webster, 1986), is not stable in the weathering environment, and hence is not considered to be involved in supergene gold mobility. However, mobility is possible by chloride complexing, which can occur under oxidizing saline conditions in arid regions. Mobility of Ag is favoured so the Au that redeposits, usually under reducing conditions, from humic materials, has a much lower Ag content (Webster, 1986). Gold geochemistry is discussed in more detail in Chapter V.3.

The platinum group elements commonly occur in a variety of minerals associated with Ni sulphide ores and from limited evidence it appears that they are mobilized and deposited in the gossan as metals (Hudson, 1986; Cowden et al., 1986). The mineral grains are difficult to locate in the gossans and the mechanisms by which they weather are not well understood. The hypotheses proposed suggest the formation of chloride complexes and rely heavily on thermodynamic data (Travis et al., 1976; Bowles, 1986).

CONCLUSION

The wide variety of supergene sulphide minerals that have been reported (see Nickel and Daniels, 1985) are an interim step on the way to gossan formation and help retain ore and pathfinder metals. Their forms and fabrics are varied; they may grow from solution with their own crystal morphology constrained by the particular solution channels—or they may replace primary minerals and be a step in the preservation of the primary texture, for example violarite developing from pyrrhotite, pentlandite or millerite. The fabrics of most secondary sulphide minerals have now been documented in the literature, and in most cases the geochemical processes involved can be understood and used as an aid in gossan evaluation.

Careful evaluation using sensitive chemical analysis techniques, coupled with the unravelling of the mineralogy by optical microscopy and electron-optical techniques can be most rewarding if this is coupled with an understanding of the processes by which these gossans could have formed. Modern electron microprobes and analytical scanning electron microscopes that can determine the trace element contents of individual gossan minerals are extremely valuable in this regard. Such an understanding is the first step in comprehending the gossanous material encountered in exploration so that a true assessment can be made of the parent material. The complexities of gossan-forming processes are

such that the Fe content, the mass of the sulphide body and the pH of the solutions involved are the major controls on the fate of the chemical elements mobilized during weathering. Subsequent physical and chemical reworking of the gossan material can cause considerable changes and many of the principles outlined in this chapter are also relevant to understanding these processes.

GOSSAN AND IRONSTONE SURVEYS

G.F. TAYLOR and M.R. THORNER

INTRODUCTION

The identification and evaluation of gossans is an important and successful technique in exploration for near-surface mineralization in northern and southern Africa, Australia, the Middle East, India, southern USSR and southern USA. Because of Pleistocene glaciation, gossans are generally not well developed in much of Canada and in northern parts of Europe, the USSR and the USA. They are also of limited significance in humid savanna and rainforest terrains. Nevertheless, as well as the obvious successes, there have been many instances of misidentification. In this chapter, the many factors controlling the geochemistry of gossans are discussed to assist in increasing the reliability of procedures for differentiating between fertile and barren gossans and other ironstones. Data from numerous deposits have been used for illustration; these are grouped into 33 case studies which are referred in the text as follows: Rosh Pinah, Namibia (18). The discussion is concerned principally with gossans and ironstones found in situ rather than as fragments in other sample media. Such fragments are, however, important contributors to anomalies located by soil, pisolith and stream sediment surveys, hence gossan geochemistry is of considerable relevance to the interpretation of data from these sources.

GOSSAN SEARCH

Ironstones commonly have contrasting physical properties to the enclosing rocks including, in particular, a colour contrast that may be utilized to locate outcrops by colour aerial photography. Glasson (1973) used this method to locate over 200 ironstones in a reconnaissance survey of 300 km² of rugged terrain north of Mount Isa, Queensland, Australia. Each outcrop was subsequently sampled from helicopter traverses and anomalous target areas defined from Cu, Pb and Zn analyses. Colour contrast is also effective during ground surveys where red-brown outcrop and float can readily be distinguished from surrounding rock or overburden. However, identification becomes more difficult where the contrast is reduced by lateritization or desert varnish, and incorrect interpretations are likely.

Prospective areas may be searched very rapidly using satellite-based techniques. For example, Landsat multispectral scanner (MSS) images have been used to identify ironstones in Saudi Arabia (Raines and Allen, 1975) and Australia (Cole, 1985). With the rapid improvement in the resolution of satellite imagery, smaller outcrops can now be located. However, it is still not possible to distinguish between gossans and other ironstones by remote sensing, even with infrared spectral imagery that can distinguish between different minerals (Raines et al., 1985).

Because of the refractory nature of the dominant minerals (Fe oxides and quartz) gossans commonly occur as resistant spines or ridges of greater relief than the host rocks. At Pegmont, northwest Queensland (12), the gossan rises some 10 m above the surrounding plain. In some instances, silicification or ferruginization of the wall rocks result in resistant ridges on either side of the gossan, giving a bowl-shaped profile as at Dugald River, northwest Queensland (11). If the gossan is not indurated or is composed of friable and less stable secondary minerals, it may occur as a trough of lower relief than the host rocks and be filled with soil or transported material. This is commonly the case for Pb-Zn-rich, Fe-poor mineralization in carbonate-rich rocks. Vegetation responds to geochemical anomalies (Cole, 1977, 1980) so that the resultant botanical variations, including natural poisoning, may be detected by MSS; thermal variations may be detected by MSS or infrared imagery. In general, such geobotanical anomalies represent gossans rather than ironstones, but may be confused by variations due simply to changes in lithology. Difficulties in gossan search by remote sensing techniques and aerial photography arise in regions with extensive colluvial overburden or where dense vegetation masks outcrop and does not respond to geochemical anomalies. In such cases, there is no alternative to surface traverses.

The size of ironstone and gossan outcrop may also cause problems. Gossans on massive sulphide mineralization within volcano-sedimentary belts such as in northwest Queensland (Scott and Taylor, 1987) and northeast Sudan (Aye et al., 1985) may be discontinuous over a strike length of many kilometres and be tens of metres wide. Alternatively, vein mineralization may be represented by very thin gossanous bands within ferruginized country rock and be very difficult to identify. In tropical terrains where there has been planation and burial by transported overburden, outcrop is minimal, with gossan occurring as rubble or float on the surface, in drainage channels or incorporated within duricrusts.

GOSSAN IDENTIFICATION: BASIC PRINCIPLES

In semi-regional and prospect exploration, the key to successful gossan identification, as with other sample media, is to use appropriate procedures for sampling, mineralogical examination, chemical analysis and data interpretation. Unlike other sample media, the heterogeneous nature of gossans requires special

field techniques. Sample preparation for chemical analyses is made difficult by the high Fe oxide content, which causes staining of crushing and grinding equipment and possible cross-contamination. In addition, many of the significant secondary minerals are not readily dissolved, necessitating specialized analytical techniques. Sample preparation and analytical techniques applicable to gossans are given in Appendices 1 and 2.

Field relationships

Regional and local geology exert considerable influence on the presence and type of mineralization. The style of mineralization and host lithologies recognized elsewhere in the region may assist in the interpretation of ironstones encountered in a new prospect. Not only do the rock types indicate the type of mineralization (e.g. quartz-eye porphyry, pyritic black shales, jasper, chert, iron formation and limestone pods are indicative of mineralization in volcano-sedimentary sequences), but their chemical and physical properties may influence gossan formation and geochemical dispersion. It may also be possible to map the nature and extent of alteration (silicification, chloritization, sericitization, pyritization) about the ironstone. The relationship of the ironstone to any structure and to the geomorphology may indicate its genesis (e.g. fault, drainage, stratigraphic or leakage ironstone) or whether it is residual, translocated, solution-deposited or of lateritic origin.

Macroscopic features

Colour is an inherent but equivocal diagnostic feature of ironstones. Many gossans derived from potentially economic mineralization are characterized by extreme local variations in colour which differ markedly from the dull uniform dark browns of barren gossans and other ironstones. There have been attempts to construct colour scales related to the underlying mineralization but this technique is subjective and highly dependent on the experience of the field geologist.

Broad-scale structural features (texture) of the ironstone, such as layering, brecciation, blocky structure, small-scale folding and slumping, reflect the nature of the primary ore. The various morphologies of solution-deposited Fe and Mn oxides on the surface of ironstones indicate leaching of the source body and are relevant in the interpretation of geochemical data.

Mesosopic features

The two most informative diagnostic features observed with a hand lens or binocular microscope are mineralogy and replicate fabric, both of which are described in detail by Blain and Andrew (1977) and Nickel and Daniels (1985). Replicate fabrics are at best a highly subjective means of identifying primary

mineralization and should be used only as a part of the process, rather than in isolation. On the other hand, the mineralogy of ironstones and gossans is often diagnostic and is of considerable importance in the interpretation of geochemical data, as outlined in Chapter II.1.

Gossans and ironstones are composed dominantly of secondary minerals, although some residual primary minerals may also be present. Goethite and hematite are the most common secondary minerals and bear an antipathetic relationship to the total silica content, i.e. both residual and fine-grained secondary quartz. The Fe oxides, together with the lesser concentrations of Mn oxides, kaolinite, sericite, allophane and phyllosilicates, have target and pathfinder elements co-precipitated within or adsorbed on them (see Chapter II.1).

The identification of accessory or trace residual minerals may help in the characterization of the primary mineralization and lithological association. Of particular significance are sulphide grains armoured against oxidation by being enclosed within residual gangue minerals such as quartz. Other common residual minerals include magnetite, gahnite, cassiterite, barite, rutile, ilmenite and various phyllosilicates. Oxidate minerals are even more diagnostic (Table II.2-1). Some of these can be recognized by hand lens or binocular microscope but others are extremely rare and can only be positively identified by X-ray diffraction or electron microprobe techniques. It is often these secondary minerals which give rise to the spectacular colours and high geochemical anomalies found in many gossans. Secondary minerals of the alunite–jarosite series, for example, may contain high concentrations of target and pathfinder elements, comparable with those commonly reported for Mn oxides (Scott, 1987). Some minerals are highly stable whereas others are soluble and are found only in arid environments. Diagnostic oxidate mineral assemblages for various styles of mineralization are discussed by Blain and Andrew (1977) and a broad coverage is given by Nickel and Daniels (1985).

The application of the study of fabrics and texture (structure) to the identification and evaluation of gossans emanated from work in North America and Australia (Blanchard, 1968), with more recent contributions by Blain and Andrew (1977), Andrew (1980) and Nickel and Daniels (1985). These papers give excellent graphic examples of the various replicate fabrics of sulphide and gangue minerals and demonstrate how a careful study may reveal important details that can assist in the interpretation of geochemical data. Ideal conditions for the formation of pseudomorphic fabrics are coarsely crystalline sulphides and a relatively high pH early in the oxidation process, as presented in Chapter II.1. Thus, if the sulphides are coarse grained, crystallographic-, cleavage- or fracture-planes are easier to recognize than in fine grained aggregates; a high pH favours in-situ precipitation of ferric oxides and hydroxides and the coprecipitation of other cations along these planes and grain boundaries before all the sulphide is oxidized. In addition to goethite and hematite precipitated in situ, the pseudomorphs may result from introduced goethite, hematite and silica, which can

dilute the geochemical signature. Where there has been colloform precipitation of solution-deposited oxides, few if any fabrics are preserved as pseudomorphs, although some structure (e.g. banding) may be apparent. Pseudomorphic fabrics after gangue minerals can also form when Fe oxides precipitate along grain boundaries as the gangue minerals weather.

Diagnostic macroscopic and mesoscopic features can enable gossans to be differentiated from other ironstones where lower levels of the gossan profile are exposed or sampled, or where the gossan is immature. However, these features may be absent or obliterated where the mineralization is fine grained or if the gossan is mature and highly leached or if it has been flooded with solution-deposited silica, Fe oxides or other secondary minerals. It is for such samples, and for the evaluation of the significance of gossans, that multielement geochemistry has proven successful.

GOSSAN EVALUATION: GEOCHEMISTRY

Ironstones and gossans are composed mainly of Fe, Si and O, with lesser and variable amounts of Al, Ca, Mg, Mn, Ti and P derived from the gangue and host rocks, together with generally minor or trace quantities of target and pathfinder elements. It is the associations of these elements and their relative concentrations that are of importance in gossan appraisal. The various factors controlling this geochemistry are examined in the following paragraphs.

Primary element associations

The element associations of primary mineralization are important both for selecting elements for analysis and for the interpretation of the data. In some cases, the associations characteristic of deposits of certain genetic types (Boyle, 1974) are overprinted by variations within and between metallogenic provinces and by post-depositional changes, including metamorphism. Some of the more common associations in deposits likely to give rise to gossans are listed in Table II.2-2, and discussed below.

Sedimentary exhalative Pb-Zn-Ag deposits may be classified into two broad groups; the Mount Isa (Australia), Howards Pass (Canada) type, which are often associated with abundant Fe sulphides, and the Broken Hill (Australia), Gamsberg (South Africa) type which are associated with Mn-rich quartz-magnetite-apatite-garnet banded iron formation (BIF). In addition to the target elements, As, Ba, Cd, Cu, Hg, Sb and Tl are commonly associated with these styles of mineralization, generally with B, Bi, Co, Ga, Ge, In and Ni. The Broken Hill-type mineralization commonly has W as a minor associate, with Mn oxides predominating over Fe oxides.

Carbonate-hosted (Mississippi Valley-type) Zn-Pb deposits have few elemental associates other than Cd, with the common Fe sulphide being marcasite.

TABLE II.2-2

Geochemical associations of elements within various types of sulphide deposits

	Volcanogenic Cu-Zn-Pb	Sedimentary black-shale hosted Cu	Porphyry Cu	Au-bearing Fe sulphides	Ultramafic Ni-Cu	Sedimentary exhalative Pb-Zn-Ag	Carbonate- hosted Zn-Pb
Ag	×	×	×	×		×	
As	×	×	×	×		×	
Au	×		×	×	×		
Ba	×					×	×
Bi	×		×				
Co		×			×		
Cr					×		
Cu	×	×	×	×	×	×	
Hg	×	×		×		×	
Ir					×		
Mn	×						×
Mo	×	×	×				
Ni		×			×		
Pb	×	×	×	×		×	
Pd					×		
Pt					×		
Re			×				
Sb	×	×	×	×		×	
Se	×			×	×		
Sn	×						
Te	×			×			
Tl	×	×		×		×	
U		×					
Zn	×	×	×			×	×

This type of mineralization gives rise to Fe-poor gossans in which secondary Zn minerals are common, and the galena often remains unaltered.

Skarn-hosted Cu-Pb-Zn mineralization commonly occurs in rocks with high Mn and Ca contents, the former forming oxides which concentrate many trace elements. Typically, this mineralization has high concentrations of Ag, As, Au, Ba, Bi, Cd, Mo, Sn and W with lesser amounts of B, Co, F, Ni and Sb. In Sn and W skarns, B, Be and F assume greater importance.

Volcanogenic massive Cu-Zn(-Pb) deposits vary in size from very large (e.g. Kidd Creek, Canada) to small, and in age from Archaean (Canada, Australia) to Miocene (Japan). The associated elements are similar to those in sedimentary exhalative deposits, except that Au, Se, Te, As, Sb, Bi, Cd, In, Th, Hg, Sn and Ba are more significant.

Porphyry Cu deposits generally have Au and Mo as associated target elements, with Re, a major constituent of molybdenite, as a pathfinder. Minor amounts of Pb, Zn, Ag, As, Sb and Hg may occur in these deposits, usually as skarn mineralization.

Shale-hosted Cu mineralization is a broad category that includes such deposits as the Kupferschiefer (Europe), White Pine (Canada) and a plethora of epigenetic, structurally-controlled deposits in sedimentary rocks. The most commonly associated elements are Ag, As, Co, Mo, Ni, Pb and Zn although some deposits may contain a wider range of trace elements, dependent on their provenance.

Massive and disseminated Ni-Cu mineralization has the least variable trace element associations with Ag, As, Au, Co, Cr, Mg, platinum group elements (PGE), Se, Te and Ti reflecting both the mineralization and the mafic to ultrabasic host rocks. In addition, there may be trace quantities of Bi, Hg and Sb.

Precious metal (i.e. Au) mineralization occurs in many styles, with those associated with pyrite most likely to form gossans. Although many elements occur in such deposits, the most common are Ag, As, Bi, Cu, Hg, Pb, Sb, Se and Te.

Zonation

Primary haloes and secondary dispersion both contribute to zonation within a gossan outcrop. Primary zonation may occur as monomineralic banding or, in metamorphosed deposits, as aggregates of various sulphide minerals. On a macroscopic scale, volcanogenic massive sulphide deposits have a distinctive vertical zonation from Cu- through Cu-Zn-Pb- to Ba-rich, commonly with an increase in Mn content along strike.

Both scales of primary zonation may be reflected in a gossan outcrop but are commonly complicated by the superimposed secondary zonation determined by the relative mobilities of the elements during weathering, groundwater composition and the nature of the secondary minerals. On a mesoscopic scale, the chemical composition of a colloform, solution-deposited gossan is often substantially different from that of a corresponding direct gossan. On a macroscopic scale, hydromorphic dispersion of the more mobile elements will enlarge the anomaly. Vertical zonation within the gossan results from the continued leaching of trace elements from the surface to deeper in the profile.

The relative mobilities of target and pathfinder elements are dependent on the solution conditions determined by the Eh, pH and presence of other soluble and partly soluble components in the gossan-forming environment, which in turn are influenced by the mineralogy of the ore, gangue and host rocks. The resultant effect is that elements react and migrate at different rates and under different conditions and can thus be segregated by secondary dispersion. These topics are discussed in detail in Chapters I.5 and II.1.

Secondary minerals

The geochemical signatures of ironstones and gossans are not dependent on the elements that have been dissolved and transported from the environment, but

on those that are retained. Thus, the major element content is determined by quartz, Fe and Mn oxides, primary and secondary silicates and accessory minerals. The retention of minor and trace elements is controlled by

- (1) the formation of discrete secondary minerals;
- (2) adsorption onto primary and secondary minerals;
- (3) coprecipitation with secondary minerals, and
- (4) binding with organic (humic) materials by processes such as chelation.

The role of humic materials in gossan formation is complex, but they can assist both the mobility and the retention of a particular element and therefore play a role in the formation of secondary minerals (see Chapters I.2 and I.5).

There are limits to the concentration of any one element that can be adsorbed onto the surface of a secondary mineral and, for crystallographic reasons, be incorporated within the lattice. Once these minerals become saturated, others begin to crystallize. The concentration of adsorbed or lattice-bound trace elements is also controlled by ageing of the host secondary mineral. Initially, such minerals may be disordered or colloidal, with a large surface area and high defect population, conducive to a high degree of "scavenging". However, as the mineral ages, the surface area is reduced and crystallographic ordering becomes greater so that the concentration of trace elements becomes less, and additional occlusions of secondary minerals may form. Thus, the intimate mixtures of secondary minerals and goethite commonly found in gossans are probably due to the ageing of Fe oxide co-precipitates and the exclusion of previously internally bound elements.

Groundwater chemistry

The composition of groundwaters at the time of gossan formation is difficult to ascertain unless oxidation is still active. It is best to assume that the groundwaters associated with weathering sulphides are in a gradient between the higher pH and Eh of the already oxidized material and the more acid, lower Eh conditions within the remnant sulphides. The concentration of total dissolved solids (T.D.S.) would be greater close to the area of chemical activity. However, because the oxidation reactions are kinetically controlled, the system may not be in equilibrium. In humid, tropical climates, groundwaters may be rich in humic acids and microorganisms but have relatively low concentrations of inorganic anions, thereby increasing the mobility, dispersion and leaching of elements released from the sulphides and associated gangue and wallrock minerals, except in sites with rapidly fluctuating water-tables or organic horizons in seepage areas and swamps.

In arid environments, groundwaters commonly have a high T.D.S. content (alkali cations with anions such as chloride, sulphate and, at high pH, carbonate) and a wide pH range, dependent on the buffering minerals. Secondary minerals precipitated when the gossan originally formed may no longer be stable, and many cations will be solubilized by an increase in chloride content. At Elura, New

South Wales, Australia (32), initial oxidation of the Pb-Zn-Ag orebody resulted in the formation of an ironstone gossan with some ferruginization of the wall rocks. Less mobile elements were retained within the gossan, e.g. as beudantite $\text{PbFe}_3(\text{AsO}_4)(\text{SO}_4)(\text{OH})_6$, some elements were concentrated at the water-table as supergene sulphides (e.g. Cu in covellite) or as native elements (Ag and Au), and the more mobile elements (Cd, Zn) were mostly leached. Subsequent increases in the T.D.S. and pH of the groundwaters due to the onset of aridity resulted in elements previously bound in beudantite being remobilized to form supergene oxidate minerals, such as mimetite, hidalgoite, cerussite and barite immediately above the water-table (Taylor et al., 1984).

Climatic and topographic modifications

The formation of gossans, as with other components of the regolith, is controlled by environmental factors determined by climate and relief. Of the climatic factors, temperature controls the rate of oxidation and rainfall controls the intensity of leaching. The relief influences the drainage status and also, therefore, the degree of leaching and dispersion. In tropically weathered terrains, the regolith, including gossans, has commonly evolved over long periods and under range of different climatic and topographic environments, as discussed in Chapters I.1, I.2 and I.3. Accordingly, the present environment is not necessarily that under which the principal characteristics of the gossan were developed. Knowledge of the weathering history, particularly the climatic history, is thus of assistance in understanding and interpreting gossan geochemistry. For the most part, this history can only be inferred from the geomorphology and features of the regolith on the country rocks, such as development and truncation of lateritic profiles, presence of introduced components (e.g. silica), and the depth and nature of transported overburden.

Climate

The most extensive studies of gossans have been confined mainly to those in semiarid to arid regions of low to moderate relief. They commonly have distinctive profiles which, when complete and mature, exhibit a vertical zonation (Fig. II.i-2) that consists of a supergene enrichment zone (sulphide minerals) at or below the water-table, an oxidate zone (sulphates, phosphates, arsenates, native elements), a zone (commonly carbonate-enriched) influenced by vadose waters, and an upper, leached, oxide zone. Overall, there is a decrease in the concentrations of target and pathfinder elements upwards through the profile so that, at the surface, the abundances of all but the immobile pathfinder elements are greatly reduced. The most mobile elements, such as Zn and Cd, tend to be leached from all zones. These profiles typically occur in deeply weathered, lateritic terrains and thus appear to be the product of intense leaching under past humid climates followed by continued oxidation under increasingly arid conditions with lowering water-tables. Elements mobilized during this second phase

reprecipitated as relatively soluble minerals, such as sulphates and carbonates, which have remained stable under the conditions of reduced leaching prevailing in the arid climate. Other components, particularly silica, may be introduced into the gossan, causing dilution.

The effects of this weathering history are reflected in the gossan geochemistry. For example, as a result of the earlier leaching, some gossans derived from Ni sulphides in now semiarid Western Australia were found to contain 0.1–2.42% Ni and 900–6000 ppm Cu (Blain and Andrew, 1977). Where they have been silicified, dilution reduces the concentrations to 0.17–0.44% Ni and 490–760 ppm Cu. In the more leached Ni gossans, the Ni/Cu ratio decreases because Cu is more strongly retained by the Fe oxides (Butt, 1981).

In very arid terrains (e.g. Sahara and Arabian deserts), any pre-existing regolith, including much of the gossan profile, has commonly been eroded. Saline groundwaters in these regions now may actively leach both fresh mineralization and any remnants of the previously-formed gossan. Under the influence of the high evaporation gradient, these waters move upwards to deposit soluble salts at the surface. Because of the low rainfall, these salts persist and accumulate. This mechanism is responsible for high concentrations of Zn in the Al Masane (3.0% Zn) and Ash Sha'ib (11% Zn) gossans in Saudi Arabia (16), compared to 2.5% in fresh mineralization. Other elements that are similarly concentrated include Cu, Pb, As, Sb, Se, Hg, Mn and Mo, whereas Ba, Co, Ni and Sn are at concentrations comparable to those in the sulphides (Ryall and Taylor, 1981).

Sulphide oxidation and leaching resulting in gossan formation are probably most active in moderately humid savanna climates similar to those that favour lateritization. However, in more humid terrains, in which the organic matter derived from decaying vegetation is more abundant, Fe derived from sulphides dissolves and becomes associated with ferrallitic soils developed over the wall rocks, rather than forming indurated gossans. Where excessive rainfall has led to the formation of stone-line profiles, any gossans that have formed will disaggregate and partially dissolve, in much the same manner as lateritic cuirasse (H. Zeegers, personal communication, 1986). These processes, together with dense vegetation, has resulted in few gossans being reported from these environments although Rose et al. (1979) give some data for gossans and ironstones (pseudo-gossans) from Sierra Leone and Borneo.

The significance of the kinetic effects of temperature have not been fully evaluated. However, gossans in temperate and cold regions tend to be less strongly leached and hence to have rather higher element concentrations than equivalent gossans in the tropics. The gossans have similar physical characteristics but differ in that only the immediate wallrocks are strongly weathered, probably by acid solutions released by sulphide oxidation, and the country rocks may well be fresh at surface. The presence of fresh rocks buffers the weathering solutions, thereby reducing the degree of leaching and the extent of secondary dispersion.

Topographic effects

Uplift may promote freer drainage and lowering of the water-table, resulting in the development of deeper gossan profiles. Conversely, however, even without climatic change, uplift may cause increased dissection of the terrain, exposing lower, less strongly leached zones of the gossan profile. As these commonly have geochemical signatures similar to those of the primary mineralization, their affiliation is seldom of any doubt (Taylor and Appleyard, 1983).

In regions of moderate to high relief, gossans may not be entirely in situ. Mechanical translocation will cause gossan fragments to disperse downslope, to be incorporated in soils and drainage sediments and possibly be recemented as translocated gossans. In humid areas, Fe and other ore-related elements may be dissolved to reprecipitate as solution-deposited gossans in seepages at the break of slope. The Al Masane Zn-Cu-Pb-Ag deposit, Saudi Arabia (16) has a good example of a relict solution-deposited gossan occurring as a thick mantle over wallrocks in the wadi. The geochemical signature of this gossan is similar to that of the in-situ gossan except that the abundances of the immobile elements are greatly reduced (Ryall and Taylor, 1981). Where relief is very high, however, erosion is so great that no gossans form and fresh sulphides occur at or very close to the surface. This situation pertains even in very humid climates (e.g. Papua New Guinea, Solomon Islands) and the only oxidized mineralization is that occurring beneath ridges and in valleys.

Element selection

The selection of elements to be used in gossan identification is of considerable importance. During the "nickel boom" (1968–1972) in Australia, it was common to analyse ironstones only for the target elements (Ni and Cu), which led to misinterpretation, unnecessary follow-up drilling and, in some instances, neglect of other types of mineralization. For example, the high Ni contents of many ironstones in the Yilgarn Block of Western Australia could be related to the high background Ni contents of lateritically weathered ultramafic rocks. At Bottle Creek, 210 km north-northwest of Kalgoorlie (26), a gossan that outcrops discontinuously over several kilometres was analysed for Ni during this period but contained only low background levels. More recently, the same gossan was found to be anomalous in Au and pathfinder elements; it has since been mined for gold. Despite the added cost, proper evaluation of gossans is only possible if a range of target and pathfinder elements are determined.

Recent experience has shown that during reconnaissance exploration or orientation surveys, samples should be analysed for a wide range of elements. The elements chosen depend in part upon the expected targets and host rocks, and should include as many as possible from the appropriate categories listed in Table II.2-3, which are related to particular lithologies. The inclusion of some negative indicator elements at this early stage of exploration may eliminate subsequent costly, detailed evaluation. For example, high concentrations of Cr in

TABLE II.2-3

Suggested suites of target pathfinder and lithophile elements to be analysed during reconnaissance surveys of gossans (elements in parentheses are negative indicators)

Host rocks	Expected mineralization	Elements
Mafic-ultramafic volcanics	Ni-Cu	Ni, Cu, Co, Pt, Pd, Ir, Te (Cr), (Mn), (Zn)
	Au	Au, Pb, As, Sb, Se, Te, Bi, W
Felsic volcanics	VMS	Cu, Pb, Ag, Au, As, Sb, Bi, Se, Hg, Sn, Ba
	Cu-Mo-Au	Cu, Mo, Au, Re
Sediments	Pb-Zn-Ag	Pb, Zn, Ag, Cu, As, Hg, Sb (Mn), (Ba), (Co), (Ni)
	Cu	Cu, As, Pb, Sb, Ag, Hg (Mn), (Zn), (Co), (Ni)
Carbonates	Pb-Zn	Pb, Zn, Cd
Lateritic ironstones	-	Al, Si, Cr, V, Ti, Mn, P
Skarns	Cu-Zn, Pb-Zn Sn, W, Au-Ag	Cu, Pb, Zn, Sn, W, Au, Ag, Mn, Ca

Ni-rich ironstones are indicative of lateritic enrichments over ultramafic rocks (see Table II.2-28). Except in alkaline environments, anomalous concentrations of Zn, Co and Ni, particularly in the presence of Mn, should be treated with some suspicion as being due to secondary enrichment. Although Ba is common in gossans associated with volcanic massive sulphide mineralization (Andrew, 1984), it may be derived the weathering of feldspars. In subsequent phases of exploration, a smaller number of elements associated with the various styles of mineralization (Table II.2-2) can be chosen for the actual gossan evaluation. As shown by Smith et al. (1984), it is seldom necessary to analyse for more than ten elements, provided that the most appropriate are chosen. The final selection may depend in part on the quality of the data and therefore the sampling, preparative and analytical techniques (see Appendices 1 and 2). With the advent of inexpensive, high quality analyses at low detection limits, it is not difficult to choose a suitable range of diagnostic elements for each stage of the evaluation programme.

DATA INTERPRETATION

Analysis of multielement geochemical data should aim to distinguish gossans from other ironstones, and ultimately to characterize various gossan types. The application of statistics to interpretation of geochemical data has been summa-

rized by Davis (1973) and Howarth (1983). Specific applications to ironstones and gossan evaluation have been described by Clema and Stevens-Hoare (1973), Joyce and Clema (1974), Bull and Mazzucchelli (1975), Moeskops (1977), Talapatra (1979), Wilhelm and Kosakevitch (1979), Ryall and Taylor (1981), Taylor and Scott (1982), Smith et al. (1983) and Andrew (1984).

Because of the high degree of overlap in the compositions of gossans and other ironstones, univariate evaluation is rarely satisfactory. This is exemplified by Ni and Cu contents in ironstones from the Yilgarn Block of Western Australia (Table II.2-28) and Cu contents in ironstones from northwest Queensland, where even the presence of secondary Cu minerals is seldom diagnostic (Tables II.2-7 and II.2-23). Two of the least mobile elements, Ba and Pb, may however be more reliable discriminants for base metal mineralization. Even though the barite at Dugald River (11) is secondary, the Ba content of the Pb-Zn gossan (Table II.2-15) is considerably higher than in host rocks or the nearby Cu gossan. High Pb contents seldom result from migration or scavenging and are extremely useful in distinguishing gossans from other ironstones. Conversely, the more mobile elements, particularly Zn, are of little value as discriminants.

The use of bivariate techniques such as correlation coefficients (Talapatra, 1979) and scattergrams (Clema and Stevens-Hoare, 1973; Joyce and Clema, 1974; Moeskops, 1977) has met with only limited success. Scattergrams do not resolve the overlap in compositions, although greater separations is achieved if group means are plotted (Andrew, 1984; Taylor and Scott, 1982).

Multivariate techniques are the most appropriate for gossan discrimination. The techniques assume that the variables have normal distributions and, as the distributions of most trace elements and some major elements are approximately log-normal, it is necessary to transform the data. Simple log transformation (base 10) is appropriate (Taylor and Scott, 1982), although power transformations (log, cube root, square root) may be preferred, depending on the distribution of each element in the various groups (Smith et al., 1983). Several statistical procedures have been used:

(1) Principal component analysis and factor analysis have only restricted application, mainly because the geological and mineralogical factors responsible for element variance are usually not well understood. Potential applications are to explain the behaviour of certain groups of elements in ironstone and gossan development under specific conditions, and to construct indices that permit factor scores to be calculated and used to compare group membership. Principal component analysis was reasonably successful in distinguishing gossans derived from Ni-Cu mineralization from other ironstones in Western Australia (Joyce and Clema, 1974). In this analysis, the first principal component of analysis (Cu and Ni) accounted for 41.6% of the variance and is related to massive Ni-Cu gossans; the second principal component (Cr, Zn and Mn), 25.9% of the variance, is related to lateritic ironstones; the third principal component (positive Zn, Cu, Mn and negative Pb, Ni and Cr), 14.6% of the variance, is unexplained. In general, the geochemical characteristics of gossans and ironstones other than those

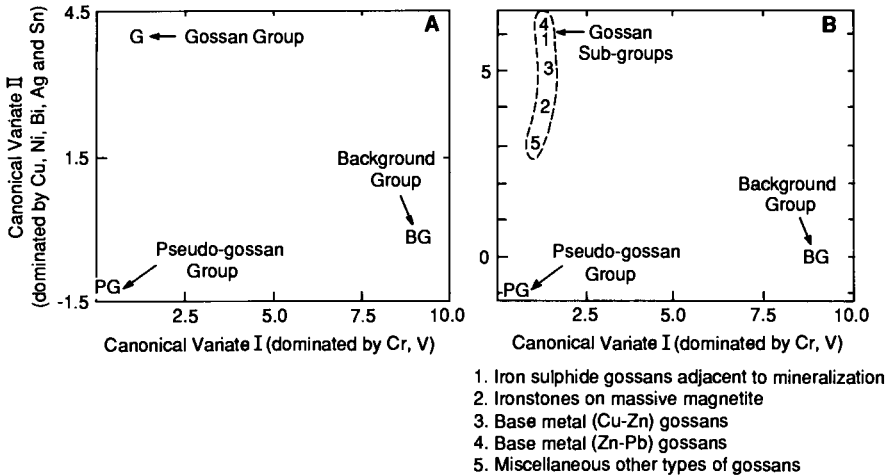


Fig. II.2-1. Canonical variate means for ironstones and gossans, Western Australia. (A) Means for three reference groups, showing marked separation. (B) The volcanogenic massive sulphide reference group subdivided into five subgroups. Redrawn from Smith et al. (1983).

related to ultramafic rocks and Ni-Cu mineralization are so variable that these techniques have little use (Taylor and Scott, 1982; Andrew, 1984).

(2) Canonical variate analysis was used successfully to discriminate between (i) Cu-Zn-Pb gossans, (ii) ironstones with anomalous geochemistry (pseudogossans) and (iii) a background ironstone group (Smith et al., 1983), all from Western Australia. All samples were analysed for 20 elements, of which 13 (Mn, Cr, V, Cu, Pb, Zn, Ni, Co, As, Bi, Ag, Sn and Ca) were used in the statistical analysis. Each element was then transformed to give a reasonable Gaussian distribution. A plot of group means for the first two canonical variates for the three reference groups (Fig. II.2-1 A) gives a marked separation. The gossan group is also separated into five subgroups (Fig. II.2-1B). The distribution of individual samples in the three reference groups is shown in Fig. II.2-2, with separation being quite distinct. Six groups of different types of ironstones and gossans were then treated as unknowns with allocations of four groups being correct, whilst one of the remaining groups has not been evaluated in the field. Samples of gossan from above the essentially barren pyrite-pyrrhotite-magnetite mineralization at Mugga Mugga (6) classified as in the gossan group, but the distinction between a barren or base metal-rich sulphide source was not made because of the absence of an appropriate reference group.

(3) Stepwise discriminant analysis has been used successfully to discriminate a variety of gossans and ironstones in southern Africa (Andrew, 1984) and to evaluate gossans in northwest Queensland (Taylor and Scott, 1982). The allocation of gossans and ironstones into six reference groups is shown in Table II.2-4 and is based upon major and trace element data. The geochemical signatures of

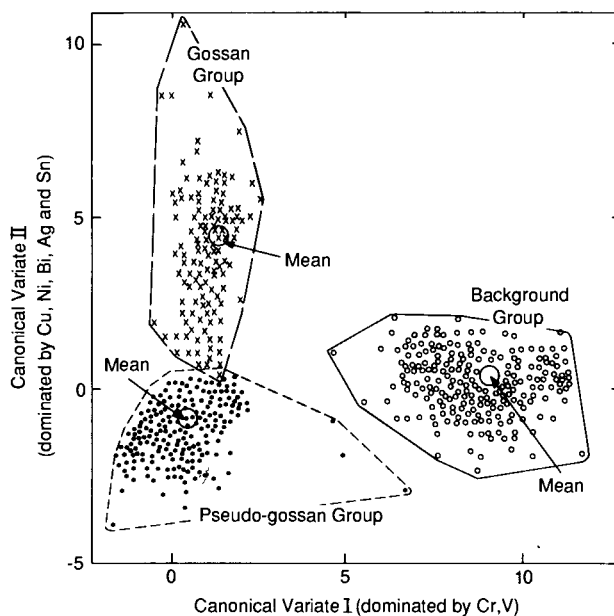


Fig. II.2-2. Plot of canonical variates I and II for individual samples of gossans, pseudogossans and ironstones from Western Australia showing separation of the three groups. Redrawn from Smith et al. (1983).

TABLE II.2-4

Classification of gossans in the Mount Isa region, northwest Queensland, Australia by discriminant analysis (figures show the numbers of samples allocated to each group by the analysis)

	Black Star	Isa Traverse	Ironstone	Dugald River	Gossan	BIF
Black Star *	18					
Isa Traverse *		36	1			
Lake Moondarra			14			2
Hilton		36	1	1		
Mount Novit		26	15	2	1	
Lady Loretta gossan		11				
Lady Loretta ironstone		20		1		
Paradise Creek Fm * (ironstone)			13			
Dugald River *		1		26		
Pegmont gossan *				1	31	
Pegmont ironstone		1	5	5		
Fairmile gossan					13	
BIF *						23
Fairmile ironstone		1				4
Soldiers Cap Fm		8	15	10	10	9
Answer Slates	4	36	2	11		5

* Type gossans and ironstones.

TABLE II.2-5

Geochemical classification of gossans from northwest Sudan derived from cluster analysis (Aye et al., 1985)

	High grade elements	Mean grade elements	Low grade elements	Probable origin
Group 1a	Cr, As, Fe ₂ O ₃	Cu, Pb, Mo	Bi, Ag, Au	Fe sulphides and/or primary oxides
Group 1b	As, Fe ₂ O ₃	Cu, Pb, TiO ₂	Cr, Bi, Ag, Au	Superficial concentration
Group 2	SiO ₂ , Bi, As, Mo, Sb	Cu, Pb, Au, Fe ₂ O ₃	Zn, K ₂ O	Cu-Zn sulphides with possible Au
Group 3	Fe ₂ O ₃ , K ₂ O	Cr, Cu, Zn, Al ₂ O ₃	As, Pb, Mo, Bi, Sb, Au	Disseminated Fe sulphides with accessory polymetallic ore
Group 4	Pb, As, Mo, Ag, Au, Ba	Cu, Zn, Bi, Sb, Fe ₂ O ₃	Cr, Ni	(Cu-Zn), Pb, Ba sulphides
Group 5	SiO ₂ (74%), Ba, Au, Sb, Sn	Bi, Pb, Mo, Ag	Fe ₂ O ₃ , K ₂ O, Ni, Cu, Zn, As	Base metals and Au sulphides
Group 6	Fe ₂ O ₃ , Mn, Co, Ni, Cu, Zn, As		Pb, Mo, Ag, Sb, Au	Gossan displaced after chemical transportation

gossans related to known genetic types or economically significant mineralization are required to maximize the characterization of the groups and hence allocate unknowns correctly. If such data are available, stepwise discriminant analysis is probably the most effective procedure for gossan identification and evaluation.

(4) Cluster analysis can be applied for exploration of completely new areas for which there are no data for comparison. In northwest Sudan, a total of 1394 gossan samples from volcano-sedimentary rocks were analysed for 32 elements (Aye et al., 1985). Cluster analysis was then used to divide the samples into seven population groups each with its distinctive geochemical signature (Table II.2-5). The groups were ranked according to their possible relationship with economic mineralization by accounting for factors such as element associations, element mobility during weathering, mineral paragenesis and known primary mineralization. The procedure distinguished (i) gossans directly related to sulphide or oxide ore, (ii) ironstones corresponding to Fe concentrations resulting from chemical transportation and (iii) three groups showing promise for base metals and Au mineralization.

LEAD ISOTOPE TECHNIQUES

The determination of Pb isotope ratios has been most commonly used for dating and in ore genesis studies, but it also has application in exploration geochemistry, particularly for the evaluation of gossans (Gulson and Mizon, 1979; Gulson, 1986). The technique is based upon recognizing the different

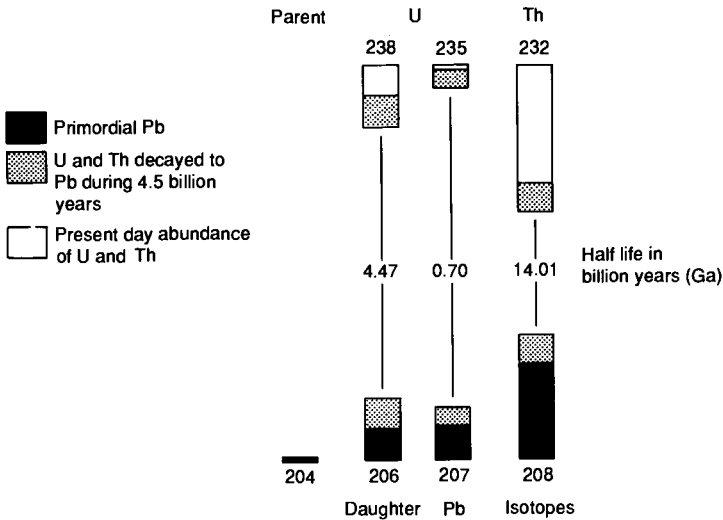


Fig. II.2-3. Radiogenic production of Pb isotopes from U and Th during the history of the Earth. N.B. The amount of ^{204}Pb has remained constant throughout the Earth's history. Modified after Gulson and Vaasjoki (1983).

isotopic signatures of country rocks, barren sulphides and potentially economic mineralization. Variations in Pb isotope ratios are due to:

- (1) radioactive decay of U and Th (Fig. II.2-3);
- (2) differences in initial U/Pb and Th/Pb ratios, arising from regional variations in the abundances of U, Th and Pb; and
- (3) mixing of Pb evolved in different environments.

Separation of Pb from U and Th to form an orebody at a particular time gives the orebody a unique set ("signature") of isotopic ratios. Most massive Pb orebodies have homogeneous isotopic signatures that lie on or close to the "growth curves" depicted in Fig. II.2-4; carbonate-hosted Mississippi Valley-type deposits, however, have anomalous signatures.

Lead-rich orebodies have very high Pb/U and Pb/Th ratios so that the isotopic ratios ($^{208}\text{Pb}/^{206}\text{Pb}$, $^{207}\text{Pb}/^{206}\text{Pb}$, $^{206}\text{Pb}/^{204}\text{Pb}$) in the orebody do not change appreciably after formation due to radioactive decay over time. In Pb-poor orebodies, however, the isotopic ratios do change with time, due to the formation of radiogenic Pb (Fig. II.2-5). The ratios may also vary markedly within the deposit, as a result of variations in initial U/Pb and Th/Pb ratios.

Isotopic signatures are not influenced by oxidation or weathering. This was demonstrated for Mount Isa-type mineralization by Gulson (1986) who showed that the isotopic signatures of six bulk gossan samples were, within experimental error, the same as those of 14 bulk samples of sulphides representing the various orebodies from which they were derived (Fig. II.2-6).

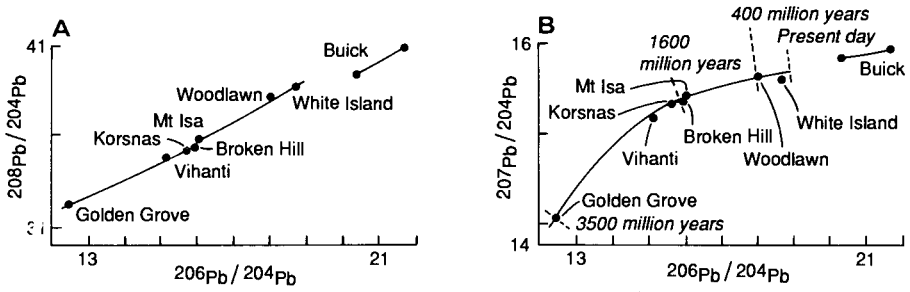


Fig. II.2-4. Lead isotopic ratio plots for the thorogenic (A) and uraniumogenic (B) isotopes illustrating the closeness of fit of major “massive” sulphide orebodies to the reference curves and their time dependence. “Buick” refers to a Mississippi Valley deposit in southeast Missouri, USA, “White Island” to a massive sulphide occurrence in New Zealand. Redrawn from Gulson and Vaasjoki (1983).

Studies of mineralization and gossans from large numbers of deposits have established the isotopic signatures for several metallogenic provinces. These signatures are significantly different from those of gossans and ironstones formed on barren Fe sulphide deposits and other Fe-rich lithologies in which the Pb and other base metals are derived from a variety of sources by remobilization during weathering. Such ironstones have a random Pb isotope signature. Based

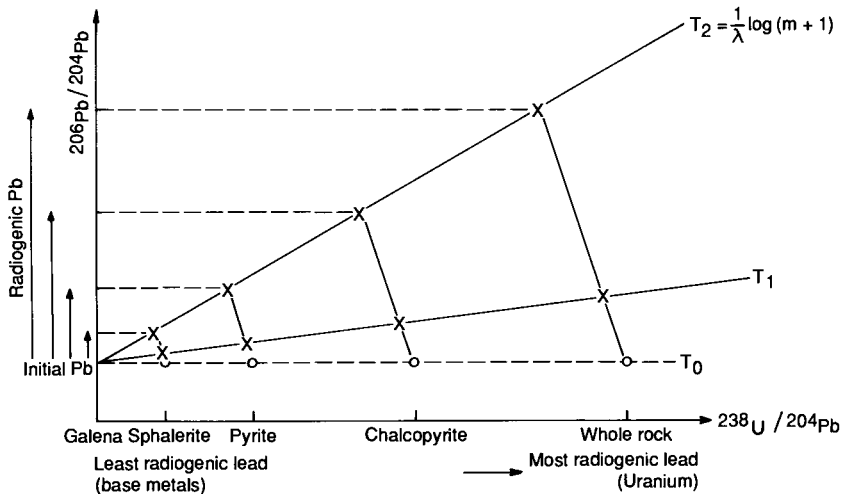


Fig. II.2-5. Evolution of Pb in a system formed at time T_0 which would then have contained isotopically identical Pb but variable amounts of Pb and U in its various components. At T_1 (or T_2), the whole rock exhibiting the highest U/Pb ratio has evolved the largest amount of radiogenic Pb, whereas the galena with negligible U has not changed at all. Sphalerite, pyrite and chalcopyrite are intermediate in behaviour. If T_2 is the present day, the different components will fall on an isochron (crosses) whose slope, m , defines the age of the system. Redrawn from Gulson and Vaasjoki (1983).

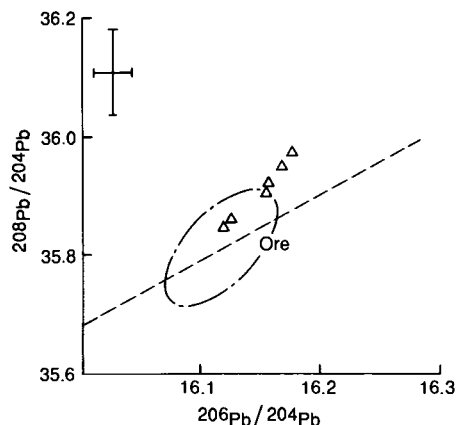


Fig. II.2-6. Ratio plot illustrating the coherence in isotopic composition from primary sulphides and gossans at Mount Isa (Gulson, 1986).

on studies of 48 case histories, comprising 21 Pb-rich orebodies, seven Pb-poor orebodies and 20 other ironstones, Gulson (1986) claimed a success rate of 80% for the classification of gossans and ironstones. The technique could, for example, discriminate ironstones with low base metal potential from gossans derived from Mount Isa-type mineralization. Similarly, ironstones from five prospects approximately 100 km south of Cloncurry were examined to determine whether

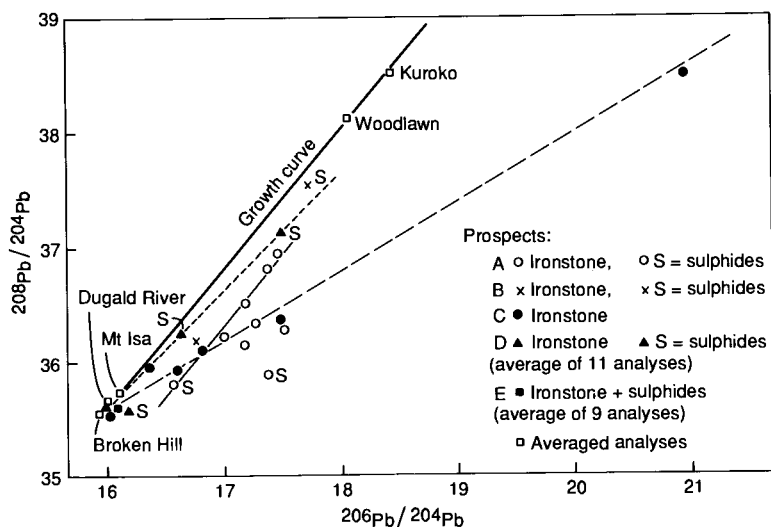


Fig. II.2-7. Ratio plot for ironstones and underlying sulphides from northwest Queensland compared with other Proterozoic base metal deposits. From Gulson and Mizon (1979).

TABLE II.2-6

Characteristics of gossans described in the text

	Climate (Köppen)	Depth of weathering m	Secondary mineralogy	Anomalous geochemistry
<i>Ironstones</i>				
1. Johnson Creek	BShw	120	gt-hm	Cu (Ba)
2. Killara	BWh	35	gt	Cu, Zn, Mn, (Co), (Ni)
3. Paradise Valley	BShw	80–100	hm-gt	Cu, As, Co
4. Western Cape Province	BSh	–	gt-(hm)	Mn, (Zn), (Co), (Ni)
5. Northeastern Algeria	BShs	–	gt-hm-al-sc	As, V, Zn, Ba, Cu, Mn, Sb
<i>Barren gossans</i>				
6. Mugga Mugga	BShs	80	hm-gt	Pb, Cu, Ag, As, Sb
7. Wadi Wassat	BSh	40	hm-gt-jr	–
8. Uniondale	Csb	–	hm-gt	Ti, Cr
<i>Pyritic envelopes</i>				
9. Mount Isa	BShw	50–55	gt-hm	Ag, As, Cu, Mo, Pb, Sb, Zn
10. Lady Loretta	BShw	100–200	gt-hm-ba-gt	Ag, As, Ba, Pb, Sb
<i>Stratiform Pb-Zn-Ag</i>				
11. Dugald River	BShw	22	gt-ba-al-jr	Ag, As, Ba, Cd, Cu, Pb, Sb,
12. Pegmont	BShw	50	hm-gt-al-jr-mu	Zn, Pb, Mu
13. Namoon	Aw	20	hm-gt-ce-an-pm al-jr-mn	Ag, As, Cd, Co, Cu, Ni, Pb, Sb, Sn, V, Zn
<i>Volcanogenic massive sulphides</i>				
14. Archaean deposits	BShs	10–75	hm-gt-al-jr	Cu, Pb, Zn, Ag, As, Bi, Mo,
15. Benambra	Cbf	variable, down-dip	hm-gt-d-jr	Sb, Se, Sn
16. Al Masane	BSh	40	hm-gt-zn	Ag, As, Ba, Bi, Cu, Hg, Pb, Zn
17. Letaba	BSh	25	hm-gt-az-ma	Zn, Cu, Pb, Mn, As, Co Cu, Pb, Zn
<i>Carbonate-hosted Pb-Zn</i>				
18. Rosh Pinah	BWn	20	mn-al-jr-zn-ba (gt)-(hm)	Ag, Ba, Cd, Cu, Mn, Pb, Zn
19. Northeastern Algeria	BShs	–	gt-hm-sm	As, Ba, Cd, Mo, Ni, Pb, Sb, Zn
20. Kamarga	BShw	20	(gt)-(hm)	As, B, Cu, Pb, Zn
<i>Copper</i>				
21. Great Australia	BShw	~ 25	hm-gt-az-ma	As, Co, Cu, Ni
22. Gunpowder	BShw	20	(hm)-(gt)	Ag, As, Cu, Hg
23. Matchless Amphibolite Belt	BWn	15–30	gt-hm-ba-ma	Ag, Ba, Cu, Pb, Ti
<i>Porphyry</i>				
24. Berg	Bsk		(gt)-(hm)	Cu, Mo, Pb, Ag
<i>Gold</i>				
25. Mount Leyshon	Caf	50	jr-al-hem	Au, Ag, As, Bi
26. Bottle Creek	BShs	80	hm-gt-jr	Au, As, Ba, Cu, Hg, Pb, Sb, Zn
27. Telfer	Bwh	100	hm-gt-qt	Au, Ag, As, Co, Cu, Ni, Pb, Se, W

TABLE II.2-6 (continued)

	Climate (Köppen)	Depth of weathering m	Secondary mineralogy	Anomalous geochemistry
<i>Nickel (-copper)</i>				
28. Yilgarn Block	BShs	various	hm-gt-qt	Co, Cr, Cu, Mn, Pb, Ir, Pt, Pd, Se, Te
29. O'Toole	Aw	-	hm-gt-qt	Co, Cr, Cu, Ni, Pt, Pd, Rh, Ir
<i>Skarn</i>				
30. Ar Ridaniyah	BWh	~ 25	gt-hm-jr-Zn	Zn, Cu, Pb, Sn Bi, Mn
31. Squirrel Hills prospects	BShw	30	gt-hm-mn- al-jr	Mn, Pb, Zn, (Cu), (P)
<i>Others</i>				
32. Elura	BShw	106	hm-gt-al-jr	Ag, As, Ba, (Cu), Hg, Pb, Sb, Sn, Zn
33. Mount Torrens	Csb	40	hm-gt-al-jr	Ag, As, Ba, Cu, Mo, Pb

gt = goethite, hm = hematite, qt = silicification, al = alunite, jr = jarosite, sc = scorodite, ba = barite, pm = pyromorphite, mn = Mn oxides, ce = cerussite, an = anglesite, zn = smithsonite, willemite, hemimorphite, az = azurite, ma = malachite, sm = smithsonite, () = trace to minor.

they were derived from Proterozoic orebodies of the Mount Isa type (Gulson and Mizon, 1979). Extensive multielement analysis indicated that prospects A, D and possibly C warranted further investigation (prospect E was not studied). On the basis of the Pb isotope data (Fig. II.2-7), only D and E are promising for base metal mineralization, with the uniformity of data for prospect E being the most encouraging.

The Pb isotope technique may lead to a reliable assessment of the potential of a particular ironstone using only five or six samples. The cost is compatible with that for multielement analysis using, for example, ICP-MS, but few laboratories offer it as a routine procedure.

CASE HISTORIES

The following case histories are representative of gossans and ironstones formed on different styles of mineralization and lithologies in different climatic and geomorphological environments. The compilation is not comprehensive, but illustrates the effects of factors previously described in this and other chapters. A synopsis based upon present climatic environment, type of mineralization and anomalous geochemistry is presented in Table II.2-6.

Ironstones

Johnson Creek, Queensland, Australia (1). Several goethite-, hematite- and quartz-rich ironstones outcrop as resistant ridges up to 2 m high in a flat area of

TABLE II.2-7

Composition of ironstones from Johnson Creek and Paradise Valley, northwest Queensland, Australia

	Johnson Creek (N = 17)		Paradise Valley (N = 22)	
	Mean ppm	Range ppm	Mean ppm	Range ppm
Ag	< 1	< 1	< 1	< 1
As	47	10-95	230	80-380
Ba	170	< 10-600	360	30-980
Co	20	< 20-60	140	40-250
Cu	1800	500-4000	6500	1300-3.2%
Mo	3	< 3-6	10	2-30
Ni	15	10-25	65	4-150
Pb	7	1-20	20	10-40
Sb			< 30	< 30
Sn	6	1-10	< 1	< 1
Zn	42	10-70	65	15-2102

mid-Proterozoic carbonate-rich siltstones approximately 65 km north-northwest of Mount Isa. These ironstones were sampled in the early 1970s and found to have anomalously high Cu concentrations (500-4000 ppm). A diamond drill hole beneath the ironstones intersected minor pyrite-chalcopyrite mineralization along bedding planes and dewatering cracks. Subsequent mineralogical examination of core samples revealed siderite-rich rocks (Taylor, 1973) which upon weathering resulted in the formation of *stratigraphic ironstones* with box-works after carbonates. Multielement analysis of the ironstones (Table II.2-7) has shown that only Cu (and possibly Ba derived from detrital feldspar) is anomalous. Lack of anomalous concentrations of any of the pathfinder elements normally associated with stratabound Cu mineralization indicates that these are not gossans. Goethite and hematite formed by weathering of siderite to a depth of 120 m (well below the regional base of oxidation at 57 m) have concentrated Cu from groundwaters leaching the surrounding country rocks. The present semiarid tropical climate has ensured that Cu is not being leached from these ironstones.

Killara, Western Australia (2). Immediately north of the Yilgarn Block and 56 km northeast of Meekatharra, lower Proterozoic volcanics, sandstones, carbonaceous shales and carbonates have been weathered to a depth of approximately 35 m. Ironstones outcrop on the pediment of a low hill capped by lateritic duricrust and were sampled on lines 10 m apart; they were analysed initially for Ag, Cu, Ni, Pb and Zn and then for a wider selection of elements by XRF and OES. The 550 ppm Cu contour defines a distinct anomaly of about 10×35 m within which the highest Cu contents (1100-1850 ppm) occur in "gossanous" samples, some with an apparent boxwork fabric (Butt, 1979). No other elements have a similar distribution to Cu; some ironstones are moderately enriched in Zn

TABLE II.2-8

Composition of ironstones from Killara, Western Australia (Butt, 1979)

	High Cu N = 4		Intermediate Cu N = 6		High Zn N = 3	
	Mean ppm	Range ppm	Mean ppm	Range ppm	Mean ppm	Range ppm
As	< 10	< 10-16	< 10	< 10-11		
Ba	418	14-1380	890	95-3115	570	80-1230
Ce	20	< 10-50	12	< 10-40	18	< 10-30
Co	65	35-90	90	75-115	105	85-120
Cr	50	< 10-80	46	10-190	25	14-40
Cu	1655	1245-1810	650	580-895	95	50-165
Fe%	52.8	42.5-57.6	47.9	31.5-57.2	52.3	48.9-56.4
Mn	205	145-330	465	50-960	270	195-345
Ni	30	25-50	55	20-120	140	120-165
Pb	16	15-20	20	< 5-25	20	15-24
TiO ₂ %	0.38	0.05-0.57	0.21	0.09-0.38	0.22	0.16-0.32
Sb	15	12-20	12	< 5-16	15	13-18
V	145	40-215	255	140-560	40	35-50
Zn	195	175-205	330	25-535	570	410-660

(maximum 690 ppm) but these are rarely enriched in Cu, and follow a different trend. Typical multielement analyses are given in Table II.2-8.

Drilling failed to locate more than traces of pyrite and chalcopyrite and it is considered that Mn and Fe oxides and oxyhydroxides precipitated on the contact between carbonaceous shale and dolerite have concentrated trace elements. It is therefore believed that the Killara pseudogossan is a *contact ironstone*, particularly as Ag, As, Bi, Cd, Zn, Mo, Sb, Sn and W are below the limit of detection of XRF and OES. The presence of minor concentrations of Zn, Co and Ni are an indication of 'scavenging' by Fe and Mn oxides.

Paradise Valley, Queensland, Australia (3). About 50 km north of Johnson Creek, Cu mineralization occurs in the Paradise Valley area. This mineralization commonly outcrops as gossan or Fe-stained rock with secondary Cu minerals. Extensive exploration in the area was aimed at finding more Cu mineralization to enhance the economics of mining the known deposits. Many ironstones were analysed and the data compared with those from above known mineralization. Typical data for samples from one such ironstone, in which many of the pathfinder elements occur in anomalous concentrations, are compared with those from Johnson Creek on Table II.2-7. Drilling beneath the 150 × 20 m ironstone outcrop failed to intersect significant Cu mineralization but did intersect a major fault. The outcrop has been interpreted as a *fault ironstone* in which groundwaters charged with elements from nearby mineralization have precipitated Fe oxides and a suite of trace elements, which are distinctively

TABLE II.2-9

Composition of ironstones from Berg River and Vredendal, western Cape Province, South Africa (Andrew, 1984)

	Berg River N = 19		Vredendal N = 10	
	Mean ppm	Range ppm	Mean ppm	Range ppm
Ag	2	<1-4	3	<1-8
Ba	35	10-850	105	55-1100
Ca	750	300-2500	1200	400-4200
Cd	1	<1-5	2	<1-3
Co	14	10-300	80	30-200
Cr	102	50-205	80	60-150
Cu	30	5-210	50	30-105
Fe%	28	2-56	55	52-58
Mg	680	130-3400	470	280-730
Mn	2100	200-1.6%	1000	120-2500
Ni	70	10-600	120	80-250
Pb	21	10-170	35	28-75
Ti	180	100-2100	250	100-800
Zn	150	30-700	550	200-2000

zoned along strike. It may also be considered as a *leakage gossan* which, although not directly related to mineralization, indicates nearby Cu sulphides.

Western Cape Province, South Africa (4). In his comprehensive study of ironstones and gossans in southern Africa, Andrew (1984) analysed ironstones from the Berg River, and from a locality near Vredendal, 100 km and 240 km respectively north-northeast of Cape Town. In both areas, the ironstones that overlie slates, phyllites and dolomites are associated with lateritization of the post-African surface. Along the Berg River, they occur as ridges 10-15 m high and up to 100 m long, whereas at Vredendal they are flat-lying and cap quartz-sericite phyllites. The ironstones are composed principally of goethite and quartz, with minor hematite and residual mica. The tabulated geochemical data for these ironstones (Table II.2-9) does not show that the high Fe-Co-Ni-Zn values are coincident, but does indicate overall rather high abundance of Mn. These elements have been leached from the underlying phyllites and concentrated in Fe and Mn oxides. However, concentrations of other elements are low and despite pseudogossanous fabrics, these ironstones should not be mistaken for gossans.

Djebel Debagh and Tadergound, northeast Algeria (5). Gossans and ironstones occur in the coastal range of northeast Algeria at moderate elevation (1000-2000 m) and high relief. The gossans are associated with varying types of

TABLE II.2-10

Composition of ironstones from Djebel Debagh and Tadergound, northeast Algeria (Hanssen and Bourezg, 1990)

	Djebel Debagh N = 15		Tadergound N = 21	
	Mean ppm	Range ppm	Mean ppm	Range ppm
As	476	96-5000	183	28-7000
Ba	58	17-534	637	104-1.8%
Cd		< 1-84		< 1-60
Co	22	17-34	13	6-34
Cu	16	< 1-333	267	< 1-6000
Fe%	59	55-63.8	31.6	7.4-66
Mg	887	544-1320	3400	1510-2.2%
Mn	169	35-291	6500	1010-3.5%
Mo	17	13-22	18	2-35
Ni	51	31-289	40	18-87
Pb			6	< 1-403
Sb	27	3-150	195	33-1354
Sr	4	< 1-16	20	< 1-1190
Ti	30	< 1-358	10	< 1-291
V	66	19-461	3	< 1-21
Zn	236	19-461	71	23-307

mineralization in carbonates and aluminosilicate rocks and are readily distinguished from ironstones by the application of factor analysis to the geochemical data (Hanssen and Bourezg, 1990). At Djebel Debagh, a goethitic ironstone overlies white halloysite with minor gibbsite and alunite in a karstic infilling. The goethite and hematite exhibit solution-deposited textures. The ironstone at Tadergound is similar to that at Johnson Creek (1) in that it is derived from the weathering of massive siderite deposits which occur along faults in Jurassic carbonates.

Both ironstones have anomalous concentrations of some elements (Table II.2-10): As, V and Zn with secondary scorodite ($\text{FeAsO}_4 \cdot 2\text{H}_2\text{O}$) at Djebel Debagh, and As, Ba, Cu, Mn and Sb together with a variety of minor secondary Cu minerals at Tadergound. The origin of scorodite and the anomalies at Djebel Debagh are unknown, although they can reasonably be assumed to be due to precipitation from acid solutions which also resulted in the formation of hydrothermal halloysite, gibbsite and alunite. The high As content may indicate a nearby deposit of Au. At Tadergound, the anomalies and secondary minerals are due to the presence of minor tetrahedrite-tennantite and barite in the replacement siderite, with little dispersion having taken place in the high pH environment.

Lateritic ironstones. Lateritic cuirasse developed over unmineralized ultramafic rocks may contain high concentrations of Ni and Cu and hence resemble gossans over Ni mineralization (see Yilgarn Block, Western Australia (28)). However, they are commonly also enriched in Cr and V, which serve to identify their origin.

Barren gossans

These are perhaps the most common form of gossans, but they are seldom described in detail because of their limited economic significance. They are developed on pyrite and pyrrhotite mineralization that contains only minor amounts of other sulphides. The concentrations of trace metals in gossans derived from such mineralization are low not only because of the low initial abundance but also because the highly acid conditions resulting from the oxidation of the Fe sulphides cause severe leaching. However, if the gangue or wall rocks are reactive (e.g. carbonate bearing), the higher pH that results may permit stable secondary minerals to form and retain base metals. Nevertheless, the absence of some pathfinder elements and subdued geochemical signatures should

TABLE II.2-11

Composition of barren gossans from Mugga Mugga (Taylor and Sylvester, 1982), Golden Grove (Smith et al., 1979) and Freddie Well (Smith et al., 1976) in the Yilgarn Block, Western Australia

	Mugga Mugga N = 16		Golden Grove				Freddie Well N = 6
	Mean ppm	Range ppm	Barren gossan N = 36		Magnetite ironstone N = 30		
			Mean ppm	Range ppm	Mean ppm	Range ppm	
Ag	5	1-14	1.6	0.2-10	0.3	< 0.1-15	< 0.1-0.1
As	370	110-600	575	< 50-3470	< 50	< 50-200	< 10
Ba	100	< 10-400	72	20-170	n.d.	n.d.	
Bi	4	< 4-16	160	< 1-560	20	< 1-175	< 1-1
Cd	< 1	< 1	< 3	< 3	< 3	< 3	< 3
Co	< 5	< 5	< 5	< 5-17	50	< 5-150	15-60
Cr	75	20-190	< 20	< 20-68	< 20	< 20-70	n.d.
Cu	140	55-230	1570	460-3060	790	< 5-1%	65-330
Mn			100	5-350	230	< 10-800	
Mo	4	1-9	< 3	< 3-10	12	< 3-250	< 3-15
Ni	5	< 5-10	< 5	< 5-10	< 5	< 5-40	< 5-5
Pb	135	19-500	70	23-150	20	5-120	5-15
Sb	15	< 4-110	33	10-90	40	15-75	5-10
Se			21	5-65	10	< 1-140	
Sn	< 4	< 4-10	270	< 1-3810	54	< 1-210	< 1-1
Te	< 1	< 1	< 1	< 1	< 1	< 1	< 1
W	25	< 10-55	34	< 10-125	45	10-105	< 10
Zn	65	35-120	195	16-580	30	< 5-215	18-250

be diagnostic of a barren gossan, particularly if multivariate statistics are used for discrimination.

Mugga Mugga, Western Australia (6). This prospect is located in the Archaean Yilgarn Block, about 50 km north of the Golden Grove (14B) Cu-Zn deposit. It occurs in felsic tuffs that have been weathered to 80 m close to the mineralization, but fresh amphibolite outcrops nearby. The massive, steeply-dipping stratabound pyrite-pyrrhotite-magnetite mineralization is capped by a massive gossan 400 m long and up to 50 m wide consisting of hematite, goethite and

TABLE II.2-12

Mineralogy and geochemistry of the barren gossan profile at Mugga Mugga, Western Australia (Taylor and Sylvester, 1982)

<i>Mineralogy (average XRD peak heights)</i>								
Depth (m)	Qtz	Kaol	Dick	Chlor	Mica	Goeth	Hem	Alun
0.00-14.4	18	6			1	19	70	
14.04-25.14	60	36	4		2	21	28	3
25.14-34.10	29	5	1		3	38	4	
34.10-52.42	59	23	2	3	27	30	8	6
52.42-68.80	160	9		1	9	34	12	4
68.80-73.39	74	5			6	27	21	3+Crist

Qtz = quartz, Kaol = kaolinite, Dick = dickite, Chlor = chlorite, Goeth = goethite, Hem = hematite, Alun = alunite, + Crist = cristobalite occurring with quartz.

Profile geochemistry (Data in ppm)

Depth (m)	Cu	Pb	Zn	Ag	As	Hg (ppb)	Sb	Co	Ni	Mo
0.00-14.04	140	150	50	8	380	20	15	55	80	5
14.04-25.14	160	440	60	4	300	30	30	105	180	15
25.14-34.10	170	170	120	8	290	30	60	60	135	11
34.10-52.42	220	2730	130	6	270	30	110	100	390	8
52.42-68.80	55	2600	125	5	200	55	140	110	200	15
68.80-73.39	15	1120	110	8	230	230	60	110	220	10
73.39-83.50	140	1100	790	2.5	65	230	11	190	320	4

	Sn	W	Ba	Sr	Ga	Ge	Cr	V	Zr	Y
0.00-14.04	1	< 8	35	3	3	3	140	35	25	< 2
14.04-25.14	2	< 8	35	3	3	3	140	35	25	< 2
25.14-34.10	2	< 8	20	6	3	2	260	170	60	7
34.10-52.42	2	< 8	160	60	4	5	380	300	80	15
52.42-68.80	3	21	90	35	4	4	400	110	140	6
68.80-73.39	2	130	250	15	3	1	120	110	180	2
73.39-83.50	1	20	1890	190	6	0.2	190	95	100	11

quartz (Taylor and Sylvester, 1982). The compositions of outcrop gossan samples (Table II.2-11) are noticeably more uniform than most other gossans and reflect the homogeneity of the mineralization. Of the elements commonly associated with volcanogenic massive sulphide (VMS) mineralization, Pb, Cu, Zn, Ag, As and Sb are present in low but anomalous concentrations in the gossan, but no Hg, Mo, Sb, Se and Sn were detected. This geochemical signature indicates that no significant base metal mineralization is present at Mugga Mugga. Geochemical data for barren gossans at Golden Grove (14B) and Freddie Well (14C) in the Yilgarn Block are included in Table II.2-11 for comparison. The higher values for Cu, As, Bi, and Sn at Golden Grove possibly reflect the proximity of the barren gossans to those on base metal mineralization.

The whole gossan profile at Mugga Mugga was sampled by a down-dip diamond drill hole. The profile was found to be distinctively zoned, with alunite-jarosite minerals at the base, a slight increase in carbonate content higher up the profile and a high hematite content in the oxide zone. The mineralogy and geochemistry of each zone is given in Table II.2-12 and indicates that, in part, element concentrations are influenced by mineralogy (e.g. Pb is associated with alunite-jarosite minerals) and that the majority of elements are depleted towards the surface. In the massive sulphide immediately below the water-table, pyrrhotite has been completely leached and some secondary siderite and marcasite have been precipitated. At the water-table, a massive ferruginous chert has formed by the deposition of silica leached from the wallrocks. Superimposed upon the oxide zone are ferruginization and mottling related to lateritization and, at 35–52 m, the influence of some sulphide-wallrock reactions.

Wadi Wassat, Saudi Arabia (7). This area in the southern part of the late Proterozoic Arabian Shield, 620 km southeast of Jeddah, is prospective for volcanogenic massive sulphide (VMS) deposits. Gossans consisting predominantly of hematite, goethite and quartz, with minor gypsum and jarosite, occur discontinuously over a strike length of 20 km. They outcrop at the crests of hills and ridges in an area of moderate relief. On steeper slopes, translocation and solution-deposition have resulted in gossans up to 100 m wide. There is some concentration of trace elements in surface gossans due to extreme aridity, as normally observed in Saudi Arabia (Table II.2-13), but their total abundance is low (Blain, 1981; Ryall and Taylor, 1981). A series of diamond drill holes revealed massive and disseminated pyrite and pyrrhotite with traces of chalcopyrite and sphalerite in a sequence of volcanoclastic and sedimentary rocks. Discriminant analysis showed the compositions of the gossans to be typical of barren gossans in the Arabian Shield and quite distinct from fertile gossans (Ryall and Taylor, 1981).

Uniondale, southern Cape Province, South Africa (8). This prospect, approximately 425 km east of Cape Town, is located where very weak pyrite mineralization occurs within steeply dipping shales of the Cape Supergroup. It lies on a

TABLE II.2-13

Composition of barren gossans from Wadi Wassat, Saudi Arabia (Ryall and Taylor, 1981) and Uniondale, South Africa (Andrew, 1984)

	Wadi Wassat			Uniondale barren gossan	
	Sulphide N = 15	Gossan N = 55		N = 20	
	Mean ppm	Mean ppm	Range ppm	Mean ppm	Range ppm
Ag	0.9	< 0.2		1	< 1-3
As	30	40	1-200		
Au	< 0.1	< 0.2			
Ba	110	550	5-2500	20	10-90
Bi	< 4	< 4			
Ca				270	50-950
Cd				3	< 1-5
Co	30	20	5-70	60	20-80
Cu	30	17	4-80	30	20-100
Cr				220	102-400
Fe%	37	30	3-62	43	12-57
Hg (ppb)	< 50	20	2-30		
Mg				170	100-500
Mn	270	100	20-2100	250	28-270
Mo	10	18	2-80		
Ni	40	20	10-140	18	10-40
Pb	10	6	1-26	40	10-70
S%	40	0.4	0.1-5.8		
Sb	25	20	2-90		
Se (ppb)	90	260	10-1240		
Sn	< 4	5	2-16		
Te (ppb)	40	< 20			
Ti				2500	1000-9000
Tl	< 10	< 10			
Zn	55	16	10-30	22	20-35

gentle slope on the flanks of an erosional surface characterized by lateritic and silcrete duricrusts (Andrew, 1980). Variably silicified red hematite-rich gossan is exposed over a strike length of 50-60 m as a low ridge, and boulders and pebbles of gossan float form an extensive halo around the outcrop. Only Cr and Ti occur in anomalous concentrations (Table II.2-13) and are derived from the weathering of the shales.

Gossans on pyritic envelopes

Base metal mineralization is commonly surrounded by an extensive primary halo or envelope of pyrite, pyrrhotite and, in places, magnetite or Fe-rich carbonates. On weathering, these envelopes form ironstones and gossans that

TABLE II.2-14

Composition of gossans formed on pyritic (Mount Isa) and pyritic/sideritic (Lady Loretta) envelopes about base metal mineralization, northwest Queensland (Taylor and Scott, 1982)

	Mount Isa				Lady Loretta		
	Orebody gossan N = 17		Pyritic gossan N = 31		Ore N = 11	Pyrite N = 4	Siderite N = 5
	Mean ppm	Range ppm	Mean ppm	Range ppm	Mean ppm	Mean ppm	Mean ppm
Ag	31	< 1-300	16	1-100	34	26	7
As	685	45-3380	540	210-1610	1080	280	76
Ba	50	< 5-825	540	10-4050	2.27%	850	510
Bi	1	< 1-7	< 1		3	< 1	< 1
Cd	20	< 1-300	7	< 1-50	< 1	< 1	< 1
Co	52	5-100	37	< 10-300	< 10	< 10	< 10
Cu	1180	390-5.75%	500	75-2500	55	9	36
Mo	53	< 3-300	14	5-70	25	3	3
Ni	87	10-300	37	< 5-100	5	< 5	5
Pb	6.9%	800-31.3%	4900	240-2.1%	1630	890	212
Sb	270	< 30-800	100	< 30-300	610	530	60
Zn	6800	450-9.2%	3250	540-770	82	123	28

have geochemical signatures characteristic of the base metal mineralization. The two examples selected illustrate Pb-Zn-Ag mineralization with envelopes of pyrite (Mount Isa) and pyrite-siderite (Lady Loretta).

Mount Isa, northwest Queensland, Australia (9). Mineralization at Mount Isa occurs as a number of orebodies (defined by a cut-off grade) in a thick sequence of mid-Proterozoic pyritic black shales. The orebodies are notably poor in Fe sulphides and are thought to represent pulses of base metal exhalation during deposition of pyrite in a sedimentary pile. The deposit was discovered by early prospectors who recognized that conspicuous ridges up to 10 m above the surrounding plain were outcropping gossans. The majority of these gossans are developed on the pyritic envelope and, because of the fine grain size of the sulphides, consist of massive goethite and hematite with no boxworks, although in some instances laminations are preserved. These gossans are highly anomalous in Ag, As, Cd, Co, Cu, Mo, Ni, Pb, Sb and Zn, concentrations well above those characteristic of barren gossans (Table II.2-14). There has been less leaching of the more mobile elements because acid produced during oxidation of the pyrite was quickly neutralized by carbonate in the gangue and wall rocks. Secondary alunite-jarosite minerals are hosts to Pb and many other elements (Scott, 1987).

The outcrop of the orebodies themselves is very restricted (Smith, 1965; Taylor and Scott, 1982). Because of the low Fe content of the ore, the gossan is

not highly ferruginous and is composed of Pb- and Zn-rich secondary minerals and has high concentrations of other trace elements. The fabric of the folded and crenulated bedding of the ore is well preserved.

Lady Loretta, Queensland, Australia (10). This deposit is near Paradise Valley (3), 115 km north-northwest of Mount Isa. The Pb-Zn-Ag mineralization occurs in mid-Proterozoic dolomitic siltstones and pyritic carbonaceous shales (Carr, 1984) and outcrops as a small gossan on the western limb of a synclinal fold. Prominent ironstone ridges of hematite, goethite, chert and barite that comprise most of the ferruginous outcrop on both limbs of the syncline are derived from the sideritic and pyritic envelope that encloses the mineralization. They occur immediately below a lateritized plateau surface approximately 60 m above the surrounding plain.

Analyses of outcrop samples (Table II.2-14) show that Ag, As, Ba, Pb and Sb are anomalous in each of the three types of ironstone, with a progressive decrease from ore gossan through pyritic gossan to ironstone after siderite. The anomalies in the siderite are due to a primary halo of target and pathfinder elements (Carr, 1984) and would themselves be sufficient to indicate base metal mineralization. Considerable mechanical and hydromorphic dispersion from these ironstone ridges gave rise to a widespread soil anomaly that led to the discovery of this deposit (see Fig. III.3-24). Initial drilling intersected 7.6 m of oxidized Pb mineralization (cerussite and anglesite) averaging 21.2% Pb, indicating a supergene enrichment in this carbonate-rich environment.

Stratiform Pb-Zn-Ag mineralization

At least two distinct styles of stratiform base metal mineralization are recognized, but both are believed to have a sedimentary exhalative origin. Apart from the large Sullivan deposit in British Columbia, Canada, which has no outcrop, a number of more recently discovered deposits (e.g. Howards Pass, northern Canada and Red Dog, Alaska) are probably related and have well-developed gossans, but unfortunately no geochemical data are available. The three case histories cited here (which are additional to Mount Isa (9) and Lady Loretta (10)) are from Australia. Gossans formed on these deposits well illustrate the effect of mineralogy on the resultant geochemistry. The generally high metal to Fe sulphide ratio results in a moderately acid to neutral pH on oxidation and the formation of a wide range of secondary Pb and Zn minerals. The presence of Mn-bearing minerals in Broken Hill style mineralization (van Moort and Swenson, 1982) results in the formation of a variety of Mn oxides, with their well-documented scavenging properties, and some distinctive Mn minerals (e.g. coronadite). Such gossans are also usually characterized by extremely high Pb contents.

Dugald River, Queensland, Australia (11). The Dugald River Zn-Pb-Ag lode is a thin (< 10 m), steeply dipping, lenticular body of pyrrhotite, pyrite, sphalerite and subordinate galena occurring in a black graphitic shale approximately 90 km northeast of Mount Isa. Outcrop is a well-defined gossan, 2.5 km long, of friable black graphitic material between more resistant, topographically higher, quartzose gossan at the contacts with the wallrocks (Taylor and Scott, 1983). Detailed analyses of part of the gossan (Table II.2-15) show that it has an extremely high content of target and pathfinder elements. They also indicate that the trace element contents of subcropping gossan are significantly greater than at the surface, reflecting leaching by downward percolating groundwaters. Gossans on the Cu mineralization in the hanging wall at Dugald River also have highly anomalous contents of target and pathfinder elements.

The gossan profile was studied by sampling a down-dip diamond core which intersected fresh mineralization at a depth of 21.65 m. Immediately above the fresh sulphide, there is a 2 m thick zone of slightly leached ore, coated with gypsum derived by acid leaching of calcite gangue. There are some mineralogical variations in the oxide zone, but it consists mainly of brown goethitic shale with yellow earthy secondary Pb minerals (Taylor and Appleyard, 1983). Barite, which is present throughout the profile, is secondary, derived from the weathering of hyalophane (Ba-feldspar). The immaturity of this gossan profile, and the consequent extremely high levels of target and pathfinder elements, are due to the relatively low Fe sulphide content of the mineralization, reactive gangue and wall rock minerals, and extensive truncation of the profile. The gossan has a distinctive geobotanical anomaly associated with it (Cole, 1977).

Pegmont, Queensland, Australia (12). Mineralization at Pegmont is similar to that at Gamsberg and Aggeneys (Cape Province, South Africa), Broken Hill (New South Wales, Australia) and elsewhere in the mid-Proterozoic Soldiers Cap Formation of northwest Queensland. The most distinctive features of this style of mineralization is the virtual absence of Fe sulphides, the presence of quartz magnetite garnet apatite BIF, and a high Mn content. Pegmont is 175 km southeast of Mount Isa in an area of low relief; oxidation extends to a depth of 50 m. The gossan forms a distinctively black, resistant ridge rising to 10 m above the plain. There has been considerable truncation of the profile and at least half of the original orebody is considered to have been eroded.

The mineralogy of the oxidized profile is complex and includes hematite, goethite, quartz, various secondary Pb minerals, Mn garnet, graphite and a variety of Mn oxides (Scott and Taylor, 1987). Apart from Pb and Zn, most pathfinder elements are at very low concentrations in the surface gossan compared to gossans from other deposits of this type (Table II.2-16), reflecting their generally low abundances in fresh mineralization at Pegmont and other prospects in the Soldiers Cap Formation. Nevertheless, these gossans are uniquely characterized by their high Mn and P contents (Taylor and Scott, 1982). They are, of course, differentiated from barren BIF by the Pb and Zn contents; Pb is at the

TABLE II.2-15
Composition of gossans formed on stratiform Zn-Pb-Ag and Cu mineralization, Dugald River, northwest Queensland (Taylor and Scott, 1983)

	Zinc-lead gossans			Copper gossans		
	Outcrop N = 4		Subcrop N = 3	Outcrop N = 5		
	Mean ppm	Range ppm	Mean ppm	Range ppm	Mean ppm	Range ppm
Ag	115	15-150	< 100	100- > 100	22	2-65
As	1900	420-4430	350	80-700	6200	360-1.1%
Ba	3.14%	0.54%-4.41%	4.0%	3.34%-4.65%	85	12-270
Cd	< 10	< 10-10	80	6-200	< 30	< 30-70
Co	< 10	< 10-10	30	< 10-50	1040	700-1500
Cu	450	50-660	740	120-1170	4.24%	1.2%-68%
Ga	20	2-30	7	0.2-20	4	< 1-10
Ge	25	15-40	5	2-8	< 1	-
Mo	30	0.3-80	10	6-15	55	10-100
Ni	6	< 4-15	15	< 4-40	320	150-500
Pb	2.75%	0.63%-6.17%	11.6%	2.99%-27.2%	1.4%	40-6.7%
Sb	440	< 30-1500	50	25-80	< 30	-
Sn	1.5	0.8-2	2	1-4	9	4-20
Tl	1	< 1-4	15	4-30	< 1	-
V	140	50-250	40	25-70	n.d.	-
Zn	0.21%	0.08%-0.28%	12.4%	1.51%-22.7%	1580	430-3500

TABLE II.2-16

Composition of gossan, Pegmont, northwest Queensland (Scott and Taylor, 1987) compared with gossans formed on BIF-hosted Pb-Zn mineralization at Broken Hill, Australia and Gamsberg and Aggeney's, South Africa

	Pegmont			Broken Hill			Gamsberg ^c			Aggeney's ^c		
	Ore	Gossan		Ore ^a	Gossan ^b		Sulphides	Gossans		Sulphides	Gossans	
		N = 3 ppm	N = 19 ppm		Range ppm	ppm		ppm	N = 5 ppm		N = 20 ppm	N = 5 ppm
Ag	6-20	6	1-40	40-300	20-420	5	1-35	5-130	2-100			
As	<10	13	<10-120	200-400	<40-300	10	10-900	10-30	30-1000			
Ba	40	52	30-2860									
Bi	1-10	<1		2-50								
Cd	200-400	<10		360-800	1-49	80-180	1-18	5-120	1-10			
Co		<10		70-140	32-160	50-120	5-40	90-900	5-600			
Cr	15-40	<15		40-100	40-100	35-75	100-180	70-110	100-180			
Cu	<10-45	83	10-180	900-20000	870-1940	30-90	55-2000	500-3800	4000-7.0%			
Ni	<4	4	<4-8	25-65	4-13	15-35	1-30	25-70	5-20			
Pb (%)	6.44-8.61	8.79	0.67-16.5	11.1	2.2-20.8	0.04-0.20	0.02-8.0	0.50-4.30	0.03-7.0			
Sb	<30	42	<30-150	70-400	200-680							
Sn	2-20	1	0.8-4									
Zn (%)	1.78-3.65	0.34	0.11-0.78	11.9	0.09-1.52	5.35-12.5	0.02-1.0	0.15-4.90	0.01-0.15			

^a Johnson and Klingner (1975)

^b Calculated from data quoted by van Moort and Swensson (1982)

^c Andrew (1980)

TABLE II.2-17

Composition of gossans formed on stratabound Pb-Zn mineralization, Namoonna, Northern Territory, Australia

	Mean N = 29 %	Range %		Mean N = 29 ppm	Range ppm
SiO ₂	28.4	0.60-73.6	Ag	990	< 5-1.55%
Al ₂ O ₃	3.97	0.50-10.1	As	2210	< 5-1.08%
Fe ₂ O ₃	38.4	1.99-72.7	Ba	115	< 5-590
CaO	0.10	< 0.01-0.20	Cd	45	< 8-400
MgO	0.51	< 0.5-1.06	Cl	385	113-2430
K ₂ O	0.66	< 0.01-2.14	Co	140	55-650
TiO ₂	0.28	< 0.1-2.08	Cr	40	< 5-175
P ₂ O ₅	0.51	< 0.1-3.38	Cu	590	20-4350
MnO	1.33	< 0.1-8.00	Mo	19	< 5-53
CO ₂	1.29	< 0.2-10.3	Ni	170	54-350
SO ₃	2.48	0.02-10.5	Pb	10.6%	300-70.8%
			Sb	450	< 5-1600
			Sn	335	< 5-1360
			V	125	< 5-455
			Zn	5150	70-2.89%
			Zr	355	45-1090

same concentration as fresh mineralization whereas Zn is depleted tenfold. Although laminations are preserved in the gossan and secondary Pb minerals are plentiful, the only boxworks are after a gangue mineral, fayalite.

Namoonna, Northern Territory, Australia (13). A 5-15 m wide gossan outcrops discontinuously over a strike length of 13 km at Namoonna, approximately 135 km southeast of Darwin. Drilling has delineated thin lenses of pyrite, galena and sphalerite, with minor manganiferous carbonate, in carbonaceous siltstones and sandstones of the Lower Proterozoic Masson Formation, which hosts other mineralization in the Pine Creek Geosyncline. Where it outcrops, the gossan forms a low ridge rising 2-5 m above the gently undulating plain, but is commonly buried by sandy red soils. The present depth of weathering is approximately 20 m, but much of the profile has been eroded.

In addition to quartz, hematite and goethite, the gossans contain a wide range of minerals including cerussite, anglesite, pyromorphite, a variety of alunite-jarosite minerals, coronanite, cassiterite, hemimorphite, sericite and chlorite. Galena is also common near the surface, having been protected from oxidation by the surrounding cerussite and other secondary Pb minerals, by its coarse grain size and by the relatively high pH environment (low pyrite and high carbonate content). The composition of the gossans is highly variable, (Table II.2-17), reflecting similar variations in the nature and grade of mineralization.

However, all samples are enriched in one or more trace elements although, in some, higher levels correspond with higher Mn oxide concentrations. This enrichment and the high mean values of P_2O_5 , CO_2 and SO_3 reflect the immaturity of these gossans. In many respects, the geochemistry and mineralogy of the Namoon gossan are similar to those at Dugald River (11), but this similarity is misleading in that it does not reflect the lower grade and tonnage of mineralization at Namoon.

Volcanogenic massive sulphide (VMS) deposits

These deposits consist mainly of pyrite, pyrrhotite, chalcopyrite and sphalerite and differ from the sedimentary exhalative deposits in that galena is generally of lesser importance and barite is a common gangue mineral. The deposits occur in recognizable volcanic suites and are commonly zoned. Gossans associated with VMS deposits commonly retain the structure and fabric of the primary sulphide and, except where highly leached, tend to have high concentrations of the target elements Cu, Zn, Pb, Ag and Au. They are usually characterized by the presence of anomalous concentrations of the volatile elements As, Bi, Hg, Sb, Se, Sn, Te and Tl and of the lithophile elements B, Ba, Cr, V and Mn with associated Co and Ni.

Archaean deposits, Western Australia (14). Although there are fewer known deposits than in the Archaean of Canada, the Yilgarn and Pilbara Blocks of Western Australia are the hosts of several well-documented VMS deposits. The mineralogy and geochemistry of gossans at Teutonic Bore (14A), Golden Grove (14B), Freddie Well (14C) and Whim Creek (14D) are described here. Golden Grove, Teutonic Bore and Freddie Well exemplify dispersion models of types A, B and C respectively and are described further in Chapter III.3.

The Teutonic Bore Cu-Zn-Pb-Ag (14A) deposit occurs in metabasaltic rocks, 300 km north of Kalgoorlie, as a steeply-dipping stratiform lens of massive sulphide and quartz. The deposit is in intensely weathered, lateritized terrain of moderate relief and has been weathered to a depth of 75 m, which is about 40 m below the present water-table. Despite the ore lens having a strike length of 320 m and a maximum width of 30 m, the gossan was only partially exposed at the surface over a strike length of about 50 m. The gossan profile is partly truncated, but it is a classic zoning of fresh sulphide, supergene sulphides, an oxide assemblage with abundant secondary ore minerals, a leached oxide zone and a surface gossan (Nickel, 1984). The surface gossan has high concentrations of target and pathfinder elements (Table II.2-18) contained in Fe oxides and secondary alunite-jarosite minerals, with cassiterite as a resistate accessory mineral. Diagnostic boxwork textures, except for those of pyrite, are not well developed. The compositions of deeper horizons in the profile are given in Table III.3-5.

The Golden Grove Cu-Zn deposit (14B) occurs in a sequence of intercalated acid pyroclastic, volcano-sedimentary rocks 380 km north-northeast of Perth.

TABLE II.2-18

Composition of gossans formed on Archaean VMS deposits at Teutonic Bore (Nickel, 1984), Golden Grove (Smith et al., 1979), Freddie Well (Smith et al., 1976) and Whim Creek (Nickel, 1982), Western Australia

	Teutonic Bore N = 12		Golden Grove		Freddie Well N = 3		Whim Creek N = 52	
	Mean ppm	Range ppm	Cu gossan N = 26		Pb-Zn gossan N = 15		Range ppm	Mean ppm
			Mean ppm	Range ppm	Mean ppm	Range ppm		
Ag	15	6-32	1.4	0.1-15	2.4	0.2-10	20	1-200
As	3100	630-6650	160	<50-1000	300	<50-2000	490	<50-7000
Bi	37	<1-250	115	<1-665	90	5-560	210	<1-1000
Cd			<3	<3	<3	<5-25		
Co			25	<5-70	5	<5-40	210	10-1000
Cr			35	<20-150	<20	<20-60	70	<20-400
Cu	1000	200-1700	990	<5-3540	1330	460-2600	4.5%	100-52.7%
Mn	170	40-350	90	<10-500	35	10-300	170	<10-800
Mo			20	<3-200	<3	<3-3	50	<3-400
Ni			5	<5-40	<5	<5-5	100	<5-400
Pb	6800	1100-2.92%	30	5-85	200	25-1700	3860	25- > 1%
Sb	725	70-3000	50	20-130	175	15-1270	90	<30-1000
Se			40	<1-300	20	8-65		
Sn	2730	60-6400	38	5-110	77	<1-520	330	<1-2000
Te			<1	<1	<1	<1		
W	800	400-1500	65	<10-280	47	<10-125	5470	30- > 1%
Zn			35	5-95	255	15-870		

Gossan Hill rises 80 m above the surrounding plain due to the presence of resistant bodies of massive magnetite associated with the sulphide lenses. Elsewhere, outcrop is rare and felsic rocks are weathered to a depth of 50 m. Whereas the barren gossans and ironstones (Table II.2-11) are maghemite-rich, those derived from base metal mineralization consist of hematite, goethite and residual quartz. Smith and Perdrix (1983) recognized two distinct gossan populations related to such mineralization, each of which has a distinctive geochemical signature (Table II.2-18). In addition to the target elements Cu, Pb and Zn, the pathfinder elements Ag, As, Bi, Mo, Sb, Se and Sn are also anomalous. The higher concentrations of many of these elements in gossans on Pb-Zn mineralization are due to the presence of stable secondary minerals.

The Freddie Well deposit (14C), about 430 km northeast of Perth, consists of a number of vertically dipping lenses of pyrrhotite, pyrite, sphalerite, chalcopyrite and magnetite in felsic schists. Gossans occur intermittently over a strike length of 5 km just below a subdued scarp at the edge of a lateritic plateau but, because of erosion, the depth of weathering over mineralization is only 10–12 m (Smith et al., 1976). These hematite-goethite-rich gossans contain anomalous Cu, Zn, Ag, Cd, In, Sn and W, but As, Sb, Bi and Pb contents are much lower than in gossans from other deposits (Table II.2-18) due mainly to low abundances in fresh sulphides (Smith et al., 1979).

The Whim Creek Cu-Zn-Pb-Ag deposit, 1250 km north-northeast of Perth, lies within argillites and siltstones that form part of the Whim Creek Group of volcanic and sedimentary rocks in the Archaean Pilbara Block. The area is a dissected plateau of moderate relief, with a hot semiarid climate. Pyrite, chalcopyrite, sphalerite, pyrrhotite and minor marcasite and galena mineralization occurs in a single horizon that can be traced for approximately 5 km. The near-surface gossan differs markedly from those in the Yilgarn Block in that it contains abundant secondary minerals, particularly carbonates (Nickel, 1982), and is geochemically anomalous in target and pathfinder elements (Table II.2-18). The immaturity of this gossan is due to erosion of upper, more leached zones of the profile, to continued weathering in the present semiarid climate and to the high pH maintained by carbonate minerals in the wallrocks.

Benambra, Victoria, Australia (15). The Wilga and Currawong massive Cu-Zn sulphide deposits are situated at Benambra, 260 km east-northeast of Melbourne. The area has very high relief and both deposits are in a steep valley at an elevation of approximately 900 m. The climate is temperate, with rainfall exceeding 900 mm per annum, most falling in the winter when snow and frosts are common; the data are included for comparison with VMS gossans in tropically weathered environments. The mineralization consists of massive sulphide lenses in Silurian volcanoclastic and sedimentary rocks, with nearby porphyritic felsic units. The sulphides are typically fine-grained pyrite, sphalerite, chalcopyrite with minor galena, arsenopyrite and tetrahedrite in a gangue of quartz, chlorite and carbonate (Robbins and Chenoweth, 1984).

The massive sulphide lenses do not appear to outcrop and the only surface expressions of the mineralization are "peripheral" gossans formed on disseminated and stringer mineralization. There is also a solution-deposited gossan below the Wilga deposit, in which Fe oxides precipitated from a spring have

TABLE II.2-19

Composition of gossans associated with VMS mineralization in the temperate climate of northeast Victoria, Australia (Robbins and Chenoweth, 1984)

Wilga				
	Gossan N = 42		Solution-deposited N = 9	
	Mean ppm	Range ppm	Mean ppm	Range ppm
Ag	20	< 1-230	1.6	< 1-3
As	420	16-1660	3650	6-1.02%
Au	0.73	< 0.05-10	< 0.05	
Ba	355	< 100-9600	130	< 100-300
Bi	220	10-460	1880	< 10-5450
Co	40	5-90		
Cu	6400	50-19.3%	410	20-720
Hg	1.3	0.003-4		
Mn	160	10-940	175	10-860
Pb	1660	90-9950	1.22%	30-4.8%
Se	90	< 1-700	5	0.3-4.8%
Sn	< 100	< 100-100		
Zn	680	20-770	210	30-1130

Currawong				
	Gossan N = 63		Barren gossan N = 15	
	Mean ppm	Range ppm	Mean ppm	Range ppm
Ag	8	< 1-90	3	1-6
As	1230	30-2.75%	520	140-1120
Au	0.5	< 0.05-8	0.18	0.05-0.25
Ba	530	< 100-1700		
Bi	73	0.5-410		
Co	28	20-50	28	10-410
Cu	630	10-3200	35	10-80
Hg	0.45	< 0.005-9.6		
Mn	360	40-1720	80	30-360
Pb	2100	40-8%	160	60-590
Se	23	< 3-170		
Sn	< 100	< 100-100		
Zn	285	30-840	110	40-180

cemented river gravels, and a barren gossan at Currawong. The target and pathfinder element signatures of the “peripheral” and solution-deposited gossan at Wilga (Table II.2-19) are clearly indicative of a VMS deposit. Because of the high rainfall, metal concentrations would be expected to be much lower, but the high relief ensures that the gossan is eroded before strong leaching can take place. The composition of the solution-deposited gossan at Wilga reflects precipitation of highly stable secondary minerals, such as Fe oxides and beudantite, in which Bi, Cu, and Zn are incorporated. The precipitation is caused by the change in pH from highly acidic conditions in spring-waters to near-neutral in the Tambo River.

Al Masane, Saudi Arabia (16). This relatively large deposit, occurring in very arid, rugged terrain 55 km southwest of Wadi Wassat, is hosted by middle Proterozoic metavolcanic and metasedimentary rocks which are exposed in steep-sided wadis. There is a prominent zone of solution-deposited gossan on the lower slopes of the wadi, but the data are not given separately in Table II.2-20. The concentrations of many target and pathfinder elements (particularly Zn) are high, occurring as secondary minerals, such as hemimorphite, smithsonite and franklinite, and within the abundant hematite and goethite. Despite the high Cu contents, no secondary Cu minerals were identified. Analysis of the fresh sulphide indicated that the concentrations of the volatile elements (As, Bi, Sb, Se, Te) and Sn are much lower than in similar deposits elsewhere in the Arabian Shield so that, despite the aridity, their abundances in gossan are lower than normally expected. Nevertheless, the application of discriminant analysis to the geochemical data correctly classified 95% of the samples as being related to VMS mineralization.

Letaba, Murchison Belt, South Africa (17). The Letaba Cu-Zn prospect lies in Archaean greenstones of the Murchison Belt some 400 km northeast of Johannesburg. The prospect is on the gently undulating Quaternary Lowveld surface at an altitude of 500 m, in a dry savanna to semiarid climate. Mineralization occurs as two vertically-dipping, massive pyrite-sphalerite-chalcopyrite lenses in quartz chlorite sericite schists. A thin (0.2–0.5 m) gossan is exposed intermittently over a strike length of 800–1100 m. The gossan is dark reddish brown, consisting of partially silicified goethite and hematite with minor subsurface malachite and azurite (Andrew, 1984).

From the limited chemical data available (Andrew, 1984), there is little doubt that the high Cu, Pb and Zn contents (Table II.2-20) are indicative of base metal mineralization. Lower than expected Ba values and the absence of As, Bi, Hg, Sb, Se, Sn, Te and Tl data makes characterization difficult. However, the anomalous concentrations of Cd, Co and Ni due to adsorption onto Mn oxides are features common to many VMS gossans and the geological setting also suggests this style of mineralization. Andrew (1980) notes that there is some element zoning within

TABLE II.2-20

Composition of gossans formed on VMS mineralization at Al Masane, Saudi Arabia (Ryall and Taylor, 1981) and Letaba, South Africa (Andrew, 1984)

	Al Masane N = 62		Letaba N = 50	
	Mean ppm	Range ppm	Mean ppm	Range ppm
Ag	10	< 0.2-90	6	< 1-30
As	400	1-2200		
Au	2	< 0.2-40		
Ba	120	5-3200	17	10-160
Bi	30	< 4-290		
Ca			750	300-1600
Cd			10	< 1-35
Co	130	10-1860	100	17-750
Cr			80	30-600
Cu	5200	50-1.9%	1%	500-34%
Fe%			35	5-58
Hg	1.5	0.002-15		
Mg			2500	450-3%
Mn	5100	30-3.1%	150	20-4000
Mo	80	< 4-1350		
Ni	20	10-100	60	10-300
Pb	2500	12-3.6%	1000	115-5000
Sb	60	< 4-400		
Se	54	< 0.02-380		
Sn	6	2-26		
Ti			400	100-2800
Zn	3.3%	110-34%	7000	1000-2%

the gossan. The surface expression of mineralization at Letaba is discussed further in Chapter III.3 (see p.348).

Carbonate-hosted base metal deposits

Exhalative deposits at Mount Isa (9), Hilton, Lady Loretta (10) and Dugald River (11) occur in carbonate-rich (often dolomitic) shales and siltstones. Many deposits, however, are hosted by nearly pure carbonate rocks, the best examples being the Mississippi Valley-type deposits of galena, sphalerite and minor marcasite. These deposits seldom form ironstone gossans, the outcrop being entirely of secondary Pb and Zn minerals such as cerussite, anglesite, smithsonite, hemimorphite and willemite and very low concentrations of pathfinder elements other than Cd. A variety of gossans from carbonate-rich environments are described in this section.

Rosh Pinah, Namibia (18). This stratiform Pb-Zn-Ag-Cu deposit is situated on the lower western slopes of the Richtersveld Massif in a region of warm, tropical desert (40 mm annual rainfall), approximately 600 km south of Windhoek. The mineralization is associated with upper Proterozoic, brecciated, Ba-rich dolomitic lenses and carbonaceous chert horizons in the Kapok Graben. It is not, therefore, a Mississippi Valley-type deposit, but is included to illustrate the effect of carbonate buffering by host rocks.

Much of the original gossan has now been removed by mining but is reported (Page and Watson, 1976) to have been a massive, manganiferous wad rich in secondary metal carbonates. Andrew (1984) analysed some of the remaining gossan, which varied from black finely-laminated quartzite gossan to massive and friable yellow-brown limonitic material. It consists of gypsum, cerussite, smithsonite, beudantite, hemimorphite, chrysocolla, azurite, barite and secondary alunite-jarosite minerals, together with some hematite and goethite. Replicate textures are after galena and carbonate. Many of the target and pathfinder elements are at extremely high concentrations (Table II.2-21), reflecting the combined effects of neutralizing host carbonates, the presence of stable secondary minerals and reduced leaching due to the arid climate.

Kherzet Youcef and Djebel Anini, northeast Algeria (19). Deposits of sphalerite, galena and some pyrite occur in barite-rich dolostones in an environment similar to that of the ironstones at Djebel Debagh (5). Mineralization at Kherzet Youcef is in a number of stratiform lenses, whereas at Djebel Anini it occurs in veins, shoots and patches in fractured carbonates. Gossans over both deposits consist of goethite, hematite and smithsonite (which is dominant at Kherzet Youcef), with many additional secondary carbonate and sulphate minerals occurring at Djebel Anini (Hanssen and Bourezg, 1990). The mineralogy and geochemistry (Table II.2-21) reflect the low leaching resulting from the high pH environment produced by the carbonate-rich wallrocks and the arid climate. The geochemistry also reflects differences in the primary mineralization; the gossan at Djebel Anini has the characteristics of a polymetallic deposit, whereas gossans at Kherzet Youcef have a geochemical signature more typical of Mississippi Valley-type deposits.

Kamarga, northwest Queensland, Australia (20). Both Pb-Zn and Cu mineralization occur within Proterozoic dolomitic siltstones at Kamarga 220 km north-northwest of Mount Isa. The area is one of rolling hills on the edge of a subdued domal structure, and has a dry savanna climate. The Pb-Zn mineralization has many of the attributes of a Mississippi Valley-type deposit, including a very low Fe sulphide content and the presence of barite and fluorite. Of the pathfinder elements, As and Tl occur with pyrite, Ag with galena, and Cd and Ge with sphalerite, all at relatively low concentrations. The Cu mineralization is probably epigenetic, being derived from underlying volcanics and has many of the geochemical characteristics of deposits described in the next section.

TABLE II.2-21

Composition of gossans formed on carbonate-hosted Pb-Zn-(Cu) mineralization at Rosh Pinah, Namibia (Andrew, 1984) and Djebel Anini and Kherzet Youcef, northeast Algeria (Hanssen and Bourezg, 1990)

	Rosh Pinah N = 50		Djebel Anini N = 30		Kherzet Youcef N = 23	
	Mean ppm	Range ppm	Mean ppm	Range ppm	Mean ppm	Range ppm
Ag	40	2-1500				
As			1.18%	770-11.8%	50	14-170
Ba	5000	100-28%	1.0%	830-5.4%	1510	30-1.5%
Ca	2000	50-11%				
Cd	300	30-1000	365	3-2230	70	<10-5300
Co	25	5-170	33	3-215	25	4-90
Cr	85	40-180	1520	310-1.7%	17	<1-400
Cu	2000	130-6%				
Fe%	12	1-41	29.2	3.9-60.9	29.0	5.0-54.8
Mg	900	70-6.5%	1050	340-11.4%	4700	1370-4.4%
Mn	1000	20-4%	120	10-2740	840	85-1.6%
Mo			29	<1-120	30	7-75
Ni	15	5-50	120	30-370	40	17-200
Pb	2.5%	3000-8%	8300	1110-9.9%	6900	265-9.1%
Sb			1050	185-6100	<10	<10-39
Sr			190	6-1190	155	20-1625
Ti			35	<1-850	85	<1-330
V			29	<1-170	85	7-2160
Zn	4%	2000-47%	1.9%	4200-34.7%	3.2%	3270-43.2%

TABLE II.2-22

Composition of ironstones formed on carbonate-hosted Zn-Pb and Cu mineralization, Kamarga Dome, northwest Queensland

	Mineralized N = 13		Unmineralized N = 9	
	Mean ppm	Range ppm	Mean ppm	Range ppm
Ag	2	< 0.1-7	0.3	< 0.1-0.5
As	150	< 10-700	55	< 10-310
Ba	175	21-590	260	75-550
Bi	1	< 1-6	< 1	< 1
Co	25	< 5-100	23	5-70
Cr	25	< 20-50	23	< 20-40
Cu	740	70-5700	150	10-340
Fe ₂ O ₃ %	36.7	6.04-77.2	33.5	4.75-82.7
Ga	< 1	< 1-2	< 1	< 1-2
Ge	1	< 1-2	1.8	< 1-10
MnO%	0.22	< 0.1-0.58	0.46	< 0.1-1.56
Mo	3	< 3-10	3	< 3-5
Ni	55	< 5-150	42	< 5-100
Pb	930	12-3200	30	10-100
Sb	< 5	< 5-11	< 5	< 5-8
Sr	< 5	< 5-34	17	< 5-38
Zn	1640	200-3500	107	25-200

Gossans are extremely rare and ironstones consist of slightly ferruginized weathered host rocks with thin ferruginous bands. They consist of quartz, goethite and hematite, with variable amounts of calcite, dolomite, muscovite, chlorite, K-feldspar and trace cerussite and an alunite-jarosite mineral. Geochemical data for "mineralized" and "unmineralized" outcrop (Table II.2-22) indicate that the contents of chalcophile elements are higher in the mineralized ironstones, whereas the lithophile elements tend to be higher in the unmineralized ironstones. The data reflect both the generally low geochemical signatures of the sulphides and that little of the mineralization was originally present in the now weathered material. In such situations, analysis of ironstones alone may be insufficient to delineate the mineralization; a statistical comparison with the surrounding country rocks is necessary to identify the subtle anomalies.

Copper mineralization

Copper sulphide mineralization occurs in many forms, including:

- (1) porphyry-style mineralization of the Circum-Pacific Rim;
- (2) deposits of the Zambian type, i.e. Cu sulphide mineralization, poor in Fe sulphides, hosted by carbonate-rich rocks;

TABLE II.2-23

Composition of gossans on copper mineralization at Great Australia, Cloncurry, Mammoth and Esperanza (Hunter, 1980), northwest Queensland

	Great Australia N = 14		Mammoth N = 6		Esperanza N = 12	
	Mean ppm	Range ppm	Mean ppm	Range ppm	Mean ppm	Range ppm
Ag	< 0.1		9	1-25	< 1	
As	420	75-890	0.55%	50-2%	285	15-1450
Ba	20	5-60	170	100-400	200	10-580
Bi			50	1-100	1	< 1-2
Co	510	150-2300	30	2-80	14	< 10-30
Cu	2.15%	4600-8.14%	1 %	230-5.6%	295	35-900
Hg			0.18	0.04-0.88		
Mo	25	10-40	6	1-30	3.5	1-10
Ni	140	30-460	40	15-100	7	4-20
Pb	35	22-47	85	8-200	32	< 5-140
Sb	< 5	-	70	15-200	< 30	< 30-40
Sn	5	< 5-15			< 0.8	< 0.8-2
Zn	16	10-30	25	5-60	10	< 5-40

(3) volcanogenic massive sulphide deposits, e.g. examples 14-17;

(4) Cu sulphides associated with substantial Fe sulphides, e.g. Mount Isa (9).

Only the VMS and pyritic deposits ((3) and (4) above) have substantial gossans developed on them. Indeed, the gossans on many of the latter, which are hosted by a variety of lithologies, are very prominent. Many contain abundant secondary sulphides and carbonates which have been mined in the past (e.g. in Rajahstan, India; northwest Queensland, Australia). The giant Mount Isa deposit, however, has no surface expression.

Great Australia, northwest Queensland, Australia (21). Gossans associated with the Great Australia deposit, 2 km south of Cloncurry were discovered in 1867 and led to mining within the Proterozoic Mount Isa Inlier. The main gossan, consisting of hematite, goethite and Cu carbonates, rose 10 m above the surrounding plain and was approximately 30 m long (Ball, 1908). This and many smaller gossans delineated lodes of pyrite-chalcopyrite mineralization in shears at the contact between shales and mafic volcanic rocks. The gossans contain well-preserved boxworks after coarse-grained pyrite and chalcopyrite. In addition to their extremely high Cu content (Table II.2-23), they are relatively rich in As, Co, Mo and Ni but poor in Pb and Zn. Such signatures are common for many of the gossans associated with the small tonnage, high grade, shear- and fault-controlled vein Cu deposits of the area.

Gunpowder, northwest Queensland, Australia (22). The Mammoth Cu deposit, located 115 km north of Mount Isa, consists of a number of discrete lenses of pyrite, chalcopyrite, chalcocite and bornite occurring in brecciated arkosic sandstone and quartzite (Scott and Taylor, 1977; Scott, 1986). The mineralization has similarities to the Mount Isa Cu deposit, with the Cu being derived from the nearby Eastern Creek volcanics (Scott and Taylor, 1982). The immediate environment of the deposit is a rugged heavily dissected plateau with prominent quartzite ridges.

The gossan, much of which was mined at the turn of the century, consists of brecciated arkosic sandstone in a groundmass of hematite and goethite, reflecting the appearance of the mineralization. Apart from Cu, the contents of both Ag and As are high but, in contrast, although Co and Ni are both associated with ore, they are barely anomalous in the gossan (Table II.2-23). In this area north of Mount Isa, the slightly anomalous Pb values also appear to be indicators of Cu mineralization although this has not yet been confirmed statistically. In other ironstones from the Gunpowder area, Hg, Cu, As, Pb, Co and Ni are characteristic of gossans associated with Cu mineralization (Ryall et al., 1981), although the abundances of Co and Ni are partly determined by the Mn contents. Gossans at the nearby Esperanza prospect (Hunter, 1980; see also p. 412) are leakage gossans and have much lower element concentrations (Table II.2-23).

Matchless Amphibolite Belt, Namibia (23). The Gorob, Matchless, Otjihase and Ongeama Cu deposits occur within the NE–SW trending, Matchless Amphibolite Belt in the Damaran Khomas Trough of Namibia. The three easterly deposits are at an altitude of approximately 2000 m on the Jurassic Gondwana plateau, which has a hot semiarid climate. Gorob is at a much lower altitude to the west of the Great Escarpment and has a cooler, tropical coastal desert climate. Mineralization at each deposit consists of massive to disseminated pyrite, pyrrhotite, chalcopyrite and minor sphalerite in magnetite quartzites and quartz chlorite schists. Barite is a common gangue mineral. The deposits have the characteristics of a submarine volcanogenic exhalative origin, with Ag as the precious metal associate. Geochemical dispersion at Otjihase is described on p. 407.

The depth of weathering varies from 15–30 m and each deposit is represented by gossanous outcrops (Andrew, 1980, 1984). The gossans consist of goethite, hematite and resistate minerals, particularly barite, together with minor malachite, chrysocolla and alunite-jarosite minerals. The gossans have remarkably similar compositions (Table II.2-24a), reflecting the uniformity of deposits within this extensive mineralized belt. Andrew (1980) notes that other elements are associated with the primary mineralization, and elevated values for As, Bi, Sb, Se and possibly Mo might be expected in these gossans. Gossans on Cu mineralization can be distinguished from those on barren pyrite on the basis of higher Ag, Ba, Cu, Pb and Zn and lower Ti contents (Table II.2-24b). Stepwise discriminant analysis was able to distinguish the various types of gossans, at these deposits,

TABLE II.2-24

(a) Composition of gossans formed on four copper deposits within the Matchless Amphibolite Belt, Namibia (Andrew, 1984)

	Ojijhase N = 68			Matchless N = 70			Gorob N = 46			Ongeama N = 25		
	Mean ppm	Range ppm		Mean ppm	Range ppm		Mean ppm	Range ppm		Mean ppm	Range ppm	
Ag	4	1-58		5	1-35		3	1-35		8	3-65	
Ba	460	10-5%		950	10-6.5%		300	10-7000		50	10-300	
Cu	500	80-6500		380	100-2800		8000	600- > 10%		350	100-1500	
Cd	2	1-3		3	1-12		7	1-200		3.5	1-15	
Co	11	5-55		25	5-70		43	5-2200		60	40-90	
Cr	105	70-530		100	50-210		120	50-300		55	30-120	
Cu	2200	300-7200		3700	320-3%		1.5%	450-25.6%		4600	700-1.2%	
Fe%	34	4-58		24	5-57		22	1-55		43	13-61	
Mg	1050	100-1.2%		1300	270-7500		2800	200-4%		1900	100-3.1%	
Mn	110	28-1000		300	55-3000		90	20-500		1900	230-1.2%	
Ni	11	5-35		30	10-80		43	5-200		23	18-30	
Pb	210	30-2000		270	30-3200		350	70-8500		420	100-3300	
Ti	1200	65-6400		900	200-6200		650	100-4200		520	200-5500	
Zn	110	32-480		500	60-4000		1000	60-1%		820	180-4000	

(b) Mean trace element concentrations for subsets of (i) the Ojijhase gossan and (ii) the Matchless gossan

	Ojijhase		Matchless	
	Copper (N = 11)	Pyrite (N = 55)	Copper (N = 20)	Pyrite (N = 40)
Ag	5	2	10	1
Ba	807	30	4943	34
Cu	2243	2198	7464	1030
Mn	112	142	409	102
Pb	293	60	544	81
Ti	1044	2281	757	1517
Zn	125	100	1054	118

one deposit from another, and these gossans from ironstones and gossans elsewhere in southern Africa (Andrew, 1984).

Porphyry Cu (Mo, Au) deposits (24). Porphyry Cu deposits commonly have Mo and Au either associated with them or occurring separately (e.g. Climax and Henderson porphyry Mo deposits, USA). Despite the importance of these deposits, there is very little information on the geochemistry of cap rock (gossans) on such deposits and a review of geochemical exploration for this type of Cu mineralization (Coope, 1973) makes no mention of gossans. Such deposits occur in a wide range of climatic and topographic situations and consequently should have a geochemical signatures that vary according to the degree of leaching and erosion of the cap rock.

The Berg deposit, British Columbia was studied to determine the effects of supergene alteration on the original hypogene geochemistry (Heberlein et al., 1983). In the absence of detailed data, the following conclusions were reached:

(1) Zinc is removed from both the supergene sulphides and the leached cap rock.

(2) Copper is concentrated in the supergene sulphide zone and may occur as a supergene oxide assemblage, but is generally leached from the capping.

(3) Molybdenum, Pb and Ag are concentrated in the leached cap, whereas Cu and Mn are enriched in the supergene zone.

(4) Highly leached deposits of this type have a Mo-Pb-Ag-F signature.

Solution-deposited ironstones in the vicinity of the deposit have variable contents of trace elements, with maximum values of 2250 ppm Mo, 950 ppm Cu, 245 ppm Zn, 375 ppm Pb, 4 ppm Ag, 480 ppm F, 155 ppm Mn and 12.4% Fe.

Gold deposits

There are many types of Au deposits (Boyle, 1979) but they are expressed as gossans only when associated with abundant sulphides. The mobility of Au during sulphide oxidation is dependent on complex S species, particularly thiosulphate, which are abundant in a gossan-forming environment only if the weathering solutions are buffered to a near-neutral or alkaline pH (Webster, 1986). As noted by Nickel and Daniels (1985), metallic Au may be present as a residual primary mineral (commonly the Au-Ag alloy, electrum) or as a secondary mineral, generally with a very low Ag content.

Mount Leyshon, northeast Queensland, Australia (25). This is one of many Au deposits of differing origins in northeast Queensland. Although the mineralogy varies, the ferruginous outcrops associated with these deposits appear to have similar geochemical signatures. At Mount Leyshon, pyrite, subordinate pyrrhotite, chalcopyrite, sphalerite and galena, with accessory Mo and Bi sulphides, occur in quartz veins within a Permian phreatomagmatic breccia complex (Morrison et al., 1987). Gold is associated with these veins. The deposit occurs at the boundary

TABLE II.2-25

Composition of ironstones formed on breccia-hosted gold mineralization, Mount Leyshon, northeast Queensland (Scott, 1987)

	Kaolinite-alunite N = 9		Jarosite N = 7	
	Mean ppm	Range ppm	Mean ppm	Range ppm
Al ₂ O ₃	6.95	1.87–10.2	6.70	2.32–15.1
Fe ₂ O ₃	40.7	31.1–63.1	53.9	37.7–74.4
MnO	0.02	< 0.01–0.04	0.03	0.01–0.12
TiO ₂	0.21	0.09–0.70	0.16	0.03–0.38
P ₂ O ₅	0.40	0.07–0.62	0.61	0.11–1.17
SO ₃	0.65	0.18–1.72	1.75	0.12–6.87
Ag	26	< 0.1–190	2	< 0.1–5
As	180	< 100–700	410	100–800
Au	14	< 3–70	4	< 3–20
Ba	230	70–540	460	120–1450
Bi	730	< 2–1500	76	2–250
Co	6	< 5–30	< 5	< 5–10
Cr	50	< 5–150	39	15–60
Cu	270	100–610	480	45–910
Mo	28	2–100	36	2–150
Ni	24	< 20–140	25	< 20–75
Pb	1170	< 50–4900	300	< 50–920
Sn	8	2–15	11	4–25
Sr	32	10–130	24	5–50
W	24	< 10–50	23	< 10–80
Zn	250	< 5–1150	690	< 5–2590
Zr	49	15–70	44	15–95

between Cambro-Ordovician metasedimentary and metavolcanic rocks and Ordovician–Devonian granites, 20 km south of Charters Towers.

The complex is extensively eroded and forms an 80 m high hill above the surrounding gently undulating plain. The depth of weathering is approximately 50 m. Oxidation of primary mineralization gave rise to ferruginous samples that were classified by Scott (1987) as jarosite- or kaolinite/alunite-rich, although the origin of the alunite/jarosite is being debated. Analytical data for the two groups of samples (Table II.2-25) indicate a wide concentration range for all trace elements, reflecting variations in primary mineralization. Statistical analysis of the data shows that Ag, Bi, Pb and, to a lesser extent, P, As, Cu and Mo are closely correlated with Au mineralization. The low pH due to the oxidation of pyrite, as indicated by the presence of alunite, jarosite and kaolinite, has resulted in dispersion of Co, Ni and Zn from the ironstones.

Bottle Creek, Western Australia (26). Bottle Creek, located 210 km north-northwest of Kalgoorlie, is one of many mines developed on residual and

supergene Au deposits in the lateritic regolith of the semiarid Archaean Yilgarn Block of Western Australia. Mineralization is represented at the surface by a subdued gossan that outcrops intermittently over a strike length of 26 km. In many places, it is covered by soil, lateritic gravels or transported overburden, or occurs as float. The gossan was first sampled and analysed, for Ni, in the early 1970s, but no significant anomalies were detected. In 1983, the area was reexamined and a widespread As anomaly with some non-coincident Au anomalies were discovered by a lateritic nodule and pisolith survey. At the same time, the gossanous outcrop was resampled, yielding As, Au, Bi, Pb and Sb anomalies (Legge et al., 1990). Extensive drilling led to the discovery of a deposit having mean grades of 3.5 g/t Au and 27 g/t Ag in weathered bedrock and laterite, which has now been mined. The primary mineralization consists of Au and electrum in a massive sulphide body containing pyrite and pyrrhotite, with minor tetrahedrite, sphalerite, arsenopyrite, chalcopyrite, galena and magnetite. The host rock is believed to be a graphitic shale associated with a felsic porphyry in a sequence of highly altered mafic volcanics.

TABLE II.2-26

Composition of gossans on gold mineralization, Bottle Creek, Western Australia

	Surface N = 12		Subsurface N = 9	
	Mean ppm	Range ppm	Mean ppm	Range ppm
Ag	< 5	< 5-25	16	< 5-39
As	5425	800-1.51%	1.04%	5260-1.56%
Au	2.53	0.05-10	18	0.03-90
Ba	2075	85-7200	615	20-3340
Bi	7	< 5-18	16	9-27
Cd	< 5	< 5	7	< 5-18
Co	16	< 5-50	210	7-1350
Cr	125	70-220	315	110-820
Cu	350	120-620	800	135-1660
Hg (ppb)	55	15-180	115	8-410
Mo	4	1-31	9	1-20
Ni	28	< 20-60	210	2.5-1050
Pb	270	50-5200	815	235-2680
Sb	615	60-1500	830	20-3000
Sn	4	1-15	7	3-15
Te	0.22	0.08-0.30	0.31	0.9-0.45
Tl	0.50	0.05-1.25	2.25	0.2-6.9
V	95	20-160	260	75-865
W	< 5	< 5	< 5	< 5
Zn	160	< 5-510	835	280-1300
Zr	62	15-165	55	16-110

Weathering is to a depth of approximately 80 m close to the mineralization. The gossan consists of variably silicified goethite, hematite, kaolinite, muscovite and beudantite and contains anomalous concentrations of a wide range of chalcophile and lithophile elements (Table II.2-26); of these, As, Ba, Cu, Hg, Pb, Sb and Zn in particular are related to the mineralization. There is a marked concentration of most elements in subsurface gossan, the exception being Ba which is present as insoluble barite at the surface. There has been only slight enrichment of both Au and Ag in the weathered zone, 30–60 m below the surface. Above and below this interval, Au and Ag appear depleted; a possible explanation for distributions of this type is discussed in Chapter V.3.

Telfer, Western Australia (27). This orebody, which for some years was Australia's largest gold mine, remained undiscovered until 1971 due in part to its remote location in the Great Sandy Desert approximately 1300 km north-north-west of Perth. During an exploration programme for base metal mineralization in the Paterson Ranges, samples of gossan were found to be auriferous—testimony to the need for multielement analysis of gossans. Below the base of complete oxidation at 100 m, the mineralization consists of a number of “reefs” of pyrite, chalcopyrite and Au in shallow marine sediments comprising sandstones, interbedded siltstones and shales, and major carbonate formations of Proterozoic age (Tyrwhitt, 1985). Folding has produced a series of gently-dipping elongate domes. Above 100 m, Au occurs in quartz-limonite gossans with large boxworks after recrystallized pyrite and carbonate. Copper has been leached from the upper parts of the gossan and is now concentrated in a supergene zone at the base of weathering. There is some evidence for recrystallization of Au, but there is no marked supergene enrichment.

Each of the four groups of gossans at Telfer has a highly anomalous Au content (Table II.2-27), consistent with the presence of visible Au in many surface samples (J.R. Wilmshurst, personal communication, 1990). Other elements which may be considered to be pathfinders are Ag, As, Co, Cu, Ni, Pb, Se and W, with Sb contents being unexpectedly low. The “discovery” outcrop is generally less anomalous because it is situated on a more siliceous part of the Middle Vale Reef, the main ore horizon. Gossans from the West Dome are developed on the less strongly mineralized “E” Reefs.

Nickel deposits

There is a considerable literature on the geochemistry of gossans associated with massive and disseminated Ni(-Cu) sulphide mineralization. It applies particularly to the Yilgarn Block of Western Australia, where much of the pioneering work on gossan and ironstone evaluation became the catalyst for the application of multielement geochemistry to gossan evaluation.

TABLE II.2-27
Composition of gossans formed on gold mineralization, Telfer, northern Western Australia (J.R. Wilmshurst, personal communication, 1990)

	MVR West Limb		MVR discovery gossan		Vein gossans, E limb		West Dome	
	N = 36		N = 9		N = 16		N = 7	
	Mean ppm	Range ppm	Mean ppm	Range ppm	Mean ppm	Range ppm	Mean ppm	Range ppm
Ag	15	8-45	8	<5-12	9	<5-30	<5	
As	3050	710-6110	3475	1160-5990	2370	75-7780	3645	2540-6760
Au	115	9.7-690	78	0.6-224	45	0.2-134	6	2.0-10.2
Ba	780	<100-3100	440	<100-1200	335	<100-2000	250	<100-870
Cd	22	6-33	7	<5-19	16	<5-30	22	13-25
Co	640	5-3540	14	<5-47	380	<5-1970	430	10-890
Cr	155	55-270	265	110-330	185	25-410	90	65-160
Cu	2450	190-5500	280	100-610	2310	120-9500	435	250-800
Mo	10	<10-20	12	<10-16	10	<10-15	<10	
Ni	240	<20-970	<20		120	<20-450	140	<20-220
Pb	320	80-110	140	<50-660	555	<50-5200	55	<50-65
Sb	6	1-75	2	<1-3	3	<1-6	2	1-4
Se	13	<5-50	9	<5-20	30	<5-300	<5	
W	670	25-4340	75	25-110	1120	50-4590	585	35-1550
Zn	85	5-480	8	20-240	55	<5-180	40	23-80

MVR: Middle Vale Reef

TABLE II.2-28

Concentrations of selected elements in gossans from the Yilgarn Block, Western Australia (Travis et al., 1976)

	A N = 6	B N = 5	C N = 10	D N = 9
Au (ppb)	4-18	100-1100	1-1600	1-30
Co	40-1400	295-1625	< 10-660	65-1900
Cr	600-1800	70-1080	20-1%	220-2800
Cu	500-2.02%	1700-1.18%	175-1.4%	200-2900
Fe%	8.9-54.1	7.4-43.0	1.9-50.0	3-54
Ir (ppb)	145-1980	165-600	70-345	6-70
Mn	30-460	30-180	30-540	205-885
Ni	240-2.78%	1200-1.14%	2.00-2.5%	900-1.7%
Pd (ppb)	180-1940	75-340	60-1700	20-335
Si%	1.4-38.0	8.2-4.3	2.7-44.4	5-390
Zn	40-60	40-100	10-90	45-360
	E N = 12	F N = 5	G N = 9	H N = 21
Au (ppb)	0.6-166	1-9.2	1.2-237	0.1-400
Co	10-1900	190-340	60-670	120-2960
Cr	515-1.39%	150-3700	55-2600	1030-2.45%
Cu	700-5.05%	900-2300	200-3700	< 100-1400
Fe%	6-56.5	31.6-54.5	24-55	9.2-54
Ir (ppb)	< 0.1-435	25-55	0.2-8.0	0.3-17
Mn	50-4100	70-590	70-1375	310-4400
Ni	100-2.7%	2800-9300	200-4200	400-9200
Pd (ppb)	6-2500	70-415	< 1-90	1.5-50
Si%	2-38.2	1-20.8	2.4-27.4	1-32.6
Zn	45-750	110-1285	30-875	80-785

A: Jan Shoot, Kambalda; B: Lunnon Shoot, Kambalda; C: Mount Clifford; D: Dunite association; E: Mafic association; F: Sediments in volcanic ultramafics; G: Other gossans in sediments; H: Lateritized unmineralized ultramafics.

Archaean Yilgarn Block, Western Australia (28). The discovery in 1966 of Ni sulphide mineralization at Kambalda by Western Mining Corporation led to the ensuing "nickel boom" (1967-1972). The collection and analysis of ironstones and gossans formed an integral part of all exploration programmes. Because of the difficulty in distinguishing between the ferruginous and silicified gossans associated with Ni(-Cu) sulphide mineralization and barren gossans, lateritized ultramafics and other ironstones, microtextural (Roberts and Travis, 1985) and geochemical techniques of evaluation were initiated (Cochrane, 1973; Clema and Stevens-Hoare, 1973; Joyce and Clema, 1974; Wilmshurst, 1975; Bull and Mazzucchelli, 1975; Travis et al., 1976; Moeskops, 1977). The geochemical data presented in Tables II.2-28 and II.2-29 are based, respectively, on a survey by Western Mining Corporation (Travis et al., 1976) and a review by Moeskops

TABLE II.2-29

Composition of nickel gossans and ironstones from the Yilgarn Block, Western Australia (Moeskops, 1977)

	Gossans N = 103		Ironstones N = 69	
	Mean ppm	Range ppm	Mean ppm	Range ppm
Ag	2	2		
As	25	20-30	25	20-30
Au	< 0.15			
Bi	45	20-60	15	~ 15
Co	280	200-400	480	200-800
Cr	750	200-2000	600	100-1800
Cu	1000	800-3000	90	80-150
Mn	300	200-400	1400	800-2000
Mo	< 5		10	~ 10
Ni	3000	1500-5000	1500	800-2500
Pb	35	30-40	30	10-40
Pd	0.15	0.1-0.3		
Pt	0.15	0.1-0.2		
Sb	30	20-40		
Se	35	20-40	< 2	
Zn	140	50-200	800	200-1500

(1977) of gossans and ironstones associated with various styles of Ni mineralization, other sulphide deposits and lateritic weathering in the Yilgarn Block.

The various types of ironstones may have similar Ni and Cu contents so that it is not possible to use these elements alone to identify the gossans. However, when more elements are used, the similarity in the compositions of the Ni gossans permits the use of principal component and discriminant analysis to distinguishing them from other gossans and ironstones. The Ni-Cu gossans are characterized by relatively high Ni and Cu, low Mn and Cr, and very low Zn and Pb contents. Lateritic ironstones, which are most commonly confused with gossans, are characterized by high Ni and Cr, medium to low Mn, and low Cu, Zn and Pb contents; ironstones and barren gossans developed on sulphidic shales and cherts have high to medium Ni, Zn and Mn contents, with medium Cu and Cr, and low Pb. Moeskops (1977) concluded that discrimination can largely be made by using Cu, Ni, Cr, Mn, Zn and Pb. Both he and Travis et al. (1976) suggested that the platinum group elements (PGE) Ir, Pd and Pt, and possibly Se and Te, would give valuable corroborative information. The PGE are commonly associated with Ni-Cu sulphide mineralization and, despite some mobility of Pt and Pd, remain at significant concentrations in gossans and have considerable importance as pathfinder elements (see also Mount Keith, p. 324).

TABLE II.2-30

Enrichment/depletion of selected pathfinder elements in gossans on nickel mineralization, O'Toole Mine, Minas Gerais, Brazil (Taufen and Marchetto, 1989)

	Fresh ore g/m ³	Gossan zone g/m ³	% Enrichment/ depletion in gossan
Ni	92.8 × 10 ³	14.8 × 10 ³	- 84
Cu	15.3 × 10 ³	9.6 × 10 ³	- 37
Co	2.0 × 10 ³	0.6 × 10 ³	- 70
Pt	1.13	0.88	- 22
Pd	1.64	1.10	- 33
Rh	0.20	0.28	+ 37
Ru	0.68	0.62	- 9
Ir	0.34	0.46	+ 35

O'Toole, Minas Gerais, Brazil (29). The O'Toole Ni-Cu orebody is situated about 500 km northwest of Rio de Janeiro on a high plateau of moderate relief. The area has a savanna climate (mean annual rainfall 1600 mm). The mineralization is hosted by a sequence of ultramafic to mafic volcanic rocks and cherts and consists of pyrrhotite, pentlandite and chalcopyrite with magnetite and minor sphalerite, ilmenite and cobaltite-gersdorffite (Taufen and Marchetto, 1989). This primary mineralization grades into a transitional zone of supergene sulphides at 40 m and into a gossanous oxide zone of variably silicified goethite and hematite above 20 m.

The gossan only outcrops over part of the deposit, the remainder being covered by red, Fe-rich soil. It is a typical Ni sulphide gossan, high in Ni and Cu and low in Zn, so that on a triangular Ni-Cu-Zn plot (Moeskops, 1977), it falls within the true Ni gossan field. The concentrations of Ni, Cu, Co and some PGE in primary ore and gossan, based on an isovolumetric calculation, are given in Table II.2-30. The calculation permits estimation of the enrichments and depletions that occurred during gossan formation. As expected, Ni and Co are highly depleted, Cu, Pt, Pd and Ru less strongly depleted and Rh and Ir are enriched. Differences in the abundance of the PGE compared to the Yilgarn Block probably reflect differences in primary mineralogy and geochemistry and in weathering history. Nevertheless, the characteristics of the gossans in both regions are broadly similar.

Skarn deposits

Skarn mineralization includes Cu-Zn, Pb-Zn, Sn, W and Au-Ag deposits, which commonly have pyrrhotite as the dominant Fe sulphide. The two examples presented here represent Zn-Cu and Zn-Pb skarns, but some large Sn deposits in Tasmania, now considered to be skarns, also had significant gossans developed on them. Unfortunately, these have been removed and no data are available. The

TABLE II.2-31

Composition of gossans on skarn Zn-Pb-Ag mineralization, Ar Ridaniyah, Saudi Arabia (Ryall and Taylor, 1981)

	Sulphide	Gossans	
	N = 8	N = 13	
	Mean	Mean	Range
	ppm	ppm	ppm
Ag	23	0.7	0.1-4.8
As	15	75	8-200
Au	< 0.1	< 0.2	
Ba	270	170	22-500
Bi	140	25	2-140
Co	70	40	30-6
Cu	2400	900	420-1300
Fe%	22	22	6-34
Hg (ppb)	< 50	17	2-45
Mn	1500	960	240-1600
Mo	13	14	6-22
Ni	20	23	20-30
Pb	1100	580	10-6100
Sb	7	< 10	
Se (ppb)	1500	920	340-1500
Sn	150	200	60-440
Te (ppb)	500	< 20	
Tl	< 10	< 10	
Zn%	6.2	1.0	0.4-1.7

presence of pyrrhotite, magnetite and carbonate as gangue minerals results in a moderately high pH upon oxidation of the ore and consequently the gossans are not very strongly leached.

Ar Ridaniyah, Saudi Arabia (30). The Ar Ridaniyah district, situated 220 km west of Riyadh on the eastern edge of the Arabian Shield, is characterized by numerous ancient Ag mines and several Zn-Pb-Ag prospects. The area has low rounded hills that commonly rise less than 50 m above the flat and sand-filled wadis. Mineralization consists of pyrrhotite, sphalerite and minor chalcopyrite and galena interlayered and intergrown with skarn minerals.

Gossan occurs as rubbly outcrop in a gently sloping area of about 200 × 30 m and is composed of quartz, goethite, hematite, plumbojarosite and, locally, calcite, gypsum and hemimorphite. It is characterized by moderate to high Zn and Sn contents (Table II.2-31), low to moderate (but clearly anomalous) Cu and Pb and low abundances of other pathfinder elements. Experience in Saudi Arabia (Ryall and Taylor, 1981) is that both Cu and Zn are generally concentrated in the surface gossans, so that not only does the composition of these gossans reflect that of the underlying mineralization but also suggests it to be subeconomic.

TABLE II.2-32

Composition of gossans on skarn-hosted base metal mineralization at four prospects at Squirrel Hills, northwest Queensland, Australia

	Cowie North N = 12 Mean ppm	Dingo N = 7 Mean ppm	Black Rock N = 7 Mean ppm	Marramungee N = 5 Mean ppm
Ag	2	32	40	2
As	400	130	190	24
Ba	150	150	170	45
Bi	27	250	1	1
Cd	< 1	< 1	< 1	< 1
Co	10	53	58	18
Cr	< 10	< 10	< 10	< 10
Cu	150	720	300	250
Fe ₂ O ₃ %	15.5	31.2	17.3	38.3
MnO%	7.99	0.26	2.34	3.10
Mo	3	5	11	1
Ni	4	4	32	4
P ₂ O ₅ %	3.97	0.28	1.07	0.21
Pb	7.58%	1.44%	1.21%	200
Sb	< 30	< 30	< 30	< 30
Sn	4	9	2	1
Sr	1060	33	50	26
Zn	6000	4100	8.62%	1180

Squirrel Hills prospects, northwest Queensland, Australia (31). These prospects are about 30 km northeast of Pegmont (12), centred around a number of geochemically anomalous gossans developed over mineralization hosted by rocks of the Lower Proterozoic Soldiers Cap Group. Unlike Pegmont, these rocks have been metamorphosed at the contact with granites of the Williams Batholith (Blake, 1987), mostly to quartz-garnet gneisses. The metamorphic ore assemblage is martite, pyrrhotite, pyrite, galena and magnetite, with some chalcopyrite at the Dingo prospect (Nisbet and Joyce, 1980). The area has low relief, with some low hills and ridges rising up to 20 m above the plains, and a semiarid climate; the depth of weathering is approximately 30 m.

Mineralization outcrops as manganiferous banded gossan consisting mainly of quartz, goethite, hematite and garnet, with minor gahnite, hemimorphite, corkite, plumbogummite, cryptomelane, coronadite, chalcophanite and variable amounts of carbonaceous matter. The gossans from the four prospects (Table II.2-32) have extremely variable Ag, Cu, Pb and Zn contents that reflect variations in primary mineralization. High Mn, P and relatively low Fe contents are similar to those at Pegmont, representing the influence of the quartz magnetite apatite garnet BIF. The Mn and P both form stable secondary minerals with the target and some pathfinder elements. Despite the generally low concentrations of the

pathfinder elements stepwise discriminant analysis effectively classifies these gossans (Taylor and Scott, 1982)

Other deposits

Elura, New South Wales, Australia (32). The Elura Mine occurs 40 km north-northwest of Cobar and 600 km west-northwest of Sydney. The massive pyrite, pyrrhotite, galena, sphalerite mineralization is a vertical pipe-like body and is weathered to a depth of 106 m. The orebody is hosted by a sequence of siltstones and sandstones in an area of low relief. The orebody was probably blind and only strongly ferruginized wallrock, which has been slightly eroded, outcropped. The outcrop is now buried beneath red colluvial soil. Geochemical dispersion at Elura is discussed further in Chapter III.3 (see p. 340).

The mineralogy, geochemistry and genesis of the gossan profile have been described by Taylor et al. (1984). The profile has many of the features of a "classical" mature gossan, with a thick, complex, supergene enrichment zone occurring between the ironstone gossan and underlying massive sulphide. Within the *ironstone gossan*, goethite, hematite and quartz are the main minerals with an increasing secondary sulphate and arsenate mineral content towards the base. No diagnostic boxworks or significant primary ore structures have been preserved. The *supergene zone* consists of approximately 15 m of oxidate minerals overlying 3 m of sulphides, the transition being marked by a 15 cm thick blanket of black/blue sooty supergene Cu sulphides. Leaching of some ore minerals continues for a further 20 m below the supergene zone.

The geochemistry of the various zones (Table II.2-33) is quite distinctive with Ag, As, Au, Ba, Bi, Cu, Hg, Pb, Sb and Sn being markedly enriched in the supergene zone. In contrast, the more mobile elements Zn, Tl and Cd have been leached from the profile. Initial oxidation of the ore resulted in the destruction of all sulphides. The mobile elements were lost from the gossan and Zn now occurs in anomalous concentrations deep in the weathered profile and for some distance downslope from the orebody. Whereas some Fe oxides formed essentially in situ by oxidation of the Fe sulphides to form direct gossan, the remaining Fe was taken into solution to be precipitated in the immediate wallrocks or as botryoidal, mammillary or stalactitic growths of Fe oxides in solution-deposited gossan. The direct gossan has significantly higher concentrations of the least soluble elements. Silver, Ba, Cu and Hg were also partially depleted in the gossan but Pb, As, Sb and Sn have largely been retained. Lead and As occur as the highly stable secondary mineral beudantite, which by analogy with other alunite-jarosite minerals may incorporate Sb as an anion and Ag, Ba and Hg by substitution for Pb.

Oxidation of the ore is no longer active, except for slight leaching below 106 m. Accordingly, water percolating through the gossan is no longer acid but has become slightly alkaline (pH 7.7–8.0), due to leaching of carbonate from the surrounding rocks, and saline (2.5% TDS). Under these conditions, beudantite is less stable and elements initially held in the ironstone are becoming mobilized,

TABLE II.2-33

Average composition of zones within the Elura Pb-Zn-Ag gossan profile, central New South Wales, Australia (Taylor et al., 1984)

	Fresh ore N = 42	Supergene sulphide N = 11	Supergene copper N = 4	Supergene oxidate N = 10	Ironstone gossan N = 14	Surface ironstone N = 5
<i>Data in %</i>						
SiO ₂	5-15	n.d.	n.d.	46.3	2.1	3.8
Al ₂ O ₃	0.5	< 0.02	0.44	0.27	1.32	5.5
Fe	15-50	29.5	5.43	17.0	54	50
MgO	0.1-0.7	0.02	0.06	0.05	< 0.1	< 0.1
CaO	0.2-0.9	< 0.01	0.04	0.04	0.22	0.09
K ₂ O	< 0.01-0.7	< 0.01	n.d.	0.07	< 0.1	0.12
TiO ₂	< 0.1	< 0.02	0.02	0.03	< 0.1	0.87
P ₂ O ₅	< 0.04	< 0.02	0.04	0.06	< 0.04	0.12
MnO	< 0.05	0.02	n.d.	< 0.01	< 0.5	< 0.5
CO ₂	0.5-9.3	0.18	0.56	0.1	< 0.2	n.d.
S	25-35	39.9	17.7	1.40	0.61	0.61
<i>Data in ppm</i>						
Ag	130	325	4200	150	< 1-100	< 1
As	5500	1735	2.67%	7.37%	2.2%	1.3%
Au	0.1-2	< 2	2	6	n.d.	n.d.
Ba	0.1-1%	810	5900	7000	400	2300
Bi	4-42	n.d.	n.d.	n.d.	< 1	< 1
Cd	90-380	42	25	< 5	< 3	< 3
Cu	1730	3750	51.5%	835	900	100
Hg (ppb)	5-100	n.d.	n.d.	n.d.	1.5	0.04
Mo	< 4-23	4	9	50	40	14
Pb	5.8%	28.5%	2.47%	16.2%	5.5%	4.3%
Sb	< 200-1200	510	140	6760	1000	600
Sn	25-120	110	1980	1840	1-300	5
Tl	25-460	500	60	3	< 1	< 1
Zn	8.4%	6500	290	740	1600	500

reprecipitating at the standing water-table in response to changes in pH and ionic composition. There now exists a complex supergene oxidate zone with transition from arsenate-rich (hidalguito, $(\text{PbAl}_3(\text{AsO}_4)_2(\text{OH})_6)$ with some beudantite, and then mimetite $(\text{Pb}_5(\text{AsO}_4)_3\text{Cl})$, to sulphate-rich (beudantite then anglesite) to supergene galena. Minor phases include native Ag (containing up to 20% Hg), native Au, electrum, cerussite, nadorite $(\text{PbSbO}_2\text{Cl})$, lanarkite $(\text{PbSO}_4\text{PbO})$ and barite. The dominant minerals in the supergene sulphide zone are primary pyrite and galena, supergene pyrite, galena, chalcocopyrite, marcasite, digenite, chalcocite, anglesite and beudantite.

Mount Torrens, South Australia (33). A number of base metal and massive pyrite prospects occur in metamorphosed siltstones and schists of Upper Pro-

TABLE II.2-34
Composition of ironstone outcrops, Mount Torrens, South Australia

	Gossan		Ferruginous metasiltstone		Gossanous metasiltstone		"Laterite"	
	Mean ppm	Range ppm	Mean ppm	Range ppm	Mean ppm	Range ppm	Mean ppm	Range ppm
Ag	40	3-100	7	1-28	<1	<1-2	<1	<1-1
As	3240	560-1.45%	1100	400-3800	30	6-85	65	25-105
Ba	2320	200-1.85%	1265	450-4750	475	20-2200	145	20-330
Bi	5	<4-16	4	<4-8	<4	<4-4	4	<4-12
Cu	2340	370-550	960	160-2000	210	80-430	120	10-370
Mo	100	50-150	12	10-15	12	8-25	7	4-15
Pb	8100	700-2.32%	1970	1050-6050	50	10-140	30	10-90
Sb	21	<4-55	16	8-26	12	<4-24	8	<4-14
Se	5	<2-14	4.7	5	7	4-10	3	<2-7
Sn	16	<4-115	5	<4-12	8	<4-14	7	<4-14
W	18	<10-50	16	<10-55	11	<10-40	10	<10-35
Zn	150	25-420	25	15-40	20	2-40	9	2-25

terozoic age (e.g. Kanmantoo Cu deposit, Nairne pyrite deposit) 30 km east of Adelaide. The discovery of a Pb-rich gossan in a creek bed led to the discovery of the Mount Torrens prospect at which there are a number of areas of ferruginous and gossanous outcrop. These have been subdivided into four groups (Table II.2-34):

(1) *Gossans*. The geochemical signature of the gossans suggested them to have been formed on base metal mineralization, which was later confirmed by diamond drilling.

(2) *Ferruginous metasiltstones*. These also have high concentrations of target and pathfinder elements but deep trenching and diamond drilling failed to locate any mineralization. It is now believed that they represent a lens of sulphide mineralization that has been eroded, with only a stringer zone remaining.

(3) *Gossanous metasiltstone*. The much lower metal concentrations in the gossanous metasiltstone indicate that this was formed on a lens of barren pyrite-pyrrhotite mineralization.

(4) *Ironstone ("laterite")*. The composition of the so-called laterite is comparable to that of the gossanous metasiltstone, but it is more ferruginous, no fine laminations are preserved, and the vermiform nature of the Fe oxides indicates that they are solution-deposited. These materials are now believed to represent reworked gossan rather than lateritic ironstones.

SUMMARY

The use of gossans to find near-surface sulphide mineralization is a cost-effective exploration technique provided that comprehensive methods of identification and evaluation of ironstones are used. Extensive research, particularly by CSIRO and exploration company personnel within Australia, has led to the following conclusions.

Prior to sampling, an ironstone outcrop should be mapped in detail, with special note being taken of the geomorphological setting and relief, the extent of possible erosion, the host rocks, the structure, size and continuity of the ironstone and the presence of secondary minerals other than hematite and goethite-including, for example, pH indicators as discussed in Chapter II.1. Samples should be collected along traverses across the outcrop at intervals that can appropriately account for the heterogeneity commonly encountered.

The fabric, mineralogy and geochemistry, of gossans is largely determined by the pH of the oxidizing environment. Boxwork fabrics are best preserved when the oxidizing sulphides are coarse grained and the environment has a high pH. Under these conditions, no Fe^{2+} can remain in solution and is immediately precipitated on crystal faces, cleavage planes and grain boundaries. If the pH is low, Fe^{2+} remains in solution and is leached, although it may precipitate nearby as a solution-deposited gossan.

The elements occurring within mineral deposits fall naturally into five groups depending on the Eh: anions (including oxyanions), cations, metals, insoluble oxides and those which have a variable oxidation state, as discussed in Chapter I.5. Target and pathfinder elements most commonly form cations that are more soluble at low pH. Such acid conditions also inhibit adsorption and co-precipitation with the Fe oxides, and only a few secondary minerals are stable. Thus, boxworks and enhanced geochemical signatures in gossans are favoured by the higher pH that develops in deposits deficient in Fe sulphides, or where the gangue and/or wallrocks are reactive.

However, in evaluating gossans and ironstones, it is not the absolute values of one or more target elements that are diagnostic but the relative concentrations of a suite of elements commonly associated with the various styles of mineralization. For example Pt, Pd, Ir and Se, commonly at concentrations below 1 ppm, occur with Ni, Cu and Co in massive Ni-Cu sulphide mineralization and associated gossans. The presence of these elements, and the absence of Zn, distinguish such gossans from lateritized ultramafics.

All multielement geochemical and, if possible, mineralogical and geological data should be entered into a computer database for evaluation. Stepwise discriminant analysis is the most effective statistical manipulation and, provided sufficient training sets are available, is able not only to separate gossans from ironstones, but also to assign the gossans to different types of mineralization. Under limited circumstances, factor analysis or cluster analysis may also prove useful.

SEASONALLY HUMID TROPICAL TERRAINS (SAVANNAS)

H. ZEEGERS and P. LECOMTE

INTRODUCTION

Savanna climates are tropical climates having an annual rainfall ranging between 600 and 1500 mm and well-contrasted dry and wet seasons. These climates occupy a wide belt bordering the equatorial zone (Fig. I.1-1) including the Brazilian Shield, West and East Africa and parts of India and northern Australia.

The landscapes of these regions are typified by the widespread presence of laterites and of the corresponding deep weathering profiles as described in Chapter I.3. One of the most conspicuous features of these profiles, when they are neither truncated nor degraded, is the presence of a thick, hard, surficial ferruginous duricrust: *cuirasse*.

As introduced in Chapter I.1 (Table I.1-6) and applied also to the rainforest and arid zones (Chapters III.2 and III.3), there are three principal series of geochemical dispersion models:

(A) the (pre-existing) lateritic profile is mostly preserved, so that the ferruginous *cuirasse* is outcropping or suboutcropping (A models);

(B) as a result of erosion, the pre-existing lateritic profile is truncated below the *cuirasse* horizon (B models);

(C) the pre-existing lateritic profile has been entirely eroded, and soil profiles are the product of weathering under more recent climates (C models).

Each of these situations results in different mineralogical composition of the weathering products, and hence largely controls the distribution and mobility of trace elements. Where profiles are complete, the Fe oxides are the key minerals, at least in the upper horizons of the profile, and the retention of those trace elements that are not incorporated in primary resistant minerals will depend largely on their affinity for goethite or hematite (Tooms et al., 1965; Zeissink, 1969; Blot et al., 1978; Esson, 1983; Schorin and Puchelt, 1987).

If the upper part of the lateritic profile has been eroded, two situations again may be distinguished (Boulet, 1974; Leprun, 1977; Zeegers and Leprun, 1979):

(1) truncation is rather high in the saprolite, and *kaolinite* inherited from the former weathering profile is the dominant secondary mineral.

(2) truncation is near the base of the pre-existing profile, where rock-forming silicates are present. Weathering of such minerals may result in the formation of *smectites*, particularly in drier savannas (annual rainfall < 1200 mm) and/or in

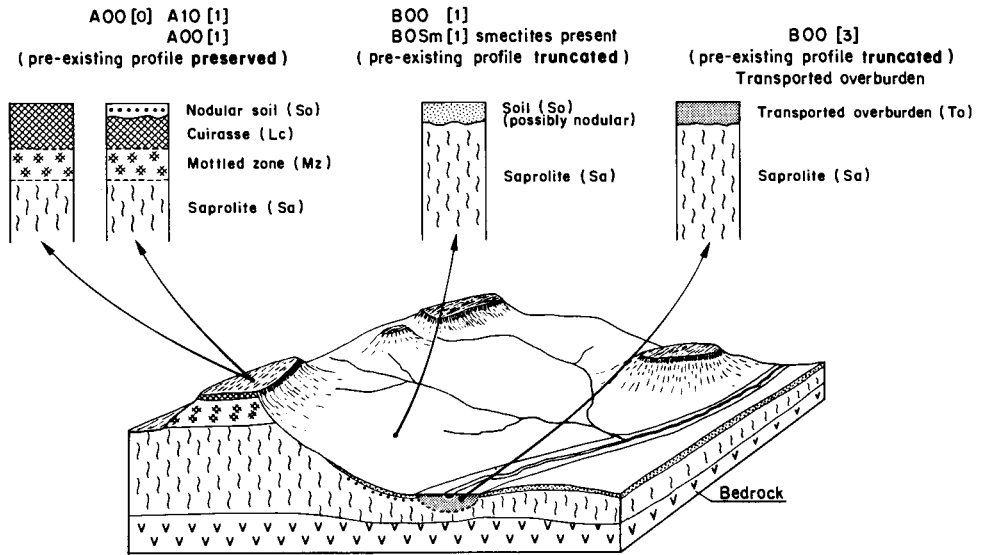


Fig. III.1-1. Diagram showing the general landscape and the weathering profile related to preserved or truncated lateritic surface. N.B. Compare with Fig. III.2-1: differences in geochemical dispersion are expressed by the model codes.

Abbreviations (for all model diagrams):

HORIZONS

To	Transported overburden
So	Soil
Lc	Lateritic cuirasse
No	Nodular horizon
Mz	Mottled zone
Sa	Saproliite
Br	Bedrock

SAMPLE TYPE

G	Gossan
G(S)	Gossan, surface
G(SS)	Gossan, subsurface
OM	Oxidized mineralization
OM(S)	Oxidized mineralization, surface
OM(SS)	Oxidized mineralization, subsurface
M	Mineralization
M(S)	Mineralization, surface
WB	Weathered bedrock
F	Fault ironstone

MECHANISMS AND ANOMALY TYPES

M	Mechanical (physical, clastic)
H	Hydromorphic (chemical)
R	Residual

PG	Pseudogossan
SL	Residual soil
TO	Transported overburden
SS	Stream sediment

poorly drained environments. Smectite-rich soils (vertisols) may form on basic rocks or on clay-rich alluvium (see Chapter I.6).

These different situations may merge one into the other over very short distances (Boulet, 1974). This is indicated on Fig. III.1-1, which depicts a landscape typical of seasonally humid tropical terrains. Accordingly, even within the small size of a single prospect, areas having different geochemical character-

istics may be encountered, requiring different interpretations of element mobilities and different decisions as to the most appropriate exploration procedure.

Uplift and/or a change to a drier climate (Chapter III.3) are not the only causes of modification to the pre-existing profile. In some regions, particularly in East Africa, stone-line profiles have been reported that resemble those described in Chapter III.2 (Webb, 1958; Tooms and Webb, 1961). These profiles have not been as strongly leached as in rainforest environments, but nevertheless were probably formed under wetter climatic episodes that prevailed between the formation of the lateritic profile and the present rather drier climate; they will be considered as belonging to B 1 * [*] (ferruginous kaolinitic) type dispersion models.

The dispersion models presented hereafter are thus based on 3 main situations:

(1) pre-existing lateritic profile mostly preserved: A 0 0 [*] (recent leaching none or minor) or A 1 0 [*] (recent leaching low) situations;

(2) pre-existing profile partly truncated:

(a) present profile mostly kaolinitic or "ferruginous kaolinitic": B 0 0 [*] or B 1 0 [*] situations;

(b) present profile mostly smectitic: B 0 Sm [*] situations;

It is emphasized, however, that irrespective of the level of truncation or the degree of modification of the profile and, therefore, the dispersion model, the different weathering horizons retain chemical characteristics inherited from the underlying bedrock and may thus be considered as lithodependent to some extent (Blot et al., 1976; Matheis and Pearson, 1982; Matheis, 1983; Wilhelm et al., 1985).

A-TYPE DISPERSION MODELS: PRE-EXISTING LATERITIC PROFILE MOSTLY PRESERVED

Profile description

General

Lateritic profiles are best preserved in areas where the former lateritic surface is rather flat or only gently undulating and at low to medium altitudes. In such situations, the present topography roughly coincides with the pre-existing lateritic surface and erosion is of low energy. Large areas having well-preserved lateritic profiles occur in central Burkina Faso, south Mali, northeast Guinea, east Central African Republic, parts of India and northern Australia—that is, mostly in old basement areas with a rather homogeneous lithology, and in zones of relative tectonic stability. When these conditions are not met, the old lateritic surfaces have been at least partly eroded, resulting in a dissected morphology where remnants of cuirasse of varying local significance may be observed.

The age or even the number of the pre-existing lateritic surfaces is a matter of considerable debate and there is as yet no general agreement (Boulet, 1970;

Michel, 1978; Millot, 1980; Grandin and Thiry, 1983) but a late Mesozoic-early Tertiary age seems widely accepted as one of the most significant.

The idealized lateritic profile, as presented Chapter I.3, can be schematically described as follows (Fig. III.1-1):

(1) *surficial soil* (0–1 m thick); greyish, silty horizon, sometimes becoming reddish towards the base, with ferruginous nodules or pisoliths, in a fine matrix consisting essentially of quartz and kaolinite. This horizon is interpreted as mostly resulting from the degradation (by dissolution and loss of Fe) of the underlying cuirasse (Nahon and Trompette, 1982; Bocquier et al., 1984).

(2) *ferruginous cuirasse* (1–5 m thick); an indurated pisolitic, lamellar or pseudo-conglomeratic horizon, with hematite, goethite and kaolinite as dominant secondary minerals and quartz as main primary residual mineral. At depth, it merges into a softer Fe-rich “carapace”. The more detailed description presented in Chapter I.3 subdivides the cuirasse or iron crust into four subhorizons.

(3) *mottled zone* (0.5–4 m thick); a kaolinite-goethite matrix with ferruginous (aluminous hematite) spots and nodules that are more or less indurated and more abundant in the transition zone with the “carapace”. No relic rock fabrics or structures are preserved in this horizon, except as lithorelics within ferruginous segregations.

(4) *saprolite* (5–60 m thick); mostly kaolinitic, with rock structures or fabrics at least partially preserved, indicating that weathering has been essentially isovolumetric. Where strongly leached, it is sometimes referred to as the “pallid zone”. At the base of the saprolite, smectites may form under some specific drainage and/or over particular lithologies; smectite formation is generally interpreted as being related more to the present climate than to past ones. In Chapter I.3, two subhorizons are distinguished: the coarse grained saprolite at the base, with some unweathered rock fragments or primary minerals, and the fine grained saprolite in the upper part, where only resistant primary minerals (such as quartz) may be found.

A simplified profile description may be considered, which includes two major horizons: the *pedolith*, comprising the upper part of the regolith, subjected to soil forming processes, and the rest of the profile, the *saprolith*.

From this description, it is evident that, even when most of the pre-existing profile is preserved, some characteristics reflect the influence of the present climate. Thus, at the top of the profile, the cuirasse may be leached and transformed into a quartz-kaolinite assemblage containing some relic nodules or pisoliths. At the base of the saprolite, rock-forming minerals have weathered to smectites rather than kaolinite. Additionally, water-table fluctuations or lateral water circulation may lead to the transformation of existing kaolinite to smectite. The former lateritic profile cannot therefore be considered as being exactly in equilibrium with the conditions prevailing in the present savannas, even if the degradation or transformation suffered are far less important than under wetter (Chapter III.2) or drier (Chapter III.3) conditions.

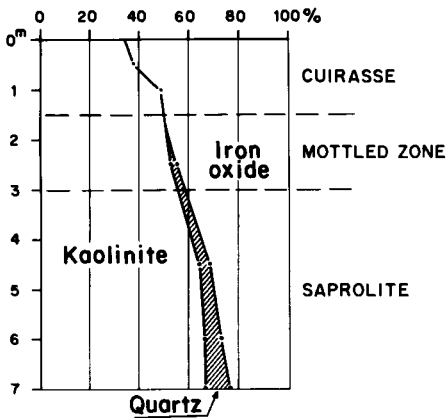


Fig. III.1-2. Generalized mineralogical compositions of the upper part of a lateritic weathering profile. Modified after Leprun (1979).

Mineralogy and chemical composition

The mineralogy of weathering profiles in savanna environments is illustrated by Leprun (1979) from a weathering profile in Burkina Faso (Fig. III.1-2). Thus, the proportion of kaolinite decreases from 66% in the saprolite to 38% in the cuirasse, whereas the Fe oxide content is 62% in the cuirasse and only 21% at the base of the saprolite. Ambrosi and Nahon (1986) have shown that the cuirasse has developed by progressive ferruginization of the kaolinitic matrix of the saprolite. Two processes, acting simultaneously, are involved. Firstly, hematite replaces kaolinite to form nodules, while secondly, the initial kaolinite is replaced by microcrystalline kaolinite and goethite.

The chemical processes involved in lateritic weathering are described in Chapters I.2–I.5. The massive accumulation of Fe and Al in the upper part of the profile corresponds to the almost complete removal of the alkaline and alkaline-earth elements. Typical vertical distributions of Al_2O_3 , Fe_2O_3 and SiO_2 are shown on Fig. III.1-3, from data from Burkina Faso (Ambrosi, 1984). Data from other examples in Senegal and Burkina Faso are given in Table III.1-1. The following trends are evident:

(1) SiO_2 contents decrease progressively from the base of the saprolite to the top of the cuirasse horizon. Whenever a surficial soil horizon is present, it has very high SiO_2 contents, correlating with losses of Al_2O_3 and Fe_2O_3 .

(2) Fe_2O_3 concentrations increase towards the top of the profile, with a strong enrichment in the cuirasse horizon.

(3) Al_2O_3 contents are highest in the kaolinitic saprolite, and then decrease in the Fe-rich horizon, except where Al-rich bauxitic cuirasses have formed.

The trace elements are retained in the lateritic profile if:

(1) they are present as stable primary minerals (e.g. Sn in cassiterite) which are preserved or even concentrated during weathering;

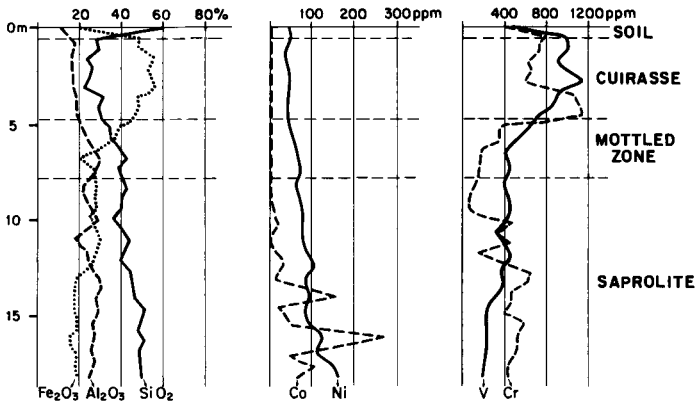


Fig. III.1-3. Average variations of selected major and trace elements contents in a lateritic weathering profile of Burkina Faso. Derived from Ambrosi (1984).

TABLE III.1-1

Means or ranges of SiO_2 , Al_2O_3 and Fe_2O_3 contents in different horizons of lateritic profiles; 1: basic to intermediate volcanics, Burkina Faso (Ambrosi, 1984); 2: shales, Burkina Faso (Leprun, 1979); 3: migmatites, Burkina Faso (Leprun, 1979); 4: sandstones, Senegal (Nahon, 1976); 5: granodiorite, Burkina Faso (Zeegers et al., 1981)

Reference	Horizon	$\text{SiO}_2\%$	$\text{Al}_2\text{O}_3\%$	$\text{Fe}_2\text{O}_3\%$	N
1	Cuirasse	26	19	48	176
	"Carapace"	31	22	39	176
	Mottled clay	38	25	27	176
	Transition	44	27	19	176
	Saprolite	53	15	17	176
2	Cuirasse	17-33	16-18	38-56	3
	Mottled clay	53	24	18	1
	Saprolite	56	23	9	1
3	Cuirasse	43-53	11-16	22-32	10
	Mottled clay	56-61	18-20	4-11	4
	Saprolite	64-69	16-17	1-3	3
4	Nodular soil	61	8	25	105
	Cuirasse	50	2	42	105
	Mottled clay	84	7	5	105
5	Soil	67	11	21	76
	Cuirasse	53	11	35	126
	Mottled clay	62	11	25	128
	Saprolite	69	11	18	248

(2) they form accessory, stable, secondary minerals;

(3) they are incorporated in one or more of the main secondary mineral phases. Such elements fall into two main groups:

(i) elements such as Cu, Zn, Ni, Co or Mn associated with kaolinite or other secondary silicates forming the saprolite. These elements are commonly strongly leached when Fe_2O_3 contents increase, in the upper horizons of the profile (Kalsotra and Prasad, 1981; Ambrosi, 1984).

(ii) elements such as V, P, Cr, Mo, Nb and As that have a strong affinity for the Fe oxides. These are retained or even enriched in the Fe-rich horizons, whereas in the saprolite their concentrations rarely exceed those observed in the bedrock.

Vertical distributions for elements representative of each of these groups are shown on Fig. III.1-3.

Because no drastic change in trace element concentrations have commonly occurred, sampling and analysis of the saprolite may indicate the geochemical characteristics of the bedrock (Mösser et al., 1985; Paquet et al., 1987). In contrast, the Fe-rich horizons (cuirasse) and, to some extent, the mottled zone, have compositions that differ greatly from those of the bedrock. Tardy et al. (1988) have shown that the characteristics of the bedrock are progressively altered as the profile evolves in such a way that the lithodependance is least where the profile is most evolved, i.e. where the Fe content is highest. Nevertheless, significant lithological contrasts or the presence of mineralization may be detected by analyzing samples collected in the strongly lateritized upper horizons of the weathering profile (Zeegers and Leprun, 1979). Similar conclusions have been reached in drier climates by Mazzucchelli and James (1966), Smith and Perdrix (1983) and Smith et al. (1987) as discussed in Chapter III.3.

Dispersion models and examples

A-type dispersion models correspond to areas of outcropping lateritic cuirasse (A 0 0 [0]) and to cuirasse covered by a thin residual or semi-residual soil (A 0 0 [1] or A 0 0 [2]) models. The situation of these models within the general landscape is presented Fig. III.1-1, and details are given on Fig. III.1-4. By comparison with dispersion models in rainforest terrain, the recent leaching of the profile is generally minor. The A 1 0 [*] models of dispersion are found only in savanna environments where the climate is or has been rather humid, such as in East Africa.

For the A 0 0 [0] model (outcropping cuirasse), the dispersion mostly proceeds from a combination of hydromorphic (H) and detrital (M) processes, both past and present, related to the formation or evolution of the lateritic profile. In the saprolite, whether kaolinitic or smectitic, many of the target elements (e.g. Cu, Pb, Mo, As) are not strongly leached and anomalies are mostly residual. However, hydromorphic processes disperse some elements (e.g. Zn). The dispersion halo widens in the mottled zone, but reaches its greatest extent in the cuirasse. The formation of this horizon involves intense chemical alteration and it

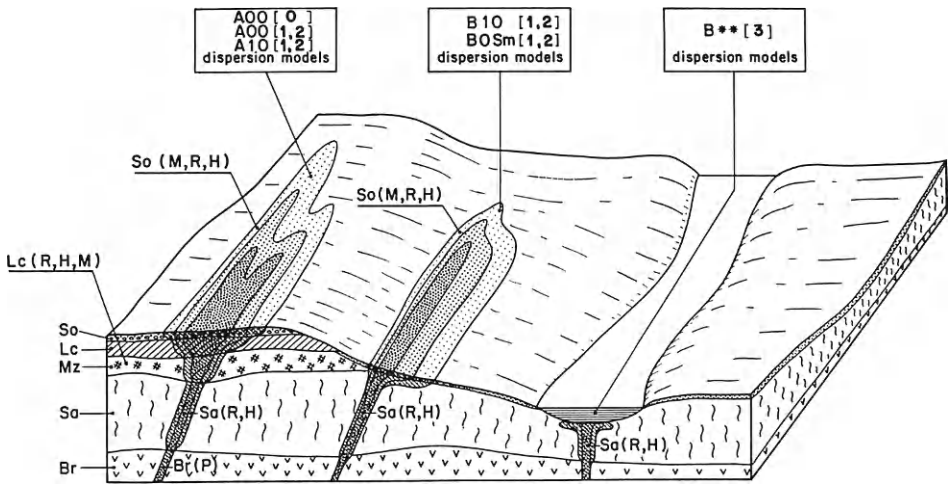


Fig. III.1-4. Diagram showing the idealized dispersion models in preserved or truncated lateritic profiles. N.B. Compare with Fig. III.2-5: differences in geochemical dispersion are expressed by the model codes. For abbreviations, see Fig. III.1-1.

is probable that at least part of the Fe accumulated in it has been transported for some distance; some of the trace elements may have behaved similarly, resulting in a large dispersion halo. Compared to bedrock, the concentrations observed in this halo may be similar (Pb, W, Sb), enriched (Mo, As, Au) or more or less depleted (Cu, Zn, Au), depending upon the stability of the host minerals and the chemical characteristics of the elements concerned.

When surface geochemical samples are collected, particular attention should be paid to the sampling medium and to sample preparation. Indeed, when the lateritic cuirasse is covered by a silty nodular soil, very different geochemical responses may be obtained depending on whether the soil or the hard laterite itself is sampled. The choice of the size fraction to be analyzed is also very important. In some circumstances, the fine fraction ($< 125 \mu\text{m}$ for instance) is mostly made of quartz, and is almost useless for exploration purposes, whereas in different situations, the same fine fraction may contain significant amounts of kaolinite, and thus be an efficient host for several target and pathfinder elements. Selection of the coarse fractions ($> 500 \mu\text{m}$ or so) may result in relying only on the ferruginous material, which may be leached or in which some elements have been concentrated, depending upon circumstances.

In some situations, it is possible to have transported overburden lying over an almost fully preserved lateritic profile. Matheis and Pearson (1982) described a profile from north Nigeria where an indurated lateritic horizon is covered by a structureless friable material, which is assumed to be water-transported and thus allochthonous. This interpretation is based on the observation that the silt horizon clearly erodes the underlying laterite. These profiles were not sampled

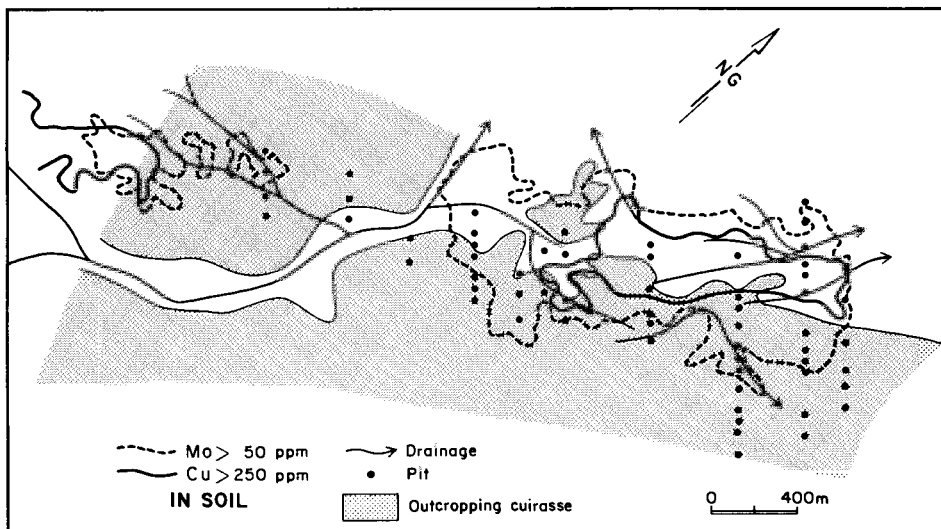


Fig. III.1-5. Goren Cu-Mo prospect, Burkina Faso. Distribution of Cu and Mo contents of soil samples collected at a 50×50 m grid. From Zeegers et al. (1981).

because it was considered that they would not contain any geochemical signature from the bedrock. Such a situation may be considered to represent the A 0 0 [3] model. Situations in which truncated lateritic profiles are buried beneath transported overburden (i.e. B * * [3] model) are described later in the chapter.

Goren Cu-Mo mineralization, Burkina Faso (A 0 0 [1], B 0 0 [1]). This prospect is situated in a dry savanna in north-central Burkina Faso. Geochemical exploration was carried out to follow-up an aeromagnetic anomaly in a Precambrian greenstone belt. This resulted in the discovery of a well-contrasted Cu-Mo soil anomaly related to disseminated molybdenite and chalcopyrite in a granodiorite stock (Zeegers et al., 1981). The mean grades in the mineralization are 0.2–0.3% Cu and about 0.03% Mo. Most of the prospect is covered by a thick and well-preserved lateritic profile; dissection has occurred only along the drainage axis, where in consequence the subcrop is predominantly saprolite.

The Cu and Mo anomalies in soil samples (30 cm depth, < 125 μm fraction) are shown in Fig. III.1-5. The distribution of Cu seems to be strictly controlled by the presence of a suboutcropping cuirasse horizon and the highest contents (> 250 ppm Cu) are found where the upper part of the lateritic profile has been removed. In comparison, the distribution of Mo shown by soil sampling is in no way influenced by the presence or the absence of a ferruginous cuirasse. High contents are found whatever the degree of truncation of the lateritic profile.

Several pits were dug to expose the weathering profile; some analytical data from samples collected from these pits are presented Table III.1-2. The mean

TABLE III.1-2

Goren Cu-Mo prospect, Burkina Faso: mean content of Fe_2O_3 , Cu and Mo in different horizons of the weathering profile

Horizon	Fe_2O_3 %	Cu ppm	Mo ppm	N
Soil	21	160	40	76
Cuirasse	35	215	120	126
Mottled clay	25	220	125	128
Saprolite	18	350	100	248

concentrations of Cu and Mo in the four horizons of the weathering profile show distinctly different trends: Cu contents decrease steadily from the saprolite to the soil, whereas Mo is concentrated with Fe in mottled zone and cuirasse horizons. In the soil, Mo content declines, following the degradation of the cuirasse and the loss of Fe.

The geochemical dispersion of Cu and Mo, as observed at Goren, is thus very different according whether the profile is preserved (A) or truncated (B). This is illustrated in Fig. III.1-6, where four situations are shown:

(1) profiles 1 (lateritic profile preserved) and 4 (lateritic profile truncated) are some distance from the mineralized granodiorite. Contents of both elements are low (< 50 ppm Mo and < 200 ppm Cu) in the saprolite and the mottled zone, but that of Mo is rather high (> 75 ppm) in the cuirasse of profile 1, because of a larger dispersion halo in that horizon.

(2) profiles 2 (lateritic profile preserved) and 3 (lateritic profile truncated) are within the mineralized envelope. Copper and Mo contents are high in the different horizons (> 700 ppm Cu and > 200 ppm Mo) but, in the cuirasse (profile 2), Cu is significantly leached, and the surface expression for that element is thus considerably subdued.

Copper and Mo thus exhibit different dispersion characteristics in the various horizons of the lateritic weathering profile. Molybdenum has a strong affinity for the Fe oxides and is therefore fixed in the cuirasse horizon, possibly after some hydromorphic migration has resulted in an enlarged dispersion halo. Conversely, Cu is less stable in the Fe-rich environment, and is relatively depleted in the cuirasse horizon.

In the situation represented by the A 0 0 [1] dispersion model, the cuirasse is commonly covered by a silty soil consisting of quartz and kaolinite, with some ferruginous nodules at the base. This soil horizon commonly represents the only readily available sampling medium. Accordingly, the quality of the geochemical responses of Cu and Mo was evaluated for different size fractions of anomalous soil samples collected at Goren (BRGM, unpublished internal reports). The distribution of the major oxides SiO_2 , Al_2O_3 and Fe_2O_3 was also determined in these samples and fractions. The results are illustrated for two samples in Fig. III.1-7.

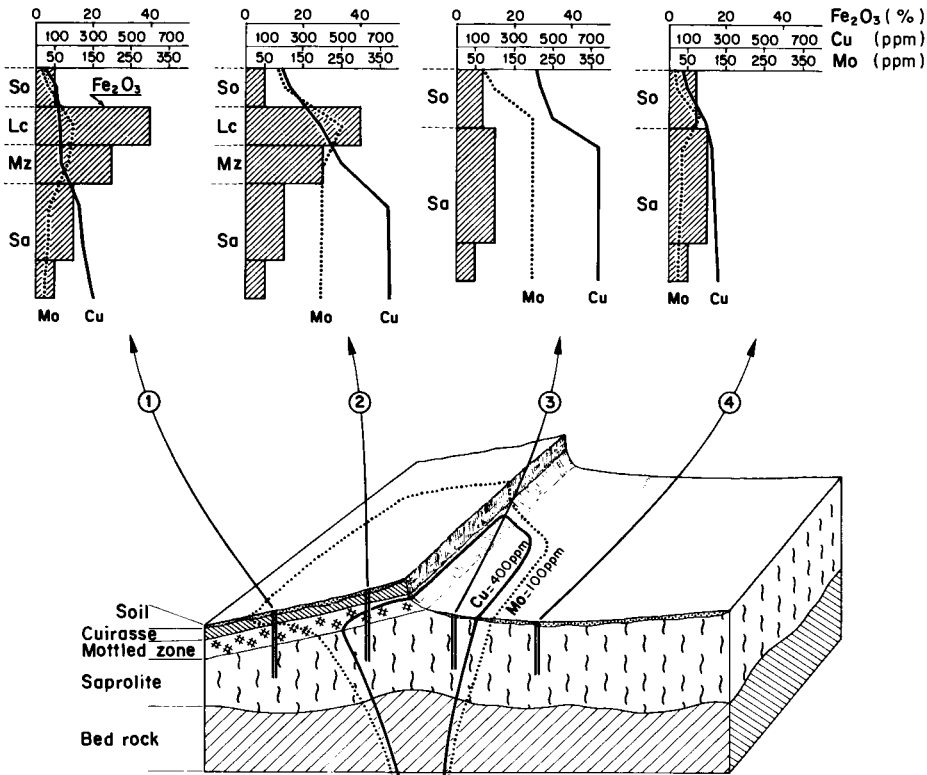


Fig. III.1-6. Goren Cu-Mo prospect, Burkina Faso. Diagrams showing the distribution of Fe_2O_3 (mean contents for each horizon except for saprolite, for which 2 samples are shown), Cu and Mo in profiles situated in different weathering situations. For abbreviations, see Fig. III.1-1.

The most striking feature is the inverse correlation between the concentrations of SiO_2 and those of Fe_2O_3 , Cu and Mo. This is most important and is due to dilution by quartz in the 63–250 μm size fractions. In the fine (< 63 μm) fraction, the Cu response is significantly improved; the high Al_2O_3 contents of these samples indicate an increased proportion of clay minerals, probably kaolinite. The coarsest fractions (> 1000 μm) which have the highest Cu and Mo contents, contain large amounts of lateritic material (as nodules and pisoliths) as reflected by the high Fe_2O_3 contents.

The most suitable size fractions for geochemical exploration purposes, therefore, are the finest (< 63 μm) or the coarsest (> 1000 μm). The main mineral phases responsible for the high metal contents are probably the clay minerals (kaolinite) in the former and Fe oxides in the latter. Using analytical data from background samples, the anomaly/background ratio for Cu and Mo in the < 125 μm and > 1000 μm size fractions indicates that the fine fraction gives the better contrast (Table III.1-3).

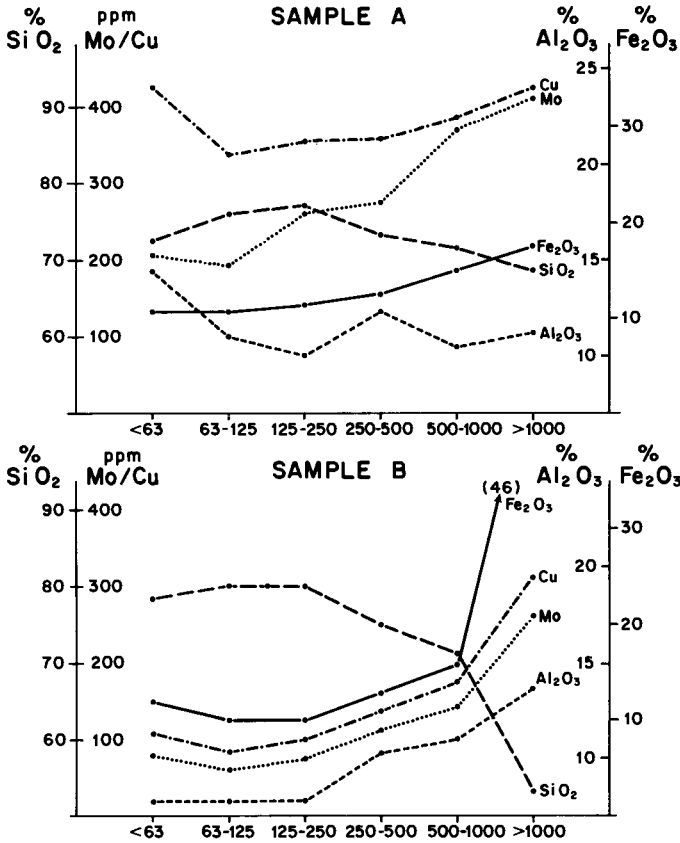


Fig. III.1-7. Goren Cu-Mo prospect, Burkina Faso. Distribution of selected major and trace elements in different size fractions of anomalous soil samples.

Wan-Rumbek area, south Sudan. A regional soil survey of an area of about 200,000 km² of mostly migmatitic and granitic basement in south Sudan demonstrates the suitability of soil sampling for regional surveys in lateritic terrain (De Vivo et al., 1981). The region has a savanna climate with an annual rainfall

TABLE III.1-3

Goren Cu-Mo prospect, Burkina Faso: ratio of threshold (mean + 2 standard deviations) to background in fine and coarse fractions of soil samples overlying the lateritic profile in the mineralized envelope

Size fraction	Cu	Mo
< 125 μm	4.00	3.74
> 1000 μm	2.15	2.95

ranging from 800 to 1600 mm, with well-contrasted seasons. Soils were sampled at a density of 1 sample per 300–350 km²; the samples were dried, sieved to minus 80-mesh (177 μm) and crushed. They were analyzed by XRF for Al, Fe, Mn, Ti, Cu, Mo, Pb, Zn, Nb and Sn. Threshold values for Nb, Sn, Mo, Zn, Pb and Cu were found to be 50, 15, 17, 87, 114 and 117 ppm respectively. Part of the area is a laterite plateau, and in these regions the survey found:

(1) clear geochemical signatures for distinct lithologies such as nepheline syenites (Ti–Nb–Al–Zn association) and basic rocks (Cu–Zn–Al association) even where there was a thick lateritic cover;

(2) a specific geochemical signature (Pb–Cu–Zn–Fe–Mn) in the lateritic environments, that could not be explained by lithological contrast. It was concluded that this association was due in part to supergene enrichment.

This example demonstrates the residual character of the lateritic cover, for geochemical characteristics of the underlying bedrock persist at the surface and are detectable by low density soil sampling. However, some specific geochemical signatures are due to lateritic weathering of unmineralized bedrock.

Kinagoni Hill Pb–Zn deposit, Kenya Coast Province (A 0 0 [1], A 1 0 [1]). This region has a typical seasonally humid climate with an annual rainfall ranging between 875 and 1125 mm. Near the Kinagoni deposit, numerous occurrences of lateritic cuirasse are known. In the 1970's, regional geological and stream sediment geochemical surveys were carried out and several mineral occurrences were discovered by following up anomalies by detailed geochemical surveys.

The Kinagoni Hill deposit, which is covered by a thick lateritic cuirasse, is indicated by a well-contrasted Pb–Zn anomaly. The dispersion halo has three components (Bugg, 1982):

(1) *residual*: at the top of the hill (Fig. III.1-8), Pb contents of up to 3000 ppm are present in the residual soil over the lateritic cuirasse;

(2) *mechanical*: soils having Pb contents up to 1000 ppm occur on the slopes of Kinagoni Hill. The soils contain relatively insoluble secondary Pb minerals, including anglesite and cerussite, derived from the mineralization at the summit;

(3) *hydromorphic*: strong Zn anomalies (up to 1000 ppm) occur in Mn-rich alkaline soils developed over barren Jurassic limestones, several hundred metres downslope from the deposit.

The three components of the anomaly again demonstrate that elements derived from the same mineralization may have different dispersion characteristics in the supergene environment, depending on their mobility during weathering. Similarly, but under drier conditions, Cox and Curtis (1977) observed that Zn leached from soils overlying the Lady Loretta deposit (Australia) were concentrated downslope, whereas Pb and Ag anomalies halos are restricted to the immediate area of the deposit. Oxidation and leaching of mineralized rocks extends to 100 m and more below surface, possibly related to a fossil weathering episode, during which the hydromorphic Zn dispersion halo could have developed. Gossan formation and geochemical dispersion at Lady Loretta are dis-

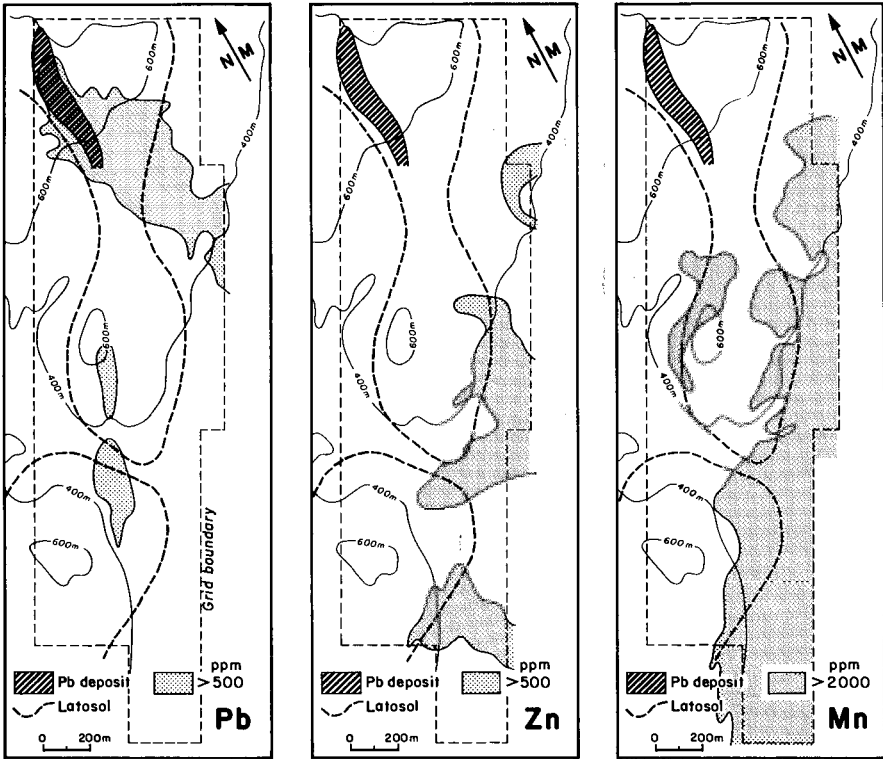


Fig. III.1-8. Kinagoni Pb-Zn prospect, Coast Province, Kenya. Distribution of Pb, Zn and Mn in soil samples (minus 80-mesh ($177\ \mu\text{m}$) fraction; HCl extraction). Modified after Bugg (1982).

cussed in Chapters II.2 and III.3 respectively. Similar conclusions were reached by Middleton and Campbell (1979) and Laville-Timsit et al. (1983) in humid rainforest environments (e.g. THR prospect, see p. 262).

Diouga area, Burkina Faso (A 0 0 [1]). Several scattered Au occurrences have been found in a deeply weathered lateritic terrain developed from Precambrian volcanics (BRGM, unpublished internal reports). The mineralogy and geochemistry of the weathering profiles have been studied in detail (Ambrosi, 1984) and show that the trace elements have been subjected to two distinct dispersion processes:

(1) some elements, such as Cr and V, are stable in the profile and may even accumulate in the cuirasse relative to the Fe concentration, forming large geochemical dispersion haloes whose formation is probably related to the development of the profile. This dispersion pattern is similar to that described for Mo at Goren (see p. 211).

(2) elements such as Cu and Ni are partially solubilized and leached from the profile.

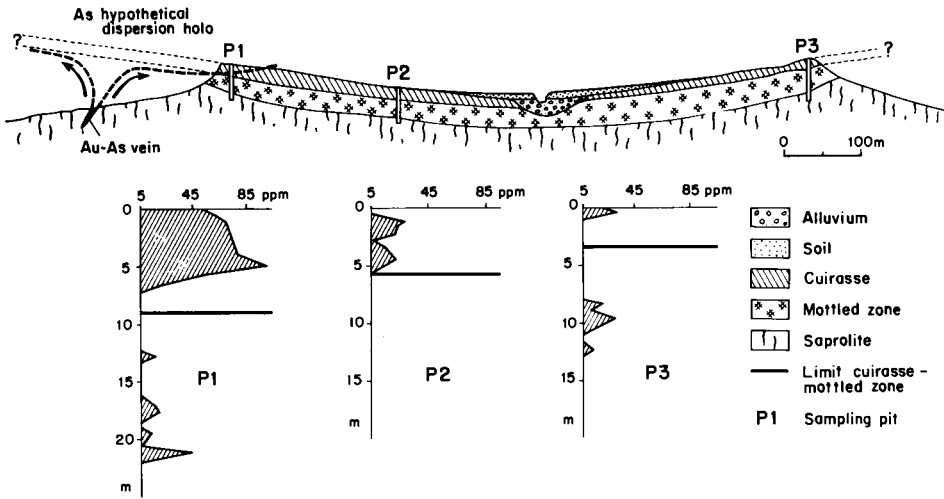


Fig. III.1-9. Diouga Au prospect, Burkina Faso. Cross section showing the dispersion of As from Au-As mineralization in different positions relative to the lateritic surface. Modified after Ambrosi (1984).

Arsenic, a key pathfinder in exploration for Au, seems to belong to the first group, i.e. retained or enriched during lateritic weathering. It has an extensive dispersion halo in the upper cuirasse horizon, around the Au-As mineralization (Fig. III.1-9). Distant from the mineralized “source” (sampling pit P1), but still within the anomalous surficial halo, the As contents decrease sharply from 80–100 ppm in the cuirasse to 5–20 ppm in the lower mottled zone and saprolite. Further away, the As content in the cuirasse declines to 20–25 ppm in pit P2 and to background level (less than 10 ppm) in pit P3. The distances of P1, P2 and P3 from mineralized source are approximately 200, 400 and 900 m.

There is no significant concentration of Au in the different horizons of the weathering profile at Diouga, even where As is anomalous. This may be due to leaching or, more probably, to the uneconomic character of the primary mineralization. Nevertheless, As may be considered as a good pathfinder for Au, the main advantage being its stability in the weathering profile and its wide dispersion in the ferruginous horizons.

Filon Bleu Au prospect, Guinea (A 0 0 [0], A 0 0 [1], B 0 0 [1]). The “Filon Bleu” prospect exemplifies the good surface geochemical response given by a small vein type Au occurrence (BRGM, unpublished internal reports) in Precambrian volcano-sedimentary rocks. Along the SE–NW traverse depicted on Fig. III.1-10, the following weathering environments are observed:

- (1) from A to B, the pre-existing lateritic profile is dissected, resulting in a B 0 0 [1] model, with suboutcropping saprolite developed over basic volcanics;
- (2) from B to C, outcropping cuirasse, i.e. model A 0 0 [0];

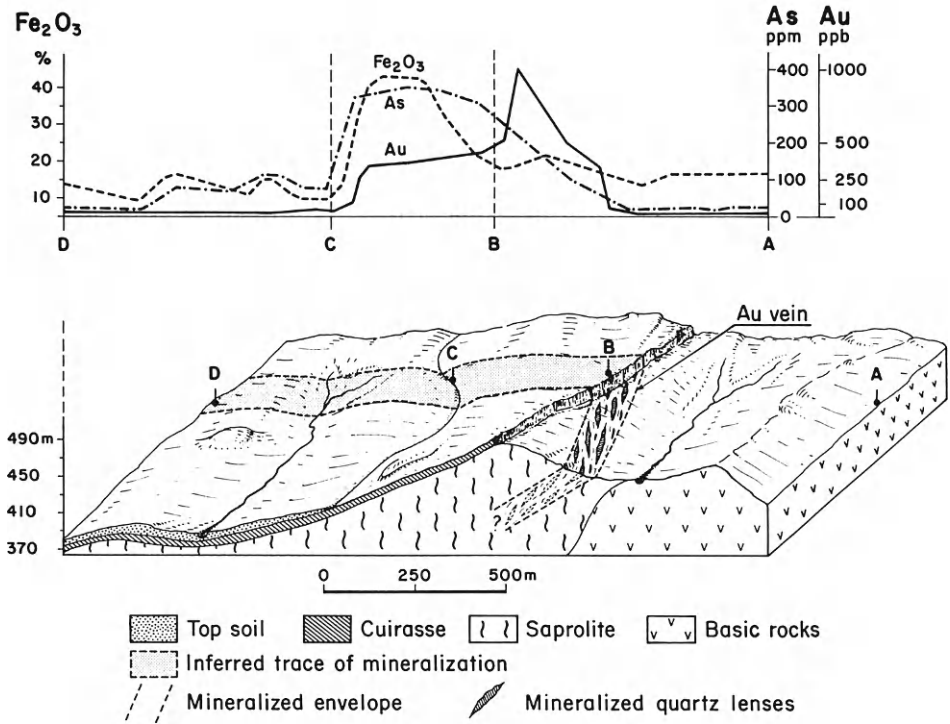


Fig. III.1-10. Filon Bleu Au prospect, Guinea. General landscape and cross section showing the distribution of Au, As and Fe_2O_3 contents in different surface conditions.

(3) from C to D, cuirasse covered by a mostly residual silty soil, 0.5 to 1 m thick, i.e. models A 0 0 [1] or locally A 1 0 [1] with some degradation of the cuirasse.

Geochemical sampling was carried out at about 30 cm depth in soils (in B 0 0 [1], A 0 0 [1] or A 1 0 [1] situations), or from cuirasse outcrops (A 0 0 [0] situation) on a 100×100 m grid. The soil samples were sieved and the fine ($< 125 \mu\text{m}$) size fraction recovered for analysis (34 elements by ICP after alkaline fusion and Au by AAS after aqua regia-HF digestion). The hard cuirasse samples, however, were crushed and pulverized before analysis. The Fe_2O_3 , As and Au contents along the traverse (Fig. III.1-10) show specific geochemical dispersion characteristics according to the different weathering situations:

(1) where the profile is truncated (AB): a strong Au anomaly (approximately 1 g/t) associated with high As contents (to 150 ppm) marks the suboutcropping vein; Fe_2O_3 contents do not exceed 20%;

(2) where the cuirasse outcrops (BC): Au contents decrease but still remain anomalous (250–350 ppb) over the mineralized vein. The As contents, however, are enhanced to about 300 ppm; Fe_2O_3 concentrations reach 40%, a normal figure for cuirasse environments;

(3) where the cuirasse is covered by a residual soil (CD): although Au is no longer anomalous, As remains so, with concentrations of up to 100 ppm compared to a local background of some 25 ppm; Fe_2O_3 contents drop down to some 15%.

The mineralized vein is thus well indicated by quite extensive Au-As anomalies in each situation. The best contrast for Au is obtained where the profile is truncated, but the anomaly almost disappears where the cuirasse is covered by a residual soil. Arsenic appears to be less influenced by the type of weathering profile present, with strong contrasts whatever the surface situation; however, maximum concentrations are obtained where the outcropping cuirasse is sampled.

Wherever the pre-existing lateritic profile is preserved, therefore, whether or not it is covered by a surficial soil, sampling should preferentially take into account the Fe-rich phases (e.g. nodules and pisoliths) for As and Au determinations. Similar conclusions have been reached in arid environments in Australia by Mazzucchelli and James (1966), and Smith et al. (1987), as discussed in Chapter III.3.

Banankoro Au prospect, Kangaba region, south Mali (A 0 0 [0], A 0 0 [1], B 0 0 [1]). Located by a regional soil and stream sediment geochemical survey (BRGM, unpublished internal reports), the Banankoro prospect consists of Au mineralization in a quartz stockwork along a fault zone, hosted by Precambrian tuff and shales. The Au anomaly, found by soil and laterite sampling on a 100×100 m grid, is some 2 km long. The anomaly, delineated by the 100 ppb Au contour, extends over preserved lateritic plateaux, where the cuirasse horizon may locally be covered by a silty residual soil, or over a truncated profile with suboutcropping saprolite (Fig. III.1-11). Distinct geochemical signatures are discerned in these different environments (Roquin et al., 1989), with a significant enrichment for elements such as P, V, Cr, As, Nb and Mo over outcropping cuirasse and high Zr, Ti, Ce or Y contents in truncated situations, mostly in the valleys.

Results obtained by trenching or percussion drilling show that the mean ratio in Au contents between the surface (cuirasse or derived soil) and saprolite is about 1 : 5 over the mineralized structure. The change in the frequency distributions of Au from the saprolite to the surface soil is shown Fig. III.1-12. The Au content of the soil appears to be strongly homogenized compared to the highly variable multimodal distributions in both the cuirasse and saprolite. In the soil and cuirasse respectively, 65% and 80% of the samples contain less than 100 ppb Au, compared with only 10% of saprolite samples.

Changes in the morphology of gold grains in the weathering profile at Banankoro (Freysinet et al., 1987) indicate that some of the gold dissolves and recrystallizes in the upper ferruginous horizons (mottled zone and cuirasse). Primary grains show progressive rounding and decrease in size from bottom to top of the profiles (Fig. III.1-13-1,2). Precipitation of secondary gold is observed

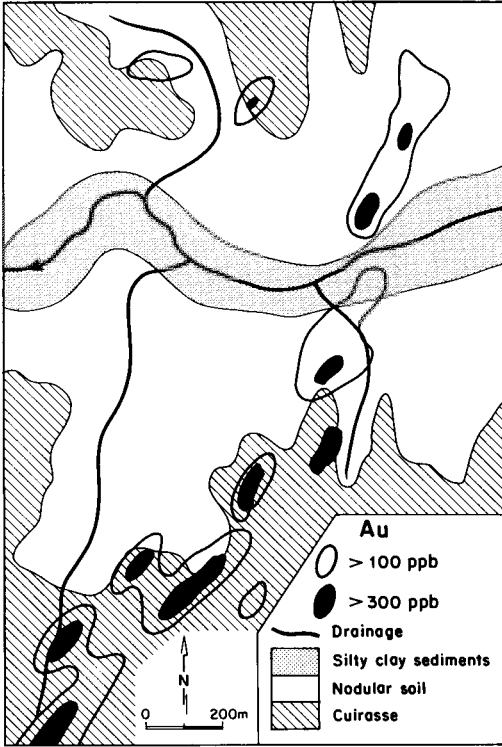


Fig. III.1-11. Banankoro Au prospect, Kangaba region, Mali. Distribution of Au in soil samples on a 100 × 100 m grid.

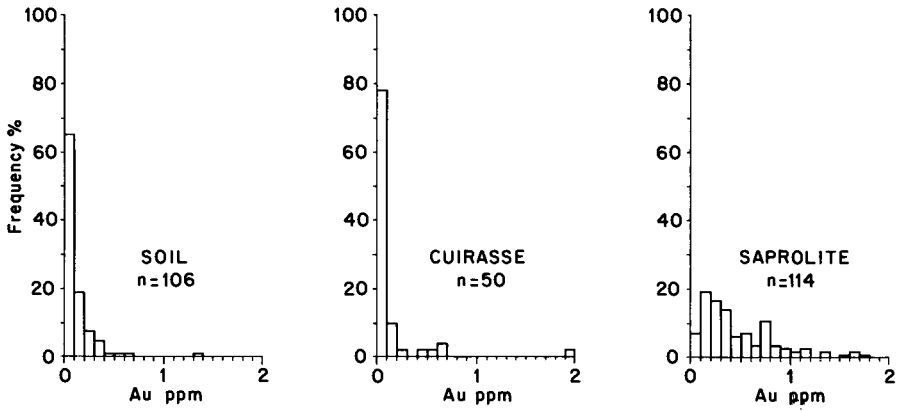


Fig. III.1-12. Banankoro Au prospect, Kangaba region, Mali. Histograms showing the distribution of Au of saprolite, cuirasse and soil samples.

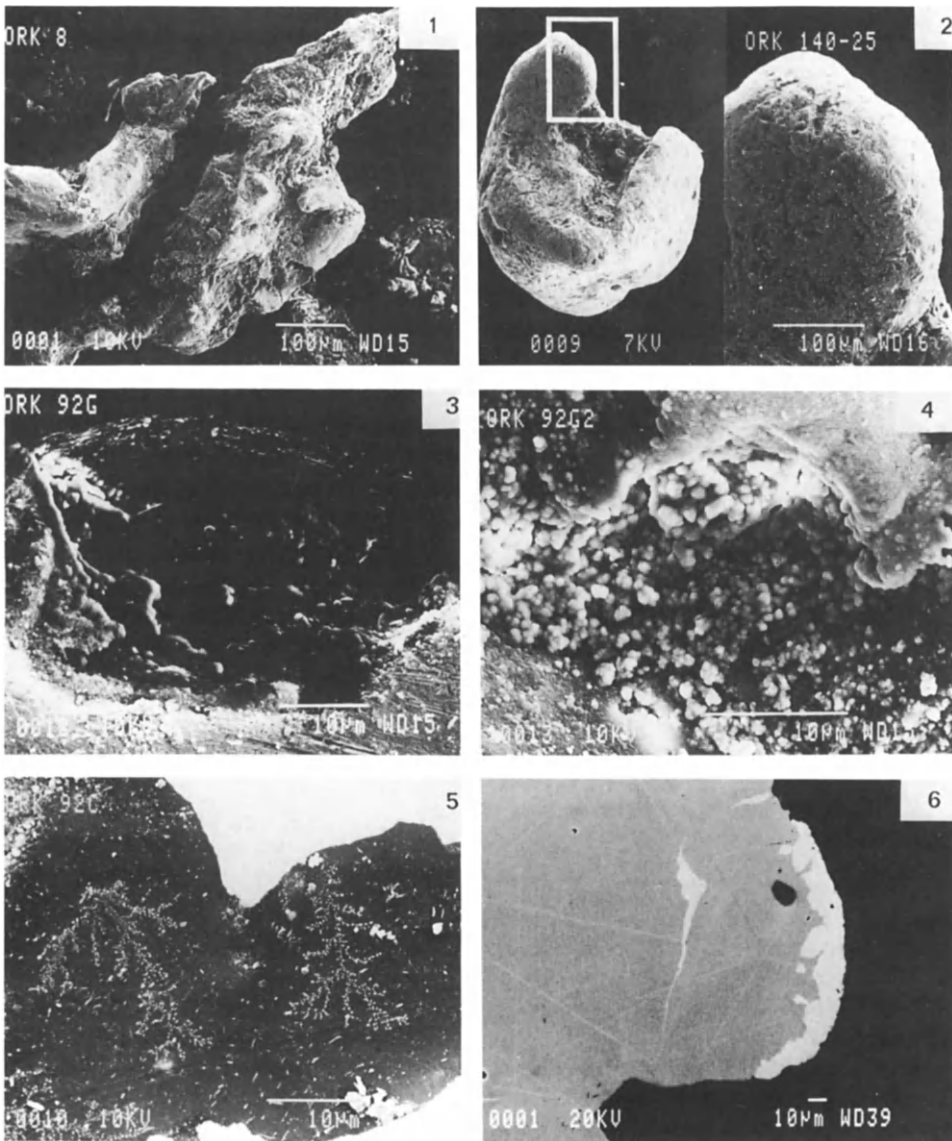


Fig. III.1-13. Banankoro Au prospect, Kangaba region, Mali. Morphological changes in gold particles collected in different horizons of the lateritic weathering profile.

on reception structures at the surface of Fe-oxides crystals, as microglobules (Fig. III.1-13-3,4) or dendrites (Fig. III.1-13-5) or, sometimes, on primary gold grains as a supposedly recently formed gold cortex (Fig. III.1-13-6) having a Ag content of less than 0.5% against 6–8% in the centre of the grain. Such low Ag

concentrations can also be explained by progressive Ag-depletion in primary grains from the rim to the centre (Bowles, 1988), in the example depicted Fig. III.1-13-6, but the sharp contact between the gold cortex and the primary grain must lead to consideration of the first hypothesis. However, the overall composition of the gold grains suggests there is a relationship between fineness and weathering intensity due to the preferential leaching of silver from gold particles during lateritization. It is shown by Freyssinet et al. (1989b) that the fineness of gold regularly increases from the base of the profile (saprolite: fineness 947 ± 10) to the top (cuirasse: fineness 959 ± 10).

Other studies (Mann, 1984a; Nair et al., 1985; Michel, 1987) similarly implicate the processes of lateritization in the supergene dispersion and concentration of gold and in the accretion of nuggets. Evans (1981) considers that the history and future potential of gold placers in Oregon and California, USA, are strictly dependant on their coincidence with a lateritically weathered Cretaceous peneplanation surface. This weathering was also responsible for the formation of Ni laterites, such as that at Riddle, Oregon (Cumberlidge and Chace, 1967; Chace et al., 1969).

The Sukulu carbonatite complex of eastern Uganda (A 1 0 [1]). The potential for economic concentrations of phosphates, niobium, REE, base metals and iron ore over carbonatites in eastern Uganda was investigated by detailed soil and stream sediments geochemical surveys, mineralogical determinations of residual soils, ground geophysics, pitting and drilling (Watts et al., 1963; Bloomfield et al., 1971; Reedman, 1974, 1984). The area is characterized by lateritic weathering in which the upper part of the profile generally consists of a red sandy and relatively thin soil, commonly overlying hard laterites or with a latosol over a patchy, near-surface duricrust (Bloomfield et al., 1971). The soil surveys located large, possibly economic, accumulations of phosphates, Nb and Fe in the weathering profile.

Several elements are strongly enriched in soils relative to concentrations in weathered carbonatites, due to the residual accumulation of relatively resistant minerals such as apatite and pyrochlore (Table III.1-4). The enrichment in soil is clearly demonstrated for P_2O_5 and Fe_2O_3 in Fig. III.1-14 (Sukulu complex; Reedman, 1984). In these ferruginous lateritic soils, there is an inverse correlation between Fe_2O_3 and P_2O_5 contents, but the average phosphate contents remain rather high, whatever the Fe_2O_3 concentrations.

This example demonstrates that surface geochemical techniques are well suited for the detection, and even the preassessment of potentially economic secondary mineralization that has been formed by the residual concentration of resistate elements during lateritization. Similar conclusions were reached in a rainforest environment by Laval et al. (1988) at Mabounié, Gabon (see p. 267). There is, however, no equivalent example from semiarid terrains, though no doubt the same general conclusions apply. The weathering profile over the

TABLE III.1-4

Sukulu rare earth prospect, Uganda: mineralogy, means and ranges values for selected oxides and trace elements (derived from Reedman, 1984)

Element or oxide	Rock samples N = 50		Soil samples N = 600		Minerals
	Range	Mean	Range	Mean	
P ₂ O ₅ %	0.0-29.2	4	1.0-25.6	9.6	Apatite
Nb ₂ O ₅ ppm	0-2800	760	500-13000	4100	Pyrochlore
Fe ₂ O ₃ %	1.5-65.0	7.2	18.2-71.2	42.7	Magnetite
Zr ppm	20-600	140	120-2000	750	Zircon Baddeleyite
Ti ppm	< 500-4000	1000	500-18000	5400	Ilmenite Magnetite
V ppm	30-200	100	5-250	80	Ilmenite Magnetite
Ba ppm	200-5000	2400	400- > 5000	1500	Barite
Sr ppm	420-2000	2400	150-1900	700	?
La ppm	< 20-5000	750	130-5000	1370	Monazite

Mount Weld carbonatite, Western Australia is similar, but it is buried beneath transported overburden and has no surface expression (Duncan, 1988; see p. 329).

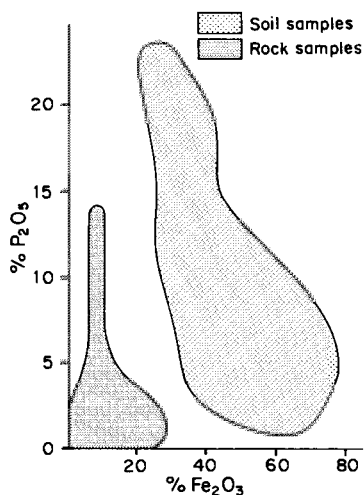


Fig. III.1-14. Sukulu REE prospect, Uganda. Schematic correlation diagram of the P₂O₅ and Fe₂O₃ contents of the fresh carbonatite and corresponding soil. Modified after Reedman (1984).

*Profile description**General*

In comparison with the preceding dispersion model (Fig. III.1-4), the main characteristic of B-type situations is the absence of the hard cuirasse horizon. The pre-existing lateritic or other deeply weathered profile has been eroded to a lower horizon, i.e. either the mottled zone or the saprolite. Depending on the depth of truncation, relicts of the pre-existing profile such as lateritic nodules or fragments may still be observed on top of the present profile, either as a surface gravel layer (lag) or within soils. More commonly, when the hard armouring cuirasse has been removed, the softer underlying horizons are more easily eroded so that lower levels of the saprolite are exposed. When erosion is intense, the bedrock may even outcrop, resulting in C-type situations in which primary haloes should be sought by lithochemical sampling. Such erosion is more common in desert environments (see Chapter III.3) in which soil development, and hence secondary geochemical dispersion, are restricted.

In areas where erosion has occurred, the remnant weathering profile is less differentiated than in A-type situations. Generally, the saprolite is overlain by a thin soil horizon or, less commonly, by a reddish nodular material corresponding to the former mottled zone. The total thickness of the profile is also reduced and may not exceed about 10–20 m. Although, in general, the present profile represents the lower part of a complete lateritic profile, some variations are observed. For example, in eastern Africa (e.g. Zambia, Zimbabwe), weathering profiles have been described having a peculiar zone of accumulation, the “stone line” (Webb, 1958; Tooms and Webb, 1961; Brown, 1970). These profiles usually have 3 principal horizons (Fig. III.1-15):

- (1) a yellow-brown sandy loam, up to 0.6 m thick, devoid of rock fragments;
- (2) a quartz or bedrock rubble line marking the contact with a “lateritic” horizon of soft dark red Fe-rich concretions in a red sandy matrix, with a total thickness not exceeding 0.5 m (the “stone line”);
- (3) a red-brown clayey sand, transitional to the underlying highly decomposed rock (saprolite).

For Tooms and Webb (1961), the residual origin of the upper horizon was demonstrated by the higher clay/sand ratios found over shales compared to arenaceous or granitic bedrock, and by the relationship between the contents of some trace elements of the upper horizon with those of the underlying bedrock (see Zambian examples below).

Such profiles closely resemble the stone-line profiles observed in rainforest environments (Lecomte, 1988; Chapter III.2), and possibly represent the very first stage of their development. It is noticeable that the total thickness of the upper horizons of these eastern African examples (about 0.6 m) is considerably less than those observed in more humid environments (3–6 m). It should be

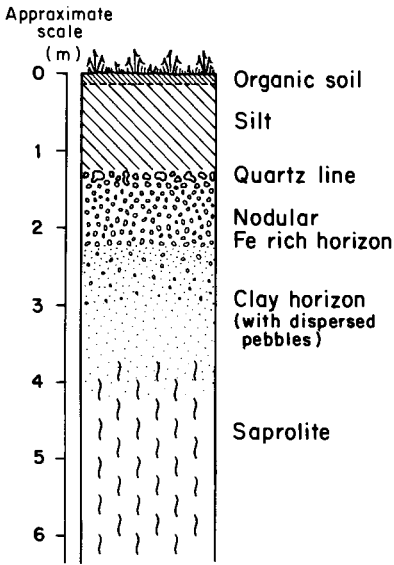


Fig. III.1-15. Idealized weathering profile with a Fe-rich nodular accumulation horizon (stone line) in Eastern Africa. Modified after Tooms and Webb (1961).

noted, of course that not all stone lines have this origin. Some are clearly sedimentary, having exotic, perhaps rounded, clasts of distant provenance and in this case the surface soils will not be residual. The soils may still be a suitable sample medium, however, if termite activity has brought deep residual material to the surface, as discussed in Chapter I.6.

Mineralogy and chemical composition

The mineralogical composition of the weathering profile mostly depends on the level of truncation (Fig. III.1-1). Thus, if truncation is relatively high in the pre-existing lateritic profile (for example in the mottled zone), the Fe oxides (goethite and hematite) are still abundant and may comprise more than 20% of the material. When truncation is within the saprolite, the dominant mineral is commonly kaolinite, coexisting with minor Fe oxides, quartz (the abundance depending upon the lithology) and possibly some untransformed primary minerals. Most of the kaolinite and Fe oxides may be considered to have been inherited from the former weathering episode.

In comparison, where truncation to the base of the former profile has occurred, a different mineral assemblage, characterized by the abundance of smectites, is observed. As described in Chapter I.2, if rock-forming minerals are weathered under poor drainage conditions, some alkaline and alkaline-earth elements may be retained in the profile as smectites. Such secondary minerals are particularly abundant in truncated weathering profiles developed on basic

TABLE III.1-5

Truncated dispersion models—B 0 0 [1], B 0 Sm [1]: behaviour of trace elements in smectitic and kaolinitic profiles, relative to bedrock contents; *E*: equivalence; *D*: Depletion; *C*: concentration (compiled from Mösser et al., 1985)

Behaviour relative to bedrock content	Kaolinitic	Smectitic
D	B, Ba, Sr Rb, Pb, Co	B, Ba, Sr
D, E	Sn, Zn	Sn
E		Rb
E, C	Cu, Cr, Ni	Cu, Cr, V Zn, Pb, Ga
C	Ga	Ni, Li
C, D	V, Li	Co

rocks (e.g. Boulet, 1974; Pion, 1979), but are also common over granites. These different mineralogical compositions suggest the existence of two distinct geochemical environments with very different pH and drainage conditions, namely acidic and freely drained where kaolinite is dominant, and alkaline and poorly drained if smectites are abundant. Consequently, quite different geochemical dispersion mechanisms exist, represented by models B 0 0 [1] (kaolinitic) and B 0 Sm [1] (smectitic). Nevertheless, smectites and kaolinite often coexist, or predominantly kaolinitic profiles merge into smectitic ones over short distances (Pion, 1979) so that this distinction is somewhat artificial.

In general, there is a clear relationship between the trace element contents of the saprolite and the bedrock from which it is derived (Mösser et al., 1985). This lithodependence may apply to kaolinite as much as to smectites, as illustrated on Table III.1-5, from results obtained in non-mineralized environments.

Dispersion models and examples: kaolinitic or "ferruginous-kaolinitic" models (B 0 0 [1], B 1 0 [1]); semi-residual profiles (B 0 0 [2], B 1 0 [2]); models with transported overburden (B 0 0 [3], B 1 0 [3])

Where profiles have been truncated (Fig. III.1-4), the geochemical dispersion halos are relatively small in size, due to the absence of the cuirasse. Depending on the topography, however, the dispersion halo may be significantly enlarged by mechanical processes in the surficial soil. Similar dispersion haloes may be found deeper in the profile if ferruginous materials derived from the degradation of pre-existing lateritic horizons are present in a stone line. The effects of chemical and mechanical dispersion of iron and associated trace elements, during and after nodule and pisolith formation, are preserved in the lateritic remnants. In such cases, the distributions of different trace elements will depend on their

affinity for these Fe-rich phases. Such “ferruginous-kaolinitic” truncated profiles, which have mostly been described from eastern Africa, are more highly evolved than normal kaolinitic profiles, and can be considered to some extent similar to the stone-line profiles of the rainforests in characteristics and origin. In comparison, despite profound chemical and mineralogical transformation, dispersion haloes in the saprolite are minimal in size, and anomalies are mostly residual.

Commonly, truncated profiles are capped by a cover of semi-residual soils or transported overburden. Such situations are discussed in the following examples.

Petite Suisse Cu prospect, Burkina Faso (B 0 0 [1]). The Cu mineralization at Petite Suisse, central Burkina Faso (Mösser and Zeegers, 1988) consists of disseminated chalcopyrite hosted by a granodioritic stock and altered felsic volcanics; grades are between 0.10 and 0.45% Cu. The area has a well-defined seasonal climate, with an annual rainfall of about 1000 mm. Weathering over the deposit is commonly to depths of about 40 m. The profiles have no hard cuirasse horizon and consist of soil about 0.5 m deep directly overlying saprolite, which is mostly either kaolinitic or smectitic, depending on the topographic situation (see p. 203). Thus, in profiles in freely drained environment, the saprolite consists principally of kaolinite, quartz, micas and minor Fe oxides. At the base of the sampled profile, at 7–10 m, some smectites appear, but kaolinite is still the dominant mineral. In lower topographic position, where drainage conditions are poor, the profiles consist of a thin soil horizon overlying a mostly smectitic saprolite (see p. 225).

The results of a size fraction analysis of the profile are shown Fig. III.1-16. It is evident that mean Cu contents are high (2000–10000 ppm) throughout the profile, particularly in the fine fractions. This illustrates the limited extent to which Cu is leached from a truncated kaolinitic profile in savanna environments. However, some leaching may be observed in the upper part of the profile (0.0–0.4 m and 0.4–1.0 m), where Cu contents are below 1000 ppm. Similar conclusions are evident at Goren (see p. 212), where Cu was shown to be leached mostly from the cuirasse horizon and retained in the saprolite, and in preserved or truncated profiles in rainforests (Chapter III.2).

The relationship between Cu and other elements depends upon the grain size and the sampling depth. Thus:

(1) in the coarse ($> 63 \mu\text{m}$) fraction, Cu shows some affinity for Fe, especially in the upper horizons. However, as shown in Table III.1-6, less than 10% of the total Cu is accounted for by this fraction, because it represents only a small proportion of the total sample;

(2) in the intermediate size fraction ($2\text{--}63 \mu\text{m}$), Cu shows a clear correlation with MgO, particularly in the upper 6 m of the profile, probably due to the presence of Mg-rich phyllic minerals;

(3) in the finest fraction ($< 2 \mu\text{m}$), there is a close relationship between Cu and MgO at depth, where smectites are present.

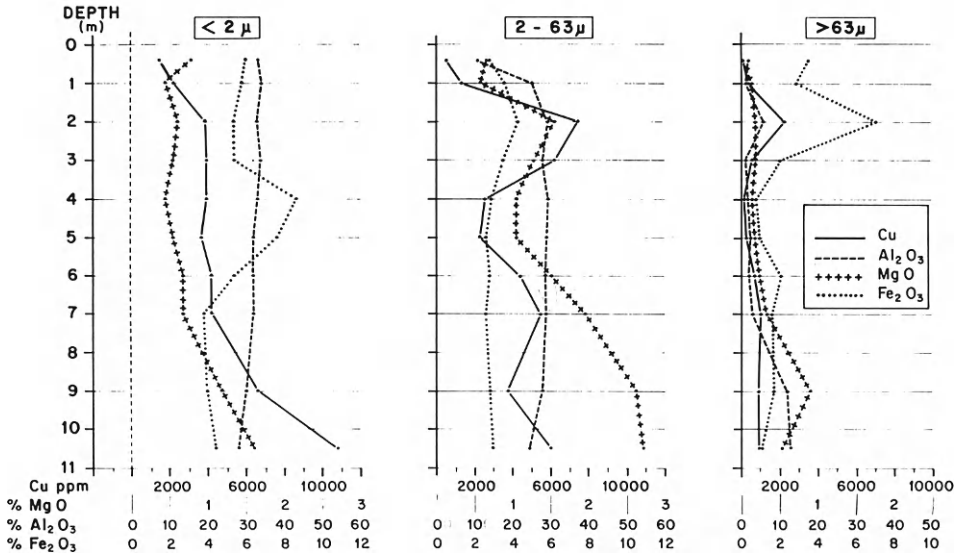


Fig. III.1-16. Petite Suisse Cu prospect, Burkina Faso. Distribution of selected elements in the 3 main size fractions in a truncated kaolinitic weathering profile. From Mösser and Zeegers (1988).

At least three minerals may thus be considered as possible hosts for Cu: *Fe oxides* in the coarse (but accessory) fraction of the samples and near the surface, *Mg-rich phyllites* at intermediate depth and *smectites* at the base of the profiles. Kaolinite is also important for Cu dispersion, having a mean Cu content about 1500 ppm.

TABLE III.1-6

Petite Suisse Cu prospect, Burkina Faso: proportion of total Cu (in %) in the 3 main size fractions of samples collected at different depths in a kaolinitic weathering profile (from Mösser and Zeegers, 1988)

Depth m	<math>< 2 \mu\text{m}</math>	$2-63 \mu\text{m}$	$> 63 \mu\text{m}$
0-0.4	69	26	5
0.5-1	56	42	2
1.5-2	28	70	2
2.5-3	28	69	3
3.5-4	27	70	3
4.5-5	51	45	4
5.5-6	32	62	6
6.5-7	20	74	6
8.5-9	40	53	7
10-10.5	47	45	8

Because most of the Cu (> 90%) is present in the fine fractions (Table III.1-6), the importance of these fractions in geochemical exploration is obvious. Moreover, much of the Cu appears to be retained in the lattices of the secondary silicates rather than adsorbed at their surface. This restricts the possibility of using weak chemical attacks for geochemical analysis.

Loulo Au deposit, Mali (B 0 0 [1]). The Loulo deposit was discovered following an integrated regional survey involving soil and stream sediment geochemistry and geological mapping (Dommanget et al., 1985; BRGM, unpublished internal reports). The deposit is situated in Proterozoic volcano-sedimentary rocks in the Kenieba area, which has long been known for its gold potential. The regional geochemical survey was based on soil sampling at a grid of 1600×500 m, and simultaneous stream sediment sampling wherever the drainage was suitable; the average sampling density was 1.5 samples/km². The fine fraction (< 125 μ m) of the samples was analyzed for Au. The 63–250 μ m paramagnetic fraction, separated following a method described by Laville-Timsit and Wilhelm (1982), was analyzed for 34 trace and major elements by direct reading emission spectrometry.

Some 40 Au anomalies were found and checked by a follow-up survey that included field geological mapping and soil geochemistry. The regional anomaly corresponding to the Loulo deposit was a single sample containing 1500 ppb Au and 1500 ppm B. The results of the follow-up survey of that anomaly are shown in Fig. III.1-17. Its significance was clearly demonstrated by the presence of several high Au values ranging between 0.5 and 1.7 g/t in soils. At the same time, a peculiar geological environment was identified, in which tourmaline-bearing sandstones were found to host the mineralization.

The geochemical dispersion characteristics of Au as indicated by drilling, trenching and surface information are as follows:

(1) in the saprolite, there is no significant primary halo: the gold mineralization is strictly confined to the weathered tourmaline sandstone unit, which is some 5–8 m thick, and does not extend in the surrounding shales at all;

(2) at the surface, in eluvium or soil (Figs. III.1-18 and 19), mechanical dispersion of gold is indicated by rather high Au contents (up to several g/t). The formation of this halo is accentuated by the greater resistance to weathering of the tourmaline sandstones, which form small hills. The existence of such a dispersion halo makes it possible to detect such narrow deposits even by using large geochemical sampling intervals.

The surface expression of the deposit includes only Au and B. Other trace elements, such as Co, As and Ni, are present in the fresh sulphidic mineralization, but not in concentrations high enough to persist in the weathered (oxidized) zone. Geochemically, therefore, the Loulo deposit is thus characterized by a mostly mechanical dispersion halo of Au and B, developed over a truncated weathering profile.

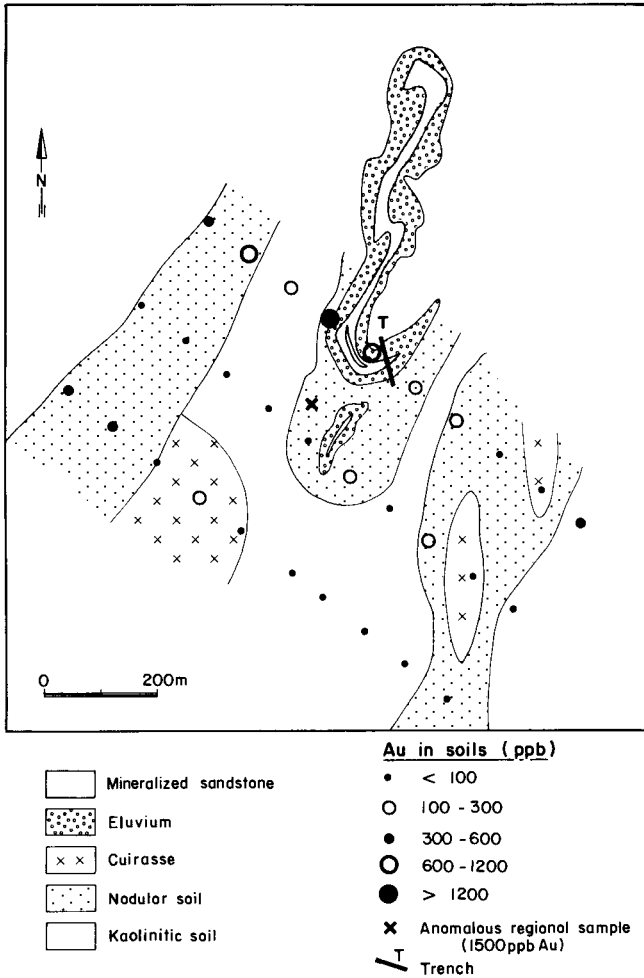


Fig. III.1-17. Loulo Au prospect, Mali. Distribution of Au related to the occurrence of different soil types.

Sabodala W prospect, west Senegal (B 0 0 [1]). Sabodala has a seasonally humid climate, with an annual rainfall of about 1200 mm. The mineralization consists of a quartz scheelite stockwork in trondhjemite, and was discovered following a regional stream sediment geochemical survey (BRGM, unpublished internal reports). The resulting anomaly was further investigated by soil geochemical surveys successively using 250×100 m and 100×10 m sampling grids. The mineralization itself was intersected by trenching but the grades were found to be uneconomic, ranging between 0.05 and 0.3% WO_3 .

The characteristics of the W distribution in samples collected at the different stages of exploration are presented Table III.1-7 and Fig. III.1-20. The regional

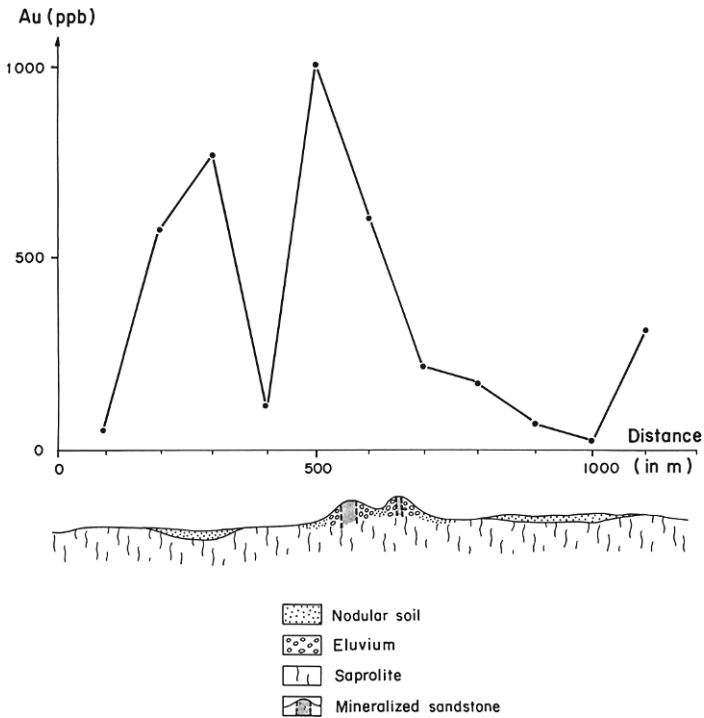


Fig. III.1-18. Loulo Au prospect, Mali. Cross section showing the weathering profile in the vicinity of the main mineralized structure and the distribution of Au in soil samples.

background value for W is estimated to be less than 5 ppm and although the soil anomaly in the vicinity of the mineralization has a high contrast, it is restricted in size, more or less coinciding with the extent of the underlying mineralization. This can be explained by considering that the upper part of the profile, from where soil samples have been collected, probably consists of a weakly evolved saprolite, in which dispersion is low and anomaly contrast high. This is confirmed by the resemblance between W distributions obtained by trenching to the saprolite and by soil sampling at 100×10 m grid. This example also demonstrates that W, as scheelite, is stable during weathering and that the anomaly is mostly residual for, because of the low relief, there has been little mechanical dispersion.

Southwest Uganda. Beryl pegmatites were successfully prospected by geochemical techniques in environments with thin and poorly developed sandy residual soils (Debnam and Webb, 1960). The background content of soils over barren country rock varies from 0.5 to 4 ppm Be. Peak values over beryl pegmatites are commonly 10–20 ppm, and more rarely 80–125 ppm. Reedman (1973) showed

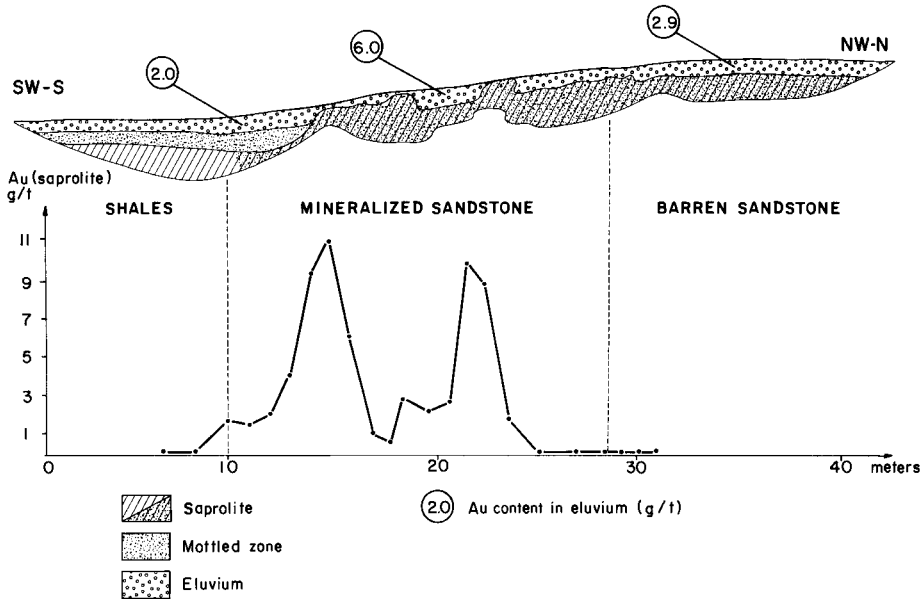


Fig. III.1-19. Loulo Au prospect, Mali. Cross section across the main mineralized structure showing the Au distribution in mineralized saprolite and eluvium.

that the lateral dispersion of Be (presumably as beryl) is very restricted in surface soils and rarely exceeds twice the width of the source pegmatite. Again, the geochemical anomaly here is mostly residual, with mechanical dispersion probably limited by the low relief. The insolubility of beryl under supergene conditions denies the possibility of hydromorphic dispersion.

North Karamoga region, northeast Uganda. A large area was covered by a reconnaissance stream sediment geochemical survey which led to recognition of numerous base metal anomalies. The more promising ones were followed up by

TABLE III.1-7

Sabodala W prospect, Senegal: main distribution parameters (ppm) for W in soil and trench samples, at different sampling intervals

Sampling mode	Sampling grid m	Mean	Minimum	Maximum
Soil	250 × 100	34	2	250
Soil	100 × 10	109	3	700
Trenching	100 × 2	612	20	3200

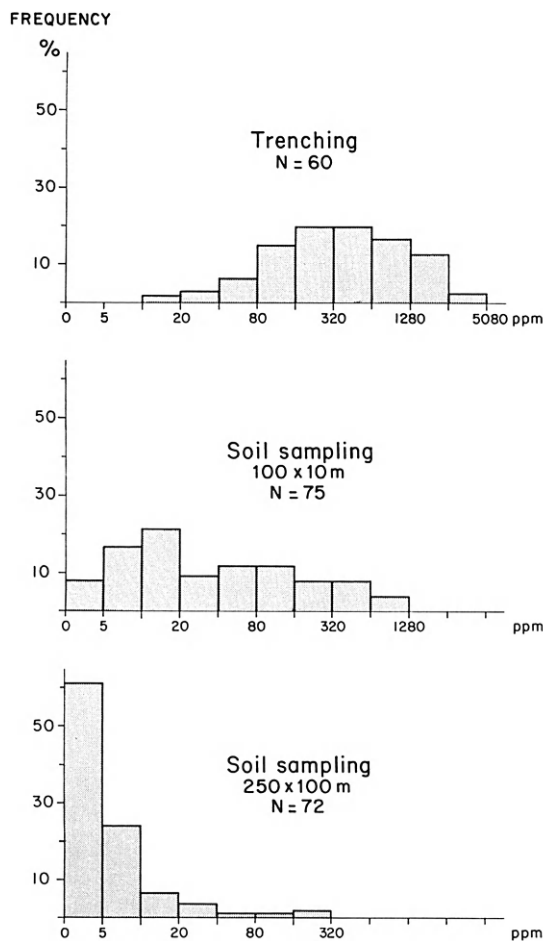


Fig. III.1-20. Sabodala W prospect, Senegal. Distribution histograms of W contents of samples collected at different stages of exploration.

detailed soil geochemistry and several Cu-Zn occurrences were discovered (Brock, 1973). In situations where the soil cover is very thin (< 1.5 m over the saprolite), it was observed that lateral geochemical dispersion in the soil is quite limited. For instance, high Cu values (800 ppm) found in the B-horizon directly above mineralization only 0.5 m wide decline sharply to background levels (< 50 ppm) within a few metres. In such a case, where the weathering profile is deeply truncated, the geochemical anomaly is mostly residual. Consequently, a very close sampling interval (3–4 m) was necessary to ensure the adequate delimitation of the mineralized units.

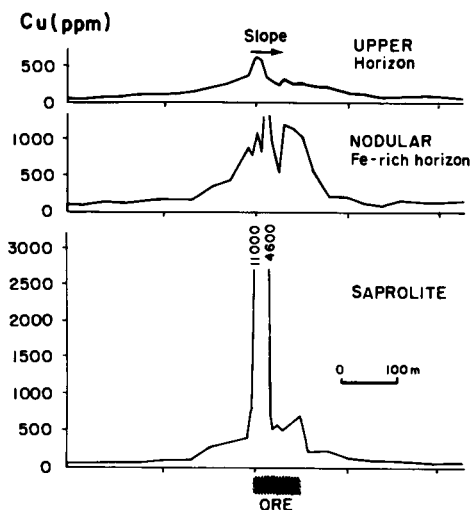


Fig. III.1-21. Baluba Cu prospect, Zambian Copperbelt. Distribution of Cu in the 3 main horizons of the weathering profile. Modified after Tooms and Webb (1961).

Baluba area, Zambian Copperbelt: "near stone-line profiles" (A 1 0 [1], B 1 0 [1]). Baluba is situated in a region with a typical seasonally humid savanna climate. There are several different types of weathering profiles, commonly merging one to the other along the same catena (Tooms and Webb, 1961, Govett, 1987). At the surface, the soil consists of grey and sandy clay but at depth there are various types of lateritic material such as Fe-rich nodules forming a rubble- or stone line, indurated ironstones and/or ferruginous concretions. These lateritic horizons are considered to be relics of an earlier weathering episode. Similar profiles have been described in Zambia by Webb and Tooms (1959), Tooms and Jay (1964) and Rose et al. (1979).

Above mineralization, Cu anomalies are generally well expressed in the three principal horizons of the weathering profile (Fig. III.1-21). The anomalies increase in width towards the surface, indicating that the greatest dispersion of Cu occurs in the Fe-rich horizons or in the soil rather than in the saprolite. Indeed, Cu is significantly enriched in the various Fe-rich horizons, and more especially in soils developed over them. These high concentrations are interpreted as representing anomalies developed during earlier weathering phases. At the surface, however, most of the Cu is hosted by the finest (clay) fraction of the soil, so that part of the present anomalous halo may be due to recent hydromorphic dispersion.

Downslope of mineralized occurrences, Cu anomalies occur in poorly drained "dambos", described by Govett (1987) as flat, seasonally swampy, grassy areas, free of tree growth. Many of these anomalies are considered to be hydromorphic in origin, but there is also evidence for mechanical dispersion. Indeed, up to 4%

of the dambo soil is coarser than 1.35 mm, and this fraction (containing Cu-rich laterite fragments) has a greater Cu concentration than any other size fraction. Such anomalies are considered (Govett, 1987) to be displaced with respect to their source mineralization, and may occur in B 1 0 [3] or B 0 Sm [3] situations, i.e. truncated profiles overlain by transported overburden.

Cu anomalies; Kasempa-Kitwe region, northwest Zambia. In northwest Zambia, on the eastern fringe of the Kalahari Sand belt, Brown (1970) studied the behaviour of Cu in 2 different pedological situations. In the first, the upper part of the profile is transported, with several tens of metres of aeolian Kalahari Sand overlying the saprolite (model B 0 0 [3]). In the second situation, the entire profile is residual and consists of a clayey red-yellow soil overlying a lateritic nodular layer, sometimes indurated at depth, developed just above the saprolite. The transition between the residual and transported situations is progressive and, even in the "residual" profiles, there is some contamination by Kalahari Sand (models A 1 0 [2] or B 0 0 [2])

In profiles developed in situ, Cu shows subtle, relative concentration in the Fe-rich horizons. In the lower horizons, anomalies are probably largely residual, with some hydromorphic component, whereas in the soils, some lateral mechanical dispersion has taken place. Where Kalahari Sand is present, the surface geochemical response of Cu is greatly reduced but, nevertheless, the silt fraction has been successfully used to detect anomalous Cu concentrations for an overburden depth of up to 15 m. The threshold value for Cu in the silt fraction of Kalahari Sand is about 50 ppm. This vertical dispersion pattern is attributed to seasonal moisture movements, with alternating upward and downward migration of water and associated metals corresponding to the wet and dry seasons. Geochemical dispersion in such overburden is thus exclusively hydromorphic, unless if, as Brown also suggests, termites are responsible for some mechanical transport of fine metal-enriched material from underlying horizons.

Liptako area, Niger (A 1 0 [0,1]; B 1 0 [2,3]). The role of termites in the geochemical dispersion of Au is emphasized by Gleeson and Poulin (1989) in a dry savanna environment in Niger. In the Liptako region, lateritic plateaux are present (A models) but are commonly dissected, resulting in a truncated situation (B models) in which the saprolite is covered by a semi-residual and transported cover of eluvial sand and aeolian and alluvial deposits, the thickness of which may exceed 5 m. Several test surveys were carried. Firstly, the optimum size fraction was found to be minus 80-mesh ($177\ \mu\text{m}$) for both soil and termitaria samples. Secondly, geochemical responses obtained in different environments using both sampling media were compared. It was evident that, whereas soil sampling is adequate where the soil cover is less than 2 m thick, termitaria sampling can be recommended where the soils are developed on semi-residual or transported overburden more than 2 m thick. Significant results were obtained in the Deba region where sampling on 300×500 m centres gave anomalous Au

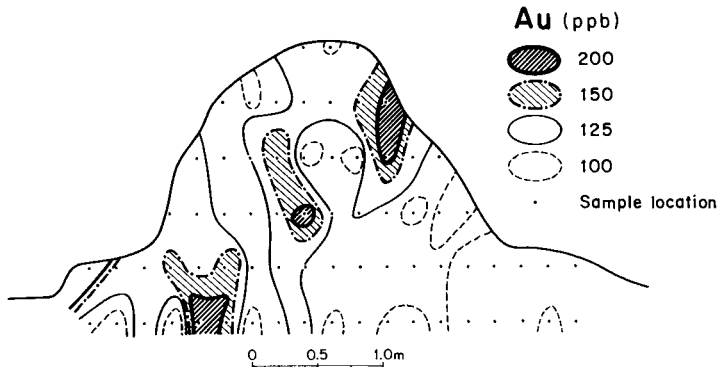


Fig. III.1-22. Koma Bangou area, Niger. Section of a termite mound showing the distribution of Au in the minus 80 mesh ($177\ \mu\text{m}$) fraction. From Gleeson and Poulin (1989). Compare with Fig. I.6-4.

values up to 200 ppb and suggest the presence of additional Au mineralization. A study of the distribution of Au in the termitaria showed that the higher values tended to be present in the cores and upper surfaces of the mounds (Fig. III.1-22). For routine surveys, therefore, these upper surfaces were sampled preferentially. The erosion of termitaria increases the residual component of the surface soils and hence, as discussed in Chapter I.6, they offer no advantage as a sampling medium unless deposition of the overburden is still active. The role of termitaria as a sampling medium in an area in Mozambique where there is active movement of colluvial overburden on steep slopes is described by d'Orey (1975) —see Chapter I.6.

Thalanga polymetallic deposit, Queensland, Australia (B 1 0 [3]). The Cu-Pb-Zn-Ag-Au mineralization at Thalanga has a truncated lateritic weathering profile that partly subcrops as a gossan and is partly buried by a thick (up to 80 m) post-mineralization cover of conglomerates and massive clays of Tertiary age. Geochemical dispersion haloes in this cover were drilled to delineate possible extensions of the known mineralization (Granier et al., 1989). Cuttings were sampled at 3 m intervals, and strong Pb, Zn, Cu and Ag anomalies were found in the Tertiary overburden up to 25 m above the mineralization. The dispersion haloes have commonly a major vertical component, where the highest contrast is observed, and a lateral one, as shown Fig. III.1-23 for Pb. Background and anomalous values in the Tertiary cover are respectively < 100 and > 800 ppm Pb; < 75 and > 600 ppm Zn; < 45 and > 360 ppm Cu and < 1.5 and > 5 ppm Ag. These high values suggest the possibility of mechanical dispersion during reworking of the basement rocks and the associated mineralization at the base of the transgressive Tertiary sediments. However, the dispersion patterns, especially that of Pb, resemble those found elsewhere in Australia, e.g. in alluvium at Dalganga, Western Australia (see p. 357) and in saprolite at

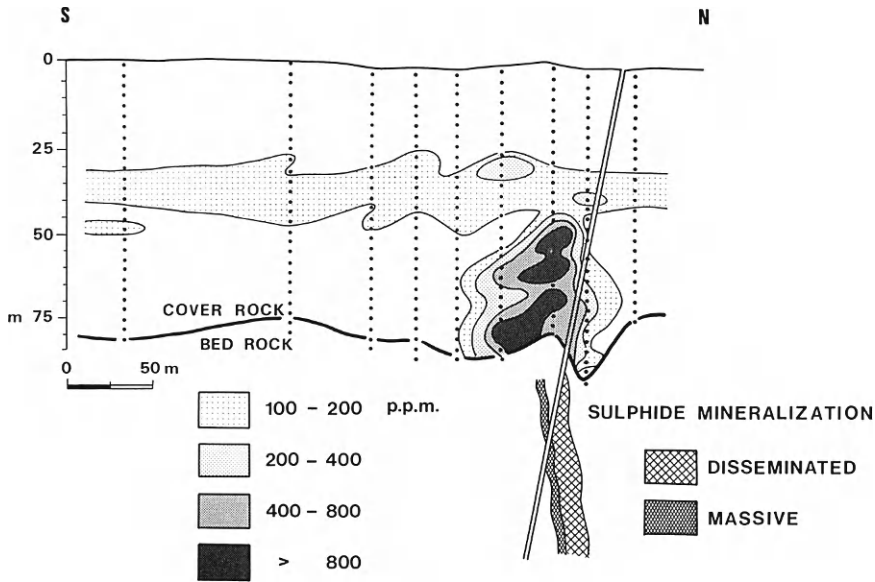


Fig. III.1-23. Thalanga, Queensland, Australia. Distribution of Pb in Tertiary sediments overlying mineralization.

Teutonic Bore, Western Australia (see p. 336), both in semiarid regions, and in saprolite at Woodcutters, Northern Territory, in a savanna climate (Taube, 1978). At each of these, the dispersion has a strong horizontal component that may be related to precipitation at an old water-table. In addition, the possible role of electrochemical dispersion at Thalanga has been discussed by Govett and Atherden (1987). This example demonstrates that significant geochemical dispersion may occur into sediments overlying mineralization, offering potential for near-surface sampling in such situations.

Dispersion models and examples: residual smectitic profiles (B 0 Sm [1])

By comparison with the preceding dispersion model (truncated, kaolinitic profiles), the smectitic environments represent conditions that favour the retention of most trace elements, including the target metals, within the weathering profile. This is demonstrated by several examples, for different elements, that illustrate the role of mineralogy in geochemical dispersion. For instance, kaolinite and smectites may fix large amounts of Cu in the profile, and Pb may be retained as secondary carbonates or phosphates. The incorporation of these metals in stable minerals results in their relative immobilization and thus restricts the size of the geochemical dispersion haloes. Indeed, chemical processes of weathering in these situations do not promote further significant hydromorphic dispersion for most elements.

TABLE III.1-8

Petite Suisse Cu prospect, Burkina Faso: estimated Cu content in the main mineral phases or fractions (from Mösser and Zeegers, 1988)

Mineral phase	Cu mean content (or range)
quartz + feldspars	50–100 ppm
Mn oxides, as MnO ₂	6%
phyllite fraction	
untransformed	6000–11000 ppm
transformed (kaolinite)	2000 ppm
hematite	2300 ppm
goethite	300 ppm
clay minerals	
kaolinite	1500–2000 ppm
smectite	7500–8300 ppm

Petite Suisse Cu prospect, Burkina Faso (B 0 Sm [1]). Dispersion of Cu in a kaolinitic weathering profile from this prospect has been presented previously (see p. 227). In the same area, however, there are situations where smectitic profiles have developed over the disseminated Cu mineralization (Mosser and Zeegers, 1988). A detailed study of a 4 m deep weathering profile showed that Cu, which is present in very high concentrations throughout the profile, is enriched in several mineral phases, depending on the grain size and the position in the profile (Table III.1-8).

Copper, present in the ore as sulphides, appears to have been transferred to several different secondary minerals during weathering. As in the more kaolinitic profiles, in over 80% of samples, the fine size fractions contain most of the total Cu, and such fractions should thus be preferentially used for geochemical exploration in similar terrains. At the base of the profile studied, smectites and, to a lesser extent, kaolinite, are the main Cu-bearing phases. Higher in the profile, smectites are progressively replaced by large kaolinites, which apparently retain only part of the Cu previously contained by the smectites. At the surface, some of the Cu is associated with Fe-Mn nodules in the coarse size fractions, but this accounts for less than 20% of the total Cu. Overall, these mineralogical changes result in progressively decreasing Cu contents, from some 2500 ppm at 4 m depth to 1000 ppm at the surface.

Gan prospect, Burkina Faso (B 0 Sm [1], B 0 Sm [3]). This Pb-Ag occurrence was discovered during a UNDP geochemical exploration programme (Goossens, 1975). The climate is typical of dry savanna environment, with less than 1000 mm annual rainfall and well-contrasted seasons. The prospect lies in a gently undulating peneplain of low relief. The overall depth of the weathering profile is about 30 m. The deposit is of vein type, with argentiferous galena and accessory Cu sulphides, within Precambrian schists and quartzites. At the surface, the sul-

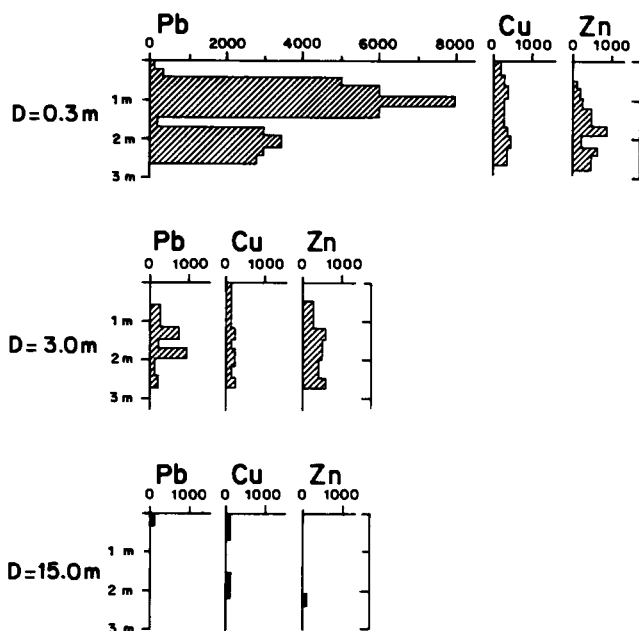


Fig. III.1-24. Gan Pb prospect, Burkina Faso. Distribution of Pb, Zn and Cu in weathering profiles at increasing distances (D , in m) from the Pb-Zn vein. Modified after Goossens (1975).

phides have been transformed into a new mineral assemblage reflecting the alkaline and oxidizing thermodynamic conditions prevailing in this rather dry climate. The following mineralogical succession was observed: sulphides (Pb, Cu) \rightarrow sulphates (Pb) \rightarrow carbonates (Pb, Cu) \rightarrow phosphates (Pb, Cu).

Trenching across the mineralization showed that the geochemical dispersion halo is very narrow (Fig. III.1-24) and that Pb, Cu and Zn are reduced to background values only 15 m from the mineralization. This explains why the main vein was barely indicated by a soil survey on a 50×50 m sampling grid. A better response was obtained using a 10 m grid, with Pb values up to 1600 ppm. The anomaly is mostly residual in the saprolite, but no anomalies are observed in the overlying soil even a few metres from the mineralization. This result is somewhat surprising and the presence of transported overburden is thus suspected (i.e. B 0 Sm [3] situation). It demonstrates that in such alkaline environments in truncated terrain with a very low relief, soil surveys with rather large sampling grids (1000×1000 or 500×500 m) tend to be inappropriate for the discovery of massive sulphide mineralization. Sampling intervals should thus be reduced to suit these very specific conditions. In addition, careful field observations to determine the nature and origin of the sample medium are essential for successful application of surface geochemical techniques. The wider grids may be applicable if ferruginous lags are present and are selectively sampled, a

procedure successfully adopted in some savanna and semiarid terrains in Australia (Carver et al., 1987; see p. 346).

CONCLUSION

Savanna climatic environments contain a wide variety of geochemical dispersion situations. When the entire pre-existing lateritic profile has been preserved, the contrast between the horizons gives an anisotropic dispersion pattern for most elements. The mineralogy of these horizons has a determinant role in the retention or leaching of trace elements in the profile. In the upper, ferruginous, horizons, goethite and hematite can probably fix large amounts of elements such as Mo and As, resulting in extensive dispersion haloes. Other elements (e.g. Zn, some Cu and Au) are less resistant to this oxidizing and freely drained environment, and are partially leached from the profile. In the lower horizons, elements such as Cu, Zn and Ni can be retained by secondary silicates (kaolinite, smectite), so that geochemical contrasts increase, but at the expense of a decline in the size of the dispersion haloes.

Where the weathering profile is truncated, with a thin soil overlying the saprolite, the conditions in dry savannas favour the retention of most of the pathfinder and target elements. Some are held in the lattices of secondary silicates, whereas others can form stable, accessory, secondary minerals, such as Pb phosphates. Such environments are indicated by the presence of smectites as the dominant clay mineral in the saprolite.

In all instances where the complete profile is residual, no situations have been identified in which the geochemical response of mineralization (including Au, base metals and REE) could not be detected by surface geochemical sampling. When transported overburden is present, however, the geochemical response is commonly obliterated, unless conditions favour hydromorphic dispersion. In appropriate situations, such dispersion may give rise to a surface expression of buried mineralization. In all situations, sampling procedures and sample preparation are critical, especially when the lateritic profile is fully preserved.

HUMID TROPICAL TERRAINS (RAINFORESTS)

Paul LECOMTE and Hubert ZEEGERS

DISTRIBUTION AND DESCRIPTION

Humid tropical terrains are characterized by a high annual rainfall (averaging 1600–> 3000 mm) and high mean temperatures. Except in monsoonal regions of Southeast Asia, there is little seasonal variation in climate, even if short dry seasons may occur as, for example, in South America (Amazon Basin) and Central Africa. The natural vegetation consists predominantly of rainforest. These terrains occupy more than 23 million km² (approximately 15% of the earth land surface) in an equatorial belt crossing three continents (see Fig. I.1-2):

- (1) South America—the Amazon basin and Guyana shield;
- (2) Africa—from the Congo basin to the Great Lakes;
- (3) Southeast Asia—parts of Indonesia, Malaysia, Burma and India.

In the past, however, these regions have experienced both cooler and drier periods. From palynological observation, Salard-Cheboldaëff (1981) demonstrated that since the Maestrichtian, there has been a progressive warming with both more and less humid periods. Although these studies were focussed on Central Africa, correlations were established with South America and Asia. Similarly, during the Quaternary, Giresse (1978) demonstrated that, in Africa, the climate has been alternately humid and dry during the last 70,000 years. Four main periods have been recognized, apparently corresponding with glaciations in Europe.

Considering the relative tectonic stability of most of the humid tropical regions it is quite clear that, very frequently, the present landscape has been subjected to several different climatic periods, leading to different weathering products. This may make it difficult to interpret the observed weathering profile simply by considering it in terms of the present climate.

Under the rainforest conditions prevailing in the equatorial tropics, most of the transformations due to weathering are related to in-situ hydrolysis, and leaching generally proceeds vertically (Millot, 1980). Landform development is mostly related to chemical processes and the resultant, characteristic “half-orange” landscape is in effect a product of chemical wasting.

The primary mineral assemblages are partly or totally transformed into a mixture of kaolinite, quartz and Fe-Al oxides (Millot et al., 1977). Aluminium, Fe and Ti are the only major elements to be maintained or even enriched in the weathering profile, whereas the others, including some of the silica, are leached,

either totally or partially (Pedro, 1966). Of the trace elements, some, such as V, Cr and P, follow the behaviour of Fe, whereas others are partly or wholly leached (Zeegers, 1979; Schorin and Puchelt, 1987).

Such mineralogical and chemical evolution is common throughout the humid tropics and the resultant "kaolinitic mantle" might be considered to be part of a developing "lateritic profile". However, the formation of ferruginous duricrusts, typical of such profiles, is not known in these regions. In general, weathering processes related to the present climate seem only to modify or extend already existing profiles that were formed earlier under different climatic conditions. Very commonly, remnants from these older episodes can be observed in the profiles—for example, as cuirasse blocks derived from an ancient indurated lateritic surface. The nature of this interaction between older and younger weathering processes in the humid tropics is important for understanding the geochemistry of these profiles and is discussed in a later section.

The overall depth of the weathering zone is commonly several tens of metres. The saprolite occupies approximately the same volume as the fresh rock, but the upper few metres are organized into distinct pedological horizons, with new structures replacing any primary or earlier fabric. In general, the chemical composition of the different horizons constituting the weathering profile is related to that of the underlying bedrock. The composition is, of course, strongly modified by the processes of profile formation, but even in the upper weathering horizons, certain characteristics can always be recognized. Such "lithodependence" also applies in mineralized environments, although the nature of the surface expression will vary according to particular environmental conditions. In this chapter, various examples have been used to establish generalized dispersion models appropriate for rainforest terrains.

The weathering profiles and the corresponding dispersion models are described and coded using the terminology introduced in Chapter I.1 (Table I.1-6). However, in comparison with drier environments (Chapters III.1 and III.3), alteration of the pre-existing profile by leaching related to the present morphoclimatic conditions is possibly at least as significant as the degree of truncation. Consequently, the models are subdivided according to the intensity of present alteration, as follows:

- (1) recent alteration low,
- (2) recent alteration moderate,
- (3) recent alteration strong, with the formation of stone-line weathering profiles.

Within these categories, further subdivision is made according to the preservation or truncation of the former lateritic profile. The following characteristics are considered for each situation:

- profile description (macroscopic scale),
- mineralogical composition,
- chemical composition: major and trace elements,
- geochemical responses, with examples and case histories.

Even if soils may locally consist of a semi-residual mixture, there are very few case histories from areas having a cover of transported overburden in rainforest environments. Such overburden occurs on a local scale in most valleys where there is slight to moderate relief. Regional exploration in such areas is commonly undertaken by stream sediment surveys, because many streams are incised to bedrock. Indeed, fresh sulphides may be present in the samples. Follow-up surveys in alluvium-covered valley floors depend upon saprolite sampling by trenching or drilling. In poorly drained environments, problems may be experienced in distinguishing between alluvial sands and the upper leached horizons of podzolic residual soils (see Chapter I.4). Very thick sequences of alluvial sediments occur in major valleys such as those of the Amazon and Congo basins. Although these may overlie prospective basement rocks, very little mineral exploration has been attempted in these regions. Accordingly, no dispersion models or case histories can be presented for such situations, but surface geochemical techniques would not be expected to have much application.

DISPERSION MODELS: LOW RECENT ALTERATION

General

Most rainforest environments are characterized by strongly leaching conditions, as described later in this chapter. Situations in which recent alteration is of relatively low intensity correspond to transitional zones between rainforest and savanna. There, transformation of the pre-existing profile, whether preserved or truncated, is indicated by pronounced chemical degradation or even disappearance of cuirasse horizons and the reworking of exposed saprolite to form ferrallitic soils. As a consequence, the thickness of the residual soil overlying the profile is generally greater than for a similar situation under drier climates.

A-type models: pre-existing profile mostly preserved

Environment, geomorphology and profile description

The position of the most commonly encountered model (A 1 0 [1]) in the generalized landscape is illustrated on Fig. III.2-1. Under such conditions, geomorphological features still include the plateau landforms inherited from former climates, because the lateritic surface is most commonly preserved. Typical profiles consist of:

- (1) an upper indurated Fe-rich horizon, sometimes transformed into nodules embedded in a clay matrix in its upper part;
- (2) an homogeneous ferruginous clay horizon;
- (3) the saprolite.

Such profiles have been described from the Ivory Coast (Nahon et al., 1980, 1982), from central Brazil (Esson and Surcan Dos Santos, 1978; Esson, 1983)

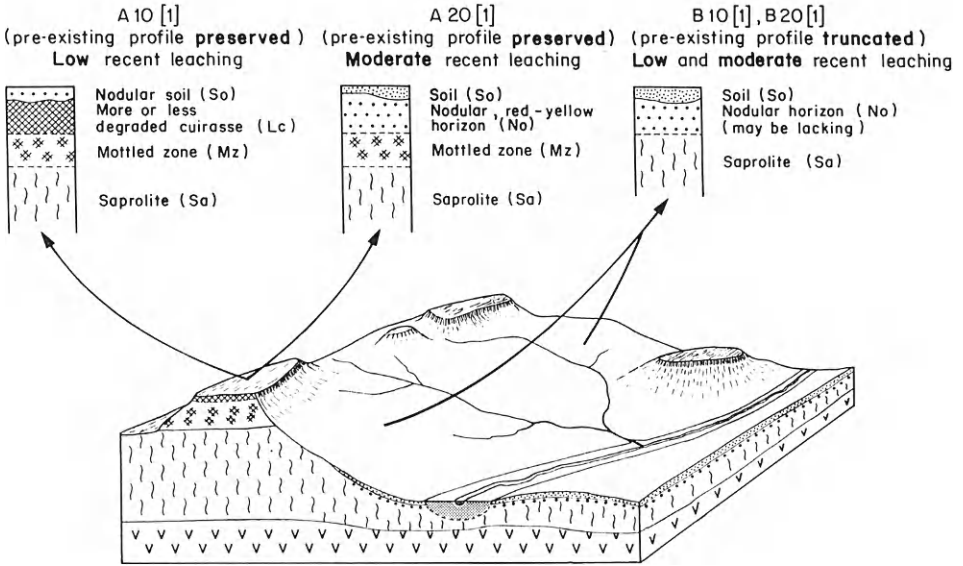


Fig. III.2-1. Diagram showing the general landscape and the weathering profiles related to the low and moderate recent leaching models. For abbreviations, see Fig. III.1-1.

and from monsoon forests of India (Sen, 1981). In these regions, weathering is less pronounced than in equatorial rainforest, so that the old lateritic profiles are well preserved. A detailed example, developed on glauconitic argillaceous sandstones, was described from the Eboina region, Ivory Coast, by Nahon et al. (1980). The profile (Fig. III.2-2) consists of:

- (1) an uppermost nodular horizon resulting from the disintegration of the iron crust;

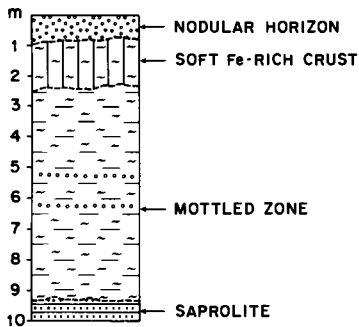


Fig. III.2-2. Generalized weathering profile of the Eboinda region, Ivory Coast. Modified from Nahon et al. (1980).

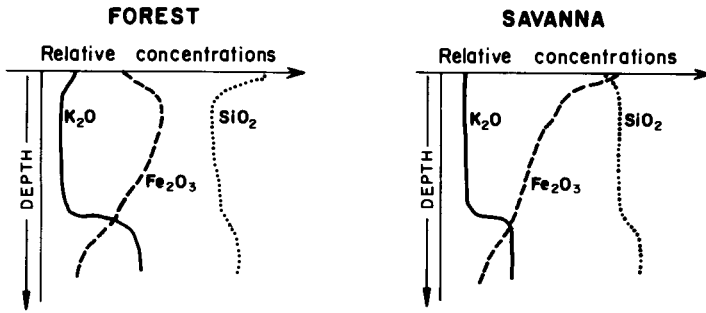


Fig. III.2-3. Idealized K_2O , Fe_2O_3 and SiO_2 distributions in the weathering profile in rainforest and savanna environment. Modified from Pasquali and Lopez (1982).

- (2) a soft, red Fe-rich crust;
- (3) a clay-rich horizon, with an increasing proportion of Fe-nodules, transitional to the upper horizon;
- (4) saprolite, at the top of which polyhedral structures replace the primary fabric.

Over granitic rocks, Pasquali and Lopez (1982) proposed two idealized weathering profiles, corresponding to rainforest and savanna environments (Fig. III.2-3). The distribution of major oxides in these profiles shows, in savannas, increasing Fe_2O_3 contents towards the surface, whereas in rainforests, some leaching of Fe may be observed in the upper horizon. Conversely, this upper horizon is relatively enriched in SiO_2 and Al_2O_3 . Very clearly, some iron is removed from the surface under the rather aggressive conditions prevailing in the humid tropics.

Over ultramafic rocks, the primary mineral assemblages (including ferromagnesian and carbonate minerals) are replaced by amorphous or crystalline iron oxides and by gibbsite (Nahon et al., 1982). These mineralogical observations are confirmed by the distribution of major elements such as MgO , which is totally leached, and Fe_2O_3 , which is strongly enriched in the middle part of the profile. In the upper horizon, Fe_2O_3 is depleted whereas SiO_2 and Al_2O_3 are enriched, probably as a result of present weathering (Fig. III.2-4).

General dispersion characteristics and examples

The most commonly encountered model (A 1 0 [1]) is detailed in Fig. III.2-5. Element mobilities and dispersion are very similar to those observed in savanna climates (see Chapter III.1); consequently, metals such as Cu and Zn might possibly be leached in the strongly weathered horizons, whereas others, such as Mo, As, Pb, Bi, Cr and V, will be retained or even concentrated in the Fe-rich horizons.

The degree of dispersion is sequential, increasing vertically upwards according to the zonation of the profile (Fig. III.2-5). In the saprolite (Sa), the width of

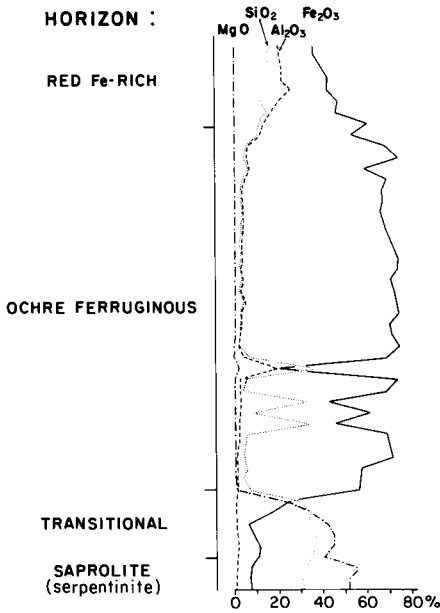


Fig. III.2-4. Distribution of selected major elements in a weathering profile over ultramafic rocks. Modified from Nahon et al. (1982).

the mineralization may appear much greater than in the bedrock, having been enlarged by hydromorphic (chemical) dispersion processes, but the geochemical expression remains dominantly residual. In the intermediate mottled and ferrugi-

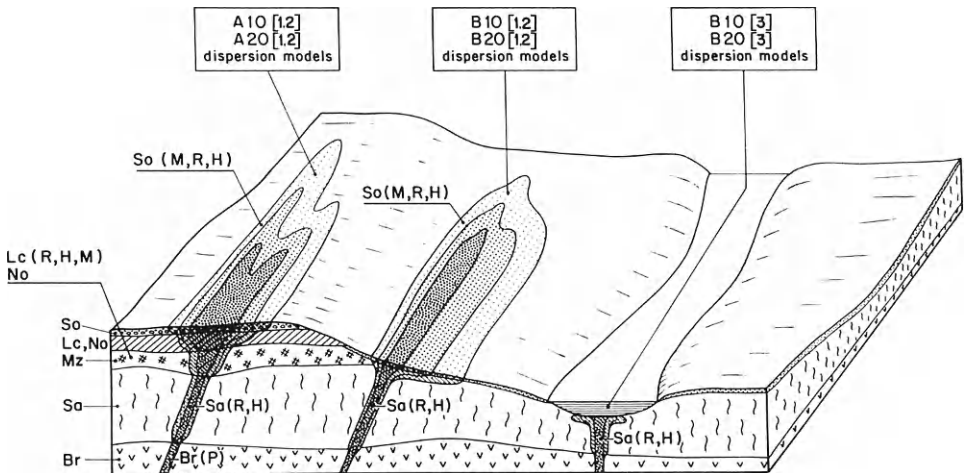


Fig. III.2-5. Diagram showing the idealized dispersion models in low and moderate recent leaching situations. For abbreviations, see Fig. III.1-1.

nous horizons (Mz), the dispersion halo widens further, again by hydromorphic processes. In the degraded cuirasse horizon (Lc), just as in drier climates, metal dispersion is mostly controlled by the chemistry and mineralogy of iron; accordingly, some leaching of mobile elements may be observed, resulting in subdued anomalies. In the soil, mechanical processes may enlarge the dispersion halo, with a simultaneous decrease in the anomaly contrast. Accordingly, if the former weathering profile is really very little truncated, a rather widespread dispersion halo of low contrast is expected. However, if such a halo is not present, it is probable that some stripping has occurred. This appears to be the case at Toulepleu, Ivory Coast, where neither Cu and Au are widely dispersed, even though the pre-existing profile appears to be present in its entirety.

Toulepleu Cu-Au prospect, Ivory Coast (A 1 0 [1]). Following a regional exploration programme carried out in the Precambrian greenstone belts of the western Ivory Coast, several stream sediment Cu anomalies were further investigated by detailed geological mapping and soil sampling. One of these anomalies was shown to be related to disseminated Cu-Au mineralization, which was subsequently intersected by drilling at about 100 m depth. The mineralization (0.1–0.6% Cu) seems to be related to a shear zone across a volcano-sedimentary series consisting of biotite-amphibole gneiss and amphibolites.

The weathering profile (Fig. III.2-6) is composed of a semi-indurated nodular lateritic horizon (0.5–3 m thick) overlying a mottled zone of similar thickness, merging to the saprolite. Locally, in a flat low-lying area, there is a surficial cover of grey sandy soil. This horizon is interpreted as representing the effects of impeded drainage, resulting in reducing conditions, together with some surface leaching.

The presence of the Cu mineralization is fairly well reflected in the minus 125 μm fraction of surface soils (30–40 cm depth) sampled at an interval of 50 \times 50 m. The anomaly, about 400 m in length, is well developed with 2 peak values of 1000 ppm Cu. Two traverses of auger holes profiles (AB and CD, Fig. III.2-6) show that the Cu anomaly in the upper nodular horizon corresponds to the anomalous Cu–Au–Ag concentrations in the saprolite. Data for Cu and Au in the principal horizons of the profile are presented in Table III.2-1. Overall, the results demonstrate that:

(1) Secondary lateral dispersion is very limited in surficial soil. As a consequence the surface anomaly, especially for Cu, has a sharp contrast and does not extend far from the position of the underlying mineralization.

(2) There is no significant difference in the mean Cu and Au contents between the mineralized bedrock, the saprolite and the upper “lateritic” horizon. Thus, many of the characteristics of the mineralization can be inferred from surface geochemical data.

Similar results were obtained from a second prospect nearby, where soil sampling delineated a 200–600 ppb Au anomaly. This was further checked by

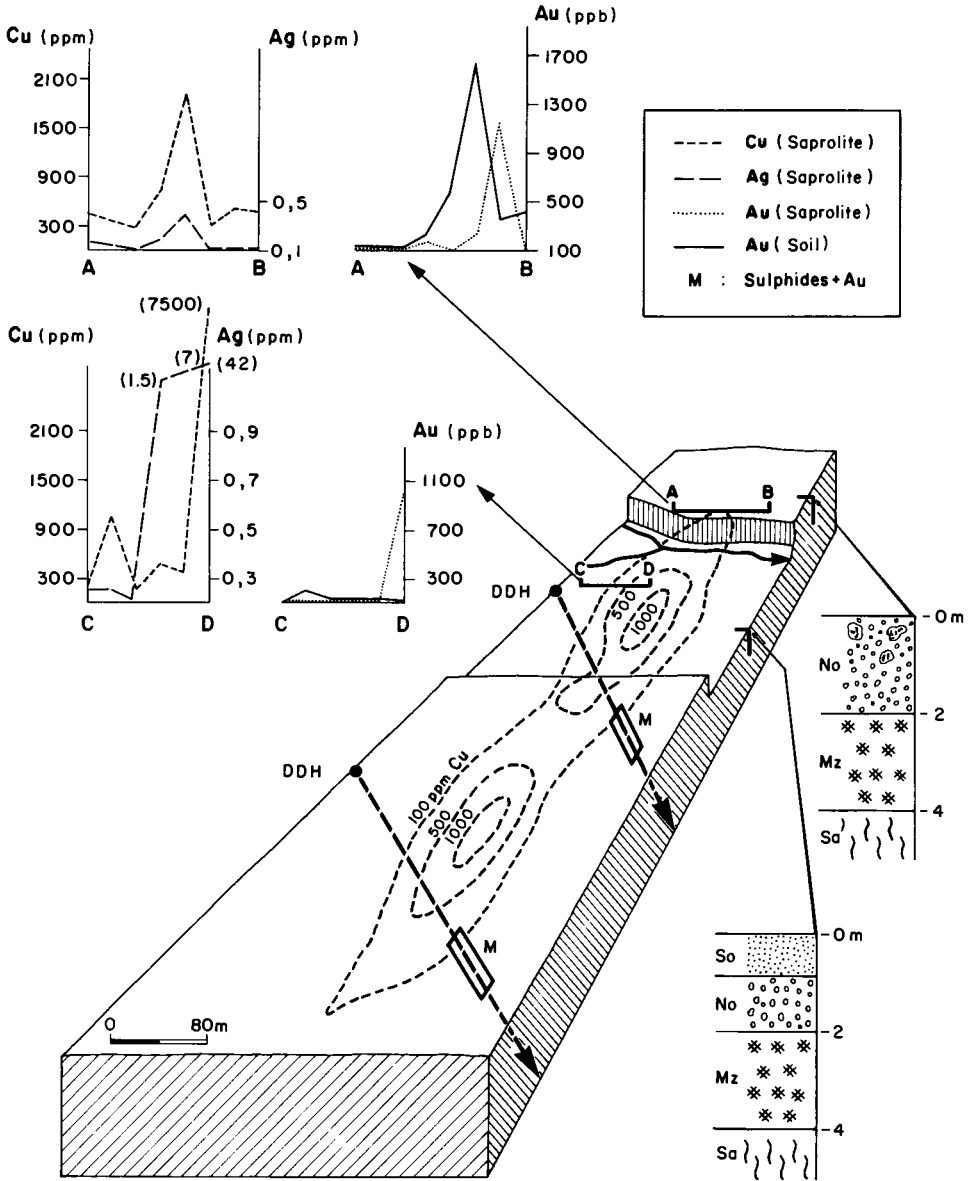


Fig. III.2-6. Toulepleu prospect, Ivory Coast. Schematic weathering profiles; Cu, Au, Ag distributions in soil and saprolite and location of diamond drill holes.

auger drilling (Fig. III.2-7), which showed good correlations between the Au contents of the red, nodular, lateritic upper horizon, the mottled zone and the saprolite.

TABLE III.2-1

Toulepleu prospect, Ivory Coast: concentrations and dimensions of Cu and Au anomalies in different sampling media

	Cu		Au	
	ppm	Dimensions m	ppm	Width m
Soil	500-1000	2 × 150 × 140	400-1800	40
Saprolite	500-7500	width: 40-70	200-1200	10-20
Ore	> 1000	width: 10	1000-16000	15

Mborguéne Au prospect, Bétaré Oya region, east Cameroun (A 1 0 [1]). Gold mineralization was discovered following a regional stream sediment geochemical survey. A multielement soil anomaly (Au, Bi, Ag, Mo, W, Pb and As) warranted further investigation by trenching and diamond drilling. The dispersion of Au and other elements from the fresh ore to the surficial soil was studied in detail (Freyssinet et al., 1989a).

The bedrock, consisting of Proterozoic volcano-sedimentary rocks, is covered by a weathering mantle 25 m thick. The saprolite is overlaid by a Fe-rich nodular horizon (2-4 m thick), in places still indurated, and a red-brown ferrallitic soil, up to 2 m thick. Primary Au mineralization is associated with abundant sulphides

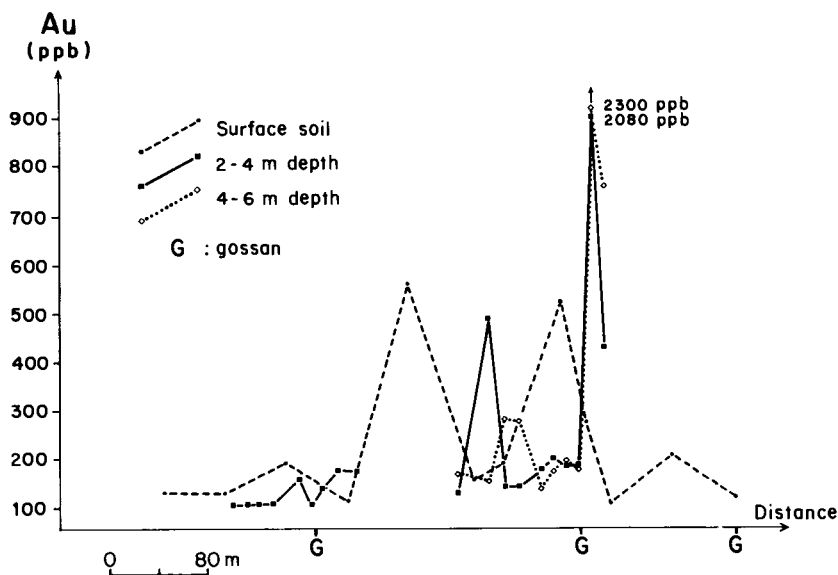


Fig. III.2-7. Toulepleu prospect, Ivory Coast. Distribution of Au in soil along a traverse across the mineralized structure.

TABLE III.2-2

Mborguéne Au prospect, Cameroun: mean contents (ppm) of Au, Ag, As, Pb, Mo, W and Bi in bedrock, saprolite and nodular horizon samples, in the mineralized zone (A) and in nearby background area (B)

Bedrock	Saprolite	Nodular horizon		
Au	A	1-15	1-3.5	0.1-4
	B	< 0.02	< 0.02	< 0.02
Ag	A	1-300	0.5-1.5	0.1-1.4
	B	< 0.1	< 0.1	< 0.1
As	A	100-2000	400-800	300-800
	B	50-150	50-150	200-300
Pb	A	100-3000	300-5000	300-4000
	B	30-50	30-50	100-200
Mo	A	20-600	10-400	50-500
	B	< 1	2-6	5-15
W	A	50-1200	100-600	50-250
	B	< 1	< 1	< 1
Bi	A	20-600	10-200	15-200
	B	< 1	< 1	< 1

and zones of silicification. There is a strong geochemical response to mineralization in each horizon of the weathering profile (Table III.2-2). The secondary dispersion halo for Au and other elements was quantified by calculating, for each horizon of the weathering profile, a dispersion index, I , in which:

$$I(i) = \log(x(i)/M(i))$$

where $x(i)$ = mean content for a given element in a given horizon and $M(i)$ = mean content for the same element in the fresh mineralization.

The distribution of I along a section across the mineralized zone is illustrated for 7 elements in Fig. III.2-8. Four types of dispersion haloes can be identified:

- Bi: mostly residual, with little or no dispersion;
- W, Mo, Pb and Au: dispersion halo progressively enlarged in the upper part of the profile, reaching a maximum in the nodular horizon;
- As, which is abundant in one of the mineralized structures and possibly forming a primary halo, is strongly dispersed in the Fe-rich nodular horizon.
- Ag: residual, and restricted to the mineralization itself, having been severely leached from the saprolite and showing no significant extension above or away from it.

The relative sizes of the dispersion halo are:

$$\text{Ag} < \text{Bi} < \text{W} < \text{Pb} = \text{Mo} < \text{Au} < \text{As}$$

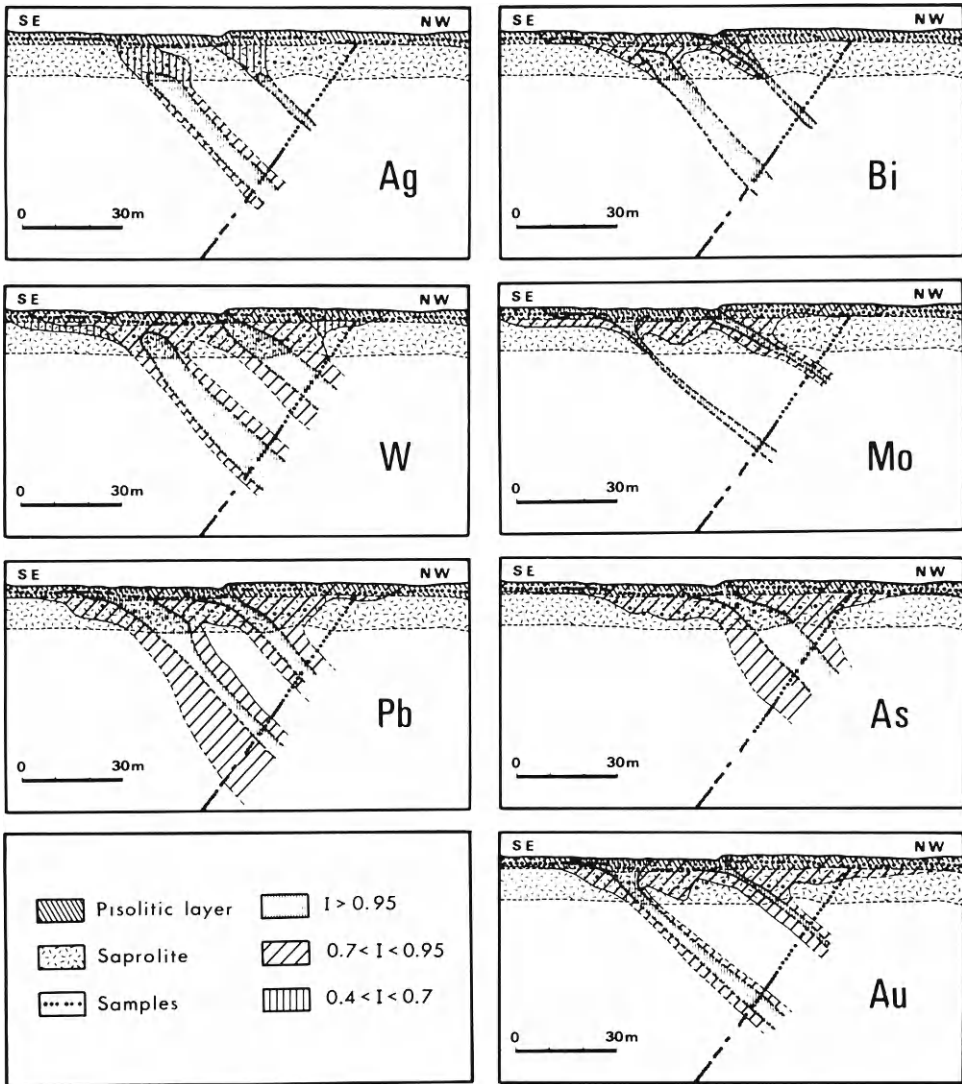


Fig. III.2-8. Mborguéné prospect, Cameroun. Distribution of metal dispersion index (I) at the surface and in depth along a traverse across the main Au and sulphides occurrences. From Freyssinet et al. (1989a).

It should be noted that although Ag and Bi have similarly narrow dispersion haloes, these arise in different ways: Ag does not form a significant halo because it is strongly leached, whereas Bi is almost immobile and therefore does not extend away from the subcrop of the mineralization. In contrast, As is strongly dispersed but its concentration is mostly controlled by the abundance of Fe

oxides in the sampled material and so its distribution is not necessarily part of the geochemical signature of the Au mineralization (Lecomte, 1990).

Gold itself has very favourable dispersion characteristics and gives a good geochemical response. The observed distribution pattern is probably the combined result of detrital and chemical (hydromorphic) processes, which have been active during past or recent weathering episodes. The (chemical) dispersion of Au in this environment has been demonstrated by Davies et al. (1989) in Sierra Leone. They show that primary gold grains may be dissolved and subsequently reprecipitated as nuggets in the different horizons of lateritic weathering profiles. These observations are similar to those made in more arid environments by Wilson (1984), Mann (1984a), Davy and El-Ansary (1986) and Freyssinet et al. (1989b), and demonstrate that Au may be secondarily mobilized in lateritic weathering profiles. However, it is not clear to what extent these processes are related to the formation of the pre-existing profile or whether they are still active under the present climatic and pedogenic environment. The mobility of gold in lateritic environments is discussed in Chapter V.3.

B-type models: pre-existing profile partly truncated

Environment, geomorphology and profile description

These models apply to areas where the former lateritic surface has been dissected, so that the present topographic surface intersects the pre-existing profile in the kaolinitic saprolite. Recent pedogenic transformations are minor, so that the horizons of the old profile that remain have not been drastically reworked. Geochemically, therefore, these models closely resemble those in equivalent geomorphological situations under seasonally humid climates (see Chapter III.1). Above the saprolite, pedogenic differentiation has resulted in the formation of distinct horizons whose total thickness seldom exceeds 1 m. Makumbi and Jackson (1977) described a typical profile, from Zaire, in which a thin humic horizon and a reddish sandy-argillaceous horizon, several tens of centimetres thick, transitionally overlie the saprolite. Where dissection has been extreme, the old profile may be entirely stripped, exposing the unweathered bedrock (C-type models).

General dispersion characteristics and examples

In situations corresponding to the B 1 0 [*] models (Fig. III.2-5), dispersion is dominantly residual (R) or hydromorphic (H) in the near-surface, where the saprolite is being transformed into a soil. However, mechanical dispersion may significantly enlarge the halo, particularly on slopes, although simultaneously causing dilution of element concentrations. There, soils may be semi-residual (B 1 0 [2] model). Along the drainage axes, the saprolite is commonly overlain by alluvium (B 1 0 [3] model). No examples are known that describe the geochemical response in such situations, but surficial sampling is probably worthless in

such circumstances and the only adequate sampling medium would be the saprolite itself.

Espérance Au prospect, French Guiana (B 1 0 [1]). The Espérance Au prospect is situated in a region of Precambrian volcano-sedimentary rocks which consist, at the prospect itself, of shales, sandy shales and sandstones. Drilling indicates mineralization exceeding 5 g/t over several metres. The prospect was discovered by a regional stream sediment survey (Zeegers, 1979) followed up by soil surveys. Soil samples were collected at a depth of 30 cm on a grid of 200×50 m and the minus 125 μm fraction analyzed for Au by AAS. The dispersion pattern for gold revealed an anomaly having a strong contrast (maxima of 200–800 ppb Au, compared to a background of less than 50 ppb) and a major E–W trend (Fig. III.2-9). The anomaly was confirmed by saprolite sampling by hand augering and was subsequently diamond drilled. Over most of the prospect, the pre-existing lateritic profile has been truncated. The characteristics of geochemical dispersion were studied by drilling ten shallow auger holes on a traverse (L1) across the geochemical anomaly overlying bedrock mineralization. Samples were collected from different horizons and analyzed for 34 elements by ICP and for Au by AAS following MIBK extraction. A size fraction analysis of the soils was also carried out, and the fractions were analyzed as above. Typically, soil profiles consist of:

- a sandy, humic horizon (5–20 cm thick),
- a red-brown silty clay horizon (30–60 cm thick),
- a transitional horizon,
- the saprolite.

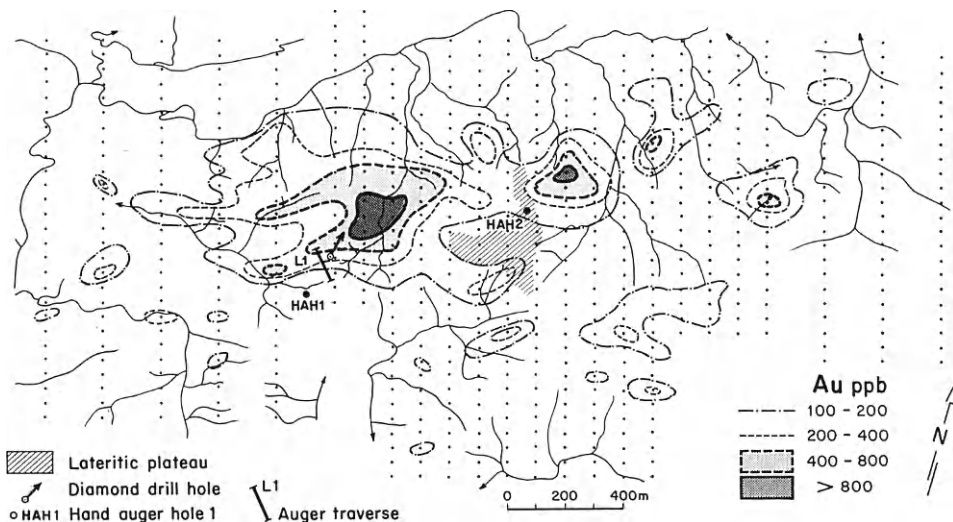


Fig. III.2-9. Espérance prospect, French Guiana. Gold contents in soils. Data from traverse L1 shown on Fig. III.2-10.

TABLE III.2-3

Espérance prospect, French Guiana: mean contents of selected trace and major elements and the proportion of $< 63 \mu\text{m}$ material ($\% < 63\mu$) in auger hole samples from the different horizons of the weathering profile

Horizon	Upper sandy humic	Silty clay brown red	Transition	Saprolite
N	10	12	8	30
SiO ₂ %	79	75	70	68
Al ₂ O ₃ %	12	13	16	18
Fe ₂ O ₃ %	6	7	10	9
K ₂ O %	0.3	0.3	0.4	1.2
% $< 63\mu$	19	29	37	48
V ppm	150	180	210	240
Cr ppm	110	120	160	160
Cu ppm	25	20	30	30
Ba ppm	230	210	240	540
Au ppb	950	1150	1100	1900

The chemical data, summarized on Table III.2-3, indicate:

(1) very low Fe₂O₃ contents, confirming the lack of a "lateritic" character in any of the horizons.

(2) high SiO₂ and low Al₂O₃ contents, denoting a high proportion of quartz in the samples. This is in agreement with information from deep drill holes, which intersected bedrock consisting predominantly of sandy shales. Some enrichment of SiO₂, coupled with a decline of the $< 63 \mu\text{m}$ fraction is observed in the upper weathering horizons. This is a consequence of recent pedogenetic activity, in which finer mineral phases, mostly clay minerals, are lost, resulting in the residual concentration of quartz.

(3) decreasing contents of trace elements (V, Cr, Ba, B) from the bottom to the top of the profile. This suggests either some surficial leaching, or dilution related to silica enrichment.

(4) almost total depletion of K₂O from the 3 upper horizons, compared to 1.2% in the saprolite. Such leaching of K₂O is common, e.g. as described by Makumbi and Jackson (1977) in a weathering profile developed over argillites in Zaire.

Although profiles at Espérance are mostly truncated, there is a small laterite-capped hill about 1 km east of line L1. Auger hole HAH2 was drilled through the preserved lateritic profile on this hill. The analytical data obtained on 1 m samples are compared in Table III.2-4 with results of auger hole HAH1, which is situated where the profile is truncated. In hole HAH1 (profile truncated), the top 2 m are strongly depleted in Fe₂O₃, Ba, Ce, B and Sr and strongly enriched in SiO₂ and Cr. The geochemical signature is thus strongly subdued near the surface. Conversely, in hole HAH2, Fe₂O₃, V and Cr are strongly enriched in the upper 2 m, in the lateritic cuirasse. However, the trace elements are strongly

TABLE III.2-4

Espérance prospect, French Guiana: mean contents of selected major and trace elements in samples from 2 auger holes (HAH1 and HAH2) at different sample depths

		Depth m					
		1	2	3	4	5	6
SiO ₂	HAH1	57	45	46	45	46	42
%	HAH2	25	26	32	36	44	47
Al ₂ O ₃	HAH1	25	30	27	27	27	23
%	HAH2	27	33	43	36	37	38
Fe ₂ O ₃	HAH1	13	16	16	16	14	24
%	HAH2	44	35	16	18	11	8
K ₂ O	HAH1	1.3	5.3	7.8	8.4	8.4	7.5
%	HAH2	2.3	3.5	3.0	3.6	4.4	4.3
Ba	HAH1	650	1850	2650	2900	3350	3300
ppm	HAH2	750	1100	1450	1800	2700	2550
Ce	HAH1	60	120	125	300	420	205
ppm	HAH2	25	20	25	15	15	15
B	HAH1	5	70	150	90	250	300
ppm	HAH2	5	5	50	15	55	40
Sr	HAH1	120	270	340	360	410	390
ppm	HAH2	60	70	90	90	120	110
V	HAH1	282	345	278	279	259	259
ppm	HAH2	719	652	329	338	291	282
Cr	HAH1	458	465	245	253	263	163
ppm	HAH2	696	554	320	298	250	250
Ni	HAH1	51	39	24	26	29	48
ppm	HAH2	32	27	31	30	35	28

depleted near the surface, as in hole HAH1. Thus, despite a different geomorphic situation, the trace elements show a similar behaviour in the soils.

The gold distribution in the upper part of the weathering profile has been assessed by averaging the data from all holes along traverse L1, which immediately overlies the mineralized zone (Table III.2-5). The mean Au content in the upper humic horizon is approximately 50% of that in the underlying saprolite. In the sandy-silt horizon at 30 cm, from which the soil geochemical samples are normally collected, the mean Au content is about 65% of that of the saprolite. The anomalous Au signature is thus only weakly depressed in the upper soil horizons compared to the saprolite.

A comparison of the Au contents of saprolite and bedrock (diamond drill hole samples) is given in Table III.2-5: surprisingly, the mean Au content is higher in

TABLE III.2-5

Espérance prospect, French Guiana. Auger and diamond drill hole samples: mean Au contents (x Au) in ppm and in g/m^3 ; proportion of the ore gold content (in g/m^3); standard deviation (s Au) and coefficient of variation (s/x) in the different horizons of the weathering profile

Horizon	N	x Au ppm	x Au g/m^3	% Au (ore) g/m^3	s Au ppm	s/x
Upper sandy humic	10	0.9	1.5	42	0.2	0.2
Silty clay brown red	12	1.2	1.9	52	0.4	0.3
Transition	8	1.1	1.7	47	0.3	0.3
Saprolite	30	1.9	3.0	83	2.2	1.2
Fresh ore (diamond drill hole)	146	1.3	3.6	100	7.4	5.5

the saprolite (1.9 g/t Au) than in fresh rock samples (1.3 g/t). However, assuming isovolumetric weathering and densities of 1.6 for saprolite and 2.7 for bedrock and by expressing the mean Au content in g/m^3 instead of in g/t , the Au contents are 3.0 g/m^3 and 3.6 g/m^3 for saprolite and fresh rock respec-

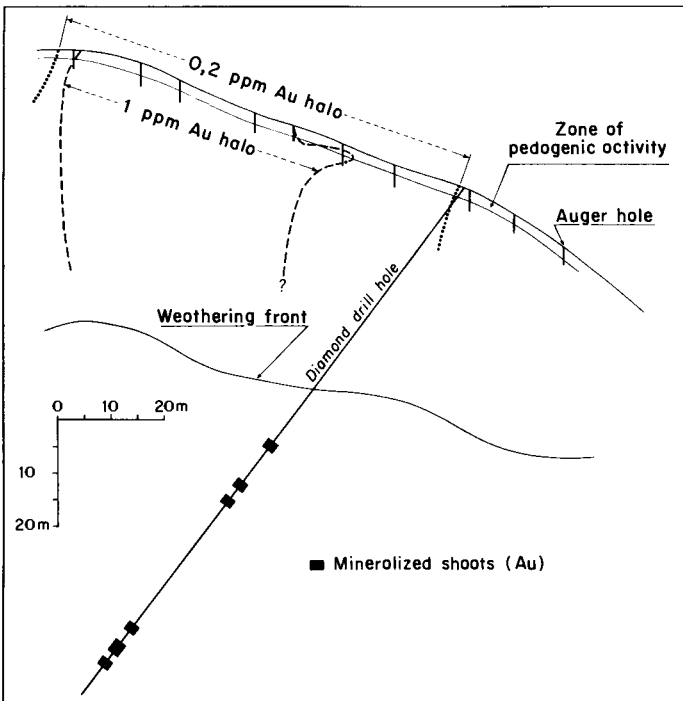


Fig. III.2-10. Espérance prospect, French Guiana. Gold dispersion along a vertical section corresponding to the auger traverse L1 (for location, see Fig. III.2-9).

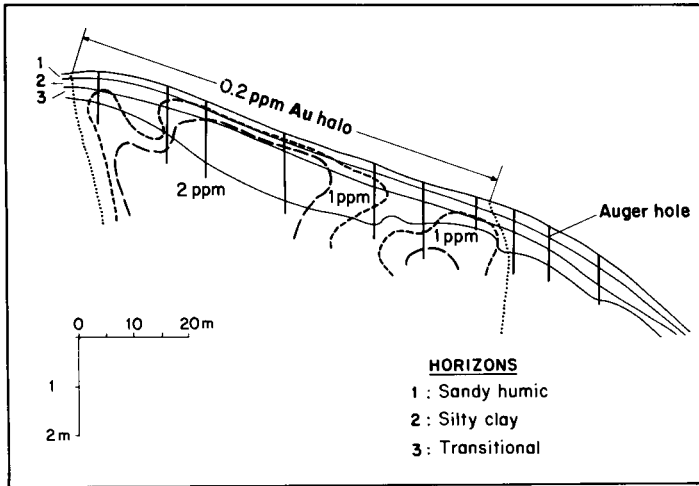


Fig. III.2-11. Espérance prospect, French Guiana. Gold dispersion in the upper part of the weathering profile; as Fig. III.2-10, with vertical scale expansion.

tively. The data thus show a *net loss* of gold from the saprolite, to about 80% of the original concentration.

The secondary dispersion patterns of Au in the weathering profile (Figs. III.2-10 and III.2-11) show that the bedrock mineralization is clearly delineated by a 0.2 ppm halo surrounding narrow zones in which Au contents may exceed 2 ppm. However, in the upper humic horizon, this halo is weakened. Despite the relatively steep slope (35%), the halo is barely distorted downslope. These data demonstrate that in a situation in which the pre-existing profile has been truncated, a prominent and accurate geochemical response for gold may be obtained from any horizon of the weathering profile. This is not unexpected, given that it is less strongly leached than the comparable situations in which the profile has been preserved (A models).

On average, the maximum gold content of soils at Espérance tends to be 50% or more of that of underlying mineralization. Where mineralization is narrow, however, dilution or homogenization in surficial horizons may reduce the contrast. Furthermore, the bulk density of the sampling media must be considered when quantifying the processes of gold dispersion. In the less dense saprolite, the Au contents, expressed as grams per tonne (g/t) or ppm, may appear significantly higher than in the corresponding bedrock. Finally, the data suggest that the transformation of bedrock into saprolite is accompanied by some redistribution and homogenization of the Au contents, most probably hydromorphically.

Céline Cu prospect, French Guiana (B10[1]). This Cu occurrence was discovered as a result of a soil and stream sediment geochemical survey; three

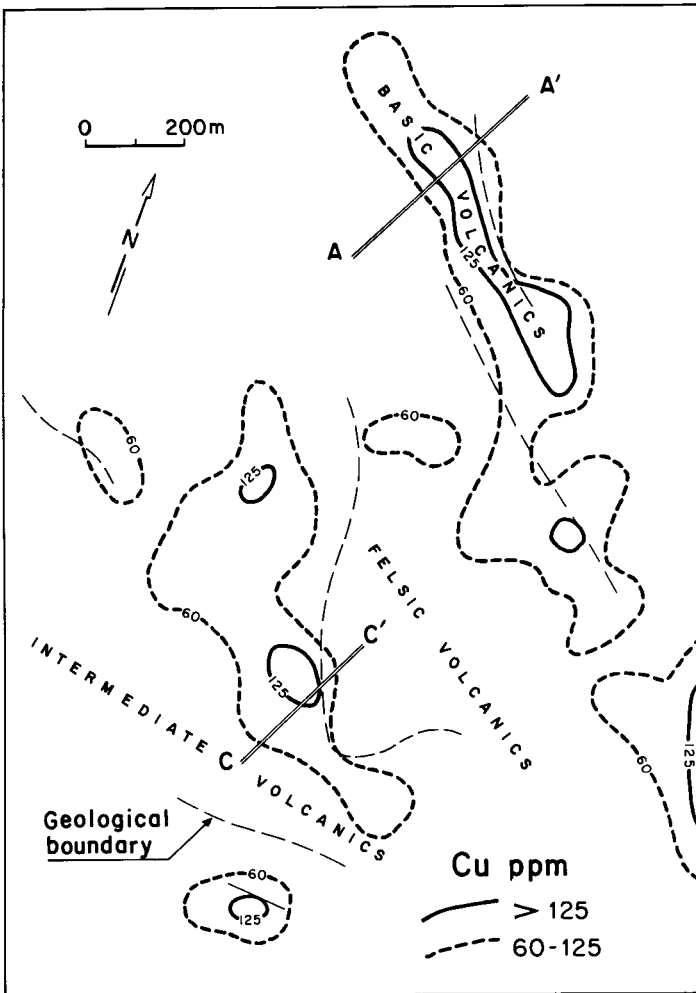


Fig. III.2-12. Céline prospect, French Guiana. Copper distribution in soils. AA' and CC': auger hole traverses (see Fig. III.2-13).

anomalous samples of 100, 120 and 200 ppm Cu were followed up by a soil survey of 3.2 km² on a grid of 100 × 100m (BRGM-COMILOG joint venture, unpublished internal report). The survey identified two elongated Cu anomalies of 1000 × 400 m (Fig. III.2-12).

The local geology consists of a volcanic sequence of rhyolites, rhyodacites, tuff, andesites and basalts, all affected by greenschist facies metamorphism. The soil Cu anomalies are coincident with the geological trends and were checked by saprolite sampling by hand auger. Holes 25 m apart were drilled to between 1.2 and 6 m depth. The results on two lines (AA' and CC' on Fig. III.2-12) show a fair

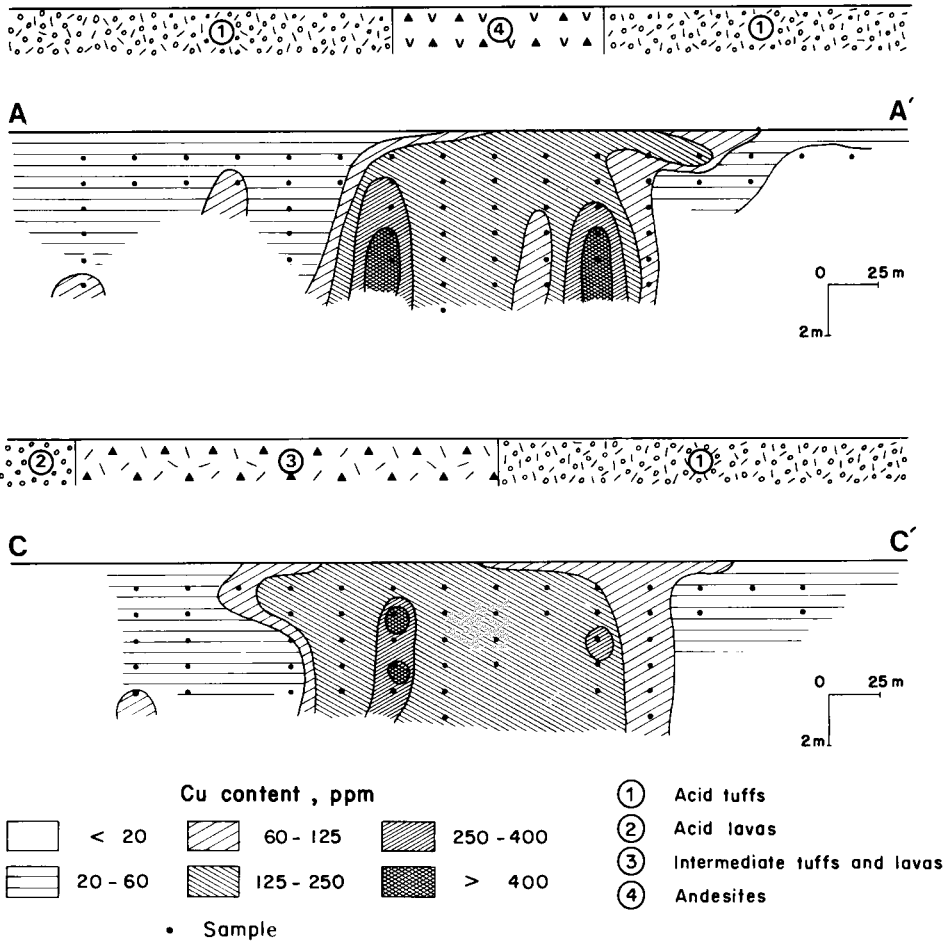


Fig. III.2-13. Céline prospect, French Guiana. Copper dispersion in the weathering profile along AA' and CC' auger hole traverses (for location see Fig. III.2-12).

continuity of the Cu anomaly from the surficial soil down to the saprolite (Fig. III.2-13). The Cu anomaly at depth indicates disseminated mineralization both in basic volcanic rocks (traverse AA') and in intermediate tuffs and lavas (traverse CC'). The dispersion of Cu is very similar to that observed for Au at Espérance, with a rather narrow dispersion halo (probably) extending from the primary mineralization to the surface.

From the analytical data, the change in Cu contents with depth can be estimated. The threshold for soil samples is 100 ppm, with peak values exceeding 150 ppm. The mean Cu contents of the soils are compared in Table III.2-6 with their equivalents within the underlying transition horizon (0.3–3 m) and the saprolite (3–5 m). In general, there is very little difference between the Cu

TABLE III.2-6

Céline prospect, French Guiana: mean Cu contents (ppm) in auger hole samples from three horizons of the weathering profile and corresponding background, threshold and anomaly peak concentrations

Horizon	Background (N)	Threshold (N)	Anomaly peak (N)
Soil	25 (3)	100 (4)	150 (2)
Transition	30 (13)	130 (9)	175 (8)
Saprolite	35 (22)	180 (25)	225 (35)

contents of soil and saprolite but, because of smoothing effect during soil formation, some high Cu values at depth are not precisely reflected at surface.

The results from Céline typify the B1 type dispersion model for regions in which the degree of leaching (of Cu) in surface soil horizons is low. However, the anomaly has not been drilled, so that the ratio between Cu values in the bedrock and in the saprolite is not yet known.

Saint-Pierre Au prospect, French Guiana (B 1 0 [1]). The Saint Pierre prospect was also discovered by the regional geochemical survey of Guiana carried out for the French Government (Zeegers, 1979). The regional anomaly was confirmed and further investigated by a soil geochemical survey, followed by a hand auger sampling programme (BRGM, unpublished internal report).

The regolith is very similar to that observed at Espérance, with a thin surficial soil (less than 1 m thick) overlying the saprolite. The Au anomaly in the soils is some 1200 m long, with Au contents of the minus 125 μm fraction ranging between 100 and 800 ppb. The auger holes were systematically drilled to the saprolite along traverses 100 to 200 m apart, with a 5 or 10 m interval between the holes. All 58 samples collected along one of these lines were analyzed for 34 elements by ICP and for gold by AAS. The results for Au, Fe_2O_3 , TiO_2 , SiO_2 , Ag, Pb and Mo are presented on Fig. III.2-14 (Zeegers, 1987). The Au mineralization itself and the associated hydrothermal alteration halo can clearly be recognized in the sampled horizons. Features of the data are:

(1) Au, Pb, Mo and Ag anomalies have the same "source" and a more or less pronounced downslope dispersion. The maximum dispersion is observed for Au, with anomalous values continuing to the northern end of the line;

(2) SiO_2 is significantly enriched with gold, probably reflecting hydrothermal silicification;

(3) where SiO_2 and Au are enriched, TiO_2 and Fe_2O_3 are depleted, possibly indicating hydrothermal leaching.

This example demonstrates the manner in which gold mineralization and its associated geochemical signature, as observed by diamond drilling, persist throughout the weathering profile. The highest contrast seems to be present in the saprolite and this is thus the preferred sampling medium at a very detailed

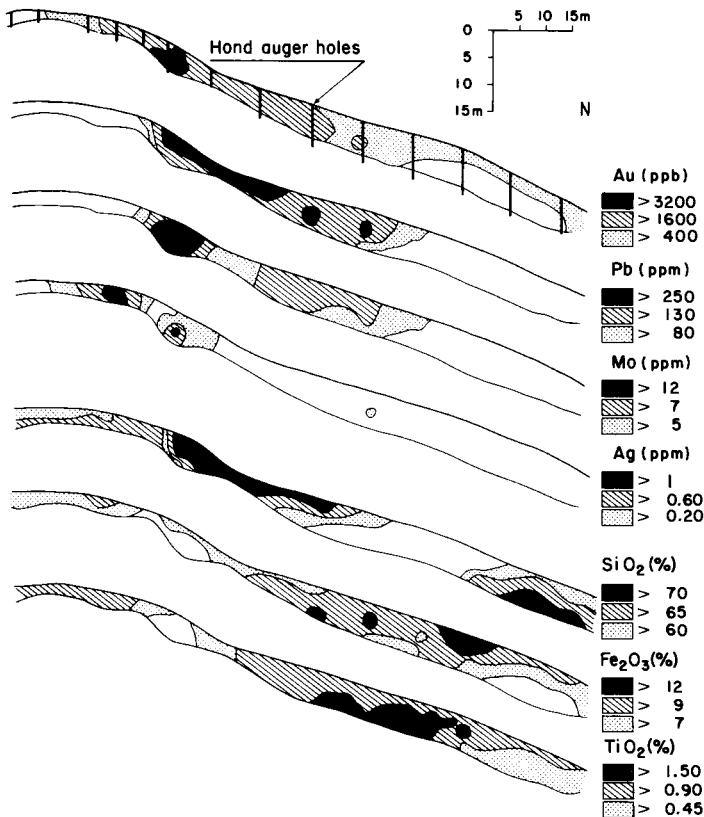


Fig. III.2-14. Saint-Pierre prospect, French Guiana. Distribution of Au and associated elements in auger hole samples (Zeegers, 1987).

scale of exploration, thereby maximizing the information obtained about the target mineralization. At Saint Pierre, multielement analysis of strongly weathered samples was helpful not only for locating the mineralized structure, but also in providing information about the associated sulphide assemblage and hydrothermal alteration.

DISPERSION MODELS: MODERATE RECENT ALTERATION

General

In areas where climatic conditions are more severe than described in the preceding section, the pre-existing lateritic profile has undergone greater transformation, resulting in the almost total degradation of the cuirasse horizon. If the

profile has been truncated, the exposed saprolite is transformed into an homogeneous ferruginous clay horizon, one or more metres thick.

Regions in which these moderately evolved weathering profiles are found are not readily defined in terms of the present climatic conditions. They are encountered both in areas where annual rainfall averages no more than 1800 mm and also where it exceeds 3 m, for example in the Guyana shield. These profiles are the net result of all climates that have prevailed since lateritization.

A-type models: pre-existing profile mostly preserved

Environment, geomorphology and profile description

Transformation of the original lateritic profile increases as a function of increasingly extreme climatic conditions, including either those presently prevailing, or an average of past climates. Most obviously, the reddish colour of the surface horizons, due to the presence of hematite, is progressively replaced by the yellow colouration indicating goethite. Moreover, the structure of the ancient profile is progressively erased and reorganized into new horizons. This was shown for instance by Muller (1978), in Cameroun, where the dominantly red soils in the north of the country under a savanna climate are replaced by dominantly yellow soils in the south, where climate is more humid. The plateau landforms characteristic of lateritic landscapes may persist, though tending to be replaced by the more evolved "half-orange" topography.

General dispersion characteristics and examples

The typical landscape of A 2 * * [*] situations (moderate recent alteration, little or no truncation) and the most common dispersion model (A 2 0 [1]) are illustrated in Fig. III.2-1, with an idealized description of the corresponding weathering profile. A lateritic tendency is still present, but the continuous cuirasse is no longer observed, having been replaced by a nodular horizon overlying soft brown-red clays corresponding to the transformation of the mottled zone and the saprolite.

Metal dispersion is not very different from that described for the A 1 0 [1] model, where recent alteration is low. However, mobile elements such as Zn may be totally leached from the surface horizons whereas others, such as Pb, are mostly retained. There is no published evidence for the development of seepage anomalies resulting from such leaching, although it is possible that mobile elements may be trapped in specific Eh-pH conditions, such as in swamps.

The THR Pb-Zn prospect, French Guiana (A 2 0 [1]). This base metal prospect, situated in a Precambrian volcano-sedimentary series, was discovered following a regional (soil and stream sediment) geochemical survey (BRGM-COMILOG, unpublished internal reports). Diamond drilling has shown that the mineralization is stratabound and contains disseminated sphalerite, galena and pyrite. The grades are subeconomic, 0.5% Pb and 1.5% Zn over widths of 100 m.

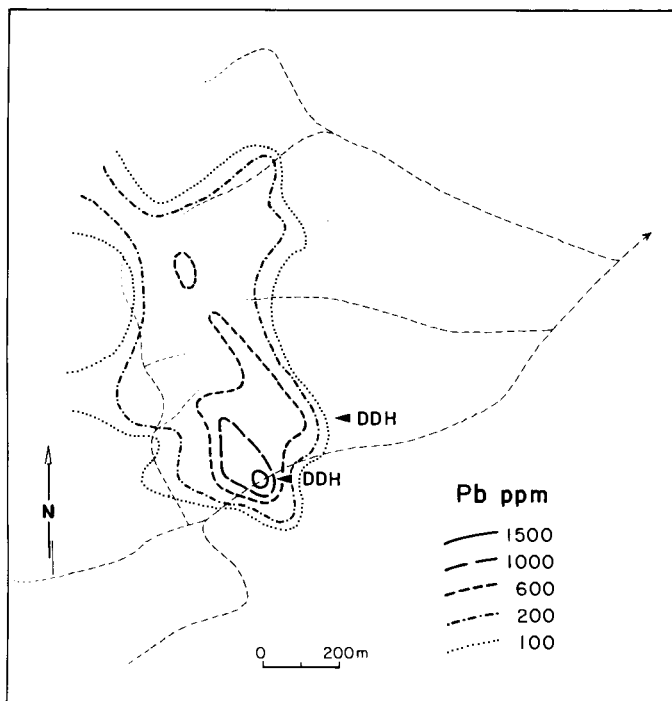


Fig. III.2-15. THR prospect, French Guiana. Lead distribution in soils and location of drill holes (DDH).

The region has a high annual rainfall (about 3 m) and a dense forest cover. It is characterized by deep ferrallitic weathering to about 50 m; the near surface horizon (4–5 m deep) is an homogeneous reddish ferruginous clay, containing a few Fe oxide nodules. The distribution of Pb shown by soil sampling (30 cm depth, $< 125 \mu\text{m}$ fraction on a 100×50 m grid) is presented on Fig. III.2-15. The anomaly has a well-defined NW–SE trend, following the major local geological structures. The Pb concentrations are rather high, with the 600 ppm halo being about 700 m long, with maximum values exceeding 1500 ppm. In contrast, the distribution of Zn, the principal ore metal, shows no significant anomalies. Concentrations are below 100 ppm and do not indicate mineralization.

The data thus demonstrate that, under these conditions, Pb and Zn behave completely differently in the supergene environment above sulphide mineralization (Laville-Timsit et al., 1983). In soils, Pb is associated with stable supergene minerals, principally phosphates and phospho-sulphates. These minerals are found not only in soil samples, but also in stream sediments, where they are responsible for strong Pb anomalies. It can thus be inferred that following the initial chemical activity leading to the formation of the secondary Pb minerals, subsequent dispersion has been predominantly mechanical. In contrast, only

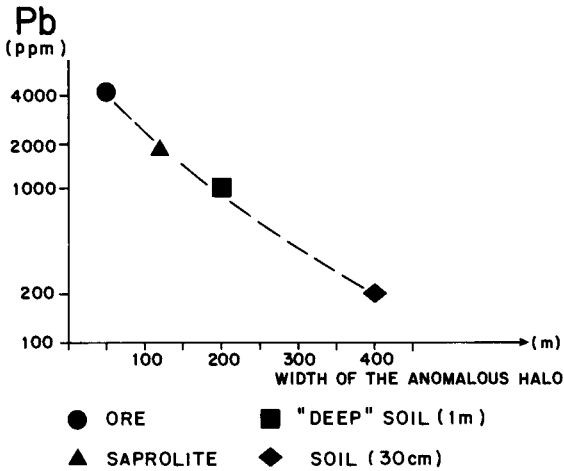


Fig. III.2-16. THR prospect, French Guiana. Comparison of Pb anomalous haloes (size and grade) in the different sampling media.

chemical mechanisms are involved in the leaching, dispersion and further immobilization of Zn, which is moderately enriched in stream sediments, associated with amorphous Fe oxides and organic matter.

The dispersion characteristics of Pb in the weathering zone can be summarized by comparing the approximate dimensions and grades of the fresh and weathered mineralization and those of the corresponding dispersion haloes in the ferruginous clay horizon and the soil (Fig. III.2-16). Primary mineralization has a true width of 50 m at grades exceeding 4000 ppm Pb, and is surrounded by only a narrow primary halo. In the weathered zone, the dispersion halo has two components:

(1) in the saprolite, mineralization has a width of 120 m, but at a reduced concentration level (2000 ppm);

(2) in the ferruginous clay (samples taken at 1 m depth) and the surficial soil (30–40 cm depth), the geochemical dispersion halo is significantly enlarged to about 400 m wide at 200 ppm Pb.

Some mineralized rock samples from deep drill holes and anomalous soil samples were analyzed for 34 major and trace elements by direct reading emission spectrometry. Selected results (Table III.2-7) show the extent to which the geochemical signature of the fresh ore samples persists into the overlying soil. For example, B (reflecting hydrothermal tourmaline), Sb, As and Ba behave similarly to Pb and remain strongly anomalous in the upper part of the weathering profile. Conversely, Ag and Cd are similar to Zn, being strongly leached from the surface.

In conclusion, it is evident that, due to different element mobilities, data obtained from soil sampling alone can give an erroneous impression of the

TABLE III.2-7

THR Pb-Zn prospect, French Guiana: comparison of selected trace elements contents of ore and overlying soil samples

Element	Ore samples N = 14 ppm	Soil samples N = 5 ppm	Ore/soil %
Pb	4000	1100	28
Zn	10000	90	1
Ag	18	2	14
Cd	110	2	2
As	800	380	48
Sb	195	95	49
B	1000	325	33
Ba	2600	1450	56

economic characteristics of the mineralization. At THR for example, it could be concluded from the surface data that the underlying mineralization is Pb-rich whereas in fact Zn is far more abundant. The different behaviour of Pb and Zn during weathering is also observed in a savanna climate at Kinagoni Hill, Kenya (see p. 215) and at Lady Loretta, Australia, where the present climate is now semiarid (see p. 351).

Mahdia area, Guyana, Cu-Mo (A 2 0 [1]). A very detailed study of the geochemical dispersion of Mo and Cu from sulphide mineralization into deeply weathered soils in rainforests was carried out by Montgomery (1971) at Mahdia in Guyana. The local geology consists of amphibolites, derived from intermediate to basic volcanic rocks, and intrusive granites. The principal sulphide minerals are molybdenite, chalcopyrite and pyrite. Molybdenite occurs disseminated or in quartz veins or veinlets, whereas chalcopyrite is mostly associated with hydrothermal alteration in the granites. The mean grades in mineralized drill cores vary from 200 to 800 ppm Mo and 100 to 400 ppm Cu.

The weathering profile consists of an upper humic horizon overlying red clays with variable amounts of ferruginous nodules. This nodular horizon, which contains 10–45% Fe_2O_3 , merges progressively with mottled zone and, finally, the saprolite. The nodular Fe-rich horizon is well developed on amphibolites but may be absent over the granites. In general, the situation corresponds to the A 2 0 [1] model, although truncated profiles (B-type models) may also be encountered, due to landscape rejuvenation.

A detailed study of the dispersion of Cu and Mo in the weathering profile was based on data from numerous soil, drill hole and pit samples. The upper humic A horizon is significantly depleted in Cu and Mo if compared to the lower horizons. The ratio of the metal content of the A horizon to the mean contents of the 3 lower horizons, calculated on data from 11 drill holes, is 0.44 for Mo and 0.42

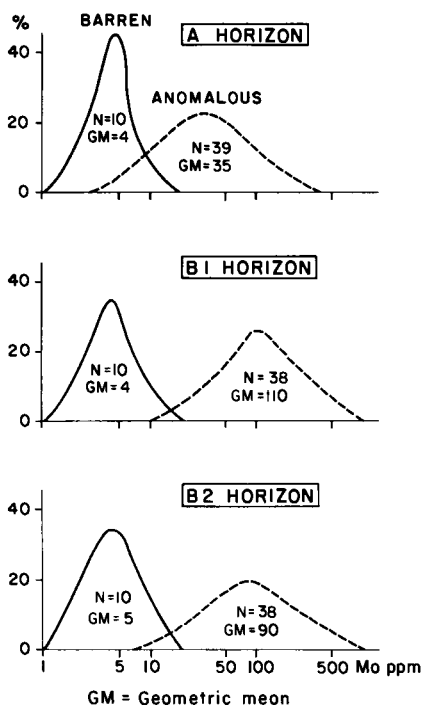


Fig. III.2-17. Mahdia area, Guyana. Frequency distribution histograms for Mo corresponding to barren and anomalous populations in the upper soil horizons: A, B1 and B2. Modified after from Montgomery (1971).

for Cu. Such an apparent leaching is probably related in part to dilution by quartz sand, which is more abundant in the soil.

The histograms presented in Fig. III.2-17 give a comparison of the Mo contents of the A, B1 (Fe-rich) and B2 (mottled) horizons. These confirm that, in the anomalous area, Mo has been leached from the A horizon and suggest that there has been some enrichment in the ferruginous B1 horizon. In contrast, in background areas, Mo distributions are similar for each horizon of the weathering profile. In the B1 and B2 horizons, in anomalous areas, the concentrations of both Mo and Cu are closely related to that of Fe. For Mo, a spectacular enrichment factor (100 to 200) was observed in the ferruginous nodules, compared to the minus 80-mesh ($180\ \mu\text{m}$) fraction of the same samples. This enrichment is possibly related to former weathering processes, if it is assumed that the ferruginous nodules observed in the B1 horizon mostly represent relics of an older lateritic surface. Nevertheless, whatever the origin and importance of secondary redistribution processes of Mo and Cu in the horizons of the weathering profile, the concentrations obtained in any of these horizons correlate fairly well to those in the bedrock, as shown in Fig. III.2-18. Furthermore, even if Mo is

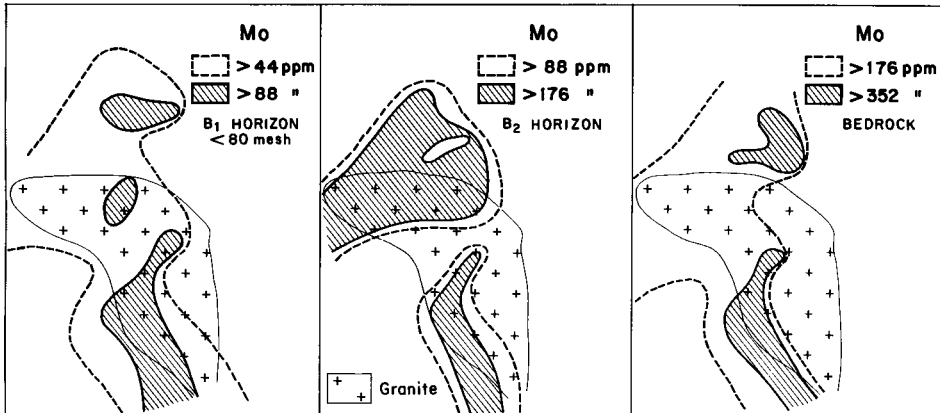


Fig. III.2-18. Mahdia area, Guyana. Molybdenum distribution in B1 and B2 soil horizons and in bedrock. Modified after Montgomery (1971).

strongly enriched in the ferruginous nodules, analysis of the minus 80-mesh fraction of soil samples proved to be very efficient in delineating bedrock mineralization. There is thus no need to utilize the coarse ferruginous fraction, by grinding the samples, even though this would have given stronger anomalies with higher contrasts.

The Mabounié phosphate, Nb and REE alkaline complex, Gabon (A 2 0 [1]). The Mabounié alkaline complex, located 40 km east-southeast of Lambaréné, Gabon, intrudes the migmatitic basement. It is a concentric system with a sövite and beforosite carbonatite at the centre, surrounded by agpaite syenites and an outer ring of fenites (Laval et al., 1988). The complex and the associated P-Nb-REE mineralization were discovered following up a regional airborne geophysical survey (Guillemot, 1988) by detailed soil and stream sediments sampling and deep drilling of the resultant anomalies (BRGM, unpublished internal reports). The economic minerals are secondary apatite (phosphate), pyrochlore (Nb) and crandallite (REE).

The weathering profile, which is relatively atypical of the rainforest environment, is composed of three main horizons:

(1) an indurated phosphate horizon with secondary apatite, directly overlying fresh rock;

(2) a mottled horizon enriched in Fe, Nb and REE and strongly depleted in P;

(3) a friable, red surficial horizon containing Fe oxide nodules, from which most elements have been partly leached.

The formation of the deposit is directly related to the weathering processes, with secondary apatite formed at the base of the profile and pyrochlore and crandallite residually concentrated in the mottled horizon.

The mineralization is clearly outlined by the soil anomaly, with the maximum concentrations of 6% P_2O_5 , 1.45% Nb_2O_5 , 350 ppm Y and 4500 ppm Ce corresponding to 24% P_2O_5 , 2% Nb_2O_5 , 500 ppm Y and 5000 ppm Ce in the deposit itself. A similarly strong contrast is shown by the soil anomaly in a savanna climate at Sukulu, Uganda (see p. 222). The Mount Weld carbonatite, Western Australia, has a similar weathering profile, but it is buried by over 15 m of transported overburden and hence has no surface geochemical expression (see p. 330).

Other examples. Bose (1982, 1984) described a weathering profile from Orissa state, India, which has a 0.5 m thick leached sandy horizon and a nodular ferruginous horizon (1–2 m thick) overlying saprolite. Exploration for Cu was carried out in this environment and it was found that the best geochemical response was obtained by sampling and analyzing the ferruginous nodules. Indeed, old workings are responsible for some Cu contamination in the fine fraction of soil samples and the use of the coarse nodular fraction eliminated this problem. In Guyana, Kilpatrick (1969) demonstrated that deeply weathered soil samples above a serpentinite gave a good geochemical response, with anomalies of up to 5000 ppm Ni and 500 ppm Co.

B2-type models: pre-existing profiles partly truncated

Environment, geomorphology and profile description

In this situation, the saprolite is intersected by the present topographic surface, but the weathering profile is still tens of metres thick. These models occupy a similar landscape position to the B1 models (Fig. III.2-1), but the saprolite has been more severely transformed. The main difference from the less leached models is that, near the surface, the saprolite has been transformed into a poorly structured reddish-orange horizon whose thickness may reach several metres. A typical profile was described from the central Ivory Coast by Verheye (1979):

- (1) reddish sand-clay soil, 1–2 m thick, with some polyhedral structures;
- (2) reddish sandy clay, about 1 m thick, containing small ferruginous nodules;
- (3) saprolite.

The mineralogy of the upper few metres of the profile is very uniform, consisting predominantly of quartz, kaolinite and Fe oxides. Trace elements of particular interest to mineral exploration are more strongly leached than for model B 1 but, nevertheless, several examples from the literature demonstrate a fair geochemical response, with high anomaly/background ratios.

General dispersion characteristics and examples

An idealized illustration of the most commonly encountered dispersion model (B 2 0 [1]) is shown on Fig. III.2-5. In general, dispersion is not very extensive either in the saprolite or in the upper sandy clays, although some hydromorphic

TABLE III.2-8

d'Artagnan prospect, French Guiana: means and ranges of copper contents of fresh ore and different horizons of the weathering profile

Horizon	Depth m	Fraction	N	Cu	
				Mean ppm	Range ppm
Soil	0.30-0.40	< 125 μm	4	700	400-1000
Fe-rich	1	Total	7	720	400-800
Saprolite	1-6	Total	31	860	800-1200
Ore	30-60	Total	4	2000	1300-3500

redistribution may have occurred. The only significant lateral dispersion is observed in the soil, due mainly to physical processes, but haloes are rarely very large. Accordingly, an excellent geochemical response is commonly obtained in these moderately leached, truncated environments, as illustrated by the following case histories. Anomalies are characteristically of high contrast but of restricted size, although very mobile elements such as Zn may be almost totally leached from the upper soil horizons. However, a less favourable response is obtained where semi-residual material or transported overburden (models B 2 0 [2] or B 2 0 [3]) are present.

d'Artagnan Cu prospect, French Guiana (B 2 0 [1]). Mineralization at this prospect consists of disseminated chalcopyrite within intermediate to basic lavas. Geochemical dispersion has been investigated by soil sampling, augering and deep drilling (BRGM-COMILOG joint venture, unpublished internal reports). Variations in Cu contents with depth are summarized on Table III.2-8. The ratio between the Cu contents of soils and fresh ore is about 1 : 3, which indicates only minor leaching. The prospect, which is typical of B2 model, is close to the THR prospect (p. 262), but has a greater degree of truncation.

Cambrouze Ni-As prospect, French Guiana (B 2 0 [1]). At Cambrouze, the weathering profile is highly truncated, and blocks of almost unweathered pyroxenite bedrock are found at 5-6 m depth. The upper horizons consist of a reddish clay containing 30% or more Fe_2O_3 . A regional soil and stream sediment survey (Zeegers, 1977) showed a strong combined anomaly of Ni (to 1000 ppm) and As (to 500 ppm), which was followed-up by a soil survey based on samples collected at about 30 cm depth on a 200×400 m grid (Fig. III.2-19). Similar distribution patterns were observed for both Ni and As, with high contrast anomalies having maxima of 1500 ppm Ni and 500 ppm As. More detailed saprolite sampling by hand auger drilling separated the Ni and As anomalies (Fig. III.2-20). Nickel and As both exhibit only very narrow lateral dispersion haloes and concentrations remain very high even near the surface (1 m depth). The source of the anomalies has not yet been established.

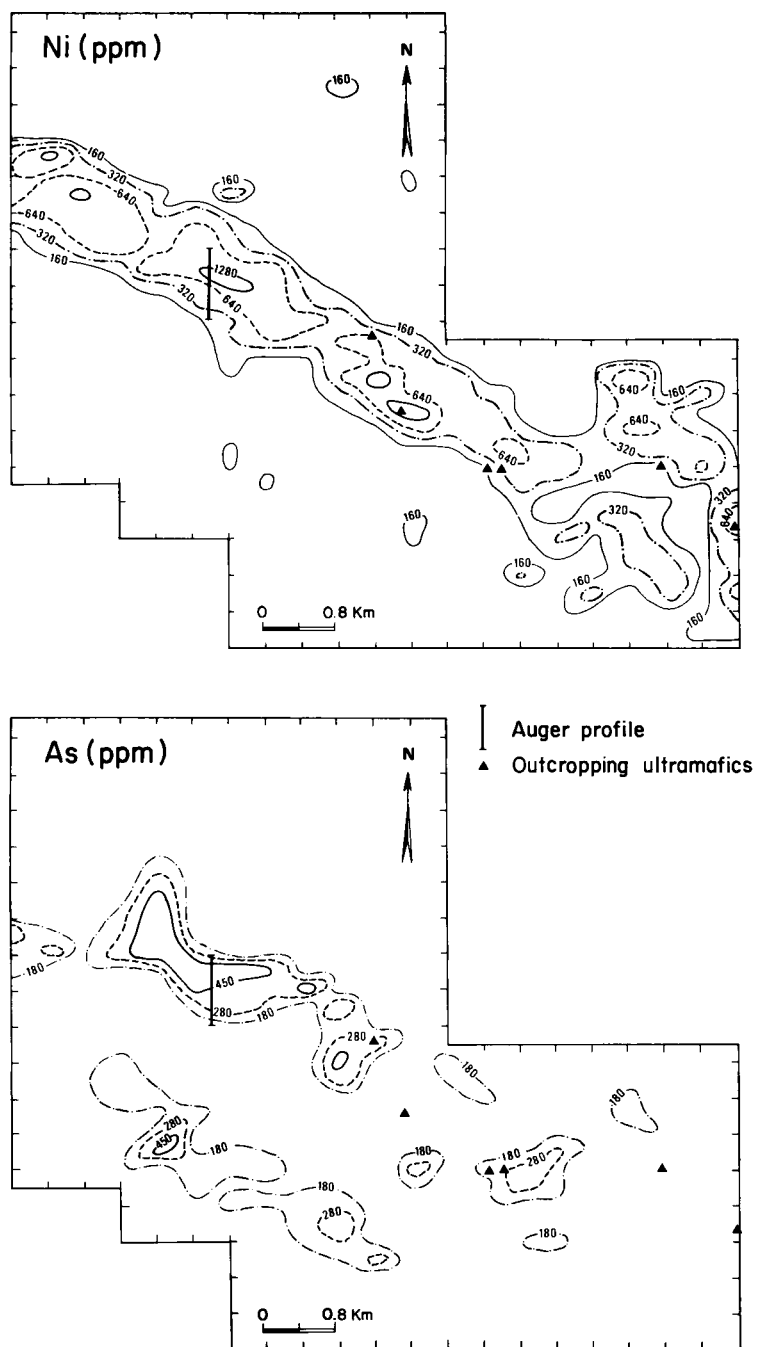


Fig. III.2-19. Cambrouze prospect, French Guiana. Nickel and As distribution in soils.

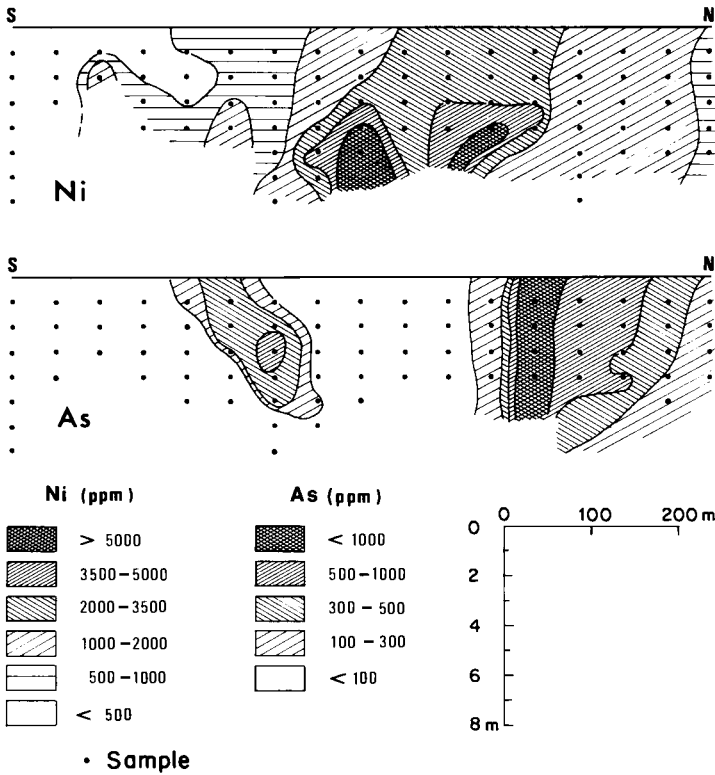


Fig. III.2-20. Cambrouze prospect, French Guiana. Nickel and As distribution in auger traverse (for location see Fig. III.2-19).

Dorlin Au prospect, French Guiana (B 2 0 [1]). Gold mineralization at Dorlin is associated with sulphides (principally pyrite and arsenopyrite) occurring in two distinct zones of hydrothermal alteration (zones A and B on Fig. III.2-21), hosted by intermediate and basic volcanic rocks of Proterozoic age. Zone A is character-

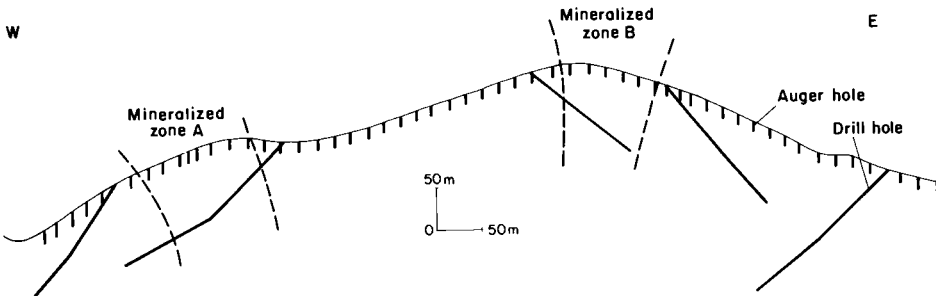


Fig. III.2-21. Dorlin prospect, French Guiana. Schematic cross-section of the main mineralized zone (see Table III.2-9).

TABLE III.2-9

Dorlin prospect, French Guiana: mean contents of selected major and trace elements in two mineralized zones (see Fig. III.2-21) (from Taylor et al., 1989)

	Zone A		Zone B	
	Bedrock	Saprolite	Bedrock	Saprolite
Fe ₂ O ₃ %	21	25	9	19
MgO %	5.6	0.8	3.1	1.8
K ₂ O %	2	1.8	3.3	4.1
B ppm	335	2580	3270	6760
As ppm	765	635	4000	545

ized by abundant quartz, chlorite and sericite, whereas zone B has dominant tourmaline. The weathering profile in the area is typically truncated but occasional cuirasse relics suggest that the former lateritic surface was probably not far above the present topographic surface. The prospect is one of the several Au anomalies found during a regional soil and stream sediment survey in 1975. Detailed soil and saprolite surveys (Taylor et al., 1989) located anomalies of Au and pathfinders elements such as As, Cu, Sb and B. The development of the geochemical signature was investigated by a traverse of shallow and deep drilling. Comparison of the different surface sample media shows that the mineralization is expressed by sharply contrasted Au anomalies, with average ratios of Au contents of primary mineralization : saprolite : soil of about 5 : 2 : 1. Consequently, surface geochemistry has an important role in delineating the mineralized bodies.

In zone A (Fig. III.2-21), the key elements characterizing the mineralization and the associated hydrothermal alteration halo in the fresh rock are MgO (chlorite), K₂O (sericite), Fe₂O₃ (pyrite), As (arsenopyrite) and Au. In the saprolite, the main difference (Table III.2-9) is a significant loss of MgO, indicating that chlorite is almost totally leached. In contrast, the high K₂O contents indicate sericite to be rather stable in the saprolite. Iron and As probably occur as sulphides in the fresh rock, and are retained as oxides in the saprolite. The low mean content of B (335 ppm) in the underlying bedrock reflects the low abundance of tourmaline, so that the high values (mean 2580 ppm) recorded in the saprolite are thus rather surprising. A possible explanation is that resistant tourmaline derived from rocks upslope has been mechanically transported by mass flow of the upper part of the saprolite (i.e. B 2 0 [2] dispersion model) and then washed deeper into the saprolite by physical eluviation (see p. 99). If so, this is one of only few examples of this process affecting minerals of direct exploration significance.

A very similar process was observed for Au on the other side of the mineralized hill (zone B), in which the surface and subsurface anomalies are far more developed than the primary mineralization. In the same zone (Fig. III.2-21), very

TABLE III.2-10

Southwestern Nigeria: comparison of mean contents of Co, Cr and Ni of rocks and corresponding soil samples, for 5 different geological environments (from Matheis, 1981)

Lithology	Co ppm		Cr ppm		Ni ppm	
	Rock	Soil	Rock	Soil	Rock	Soil
Schists, quartzites	9	< 10	5	< 10	7	< 10
Biotite gneisses	20	10-25	11	10-25	15	10-25
Hornblende gneisses	40	25-50	40	40-60	40	25-50
Amphibolites	85	50-70	90	50-70	100	50-70
Ultramafic rocks	85	> 70	500	> 70	210	> 70

high B concentrations (several thousand ppm) and relatively high MgO concentrations (up to 3%) in the saprolite samples reflect the high abundance of tourmaline in the fresh rock.

Each of the mineralized zones is therefore characterized by a different geochemical signature, reflecting its specific hydrothermal fingerprint. Even in the saprolite, the multielement geochemical data is sufficiently clear to allow the type of mineralization to be recognized.

Regional geochemical exploration in Nigeria. Matheis (1981) showed that soil geochemistry is an efficient tool for identifying potential source rocks in the geological and morphoclimatic conditions of southwestern Nigeria. The geology of the area consists of Precambrian volcano-sedimentary belts and Sn-Nb-Ta-bearing pegmatites. It was found that certain lithologies could readily be mapped by analyzing selected trace elements retained in latosols. For example, in the volcano-sedimentary environments, the increasing concentrations of Co, Cr and Ni in more and more basic rocks were found to result in similarly increasing concentrations in corresponding soils (Table III.2-10). In some instances, however, elements ratios were more useful than the individual elements. Thus, relatively low values of the Mg/Li ratio delineates the extension of Sn-Ta-Nb pegmatites with a anomaly/background ratio higher than that of Li (Fig. III.2-22).

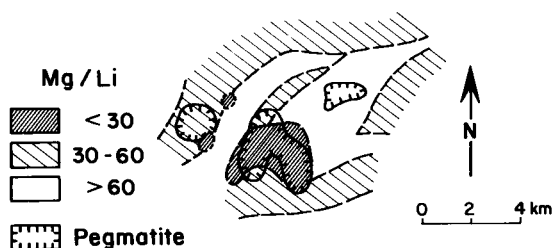


Fig. III.2-22. Regional soil survey of southwestern Nigeria. Distribution of Mg/Li ratio in soils. Modified from Matheis (1981).

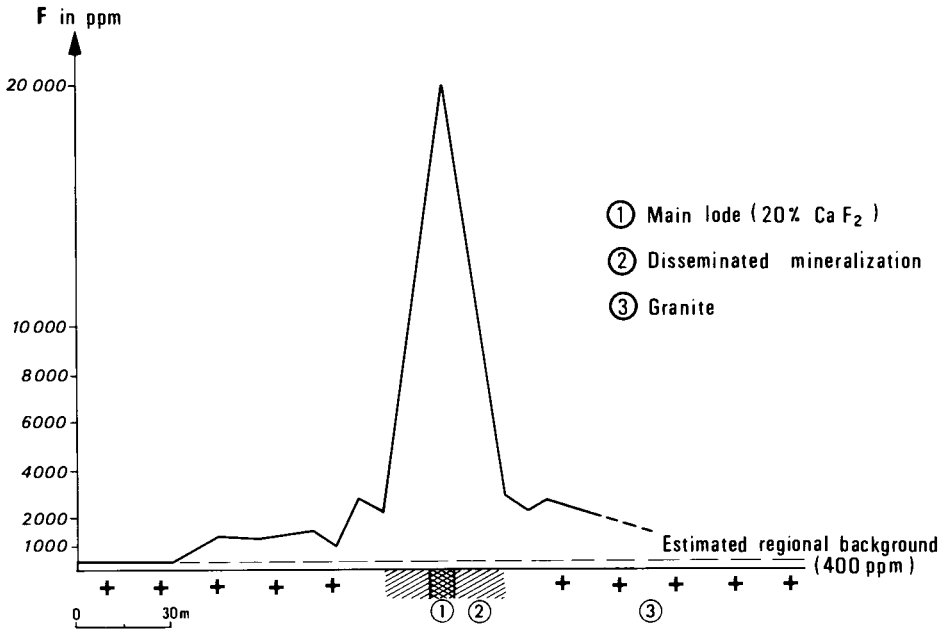


Fig. III.2-23. Fluorine dispersion in a soil traverse across a fluorite deposit in central India. Modified after adapted from Mukherjee (1979).

Exploration for Cu in western Suriname. Exploration in the Upper Nickerie region demonstrated a fair geochemical response for Cu where the pre-existing profile has been truncated (Dahlberg, 1982; Pollack and Zeegers, 1983). Indeed, over rocks containing about 0.3% Cu as disseminated sulphides, concentrations of 400–3000 ppm Cu are found in the saprolite and the corresponding soil anomaly ranges from 400 to 2000 ppm. However, the dispersion halo is very narrow, and the areal dimensions of the soil anomaly hardly exceed those of the primary mineralization. Most of the Cu initially contained in the sulphides has been transferred to secondary minerals, principally iron oxides. Hydromorphic dispersion of Cu, that could have resulted in a large dispersion halo, has been restricted by its relative immobility in the prevailing conditions.

Chandidongri fluorite mineralization, central India (B 20 [1]). Fluorite mineralization occurs in K feldspar-rich pegmatites traversed by a silicified shear zone. Freely drained residual latosolic soils were collected in the B-horizon along traverses perpendicular to the strike of the mineralization (Mukherjee, 1979). The results show an excellent geochemical response for F (Fig. III.2-23) and also for Pb, Cu and Zn. The maximum contents in soil samples reach nearly 2% F, about one tenth of the grade of the main lode, 700 ppm Zn, 300 ppm Cu and > 2000 ppm Pb. The width of the anomalous halo is about 200 m, taking 1000 ppm F as the local threshold value.

DISPERSION MODELS: STRONG RECENT ALTERATION ("STONE-LINE" WEATHERING PROFILES)

General

The spectacular stone-line weathering profiles, as described by Lecomte (1988), are mostly found where present climatic conditions are extreme, with high mean temperatures (about 25°C) and annual rainfall greater than 2000 mm (Fig. I.1-1). The resulting pedogenic evolution may affect either a pre-existing lateritic surface or a truncated profile. The corresponding dispersion models are referred to as A 3 * [*] and B 3 * [*] models.

Compared with the preceding models, which correspond to a lesser degree of recent alteration, the most noticeable characteristics are *firstly* the destruction of previous pedogenic features and the remobilization of iron in the upper part of the profile and, *secondly*, the presence below of the stone line itself. This latter horizon consists of coarse fragments such as ferruginous nodules, quartz and lithorelics embedded in a clay matrix, and may include a high proportion of material inherited from earlier lateritic episodes. The profiles are typified by yellowish colours in the upper horizon (above the stone line) and reddish colours in lower horizons, probably corresponding to the dominant iron oxide phases, namely goethite and hematite respectively.

There appear to be two types of stone line according to the material from which the fragments are derived (Lecomte, 1988). *Lateritic stone lines* consist predominantly of ferruginous material including degraded cuirasse blocks. *Quartz stone lines* consist predominantly of quartz fragments and more or less indurated lithorelics (Fig. III.2-24). These stone lines are considered to have been formed by the reworking, respectively, of complete and truncated lateritic profiles and hence correspond to the principal model subdivision. Much of this reworking is probably chemical in nature (Muller et al., 1980; Bocquier et al., 1984) but the accumulation of coarse fragments in the stone line itself implies the involvement of physical processes. Downward migration of these fragments, first suggested by Laporte (1962) and Moeyersons (1978), may occur as the result of enhanced plasticity due to high rainfall (Boulet, 1978; Lecomte, 1988), or by bioturbation, e.g. by termites (Stoops, 1967, Lévêque, 1978). It is now considered, therefore, that these very peculiar weathering profiles were formed by a combination of chemical, physical and biological processes, although the precise mechanism is uncertain. Nevertheless, most authors now consider them to be residual.

Within the humid tropics, stone-line profiles are commonly observed in the large planation zones corresponding to old basement areas (Central Africa, Madagascar, part of South America) but are generally absent from regions with recent orogenic activity, such as most of southern Asia and the eastern Andes. In these regions, the rate of mechanical erosion probably exceeds that of chemical reworking and downward migration, so that the stone line cannot develop (see

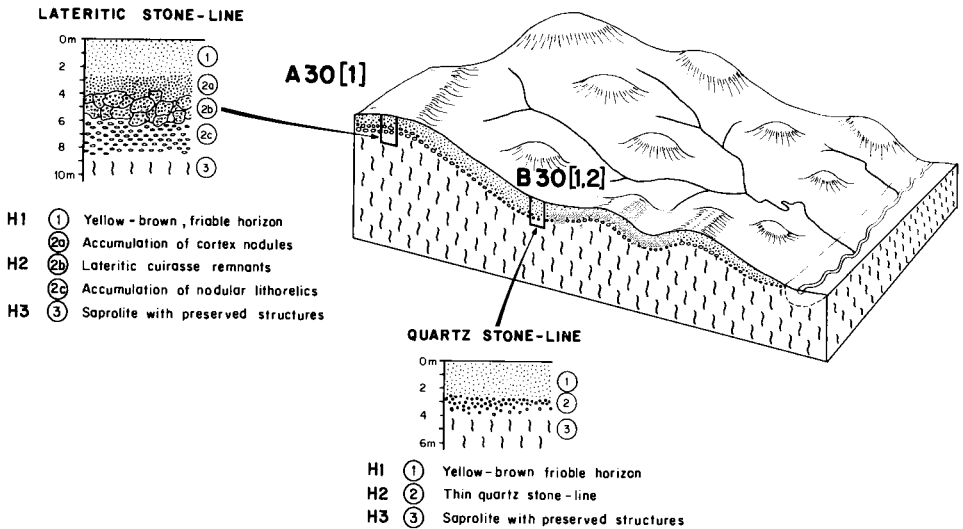


Fig. III.2-24. Diagram showing the general landscape and the weathering profile related to models for situations subject to strong recent leaching (models A3 and B3). For abbreviations, see Fig. III.1-1.

Chapter IV.1). Stone-line profiles may also be present in some regions where the present climate is less humid, such as the central Ivory Coast and East Africa, in transitional zones between savanna and forest. Matheis and Pearson (1982) even describe stone-line weathering profiles in northern Nigeria, under present-day dry savanna climate with less than 1200 mm annual rainfall. Stone-line profiles in these climates are discussed in Chapter III.1. However, not all stone lines, particularly those in savanna and semiarid climates, have this vertically residual origin. Some mark the base of colluvial mass flow and others are clearly detrital (see p. 103). Even in rainforests, quartz stone lines may include alluvial gravels and cobbles near to drainage axes (Collinet, 1969).

A-type models: pre-existing profiles mostly preserved. Lateritic stone-line profiles

Environment, geomorphology and profile description

The situation of this model (A 3 0 [1]) within the general landscape is illustrated on Fig. III.2-24. Data from Muller et al. (1980) and Lecomte and Colin (1989) suggest the following idealized profile:

(1) *Horizon H1* (1 to 6 m thick): yellowish, homogeneous, friable sandy clay, free of coarse fragments, with the upper part commonly differentiated into a humic soil.

(2) *Horizon H2*, the stone-line horizon (0.5 to 2 m thick): subdivided according to the nature of the coarse material:

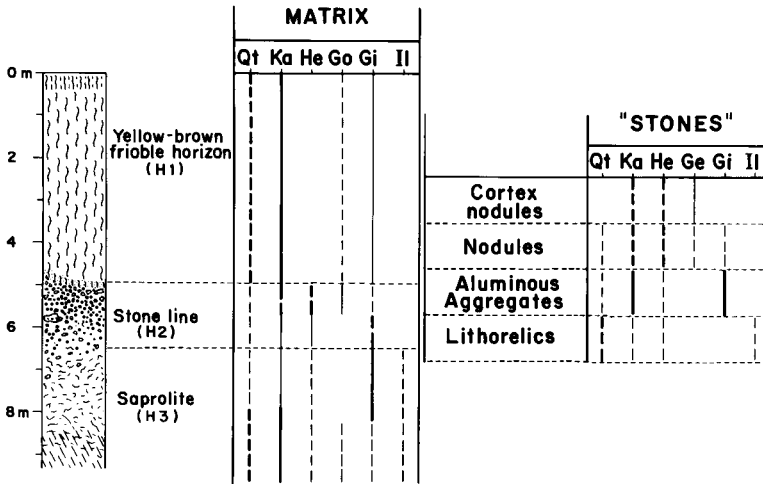


Fig. III.2-25. Stone-line weathering profiles, Gabon. Schematic mineralogical composition in the different horizons and constituents. From Lecomte (1988).

- (a) spherical ferruginous nodules and pisoliths;
 - (b) lateritic blocks of various sizes;
 - (c) more or less ferruginized, commonly elongated lithorelics.
- (3) *Horizon H3*: the saprolite.

The contact between the sandy clay soil and the stone line is normally sharp, although a thin transitional horizon may be observed, characterized by the increasing size of the quartz grains (to more than 1 mm) and the appearance of small, soft, ferruginous nodules. In comparison, the transition between the stone line and the saprolite is progressive, with a decreasing proportion of nodules and lithorelics.

The average mineralogical composition of the different horizons and constituents of the stone-line profiles is shown on Fig. III.2-25. Most of the rock-forming minerals have been transformed into a secondary assemblage comprising quartz, kaolinite, gibbsite and Fe oxides in rather constant proportions throughout the weathering profile. Detailed chemical data, principally from Gabon (Lecomte, 1988; Lecomte and Colin, 1989) confirm the general trends noted for lateritic profiles including, for example, the almost total removal of the alkaline and alkaline-earth elements from at least the soil and the stone line. For this reason, only the three major oxides Fe_2O_3 , Al_2O_3 and SiO_2 are considered in the following discussion of the origin of the profile. As with the mineralogy, the chemical composition of the fine matrix (minus $63 \mu\text{m}$ fraction) appears to be fairly homogeneous from one horizon to another. Nevertheless, as shown on Fig. III.2-26, differences related to lithology are obvious even in the upper, strongly leached H1 horizon. A comparison between 6 sets of samples corresponding to different geological environments using $\text{Al}_2\text{O}_3/\text{Fe}_2\text{O}_3$ and $\text{SiO}_2/\text{Al}_2\text{O}_3 + \text{Fe}_2\text{O}_3$

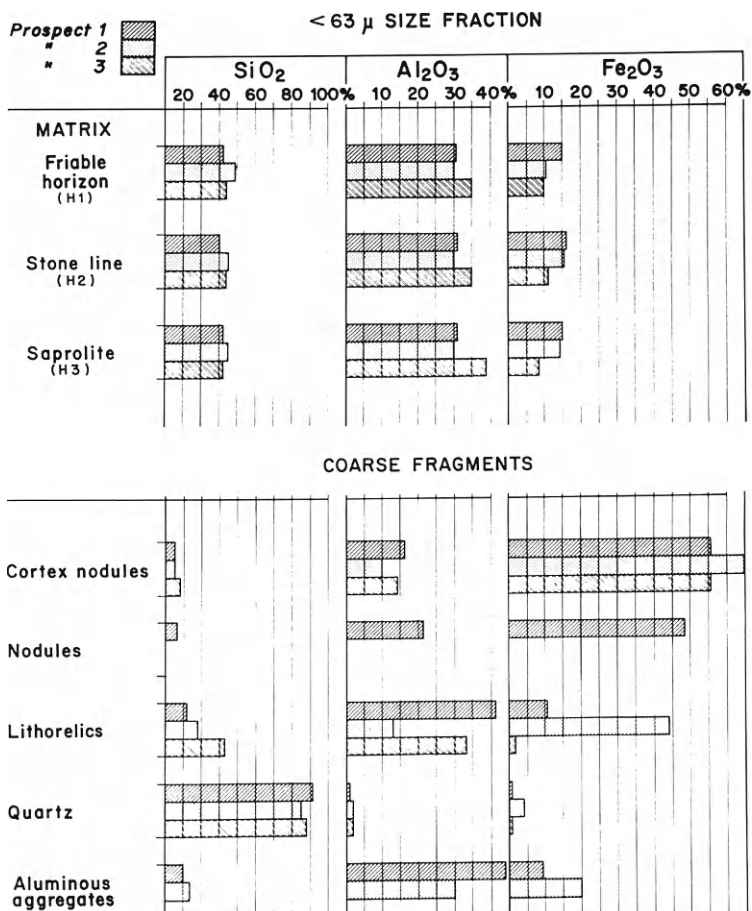


Fig. III.2-26. Stone-line weathering profiles, Gabon. Distribution of SiO_2 , Al_2O_3 and Fe_2O_3 in the different horizons and constituents.

TABLE III.2-11

Gabon: mean $\text{Al}_2\text{O}_3/\text{Fe}_2\text{O}_3$ and $\text{SiO}_2/(\text{Al}_2\text{O}_3 + \text{Fe}_2\text{O}_3)$ ratios in H1 (upper yellow friable), H2 (stone line) and H3 (saprolite) horizons of stone-line weathering profiles developed over 6 different lithologies

Lithology	$\text{Al}_2\text{O}_3/\text{Fe}_2\text{O}_3$			$\text{SiO}_2/(\text{Al}_2\text{O}_3 + \text{Fe}_2\text{O}_3)$		
	H1	H2	H3	H1	H2	H3
1 Granites	3.6	2.9	4.6	1	0.9	0.9
2 Acidic gneisses	2	1.8	2.2	0.9	1	0.9
3 Schists, gneisses	2.6	1.9	2.1	1.2	1	1
4 Amphibolites	1.4	1	1.3	0.4	0.4	0.5
5 Ultramafics	1.4	1.1	0.5	0.7	0.6	0.4
6 Black shales	3.5	2.4	2.9	1.7	1.4	1.3

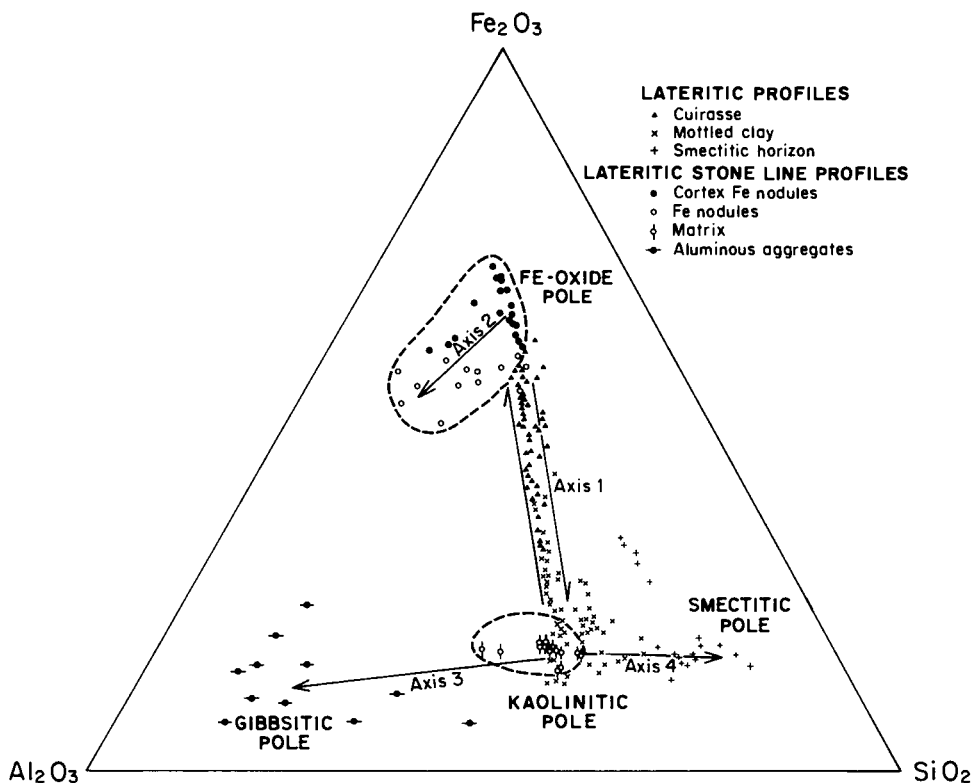


Fig. III.2-27. Fe_2O_3 - SiO_2 - Al_2O_3 diagram. Comparison between samples from lateritic profiles in savanna environment, West Africa and lateritic stone-line profiles in rainforest of Gabon.

ratios is given Table III.2-11. The values obtained for these ratios in horizons H1, H2 and H3 reflect the more or less basic or siliceous composition of the underlying bedrock. These data demonstrate that the chemical composition of the matrix component of the three horizons constituting the stone-line profiles is at least partly inherited from that of the bedrock, from which it is inferred that these profiles are mostly residual.

The major element composition of the coarse fraction (> 1 mm) is more heterogeneous than that of the fine fraction. This is demonstrated in Fig. III.2-26 in which the compositions of stone-line fragments are compared with those of the fine fraction material from the same locations. The Al_2O_3 contents in particular show some relationship with the lithology.

The relationship between past and present weathering episodes can be demonstrated (Lecomte, 1988) by comparing analytical data from stone-line profiles in Gabon with preserved and non-transformed lateritic profiles in Burkina Faso (Ambrosi, 1984) on a single Fe_2O_3 - SiO_2 - Al_2O_3 triangular diagram (Fig. III.2-27). These data appear to cluster along axes that correspond to the principal evolu-

tionary trends, both mineralogical and chemical, of the main weathering processes, the combined actions of which have resulted in the formation of the present profile:

Axis 1 links a kaolinitic pole (mottled zone and saprolite from lateritic profiles, fine matrix from stone-line profiles) with a ferruginous pole (cuirasse samples from lateritic profiles, nodules and pisoliths from stone-line profiles). All the samples lying along this axis may be considered to reflect the influence of a similar major weathering process, probably not a recent one, the main mineralogical effect of which has been the massive neoformation of kaolinite and Fe oxides.

Axes 2 and 3 mark the increase of Al_2O_3 contents observed when the different constituents of the former lateritic profile are submitted to more recent pedogenetic processes, under more humid climates.

Axis 4 is defined by samples from rather dry savanna environments (Burkina Faso) characterized by the presence of smectites, probably formed under recent morphoclimatic conditions (Mosser and Zeegers, 1988). This situation is discussed in Chapter III.1.

General dispersion characteristics and examples

In terms of dispersion models, the "lateritic" stone-line profiles must be considered as being the result of at least two distinct weathering episodes, namely formation of the laterite profile, presumably in a former humid savanna climate, followed by modification due to the recent change to a rainforest climate.

In the saprolite (Fig. III.2-28), which is less affected by the recent pedogenic processes, geochemical dispersion is not expected to be any greater than in A-type models from other areas having a lesser degree of recent alteration.

In the stone line itself (H2), the dispersion halo "mushrooms" strongly, probably under the combined effects of mechanical and hydromorphic processes

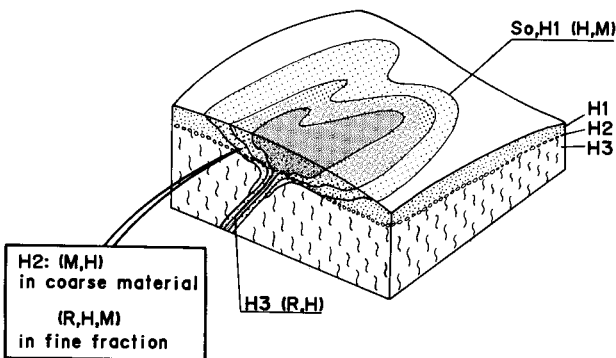


Fig. III.2-28. Diagram showing the dispersion model in regions with strong recent leaching. For abbreviations, see Fig. III.1-1.

(Lecomte, 1988). The coarse and fine size fractions give different geochemical responses. The coarse fraction mostly reflects the dispersion halo as it was in the pre-existing lateritic weathering profile, but with modifications that possibly include some mechanical transport. Accordingly, some elements, such as V, Cr, Cu, Mo, Ag, Cd, As and W, are more strongly retained, and even enriched, in the coarse ferruginous material than in the more strongly leached, less ferruginous clay matrix (see below, Mavikou).

The upper yellowish (H1) horizon is so strongly leached that some of the Fe oxides have been removed or transformed from hematite to goethite (Chatelin, 1968; Nahon, 1976; Bocquier et al., 1984); in addition, trace element contents are significantly depleted, by comparison with the saprolite (see Mebaga, p. 284). The geochemical response may thus be strongly subdued, not only for base metals but also for Au, which shows decreasing abundance and increasing crystal dissolution and corrosion in the upper part of the profile (see Dondo Mobi, p. 286). In addition, hydromorphic dispersion may result in marked homogenization in the H1 horizon (e.g. at Mebaga). The dispersion halo in the surface soil, at the top of the H1 horizon, is probably better developed and more widespread than in any other situation. However, the usefulness of such haloes for exploration may be strongly hampered by leaching, which can reduce metal abundances to close to analytical detection limits. The examples presented hereafter demonstrate that such leaching may vary markedly in intensity from place to place under apparently very similar conditions. It is probable that extreme situations might exist in which leaching almost totally cancels the geochemical response of even significant mineralization in depth.

Mavikou Cu-Au prospect, southwest Gabon (A 3 0 [1]). This prospect is hosted by Precambrian gneisses and amphibolites. Gold mineralization occurs both as alluvial deposits which have been exploited previously and as bedrock occurrences indicated by geochemical anomalies (BRGM, unpublished internal reports). Variations in the abundances of major and trace elements in a representative profile are shown in Fig. III.2-29. The data indicate:

(1) an increase in concentrations of elements such as Fe, Ni, V and Cr in the stone line (H2), probably related to the presence of Fe-rich lateritic material;

(2) decreasing concentrations of Al_2O_3 , K_2O and associated trace or minor elements (e.g. Ba) from the saprolite to the surface, reflecting the pronounced hydrolysis of K-minerals such as muscovite and feldspars in the upper two horizons of the weathering profile.

Despite these variations in concentration with depth, the distributions of major and trace elements shown by sampling the surface horizon (H1) have a reasonable relationship with the underlying lithology (Lecomte, 1988). Thus, the concentrations of V, Ni and Ba appear to be strictly controlled by the presence of amphibolites (V, Ni) or feldspathic gneisses (Ba) (Fig. III.2-30). The close relationship between the major and trace elements contents of bedrock and soils is also evident from comparisons of data over gneissic and amphibolitic base-

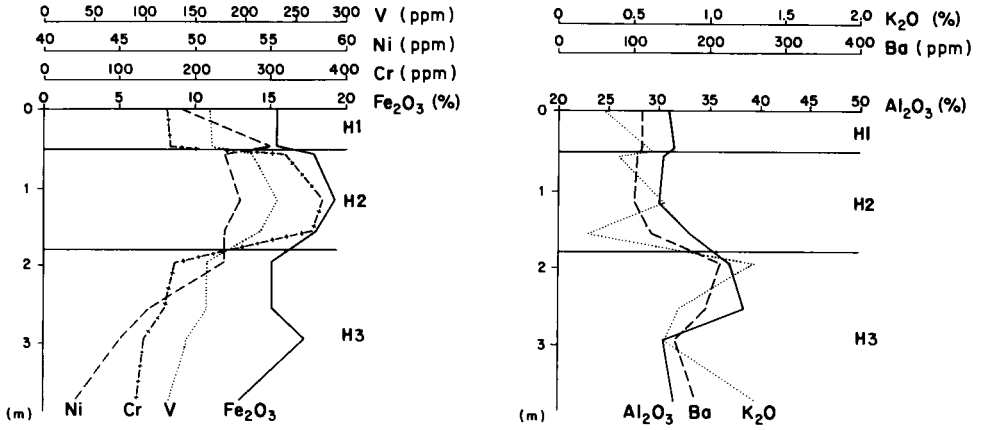


Fig. III.2-29. Mavikou prospect, Gabon. Vertical distribution of some major and trace elements in the weathering profile. H1, H2, H3: horizons, see text for explanation.

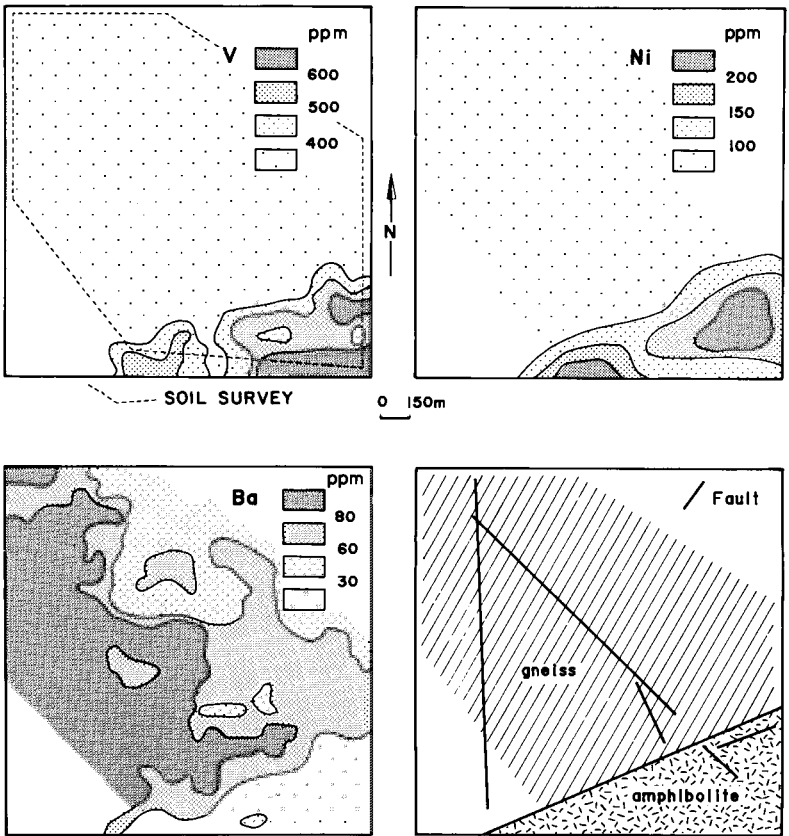


Fig. III.2-30. Mavikou prospect, Gabon. Distribution of V, Ni and Ba in soils; simplified geological sketch map.

TABLE III.2-12

Mavikou Au prospect, Gabon: comparison of mean contents of selected major and trace elements in soils from different geological environments

	Gneisses		Amphibolites	
	Soil N = 433	Bedrock N = 61	Soil N = 77	Bedrock N = 60
SiO ₂ %	63	77	49	46
Al ₂ O ₃ %	21	8	20	9
Fe ₂ O ₃ %	12	3	28	6
Cr ppm	250	260	750	1200
Ni ppm	35	30	160	500
V ppm	190	55	520	95
Ba ppm	100	580	25	320
Sr ppm	5	85	5	55

ment (Table III.2-12). Nevertheless, the bedrock geochemical signature is significantly modified in the soil; for example, Ba and Sr are strongly leached whereas Fe, V and Cr are enriched.

Soil sampling revealed a Cu-Au anomaly of high contrast, confirmed in the saprolite by auger drilling. Data from samples collected over mineralization from the different horizons are compared on Table III.2-13 with data from a nearby background area situated in a very similar geological and weathering environment. The anomalous natures of both Cu and Au are well expressed in each horizon of the weathering profile over mineralization. Interestingly, the Au anomaly in the fine fraction of the leached H1 horizon has a higher contrast than those of the deeper horizons or than the coarser fractions of the stone line, the latter being commonly enriched in V, Cr, Cu, Mo, Ag, Cd, As and W.

TABLE III.2-13

Mavikou Au prospect, Gabon: anomalous concentrations of Au and Cu in the different horizons and materials of the weathering profile, compared to a nearby background area (na: not analyzed)

Horizon	Material	Anomaly		Background	
		Au ppb	Cu ppm	Au ppb	Cu ppm
H1	Matrix	310	280	< 20	10
H2	Matrix	290	330	< 20	10
H2	Fe-rich nodules	70	410	< 20	20
H2	Lithorelics	20	160	< 20	5
H2	Al-aggregates	500	170	na	na
H3	Matrix	180	270	< 20	10

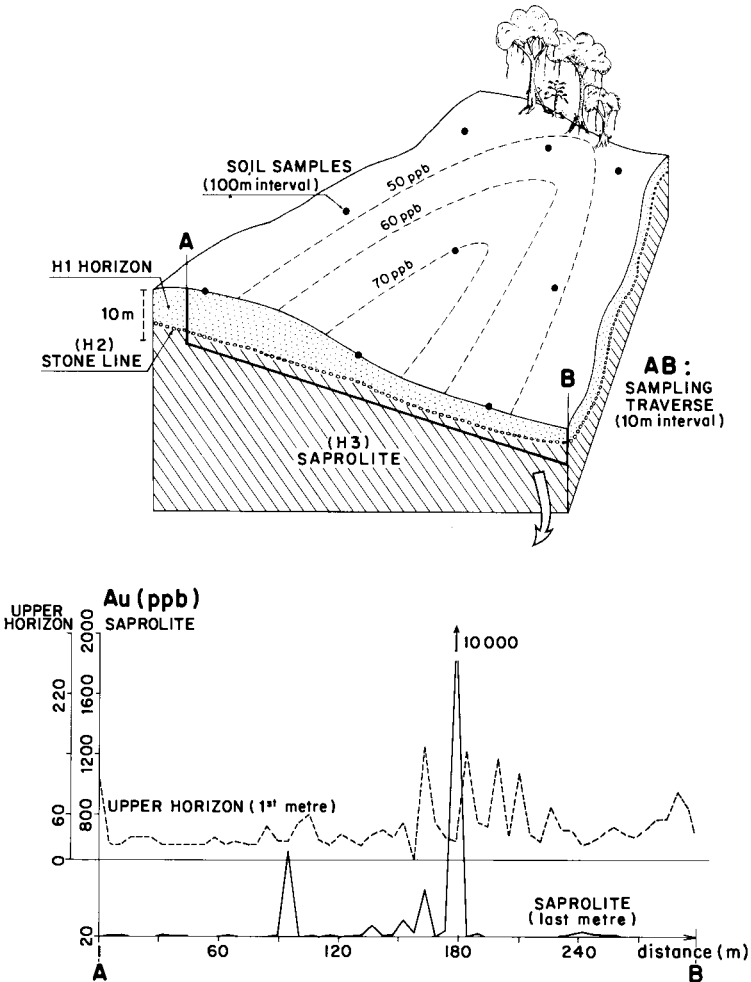


Fig. III.2-31. Mébaga prospect, Gabon. Soil Au anomaly and the location and results of auger sampling at the surface (H1 horizon) and in the saprolite (H3 horizon).

Mébaga Au prospect, Gabon (A 3 0 [1]). The Mébaga prospect is located within an Archaean greenstone belt, comprising volcano-sedimentary rocks, banded iron formations and minor pegmatitic intrusions. The stone-line horizon, some 2 m thick and overlain by 5 to 10 m of the friable, yellow H1 horizon, consists mainly of ferruginous nodules in a clay matrix. A soil geochemical survey, which followed-up regional drainage surveys (heavy minerals and stream sediment geochemistry), showed a distinct but poorly contrasted anomaly (maxima 40–80 ppb Au, Fig. III.2-31). This was investigated further by collecting saprolite samples by powered auger drilling, at 5 m intervals on sampling lines 100 to 200 m apart (BRGM, unpublished internal reports).

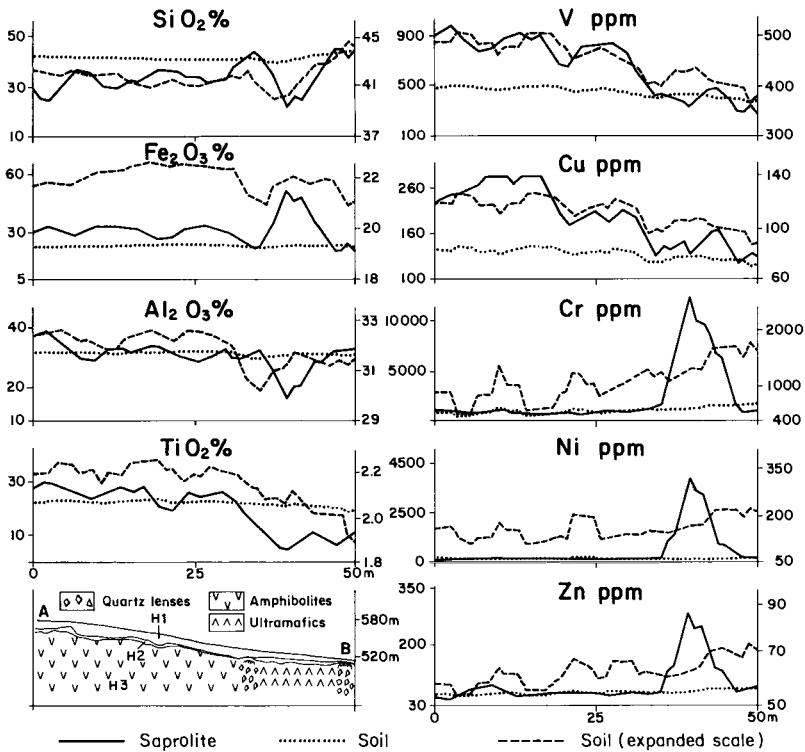


Fig. III.2-32. Mébaga prospect, Gabon. Distribution of selected major and trace elements contents in the H1 upper horizon and in the H3 (saprolite) horizon, along traverse AB (see Fig. III.2-31)

The data for SiO_2 , Fe_2O_3 , Al_2O_3 , TiO_2 , Cr, V, Ni, Cu and Zn in soil and saprolite samples along a traverse (AB on Fig. III.2-31) across the Au anomaly are shown in Fig. III.2-32. In the saprolite, well-defined enrichments of several elements (such as Cr and Ni) indicate that little homogenization or dispersion has occurred. Three main lithologies can be distinguished: amphibolites having $> 3\%$ TiO_2 and elevated Cu and V contents; ultramafics containing > 2000 ppm Cr or Ni, and quartz-feldspar lenses with high SiO_2 contents (Lecomte, 1988; Colin and Lecomte, 1988). In contrast, the geochemical response in the soils, displayed on the same concentration scale, is considerably smoothed for all elements, so that most geochemical contrasts evident in the saprolite disappear. This is discouraging for the application of surface geochemical sampling in such environments, but by replotting data on a more suitable concentration scale, subtle but significant variations appear for several elements (e.g. SiO_2 , Al_2O_3 , TiO_2 , Fe_2O_3 , V and Cu) in fair agreement with the saprolite data. However, the geochemical response of Ni, Zn and, to some extent, Cr is lost. Chromium concentrations are far lower in soil samples (Table III.2-14) and the peak values, which correspond to the ultramafic rocks, are slightly displaced downslope,

TABLE III.2-14

Mébaga Au prospect, Gabon: comparison of the mean concentrations of selected major and trace elements in soil and saprolite (auger hole samples)

	Saprolite	Soil	Difference %
SiO ₂ %	35	42	+20
Al ₂ O ₃ %	31	32	+3
Fe ₂ O ₃ %	30	23	-23
TiO ₂ %	1.9	2.2	+16
Cr ppm	2200	1100	-50
Ni ppm	490	150	-70
V ppm	660	460	-30
Cu ppm	200	110	-45
Zn ppm	85	65	-23

making it difficult to use soil Cr data for the accurate location of specific ultramafic units. The lower Cr concentrations may be due in part to leaching of Cr-bearing phases less resistant to weathering than chromite, and in part to dilution. These data demonstrate both the residual character of the deeply weathered stone-line profile, and the high degree of alteration by leaching to which they are subjected. Some elements cannot resist such leaching, and thus become unsuitable for geochemical exploration purposes.

The behaviour of Au in the different surface sample media at Mébaga is shown on Fig. III.2-31. The very weak soil anomaly detected on a 100 × 100 m grid corresponds to two narrow mineralized zones containing several g/t Au in the saprolite. Even by soil sampling at very close intervals (5 m) the maximum Au contents do not exceed 150 ppb. Indeed, reducing the sample interval from 100 m to 5 m does not seem to define the location of Au mineralization more precisely. It is probable that homogenization of the Au contents in the H1 horizon is such that sampling intervals closer than 100 m are meaningless (Colin and Lecomte, 1988). Consequently, soil anomalies are best checked by saprolite sampling rather than by more detailed soil sampling.

Dondo Mobi Au prospect, Gabon (A 30 [1]). A soil survey centred on old alluvial gold workings revealed an anomaly, about 700 m long, having 200 to 1000 ppb Au (Fig. III.2-33). The anomaly was confirmed by auger drilling to collect saprolite samples. Basement gold mineralization was subsequently discovered by diamond drilling, at depths of 30–120 m. Thus, despite the intense near-surface leaching, bedrock Au mineralization is clearly reflected in the soils. The weathering profile is similar to that at Mébaga, with a well-developed lateritic stone line. The dispersion of gold from the bedrock to surficial soil, shown in Fig. III.2-34, is as follows (Lecomte and Colin, 1989):

(1) In the bedrock, most of the gold is present in scattered quartz lenses within amphibolites, over a total width of some 50 m.

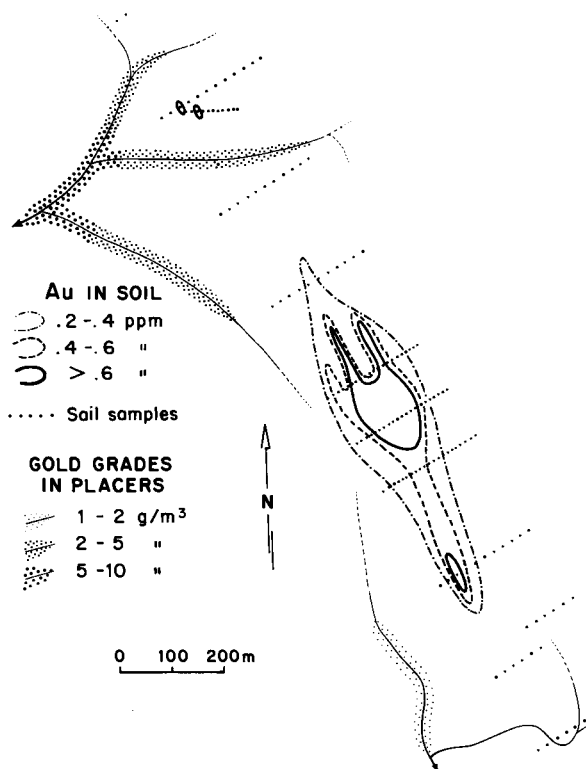


Fig. III.2-33. Dondo Mobi prospect, Gabon. Gold soil anomaly and gold grades in previously worked placers.

(2) In the saprolite, there is no evidence for a significant enlargement of the mineralized zone. Anomalous gold values in the saprolite are also observed over a width of 50 m, without any significant leaching, enrichment or lateral dispersion.

(3) In the stone line (H2) and friable yellow sandy clay (H1) horizons, in contrast, the Au dispersion halo is significantly enlarged but the Au concentrations decrease. The dispersion halo at the top of H1 horizon has a width of about 220 m defined by the 150 ppb contour, 100 m at 500 ppb and 50 m at 1000 ppb.

Gold grains from different horizons of the weathering profile have been studied by SEM (Colin and Lecomte, 1986; Colin et al., 1989). The grains show an increasing degree of dissolution and corrosion from the base to the top of the profile (Fig. III.2-35). In the saprolite (Fig. III.2-35-2), the morphology of the grains is very similar to that observed in the bedrock mineralization (Fig. III.2-35-1) with fairly well-preserved crystalline forms. Above the base of stone-line horizon, some corrosion and dissolution is observed, particularly on crystal edges (Fig. III.2-35-3) and faces (Fig. III.2-35-4). In the upper yellow horizon

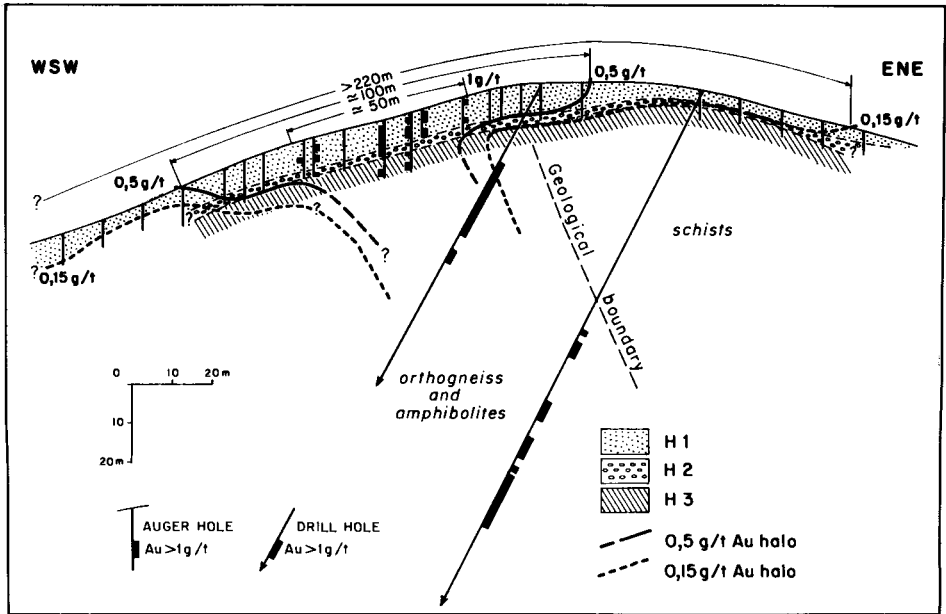


Fig. III.2-34. Dondo Mobi prospect, Gabon. Mushroom-like Au dispersion in the weathering profile; H1, H2, H3: horizons, see text for explanation.

(H1), the crystalline forms can no longer be recognized, due to a higher degree of degradation of the gold grains (Fig. III.2-35–5,6). These results, which should be compared with those from savanna (Banankoro, Mali, Fig. III.1-13) and semiarid environments (Bardoc, Western Australia, Fig. III.3-9), are discussed further in Chapter V.3.

Ity Au deposit, Ivory Coast (A 3 0 [1]). The mushroom-like dispersion halo of Au described by Granier et al. (1963) at Ity (Fig. III.2-36) is developed in a lateritic stone-line profile. The saprolite is some 70 m thick and the stone-line horizon includes a high proportion of lateritic material. Here again, dispersion is not very extensive in the saprolite, but increases in the H2 horizon and, particularly, the upper H1 horizon, with some displacement downslope.

B-type models: pre-existing profiles partly truncated. "Quartz" stone-line profiles

Environment, geomorphology and profile description

These models become increasingly common (i) lower in the landscape (Fig. III.2-24), and thus further from the former landsurfaces, and (ii) on a regional scale, where recent block faulting and uplift have resulted in rejuvenation of the drainage and the complete removal of any weathering palaeosurface. Conse-

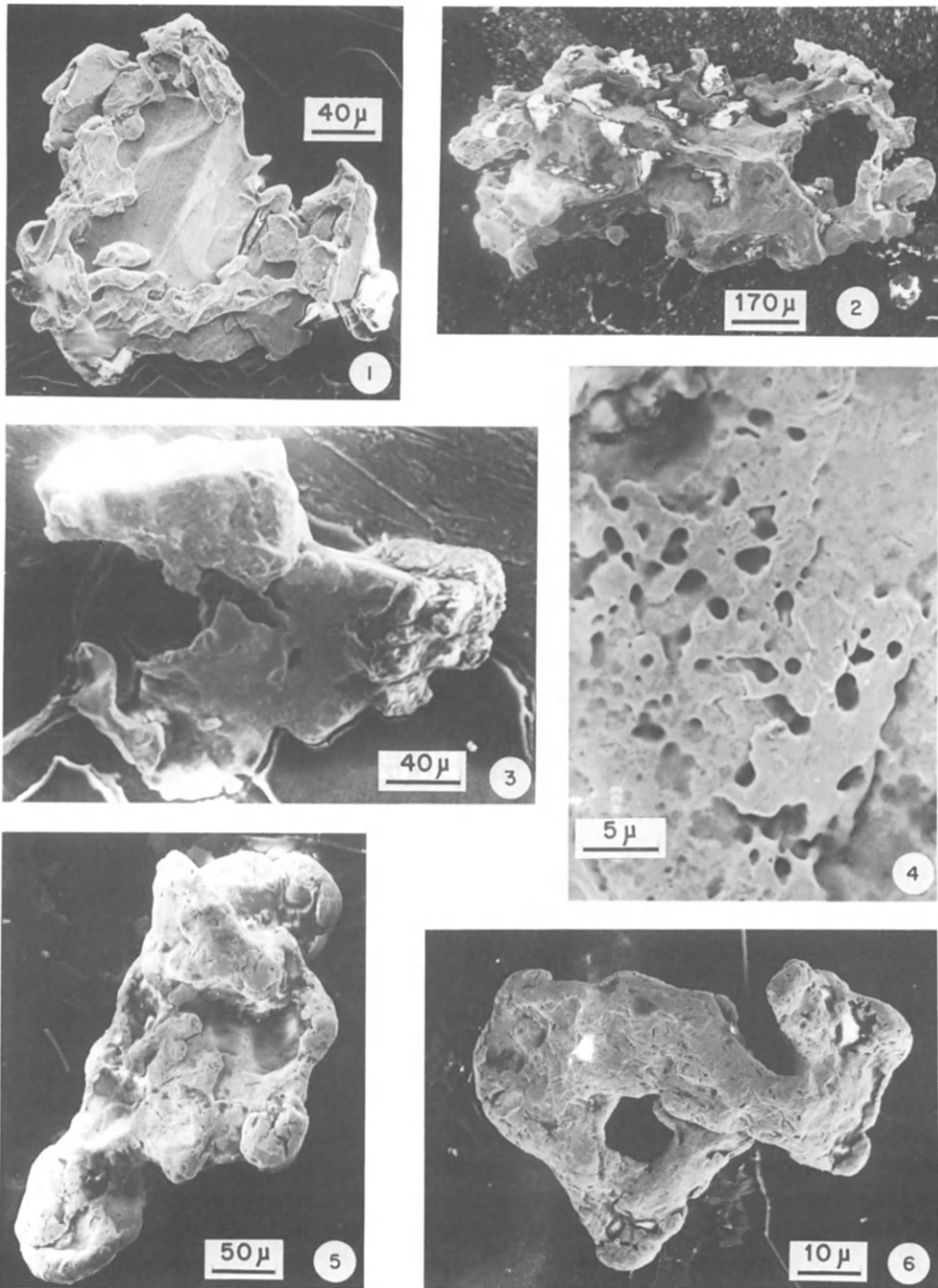


Fig. III.2-35. Dondo Mobi prospect, Gabon. Morphological evolution of gold particles in the weathering profile.

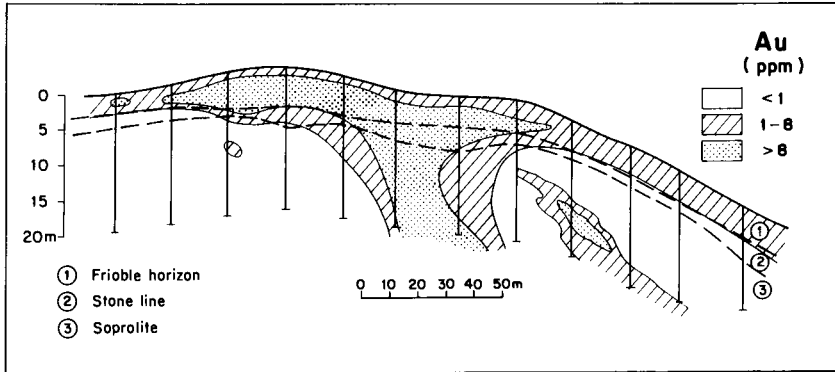


Fig. III.2-36. Ity prospect, Ivory Coast. Mushroom-like Au dispersion in the weathering profile. Modified after Granier et al. (1963).

quently, the stone-line horizon (H2) mostly contains quartz fragments and has almost no lateritic material such as nodules, pisoliths and cuirasse blocks. Near the drainage axes, the stone line may also eventually include alluvial gravel and cobbles (Collinet, 1969). The total thickness of the soil profile is less than for the A3 models: the H1 horizon (friable yellow sandy clay) is usually between 1 and 4 m thick and the H2 horizon (stone line) rarely exceeds 0.5 m.

General dispersion characteristics and examples

The mineralogy of the truncated profiles of the B3 [*] models is broadly similar to the equivalent complete profiles. The main differences are a lower proportion of Fe oxides, because of the almost complete absence of lateritic remnants, and a less complete development of the profile. Accordingly, geochemical dispersion is less pronounced, with respect both to the degree of leaching and to the extent of the dispersion haloes, as shown by the examples that follow. In these situations, most elements, including Au, are only slightly affected by surficial leaching. As a result, even minor mineralization may be detected by regional geochemical surveys. The depletion factor between soil and saprolite samples is not high and the size of the secondary dispersion halo is little larger than the primary mineralization. Thus, in comparison with the A3 dispersion models, the surface geochemical expression shows a stronger contrast but the dispersion halo is significantly smaller. Indeed, it is not always possible to distinguish between the B3 and B1-B2 models based only on geochemical characteristics. The greater degree of evolution of the profile is indicated by the presence of the stone line and by some subtle differences in mineralogy, such as the lower abundance of Fe oxide minerals and the occurrence of some resistant primary silicates (e.g. sericite).

TABLE III.2-15

Mokékou prospect, Gabon: mean contents of selected major and trace elements of the upper yellow friable soil (H1), stone line (H2) and saprolite (H3)

Horizon	SiO ₂ %	Al ₂ O ₃ %	Fe ₂ O ₃ %	K ₂ O %	Ba ppm	Sr ppm	Cr ppm	Cu ppm
H1 (N = 41)	57	26	8	4.2	720	55	170	65
H2 (N = 31)	54	26	11	4.6	750	60	200	85
H3 (N = 28)	51	29	10	6.9	1100	80	200	100

Mokékou base metal prospect, central Gabon (B 3 0 [1]). This was discovered by a regional stream sediment geochemical survey (BRGM, unpublished reports). Several Cu-Pb-Zn-Ag anomalies were found, mostly derived from black shales containing uneconomic, disseminated polymetallic sulphide mineralization. The weathering profile in the area is rather shallow, having

- (1) the yellow, friable sandy clay horizon (H1), 1–2 m thick,
- (2) a red ochre quartz stone line (H2), 0.5 to 1 m thick and,
- (3) the saprolite, in which the black shales may be recognized.

Some of the multielement geochemical anomalies were followed up by soil and auger surveys, with samples collected in the surficial soil and in the different horizons of the profile. The mean concentrations of several major and trace elements in the three principal horizons are listed in Table III.2-15. The abundances of most elements, with exception of SiO₂, decline from the saprolite to the soil. However, this surface leaching is not very strong and concentrations in the soils are generally at least 60% of those in the saprolite. Significantly, and unlike the lateritic A3 models, there is no enrichment of Fe₂O₃ in the stone line. The K₂O–SiO₂ diagram (Fig. III.2-37) illustrates the same surficial leaching process, with the samples from the H1 (upper friable sandy clay) and H2 (stone line) horizons having the higher SiO₂ and the lower K₂O contents. Nevertheless, the K₂O contents (3–5%) of the two upper horizons are rather high, suggesting that some primary rock-forming silicates have been preserved.

Mikongo Au prospect, Gabon (B 3 0 [1]). This prospect was discovered following a regional stream sediment and heavy minerals survey (BRGM, unpublished reports); a low contrast Au soil anomaly was followed up by auger sampling. Soil samples were collected at 30 cm depth, on a 100 × 100 or 100 × 200 m grid. Saprolite samples were collected at about 3 m depth, every 20 m along traverses 100 m apart. The soil profile is similar to that at Mokékou.

A summary of the results of the soil and saprolite sampling is presented in Fig. III.2-38. The soil Au anomaly has several values ranging between 25 and 210 ppb, with the three highest showing a possible NE–SW trend. In the saprolite, only a low grade Au anomaly was found, with a maximum value of 480 ppb Au and no clear orientation. Thus, a weak Au anomaly in soils was

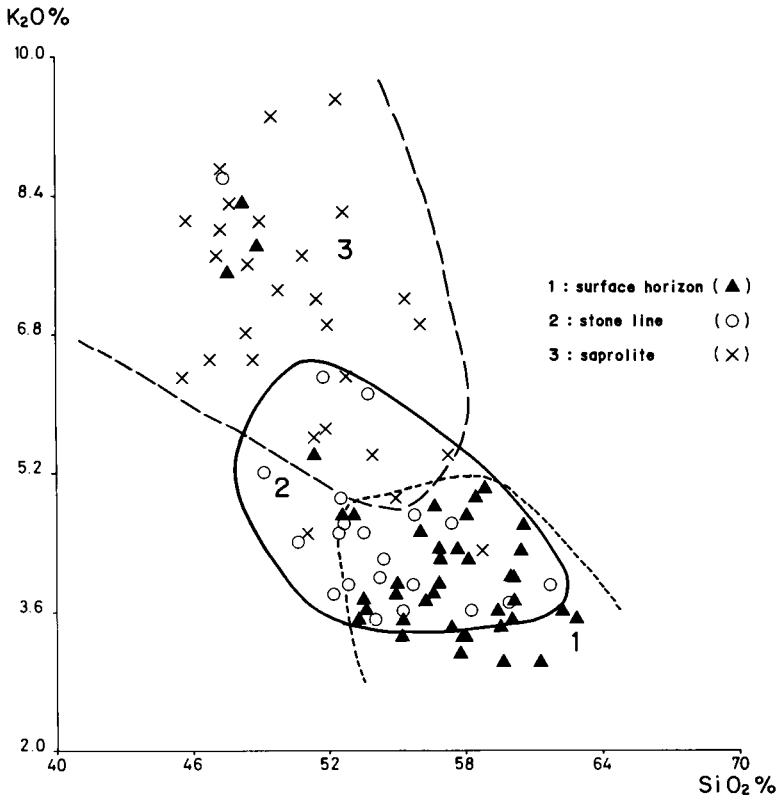


Fig. III.2-37. Mokékou area, Gabon. K₂O-SiO₂ diagram for samples collected in the different horizons of the weathering profile.

proved to correspond to equally uninteresting mineralization at depth. These results suggest that in truncated environments (B models), the significance of a surface geochemical anomaly may be more reliably assessed by such quantitative reasoning than where the profile is complete and more evolved (A models).

CONCLUSIONS

Under humid tropical climates, geochemical dispersion processes are dominated by the interaction of past and recent climates. The high rainfall induces severe leaching of the different horizons of the weathering profile, but the maximum intensity of such leaching is only achieved when imposed on already weathered material. The "stone-line" weathering profiles and, more especially, the A 3 0 [1] type (that is where the pre-existing lateritic profile is mostly preserved, but subjected to strong recent alteration) are some of the most strongly leached surface environments. Even under these extreme weathering

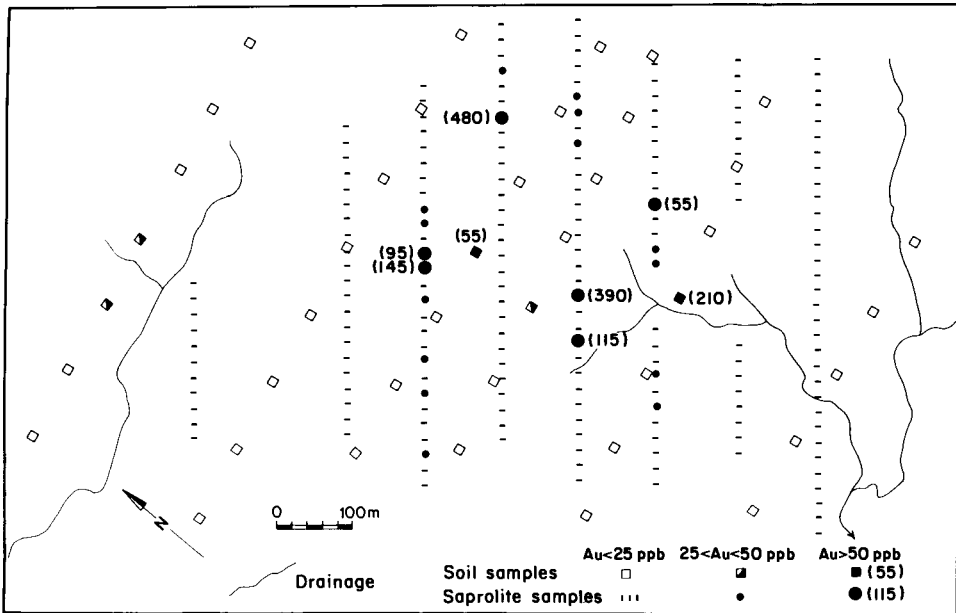


Fig. III.2-38. Mikongo area, Gabon. Gold distribution in soil and saprolite samples.

conditions, however, the geochemical signature of the bedrock or of primary mineralization is preserved in the surface horizons from which routine geochemical samples are normally collected. Nevertheless, the data from Mébaga (see p. 284) show that the geochemical response is very subdued, and may therefore be missed if unsuitable analytical or sampling techniques are used. The persistence of such weak but significant geochemical responses in deeply weathered environments is valid for several elements, including Au. Conversely in truncated profiles, even where the climate has resulted in the formation of stone lines, surface leaching is far less pronounced for most of the key elements used in exploration geochemistry, and the size of the geochemical dispersion haloes is reduced.

Where the A 1 0 [1] model prevails (pre-existing lateritic profile mostly preserved, recent alteration moderate), the dispersion models are very similar to those observed under seasonal humid climates (savanna environments) as described Chapter III.1.

The humid tropical (or rainforest) environments are thus characterized by very deep weathering, but the use of geochemical exploration techniques is not greatly hampered by such apparently adverse factors. If any given morphoclimatic environment is well understood by the exploration geochemist, and if it is recognized that the soils formed under these extreme conditions are, for the most part, residual, geochemical techniques may be as successful here as anywhere else.

The quality of the geochemical response that is obtained strictly depends on the horizon which is sampled. The poorest responses are obtained in the surficial, more or less humic soil horizons. These are commonly strongly leached and, furthermore, relative enrichment of quartz causes dilution of other minerals, including those supporting the geochemical information. Conversely, if saprolite is sampled, strongly contrasting and highly descriptive geochemical responses are obtained, commonly providing detailed information of the lithology, the mineralization itself or any associated primary halo or hydrothermal alteration. Nevertheless, the use of saprolite as a sampling medium is restricted because of the close sampling intervals that are required in the absence of significant secondary dispersion.

In summary, in these environments where the thick weathering profile and the forest cover severely hamper direct prospecting and geological mapping, geochemical prospecting, if tuned to suit these specific environments, is one of the most effective and reliable techniques of mineral exploration.

SEMIARID AND ARID TERRAINS

C.R.M. BUTT

THE WARM ARID ZONE

Definition and distribution

The semiarid to arid regions considered in this and the next chapter are the trade wind deserts of the tropics and subtropics. These are depicted as BSh (semiarid or steppe) and BWh (arid or desert) climates in the Köppen classification (Table I.1-1 and Fig. I.1-1), and for the most part comprise the warm arid zone in Budel's morphoclimatic map (Fig. I.1-2). They occur along the continental west coasts and interiors, centred about the latitudes of the Tropics of Cancer and Capricorn. The largest area of aridity is that of North Africa and Asia, consisting of the Sahara and Arabian deserts, extending through southern Iran to the west and centre of the Indian subcontinent. Smaller but still very extensive arid zones are those of Australia, southern Africa (Namibian and Kalahari deserts), North America (Mexico and southwestern USA) and South America (Atacama desert, and the caatinga of northeast Brazil). These are areas having a mean annual rainfall of less than 600 mm, the isohyet that most closely corresponds to the pedological boundary between leached soils (pedalfers) and those in which carbonate is retained (pedocals) (Young, 1976). They thus range from semiarid areas that have a more or less reliable, though seasonal, rainfall to the inner deserts that may have no measurable rain for decades. In each case, the warm arid zones are marginal to the humid seasonal tropics (savannas) in the lower latitudes and to humid subtropical or temperate regions, mostly having seasonal (Mediterranean) climates, in higher latitudes.

Evidence for widespread humid tropical conditions in the past is found in the landforms and regoliths of the warm arid zone. Their geochemical characteristics, therefore, are due to weathering under such conditions, modified by the processes of the arid environment. The link to past humid, tropical conditions is tenuous or absent in the winter cold deserts that occur principally in Central Asia and North America. Consequently, such deserts are not specifically considered, although the dispersion processes associated with these arid conditions are similar.

The influence of past humid tropical climates on the landforms and regoliths of present day arid zones is particularly important where the relief is low.

Broadly, these are arid zones on the shields and platforms comprising the Gondwanaland fragment of Africa, South America, Arabia, Australia and India, although small areas with similar characteristics are present in more mountainous areas. The shields have had broadly similar climatic and geomorphological histories and their tectonic stability has preserved old landforms and weathering products. Extensive planation occurred under savanna climates until the early to mid Tertiary and was followed by stripping of weathered zones from higher ground and sedimentation on lower ground under the predominantly arid climates that continue to the present (Mabbutt, 1977).

Ancient landforms and regoliths are less common in arid areas of high relief, because of the greater degree of stripping and erosion. Such areas correspond to the basin and range deserts of tectonically active regions, such as the Pacific mountain belt of the Americas, but also include mountainous and deeply dissected regions of the shields.

The semiarid to arid regions of low to moderate relief and landform preservation, predominantly in the shields and platforms, are discussed in this chapter. The regions of moderate to high relief are discussed in Chapter IV.1.

Geomorphological history of warm arid regions of low relief

Many of the geomorphological features of the warm arid regions have been inherited from pre-Pleistocene tropical periods. They consist of broad etchplains, mostly of low relief, which, depending upon the degree of stripping may (i) retain much of the mantle of deep weathering at the surface or buried beneath later deposits, or (ii) be reduced to an etch surface, being essentially the weathering front beneath the pre-existing profile, with a thin veneer of surficial sediments. In the former case, the geochemical characteristics of the earlier humid period have considerable significance, whereas in the latter, only those pertaining to later periods have importance.

The influence of deep tropical weathering is probably greatest in the Australian arid zone. Parts of Australia have been continuously subaerial since at least the Permian (Ollier, 1978) and locally perhaps since the late Proterozoic; elsewhere epeirogenic subsidence allowed marine sedimentation in the Mesozoic and Tertiary, with subaerial weathering during intervening periods of uplift. Broadly, climates tended to be temperate to warm in the Mesozoic–early Tertiary and humid tropical in the Oligocene–Miocene, with a subsequent trend to aridity extending from the centre of the continent. The long periods of humid weathering conditions and tectonic stability led to the development of a deep kaolinitic and lateritic regolith which has been largely preserved, despite some erosion during the continuing arid periods (Mabbutt, 1980). The resultant landscape has a low altitude and, generally, a low relief. Relict profiles, either complete or partly truncated, are widespread. They may form the present surface, commonly preserved by indurated upper horizons (ferruginous, siliceous or calcareous), or be overlain by a variety of aeolian, colluvial or alluvial deposits—commonly

erosion products of the weathered mantle. This landscape has many of the characteristics illustrated in Fig. I.1-3.

In North Africa, a deeply weathered relict mantle is widespread on the dry margins of the savannas and semiarid Sahel, becoming discontinuous and fragmentary in the Sahara itself. The age of the mantle varies; in the savannas, active deep weathering or reweathering may have occurred during pluvial periods in the Quaternary. Further north, it is clearly older, protected by Miocene basalts in the Hoggar (Budel, 1982) and Cretaceous sandstones in the Red Sea Hills (Fletcher, 1985), although here weathering through the sandstones may be responsible for the "buried" profile. There is overwhelming evidence for pre-Pleistocene tropical deep weathering extending from Africa to northern Europe (Thomas, 1974) and this is considered to have had a major influence on the development of Saharan and Arabian desert landscapes. A marked change in climate occurred in the late Tertiary, coincident with the development of the polar ice sheets and the onset of glaciation. There was a succession of pluvial and interpluvial periods during the Quaternary; sometimes arid conditions extended south to the present savanna-rainforest transition and, at other times, humid conditions affected the present desert core. In the latter areas, extreme erosion has left only traces of the old regolith, although the material of which it was composed has probably contributed to the extensive fluvio-aeolian sandplains. An inselberg-studded etch surface may now be the only evidence of humid, deep weathering, although further exploration and drilling may reveal weathered material beneath the sedimentary veneer.

The Arabian deserts have a similar geomorphological history. Deep tropical weathering prior to the mid-Tertiary caused considerable planation of the Precambrian basement; remnants of the regolith are preserved as fossil laterites in and beneath Mesozoic cover rocks, especially to the north and east of the Arabian Shield (Overstreet et al., 1977; Harvey, 1985). More recent weathering, to depths of 10–50 m, is also present, particularly in soft, porous or sheared rocks in which the oxidation of pyrite has resulted in acidic groundwaters. Resistant rocks remain virtually unaltered, however, with fresh sulphides preserved close to the surface (Harvey, 1985).

In general, the influence of past deep weathering on geochemical dispersion diminishes from the margins to the core of the Sahara-Arabian desert, and the processes of Quaternary aridity—such as aeolian and fluvial erosion, carbonate precipitation—become dominant. Similarly, in the Indian subcontinent, the influence of past deep weathering on the geomorphology and geochemistry of the semiarid terrains in the peninsula become subordinate to the influence of the extreme aridity of the Thar desert in the northwest. However, prominent gossans on the eastern margin of the desert are probably relicts of earlier deep weathering (Hore and Harpavat, 1980).

The Kalahari and Namib deserts of southern Africa generally show little evidence of pre-Quaternary tropical weathering, except on the margins. There had been extensive deep weathering and planation before the early Tertiary and

downwarping resulted in the deposition of over 200 m of aeolian, fluvial and lacustrine sediments (the Kalahari Beds) over much of the area in the late Tertiary and Quaternary (Grove, 1969; Cooke, 1981). Within these sediments, thick silcretes and calcretes developed (Goudie, 1973). The Kalahari, like the Sahara, was subjected to both more arid and more humid phases in the Quaternary than prevail at present. Windblown Kalahari sands became widely distributed during arid periods and buried pre-existing deeply weathered profiles in surrounding areas. To the north, in the Copperbelt of western Zambia, aeolian sands more than 30 m thick overlie weathered bedrock and are themselves being reweathered under the present savanna humid climate (Brown, 1970). To the south, present arid soils are composed of a mixture of aeolian Kalahari sands and residual saprolite. Elsewhere in arid and semiarid regions of southern Africa, where Kalahari sediments are absent, deep weathering profiles developed in the Tertiary and humid phases in the Quaternary are preserved, commonly partly truncated.

In the Americas, relict deep weathering, probably Quaternary, is recognized in semiarid northeast Brazil (de Oliveira, 1983). However, most of the warm arid regions, e.g. the Atacama desert, northern Mexico and southwestern USA, have been subjected to tectonic and volcanic activity in the Quaternary, mostly under arid climates. Relicts of earlier, humid weathering episodes are few because of the ensuing erosion, although important supergene enrichments of Cu are associated with them. In the Atacama desert in Chile, supergene enrichment in deeply weathered regoliths has occurred either during deep weathering in the mid-Tertiary (Segerstrom, 1963) or during subsequent arid periods of dissection and lowered water-tables (Clark et al., 1967).

Weathering and sedimentary deposits

Most arid shield areas have extensive tracts of sedimentary terrain. Much of this consists of aeolian, colluvial, alluvial, lacustrine and evaporitic sediments derived from the erosion and incomplete removal of a pre-existing regolith, and the accumulation of soluble salts derived from continuing weathering and rainfall. Some sediments may predate deep weathering or be contemporaneous with it, so that several stratigraphic sequences are possible:

(1) Sedimentation predates weathering, so that weathering proceeds through the cover rocks, particularly sandstones, to the basement. Ferruginization along the unconformity may appear "lateritic", but the complete profile actually incorporates both units. For example, on the Yilgarn Block, Western Australia, weathered Archaean rocks are known beneath Permian glacial deposits and > 100 m of Proterozoic sandstones; weathering beneath the Nubian Sandstone in Sudan may have a similar explanation (see Um Nabardi, p. 343).

(2) Sedimentation occurred during deep weathering, so that upper horizons are developed in transported material and lower horizons in residuum. The lateritic ferruginous horizon may be enriched with iron leached from upland

areas in the catchment, possibly leading to additional cementation, resistance to erosion and topographic inversion.

(3) Sedimentation occurred during phases of deep weathering, so that both overburden and residuum have essentially complete profiles within them. This situation may occur at Mount Keith, Western Australia (see p. 324).

(4) Sedimentation has occurred in arid periods after deep weathering; buried profiles may be complete or partially or wholly truncated. This situation is the most common, with sediments ranging in thickness from a thin veneer to a hundred metres or more. Erosion of uplands and gradual filling of valleys contribute to the flatness of many arid terrains.

The later sedimentary sequences commonly preserve evidence of Cainozoic climatic fluctuations—for example, former shorelines of Lake Chad and of the Kalahari. Similarly, ancient river systems, dating from the Tertiary or before, and intermittently active in the Quaternary, are known in the Sahara, Kalahari and Thar deserts and in Australia. Such palaeochannels have economic importance not only as potential sources of water but as sites for lignite, clays, evaporite minerals, uranium and placer deposits.

CHARACTERISTICS OF THE WEATHERING PROFILE

C.R.M. Butt and R.E. Smith

Mineralogy and geochemistry

The principal chemical and mineralogical characteristics of deeply weathered profiles in arid terrains are similar to those described for equivalent complete and partially truncated profiles in other climates (see Chapters I.3, I.4, III.1 and III.2). Thus, the mineralogy of lateritic profiles in semiarid Western Australia, illustrated schematically for several lithologies in Fig. III.3-1, is broadly similar to those in humid environments. Saprolites are dominantly kaolinitic, passing upwards into mottled and ferruginous zones composed principally of goethite and/or hematite. Gibbsite is only a minor component, with most Al occurring in residual kaolinite or, to a lesser extent, in Al-goethite and Al-hematite. These profiles are undoubtedly continuing to develop by on-going weathering at the base, but the slow throughput of water ensures that the rate of weathering is also slow. Indeed, rather than being leached, some elements are retained in smectites (e.g. Ca, Mg) as in dry savanna environments, or concentrated by evaporation and reprecipitation in the profile or toposequence, e.g. as silcrete (Si) and calcrete (Ca, Mg). In general, many features due to the arid climate simply modify the profiles that developed under previous humid climates. The modifications are due to the combined effects of a reduction in the biomass (see Table I.1-2), lowering of the water-table and changes in the hydrology and geochemistry of the groundwater. The effects are summarized in Table III.3-1. The profiles thus have mineralogical and geochemical characteristics of earlier lat-

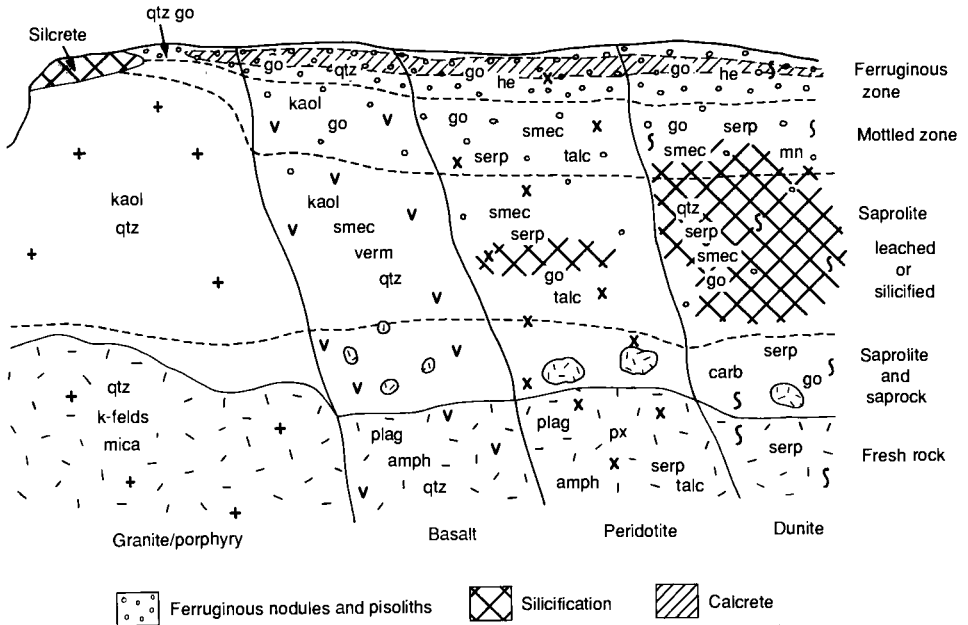


Fig. III.3-1. Typical zonation and mineralogy of complete lateritic weathering profiles in arid terrains (qtz = quartz; K-felds = K-feldspar; plag = plagioclase; amph = amphibole; serp = lizardite, antigorite; px = pyroxene; carb = calcite, dolomite; kaol = kaolin minerals; smec = smectites; verm = vermiculite; go = goethite; he = hematite; mn = manganese oxides).

eritic deep weathering and of the present evaporitic, commonly alkaline environment. Precipitation of Fe oxyhydroxides may also have occurred at intervals during the modification of the lateritic residuum, especially at water-tables, redox interfaces and porosity boundaries.

The change to an arid climate leads to a reduction in the density of vegetation, which in turn results in instability of the land surface and increased erosion. However, this may be offset, at least in part, by lowering of the water-table and irreversible dehydration and hardening of the lateritic ferruginous horizon to form an armouring cuirasse. The reduction in biomass also decreases the significance of organic matter in weathering and geochemical dispersion. Lower rainfall and higher evaporation greatly reduce the water flux, so that elements released by continued weathering or added by rainfall concentrate in the groundwater. Many of the modifications of the profile due to the change to aridity are therefore expressed as *additions* of chemical components, principally silica, aluminosilicates, carbonates, sulphates and halides. Accordingly, chemical modification of the ferruginous zone is possibly less intensive in semiarid and arid areas than in very humid climates. Nevertheless, post-lateritic hydromorphic action may have caused additional leaching of base metals and Au from the top metre or so where the ferruginous horizon is exposed. In contrast, saprolites may

TABLE III.3-1

Some effects of increasing aridity on a lateritic weathering profile

Reduction in biomass

Reduction in soil organic matter.

Increase in runoff and erosion by sheetwash.

Lowering of the water-table

Leaching of vadose zone under oxidizing and saline conditions.

Dehydration and irreversible hardening to form duricrusts,
e.g. ferruginous cuirasse, pedogenic silcrete.*Cementation by introduced components**Humid*

Iron oxides	Acid	Cuirasse.
Silica	Acid	Pedogenic silcrete (with TiO ₂).
Aluminosilicates	Acid-neutral	Hardpans; cemented saprolite.
Silica	Neutral-alkaline	Red-brown hardpans; groundwater silcrete.
Carbonates, sulphates.	Alkaline	Calcretes, gypcretes.
Halides, nitrates etc.	Alkaline, hyper- alkaline	Evaporites.

Arid

be more strongly leached due to progressive lowering of the water-table and an increase in the salinity of the groundwater. The mobilities of Mo, As and U are greater in the now more generally prevailing alkaline environments, whereas Au and some PGE are mobile only where saline groundwaters become acid and highly oxidizing (Mann, 1984a).

The addition of major, usually cementing, constituents such as silica and Ca-Mg carbonates may result only in the dilution of components already present; this is evident for Ni in silicified saprolite over dunites, and for base metals in calcretes. Conversely, enrichments may occur of elements mobile under the same conditions as these cements. Thus, silcretes (silicified saprolite) over dunite may be enriched in Cr and pedogenic silcretes formed in very acid environments over granitoids and sandstones are characteristically enriched in Ti, as secondary anatase, and Zr, as residual zircon. Enrichments of Au, U and V, in pedogenic and groundwater calcretes are discussed later in the chapter. Despite such changes, the profiles have many of the geochemical characteristics of equivalent profiles in the humid tropics, especially the savannas, and may be almost indistinguishable from them.

General features of geochemical dispersion

Continuing or intermittent episodes of leaching, hydromorphic dispersion and secondary concentration are fundamental to the long evolutionary history of the

lateritic regolith. Some of the most profound alterations, such as kaolinization and pisolith and cuirasse formation, are the products of humid, lateritic weathering. These are largely unaffected by the new chemical environments imposed by climatic change and, accordingly, their mineralogical and geochemical signatures are retained. Thus, many aspects of the geochemical expression of primary mineralization, and the development of secondary mineralization, are much the same in all lateritic terrains. The similarities are illustrated in Figs. I.1-6 and I.1-7. Conversely, some features are specific to lateritic regoliths that have been modified under arid conditions, and these are of particular concern in this chapter. The similarities and differences of concern to geochemical exploration are expressed in the model codes.

Oxidation of primary mineralization is an integral part of lateritic weathering and, over sulphide bodies, results in the formation of gossans. These seem to be best developed in arid environments, with a profile having a strongly leached oxide zone overlying sulphate, carbonate and supergene zones. The formation of gossans and their evaluation during exploration are discussed in detail in Chapters II.1 and II.2. Hydromorphic dispersion haloes of elements such as As, Sb, Cu, Pb, Mo and Zn, leached during sulphide oxidation, are best developed in the ferruginous lateritic horizon (e.g. Golden Grove, Western Australia, see p. 310), probably due to coprecipitation with relatively stable Fe oxyhydroxides. Dispersion haloes into transported overburden and into saprolite are possible, but few have been documented even for Au, perhaps because of the paucity of relevant case histories. They are known for sites in which the profile has been partly truncated (e.g. Elura, see p.340, Teutonic Bore, see p. 336 and Dalgara, see p. 357).

Primary haloes around mineralization are important in enlarging the exploration target. However, due to the intensity and duration of lateritic weathering, many of their characteristics, such as the enrichment or depletion of alkalis, or variations in K/Na ratios, are unlikely to be preserved. Only where very resistant minerals (e.g. tourmaline, muscovite) are essential ingredients of the haloes, as at Teutonic Bore, can an imprint be preserved in the saprolite and perhaps be retained in the lateritic residuum during the course of land surface reduction. Some of the geochemical characteristics of a primary halo may also be preserved by the sorption of indicator elements by Fe oxyhydroxides, such as As, Bi, Co, Cu, Ni, Pb, Zn and Mn in the Fe-rich bands at Elura.

The residual enrichment of "immobile" elements (e.g. Cr, Ti, Sn, Au, REE and P) in resistant minerals and the absolute enrichment of more mobile elements (e.g. Al, Fe, Mn, Co, Ni and, perhaps, Au) are common features in any lateritic terrain. In places, these may be sufficiently concentrated to form secondary mineral deposits. The residual concentrations of apatite over carbonatites at Mount Weld, Western Australia (see p. 329) and Mabounié, Gabon (see p. 267), and the presence of lateritic Ni and Au deposits and enrichments in all climatic environments provide ample evidence. In addition, Ni and other elements sorbed on Fe and Mn oxides may form false or non-significant anomalies that complicate

exploration. Enrichments of silica and alkaline elements, however, are a feature of lateritic regoliths in arid terrains, and it is probable that many saprolitic supergene deposits of base metals and Au formed in response to a change to aridity.

Distribution of preserved and truncated lateritic regoliths

There is a continuum between terrain dominated by mostly completely preserved lateritic regoliths, partly stripped terrain dominated by the outcrop and subcrop of saprolite and fresh rock with only a few remnants of duricrust, and almost fully stripped terrain in which even saprolite is only rarely preserved. The most widespread terrains are those in which the lateritic duricrust has been partly dismantled. In these, patches of outcropping saprolite, ranging in size from < 100 m to several kilometres across, are surrounded by alluvial tracts or lateritic remnants. In extremely arid regions in which erosional stripping has been very strong, there may be no fully preserved lateritic regoliths and the terrain consists predominantly of fresh bedrock, with only isolated patches of saprolite, either outcropping or concealed by juvenile soils or transported overburden.

Dismantling of lateritic duricrusts commences in a variety of places, such as hill slopes, crests and drainage divides. The dominant cause is the long-term change to arid conditions and the destabilization of the original protective cover of vegetation. Other contributing factors include random and systematic variations in the thickness of duricrust and its degree of induration. Surface flow (sheetwash) and the shallow subsurface piping and pervasive flow of groundwater are important erosional agents during intermittent high rainfall in arid and semiarid climates. In some regions, headward erosion by streams has occurred in response to tectonic uplift, commonly leaving duricrust remnants as plateaux.

Incomplete removal of detritus eroded from the regolith in local and district-scale uplands leaves a widespread sedimentary cover. In places, the detritus is dominated by lateritic nodules and pisoliths. The sediments may be only a very thin veneer or be tens of metres thick beneath some colluvial-alluvial plains and drainages. Such sediments may bury both near-complete and partly truncated profiles but these can usually only be recognized after drilling. Where the cover is extensive, some stratigraphic drilling is essential and can be used, inter alia, to establish local criteria for distinguishing between residual units of the regolith and transported lateritic detritus. Such criteria are indispensable when only percussion or rotary air blast (RAB) drill cuttings are available and must be applied carefully. This is particularly important in exploration directed at recognizing and delineating buried geochemical haloes in residual laterite. The distinction between areas of residual versus transported regolith is also critical in deciding where soil surveys will be meaningful.

Geochemical dispersion models

Arid landscapes consist of a mosaic of areas with different degrees of erosion and deposition for which different geochemical dispersion models may apply. There are three principal series of models, based on the degree of preservation of the lateritic regolith, as introduced in Chapter I.1 (see Table I.1-6) and followed in Chapters III.1 and III.2. A-type models apply where the profile is mostly preserved, B-type models apply where the profile is truncated below the ferruginous horizon and C-type models apply where the lateritic profile is entirely absent. The situations represented by these series of models are discussed in turn in the remainder of the chapter, with an additional discussion focussing on problems associated with calcrete development. The majority of the examples for the A and B models are drawn from Australia, the most extensively explored terrain of this type. However, the conclusions are readily applicable to all equivalent arid (and dry savanna) regions.

A-TYPE MODELS: PRE-EXISTING PROFILE ESSENTIALLY PRESERVED

C.R.M. Butt and R.E. Smith

General

The lateritic regolith is developed on an undulating surface and consequently A-type models occur in landforms ranging from upland plateaux, hill crests and slopes to lowland plains and valleys. The relief reflects differences in the rate of land-surface reduction due to the preferential deep weathering of some lithologies, certain types of alteration (e.g. chlorite-carbonate) and along shears and, conversely, the resistance to weathering of certain lithologies and some intermediate weathering products, e.g. cuirasse and silcretes, the latter possibly resulting in relief inversions. Tectonic block disturbances also contribute to the surface topography, even in stable shield areas. The only examples of these models are from Western Australia, although similar situations exist elsewhere: thus, the terrain described by Gleeson and Poulin (1989) on the dry savanna margins in Niger has close equivalence (see p. 235).

Dispersion characteristics

All A-type models have characteristics related to the preservation of a complete profile (Fig. III.3-2). The principal differences between them, particularly that affect the surface expression of mineralization, depend upon the nature of any overburden and this is recorded in the model code. Thus, model A * * [0] is typical of uplands where a duricrust (cuirasse) and/or a loose pisolitic or nodular lateritic unit occurs at surface. Models A * * [1] and A * * [2] refer to areas where an essentially complete profile is covered by up to few metres of

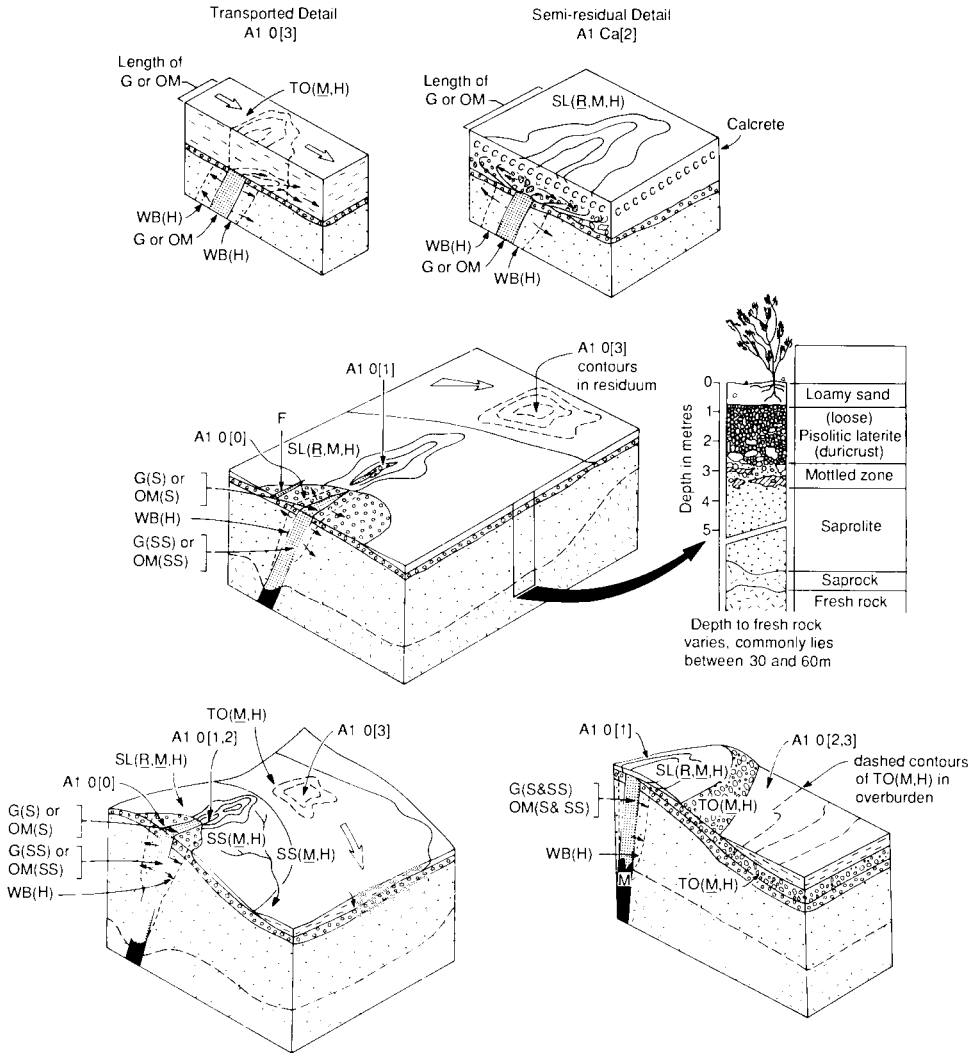


Fig. III.3-2. Block diagrams illustrating the principal A-type dispersion models in arid terrains. For abbreviations see Fig. III.1-1. Contours show general nature of anomaly; broken contours show subsurface anomaly. Derived in part from Butt and Smith (1980) and Butt (1987).

residual or semi-residual soils, whereas model A * * [3] applies to profiles buried beneath alluvial or colluvial sediments, as much as 30 m or more thick. A particular problem occurs when the sediments consist of lateritic gravels, which must therefore be distinguished from similar, residual material (e.g. by the presence of exotic pebbles). Because of the undulating nature of lateritic surfaces, it is common for several landform situations to occur within a district (Fig. III.3-3) and it is prudent to anticipate a variety of models.

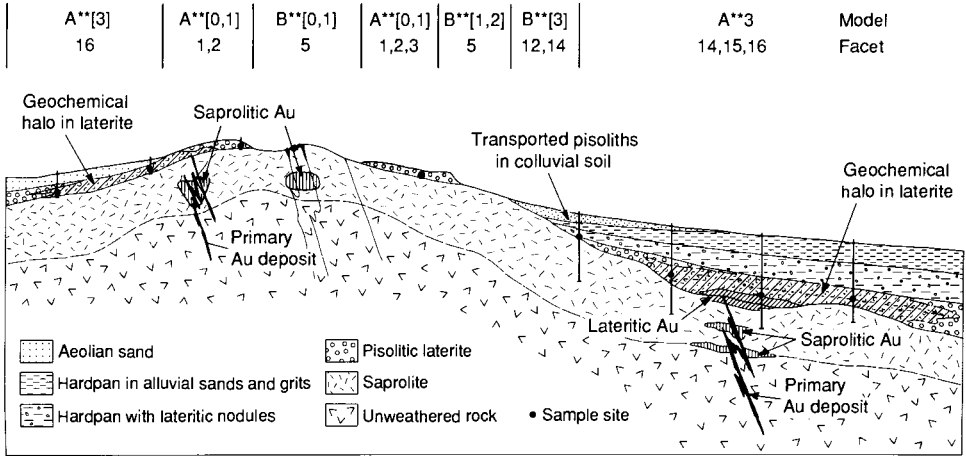


Fig. III.3-3. Landscape section illustrating the interrelationships of dispersion models in partly eroded, arid lateritic terrain, and appropriate laterite sampling locations. The dispersion and secondary accumulation of gold is used as an example. For facets, see Table I.1-4.

The upper horizons of lateritic profiles have been affected by both vertical and lateral disturbance. Continual settling and consolidation (see p. 102) have taken place in response to dissolution and eluviation, and disaggregation and colluvial transport are commonly seen above the saprolite. The lateral extent of this transport is greatest in the pisolitic horizon, ranging from a few metres to several hundred metres. The introduction of extraneous detritus (e.g. rounded pebbles of quartz and rocks) is sometimes recognized. Lateral movement is attributed to mass flow and sheetwash and depends upon local factors such as the slope and density of vegetation.

Land-surface reduction during lateritization supplied a variety of relatively resistant materials for incorporation in lateritic residuum. These include partly weathered ferruginized and/or silicified lithorelics, resistant primary minerals (e.g. Au grains, cassiterite, tantalite, chromite, tourmaline, beryl, scheelite and zircon) and Fe oxide segregations such as those formed in the mottled zone. Where oxidized massive sulphides are present, blocks and fragments of gossan may be incorporated within the lateritic duricrust. Small gossan fragments may form the cores of concretionary nodules and pisoliths. The geochemical, mineralogical and textural characteristics of the gossan fragments, and of the nodules that enclose them, are similar to those of the leached upper horizons of the gossan profile rather than the deeper sulphate, carbonate or supergene zones, which are generally much more geochemically anomalous.

The combined processes of residual accumulation and mechanical and hydro-morphic dispersion result in geochemical patterns related to concealed ore deposits being contained within the uppermost, ferruginous horizons of complete, residual or semi-residual lateritic regoliths. These geochemical and miner-

alogical patterns are invariably merged with patterns arising from the host and country rocks. The dispersion haloes that are most useful at reconnaissance and early stages of prospect evaluation are therefore usually those preserved within the ferruginous horizons. They tend to be large relative to the mineralized source and, in many cases, have internal consistency and a regular, interpretable geometry.

Reconnaissance sampling should be directed at the upper pisolitic laterite, rather than at the mid to lower duricrust, in order to utilize the maximum extent of mechanical and hydromorphic dispersion and the most homogeneous geochemical signatures. Sample spacings of 1 km to as much as 3 km can be used for reconnaissance surveys, particularly where large deposits are sought or expected.

Sampling for prospect evaluation should be directed progressively to lower horizons of the duricrust to reduce the influence of mechanical dispersion. Nodular laterite, rather than the upper pisolitic zone, is favoured, sampled at 400 m centres, and closer as exploration progresses. For more detailed prospect evaluation and the delineation of drilling targets, sampling should be directed at the massive, vermiform or brecciated base of the lateritic duricrust (cuirasse), with samples collected at intervals of 100 m or less. Once targets are delineated, further exploration is by drilling to intersect mineralization in the saprolite or unweathered bedrock.

*Models A**[0], A**[1] and A**[2], residual laterite at surface or beneath residual and semi-residual soil*

These models generally typify occurrences in upland parts of an undulating landscape. The original lateritic profile is essentially complete, and the surface exposure consists of the ferruginous duricrust and/or overlying residual or semi-residual soils. The residual cover may comprise remnants of the soil present during the formation of the lateritic profile and material developed by reweathering of the ferruginous horizon. The duricrust is exposed where the finer fractions are removed by sheetwash or wind, leaving the gravel-sized and coarser material as a lag. Some pisoliths and nodules are moved down slopes by colluvial mass flow or by surface water as sheetwash, braided wash channelling and local gullyng, and by animal disturbance. This combination of recent mechanical dispersion processes can move centimetre-sized material 100–300 m or more, supplementing the mixing and homogenizing of the surface pisolitic and nodular horizon that occurred during lateritization and further increasing the size of dispersion haloes. The eroded fine fractions are mixed with otherwise residual soils or deposited as aeolian, colluvial or alluvial sediments in surrounding plains.

In the A**[0] model, a surface veneer of loose pisoliths and nodules is commonly strewn over various types of cemented duricrust (e.g. massive, vermiform, fragmental, mottled) into which it merges. These duricrust types may be

exposed by partial truncation but complete loss of the pisolitic unit is detrimental because it removes the broadest geochemical haloes. The cemented units are also slower to sample and representative samples are less readily obtained than from loose, relatively homogeneous units. In the A * * [1], A * * [2] and A * * [3] situations, these units are concealed and must be sampled by shallow pitting or drilling.

Geochemical anomalies located by pisolith sampling may range from prospect to district scale, revealing dispersion from individual orebodies (e.g. Golden Grove, see p. 310) to large scale features related to metallogenic provinces (e.g. "chalcophile corridors" (Smith et al., 1989); see Fig. III.3-5). The procedure is thus equivalent in scope to stream sediment sampling. The size and homogeneity of the anomalies allows sampling at centres as wide as 1–3 km, yet spacings as close as 100 m remain suitable for detailed follow-up.

As with all sample media, a constant sample type should be collected if possible. Pisoliths and nodules can be classified by characteristics including size, colour, presence of skins or coatings, lustre of fracture surface, density and magnetic properties. However, it is uncertain that any of these has great significance. Although the selection of magnetic pisoliths and nodules (or lag, see p. 346), for example, increases the mineralogical and chemical homogeneity of the sample, greater crystallinity of the material can result in lower concentrations of associated target and pathfinder elements and weaker anomalies of lower contrast. Nevertheless, samples must be taken with care. Sampling of outcrop or scree derived from Fe-rich lithologies such as banded iron formations, "non-lateritic" ironstones and possible gossans should be recorded and the data treated separately.

Soils have been preferred to pisoliths for many surveys of these terrains, choosing either the total sample or a coarse fraction for analysis (e.g. Callion, see p. 319). If a fine soil fraction is used, the abundances of As, Sb, Bi and Cu, for example, may be an order of magnitude lower than in associated pisoliths. Where pisoliths are abundant in soils, similar results to pisolith sampling are obtained, and anomalies may even be enhanced if other soil components host important elements, such as pedogenic carbonates for Au. However, if the abundance of pisoliths varies significantly, this may impart a high variance to the analytical data and mask subtle responses. Carver et al. (1987) noted an equivalent problem when lag samples had high contents of barren, non-ferruginous material and found that regression for the Fe content partly overcame the problem.

Bulk leach extraction of gold (BLEG; or bulk cyanide leach, BCL) from drainage and wash sediments and soils has been widely used in Australia for regional gold exploration. The technique has met with a number of successes but the effectiveness of widespread application is limited by the uncertainties associated with any partial extraction technique applied to heterogeneous samples and by the absence of any multielement data. In regions in which the lateritic profiles are generally well preserved, anomalies as large as those from laterite sampling have been obtained. However, results can be difficult to interpret unless a large

Au anomaly is also present in the laterite, in which case laterite geochemistry would have been equally effective. Interpretational problems arise where laterite is not uniformly present because background levels for Au are higher in the laterite than the upper saprolite; the BLEG response, in consequence, has numerous misleading anomalies. The fine fractions of stream sediments appear to be as effective as BLEG and, although requiring more samples, are of lower mass and less costly to analyse for Au alone (Mazzucchelli, 1987); they are also suitable for multielement surveys. Nevertheless, direct sampling of residual and semi-residual lateritic pisoliths and nodules is generally more effective and appropriate. BLEG from soils can be used at the prospect evaluation stage, as can conventional total analysis. Unless there is a high proportion of lateritic pisoliths in the sample, total contents of Au in soils may be an order of magnitude lower than in the pisoliths alone.

It is important that the situations represented by these models be recognized correctly when designing exploration programmes, so as to make best use of the ease of laterite sampling and the proven benefits of the relatively large, consistent dispersion haloes. Areas of transported lateritic gravels must be considered separately, however, for they may only contain the regional signature from eroded uplands, perhaps a considerable distance away.

Regional laterite geochemistry surveys in southwestern Australia

Most of the Yilgarn Block of southwestern Australia appears to have experienced deep lateritic weathering during the early Tertiary. The lateritic regolith is now undergoing modification, both physical and chemical, following minor epeirogenic uplift and climatic change. The regolith is widely preserved and there are large areas with complete or sporadically complete profiles. The present climates range from temperate Mediterranean, having moderate winter rainfall (over 1000 mm p.a.) in the southwest, to warm to hot semiarid in the north and E. An equivalent climatic range may have existed in the past, so there are regional variations both in the nature of the lateritic regolith and in the soils more recently developed from them. A series of orientation studies has demonstrated that lateritic gravels and duricrusts are highly effective sample media throughout the Yilgarn Block, not only for local to district scale exploration, but also for demonstrating regional geochemical features (Mazzucchelli and James, 1966; Smith and Perdrix, 1983; Smith et al., 1987; Smith et al., 1989; see Golden Grove, p. 310 and Mount Gibson, p. 313). The application to regional surveys arises because the lateritic materials, especially the pisoliths and nodules, smooth the geochemical variations.

Use of regional laterite sampling in the Yilgarn Block has been described by Smith et al. (1989) for surveys concentrating upon greenstone belts and complex metamorphic terrain. One kg samples of pisoliths and nodules, ideally 1–2 cm in size, were collected from the ground surface over a 5–10 m radius. A 3 km triangular sampling grid was used initially with follow-up sampling at 1 km.

Samples were prepared for analysis by non-metallic procedures and analysed for up to 30 elements. The regional programme defined numerous specific anomalies but also showed that many of the chalcophile or partly chalcophile elements formed geochemical patterns ("chalcophile corridors") commonly 15–30 km wide and 50–100 km or more long. Typical of these are the patterns in the western gneiss terrain, based on a set of 1600 samples. They are illustrated on Fig. III.3-4 by the distributions of anomalous As, Sn and Sb and two weighted additive indices computed to emphasize centres of possible chalcophile and pegmatite mineralization. Two regional patterns are seen:

(1) The Marradong–Duncan chalcophile corridor. This covers the Saddleback greenstone belt, but seems to cross-cut the mapped stratigraphy. It has a regional association of As, Sb, Bi and Sn, with coincident anomalies of As, Sb, Bi, Mo, Sn, W and Au over the Boddington gold deposit (Smith, 1989). The chalcophile index $CHI = 6 * X$ depicts a far larger anomaly than Au alone.

(2) The southwest chalcophile corridor, which includes the Greenbushes rare-metal pegmatite system, the Smithfield pegmatite system and the Donnybrook epithermal-style Au deposits. It shows a strong regional association of As, Sb, Be and Sn, together with Nb, Ta, Li and B close to the pegmatite. The regional extent of this multielement anomaly can be expressed by a pegmatophile index, $PEG = 4 * X$.

Other surveys showed that the Golden Grove Cu-Zn deposits (see below), the Mount Mulgine Mo-W-(Au) deposit and the Mount Gibson Au deposit (see p. 313) lie in the Warrieadar chalcophile corridor (Fig. III.3-5). The origin of these patterns is not established, but it is possible that they reflect metallogenic provinces within the Archaean basement. As such, they have important implications in mineral exploration, particularly at the reconnaissance stage.

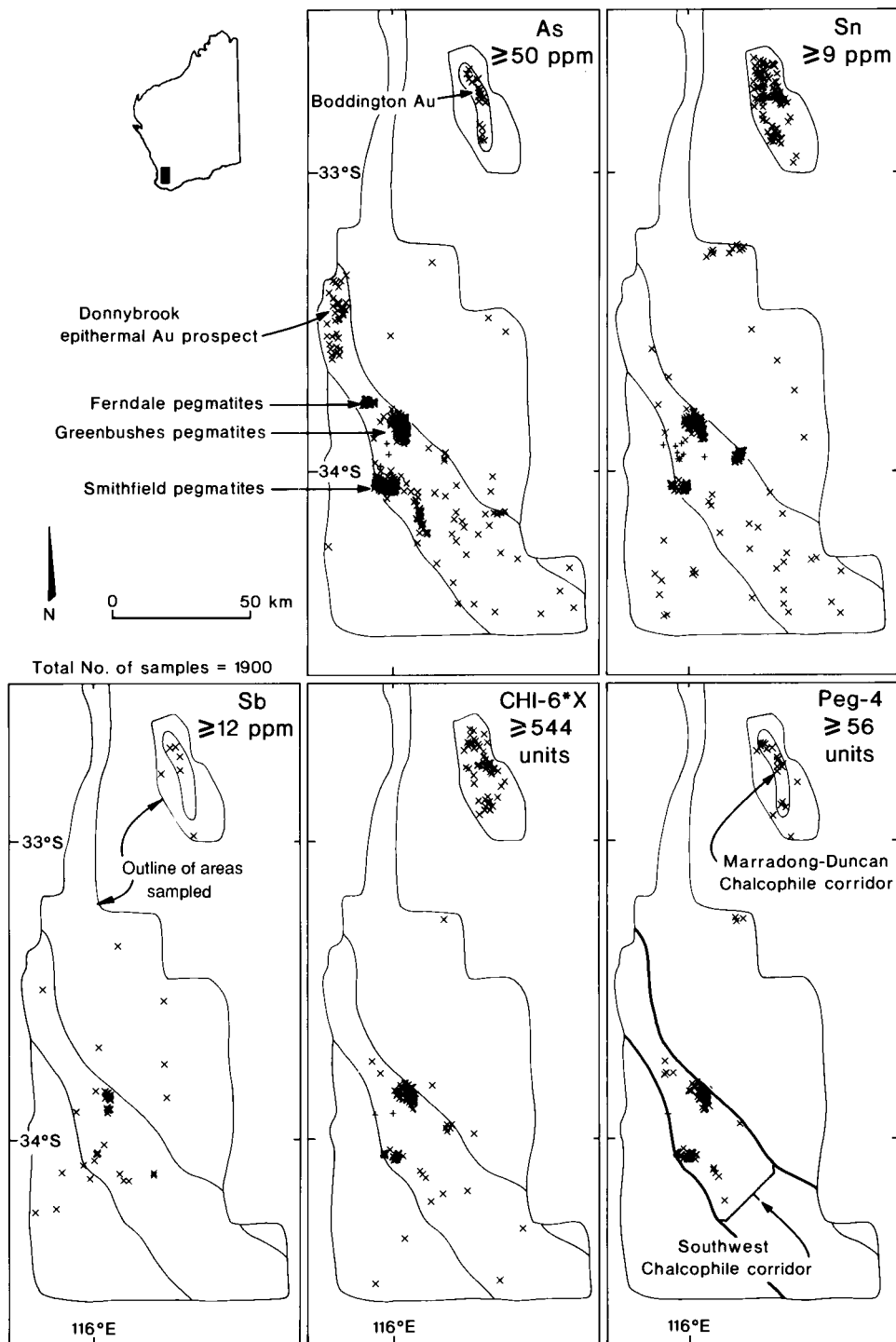
Golden Grove Cu-Zn-Ag deposits, Western Australia: Gossan Hill (B 1 0 [0,1,2]) and Scuddles (A 1 0 [1,2,3])

The Golden Grove deposits are situated in a sequence of felsic volcano-sedimentary rocks in the Murchison Province of the Archaean Yilgarn Block, 380 km north-northeast of Perth. The Gossan Hill deposits consist of massive pyrite, magnetite and pyrrhotite lodes containing variable chalcopyrite and minor sphalerite; the estimated resource is 12 Mt averaging 3.4% Cu, 12 g/t Ag and 0.1 g/t Au for the Cu zone and 2.3 Mt averaging 10.5% Zn, 0.5% Cu, 92 g/t Ag and 1.7 g/t Au for the Zn zone. The three deposits at Scuddles have combined reserves of 10.5 Mt averaging 11.7% Zn, 1.2% Cu, 0.8% Pb, 89 g/t Ag and 1.1 g/t Au.

Fig. III.3-4. Chalcophile corridors in the south western part of the Yilgarn Block, Western Australia, as defined by laterite geochemistry. From Smith et al. (1989). Only those samples exceeding the threshold limit for the particular element or index are shown.

$CHI - 6 * X = As + 3Sb + 10Bi + 3Mo + 30Ag + 30Sn + 10W + 3Se$.

$PEG - 4 = 0.09As + 1.33Sb + Sn + 0.14Ga + 0.4W + 0.6Nb + Ta$.



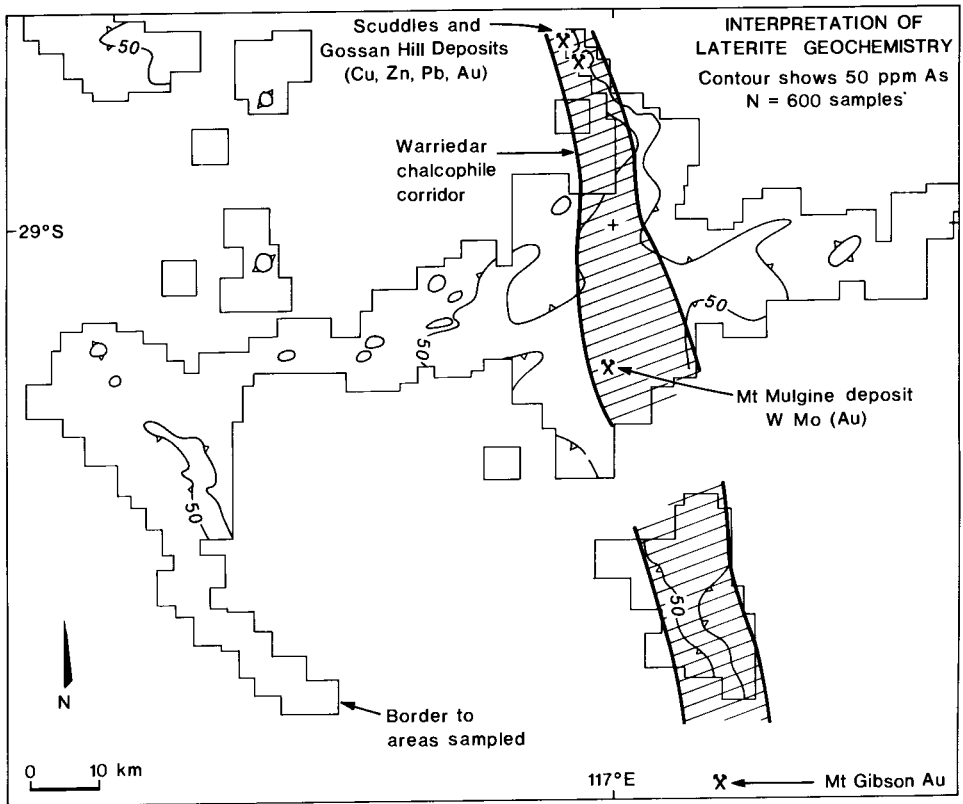


Fig. III.3-5. The Warriedar chalcophile corridor, Western Australia (hatched), as defined by laterite geochemistry, showing the locations of the Golden Grove and Mount Gibson deposits. Redrawn from Smith et al. (1989).

Much of the area is mantled by a more or less complete lateritic regolith, typically comprising:

(1) Sandy loam, 0–1 m: semi-residual to transported, with colluvial, alluvial and aeolian components.

(2) Pisolitic laterite, 1–2.5 m: a grain-supported semi-residual horizon of pisoliths, loose near the surface, cemented and increasingly nodular towards the base.

(3) Mottled zone, 2.5–3.5 m: sandy clays with isolated pisoliths and nodules; locally arenose and silicified.

(4) Saprolite, 3.5–> 30 m: kaolinitic weathered bedrock.

(5) Saprocks to fresh bedrock, > 30 m: transitional weathering zone, corresponding approximately to the present water-table.

There are few outcrops, even of saprolite, except where the prospective sequence rises 80 m above the plain as Gossan Hill or where the profile has been

partly dissected by active drainages. The deposits here were found following the recognition of outcropping gossans (Chapter II.2, case history 14B). Although these are strongly leached of Cu and Zn, many other elements are anomalous, including As, Sb, Bi, Mo, Ag, Sn and Se (Table II.2-18). The Scuddles deposits do not outcrop, and were discovered by location of a Pb anomaly in saprolite during systematic RAB drilling along strike from Gossan Hill.

Both the Gossan Hill and the Scuddles deposits may formerly have been concealed by a continuous cover of pisolitic laterite. They were selected for studies of pisolith sampling as an alternative to drilling for effective exploration of laterite covered terrains (Smith et al., 1980; Smith and Perdrix, 1983). Detailed orientation around Gossan Hill revealed a multielement anomaly extending 400 m downslope and a further 300 m across the plain. The anomaly was found to be due in part to gossan fragments forming the cores of the pisoliths, together with detrital cassiterite and adsorbed Cu, As and Zn in the concretionary Fe oxide coatings. This distribution indicates that the anomaly formed by hydromorphic and mechanical dispersion contemporaneous with pisolith formation, and was followed by predominantly mechanical dispersion during the erosion of the pisolitic horizon. The size of the anomaly, particularly that on the plain, indicated the appropriateness of a low sample density for exploration. A triangular sampling grid of 320 m was used initially, based on the anticipated minimum size of dispersion from significant mineralization, with a closer interval (160 m) used for follow-up. Samples were collected from cuttings from earlier RAB drilling. Samples were prepared for analysis by non-metallic procedures.

The results show that although the principal target elements, Cu and Zn, show distinct anomalies around Gossan Hill, neither are anomalous at Scuddles (Fig. III.3-6). However, several pathfinder elements, particularly As, Sb, Bi, Se, Sn and Mo, are distinctly anomalous over both deposits. The maxima of these anomalies are, however, displaced as much as 1 km west, which may be due either entirely to dispersion downslope or in part reflect the zoning of a primary halo. Nevertheless, the dispersion halo at Scuddles continues down a 1:85 slope for about 1.5 km (see Fig. I.6-5). The multielement anomaly can be summarized as a weighted additive index that merges and smooths the commonly erratic distribution of the pathfinder elements. On a regional basis, these indices seem to define broad geochemical patterns—the chalcophile corridors described in the previous section. One such pattern appears to link Golden Grove with the Mount Gibson Au deposit (Fig. III.3-5).

Mount Gibson Au deposit, Western Australia (A 1 Ca, Si [1,2,3])

R.E. Smith and R.R. Anand

Location and geology. Mount Gibson is about 300 km north-northeast of Perth, at the southern end of the Retaliation–Yandanoo greenstone belt in the Archaean Yilgarn Block of Western Australia. The area has a semiarid climate, with an average annual rainfall of 250 mm, falling mostly during the cooler winter months (May to August). The Mount Gibson gold mine commenced operations in

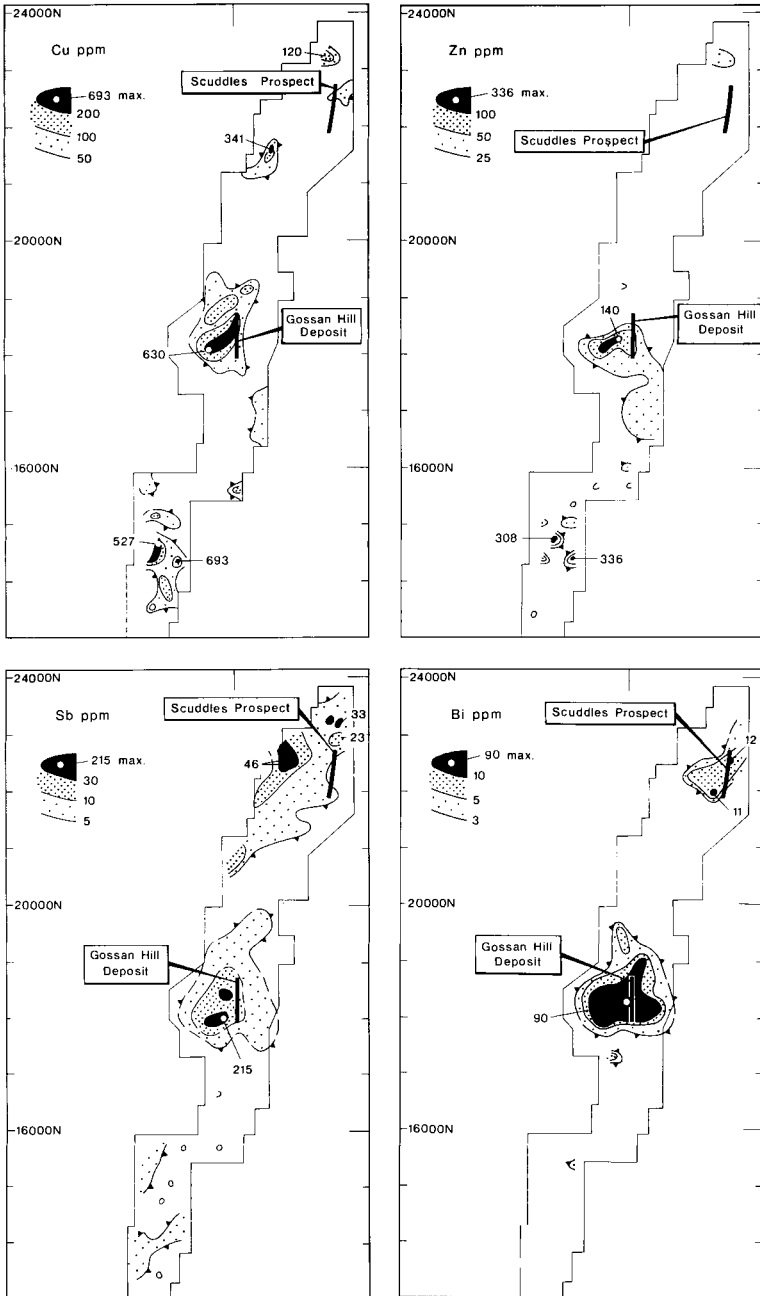


Fig. III.3-6. Distributions of Cu, Zn, Sb and Bi in pisolitic laterite near the Gossan Hill and Scuddles deposits, Golden Grove, Western Australia. Redrawn from Smith and Perdrix (1983). Gossan Hill rises 70 m above the plain; relief at Scuddles is very low.

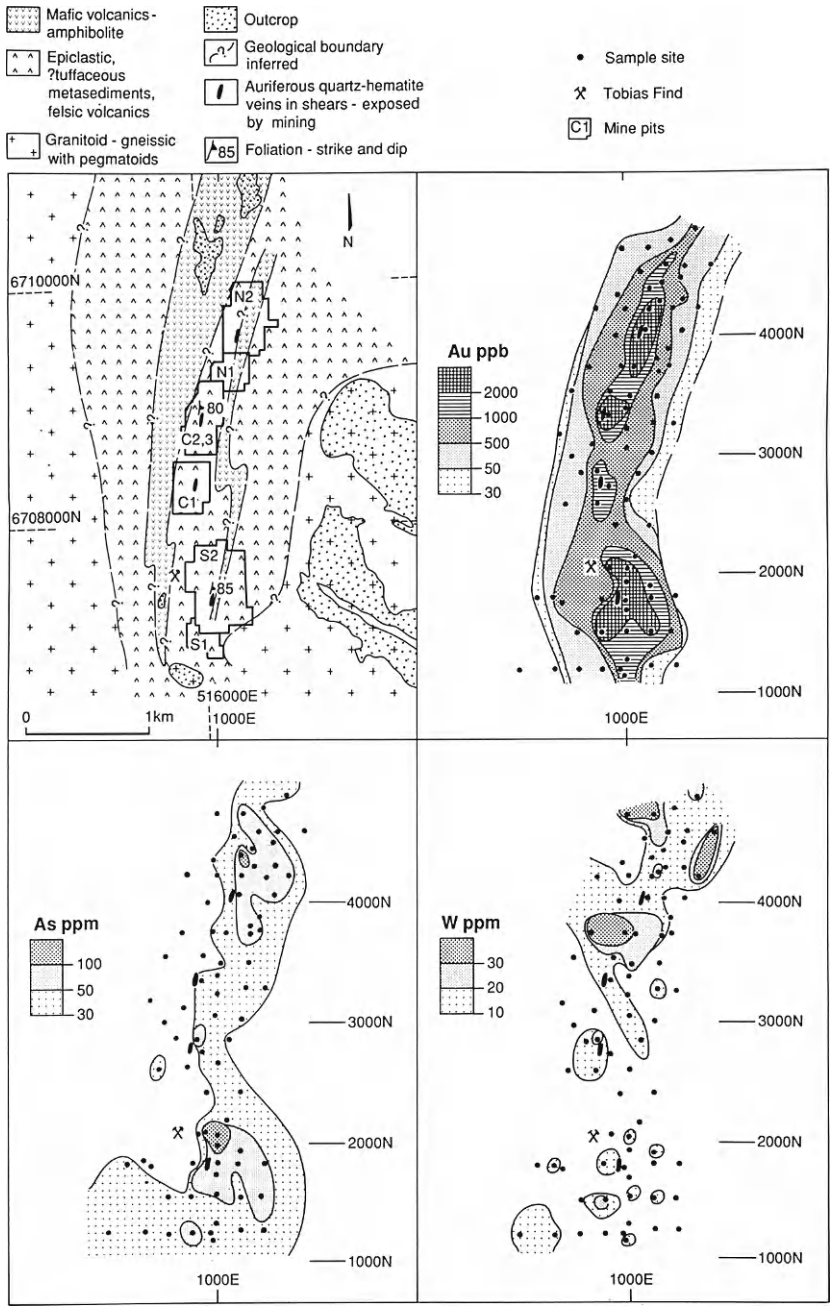


Fig. III.3-7. Geology and the distributions of Au, As and W in lateritic gravels, Mount Gibson gold deposit, Western Australia.

1985 based on lateritic ore, generally of low grade. Continued exploration led to delineation of a series of deposits with resources of 6 tonnes of Au, including some primary mineralization. (Gee, 1989, 1990). The ores are the strongest parts of a geochemical anomaly of more than 7×1 km developed above intermittent shoots of primary Au and disseminated sulphide mineralization. A small prospect, Tobias Find, discovered during the period 1910–1916, is 100 m from one of the present pits but production (1 kg Au) was not significant. The auriferous nature of the laterites was not recognized until 1982. This account is derived largely from reports by Anand et al. (1989; 1991), Davy et al. (1988; 1989), Gee (1990) and Brabham et al. (1990).

Sporadic secondary mineralization has been found along 7 km of strike (Fig. III.3-7), with individual deposits known in the SCN area (southern, central and northern pits) and at Midway North (Hornet Zone). Primary mineralization is associated with quartz veins in shears within a sequence of weathered mafic and felsic rocks, metamorphosed to lower amphibolite and greenschist facies. In the Hornet zone, Au occurs at the structural contact of a western suite of sheared basic rocks, quartz-phyric felsic schist and possible Fe-rich sediments against an eastern suite of less deformed basalts (Gee, 1989). Gold is found particularly in K-Si-S alteration zones within and marginal to the quartz-phyric rock and with sulphidic laminae (pyrite and pyrrhotite with minor chalcopyrite and sphalerite) in chlorite tremolite (cordierite garnet) schists. Preliminary geochemical studies suggest a variable primary association of Au with Ag, Cu, Pb, Zn, As, Sb, Bi, W, Se and Ge.

Regolith. Regolith-landform mapping has demonstrated the importance of understanding the erosional and depositional dynamics of the geochemical dispersion. The principal regolith units are:

Soils. There are two main soil types:

(a) yellow sands and orange sandy clays, typically gravelly below 20–50 cm, directly overlying residual lateritic gravels and duricrust.

(b) red clays, which overlie either saprolite in the erosional regimes or clay and sandy materials transported for up to 500 m and deposited upon relatively complete laterite profiles.

The red clay soils are characterized by eucalyptus woodland vegetation, whereas the yellow and orange soils derived from the lateritic residuum support an acacia shrubland.

Hardpan. Hardpan, formed by silica cementation of colluvium and alluvium, is up to 3 m thick in parts of the SCN area and reaches 6 m near Midway. In the SCN area, the colluvium is locally derived and contains an abundance of lateritic pisoliths, nodules and saprolite-derived silty, sandy clay.

Lateritic residuum. There are two principal units:

(a) loose pisolitic and nodular gravels with a yellow to red sandy clay matrix. This unit generally occurs as a blanket 1–2 m thick that overlies and grades downwards into pisolitic or nodular duricrust. The pisoliths and nodules are

commonly 5–20 mm in diameter and have pale brown, brown or nearly black cores composed of Al-goethite, Al-hematite, Al-maghemite and kaolinite with abundant residual quartz grains. The outer coatings are paler and consist of Al-goethite, kaolinite and gibbsite.

(b) lateritic duricrust, typically the substrate to the lateritic gravels. It is generally 1 to 2 m thick in the SCN area, and has a pisolitic, nodular, vermiform or fragmental fabric. The pisoliths and nodules, which are commonly spaced within a hardened sandy clay matrix, have a similar mineralogy to those in the lateritic gravels. Secondary calcium carbonate and/or opaline silica cements, related to post-laterite groundwater regimes, are present in places.

Mottled zone. The lateritic mottled zone has been exposed sporadically by mining and erosion. Pronounced mottling is present on foliated metasedimentary or metavolcanic rocks rather than on metadolerites. The mottling, typically on a 10 cm scale, is due to the heterogeneous distribution of ferruginous material within a clay-rich, Fe-poor matrix; in places, it is related to recent penetration of tree roots and associated leaching of Fe.

Saprolite. Saprolite thickness depends on lithology, the intensity of shearing and the degree of truncation of the lateritic profile. In the Hornet zone, at Midway North, the main mineralized shear is weathered to 60 m, whereas mafic volcanics to the east are weathered only to 20 m. In some severely truncated areas, mafic amphibolite is fresh at outcrop.

Supergene Au mineralization. Gold at Mount Gibson occurs at mineable grades in several regolith units. Prior to mining, some of the auriferous laterite occurred within 15–50 cm of the ground surface in the south and central pit areas. Elsewhere, it lay buried beneath several metres of partly consolidated sediments of local origin. In the SCN area, the pits are situated centrally within the geochemical anomaly, and loose lateritic gravel has been the most important ore. The high Au price, coupled with free-digging ore and efficient extractive metallurgy, allowed the mines to be worked profitably in 1985 using a cut-off of only 0.75 g/t Au, although higher cut-off grades were necessary later. Duricrust reserves are also widespread and have similar grades, but require ripping, blasting and crushing. In the Midway North area, a substantial saprolite orebody with some supergene enrichment has been mined. This lies beneath a 20 m thick depletion zone and is the weathered expression of the primary Hornet zone mineralization, together with some enrichment of the wallrocks close to the weathering front. Some lateritic ore also occurred within 10 m of the surface.

Geochemical dispersion. Orientation sampling has focussed principally upon the lateritic gravels and the underlying lateritic duricrust. Samples were categorized accordingly and each data set was treated separately. However, a broader coverage was obtained for the gravels and, as the geochemical patterns are similar for both units, the discussion is restricted to the gravels.

The large Au anomaly is shown in Fig. III.3-7. Using a threshold of 30–50 ppb Au, a concentration that seems to be generally applicable for regional surveys of lateritic terrain in the Yilgarn Block, the anomaly is 1 km wide and extends beyond the area depicted for 7 km along strike. The strongest parts of the anomaly in the SCN area are centred on a line of quartz-hematite veins. Because a number of chalcophile and associated elements (Ag, Pb, As, Sb, Bi and W) show coincident anomalies also centred upon this veining, it is concluded that there is an important and close genetic link between the lateritic gravel and duricrust and the bedrock source(s). There is evidence for lateral dispersion of some Au, possibly by a combination of mechanical and hydromorphic mechanisms, with additional sources possibly 200–400 m upslope from the main axis of the anomaly.

The distribution of As (Fig. III.3-7) is probably related to the quartz-hematite veining, but appears to be displaced asymmetrically downslope by about 200 m, similar to the patterns at Golden Grove and Scuddles (Smith and Perdrix, 1983). The As abundance, as at Golden Grove, is anomalous but is low relative to many deposits elsewhere in the Yilgarn Block. Although the Au anomaly in lateritic gravels is relatively continuous, the distribution patterns for W (Fig. III.3-7) Ag, Pb and Sb (Anand et al., 1989) are zoned, with higher relative abundances in the north. This most probably reflects zoning in the primary mineralization. The multielement chalcophile association is typical of a Au-bearing base metal or polymetallic sulphide source. The sulphides are most probably disseminated because no massive sulphide gossans have been found in the SCN area where saprolite has been exposed by mining or erosion.

Only limited data are available for the saprolite: Au mean 435 ppb, (maximum 3520 ppb); As 14 ppm, (85 ppm); Bi 6 ppm, (70 ppm); Cu 35 ppm, (160 ppm); Pb 105 ppm, (780 ppm). However, these data are compatible with the expectation that geochemical patterns in the saprolite, arising from both secondary dispersion and the weathering of the mineralization, will be stronger, more variable and narrower across strike than in the lateritic residuum.

The most notable features of the geochemical expression of mineralization at Mount Gibson are the size and regularity of the Au anomaly in the lateritic residuum. These are probably due in part to the restriction of sampling to a specific unit of the regolith, whether near the surface or buried by several metres of surficial sediments. These features confirm the validity of using wide sample spacings, such as a 500 m triangular grid, for reconnaissance exploration. Even a spacing of 1 km would detect an anomaly as large as that at Mount Gibson. Even if Au had been leached to low and erratic levels in the lateritic residuum, the multielement geochemical anomaly would still be identifiable using Pb, As, Sb, Bi and W, provided these elements were not also significantly depleted (Anand et al., 1989). In this case, a sample spacing of 300–400 m would have been appropriate.

Callion Au deposit, Western Australia (A 1 Ca, Si [0,1])

The Callion gold deposit is typical of the many supergene (lateritic and saprolitic) gold deposits that have been mined in Western Australia in the last decade. Callion is an old mining centre 100 km north-northwest of Kalgoorlie which was worked intermittently between 1899 and 1956. Gold occurs in quartz-filled shear zones within a sequence of metamorphosed (amphibolite facies) basalts, interflow sediments and acid tuffs within the Archaean Wiluna-Norseman greenstone belt (Glasson et al., 1988). The area has a subdued relief with low laterite-covered hills rising to a maximum of 20 m above colluvial-alluvial plains. Weathering commonly extends to depths of 40–60 m and, where complete on the hills, the profile over metabasaltic rocks consists of:

red brown clay loam soil, up to 0.3 m thick;

coarse pisolitic laterite, 1.0–3.0 m thick, with pisoliths to 50 mm diameter, commonly including a pedogenic calcrete horizon;

mottled zone, with ferruginous nodules and fragments in a kaolinitic and commonly silicified matrix;

saprolite, bleached and kaolinitic in the upper 10–20 m and passing downwards to yellow to red-brown and pale green clays, probably smectitic in part.

A reconnaissance survey was carried out by soil sampling on a single traverse across each of the thirteen laterite-covered hills on the tenements. One kg samples of soil and pisoliths were collected at 50 m intervals and, on one hill, two adjacent samples were found to be anomalous (530 and 350 ppb Au) compared to the background of 60 ppb Au. A detailed soil survey on a 25 × 50 m grid outlined a 200 × 600 m anomaly, defined by the 100 ppb contour, elongated parallel to the N–S structural trend. The 1000 ppb contour of the anomaly, 70 × 340 m, defines the cut-off of the small lateritic Au deposit. This deposit was evaluated by reverse cycle percussion (RCP) drilling to the base of the mottled zone (5 to 10 m) on a 25 × 25 m grid, locally infilled at 12.5 m intervals. Reserves were estimated to be 71000 t at 2.0 g/t, with an average thickness of 3 m. Gold occurs as the free metal, associated mostly with Fe oxides, and includes some clearly secondary forms. The highest concentration of gold, however, was found in pedogenic calcrete near the centre of the anomaly. In general, the Au contents of the soils were about 50% of those of the underlying laterite deposit, due to dilution (e.g. by transported clays and sand) and possible leaching during soil formation. The coincident distributions of Au, As and, to a lesser extent, Pb in soils reflect the occurrence of arsenopyrite and galena in the primary mineralization.

Subsequent exploration resulted in the discovery of the primary mineralization underlying the soil anomaly and lateritic deposit. A quartz-veined shear was located by deep diamond drilling after an initial programme of RCP drilling to 30 m depth had been unsuccessful. Thereafter, RCP drilling on 25 m centres proved a saprolite resource of 104,000 t at 7.9 g/t Au with a 2 g/t cut-off. The 3 m wide ore zone was found to occur over a strike length of 300 m and to extend to the base of weathering at 60–70 m. Although the deposit is very small,

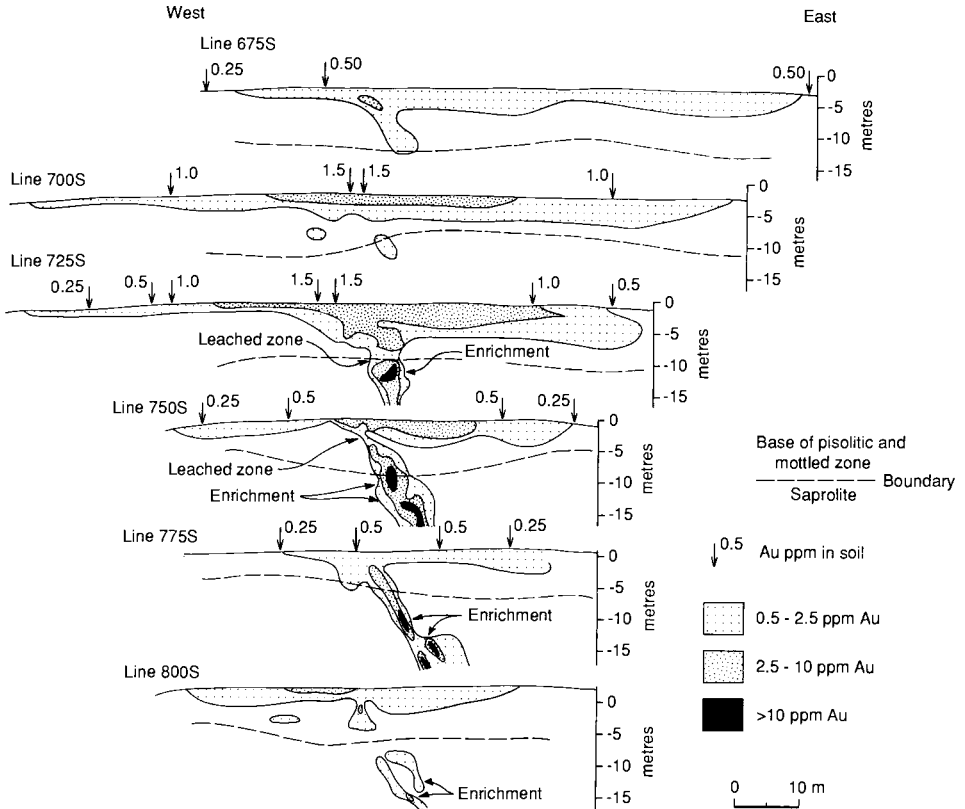


Fig. III.3-8. Stacked profiles of smoothed Au grade contours across the main Au-quartz vein, Callion, Western Australia. Modified after Glasson et al. (1988).

the Au distribution, shown in Fig. III.3-8, illustrates many of the features typical of supergene Au deposits in semiarid lateritic terrains:

(1) There is a "mushroom-like" dispersion of Au into the mottled and pisolitic horizons of the profile.

(2) Gold is largely depleted between 3 and 9 m in the upper saprolite.

(3) Gold in the saprolite is more or less confined to the shear, with some very high values (e.g. to 54 g/t) suggesting enrichment, possibly at an old water-table level. However, as the primary mineralization is vertically zoned and is poorly developed in the unweathered zone despite the continuation of the shear, the degree of enrichment cannot be estimated.

(4) There is an increase in Au fineness towards the surface, from 810 below 40 m to 920 above.

(5) Secondary forms of Au, including crystals, are present in the lateritic horizon.

These features are evidence for Au mobilization during weathering and are discussed more fully in Chapter V.3.

Morphology and composition of gold, Bardoc, Western Australia (A 1 Ca [0,1])

The Bardoc gold deposits are located in the Archaean Norseman–Wiluna greenstone belt, 50 km north of Kalgoorlie, Western Australia. Primary mineralization occurs with quartz veins in a metadolerite host rock, associated with pyrite and arsenopyrite. The deposits had earlier been mined underground, but open pit methods have since been used to exploit the low grade mineralization present in the regolith. The weathering profile, 50–60 m thick, consists of a dark red to brown saprolite overlain by a paler mottled clay zone. The former lateritic cuirasse has been degraded and the surface horizon is a ferruginous soil, 1–3 m thick, containing Fe oxide nodules and pisoliths, loose and in cemented blocks, and some pedogenic calcrete. There has been some erosion and the site is transitional between the A and B models.

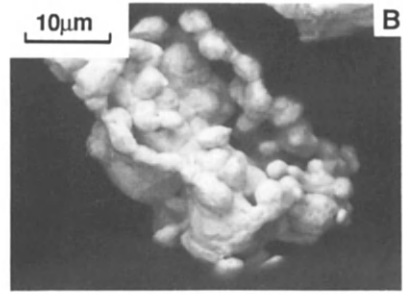
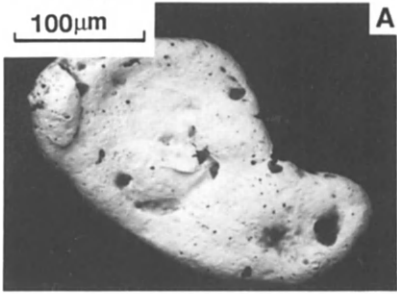
Particulate gold was recovered from 10–15 kg samples from several depths in the profile on the mineralized lode and wallrocks, and examined by electron optical techniques to determine the morphology and composition of the grains (Freyssinet and Butt, 1988b). Primary and secondary gold were found at each horizon and have the following characteristics:

Primary gold grains contain 2–11% Ag and occur either as unweathered xenomorphic forms with smooth and bright faces showing the imprint of adjacent crystals, or are dull, rounded and etched. All grains containing < 6% Ag are etched and many exhibit progressive Ag depletion on grain boundaries and along cracks.

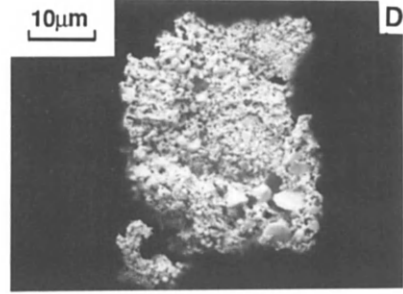
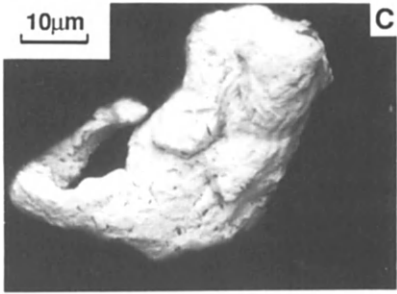
Secondary gold grains contain < 0.07% Ag and have several morphological types, including xenomorphic forms, individual or intergrown subhedral to euhedral prismatic and flat pseudo-hexagonal crystals, and complex irregular aggregates. The grains may be pristine or corroded, and commonly have a later generation of fine Au crystals or spherules adhering to them.

Some examples of the grains are shown on Fig. III.3-9. The proportions of primary grains recovered from each horizon of the weathering profile (Fig. III.3-10) demonstrate that only a few have survived the intense leaching of the upper saprolite and the mottled zone; most of these are strongly etched. In comparison, over 40% of the grains in the ferruginous horizon are primary. They were presumably preserved within vein quartz or protected by Fe oxides. Corrosion of the secondary grains is greatest in the lower saprolite and mottled zone, whereas those in the upper saprolite are predominantly pristine. In the mottled zone and upper saprolite, Au is mainly as irregular aggregates. These are strongly corroded in the mottled zone but commonly have numerous uncorroded crystals developed on them. Apart from Ag, there is no significant difference in the compositions of primary and secondary grains.

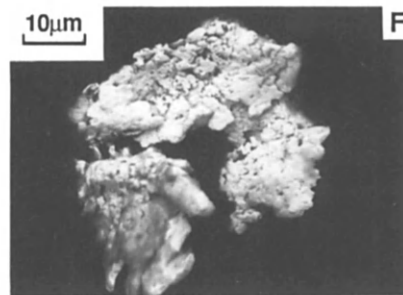
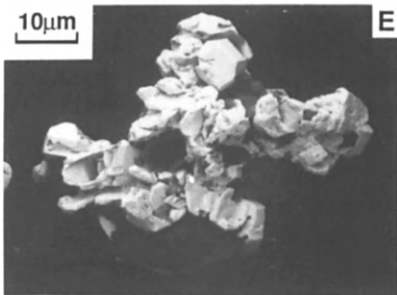
Ferruginous horizon



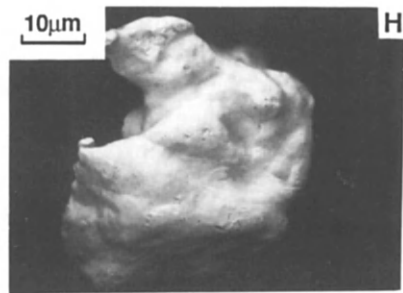
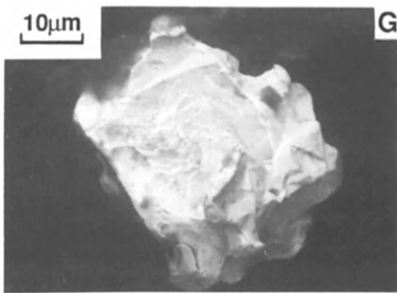
Mottled clay zone



Saprolite



Base of saprolite



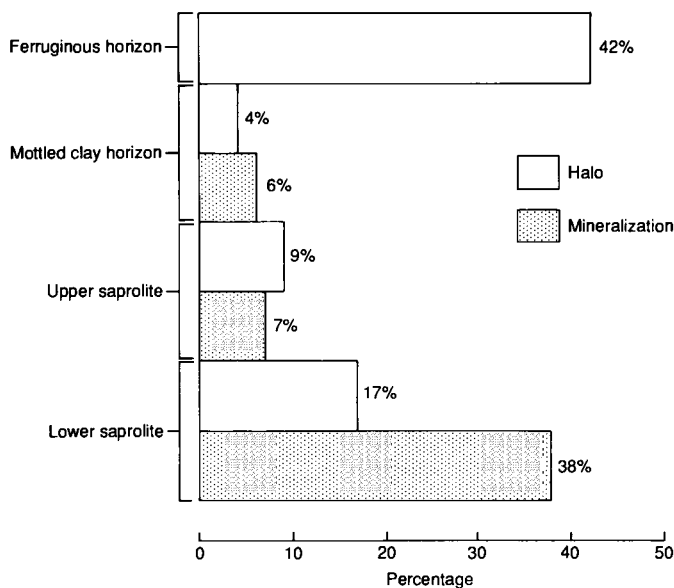


Fig. III.3-10. Percentages of Ag-bearing (primary) Au grains in different horizons of the weathering profile at Bardoc, Western Australia. Redrawn from Freyssinet and Butt (1988b).

These observations can best be explained by Au having been mobilized by different processes at different times. During lateritization, Au was probably mobilized as organic complexes at the top of the profile, mainly in the ferruginous horizon. The dissolved and colloidal Au became dispersed in this horizon, to create a secondary halo, augmented by physical movement of primary Au grains and of Fe oxide segregations such as pisoliths and nodules that contain Au. Later remobilization probably occurred under arid conditions, when groundwaters were saline. Gold solubilization was probably greater than during lateritization and took place mainly in the saprolite and mottled zone. Most of the primary Au in these zones was dissolved and reprecipitated as secondary Au of high fineness within the original mineralized zone and as minor enrichments in the wallrocks. Similar studies in humid environments (see p. 219) show that primary Au is better preserved in the saprolite and secondary Au is found only in the ferruginous zone. Gold mobility is discussed more fully in Chapter V.3.

Fig. III.3-9. Examples of different morphologies of Au grains from the weathering profile, Bardoc mine, Western Australia. Derived from Freyssinet and Butt (1988b). (A) Etched primary grain. (B) Aggregate of spherules and near-octahedra of secondary gold. (C) Etched secondary grain. (D) Etched secondary particle with later spherules and pseudo-hexagonal plates adhering to it. (E) Aggregate of secondary euhedral crystals. (F) Etched secondary grain with later spherules adhering to it. (G) Xenomorphic primary grain. (H) Corroded primary grain with small secondary spherules.

*Model A * * [3]: complete or near-complete laterite profile buried*

The principal feature of this model is that the residual profile is buried by varying thicknesses of mostly post-lateritic colluvial and alluvial sediments so that there is no surface expression of mineralization. Prior to burial, unconsolidated soil and pisoliths will have been redistributed or removed and, locally, erosion to the saprolite may have occurred. Few examples are known because of the difficulty of exploration, but it appears that the residual profiles have most of the characteristics described for the previous models; however, they are protected from the direct effects of rainfall and may have been less strongly leached. Geochemical dispersion into the overburden from individual deposits is unlikely to be detectable, but if there are several deposits in an area of a few square kilometres that contribute to the provenance of the sediments, broad patterns may be present. It is also possible that surface horizons could contain superjacent hydromorphic or biogenic anomalies arising, for example, from evapotranspiration, but no cases have been described. Similar models apply to terrains in North America in which a deeply weathered, lateritic regolith is overlain by glacial overburden (Smith, 1987b).

Exploration can be very effectively carried out by drilling for geochemical haloes in the buried lateritic duricrust. In such situations, it is usually critical to establish criteria for distinguishing regolith stratigraphy and particularly for the recognition of residual horizons from units containing transported nodular and pisolitic laterite detritus. Drill spacings can be similar to the sample density required for the A * * [0] model, although to maximize information (e.g. for geological mapping), it is common practice to drill deep into the saprolite. In general, the drilling density required to detect geochemical haloes in lateritic duricrusts can be less than 1% of that required to detect haloes in saprolite because of their relatively large size. Further savings can result where the regolith stratigraphy is accurately logged; the choice of a specific horizon or facies permits fewer samples to be analyzed per hole.

Mount Keith disseminated Ni sulphide deposit, Western Australia: Ni, Cu, Pt and Pd in the regolith (A 1 Si [3])

The Mount Keith Ni sulphide deposit is concealed by up to 35 m of transported overburden above a complete lateritic profile of similar thickness. It was discovered in 1971 by pattern drilling on a magnetic anomaly, after earlier drilling beneath a ferruginous outcrop 3 km south along strike had found ultramafic rocks containing disseminated sulphides (Butt and Sheppy, 1975). The deposit lies within the Archaean Norseman–Wiluna greenstone belt, 400 km north-northwest of Kalgoorlie. It is a large, low grade body of disseminated sulphides (pentlandite and pyrrhotite) in a serpentinized dunite. Nickel mineralization is confined to a central zone in the dunite and has horizontal dimensions of 1675×100 –300 m. Published reserves indicate a resource of about 290 mt at 0.60% Ni, with a Ni/Cu ratio of about 60:1. The deposit also represents a low

Table III.3-2

Principal weathering horizons developed over mineralized serpentinitized dunite, Mount Keith, Western Australia (after Butt and Sheppy, 1975; Butt and Nickel, 1981)

Depth, m	Description
<i>Hardpan clay zone</i>	
0–12.3	Hardpan: weakly bedded, silica-cemented red to reddish yellow conglomeratic colluvium, with quartzose, chalcedonic and ferruginous pebbles in an earthy sand matrix. Ferruginous pisoliths and accretions dominant below 5 m; MnO ₂ on partings.
12.3–25.3	Clays: pale green-grey with yellow and dark red mottles. Pisoliths and nodules in upper 2 m and lower 2.5 m.
<i>Ferruginous zone</i>	
25.3–28.3	Ferruginous pisoliths: usually cemented, with up to 30% mottled interstitial clay.
28.3–39.0	Clays: grey, green and white, usually strongly mottled yellow, ochre, brown and red. Clays are matrix to ferruginous pisoliths and nodules. Probably transported above 35 m.
39.0–42.7	Massively ferruginized saprolite/lithorelics and nodules and some strongly mottled greenish clays, commonly with relic fabrics.
42.7–45.4	Manganiferous horizon: Mn oxide veins, nodules and mottles associated with ferruginous saprolite and nodules, green clays and silica pans.
<i>Quartz-dolomite zone</i>	
45.4–62.5	Weathered serpentinite with abundant mostly brown, silica (quartz) pans to 30 cm thick. Interstitial clays have bulk density 0.85–1.5. Silica and clays preserve primary fabrics, with altered green stichtite and iron oxides pseudomorphs after sulphides and serpentinitized olivine visible throughout.
62.5–66.1	Weathered serpentinite with occasional silica pans. Dolomite crystals in voids.
<i>Supergene zone</i>	
66.1–88.7	Partly weathered, slightly bleached grey-green serpentinite with secondary sulphides (violarite and pyrite) disseminated and in veinlets. Some sulphides replaced by iron oxides. Silica veinlets becoming rare. Stichtite pink at base of zone, green at top.
<i>Primary zone</i>	
Below 88.7	Black and green serpentinitized dunite with characteristic cumulate fabric. Disseminated pentlandite and pyrhotite; stichtite pink.

grade source of platinum group elements (PGE). Although these are present in concentrations far too low to be of economic significance except, perhaps, as a minor by-product, their distribution in the regolith is of interest (Butt, 1986).

The principal horizons and mineralogy of the regolith are given in Table III.3-2 and Fig. III.3-11. The contact between the transported and residual parts of the regolith, at about 35 m, is within the pisolitic ferruginous horizon and is indicated by the presence of coarse chromite in the sediments, derived from

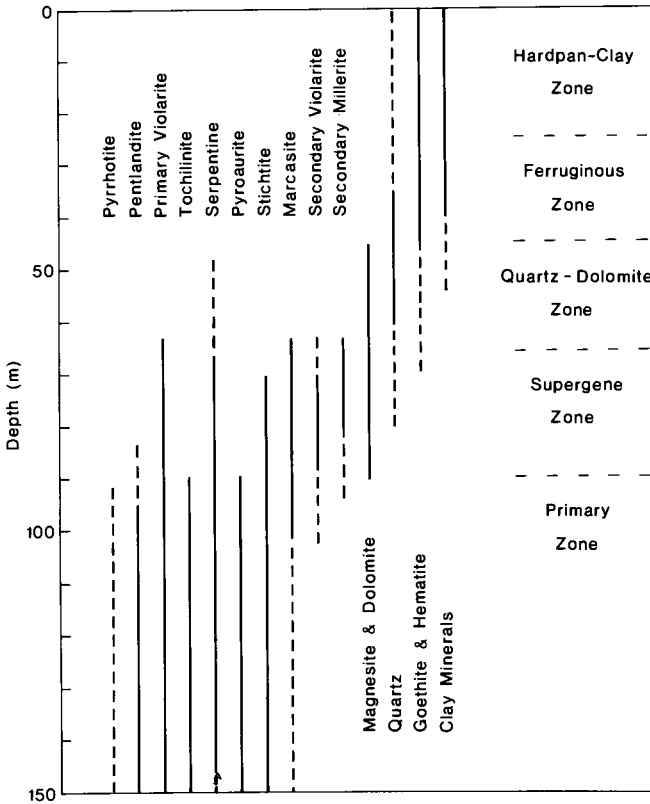


Fig. III.3-11. Mineralogy of the regolith over part of the Mount Keith dunite, Western Australia. Full lines indicate the range of maximum abundance; dashed lines indicate lesser abundance. Reproduced from Butt and Nickel (1981), *Econ. Geol.*, 76: Fig. 1, p. 1738.

ultramafic rocks upslope (Butt and Nickel, 1981). The overlying clays and silicified hardpan are probably derived from felsic rocks. The residual profile is typical of those formed on serpentinized dunites, with characteristic silicification of the saprolite. Silica is released during the weathering of the serpentine and, in the absence of Al, is precipitated as quartz. Other dunites at Mount Keith, however, contain 2–5% Al_2O_3 so that saponite and other smectites are formed instead. The silica has two important effects on the geochemical expression of the dunite and associated mineralization:

(a) it is a diluent, with the Ni, Cr, Fe and, in part, Cu contents in the silicified zone inversely related to that of Si;

(b) it is impermeable and acts as an aquiclude for a perched water-table. The zone immediately overlying the silicification is commonly greatly enriched in Mn oxides and coprecipitated Ni, Co, Cu and PGE.

The extent of the Ni sulphide mineralization was determined by drilling to clearly identifiable rock (usually 30 m or more deep) on centres at 15 to 100 m

Table III.3-3

Nickel, copper, platinum and palladium in the weathering profile, Mount Keith, Western Australia (data expressed as both mass and volume concentrations (from Butt, 1986))

	Num- ber	Mass concentration				Volume concentration				Pd/ Pt
		Pd	Pt	Cu	Ni	Pd	Pt	Cu	Ni	
		ppb	ppb	ppm	ppm	mg/ m ³	mg/ m ³	g/ m ³	g/ m ³	
Transported overburden	3	0-15	0-22	180	1030	0-38	0-55	500	2895	
Ferruginous zone	M 5	115	70	995	4760	325	195	2880	13980	1.65
	S	24	18	530	4745	87	54	1715	15180	
Manganiferous horizon	M 2	295	125	1505	21595	850	360	4300	61745	2.33
	S	41	89	360	6420	150	240	875	16170	
Quartz- dolomite zone	M 12	95	40	690	14420	140	80	1030	21010	2.35
	S	58	14	240	5520	65	35	240	5930	
Dolomite horizon	M 3	37	14	260	8275	80	30	550	17375	2.62
	S	17	7	22	875	35	15	45	1840	
Supergene zone	M 6	63	27	360	6020	150	65	870	14515	2.34
	S	17	6	53	1685	44	13	135	1440	
Primary zone	M 5	47	19	295	4495	120	50	760	11785	2.47
	S	22	8	105	1320	55	18	275	3700	

M = mean; S = standard deviation.

intervals on lines 150 or 300 m apart. Up to 10 samples, each representing 1.5 m, were analysed throughout each hole. In general, the main mineralized zone was found to be delineated by the 4000 ppm Ni and 300 ppm Cu contours in samples at 30 m depth. This depth does not, however, represent a constant horizon for sampling. Misleadingly low results were obtained where (i) the overburden was very deep, so that only the ferruginous horizon was sampled or (ii) the sample was silicified and strongly diluted. High results were obtained from the Mn-rich horizon. As a practical compromise, since several samples from each hole were analysed, the maximum value attained close to 30 m depth was used, assuming in part that this represented a constant, enriched horizon. This tended to broaden and intensify the anomaly, although very low values persisted in zones of strong silicification. However, the target was so large that these were of little significance.

Despite their low abundance, the distributions of Pt and Pd at Mount Keith indicate the behaviour of these elements in a lateritic environment. The mass concentrations of Pt and Pd steadily increase upwards through the regolith, reaching maxima in the Mn-rich horizon of the ferruginous zone (Table III.3-3). The carbonate-rich horizon overlying the supergene zone is an exception, where dilution by dolomite is possible. If concentrations are calculated isovolumetrically, however, the upward increase is less evident. There appears to be minor

enrichment of the PGE in the supergene sulphides and dilution in the carbonate horizon, but the concentrations in the saprolitic quartz-dolomite zone, whether silicified or as clays, seem little different from those in the primary zone. Platinum and Pd are enriched by a factor of seven in the ferruginous zone, particularly where it is Mn-rich. However, there has been some loss of fabric above 40 m, so that some of the enrichment may be due to residual concentration and compaction rather than absolute accumulation during isovolumetric weathering. Similar calculations suggest that Ni and, to a lesser extent, Cu are enriched about twofold in the supergene and quartz-dolomite zones and fivefold in the Mn-rich horizon. The Pd/Pt ratio remains more or less constant throughout the profile, but the lower value in the ferruginous horizon suggests some preferential loss of Pd.

Overall, the available data imply that Pd and Pt are relatively inert during weathering and that there is less scope for secondary enrichment of PGE than for Au. Nevertheless, some chemical mobility of these PGE is indicated at Mount Keith by:

- (a) minor enrichment in the supergene zone, probably associated with Ni in secondary sulphides;
- (b) enrichment and a lower Pd/Pt ratio in the ferruginous zone;
- (c) marked enrichment in the manganiferous horizon.

The enrichment with Mn is the most significant, for it suggests that these PGE can be concentrated in rather specific environments, presumably by coprecipitation or adsorption by Mn oxides in the same way as Ni, Co and Cu. Data for a similar profile over serpentized dunite at Gilgarna, near Kalgoorlie, show enrichment in the same zones, with concentrations of 5–10 ppb Pd, 30 ppb Ir in the ferruginous zone and 20–25 ppb Pd and 30 ppb Ir in the manganiferous horizon, relative to bedrock concentrations of 2 ppb Pd and 2 ppb Ir (Travis et al., 1976). Such part-residual (especially for Ir) and part-absolute enrichment is probably general in residual lateritic profiles and represents a possible exploration target for supergene PGE over suitable source rocks. The Co-Ni laterites at Bulong and Siberia, near Kalgoorlie, demonstrate that an appropriate host can develop. Discontinuous horizons up to 3 m thick contain, 1–20% Mn, 0.5–2.0% Co and 1–4% Ni (Elias et al., 1981); PGE data were not reported.

Because of the small number of sites examined in detail and the variability of PGE distributions, the existence of other enrichment zones, especially at past or present water-tables or redox interfaces, is not excluded. The weathering chemistry of Pt and, especially, Pd appears to be similar to Au (see Chapters I.5 and V.3), with mobility as thiosulphate and chloride complexes, hence precipitation may be expected at similar sites. (N.B. The platinoid nuggets associated with similarly silicified dunites in Ethiopia (Ottemann and Augustithis, 1967) and at Fifield, New South Wales, Australia, are thought to be residual, primary nuggets, rather than secondary.

Table III.3-4

Summary of resources in the regolith derived from the Mount Weld carbonatite, Western Australia (revised from Duncan, 1988)

Commodity	Tonnage Mt	Average grade%	Cut-off grade%
Phosphate (as apatite)	250	18.1	10.0
Niobium (Nb ₂ O ₅)	273	19.2	10.0
Tantalum (Ta ₂ O ₅)	145	0.9	0.5
Rare earths and yttria	6.2	17.2	10.0

Mount Weld Carbonatite, Western Australia (A 1 Si,Ca [3])

The Mount Weld carbonatite is intruded into an Archaean greenstone belt in the Laverton tectonic zone in the northeast Yilgarn Block, Western Australia. It is a 3–4 km diameter pipe-like intrusion of Proterozoic age that has been deeply weathered and buried by 15–70 m of transported overburden. Considerable reserves of REE, phosphates, Ta, Nb and Y have been concentrated in the regolith (Table III.3-4) and it thus broadly resembles Mabounié, Gabon (Laval et al., 1988; see p. 267), Araxa, Brazil, and other carbonatites in similarly deeply weathered terrains. The carbonatite is dominantly a fine to medium-grained sovite (i.e. calcitic), with subordinate beforosite (i.e. dolomitic) and intermediate lithologies (Duncan, 1988). The intrusion contains numerous variably assimilated xenoliths of wallrock and is surrounded by a 500 m alteration zone. Economically important primary minerals include apatite, magnetite, ilmenite, pyrochlore, monazite and zircon.

Glaciation during the Permian presumably removed any pre-existing regolith but left scattered tillites and fluvio-glacial sediments throughout the region. Subaerial weathering during the Mesozoic to mid-Tertiary resulted in the development of a deep lateritic regolith within which resistant minerals and immobile elements have been concentrated by residual and supergene processes. The in-situ regolith has been arbitrarily subdivided into lower residual and upper supergene zones above a relatively sharp and karst-like weathering front, 40–> 100 m below the present surface (Duncan, 1988; see Fig. III.3–12). The residual zone is characterized by resistant primary minerals concentrated by the solution of carbonate, with some minor ferruginization and silicification. Economic deposits in this zone include, in particular, considerable reserves of apatite-rich sands containing over 10% P₂O₅. The supergene zone is composed principally of secondary minerals, including clays, Al, Fe and Mn oxides, phosphates and REE oxides, but few primary minerals remain (Lottermoser, 1988). Niobium, Ta, REE, Y, Ba and Sr have been coprecipitated in crandallite, commonly pseudomorphing primary apatite and pyrochlore, and in the Fe and Mn oxides. There has also been some partitioning of the REE during weathering, with the lighter REE in secondary calcite and heavier REE in secondary monazite and churchite.

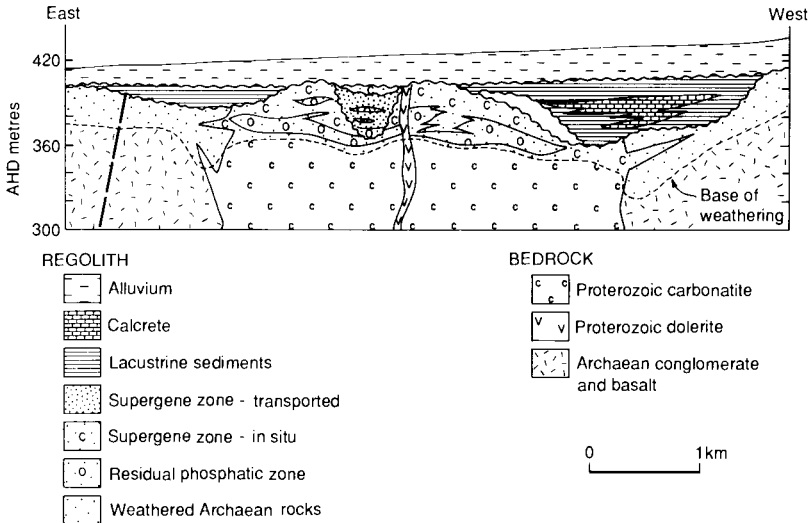


Fig. III.3-12. Section across the Mount Weld carbonatite, Western Australia, showing the principal horizons of the regolith. Modified after Duncan (1988).

In broad terms, the zonation and mineralogy of the regolith at Mount Weld resembles that at Mabounié, except that in the latter the apatite in the lower horizon is secondary. Mount Weld is also entirely concealed. Locally, the supergene zone has been reworked by sedimentary processes prior to burial under lacustrine clays and sands, groundwater calcretes, and alluvium derived from the erosion of lateritic regolith from low hills surrounding the carbonatite. Because of the sedimentary cover, the deposit has no surface geochemical expression and its discovery and exploration have been by geophysical surveys and drilling. It was discovered initially during the investigation of a prominent magnetic feature as part of a Ni exploration programme and was subsequently explored for Nb, U and, finally, apatite and REE. The sedimentary cover has also restricted the application of geophysical techniques. Variations in the abundance of magnetite in the carbonatite and, particularly, concentrations of residual and transported magnetite sands up to 12 m thick have interfered with the detailed interpretation of magnetic surveys. The presence of lacustrine sediments has affected gravity surveys, with reduced anomalies present over thick sequences of clays. The sedimentary cover is also an effective barrier for radiometric techniques, shielding gamma radiation and masking Rn emanation, both of which would be expected to give significant anomalies, especially where residual or supergene monazite are abundant. Groundwater He surveys, aimed at detecting He derived from the alpha-decay of U and Th, gave initially promising results as a regional exploration technique (Butt and Gole, 1986). The carbonatite appears to be central to a significant regional He anomaly (Fig. III.3-13). However, other

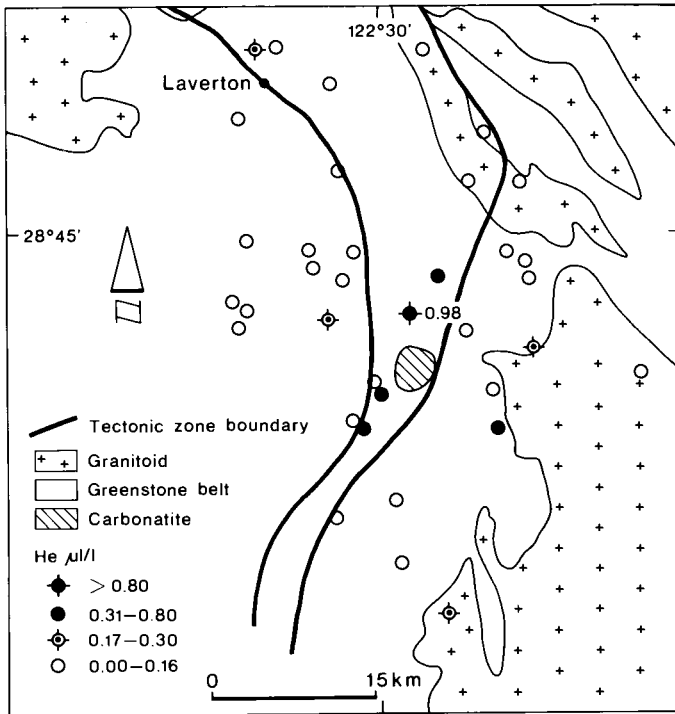


Fig. III.3-13. Regional groundwater He survey, Mount Weld area, Western Australia. Redrawn from Butt and Gole (1986).

anomalies of similar or larger dimensions and concentrations were found to be related to aquifer characteristics and, possibly, to basement faulting, and to have no direct exploration significance. Similarly, overburden gas He surveys gave no significant anomalies.

B-TYPE MODELS: PRE-EXISTING PROFILE PARTLY TRUNCATED

General

Partly truncated profiles are widespread in semiarid climatic regions. To some degree, all deeply weathered profiles in such regions are truncated, but B models refer to profiles that have been eroded to the mottled zone (or its equivalent) or deeper. In general, such models apply particularly in areas of moderate relief; the degree of truncation increases both with the relief and with greater aridity, so that in uplifted, dissected and very arid regions, only basal remnants of the pre-existing profile are preserved. The degree of truncation is dependent also on bedrock lithology, so that even where the relief is very low, deep saprolite may

be adjacent to almost unweathered rocks. The truncated profiles may (i) outcrop directly as saprolite, commonly surface-hardened by silica or alumino-silicate cementation, (ii) be covered by residual or semi-residual soil, for which saprolite is the parent material, or (iii) be buried beneath transported overburden of various types.

Dispersion characteristics

The principal B-type dispersion models are illustrated in Fig. III.3-14. An important feature is the small areal extent of surface geochemical anomalies. The lateral dispersion of many elements that occurs in the ferruginous horizon and soils derived from it, as described for A-type models, is commonly absent or poorly developed deeper in the profile. Accordingly, where saprolite outcrops or is the parent material for residual or semi-residual soils, dispersion haloes are very restricted, limited to a few metres or tens of metres from outcrop or subcrop of the source. Thus, the mechanical dispersion of fragments derived from the ironstone at Killara, Western Australia, is detectable for 50 m downslope in the coarse fraction only (Butt, 1979), and there is virtually no soil anomaly over the Teutonic Bore Cu-Zn deposit, also in Western Australia (Greig, 1983 and p. 336). There are, however, some important exceptions, which demonstrate that widespread dispersion haloes can be present:

(1) Mechanical, and perhaps some chemical, dispersion giving rise to very low contrast Pb anomalies in "soils" in braided drainage channels, e.g. from the Elura Pb-Zn deposit, New South Wales, Australia (Dunlop et al., 1983; see p. 340).

(2) Low contrast Au anomalies detected by bulk cyanide leaches (BCL or BLEG) of very shallow soils. Gold is presumed to have been transported by sheetwash, with anomalies apparently detectable up to 10 km distant from the source (G. Hall, Placer Pacific, verbal communication, 1989).

(3) Anomalies present in coarse fragments, or lag, scattered on the ground surface or in soils. Lag gravels consist of ferruginous nodules, pisoliths and lithorelics, quartz, silcrete, calcrete and other resistant materials. They are considered to be a "deflation" residue, left after the physical and chemical dismantling of the upper horizons of the profile and the removal of fine materials in solution or by sheetwash or wind, supplemented by particles moving upwards by a mechanism similar to that in vertisols (Fig. I.6-2). Lag is thus most abundant where profiles have been truncated to the mottled zone or upper saprolite. The use of lag as a geochemical sampling medium, described by Carver et al. (1987), is similar in approach to that of pisolith or nodule sampling and extends that technique to partially truncated regions. The procedure may detect extensive anomalies of low contrast and gives optimum results when ferruginous fragments are sampled selectively (see p. 345).

The widespread occurrence of transported overburden in semiarid regions, and the difficulty of recognizing residual and semi-residual soils, has encouraged

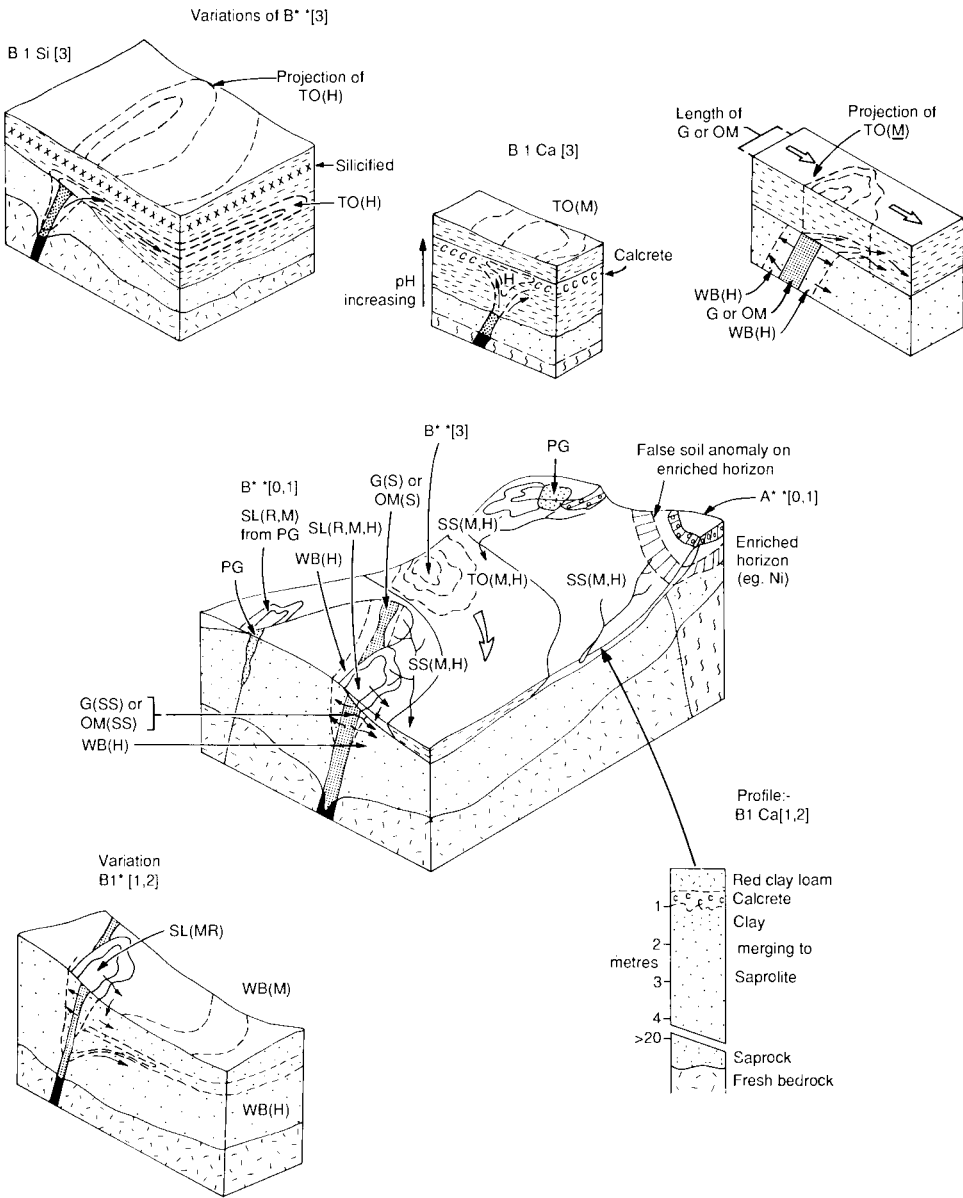


Fig. III.3-14. Block diagrams illustrating the principal B-type dispersion models in arid terrains. For abbreviations see Fig. III.1-1. Contours show general nature of anomaly; broken contours show subsurface anomaly. Derived in part from Butt and Smith (1980) and Butt (1987).

the use of drilling to identifiable saprolite for geochemical sampling. Although useful for geological mapping, this procedure ignores the broader target of any surface dispersion and relies on either intersecting weathered mineralization or

detecting haloes in the saprolite. For some elements, such as Au and Zn, leaching in the upper saprolite is so severe that even if weathered mineralization is intersected, it may be geochemically unrecognizable.

The detection and recognition of possible primary and secondary geochemical haloes in saprolite remains a challenge for the exploration of deeply weathered terrains in all climatic environments. The only examples of such haloes that have been described are for Au, deep in the profile, (e.g. Um Nabardi, see p. 343; Hannan South, Fig. V.3-4), Zn (Elura, see p. 340) and Pb (Teutonic Bore, see p. 336), apparently associated with past water-table levels. Lead dispersion has also been reported from dry savanna environments in Australia at Woodcutters, Northern Territory (Taube, 1978) and Thalanga, Queensland (Granier et al., 1989; see p. 236). Such haloes have mostly been recognized from drilling rather than in outcropping saprolite or derived soils, due to the effects of recent leaching, although the displaced Zn anomaly at Lady Loretta, Queensland (see p. 351) may relate to dispersion during past humid periods during which Pb, in contrast, was immobile. In the absence of usable secondary haloes in soils or upper saprolite, drilling at intervals as close as 5 m across strike has to be employed (e.g. see Transvaal Au deposit, p. 351; for Ni, see Leggo and McKay, 1980). In such circumstances, overlapping angle drilling is the most effective procedure.

Conversely, secondary enrichments of base metals are a feature of deeply weathered arid terrains and may pose problems in exploration for sulphide mineralization. Copper, Ni and Pb may be concentrated in ironstones which then resemble gossans. Gossans can generally be identified by their pathfinder element association, as discussed in Chapters II.1 and II.2. Nickel may also be concentrated at the base of the mottled zone or in the saprolite over ultramafic rocks. Such lateritic Ni enrichments, similar to those found in more humid areas, may reach 1–2% or more; they can give rise to soil anomalies where erosion has exposed the enriched horizon or may be intersected by drilling to the saprolite. Anomalies related to Ni sulphide mineralization may be distinguished by their distribution patterns, higher Cu/Ni ratios and, in ironstones, by elevated PGE contents.

*Models B * * [0], B * * [1] and B * * [2]. Partly truncated profile outcropping at surface or with a cover of residual and semi-residual soils*

The B * * [0] model describes the situation where gossans, oxidized mineralization and saprolite outcrop, with little or no cover of soil or other overburden. Gossan search has proved to be the most effective exploration technique and has contributed directly to the discovery of many sulphide deposits. The geochemical signature of the outcropping gossan or oxidized mineralization depends on the degree of truncation. Where truncation has been severe, exposing zones deep in the profile, the signature is simple, with high concentrations of ore-related elements. There may even be some supergene enrichment, giving an over-opti-

mistic estimate of primary grade. Where truncation is less far advanced and upper, leached zones of the profile are exposed, base metal concentrations are strongly depleted to levels similar to or lower than those in secondarily enriched ironstones (pseudogossans), so that multielement analyses and statistical interpretation may be necessary to aid identification. Rock-chip surveys may also be applied, but secondary dispersion haloes are generally restricted, so that close sampling intervals are necessary. Such surveys are inevitably biased towards more resistant units.

The situations represented by models B * * [1] and B * * [2] are commonly associated with that of the previous model B * * [0], but are areally more extensive. Search for small outcrops or semi-residual gossan float remains an important exploration procedure but soil anomalies provide a larger and more reliable target. Soils may contain fragments of gossan, oxidized mineralization and/or material derived from saprolites containing relict primary and secondary haloes, or be the host for elements undergoing active secondary dispersion. Where the weathering profile is deep and strongly leached of target and pathfinder elements (e.g. Cu, Zn, Ni, U, Ag, Cd, In, Mo) only relatively weak soil anomalies can be expected and elements such as As, Sb, Cr, Au, Pt, Sn, W and V that are chemically less mobile or are held by resistant minerals may be a better guide. Where erosion is advanced, outcropping or subcropping weathered mineralization is less strongly leached, so that strong geochemical anomalies can be expected for most ore-related elements. Strong Ni anomalies, however, may reflect lateritic enrichments in saprolites on ultramafic rocks.

Presently active dispersion is commonly mechanical, with the strongest anomalies shown by coarse fractions that contain gossan fragments, enriched lithorelics or lag gravels. Nevertheless, anomalies are also indicated by fine fractions composed of clays and fine Fe oxyhydroxides, perhaps reflecting primary or secondary hydromorphic haloes in saprolitic wallrocks. In comparison, the soil anomaly at the Killara pseudogossan, Western Australia (Butt, 1979) is present only in the coarse fractions which contain ironstone fragments. The Cu in this ironstone (1100–1700 ppm) is a spurious secondary concentration and the clays derived from the wallrocks have background Cu contents. High concentrations of Ni in fine fractions of soils in ultramafic terrains, however, may be derived from lateritic enrichments in exhumed saprolites.

Active hydromorphic dispersion into soils can sometimes be demonstrated, particularly for Au. Thus, low contrast Au anomalies are present in the top 1–2 m of soils, although underlying saprolites may be depleted to depths of 7–20 m. Such Au anomalies are commonly, but not always, associated with calcareous soils and pedogenic calcrete. The surface enrichment of Au is illustrated by the case histories for Mararoa (see p. 381), Bounty (see p. 351) and Mount Pleasant (see p. 365), and discussed further in Chapter V.3. Exploration in calcrete terrain is considered more fully later in this chapter (see p. 375).

Many soils in arid environments are semi-residual, consisting of a mixture of residual soil and introduced, typically fine-grained, aeolian and water-borne

material. Consequently, the coarse fraction of the soils or the lag gravels are commonly sampled. This procedure is adequate in eroded lateritic terrain in which these samples are usually ferruginous. In some instances, such as where the introduced materials are coarse sands, or residual clays remain, or hydromorphic dispersion is possible, a fine fraction, possibly analysed by partial extraction, may be more suitable (Mazzucchelli, 1980). Similarly, fine ($< 160 \mu\text{m}$), fractions have been used in very arid areas in Saudi Arabia where no lateritic remnants remain (Salpeteur and Sabir, 1989; see p. 370).

Lag sampling is particularly appropriate in partly truncated regions with residual and semi-residual soils. Such regions commonly have a surface pavement of coarse fragments in the range 1 mm to over 25 cm, consisting mainly of ferruginous and siliceous pisoliths, nodules and lithorelics, quartz and calcrete. A coarse (e.g. 2–6 mm) fraction of this gravel can be used as an exploration sample medium that, in many ways, is equivalent to pisoliths and nodules used in areas where lateritic profiles are complete. It shares the advantages of pisolith sampling in that anomalies are commonly larger and of higher contrast than those in soils, factors which outweigh the disadvantages of slow sampling and higher cost of sample preparation.

Several case histories illustrating the use of lag in exploration for Au, Ni and base metals in semiarid and savanna regions in Australia are described by Carver et al. (1987)—see p. 346. They suggest collection of the surface layer using a plastic dustpan and brush, sieving, crushing to minus $75 \mu\text{m}$ and analysing for the total metal content. The concentrations of many elements in lags are controlled by the Fe and/or Mn content, so that it is desirable either to hand pick Fe-rich material for analysis or to calculate regressions to correct for sample variability. An equivalent approach was used by Dunlop et al. (1983) who separated the coarse, ferruginous fraction (1.18–2.12 mm) from soils in drainage channels near the Elura Pb-Zn-Ag deposit, New South Wales, Australia (see p. 340). Contrasts were improved by regressing for Fe content and plotting residual Pb contents.

Teutonic Bore Cu-Zn-Ag-Pb deposit, Western Australia (B 1 0 [0,1])

The Teutonic Bore deposit was discovered in 1976 by regional gossan sampling and mined from 1980 to 1986. It was located 300 km north of Kalgoorlie in the Wiluna–Norseman Greenstone Belt of the Archaean Yilgarn Block of Western Australia. The deposit occurred near the base of a series of altered tholeiitic metabasalts, close to a contact with a suite of felsic volcanics. It was a steeply dipping lens of massive sulphides, 280 m long, 320 m down dip and up to 30 m thick; it contained 1.4 Mt at grades of 4.16% Cu, 16.4% Zn, 1.22% Pb and 203 g/t Ag. The lens was underlain by an extensive zone of stringer mineralization and intense hydrothermal alteration extending for 100–300 m into the footwall. The massive orebody consisted mainly of pyrite, chalcopyrite, sphalerite and galena, minor arsenopyrite and argentiferous tetrahedrite, and cassiterite as an important accessory mineral. Alteration of the footwall resulted in

replacement by quartz, sericite, chlorite and carbonates and is reflected by depletion of Na_2O , CaO and Sr and enrichment of base metals K_2O , Ba , F , Fe and MgO . The weathering of the sulphides and the characteristics of the primary and secondary dispersion haloes have been described by Greig (1983) and Nickel (1984). (See also case history 14A, Chapter II.2; Table II.2–18.)

The deposit was situated in a locally flat, topographically low site in a terrain of low to moderate relief. It was weathered to 70–80 m depth, well below the present water-table at 35 m. The primary ore was weathered to a typical gossan profile consisting of a basal zone of secondary ore minerals overlain by leached oxides and a surface gossan which outcropped intermittently over a strike of 50 m. At the surface, the gossan was strongly leached of the principal ore elements, although the mean contents of Pb (0.68%, present as plumbogummite) and Ag (15 ppm) remain anomalous (Table III.3-5). The concentrations of minor elements, especially As , Sn , Bi and Sb , however, are highly diagnostic of massive sulphides and typify the value of analysing for a suite of pathfinder elements during base metal exploration. The profile is partly truncated and much lower concentrations of all these elements would be expected if it were more complete. The effects of leaching extend to at least 16 m depth, below which a variety of secondary and relict primary minerals are present. The heterogeneity of the mineral assemblage accounts for the high variability in the composition of the gossan.

Secondary dispersion of selected elements about the massive sulphide deposit was studied using samples collected at 10 m intervals on 7.5 m benches during the course of open pit mining (Fig. III.3-15). The data show Cu and Zn to be severely depleted in the top 10–20 m over both the massive and stringer mineralization, with concentrations commonly < 100 ppm in the surface horizons. The 250 ppm Cu and 500 ppm Zn contours define the original sulphide zones in the saprolite; lateral dispersion appears to have been minimal, extending only 15–40 m into the hanging wall (250 ppm Zn contour). In contrast, the As and Pb anomaly associated with the sulphides continued to the surface. Lead showed a distinct lateral dispersion anomaly at about 20 m depth, extending 200 m laterally into the hanging wall (250 ppm). A similar anomaly may have been present in the footwall but this was not sampled; there is, however, an enrichment at this level over the stringer mineralization. This anomaly is ascribed to dispersion and reprecipitation associated with an earlier, higher water-table (Greig, 1983). It is analogous to the Au enrichments observed in this region and may have been similarly formed by chloride-rich groundwaters. The potassic enrichment in the footwall alteration zone also persisted to surface, due to the resistance of sericite during weathering but the other alkalis have been leached. The results illustrate that base metal sulphides in this environment present a small, low contrast anomaly expressed in the near-surface mainly by relatively immobile elements in the ore and primary alteration zone. Apart from some dispersion of Pb and As , there is no enlargement of the target and, if exploration depends on saprolite sampling, drilling to at least 20 m is necessary to intersect

Table III.3-5
Element concentrations at various depths in the gossan profile at Teutonic Bore, Western Australia (from Nickel, 1984)

Depth	Number	Fe ₂ O ₃ %	Cu%	Zn%	Pb%	Sn ppm	Ag ppm	As ppm	Sb ppm	Bi ppm
Surface gossan	R 12	40.0-92.6	0.02-0.17	0.04-0.15	0.11-2.92	60-6400	6-32	630-6650	70-3000	<1-250
	M	76.1	0.10	0.08	0.68	2730	15	3100	725	37
	S	16.1	0.05	0.04	0.85	2145	7	2020	805	70
2-16 m	R 10	3.7-49.9	0.01-0.32	0.02-0.21	0.06-1.30	150-4690	<1-14	175-1340	115-2130	<1-150
	M	25.2	0.06	0.08	0.46	1240	14	640	940	45
	S	21.1	0.09	0.07	0.38	1385	15	395	895	50
21-34 m	R 18	2.1-68.9	0.01-1.89	0.02-5.44	0.02-21.9	150-6805	4-2420	40-2400	85-1470	<1-515
	M	26.1	0.37	0.48	3.67	2275	265	520	570	75
	S	18.9	0.43	1.24	5.77	1905	590	555	570	130
43-48 m	R 21	4.6-58.9	0.08-4.55	0.06-0.47	0.24-10.31	4-5050	5-320	420-8670	2-4170	1-210
	M	33.0	0.68	0.23	3.10	1180	37	2185	690	50
	S	15.2	0.99	0.10	2.56	1315	65	2475	890	50
59-83 m	R 20	15.2-62.1	0.03-0.84	0.07-0.85	0.15-7.44	145-3760	9-905	400-8750	65-915	<1-800
	M	36.5	0.32	0.29	1.81	1020	90	3085	460	70
	S	13.5	0.29	0.27	2.03	880	195	2975	270	205
Primary one	R 12	11.7-25.1	1.20-19.5	0.20-27.6	0.01-2.70	135-3255	65-1825	210-2510	29-980	<1-2545
	M	17.1	7.6	11.0	0.8	935	385	800	270	315
	S	4.5	5.5	9.3	0.9	835	490	595	270	710

R = Range; M = Mean; S = Standard deviation.

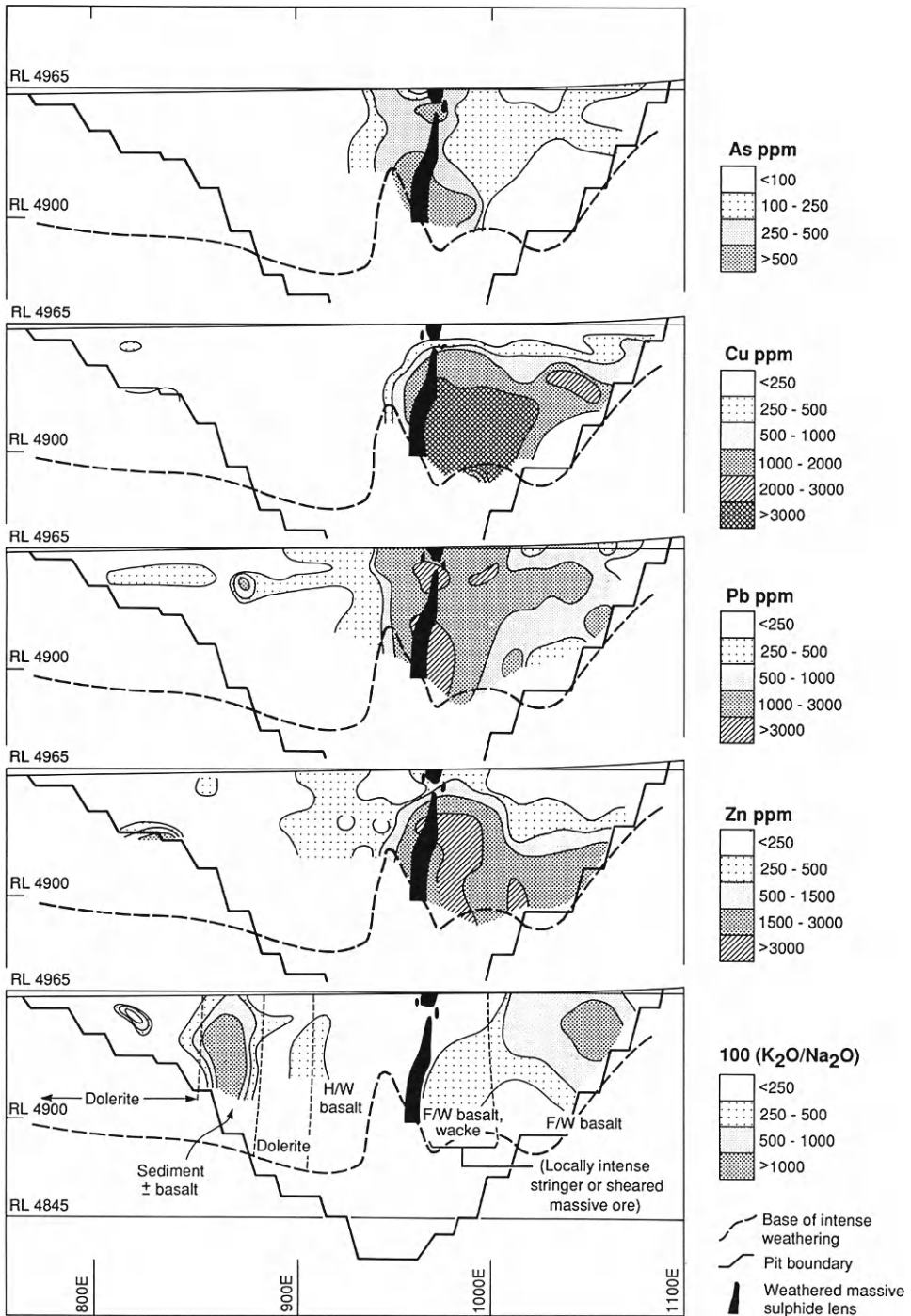


Fig. III.3-15. Distribution of As, Cu, Pb, Zn and the 100(K₂O/Na₂O) ratio on a section across the Teutonic Bore Cu-Zn deposit, Western Australia. Modified after Greig (1983).

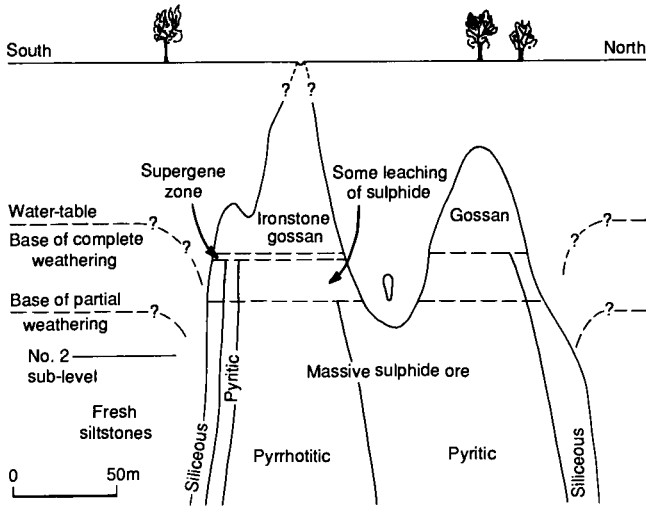


Fig. III.3-16. Longitudinal section through the Elura orebody, New South Wales, Australia, indicating the principal weathering zones. The deposit does not outcrop. Redrawn from Taylor et al. (1984).

less strongly leached weathered mineralization. No lag or soil sampling was undertaken at the site.

Elura Zn-Pb-Ag deposit, Cobar, New South Wales, Australia (B 1 Ca [2,3])

The Elura deposit, 43 km north of Cobar, was discovered in 1972 by soil and saprolite (RAB drilling) geochemistry and ground geophysical surveys following an airborne magnetic survey. It is hosted by the Lower Devonian CSA Siltstone Unit of the Cobar Supergroup and contains over 27 Mt of sulphide-rich ore (pyrite, pyrrhotite, sphalerite and galena, with minor chalcopyrite, arsenopyrite and tetrahedrite) at a grade of 8.3% Zn, 5.6% Pb and 150 g/t Ag. The mineralization forms a vertical pipe, 200 × 120 m, which bifurcates towards the surface and has only a minor suboutcrop of ferruginized wallrock (Dunlop et al., 1983; Taylor et al., 1984; Fig. III.3-16). The deposit is situated in the gently undulating Cobar pediplain, which is developed on a lateritic weathering surface of possible Miocene age. Outcrop is poor and weathered bedrock is covered by 2 m of red earths that contain layers of Fe-rich gravels, particularly in the ill-defined drainage channels.

The sulphides have been completely oxidized to 100 m, leading to local ferruginization of the host rocks which are themselves weathered to 75–120 m; the water-table is at 80 m. There is a well-developed gossan profile, with strong sulphide and oxidate supergene enrichment of Cu, Ag, Tl, As, Bi, Pb, Ba, Mo and Hg (Table III.3-6; see also case history 32, Chapter II.2 and Table II.2-33). The subcropping gossans are strongly anomalous in Pb, As and Sb, moderately in Cu,

Table III.3-6

Compositions of fresh and weathered ore and wallrocks, Elura, New South Wales, Australia (from Taylor et al., 1984)

Horizon	Number	Fe ₂ O ₃ %	Ag ppm	As ppm	Bi ppm	Cu ppm	Hg ppm	Pb ppm	Sb ppm	Sn ppm	Zn ppm
<i>Oxide zone</i>											
Surface ironstone	5	71.5	<1	1.3%	<1	100	0.04	4.3%	600	5	500
Ironstone gossan	14	77.2	<1-100	2.2%	<1	900	1.5	5.5%	1000	1-300	1600
<i>Supergene mineralization</i>											
Oxidate	1	15.7	3000	1.3%	<1	1400	420	56%	9000	900	700
Sulphide	1	34.3	1110	2.24%	95	19.1%	130	11.6%	825	12	1700
Sulphide	1	50.0	105	2.82%	4	2.28%	20	7.5%	935	18	6400
<i>Primary mineralization</i>											
Sulphide ^a ore	42	21.4-71.5	130	5500	4-42	1730	5-100	5.8%	<200-1200	25-120	8.4%
<i>Siltstone wallrocks</i>											
Regional background	26	5.40	-	10	8	25	0.0010	45	<5	<3	75
Weathered	42	6.23	-	<10	1	30	0.0017	32	0.8	-	115
Fresh											
Local background	19	2.60	-	<10	5	18	0.0010	38	5	8	50
Weathered	30	28.8	-	17	18	53	0.0005	60	5	8	275
Fe bands	26	5.92	-	<10	5	30	0.0030	35	<5	6	220
Fresh											

^a Ag, As, Cu, Pb, and Zn: mean of > 1000 samples.

- not determined.

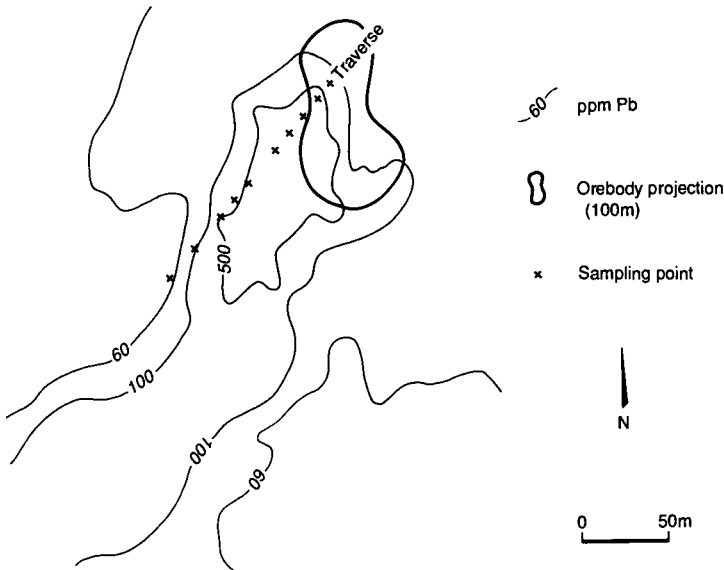


Fig. III.3-17. Lead distribution in near-surface weathered bedrock, Elura Zn-Pb-Ag mine, New South Wales, Australia. The dispersion pattern defines the trend of an inferred palaeodrainage channel. Traverse locates sample sites of Fig. III.3-18. Modified after Taylor et al. (1984) using data from geochemical survey by the Electrolytic Zinc Co. of Australasia Pty. Ltd.

Zn, Mo and Sn, and depleted in Ag, Bi, Cd, Hg and Tl. The siltstone host rocks consist of an assemblage of quartz, muscovite, chlorite, albite and calcite. Alteration near the orebody has led to the destruction of albite and the replacement of chlorite by ankerite and siderite. The weathered assemblage is quartz, muscovite, goethite, hematite, anatase and minor halite. Iron oxides form conformable and transgressive bands up to 0.5 m thick in the saprolitic siltstones. The bands average 29% Fe_2O_3 and have slightly anomalous concentrations of As, Bi, Co, Cu, Ni, Pb, Zn and Mn. These anomalies persist over 300 m from the orebody and are thought to be derived from a primary halo (Taylor et al., 1984).

In addition to the magnetic anomaly, the deposit was defined during exploration by a distinctive Pb anomaly, in shallow saprolite, that was 200 m wide (60 ppm contour) extended over 600 m to the southwest (Fig. III.3-17). The anomaly follows a drainage channel and Dunlop et al. (1983) subsequently showed that anomalous Pb concentrations are also detectable in the soils in these channels, giving a fan-shaped dispersion train of at least 5 km. The anomaly is shown by the ferruginous coarse fraction (1.18–2.12 mm) of the channel soils and represents mechanical dispersion during the formation and dissection of an earlier, possibly lateritic, surface horizon. The sample medium is essentially the same as that recommended for lag surveys (see p. 346). It offers

potential as an effective procedure for exploring interfluvial areas, although less suited for areas having a thicker transported cover in which the relationship between soil components and bedrock is more tenuous and dilution is greater.

The distribution of seven chalcophile elements in shallow weathered bedrock downslope from the orebody is illustrated by the drill traverse along the drainage (Fig. III.3-18). The concentrations of all elements are mostly at or below background in the near-surface (0–1 m) horizons. However, concentrations increase with depth and at 5–6 m each element is markedly anomalous. The anomalies for As, Bi, Hg, Pb and Sb are strongest 50–100 m from the orebody, coinciding with the development of hidalgoite ($\text{PbAl}_3(\text{AsO}_4)(\text{SO}_4)(\text{OH})_6$). Copper and Zn are more widely dispersed, implying greater mobility. There is little information about dispersion deeper in the saprolite. Dispersion into the wallrocks appears to be minimal, being restricted to a zone of ferruginization about 1 m wide. High concentrations of Mn and Zn (≥ 2500 ppm) occur at the water-table at least 350 m from the orebody. The Pb content also increases, but less markedly, whereas As, Cu and Ag are not enriched. There is no evidence for Pb dispersion or enrichment at palaeo-water-tables, as at Teutonic Bore (see p. 337).

The element distribution in the weathered zone has been attributed to dispersion during at least two distinct episodes (Taylor et al., 1984): *firstly*, during the deep weathering under humid conditions associated with the formation of the Cobar Pediplain and *secondly*, during subsequent arid periods continuing to the present. Sulphide oxidation during the earlier episode resulted in acid conditions and strong leaching of Zn, Bi, Cd, Tl and, to a lesser extent, Ag, Ba, Cu and Hg from the gossan. Because of the low carbonate content of the siltstones away from the ore and alteration zone, the acid solutions would have been little buffered and except where the ferruginized wallrocks in contact with the gossan are enriched, these elements have been widely dispersed. The lower water-tables and alkaline, saline groundwaters caused by the gradual change to aridity led to the dissolution of previously less mobile elements such as As, Sb, Ba, Pb, Hg and Sn from upper zones of the gossan and their concentration at the base in the supergene oxidate zone as chloride, carbonate and sulphate minerals. Ore elements in fragments of eroded gossan and ferruginized wallrock in drainage sediments were similarly mobilized by these saline groundwaters and reprecipitated in the upper saprolite. The Zn concentration at the water-table may have been derived from downward leaching of a previous dispersion halo or be related to still active dispersion from weathering sulphides. Mercury, a potentially useful pathfinder element present in the ore and the primary halo, has been very strongly leached by the chloride-rich groundwaters.

Gebeit and Um Nabardi Au deposits, Sudan (B 1 Ca [1,2])

The Gebeit and Um Nabardi gold mines, situated about 700 km from Khartoum in the Red Sea Hills province of northeast Sudan, are two of numerous deposits that have been worked since ancient times. The province is a late Proterozoic mobile belt, composed of andesitic volcanoclastic rocks, intruded by

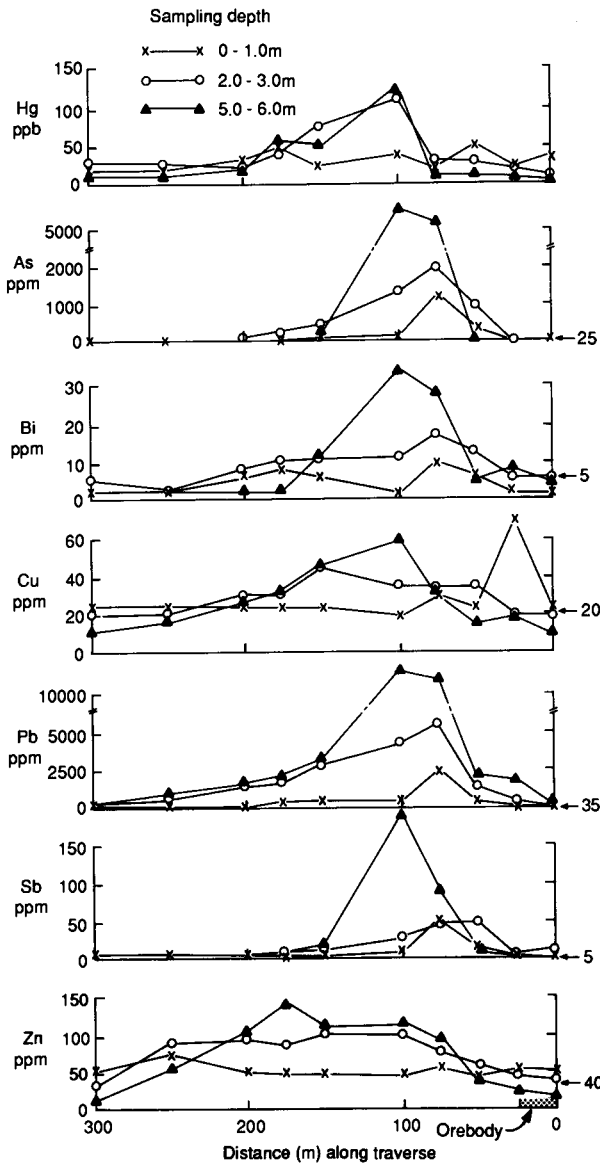


Fig. III.3-18. Distribution of some important ore metals at various depths in weathered bedrock southwest from the Elura Zn-Pb-Ag deposit (see Fig. III.3-17 for location). Arrowed values indicate background concentrations. Redrawn from Taylor et al. (1984).

a variety of igneous rocks. Gold mineralization is found with quartz veins in shears, commonly close to the andesite-rhyolite contacts. Pyrite, arsenopyrite, chalcopyrite, galena and scheelite are accessory minerals and some wallrocks

have pyritic and carbonate alteration (Fletcher, 1985). The region was subjected to severe planation prior to the deposition of the flat-lying Cretaceous Nubian Sandstone, which is itself largely eroded and now mainly occurs as remnant outliers.

The province forms a plateau sloping westwards from an escarpment 25–50 km inland from the Red Sea. The escarpment, which rises to 500–1000 m and locally to 2200 m, is deeply dissected to the east, but on the plateau to the west, there is a partly truncated lateritic regolith, 30 m or more thick. Fletcher (1985) implies that this regolith is present beneath the Nubian Sandstone and that the weathering predates deposition. However, it is possible that weathering proceeded *through* the Sandstone cover, as is observed in other terrains (e.g. through Proterozoic and Permian cover in the northern Yilgarn Block, Western Australia). Nevertheless, it appears that the cover rocks have helped to preserve the regolith, in contrast to most other regions that now have a climate of such extreme aridity. Accordingly, dispersion patterns in the regolith appear to be independent of the present topography and weathering regime.

Regional exploration of the region has been by geochemical and heavy mineral surveys of wadi (drainage) sediments, which could therefore potentially locate alluvial as well as primary and supergene mineralization. Soil sampling was used for more detailed exploration. At Gebeit, for example, much of the surface is covered by 1 m of scree and soil. The soil was sampled on 50 × 100 m centres and the minus 80-mesh (180 μm) fraction analysed for Au, As, Cu, Pb and Zn; ranges and background data are given in Table III.3-7. Copper, Pb and Zn were not significantly anomalous but the Au distribution delineated some widespread anomalies (> 100 ppb) over a 1000 × 2000 m area. The As distribution is more restricted and intense and is closely related to the known Au mineralization. The wider pattern recorded for Au reflects greater dispersion, probably related to chemical mobility during earlier weathering episodes. The effects of such mobility are illustrated at the Um Nabardi mine, where Au has been concentrated in a subhorizontal zone at the water-table, at about 50 m depth (Fig. III.3-19). This is similar to concentrations in semiarid environments in Western Australia (Butt, 1989b; see Chapter V.3).

Table III.3-7

Range and background concentrations of selected elements in soil samples, Gebeit mine, Sudan (from Fletcher, 1985)

Element	Minimum	Maximum	Background
Au ppb	100	54450	100
As ppm	5	2450	25
Cu ppm	20	220	40
Pb ppm	5	50	5
Zn ppm	35	350	65

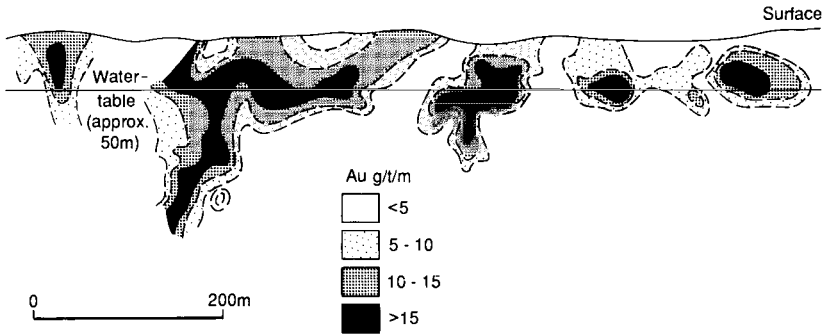


Fig. III.3-19. Section along the main vein of the Um Nabardi gold deposit, Sudan, showing accumulation of gold at the water-table. Modified after Fletcher (1985).

Lag sampling in gold and base metal exploration

In partly truncated terrains in which the lateritic ferruginous horizon has been eroded, the coarse fragments of the desert pavement (lag) commonly relate quite closely to underlying bedrock and can substitute for pisoliths and nodules as a sample medium. Carver et al. (1987) described several case histories illustrating the use of lag sampling in a range of environments in Australia, comparing data from a standard 2–6 mm fraction with those from soil samples. The lag samples were collected from the land surface, swept from an area of up to 1 m², sieved, crushed and analysed for their total metal contents. In general, the geochemical response comes from elements held by the ferruginous components, which include pisoliths, nodules and fragments of lateritic duricrust (cuirasse) and gossan. Accordingly, the best results are obtained if this material is preferentially sampled or, if this is not possible, the data are normalized for Fe content.

1. Minyari Au prospect, Paterson Province, Western Australia (B 1 Si [2])

The area is within the Great Sandy Desert and a truncated lateritic regolith developed on Proterozoic sedimentary rocks and Permian tillites is overlain by aeolian sand. The sand is about 5 m thick, with regionally extensive parallel dunes up to 15 m high occurring at 1 km intervals. Where the sand cover is thin, both soil and lag sampling revealed prominent Au, As and Pb anomalies over stockwork Au-quartz mineralization in siltstones (Fig. III.3-20). The lag samples contain coarse pisoliths, together with finer particles of lateritic material, weathered bedrock and quartz, possibly redistributed from termitaria. The lag gives a broader anomaly than the soil, particularly for Au, and is expected to give more persistent results where the sand cover is thicker. Even where there is no transported cover, lag sampling tends to give a broader anomaly: Carver et al. (1987) found that lags (2–6 mm) collected on a 50 × 400 m grid gave an

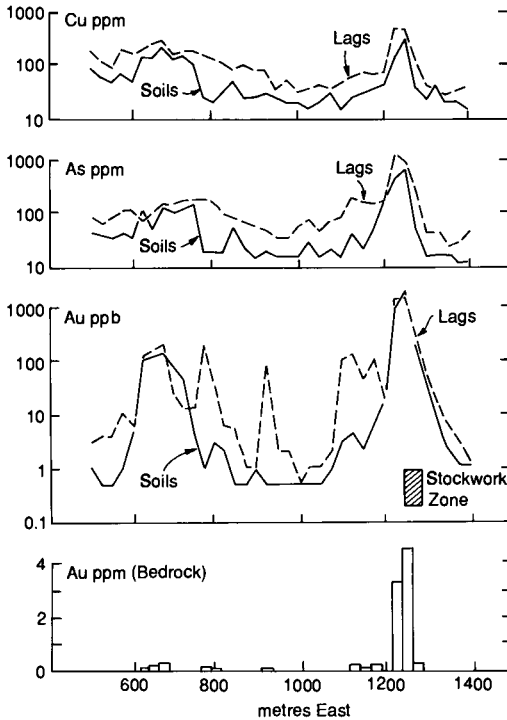


Fig. III.3-20. Traverse comparing Cu, As and Au concentrations in lag (2–6 mm) and soil (minus 130 μm) samples, Minyari Au prospect, Paterson Province, Western Australia. Redrawn from Carver et al. (1987).

anomaly of 1.7 km² compared to 0.5 km² in soil (minus 6 mm), both defined by the 5 ppb Au contour.

2. Blair Ni deposit, Kalgoorlie area, Western Australia (B 1 Ca [0])

Nickel sulphide mineralization (pyrrhotite, pentlandite and minor chalcopyrite) in the region has well-developed gossan profiles (Nickel et al., 1974; Fig. II/i-2). At this site, the supergene violarite-pyrite zone occurs at 80–140 m and the mineralization outcrops as a discontinuous ferruginous and siliceous gossan 0.5 m wide for about 250 m on a low ridge, 8–10 m above an alluvial plain. Lag (2–6 mm) and soil (minus 200 μm) sampling demonstrated that Ni and Cu derived from the ultramafic host rocks and the mineralization (or gossan) are preferentially concentrated in the coarse fraction (Fig. III.3-21). Such concentration in the plus 2 mm fraction of soils was noted by Mazzucchelli (1972) at Kambalda (see p. 362) and lag sampling is an application of this observation.

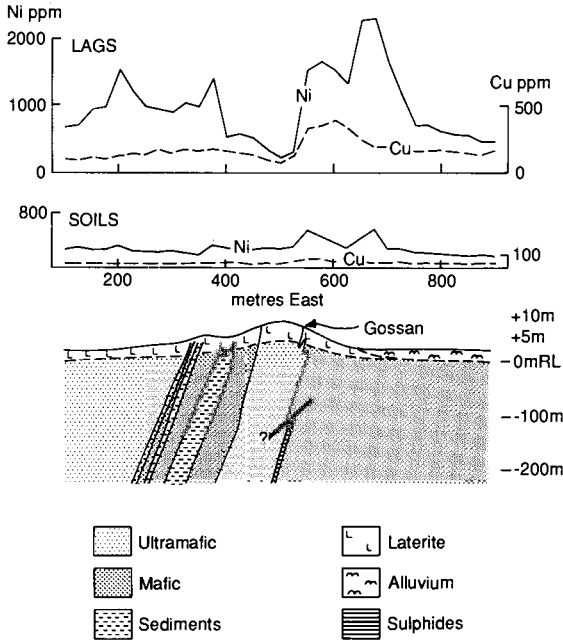


Fig. III.3-21. Traverse comparing Ni and Cu concentrations in lag (2–6 mm) and soil (minus 200 μm) samples over the Blair Ni deposit, Kalgoorlie area, Western Australia. Redrawn from Carver et al. (1987).

3. Dora Creek Pb-Zn prospect, Pine Creek Geosyncline, Northern Territory, Australia (B 1 0 [0])

The area consists of extensive plains with a few low hills of outcropping, weathered Proterozoic sedimentary rocks. The regolith is over 30 m thick and consists of a truncated lateritic profile covered by 10–100 cm thick residual lithosols. There is a surficial lag of pisoliths, quartz and ferruginous shales and siltstones, all with desert varnish. A detailed lag and soil survey close to Pb-Zn mineralization showed a good response in all size fractions, especially the plus 2 mm fraction, but the lag gave a broader anomaly with generally higher concentrations (Fig. III.3-22).

Letaba Cu-Zn deposit, northern Transvaal, South Africa (B 1 0 [1,2])

Mineralization in the vicinity of the abandoned Letaba Cu-Zn mine is situated in a flat plain in which the regolith varies from 2 to 50 m in depth. There is intermittent gossan outcrop above the mineralization, but in many places along strike the residual profile is overlain by transported overburden, the contact being marked by a stone line. Geochemical data (Frick et al., 1989) suggest colluvial overburden, displaced downslope by as much as 200–300 m. The area

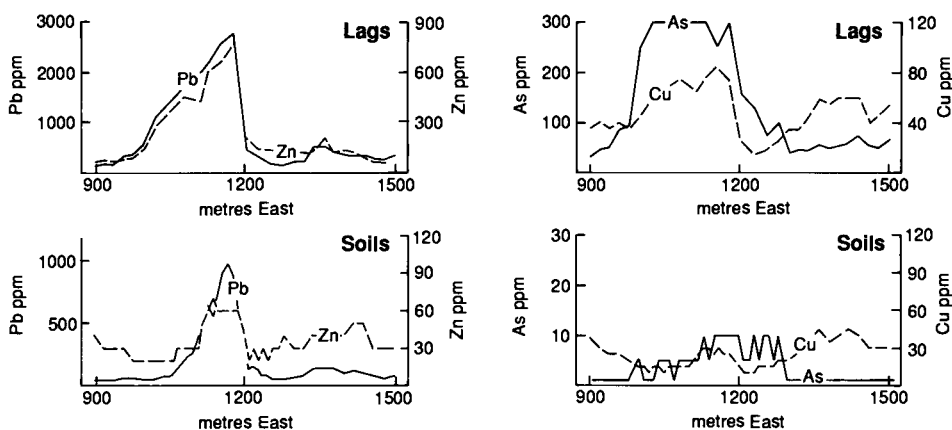


Fig. III.3-22. Traverse comparing Cu, As, Pb and Zn concentrations in lag (2–6 mm) and soil (minus 80 μm) samples, Dora Creek Pb-Zn prospect, Pine Creek Geosyncline, Northern Territory, Australia. Redrawn from Carver et al. (1987).

now has a semiarid seasonal climate and the deep weathering and stone-line formation (see p. 224 and 275) presumably date from earlier, more humid periods.

Mineralization occurs in the Archaean Murchison greenstone belt in shears within a sequence of steeply dipping quartz-sericite and chlorite-talc schists intruded by serpentinite, dolerite and diorite and is composed of Fe sulphides, sphalerite, primary and secondary Cu sulphides and minor galena. In the mine area, average grades are about 9% Zn, 0.42% Cu, 0.14 g/t Au and 7 g/t Ag over a width of 1.5–7.0 m. The mineralization is considered to be hydrothermal and hence may have had significant concentrations of halogens in the mineralizing fluids.

The compositions of outcropping gossans (Table II.2-21; see case history 17, Chapter II.2) are indicative of base metal mineralization, but the geochemical response in areas of soil and colluvial cover is less clear. Frick et al. (1989) collected 5 kg soil samples at 5 cm depth at 30 and 50 m intervals across the mineralization and analysed the minus 30 μm fraction for total contents of a range of base metals by XRF and for water-soluble halogens by ion chromatography. Results (Fig. III.3-23) showed that mineralization is indicated by anomalous concentrations of Cu and Zn in residual soils but, where soils are derived from colluvium, anomalies are either displaced or absent. In contrast, the halogens (Br, F, Cl) tend to yield ambiguous results over shallow or residual soils but give characteristic anomalies above mineralization buried beneath transported overburden; Cl and F commonly give double peak or “rabbit-ear” anomalies either side of the subcrop of the mineralization and Br a single peak immediately over it. Although the double peak anomalies are reminiscent of those of H^+ attributed by Govett (1976) to electrochemical dispersion from an oxidizing sulphide

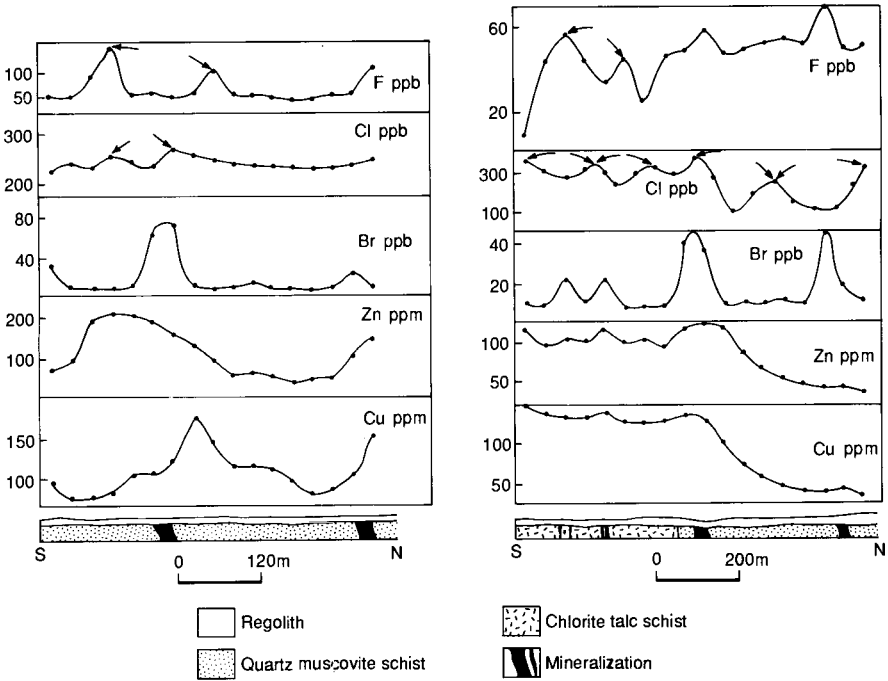


Fig. III.3-23. Base metal and halogen contents of the minus 30 μm fraction of soils on two traverses across the Letaba Cu-Zn deposit, South Africa. Anomalies in Cu and Zn are present only where soils are residual. In soils developed on colluvium, Cu and Zn anomalies are displaced or absent, but Cl and F give double-peaked "rabbit-ear" anomalies (arrowed) and Br a single-peaked anomaly directly above mineralization. Derived from Frick et al. (1989).

deposit, Frick et al. (1989) interpreted them as being due to the release of halogens during continuing weathering and their transport to the surface in ionic solution, possibly under an evaporation gradient. The double peaks correspond to the primary distribution of Cl and F in an envelope around the deposit and the single Br peak to the concentration of that element in the mineralization itself. The poor halogen response in shallow and residual soils is unexplained but may be due to a different hydrological regime. Few traverse lines extended more than 200 m from mineralization, hence the regional significance of the halogen anomalies is difficult to evaluate. Similarly, the absence of base metal data for other size fractions, such as a coarse fraction that may contain gossan fragments restricts any assessment of the relative usefulness of the halogens as pathfinders. However, the results hold promise that they give a readily detectable surface expression to blind mineralization which might otherwise only be found by drilling, although problems will obviously be experienced where groundwaters or soils are saline.

Lady Loretta Zn-Pb-Ag deposit, Queensland, Australia (B 1 Ca [0,1])

Mineralization at Lady Loretta was located by soil sampling in 1968 and, by 1973, drilling had indicated reserves of 8.69 Mt at 18.1% Zn, 6.7% Pb and 110 g/t Ag (Cox and Curtis, 1977). The deposit, which has a strike length of 720 m and a maximum true width of 41 m, is confined within a sequence of dolomitic-sideritic and carbonaceous pyritic shales in the Proterozoic Paradise Creek Formation. The primary sulphides consist of pyrite, sphalerite, galena and minor tetrahedrite.

The deposit is located on an eroded and dissected plateau of generally low relief, with lateritic surfaces preserved as cappings on small mesas. Weathering has extended to below 100 m depth, reaching over 300 m near faults. Surface soils are shallow (15 cm), stony lithosols on steeper slopes and resistant lithologies, and deeper (5–25 cm), clay-rich soils with carbonate nodules on gentler slopes. The mineralization and the pyritic unit both outcrop as ferruginous and siliceous gossans on a ridge capped by lateritic remnants, but only those laterites over the mineralization have anomalous Pb and Ag concentrations. Lead occurs as anglesite and cerussite, with concentrations ranging from 1% Pb in the gossan to over 20% in the oxide zone. No secondary Zn minerals have been reported and Zn is almost completely leached above 100 m (see Chapter II.2, case history 10; Table II.2-14).

Regional and detailed soil samples were collected within 10 cm of the surface on grids of approximately 120 × 30 m to 15 × 60 m. Total samples were analysed because Pb and Ag were enriched in the coarse fractions, probably as gossan and rock fragments. Combined results of these surveys are shown for Pb and Zn on Fig. III.3-24. Neither Pb nor Ag appear to be strongly leached and they have similar distributions, closely related to the outcrop of the mineralization and its host rocks. Lateral dispersion of Pb has been minimal but there has been some downslope mobility of Ag. In contrast, Zn has been strongly leached and remobilized. Anomalous Zn contents (> 240 ppm) are associated only with the maximum Pb-Ag values, but the highest concentrations are downslope from the mineralization. The timing of dispersion is not known, but may relate to mobility under earlier, more humid conditions; a possible present-day equivalent is the THR prospect, French Guiana (see p. 262). There is no Cu mineralization and no soil Cu anomalies, although elsewhere in the region, soil Cu anomalies broadly indicate stratabound and fault-bounded secondary mineralization.

Bounty and Transvaal Au deposits, Western Australia (B 1 Ca [1,2])

M.J. Lintern, P.M. Downes and C.R.M. Butt

These two deposits were found by soil surveys using very sensitive Au analyses and are typical of the many low grade supergene-enriched Au deposits that have been found in Western Australia since 1980. Transvaal is close to some old workings, but Bounty (Smith, 1987a) is an entirely new discovery.

The two deposits are in the Southern Cross greenstone belt in the Archaean Yilgarn Block, 5 km (Transvaal) and 115 km (Bounty) south-southeast of South-

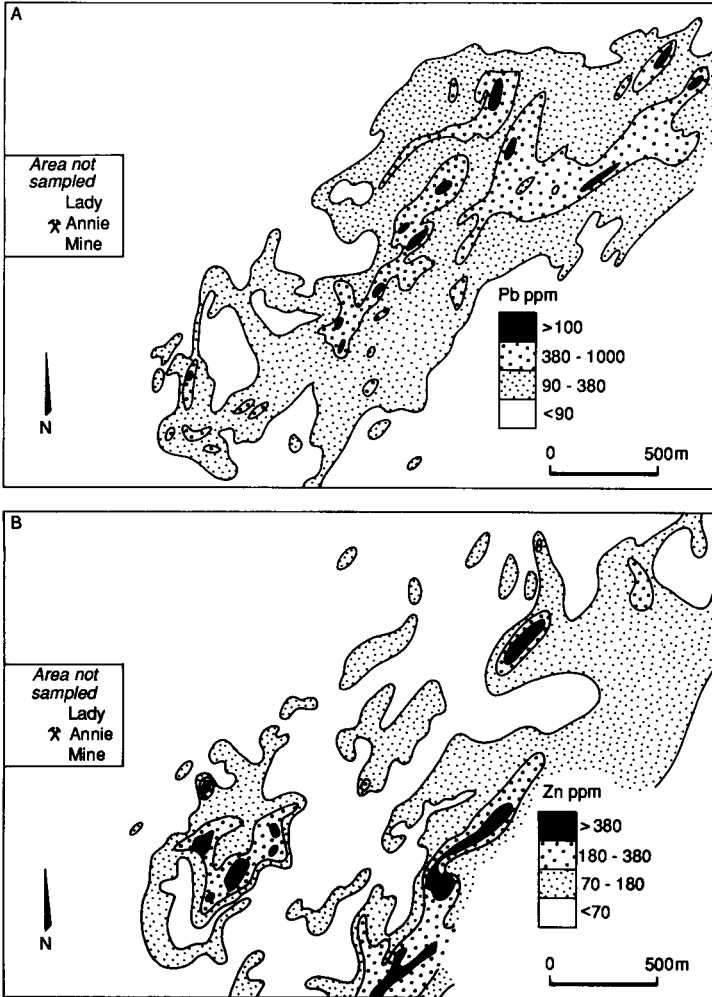


Fig. III.3-24. Distributions of Pb and Zn in soil, Lady Loretta, Queensland, Australia. Redrawn from Cox and Curtis (1977).

ern Cross. The Transvaal deposit is within a sequence of metamorphosed pelites, amphibolites and ultramafic rocks with thin interlayers of arenites. Gold is associated with disseminated pyrite and arsenopyrite in shears and, at higher grades, with quartz veins. There are two mineralized zones, occurring mainly along contacts between the pelitic and ultramafic or amphibolitic units. At the Bounty mine, Au mineralization occurs in shears within cherts and banded iron formation bounded by a mafic intrusion and a komatiitic flow sequence. In both areas, the regolith has been partly truncated, and lateritic duricrusts and gravels

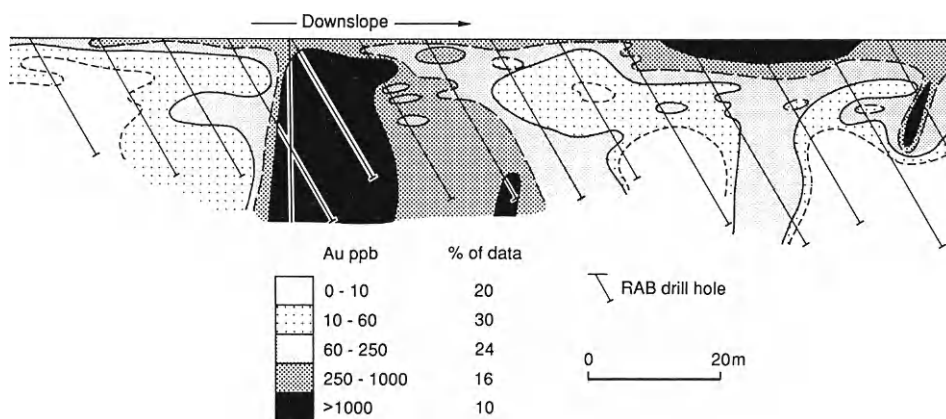


Fig. III.3-25. Section across the Bounty Au deposit, Western Australia, illustrating the concentration of gold in the top 1–2 m of the regolith and some near-surface depletion over the mineralized shear. Modified after Smith (1987a).

are now restricted to upland areas. The soils are predominantly residual and semi-residual calcareous red earths, overlying leached saprolites 40–70 m thick. Sandy clay loams with ferruginous pisoliths and nodules are developed over lateritic gravels in the upland areas.

Soil surveys were carried out on 200×50 m centres by either surface sampling or sampling by power auger, and analysing material between 0.15 and 1.5 m depth. Mineralization at Bounty was indicated by a broad anomaly, exceeding 100 ppb Au, extending for over 700 m downslope, with a peak concentration in excess of 1 ppm Au displaced over 50 m downslope from the surface projection of the mineralization. The soil anomaly was followed-up by angle RAB drilling. The combined results (Fig. III.3-25) show that the anomaly is largely restricted to the upper soil horizons away from the subcrop of the mineralized shear, which itself is depleted of Au within 2–5 m of the surface. Subsequent investigations (Lintern, 1989) have demonstrated that the Au distribution is closely related to that of pedogenic carbonate (Fig. III.3-26), so that successful soil sampling in this region requires inclusion of the calcareous horizon within the sample interval. Samples that exclude this material will give a smaller, low contrast anomaly or perhaps fail to locate one at all. This recommendation does not apply to soils on complete lateritic profiles (A-type models) which are non-calcareous and tend to have Au associated with ferruginous pisoliths. In other areas (e.g. Callion, see p. 319), calcretes are known to invade and replace pisolitic laterites and Au is present both in pisoliths and the calcareous matrix.

The regional survey around Transvaal yielded a much more subtle anomaly even though calcareous soils were sampled here also. The 10300N orebody,

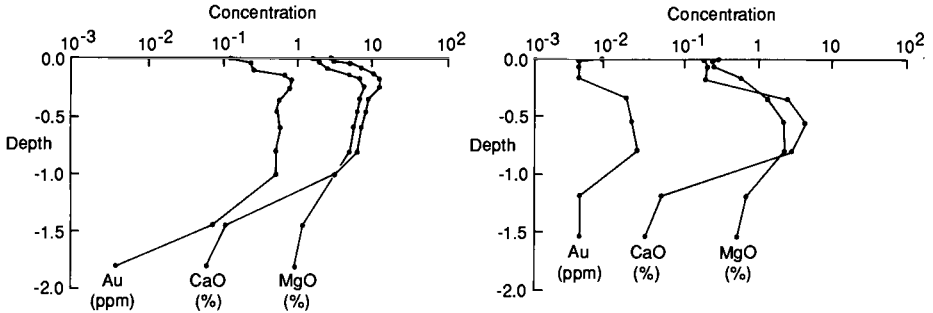


Fig. III.3-26. The association of Au with Ca and Mg in pedogenic carbonates, Bounty gold deposit, Western Australia. Redrawn from Lintern (1989).

north of the previously known mineralization, was indicated by a single sample containing 120 ppb Au (Fig. III.3-27). Investigation of this anomaly by sampling on 50×25 m centres defined drilling targets over separate zones of mineralization, but the maximum Au content (250 ppb) was not significantly greater than originally found. It was concluded that in areas where such subtle and areally restricted anomalies are present, sampling was better conducted on 100×50 or 100×25 m centres. The soil anomaly was tested initially by angle RAB drilling to

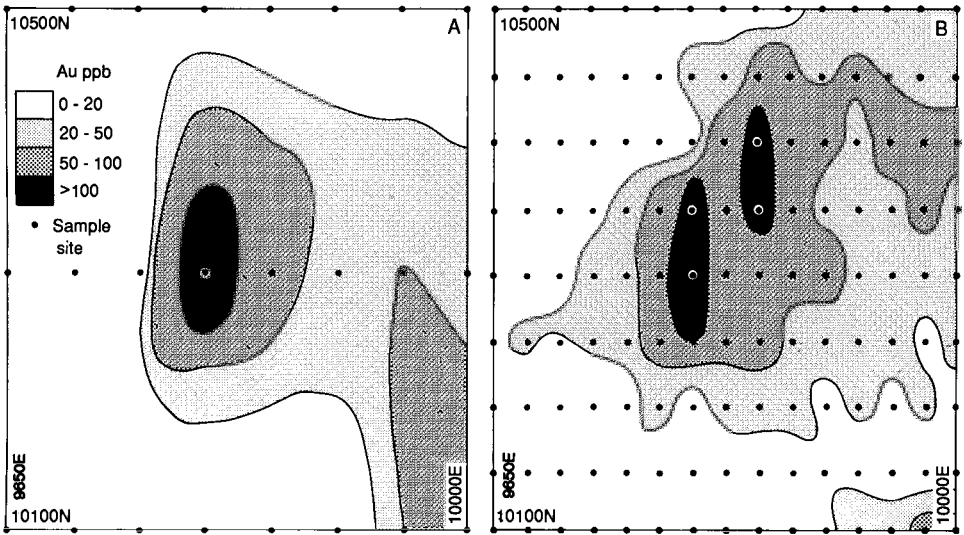


Fig. III.3-27. Distribution of Au in soils (0.15–1.5 m), Transvaal gold mine, Western Australia. (A) Discovery survey, 50×200 m grid. (B) Detailed orientation survey, 25×50 m grid.

Table III.3-8

Variations in drill-indicated grades and tonnages of gold in 10300N orebody, Transvaal mine, Western Australia, demonstrating depletion in the top 20 m; data calculated by kriging on 10×4×5 m blocks (from V. Snowden, 1987, unpublished report to Western United Mining Services Pty. Ltd.)

Mean depth m	Number of blocks	Cut-off grade					
		0.0 g/t Au		1.0 g/t Au		2.0 g/t Au	
		Grade g/t	Tonnes	Grade g/t	Tonnes	Grade g/t	Tonnes
2.5	30	0.67	13800	1.66	2530	2.87	512
7.5	40	0.82	18400	1.81	4740	3.03	1240
12.5	59	1.06	27140	2.11	9410	3.41	3345
17.5	88	1.35	40480	2.55	16805	3.95	7550
22.5	107	1.70	49220	3.02	23405	4.58	11820
27.5	112	1.92	51520	3.33	25630	4.99	13720
32.5	123	1.70	56580	3.07	26505	4.65	13550
37.5	129	1.59	59340	2.90	26920	4.45	13200
42.5	133	1.65	61180	3.07	27450	4.68	13915
47.5	133	1.72	61180	3.28	26965	5.05	13830
52.5	121	1.66	55660	3.20	24115	4.90	12325
Total	1075	1.58	344600	2.99	214470	4.63	145350

8–20 m vertical depth, but the results were disappointing, with the best intersection being 4 m assaying 1.4 g/t Au. However, it was later recognized that the drilling programme had been inadequate, having tested for potential mineralization in the depleted zone of the leached saprolite, which here extends 15–20 m below surface. Accordingly, deep reverse circulation percussion drilling was undertaken, and ultimately a resource of 214,000 tonnes at 3.0 g/t Au was proved in the regolith, to a depth of about 80 m. Depletion in the saprolite is demonstrated by the increase with depth of the ore reserves (Table III.3-8). Gold is not totally leached, but the reductions in overall grade and tonnage are considerable in the top 15–20 m. The depleted zone is far thicker than at Bounty and the marked leaching may be responsible for the smaller size and lower tenor of the soil anomaly.

The discovery of the Transvaal deposit in particular illustrates the necessity to:

- (1) investigate low order anomalies that have an attractive geological setting;
- (2) re-evaluate previously successful procedures for potential deficiencies, such as sampling density, inclusion of specific soil horizons and regional variations in threshold;
- (3) assess the adequacy of follow-up procedures, in this case shallow RAB drilling, in view of known geochemical characteristics such as the extent of depletion.

*Model B * * [3]: partly truncated profile overlain by transported overburden*

Deeply weathered arid terrains commonly have a widespread cover of transported overburden, ranging from a veneer of semi-residual colluvium of less than a metre to alluvial and lacustrine sequences over 50 m thick. This overburden may include sediments deposited during deep weathering and, more commonly, those derived from the dismantling of the regolith during later arid phases. Exploration of these covered terrains has tended to rely on geophysical surveys and drilling to residuum, on the assumption that there is unlikely to be any significant dispersion into the sediments. This assumption is probably correct in many areas, but has rarely been tested.

Although a mechanical dispersion train may be present at the base of the overburden, the local input to the detritus is usually insignificant compared to the regional contributions, so that anomalies, if present at all, are likely to be very weak. Hydromorphic dispersion haloes of various elements have been found in alluvial sediments and overlying soils and calcretes at a number of sites in Australia, such as at Dalgarranga and Redross, described below, Mount Pleasant (see p. 365) and Kadina (see p. 385). Similarly, Cu-Zn anomalies (mostly 100–200 ppm, with maxima of 1200 ppm Cu and 640 ppm Zn) are present in muddy basal sediments in Pernatty Lagoon, a playa in South Australia (Rattigan et al., 1977). These were related to an underlying dolomite in bedrock rather than to mineralization, but demonstrate that detectable dispersion has taken place. Conversely, no dispersion was found in thin (1–3 m) playa sediments above subcropping pyrite-base metal mineralization at Yindarlgooda, Western Australia, although significant anomalies are present in the underlying weathered bedrock (Friedrich and Christensen, 1977).

“Mushroom-like” dispersion haloes of Au occur in saprolite beneath playa sediments (e.g. Hannan South, Lawrance, 1991; see Fig. V.3-4). Although these may have developed after burial, at Hannan South, at least, there is no detectable Au anomaly in the sediments. Such haloes provide a large exploration target even if drilling through more than 20 m of leached sediments and saprolite may be necessary.

Development of hydromorphic dispersion haloes in transported overburden is dependent on whether, after burial, (i) elements that remain in the residual oxidized mineralization can be mobilized or (ii) conditions permit continued weathering of primary mineralization. In both circumstances, the hydrology and hydrogeochemistry of the groundwater are critical. In the cases cited, it is probable that the base metal haloes have developed from weathering of primary mineralization preserved at relatively shallow depth beneath the unconformity. Where mineralization is at greater depth, however, weathering may be slow or dispersion weaker, so that readily detectable anomalies do not form in the sediments, although they may be present in the saprolite. (At Hannan South, Au may have been mobilized from already partly oxidized mineralization, following

salinization of the groundwater.) In general, it is not certain that dispersion into either the sediments or the saprolite can be depended on, so that costly, deep, closely spaced drilling deep is at present the most reliable exploration procedure.

Dalgaranga Cu-Pb-Zn prospect (B 1 Si [3])

This prospect is about 110 km north-northeast of the Golden Grove Cu-Zn deposit (see p. 310), within an Archaean acid volcanic sequence situated between gneisses to the west and the intrusive Dalgaranga layered gabbro to the east. The prospect is in an alluvial plain in a small drainage basin and was discovered by reconnaissance drilling which detected anomalous base metal concentrations in alluvium and weathered bedrock. Subsequent exploration was by RAB drilling to depths of 36 m on 25 and 50 m centres on lines 200 m apart. A typical profile is:

0–1 m: red brown soil;

1–4 m: transported red brown silicified pebbly clays (hardpan) containing ferruginous lithorelics, nodules and pisoliths in a silty clay matrix. Becoming sandy up-drainage; no muscovite.

4–16 m: transported pale grey silty clays, with diffuse red brown and ochre mottling. Ochre mottling strong 10–16 m; no muscovite.

> 16 m: saprolite, commonly with muscovite.

The prospective sequence is on the side of a buried valley and the depth of the unconformity increases from 3–4 m in the east to over 30 m in the west. Bedrock consists of amphibolites, carbonaceous shales, muscovite schists and, in the west, granitic gneiss.

Strong, subhorizontal coincident anomalies of Cu (400–2000 ppm), Zn (500–1500 ppm) and, locally As and Pb (both to 1100 ppm) are present in the silty clays above the unconformity (Fig. III.3-28; C.R.M. Butt, unpublished data). The anomalies are largely confined to the zone of ochre mottling, increasing from 4 to > 20 m thick towards the centre of the buried channel to the west. The anomalies commonly terminate at or just below the unconformity, although possible source units were intersected in saprolite in some holes. One of the principal bedrock intersections, containing gossanous fragments, had mean concentrations of 2485 ppm Pb (range 1100–5000 ppm), 2120 ppm As (685–4310 ppm), 700 ppm Ba (475–1080 ppm), 380 ppm Cu (140–620 ppm), 305 ppm Zn (160–475 ppm) and 35 ppm Sb (13–65 ppm) over 10 m. Deeper drilling, however, has failed to locate any primary mineralization, the holes ending in unweathered gneiss. Other saprolite anomalies, particularly those of Cu and Zn, appear to be related to pyritic carbonaceous shales.

The sources of these anomalies have thus not been unequivocally located and it has been concluded that the primary mineralization has been entirely weathered or faulted out, or that the anomalies represent secondary enrichments from the relatively low grade mineralization represented by the shales. The presence of these anomalies demonstrates that dispersion into transported overburden can

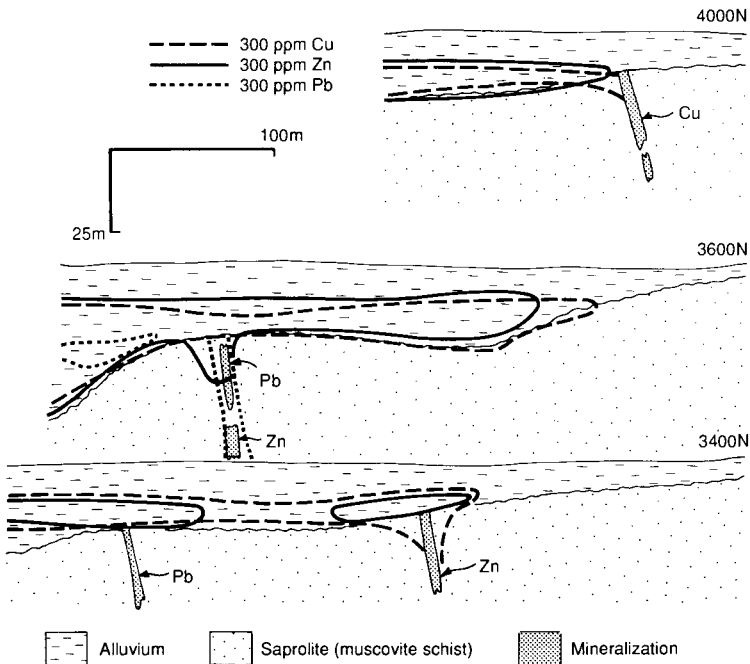


Fig. III.3-28. Sections across the Dalgara Cu-Pb-Zn prospect, Western Australia, showing the distribution of metals in transported overburden in relation to possible sources in weathered bedrock.

occur and may yield widespread geochemical expression to otherwise concealed mineralization.

Redross Ni sulphide deposit, Western Australia (B 1 Ca [0,1,3])

The Redross Ni sulphide deposit lies in an Archaean greenstone sequence similar to that at Kambalda, 50 km north (see p. 362). Massive and breccia-textured Ni sulphide ore, 0.5–5.0 m thick, occurs at the base of a komatiitic unit, against a basaltic footwall, with a narrow zone of disseminated sulphides in a talc carbonate hanging-wall. Mineralization consists of pyrrhotite, pentlandite and accessory chalcopyrite, with a supergene assemblage of pyrite, violarite and chalcocite. The deposit contained about 1 Mt of ore at 3.5% Ni and 0.25% Cu, with concentrations of up to 18% Ni and 1.0% Cu in the supergene zone. Redross was found in 1967 following the discovery of an outcropping gossan containing 0.41% Ni (range 0.04–0.96%) and 0.15% Cu (range 0.03–0.27%). Subsequent soil sampling demonstrated that in areas of residual soil, the mineralization is delineated by the 300 ppm Ni and 100 ppm Cu contours, using the minus 180 μm fraction, although better anomaly definition for Ni is given by the plus 500 μm fraction (Knowles, 1976; C.R. Dalgarno and A.R. Knowles, written communication, 1973). Along strike, oxidized mineralization subcrops beneath alluvium

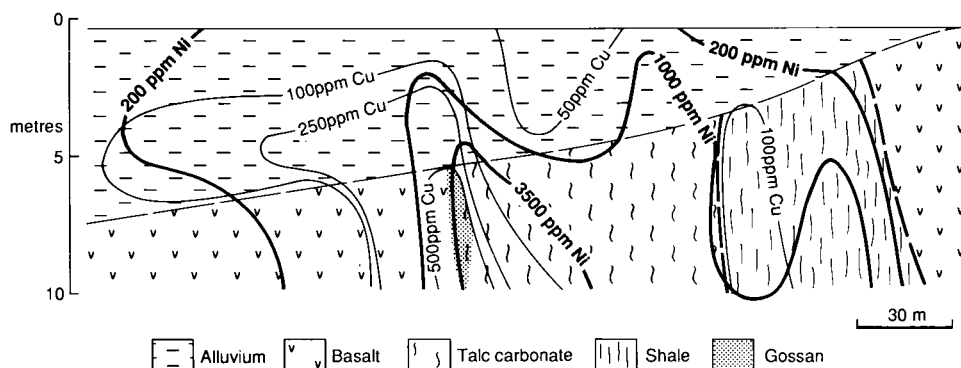


Fig. III.3-29. Section across part of the Redross Ni sulphide deposit, Western Australia, showing the dispersion of Ni and Cu into weathered bedrock and alluvium from massive Ni-Cu sulphide mineralization. Derived from C.R. Dalgarno and A.R. Knowles, written communication (1973).

up to 6 m thick. Here, auger sampling showed some hydromorphic dispersion into the alluvium, with an anomaly, defined by the 100 ppm Cu and 200 ppm Ni contours, extending about 50 m downslope (Fig. III.3-29). This dispersion probably has little direct significance for Ni exploration in this environment, given the complexities of identifying clay-rich regolith units and interpreting Cu-Ni data from deeply weathered ultrabasic rocks, but it illustrates that post-depositional dispersion has taken place.

MODEL C: PROFILE COMPLETELY TRUNCATED

Distribution

In all arid terrains, some areas have been completely stripped so that no remnants of an earlier deeply weathered regolith remain. Such erosion, by headward stream erosion, sheetwash and wind (Chapter I.6), is, of course, particularly evident where relief is high, as discussed in Part IV, but has also occurred in regions of low to moderate relief. Fully stripped areas of quite restricted extent are found in semiarid terrains, such as in southwestern Australia, principally where more resistant rocks (e.g. amphibolites, banded iron-formation) form low hills or where there has been relative lowering of erosional base levels by epirogenic movements or, more locally, by deflation of playas. Extensive areas from which any pre-existing regolith has been almost completely removed form the Sahara and Arabian deserts, where predominantly arid conditions have prevailed for a very long time and are now extreme. Indications of earlier lateritic weathering are indirect. For example, gross features of the geomorphology of these deserts may be interpreted as an etchplain-inselberg

relief, in which the present land surface is an etch surface corresponding approximately to the original weathering front (Budell, 1982). In Saudi Arabia, this implication is supported by the preservation of bauxites and palaeosols of humid tropical origin in and beneath Mesozoic cover rocks (Overstreet et al., 1977; Harvey, 1985) from which it is inferred that a deeply weathered regolith once covered much of the region.

Tropical weathering and soil formation were also associated with more recent, intermittent pluvial periods, for example during the Quaternary. The products, such as the red kaolinite- and illite-rich soils known from the Sahara and Arabian desert (Budell, 1982), may only be recognizable when preserved as palaeosols in alluvial deposits. When developed in residuum, they may be difficult to distinguish from the remnants of either older or younger weathering. Red soils are commonly formed in present-day Mediterranean and adjacent semiarid regions, especially over basic and calcareous rocks (terra rossa soils). In S.W. Australia, such soils are found in stripped areas within a terrain in which deep weathering profiles are generally well preserved (Mulcahy, 1967).

Most residual soils in strongly stripped terrains have been developed from the weathering of bedrock, rather than pre-existing regolith, under the prevailing arid or semiarid climates. They tend to be the products of physical, not chemical, weathering, to have little differentiation into horizons and to be shallow in depth and alkaline in reaction. Consequently, chemical dispersion is minimal for most elements and the soils reflect the geochemical characteristics of the bedrock quite closely. This weathering history also affects the gossans. In Saudi Arabia, only the larger gossans that correlate with palaeosurfaces exhibit the full vertical zonation described in Part II (Salpeteur and Sabir, 1989). The smaller gossans on the pediplain have developed since erosion in the Miocene, and pluvial episodes in the Quaternary were too short for a complete gossan profile to form.

Even in elevated parts of the landscape, soils are rarely totally residual but contain varying amounts of transported material, principally of aeolian and colluvial origin. Transported overburden becomes dominant in lower parts of the landscape, and considerable thicknesses of erosion products, including those derived from stripping of the deeply weathered regolith, and evaporites, may accumulate in valleys and depressions. On the Arabian Shield, for example, fluvial and lacustrine material forms vast fan deposits, 5–10 m thick, over the generally flat basement of plains and large drainage basins. Deposition occurred under previous more humid periods and have subsequently been reworked by aeolian action to form dune fields (Barbier, 1987).

Dispersion models

Arid terrains of low to moderate relief, from which the pre-existing regolith has been stripped can present considerable problems in exploration, even in areas of outcrop and shallow residual soils. Anomalies are generally restricted both in size, due to the lack of dispersion during soil formation, and in intensity,

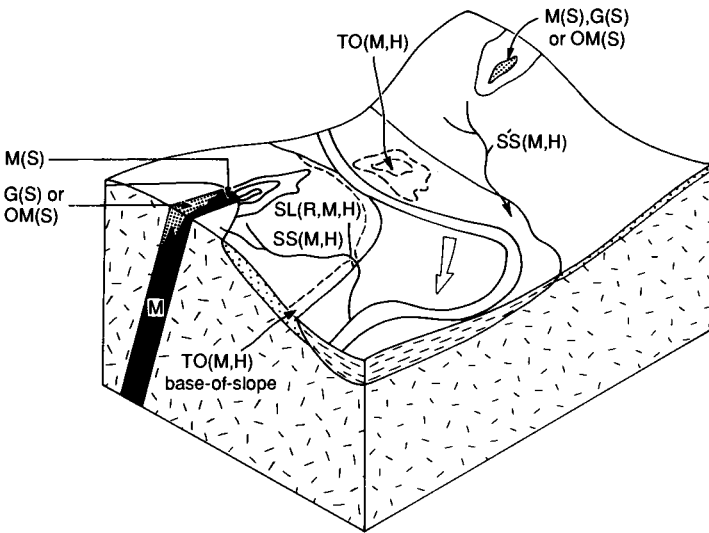


Fig. III.3-30. Dispersion model (C-type) for completely stripped terrain in a semi-arid environment. Modified after Butt and Smith (1980); for abbreviations, see Fig. III.1-1. Contours show general nature of anomaly; broken contours show subsurface anomaly.

due to dilution by aeolian or other transported overburden. In low-lying areas, mineralization may be buried by transported overburden and surface sampling becomes ineffective unless hydrogeochemical or biological processes result in the recycling of mobile elements (Fig. III.3-30).

Gossan search can be effective in base metal exploration (e.g. in Saudi Arabia, Ryall and Taylor, 1981; see Chapter II.2) because gossans commonly have positive relief. However, where they are unsilicified and the iron oxides of which they are composed are less resistant than the country rocks, they may form depressions and be obscured by windblown sand or surface rubble (Fletcher, 1985). In the more arid and non-lateritic terrains, gossans may exhibit a colour contrast with country rocks, even if there is a thin cover, so that colour aerial photography and airborne multispectral scanning have application. Reliance on purely visual evidence, however, is inappropriate, for even outcropping gossans can be small and easy to overlook, and ferruginous gossans cannot form from mineralization that is disseminated or deficient in Fe sulphides. Soil sampling is an extension of gossan search, as anomalies are due to the mechanical dispersion of gossan fragments, including stable primary or secondary minerals. The anomalies present a larger target than the gossans, so that soil surveys are very effective. Soil sampling for sulphide-poor mineralization is typified by PGE exploration in the Windimurra Complex, Western Australia, where the use of highly sensitive and reliable analysis revealed an anomaly two- to three-fold wider than the mineralized source (see p. 383)

In areas where transported overburden of various types rests directly on relatively unweathered bedrock, conventional geochemical exploration procedures may not be applicable. Soil sampling is generally not suitable in extensive sand seas and dune fields, so that rock geochemistry may be the only option, utilizing any outcrops and drilling where necessary. Similarly, surface sampling of colluvial-alluvial plains and drainage axes is of little value, except when the drainages are small and the soils can be considered to be stream sediments. In such cases, coarse fraction sampling for mechanically dispersed resistant minerals and gossan fragments, or fine (minus 75 μm) fraction sampling for chemically dispersed elements may be applicable.

Soils developed on transported overburden may give a surface expression to mineralization only if conditions permit hydromorphic, biological or gaseous transport of ore-related components. Hydromorphic anomalies have been noted where calcretes have formed, especially for Au. They might also be expected for chalcophile elements where there is a pH contrast (see p. 385), and for Mo and U in drainages. Biogenic anomalies have been noted in soils where bioturbation has occurred, e.g. termites bringing diamond indicator minerals to surface from 70 m in the Kalahari (Lock, 1985; see p. 435) and may also form where plants contribute metal-enriched litter to the soil. Atmogenic anomalies arise by the upward migration of gases to enrich soil gas or be adsorbed to soil particles. The application of gas geochemistry to exploration in the arid zone is beyond the scope of this volume, but the techniques are described in a companion volume of the Handbook of Exploration Geochemistry (Hale, in preparation).

Semiarid environments

In apparently fully stripped areas in semiarid environments, some chemical weathering and dispersion may be evident. However, it may be difficult to discern whether this is a remnant of the earlier deep weathering, whether it occurred during later pluvial episodes or is still active.

Kambalda Ni sulphide deposit, Western Australia (C 1 Ca, Sm [0,1])

Kambalda, 55 km south of Kalgoorlie, Western Australia, has an annual, mainly winter, rainfall of about 240 mm. The deposit is on the northwest shore of a large playa and bedrock exposure is unusually high for the region. Although the Ni sulphide mineralization and its ultramafic host are oxidized to the present water-table at a depth of 25 m or more, barren ultramafic rocks, interflow sedimentary rocks and basalts either outcrop or are mantled by shallow residual soils (Mazzucchelli, 1972). Weathering of the mineralization, which has resulted in the formation of the gossans and underlying supergene sulphides probably dates in part from the Tertiary. In contrast, the soils, formed from previously unweathered rock, are more recent. They are solonized brown soils (pH 8–9.5),

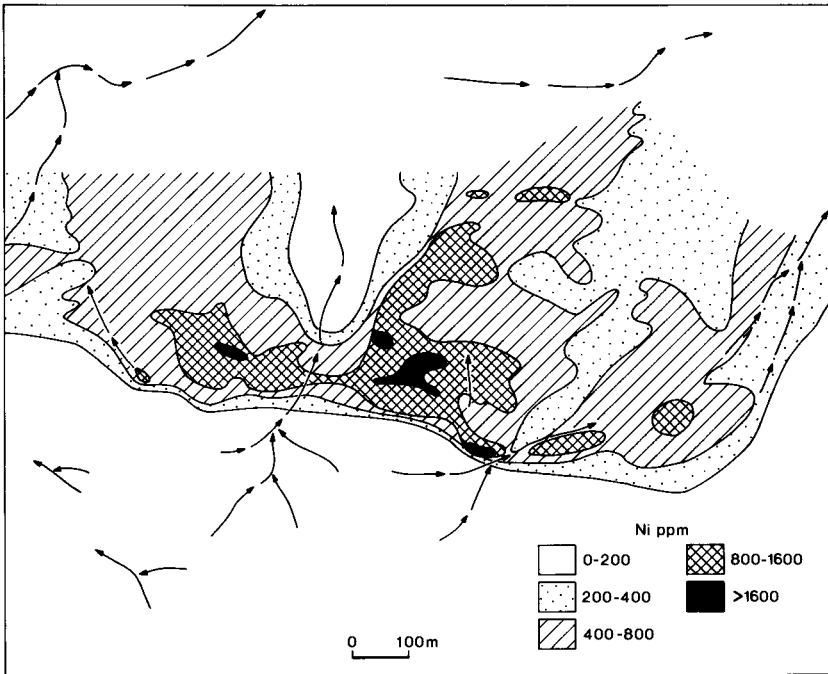


Fig. III.3-31. Distribution of Ni in soils, Kambalda, Western Australia. Modified after Mazzucchelli (1972).

generally 15–60 cm deep, that contain residual primary minerals including talc, chlorite amphibole and albite.

Mineralization at Kambalda was initially discovered by the recognition of the gossans (case history 28, Chapter II.2, Table II.2-28). Subsequently, orientation surveys were carried out to determine the effectiveness of soil sampling. The greatest response was obtained at depths of 15–30 cm, avoiding dilution by wash at the surface and by calcrete in the zone above bedrock. Regional sampling was carried out on a 425×15 m grid, with anomalous zones resampled on a 30×15 m grid; shallow drilling was necessary in areas of colluvial cover. Samples were analysed by AAS following a nitric-perchloric acid digestion. The 200 ppm Ni contour effectively outlined the ultramafic/basalt footwall contact and the highest values (> 800 ppm) indicated mineralization (Fig. III.3-31) outcropping as gossans. The minus 80-mesh ($175 \mu\text{m}$) fraction was chosen for convenience and economy, although it was found that Ni contents and contrasts were greater in the minus 200- and plus 10-mesh (75 and $2000 \mu\text{m}$) fractions. In the plus $2000 \mu\text{m}$ fraction, Ni is contained largely in ferruginous and siliceous gossan fragments. The soil anomaly, which has widths of 50 to 150 m, is the product of the breakdown and mechanical dispersion of such fragments. Copper, Zn and Cr also gave information useful for recognizing anomalies and establishing their

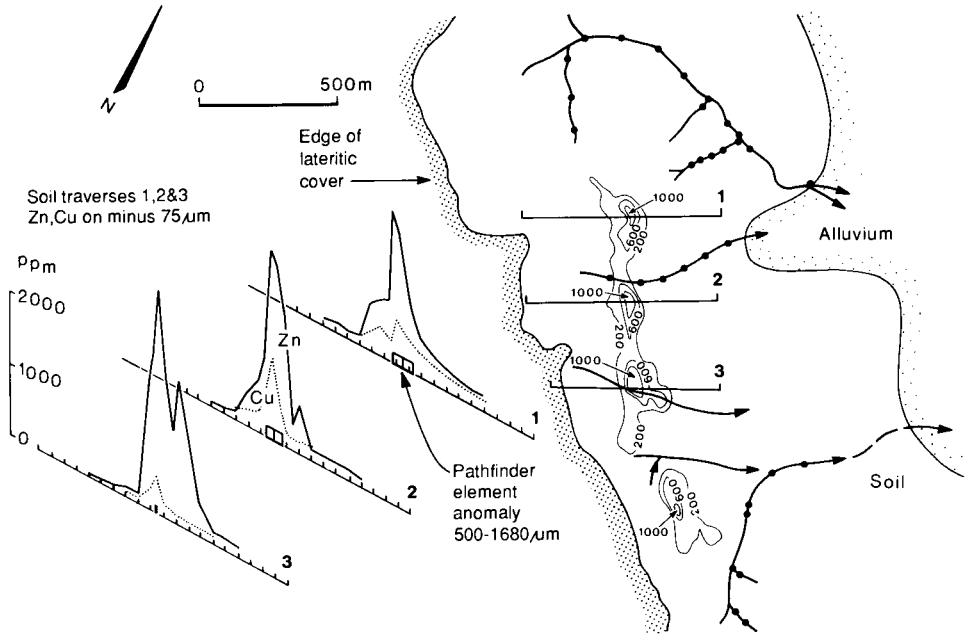


Fig. III.3-32. Dispersion of Cu, Pb and pathfinder elements in shallow residual soils over base metal mineralization at Freddie Well, Western Australia. Modified after Smith et al. (1976).

significance. Nickel sulphide mineralization at Kambalda contains 0.1–1.0% Cu, giving rise to soil Cu contents > 100 ppm over widths of 10–50 m, coincident with the Ni anomalies. Nickel-Cu anomalies in soils derived from sulphides of sedimentary origin, however, are distinguished by high Zn contents. Chromium concentrations > 200 ppm indicated soils developed over ultramafic rocks.

Freddie Well Cu-Zn deposit, Western Australia (C O Ca [0,1])

Freddie Well, 430 km northeast of Perth, Western Australia, is situated on the pediment of an eroded lateritic surface where the pre-existing profile is locally completely stripped (Smith et al., 1976). Felsic volcanic rocks are weathered, but gabbro and dolerite are fresh at outcrop. Mineralization outcrops as gossans, but sulphides occur at 10–12 m in two shoots 5–6 m wide, 8 m apart, grading 10% Zn and 0.25% Cu. The gossans contain 0.02–0.25% Cu, 0.05– $> 2\%$ Zn and very variable concentrations of up to 30–50 ppm each of Pb, Cd, In, Mo, Ag, Sn and W (case history 14C, Chapter II.2, Tables II.2-11 and 18). Soils in the mineralized area are residual, thin (10–20 cm) red brown earths with some carbonate. Soil sampling at 5–10 cm depth showed prominent Cu and Zn anomalies (Fig. III.3-32) in all size fractions. However, although intense (to 8000 ppm Zn), the anomalies are narrow, with the 200 ppm Zn contour indicating dispersion of about 50 m. The minus 200-mesh ($75 \mu\text{m}$) fraction gave the best compromise of

anomaly width and contrast for Cu and Zn but the pathfinder elements such as Ag, Sn and W are generally only detectable (1–5 ppm) in the minus 10- plus 30-mesh (500–2000 μm) fraction, probably reflecting their occurrence in gossan fragments. The narrow, intense nature of the anomalies is typical of juvenile soils formed under arid conditions, with predominantly mechanical dispersion by sheetwash and dilution by barren detritus.

Mount Pleasant Au deposit, Western Australia (C 0 Ca,Sm [2,3])

L.M. Lawrance and C.R.M. Butt

The Mount Pleasant Au deposit is a quartz vein system hosted by a differentiated layered gabbro, within the Archaean Norseman-Wiluna greenstone belt, 35 km northwest of Kalgoorlie, Western Australia. The area has an annual, mainly winter, rainfall of about 220 mm. Gold-pyrite mineralization occurs within carbonate-sericite alteration around the vein; accessory sulphides include galena, sphalerite and chalcopyrite. Much of the deposit is within a wide, flat drainage channel and is overlain by alluvial and colluvial sediments up to 6 m thick. The deep lateritic regolith present over much of the area has been truncated and the sediments rest on fresh rock and basal saprolitic zones. Unweathered gabbro commonly occurs at depths of 2–4 m beneath the unconformity, although weathering may extend to as much as 30 m close to the lode. The sediments include graded and trough-bedded pisolitic and lithic gravels, with a clay loam soil at surface; the upper 1–2 m of the regolith are calcareous.

Dispersion of Au and associated elements in residual and transported horizons of the regolith have been studied by Lawrance (1988a). The ore and alteration zones are enriched in As, W, Pb, Zn, Cu, Ba and, to a lesser extent, Ag, Mo, Bi and Sb. Within the residual horizons of the profile, Au is confined to the lode and the carbonate-sericite alteration zone, with little lateral dispersion. However, in the transported overburden, it is dispersed directly over the lode, with a considerable lateral spread in the top metre. The resultant anomaly at 0.5 m depth (threshold 10 ppb) is at least 600×100 m and, although at a far lower concentration than the primary lode, is more homogenous and represents a far larger exploration target than the subcrop of mineralization (Figs. III.3-33 and III.3-34). Tungsten, Zn, Pb, Mo and Bi are also present in the overburden, with subtle, elongate Zn, Cu and Mo anomalies over the primary mineralization. Dispersion patterns for As, W, Pb, Ba, Bi and Sb do not indicate the mineralization reliably, although those for As, Ba and Sb are more coherent where weathering is deeper. Silver is relatively abundant (11 ppm) in the primary ore, but it has been strongly leached during weathering. A comparison of dispersion patterns shows relative halo sizes are:

Ba > Zn > Cu > Pb > As > W > Mo > Sb > Bi > Ag.

The presence of this superjacent anomaly suggests that Au and other mobile ore-elements have been dispersed by near-vertical hydromorphic processes after

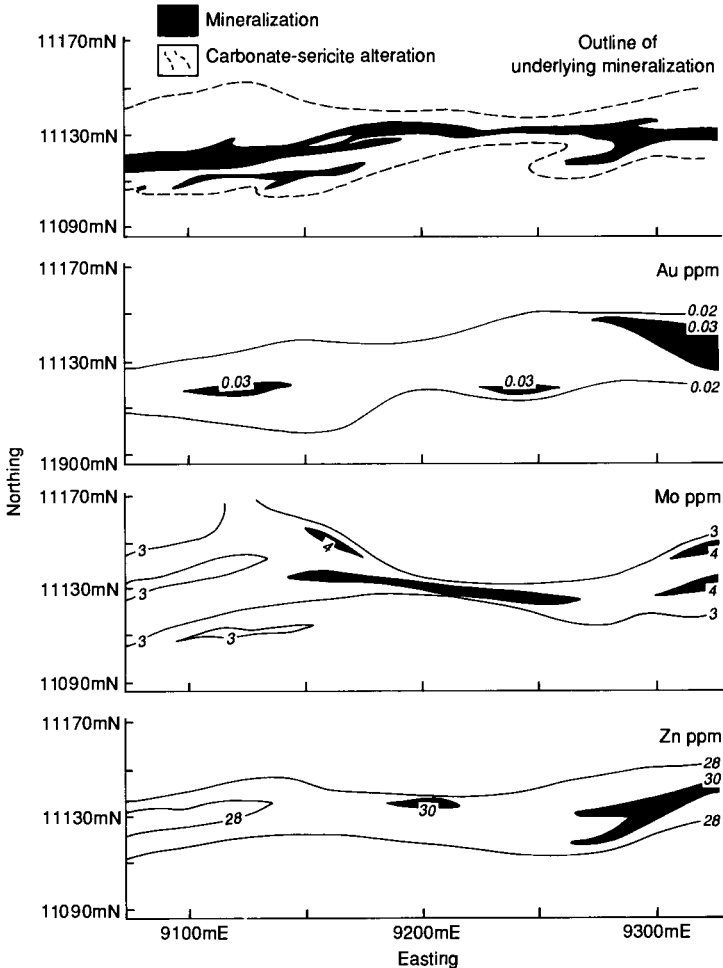


Fig. III.3-33. Distribution of Au, Mo and Zn in transported overburden at 2.5 m depth over the Mount Pleasant Au deposit, Western Australia. The outline of the lode and alteration envelope is projected from the subcrop at 5–8 m depth. Redrawn from Lawrance (1988a).

deposition of the overburden, rather than by the mechanical reworking of weathered lode material. The direction of sediment transport is normal to the strike of the mineralization and there is no evidence for displacement of the anomaly down drainage. This implies that mobilization has occurred under the recent semiarid climatic conditions, in response to the strong evaporation gradients, probably accelerated by plant evapotranspiration. Precipitation of calcretes in the surface metre of the profile may also be indicative of these processes.

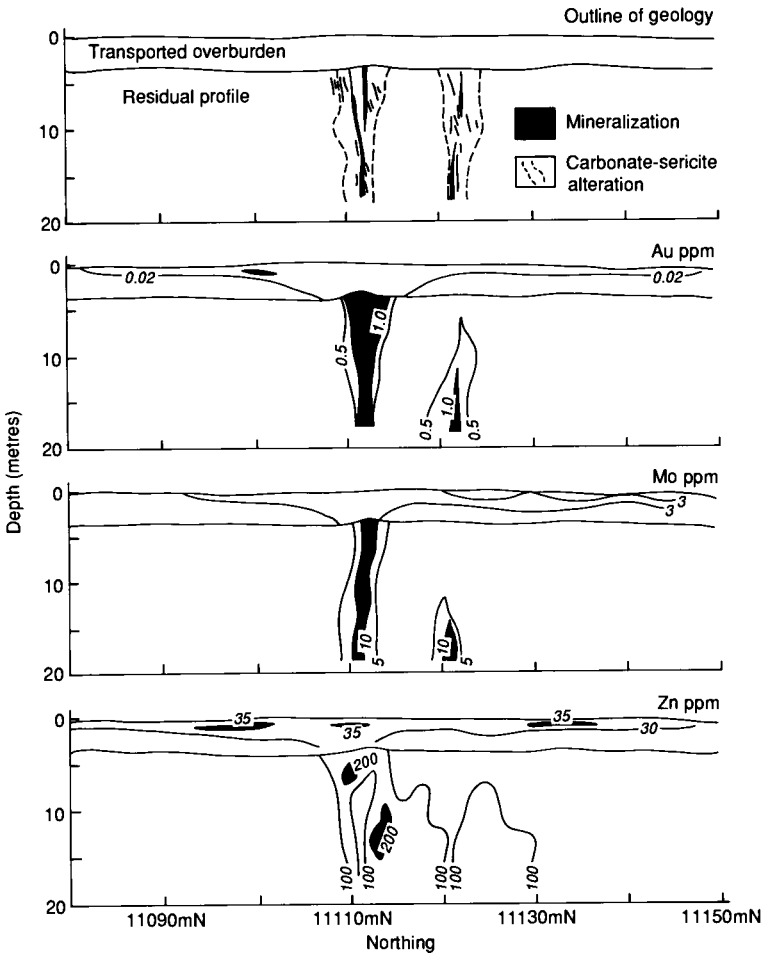


Fig. III.3-34. Dispersion of Au, Mo and Zn around the lode system and into the overlying transported overburden, Mount Pleasant Au deposit, Western Australia. Redrawn from Lawrance (1988a).

Arid environments

In extremely arid environments, widespread transported overburden, dilution and restricted dispersion cause severe exploration problems. Wadi sediment sampling has been the main geochemical exploration procedure. Soil sampling has not been widely used except for detailed follow-up, although Barbier (1987) recommended it for regional surveys of the Nadj pediplain in Saudi Arabia. Residual soils and colluvium suitable for geochemical sampling are mostly confined to areas of subdued relief, smooth hill slopes and uplands, forming a loose mantle 5–60 cm thick. They tend to be immature and skeletal, consisting

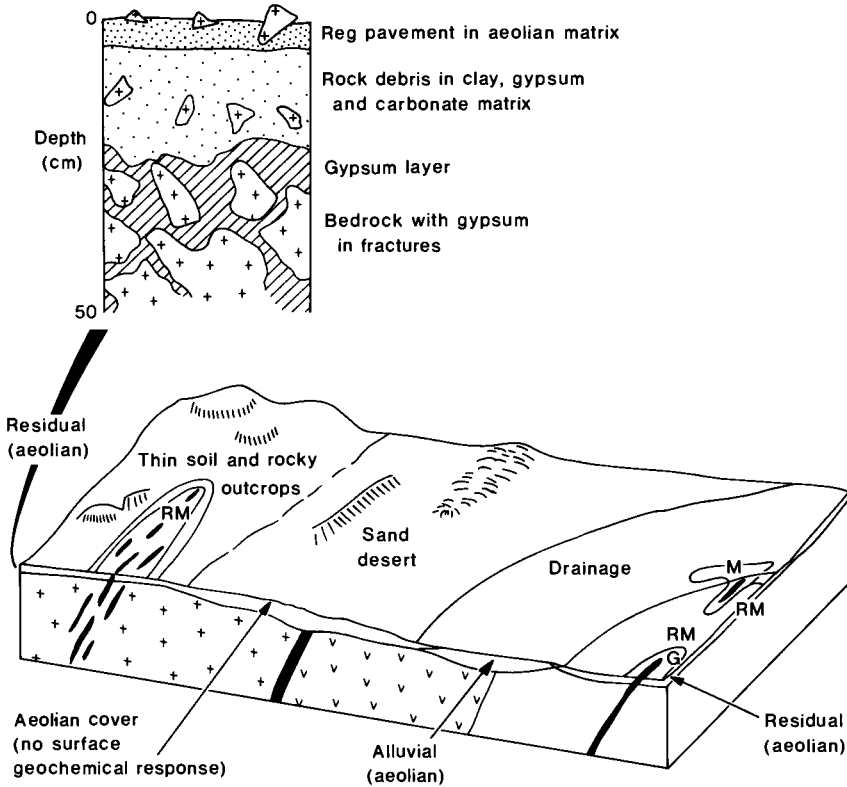


Fig. III.3-35. Dispersion model for completely stripped terrain in very arid environments. The nature of the semi-residual surface soils is shown by the inset. After Salpeteur (1985); for abbreviations, see Fig. III.1-1.

of coarse detritus, pedogenic carbonates and gypsum, and a relatively small proportion of fine, generally aeolian, material (Fig. III.3-35). Where aeolian dust comprises about 50% of the soil, its dilutant effects can be reduced by sieving, thereby concentrating resistant heavy minerals and Fe oxide pseudomorphs of some ore minerals. This procedure is best suited to exploration for mineralization containing As, Sb, Mo, Pb, Sn, W, Ta, Nb, Zr, Ti, Be, Y and REE as ore or pathfinder elements, particularly where these are preserved in primary or secondary minerals (including Fe oxides) in detrital vein quartz. Gossan fragments may also be concentrated in the coarse fraction, hence massive sulphide mineralization may give a response. In the absence of coarse host minerals, finer fractions may be more useful. Most ore minerals and accessory heavy minerals are finer than 1 mm, initially or after abrasion. Wolframite, for example, is quite brittle and breaks down within a short distance and grains of native Au are commonly smaller than 100 μm .

Anomaly enhancement by sieving is less effective for elements such as Sn (from stannite), As, Co, Cu, Li, Mo, Ni, U and Zn that may have some chemical mobility and become concentrated in the Fe and Mn oxides, clays, carbonates and sulphates that constitute the fine fractions, particularly of deeper samples. Although the coarse fractions have been the most widely recommended and used, provided that the sample is sufficiently large (> 1 kg) to be representative, the finest fractions ($< 80 \mu\text{m}$) may give a good anomalous response, especially for the chalcophile elements. The most appropriate fraction will depend on the fineness of the aeolian component; use of the plus 1 mm fraction is advised when sampling in plains with abundant aeolian sand but, in uplands, the exotic component is generally finer, so that the plus 0.3 or 0.5 mm fraction may be suitable (Barbier, 1987). The two fractions may differ in colour, the fine aeolian material being paler than the residual coarse fraction. Shallow sampling, at 2–3 cm (Barbier, 1987) or 10 cm (Salpeteur, 1985) is recommended, to avoid aggregated and gypsum- or carbonate-cemented material at depth. Deflation hollows and thin colluvial horizons having heavy mineral concentrates should be avoided, as they give rise to spurious anomalies, unless the data can be normalized, e.g. against Zr. Grid dimensions are determined by the size of the target and the expected response; whereas regular grids of 0.5 to 1 km may be suitable for large, low grade deposits having resistant minerals, closer spacings (50–100 m) will be necessary for small, high grade massive sulphide deposits.

The suitability of the coarse fraction has been disputed by Salpeteur and Sabir (1989) following orientation studies for Au exploration on the Nadj Pediplain of Saudi Arabia. These authors found that the fine fraction (preferably $< 80 \mu\text{m}$) of the argillaceous surface horizon (top 10–15 cm) is a better sample, capable of higher anomaly contrasts, better reproducibility and longer dispersion trains than the coarse fraction, for base metals as well as for Au. They concluded that use of the coarse fraction selectively *discards* these and other trace elements contained in heavy minerals and Fe oxides concentrated in the surface horizon. A 100×100 m grid is suggested for sub-regional sampling, with each sample preferably being a composite of several subsamples collected within a 15–25 m radius. Wet sieving might be necessary if secondary aggregates (e.g. of gypsum and clay) entrap fine particles and retain them in the coarse fraction. The geochemical responses are weak but can be enhanced by partial extraction (Bugrov, 1974) or by more sensitive and precise analysis (Salpeteur, 1985; Salpeteur and Sabir, 1989) to improve contrasts and detect the wider anomalies produced by sheetwash and wind action.

The use of heavy mineral concentrates eliminates the aeolian and evaporitic diluents and takes advantage of the winnowing effect of the wind. This procedure has been widely used in arid environments, particularly in drainage sediment sampling. However, heavy concentrates are costly to produce, use valuable water if panned in the field and eliminate elements in low density minerals (e.g. Li in mica); in addition, very fine minerals, particularly free Au, may be lost during panning, so that soil sampling is preferred.

Table III.3-9

Distribution of Sn, Mo and Cu in different soil fractions, Hamr Akarem, Egypt (after Bugrov, 1974)

Element	Sn			Mo			Cu		
	-1	-1 +0.25	-0.25	-1	-1 +0.25	-0.25	-1	-1 +0.25	-0.25
Number of samples	58	110	29	5	13	5	15	25	10
Background ppm	20	30	20	3	5	3	10	10	10
Threshold ppm	50	80	50	10	10	10	30	30	30
Maximum ppm	1000	3000	500	50	80	30	200	300	200

Eastern Desert, Egypt (C 0 0 [0,2,3])

Bugrov (1974) found that by using the 0.25–1 mm fraction, the areas of anomalies doubled for Sn, Mo and Cu and contrasts were increased (Table III.3-9) compared to finer fractions or whole samples. A reconnaissance survey using this fraction led to the discovery of Sn mineralization in quartz veins and a Mo-Cu stockwork. Massive Cu-Ni-Co sulphides in a gabbro-peridotite complex were found by stream sediment and soil surveys using the minus 1 mm fraction (Bugrov and Shalaby, 1975). Dispersion trains up to 1.5–2.0 km long (threshold 60 ppm Cu + Ni) in stream sediments outlined mineralized areas and were followed up by a soil/colluvium survey on a 100 × 50 m grid. Peridotites were indicated by 100 ppm Cu + Ni, and maxima of 500–4000 ppm Cu + Ni over widths of 100–350 m corresponded to the occurrence of gossans and ferruginized rock. These were derived from sulphide bodies up to 13 m thick and containing up to 4% Cu + Ni (Fig. III.3-36).

Nadj Pediplain, Saudi Arabia (C 0 Gy [2,3])

Initially, the use of the coarse fraction was recommended as an effective sampling procedure in the Nadj Pediplain by Salpeteur (1985) and Barbier (1987). The region is a gently undulating plain characterized by pebbly semi-residual soils (reg) and broad drainages (wadis) choked by alluvial and aeolian sediments. The reg soils tend to be grey due to manganiferous desert varnish whereas the wadi sediments are beige. The colour difference clearly shows the drainage network on aerial photographs as well as having significance within individual soil and sediment samples; the grey colours are typical of the coarser fractions favoured as sample media and yellowish-beige typifies the finer aeolian material.

Detailed geochemical dispersion studies have been conducted at the Bir Tawilah W and Au prospects, situated in an area of very low relief in the Arabian Shield. There are two sets of quartz veins; an earlier set, parallel to a regional N–S wrench fault, hosting Au-pyrite mineralization and a later series of W-trending veins up to 150 cm thick, in porphyritic granite and quartz diorite, containing wolframite, sulpharsenides and sulphides (Salpeteur, 1985). At the W prospects, soil samples were collected at 0–10 cm in the silty layer below the reg (pebble)

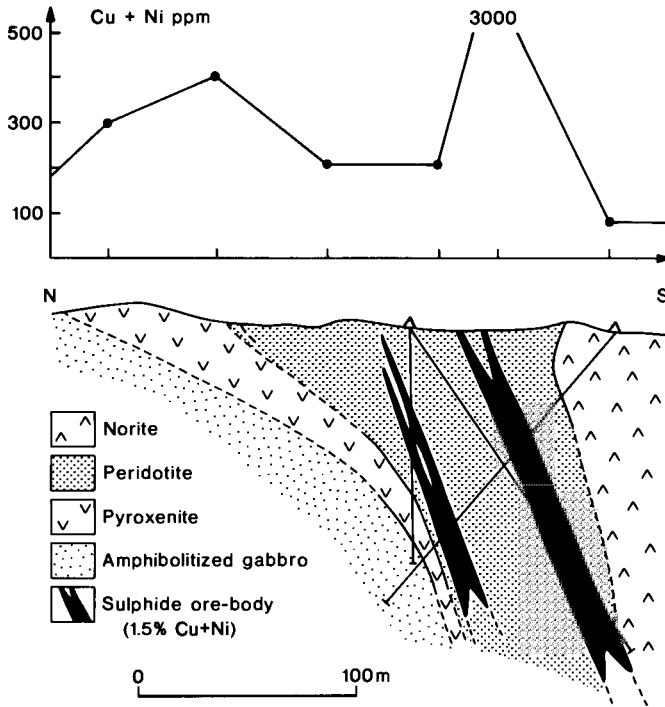


Fig. III.3-36. Dispersion of Cu and Ni in the minus 1 mm fraction of colluvium overlying the Fe-Ni massive sulphide deposit at Gabbro Akaram, Egypt. Redrawn from Bugrov and Shalaby (1975).

pavement and at 10–40 cm in an arenaceous layer containing poorly weathered bedrock gypsum and carbonate. For both sample sets and in all size fractions, the following element associations were found:

Si-W-Sn-Pb-Sb-Li-Zn:	mineralized quartz debris;
As-Co-Ni-Cu:	weathered Ni, As, Cu, Co sulphides;
Mg-Fe-Ti-V-Cr(-Ca)-Ce:	ultrabasic rocks;
Sr-Al; K-Ba:	feldspars;
B-Y:	black sericite schist.

For the possible (immobile) pathfinder elements (e.g. W, Sn, As, Li, F, Pb), the coarse fraction (1.0–3.15 mm) of the shallow (0–10 cm) reg soils gave the highest values (Fig. III.3-37) and widest anomalies, with dispersion of up to 1 km. The deeper (10–40 cm) soils, which contained many bedrock fragments, tended to give a stronger ($\times 3$) response but a dispersion of < 0.5 km. The wide outcrop area (1200 \times 400 m) of the mineralization and the flat terrain have permitted strong wind action, resulting in the loss of the fine fraction and the

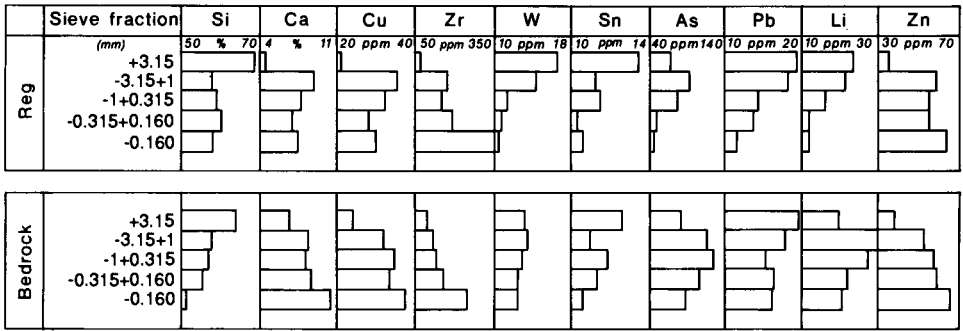


Fig. III.3-37. Size distribution of selected elements in reg soils and partly weathered bedrock, Bir Tawilah, Saudi Arabia. Modified after Salpeteur (1985).

preservation of the anomaly in the coarse fraction, displaced downwind and downslope to the E.

The coarsest soil fractions (particularly plus 1 mm) reflected the major and base metal composition of gossans at Jabal Sa'id (Table III.3-10) and 'Afif (Barbier, 1987). These results prompted the use of soil sampling for a regional survey of the Nadj plain. Samples were collected on a 400 × 400 m grid over a 600 km² area and analysis of the 1–5 mm fraction led to the discovery of hitherto unknown Pb-Zn mineralization. Subsequently, however, Salpeteur and Sabir (1989) have reported that, despite these earlier results, regional sampling for Au using the coarse fraction was unsuccessful. They ascribed this failure to reliance on orientation surveys at sites contaminated by mining. Investigations around unworked Au-pyrite mineralization in quartz veins at Bir Tawilah showed that Au tends to concentrate in the finer fraction. In a 60 cm deep soil profile 5 m from the vein, Au contents generally increase in the fine fractions (< 160 μm), particularly in the deepest horizons (Fig. III.3-38). Ten metres from the vein, however, Au is concentrated in the coarse fractions (315–2000 μm) in the top

Table III.3-10

Compositions of different fractions of soil at 1–2 cm depth over the Jabal Sa'id gossan, Saudi Arabia (from Barbier, 1987)

Fraction (μm)	Al ₂ O ₃ (%)	Fe ₂ O ₃ (%)	MgO (%)	CaO (%)	Na ₂ O (%)	K ₂ O (%)	TiO ₂ (%)	Mn (ppm)	Cu (ppm)	Pb (ppm)	Zn (ppm)	As (ppm)	Mo (ppm)	Ag (ppm)
< 160	10.2	7.7	3.2	8.8	0.9	1.0	1.6	1290	65	35	110	–	4	–
160–315	9.8	6.5	3.0	7.6	0.9	1.0	1.6	1135	60	35	100	–	5	–
315–500	7.0	8.0	2.6	13.2	0.5	0.6	0.7	910	95	80	130	–	7	–
500–1000	4.5	12.4	2.0	16.1	0.2	0.5	0.6	705	130	145	165	–	11	–
> 1000	1.5	24.3	0.6	12.3	0.1	0.1	0.2	315	180	585	185	175	28	–

– below detection limit.

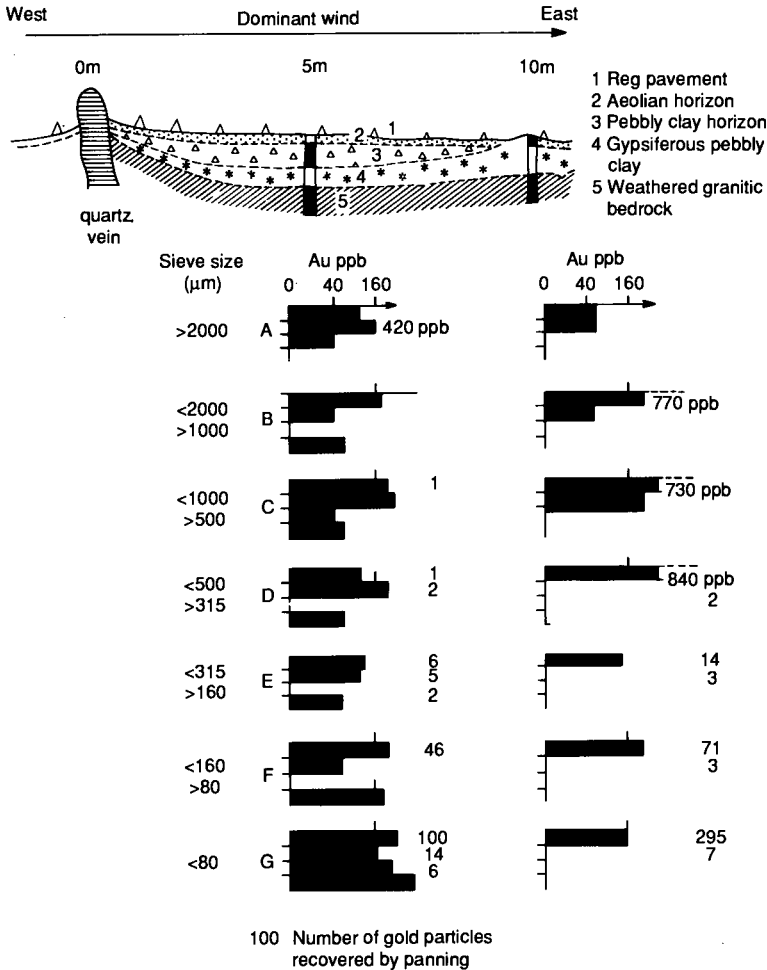


Fig. III.3-38. Dispersion and size distribution of Au in semi-residual soils downwind from an unworked quartz reef, Bir Tawilah, Saudi Arabia. Modified after Salpateur and Sabir (1989).

30 cm. At both sites, over 90% of Au particles recovered by panning were in the minus 160 μm fractions, and 10 m from the vein they were confined to the surface horizons, associated with a general increase in the abundance of heavy minerals. This difference is because the gold particles are enclosed by gypsiferous clay aggregates which are retained in the coarse sieve fraction but disintegrate in water during panning. At other prospects, it was found that the fraction hosting Au in wadi sediments changed abruptly from coarse to fine within 150 m of the source. Dispersion trains were generally very short, with anomalous values of 30–50 ppb (background 3–4 ppb) restricted to 500 m from source. These authors concluded that the fine fractions of soil and wadi sediment were statisti-

cally better samples than the previously recommended coarse fraction, giving higher contrasts and more reproducible results, particularly when coupled with more sensitive analytical procedures.

EXPLORATION IN CALCRETE TERRAIN

Nature and distribution of calcrete

Most semiarid and arid regions are characterized by the retention and accumulation of carbonates in the regolith. Their presence has been noted in several examples and model codes in the preceding sections and, in some localities, has particular exploration significance. Carbonate accumulations have a variety of regional names—e.g. caliche (North America), kunkar (India), crôte calcaire (France)—but are referred to herein as calcretes. Calcrete is defined as “terrestrial material composed dominantly, but not exclusively, of calcium carbonate, and involving the cementation of, accumulation in and/or replacement of greater or lesser quantities of soil, rock or weathered material” (after Goudie, 1972). Calcretes are composed principally of calcite and/or dolomite, either of which may be dominant, and very rarely of aragonite; in addition, siliceous smectites and gypsum may be present or even abundant.

Significant calcrete development on rocks other than limestones and dolomites typifies arid climates having 100 to 500–600 mm annual rainfall and their occurrence outside this range is interpreted as evidence for climatic change (Goudie, 1973; Mabbutt, 1977). Carbonate accumulation and the formation of calcretes may occur in either the vadose or phreatic zones and vary in nature and abundance from thin encrustations—for example, on freshly weathering (commonly basic) rocks—to minor, diffuse enrichments, friable powders, nodules and concretions in soils, to cements in hardpans and to massive limestone. A genetic classification of calcrete is given in Fig. III.3-39 (Carlisle, 1983). Upon later exhumation by dissection, massive calcretes, especially if silicified, form cap rocks or duricrusts, resulting in erosional landforms such as mesas and cuestas, similar to those in lateritic terrains. In North Africa, weathering and replacement of minerals during calcrete formation is considered to be an important erosional mechanism (Nahon et al., 1977; Ruellan et al., 1979).

Pedogenic (vadose) calcretes are especially well developed in areas of winter rainfall where high carbonic acid concentrations in soil moisture are maintained by CO₂ evolution from plant root respiration during the growing season. Carbonate enrichment occurs in the upper 10 m of the regolith, most commonly in the top metre, irrespective of whether material is in situ or transported, or the pre-existing profile is truncated or complete. Precipitation is caused by loss of water by evapotranspiration and/or degassing of CO₂ in response to lower CO₂ partial pressures (in turn due to the decline of respiration at the end of the

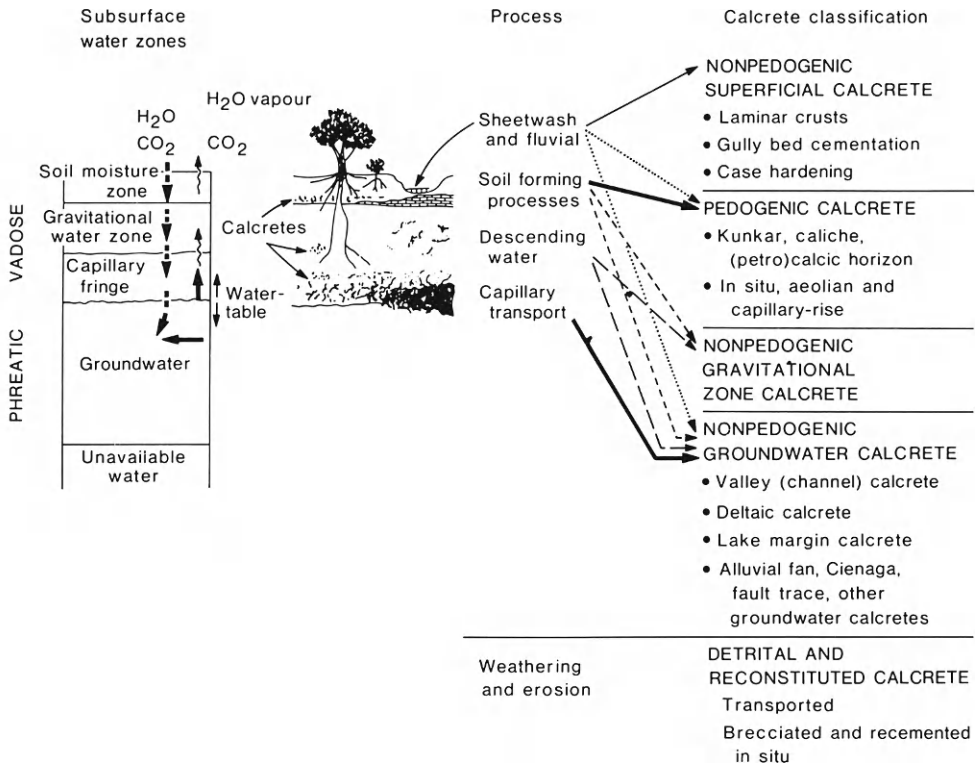


Fig. III.3-39. A genetic classification of calcrete. Modified after Carlisle (1983). A given calcrete may be formed by several processes, as indicated by the arrows.

growing season or percolation of water below the root zone):



Where pre-existing weathering profiles have been partly or completely stripped, the Ca is largely derived from the weathering of primary minerals; in such areas, there is a marked lithodependence, with calcrete development strongest on basic rocks. However, calcrete may also develop in highly leached, fully preserved, lateritic profiles, even in upland sites. Here, the derivation of the calcium is less clear, but it is probably from:

- (1) aeolian accession of calcium carbonate deflated from coastal deposits or calcareous soils and sediments lower in the landscape;
- (2) accession, with other ions, as aerosols with rainwater;
- (3) capillary rise and surface concentration under an evaporation gradient;
- (4) uptake by plants from deep in the profile and surface deposition from their eventual decay.

Mechanism (4) is probably the most significant; dry plant matter commonly contains about 1% Ca and phreatophytic plants are able to obtain nutrients from deep water-tables. The other mechanisms probably have only local importance.

Groundwater (phreatic) calcretes occur in areas of summer rainfall, where runoff, rapid infiltration and high evapotranspiration limit the period of soil dampness and plant respiration. Dissolved Ca, Mg and bicarbonate remain in solution and enter the groundwater, only precipitating in drainage axes and depressions after concentration by evaporation or CO₂ degassing due to upwelling or capillary rise. Although the distinction between pedogenic and groundwater calcretes is not always clear-cut, this broad subdivision is significant in understanding the distribution of potentially economic concentrations of uranium in calcretes and associated sediments in southern Africa and Western Australia.

Exploration significance of calcrete development

The presence of calcrete has both disadvantages and advantages for mineral exploration. The principal disadvantages are:

(1) Many pedogenic calcretes represent absolute additions to soils developed on pre-existing deep weathering profiles which, in many instances, may have been partly truncated prior to soil and calcrete formation. The concentrations of most mobile elements (except, perhaps, Fe) associated with economic mineralization are already reduced by leaching during the initial deep weathering and later pedogenesis, so that calcrete precipitation causes dilution and depresses anomaly contrasts still further. The replacement of primary and secondary minerals by carbonates may lead to the mobilization and loss of some elements, including Pb and Zn.

(2) The high pH commonly prevailing in the regolith of calcrete terrains reduces the chemical mobility of many elements and hence restricts the development of epigenetic anomalies.

Studies addressing these problems in Australia and Africa, illustrated by the case histories that follow, have shown that the options are to:

(a) sample calcrete-free surficial horizons to obtain low contrast anomalies having some lateral dispersion but possibly diluted by clastic particles;

(b) sample deep horizons below the calcrete to obtain higher contrast anomalies with minimal lateral dispersion;

(c) use the calcrete horizon as a constant sample medium and search the data for restricted, low contrast anomalies. The dilution effect may be reduced by using a carbonate-poor fraction, by normalizing the data or by dissolving the carbonate and analyzing the residue (see p. 381).

Calcrete formation may be advantageous to exploration in the following circumstances:

(1) In some environments, the calcrete represents a pH contrast to underlying neutral to acid regolith and may cause the precipitation and concentration of leached metals, hence forming epigenetic anomalies (e.g. Kadina, p. 385).

(2) Gold can be enriched in the calcareous horizons of soils and may give rise to or enhance a near-surface expression to concealed primary or secondary mineralization (e.g. Bounty, Fig. III.3-26; Mount Pleasant, Fig. III.3-34).

(3) Groundwater calcretes in particular may be the aquifer and host rock for the transport and precipitation of potentially economic U concentrations (p. 386).

Pre-existing profile mostly preserved: A-type models

The presence of pedogenic calcrete in complete lateritic profiles has rarely been described, but it occurs in Mauritania (Nahon et al., 1977) and southwestern Australia and is probably present in equivalent regions elsewhere. Continued calcrete precipitation is important in the destruction of the indurated lateritic horizon both physically, by growth of carbonate segregations, and chemically, by replacement of existing minerals. This forms a fragmentary surface horizon or calcareous soil subject to erosion and mechanical dispersion.

Introduced calcrete is a diluent for most elements retained or concentrated in Fe oxides. In the Kalgoorlie region of Western Australia, Mazzucchelli and James (1966) found that As, an effective Au pathfinder, is concentrated in lateritic fragments (220 ppm) compared to calcrete (40 ppm). Arsenic anomalies can be enhanced by preferentially sampling either the surface ironstone fragments, mostly free of carbonate coatings, or the coarse (plus 840 μm) soil fraction, in which these fragments accumulate; whole samples or the minus 175 μm fraction are diluted by calcrete (Fig. III.3-40). The surface fragments also give a wider

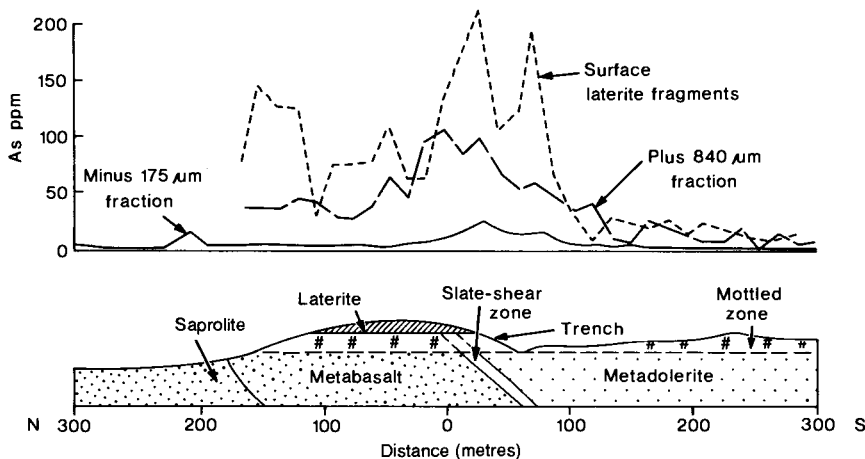


Fig. III.3-40. Lateral dispersion of As in lateritic gravels at the surface and other size fractions at 15–30 cm depth in the Kalgoorlie region, Western Australia. Modified after Mazzucchelli and James (1966).

anomaly, due to dispersion by sheetwash, as described for pisoliths and lags. Nevertheless, it is evident in the same area of Western Australia that Au concentrates in the carbonate horizon, implying that some Au mobility is concurrent with calcrete formation and still active under the present semiarid conditions. Thus, in some samples from a lateritic Au deposit, the pisoliths contain 1.5–3.0 ppm Au whereas the associated calcrete contains 0.7–1.5 ppm Au. At Callion, the highest Au contents were in the calcrete (see p. 319) and elsewhere calcretes are a minor ore type.

Pre-existing profile partly or wholly truncated and without pH contrast: B- and C-type models

Where the pH of soils and saprolite remain alkaline throughout the profile, pedogenic calcrete deposited in and partially replacing previously leached horizons of partly truncated profiles and more recent soils reduces element concentrations and depresses contrasts still further. Nevertheless, most studies have concluded that, provided that either the surface soil or the calcrete are residual, the data are valid if interpreted with care. Deep sampling gives the most consistent results for base metals but it is costly, for anomalies are restricted in size and drilling on closely spaced grids is necessary.

Pioneer Ni sulphide deposits, Western Australia (B 0 Ca [1])

The Ni-Cu sulphide deposits at Pioneer, Western Australia, 85 km south-southwest of Kambalda, are small bodies of massive pentlandite, pyrrhotite and chalcopyrite situated at the base of serpentinized ultramafics in the Archaean Kalgoorlie-Norseman greenstone belt. Soils are essentially residual, 0.1–1.0 m deep developed over partly truncated profiles 25–100 m deep (Cox, 1975). A calcrete horizon, 0.5–1.5 m thick, is developed below about 0.2 m depth, across the soil-saprolite transition, and consists of calcrete-coated lithorelics in a white matrix of calcareous smectitic clays. The mineralization subcrops as a gossan, also overlain by calcrete and soil. Traverses across it showed that metal concentrations in the soil (minus 80-mesh (180 μm)) and calcrete horizon (whole sample) were greatly reduced compared to those in saprolite and gossan (whole samples) (Fig. III.3-41). Nevertheless, the maximum Ni, Cu, Co and Zn contents and Ni/Cr ratios in soils were found to be coincident with those in saprolite but had a greater lateral spread, particularly downslope. Metal concentrations were higher in the calcrete horizon than the soil but lateral dispersion was less. Dispersion in the weathered bedrock was minimal. The minus 80-mesh (180 μm) fraction was appropriate for it was found that Ni and Co were incorporated in Mn oxides, and Zn and Cu in smectites, which comprise the fine fraction, whereas the coarse fraction contained clastic diluents such as quartz. This contrasts with the finding at Kambalda, where gossan fragments increase the metal contents of coarse soil fractions (see p. 362).

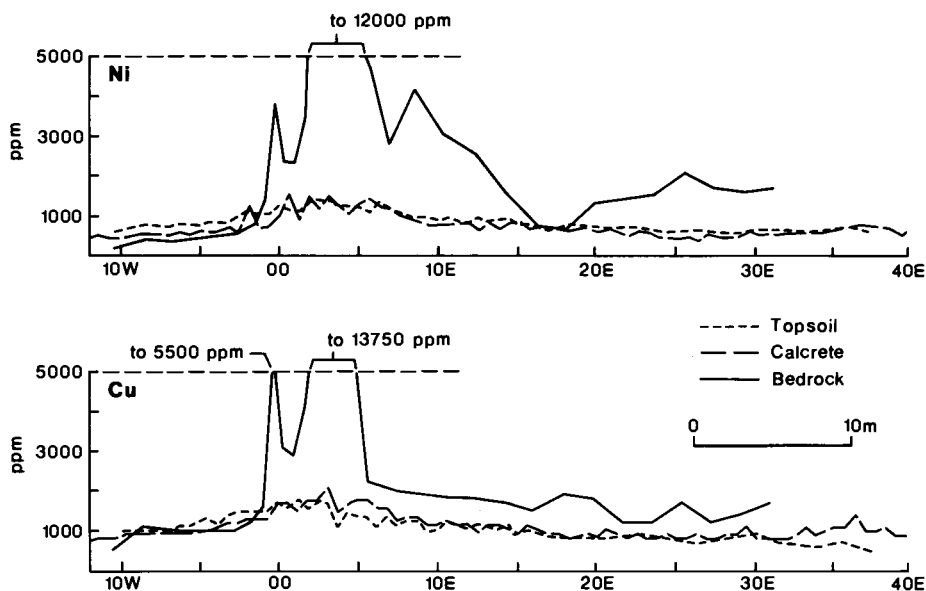


Fig. III.3-41. Copper and Ni contents of topsoil, calcrete and weathered bedrock in channel samples from a trench over Ni sulphide mineralization, Pioneer, Western Australia. Modified after Cox (1975).

Jacomynspan and Putsberg deposits, South Africa (B 0 Ca [1,2])

Danchin (1972), Garnett et al. (1982), Vermaak (1984) and Tordiffe et al. (1989) specifically addressed the problem of exploration for base metals in calcrete terrain in the northwest Cape Province of South Africa. The calcretes are thicker than those described from Australia and the total depth of the regolith is less, but the conclusions are similar. Thus, at the Jacomynspan Cu-Ni prospect, anomalies of Cu, Ni and Co in the calcrete are very intense but limited in size, reaching background concentrations within 30 m of subcropping mineralization. Vermaak (1984) found that metal concentrations in soil (30–200 ppm Cu, 45–205 ppm Ni) and calcrete (40–1730 ppm Cu, 45–2330 ppm Ni) were greatly reduced relative to mineralized schist (0.10–0.49% Cu, 0.15–2.30% Ni). However, as at Pioneer, Western Australia, soil and calcrete both defined the subcrop of mineralization and retained the Fe-Mn-Co-Cu-Ni association that reflects the mafic host rocks and the association with secondary Fe oxides. The latter are presumed to have formed by weathering under more humid conditions prior to calcrete formation.

Garnett et al. (1982) studied dispersion at the Putsberg Cu deposit and examined the causes of the weak surface expression. The deposit is concealed by thick calcrete (mostly 2 to 7m thick, locally as much as 15 m) developed on and within weathered bedrock. The calcrete consists mostly of nodules (up to 50 cm), having calcareous silty cores and laminated carbonate skins, in a silty calcareous groundmass. The calcrete horizon is abruptly overlain by a sandy soil that has

TABLE III.3-11

Metal distribution in soil and calcretes at Putsberg, South Africa (from Garnett et al., 1982)

Horizon	Fraction	N	Copper ppm		Lead ppm		Zinc ppm		Cadmium ppm		Silver ppm	
			Max Min	Med- ian	Max Min	Med- ian	Max Min	Med- ian	Max Min	Med- ian	Max Min	Med- ian
Soil	1- 2 mm	43	800 10	46	340 10	36	200 10	7	nd nd	0	nd nd	0
	75-180 μ m	43	800 20	135	180 20	52	230 50	110	nd nd	0	nd nd	0
Top of calcrete	> 5 cm boulder calcrete	52	6200 30	95	450 30	60	1300 20	52	7 0	0.58	6 0	0.56
	1- 5 cm nodules	38	1600 30	160	310 10	70	2100 20	65	3 0	0.70	4 0	0.50
	2- 10 mm calcrete chips	38	1900 30	200	620 30	100	870 20	105	4 0	0.60	4 0	0.60
	1- 2 mm	43	3100 20	65	350 30	80	600 20	80	nd nd	0	nd nd	0
	75-100 μ m	43	3000 50	195	480 60	85	460 60	120	nd nd	0	nd nd	0
	> 5 cm boulder calcrete	15	3000 30	85	620 20	55	2800 20	20	5 0	0.70	7 0	0.60
Base of calcrete	1- 5 cm nodules	39	1700 30	330	1300 20	95	1100 20	150	44 0	0.75	6 0	1.05
	2- 10 mm calcrete chips	40	3700 30	400	2000 30	165	2900 20	190	5 0	0.80	4 0	1.10
	1- 2 mm	43	3500 20	355	1800 40	130	1400 20	270	2 0	1.00	1 0	0.40
	75-180 μ m	43	6500 50	425	2700 50	70	1500 50	245	2 0	1.00	1 0	1.00
	> 2 mm rock chips	43	9800 20	1745	5300 30	365	3500 10	620	2 0	0.50	17 0	1.00

nd = not determined.

residual, aeolian and colluvial components. Over mineralization, gossan fragments are present within calcrete nodules, in the soil and in the surface lag, so that soil sampling (minus 180 μ m fraction) gave a response, though contrasts were very subdued. Thus, with a mean background of 25 ppm Cu, the mineralized zone was delineated by the 40 ppm contour, with scattered maxima greater than 200 ppm. Comparison of the various fractions of the soils and calcretes showed that the calcretes gave a significantly greater response, mainly in the finer fractions (Table III.3-11). Nevertheless, Cu, Zn and Pb contents were still greatly depleted relative to bedrock and Cd and Ag were anomalous only in the coarse fraction.

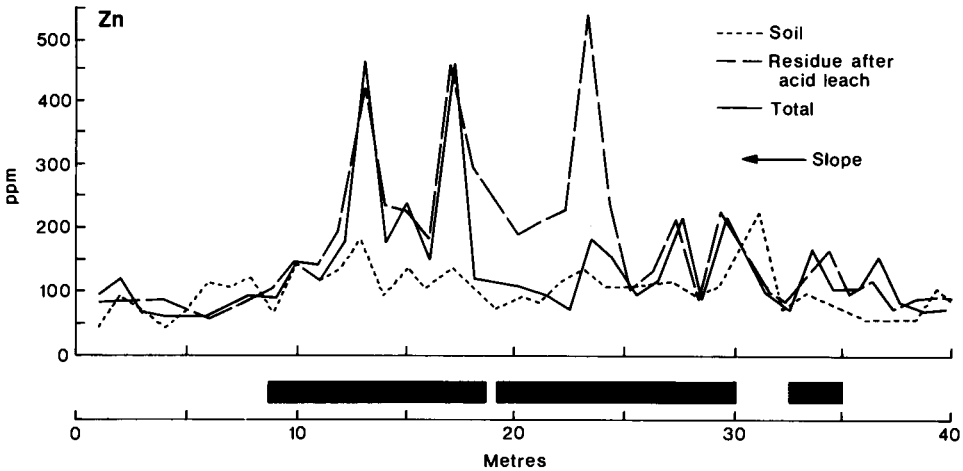


Fig. III.3-42. Zinc contents of 75–180 μm fractions of soils, calcrete (total analysis) and calcrete residue (after ammonium acetate leach) over subcropping mineralization, Putsberg, South Africa. Solid bars represent the location of mineralization beneath the calcrete. After Garnett et al. (1982).

Most of the decrease in base metal contents from saprolite to calcrete and calcrete to soil can be explained by dilution by carbonates and mechanically-derived quartz respectively, although some leaching may have occurred during calcrete formation. Garnett et al. (1982) and Vermaak (1984) both recommended the top of the calcrete horizon for regional sampling, because of the higher metal content of the calcrete and because in places the soil may either be absent or composed entirely of transported material. The disadvantage of restricted anomaly size due to the lack of mechanical dispersion in the calcrete can be partly offset by removal of the carbonate diluent using an ammonium acetate leach and analyzing the residue (Fig. III.3-42).

Mararoa Reef Au mineralization, Norseman, Western Australia (B 1 Ca [1])

The effects of dilution by calcrete or clastic material (aeolian or colluvial) may be reduced by data manipulation. For example, analytical data for As may be adjusted according to variations in Fe content because As is generally concentrated in ferruginous segregations. At Norseman, Western Australia, As- and Au-bearing quartz reefs occur in shear zones cross-cutting an Archaean greenstone belt. Smith and Keele (1984) showed that the geochemical expression of known mineralization could be distinguished in the calcrete-rich surface (0–1 m) horizon (Fig. III.3-43) by normalizing As data with respect to Fe. Such normalization is neither applicable nor necessary, however, if As dispersion is still active for in calcareous soils, it can be trapped by carbonates rather than Fe oxides (Frick, 1985; see Plat Reef, p. 383).

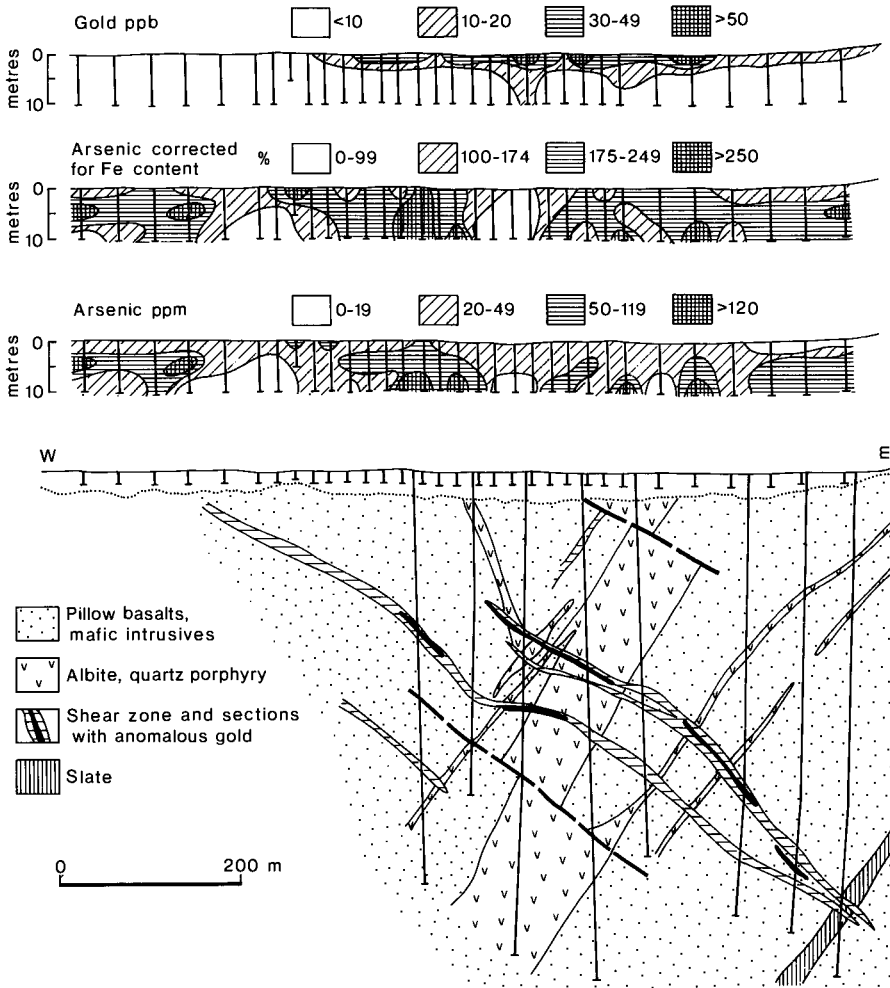


Fig. III.3-43. Distributions of Au, As and corrected As in surficial horizons of the regolith overlying Au mineralization, Mararoa Reef, Western Australia. Modified after Smith and Keele (1984). Corrected As values are actual values as percentages of expected value based on Fe content, derived from an As-Fe regression.

At Mararoa, Au is concentrated in the surface horizon, with maximum values (30–> 50 ppb) directly over the mineralization itself, rather than over the barren subcrop of the shear. Similar surface indications in carbonate soils of otherwise concealed Au mineralization are known (e.g. Bounty, see p. 351), even where the overburden is transported (e.g. Mount Pleasant, see p. 365). A possible mechanism of enrichment is discussed in Chapter V.3.

Bou Grine Pb-Zn deposit, Tunisia (C 1 Ca [1])

Studies at the Bou Grine deposit in Tunisia (Leduc, 1986; Guedria et al., 1989) suggest that dilution alone does not account for the reduction in Pb and Zn contents during calcrete formation but that leaching has also occurred. The mineralization consists of stratiform bodies of massive and disseminated sphalerite, galena and pyrite associated with barite and celestite. These bodies are situated in Triassic and Cretaceous claystones, sandstones and laminated limestones draped around diapirs of Triassic evaporites. The relief is moderate but with steep slopes around some diapirs. The area has a semiarid Mediterranean climate, with an annual rainfall of 500 mm. The soils are thin, usually less than 1 m deep, comprising:

humic loam, 0–30 cm thick, partly colluvial in origin and thicker at the base of slope. There is a sharp boundary to:

calcrete, 50–150 cm thick, with nodular, laminated and massive fabrics; this merges to:

saprolite, derived from Triassic and Cretaceous bedrock.

The humic loam gave the strongest contrasts and the area was explored using the minus 100 μm fraction sampled on a 25 \times 50 m grid. Mineralization was indicated by concentrations exceeding 2000 ppm Zn and 400 ppm Pb, compared to backgrounds of less than 100 ppm. Petrographic study of the calcrete suggests that it postdates the soil and has proceeded by infilling voids and by replacing pre-existing minerals. Fabric preservation implies that the replacement has been at least partially isovolumetric; recalculation of geochemical data on this basis from several soil profiles shows that there has been a net loss of Pb and Zn from the calcrete horizon compared to the underlying saprolite and fresh rock (Table III.3-12). Where no calcrete is present (profile A), Pb and Zn concentrations are highest in the saprolite and lower humic horizon, whereas in calcrete profiles, Pb and Zn are depleted. Partial extraction analyses demonstrated that in the calcrete horizons, most of the Pb and Zn is associated with the HCl-soluble fraction (predominantly carbonate) whereas in the soils, they are associated with the Na-dithionite soluble fraction (mostly Fe oxides). In the saprolite, the metals are distributed between both fractions. This suggests that Pb and Zn are dissolved when their host minerals are replaced by calcrete and that, although some metal is reprecipitated with calcite, the remainder is leached. The calcretes at Bou Grine are developed over highly calcareous rocks, including limestone; although there is an absolute increase in CaCO_3 content, much of calcrete, including the isovolumetric replacement of existing minerals, is due to recrystallization of original calcite. Mineral replacement and remobilization of base metals may be less evident over Ca-poor rocks, particularly where these have been deeply weathered.

PGE exploration. Plat Reef, Bushveld Complex, South Africa and Windimurra Complex, Western Australia (C 0 Ca [1])

Active concentration of As in calcretes is found in juvenile soils over the sulphide-bearing Plat Reef in the Bushveld Complex and, together with Hg, may

TABLE III.3-12

Contents of some major and trace elements in soil profiles at Bou Grine, Tunisia, assuming isovolumetric weathering (derived from Guedria et al., 1989); the soils are developed on limestones, hence there is only a minor increase in CaCO_3 content in the calcrete horizon

Horizon	Depth cm	Density $\text{g}\cdot\text{cm}^{-3}$	SiO_2 $\text{cg}\cdot\text{cm}^{-3}$	Al_2O_3 $\text{cg}\cdot\text{cm}^{-3}$	Fe_2O_3 $\text{cg}\cdot\text{cm}^{-3}$	MgO $\text{cg}\cdot\text{cm}^{-3}$	CaCO_3 $\text{cg}\cdot\text{cm}^{-3}$	Pb $\text{cg}\cdot 100$ cm^{-3}	Zn $\text{cg}\cdot 100$ cm^{-3}
<i>Profile A</i>									
Humic	20	2.05	67.7	9.64	7.8	2.67	110	36	123
Humic	40	2.21	29.2	3.54	7.5	1.33	169	168	270
Saprolite	60	2.28	46.5	2.74	11.2	2.05	157	107	307
Bedrock	100	2.55	20.4	4.08	1.79	0.76	221	38	210
<i>Profile B</i>									
Humic	10	2.14	62.9	9.20	7.06	2.56	128	26	47
Calcrete	20	2.29	21.6	5.04	3.21	0.69	197	5	6
Saprolite	30	2.26	39.1	8.36	4.75	0.68	171	6	5
Bedrock	80	2.45	44.3	8.58	3.19	0.74	187	7	8
<i>Profile C</i>									
Humic	7	2.14	49.2	7.70	5.56	1.93	146	14	30
Upper									
Calcrete	15	2.47	18.3	2.47	3.80	1.24	220	4	4
Calcrete	50	2.29	19.0	5.73	2.29	0.69	200	4	3
Saprolite	70	2.26	43.6	10.62	3.16	0.68	167	7	7
Bedrock	100	2.45	72.0	17.40	3.43	0.74	148	12	7

give the only surface geochemical expression of the mineralization (Frick, 1985). During weathering, elements such as Ni, Co, Cu and, in part, As, have limited mobility, being adsorbed to Fe oxides. These elements, after correction for soil Fe content, only indicate the presence of the Plat Reef where soils are both thin (less than 2 m) and dominantly residual but give no anomaly where soils are thicker or composed mainly of transported material. Anomalous concentrations of the mobile elements Hg and As occur directly over the mineralization, whether the soils are residual or transported, presumably due to active, upward migration. Arsenic gives the more erratic response, apparently because of adsorption to a greater variety of soil components than Hg, but is present particularly where calcrete is developed. Frick (1985) considers this to be the result of the reaction between arsenious acid and calcite to form minerals of the weilite group ($\text{CaH}\cdot(\text{AsO}_4)\cdot n\text{H}_2\text{O}$). It also appears that As and Hg may be flushed from the soil by rain; subsequent replenishment seems to confirm the active nature of the dispersion.

With the advent of highly sensitive analysis (Appendix 2), the PGE themselves may be determined. This has been demonstrated during exploration of the gabbroic Windimurra Complex, Western Australia (Harrison, 1990; R.J. Perring, verbal communication, 1990). Mineralization containing > 2 ppm PGE is associ-

ated with narrow (0.8–2.0 m) bands of disseminated and massive chromite, 50 m apart. The mineralized sequence is covered by shallow residual lithosols containing coarse fragments coated by calcrete. The minus 180 μm fractions of these soils, collected at 5–30 cm depth at 10 m intervals across strike, were analysed by fire assay fusion followed by ICP-MS. On the traverse illustrated by Harrison (1990), mineralization was indicated by an anomaly 130 m wide (maxima 43 ppb Pt, 37 ppb Pd), defined by a threshold of 8 ppb compared to a background of 2 ppb, for both Pt and Pd. In comparison, Cu and Ni gave single point anomalies of 230 ppm and 300 ppm respectively. Inspection of the data suggested that soil anomaly was accurately reflecting mineralization and a zone with high-background PGE contents; the extent of the anomaly is such that a wider sample spacing (e.g. 20 m) may have been adequate. The role, if any, of the soil carbonates in PGE dispersion has not been assessed. Mineralization was also detectable in stream sediment samples (minus 180 μm fraction), using the same threshold values.

Pre-existing profile partly or wholly truncated: profiles with pH contrast

Some calcretes are developed in regoliths that exhibit a marked pH contrast between surface and underlying horizons. If dispersion is active in the underlying horizons, the pH change at the interface may cause mobilized metals to precipitate, giving surface expression to mineralization, even where this is concealed by transported overburden.

Kadina Cu deposit, South Australia (B 0 Ca [3])

Sulphide mineralization (2% Cu) at Kadina, South Australia, is obscured by up to 70 m of transported and residual overburden (Mazzucchelli et al., 1980). Nodular and massive calcretes (0.6–2.0 m thick) beneath shallow clay loam soils overlie up to 40 m of transported clays deposited on saprolite. The calcretes are highly alkaline (up to pH 9.5), whereas underlying units are acid (pH 4.5–6.0). The distribution of total Cu was focussed in saprolite as narrow zones (to 15 m wide) containing > 1000 ppm Cu surrounded by dispersion haloes about 90 m wide defined by the 250 ppm Cu contour. Analysis for cold-extractable (acid ammonium acetate) Cu gave a “mushroom-shaped” pattern, with the strongest part of the anomaly immediately beneath the calcrete-clay interface (Fig. III.3-44). Low order anomalies extended through the calcrete and were evident in the topmost samples at 1.5 m depth. The cxCu response at the calcrete-clay contact was similar in location and dimensions to that obtained by saprolite sampling, but is more evenly distributed. Accordingly, shallower, more widely spaced drilling could have been used in the initial stages of exploration without appreciable risk of missing significant anomalies. The cxCu pattern is considered to be due to (continuing) upward migration of Cu in highly saline acidic groundwaters, with some lateral dispersion occurring prior to fixation in the zone of high pH.

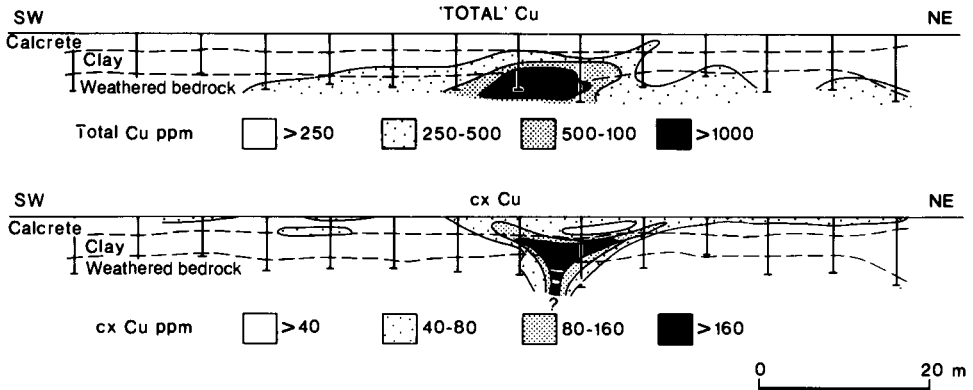


Fig. III.3-44. Distribution of total and cold extractable Cu (cxCu) in transported overburden and weathered bedrock, Kadina, South Australia. From Mazzucchelli et al. (1980).

Rocky Range Cu deposit, Utah, USA (C 1 Ca [3])

A similar hydromorphic mechanism is considered to have formed an epigenetic Cu anomaly in calcrete coatings on pebbles in alluvium overlying mineralization in Utah, USA. A chalcopyrite-bearing skarn is overlain by 6–70 m of alluvium, on a gently sloping (7°) pediment footslope in the Rocky Range mountains (Erickson and Marranzino, 1960). The Cu distribution and anomalies (greater than 300 ppm), shown by the minus 80-mesh fraction ($175 \mu\text{m}$) of the alluvial soil (Fig. III.3-45), probably indicate detrital Cu minerals derived from old workings upslope, although a few isolated high values were present above the buried mineralization. In contrast, the Cu contents of calcareous crusts scraped from pebbles were highest (200–> 400 ppm) close to the mineralization, and the ratio Cu in calcrete/Cu in alluvium exceeded 1.5 at sites overlying or downslope from it. Copper is considered to have been liberated from the sulphide mineralization under acid conditions and precipitated in the neutral to alkaline environment of the calcrete.

Surficial uranium deposits associated with calcretes

Epigenetic U enrichment of calcretes and carbonate-cemented sediments and overburden during the Pleistocene and Recent has resulted in potentially economic surficial deposits. Such deposits are known in arid terrains in Africa, the Americas and Australia (IAEA, 1984). They have formed by the solution and transport of U from a dispersed source—usually weathering granitic rocks—followed by concentration and precipitation in a relatively confined site, commonly as carnotite ($\text{K}_2(\text{UO}_2)_2\text{V}_2\text{O}_8 \cdot 3\text{H}_2\text{O}$). The deposits are classified as follows (Toens and Hambleton-Jones, 1984):

(1) Fluvialite: in palaeovalleys and drainages containing sediments having aeolian, colluvial, alluvial, lacustrine or evaporitic components.

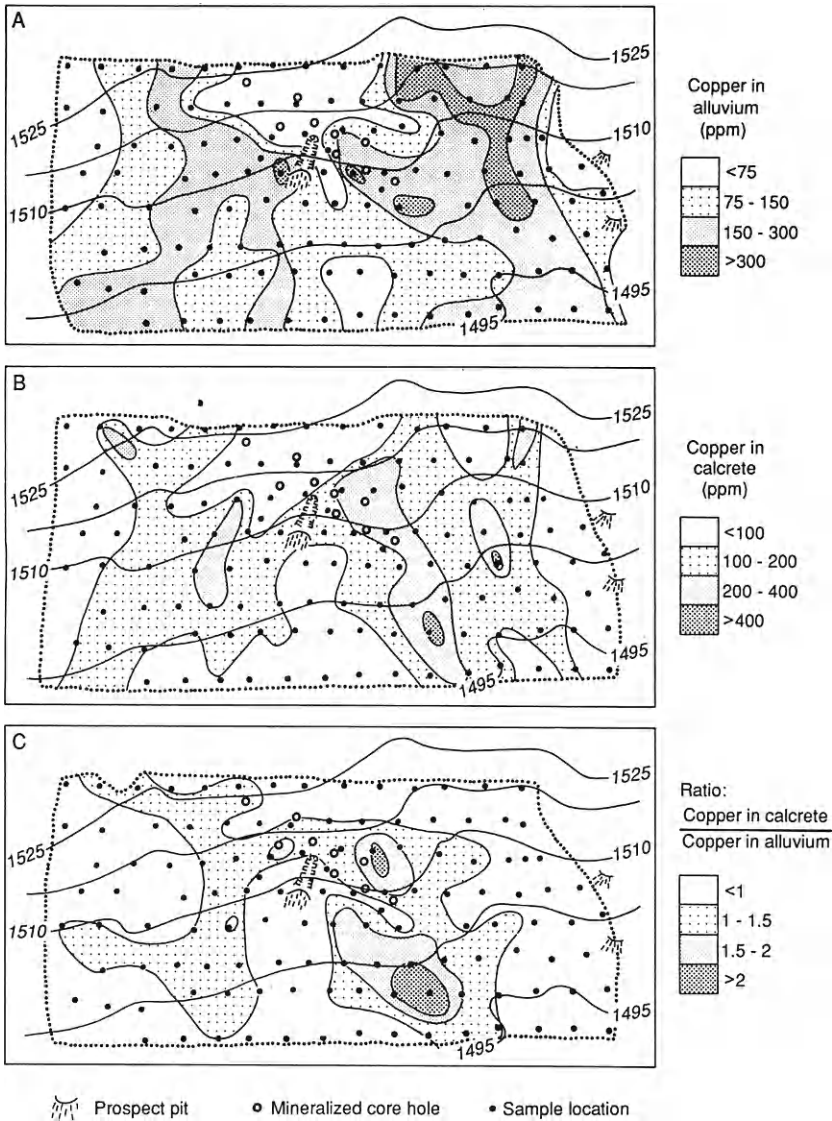


Fig. III.3-45. Copper distribution, Rocky Range, Utah, USA. (A) In alluvium (minus 175 μm fraction). (B) In calcrete coatings. (C) Ratio of Cu in coatings and alluvium. Modified after Erickson and Marranzino (1960).

(2) Lacustrine/playa: in dry or ephemeral lakes with evaporitic and fine-grained clastic sediments.

(3) Pedogenic: in residual or transported regolith, associated with calcrete, dolocrete or gypcrete.

The only known deposits with economic significance are of the fluviatile type, with the carnotite associated with non-pedogenic, valley calcretes (Australia, Somalia) and calcareous and/or gypsiferous sands and gravels (Namibia and South Africa).

Exploration for these deposits has depended upon radiometric surveys of favourable geological and geomorphological environments, followed by reconnaissance drilling of the anomalies, which themselves constitute the deposits. Soil or regolith sampling to search for a dispersion halo has been unnecessary. Future exploration may focus on concealed deposits that have formed as precipitates within undisturbed sediments, and those that have no radiometric expression because either they are very recent (and have not reached radiometric equilibrium) or differences in mobility have separated the daughter products from the parent U. Conversely, strong anomalies may be due to the concentration and deposition of Ra either distant from the U deposit, or where no U deposition has occurred at all. Consequently, understanding the genesis of these deposits, which involves weathering and dispersion in the regolith, is important for the interpretation of hydrogeochemical data in the exploration for buried and radiometrically blind deposits. The distribution, nature and origins of surficial U deposits and of appropriate exploration techniques are described in IAEA (1984).

Fluviatile and lacustrine deposits

A number of factors may be involved in the genesis of fluviatile and lacustrine deposits (Mann and Deutscher, 1978) but the most important, especially for those in Australia, are the evaporative concentration U, V and K in groundwaters and the redox control of V mobility; a lesser role is ascribed to changes in pH and in CO₂ partial pressures that cause dissociation of uranyl carbonate complexes. The cations (U, V, K) are all derived from weathered granitoids and transported in groundwaters to the valley axis (Fig. III.3-46). Uranium is solubilized as uranyl carbonate complexes and V as a four-valent cation. Precipitation of carnotite occurs where concentrations of U and K have been elevated by evaporation and where V is oxidized to the five-valent state. This may be where V has diffused upwards from depth under a redox gradient or where a subsurface bar has caused upwelling of groundwaters to relatively oxidizing conditions, accompanying effects being mounding and spread of calcrete. However, calcrete is not the only host to mineralization and in many deposits carnotite is precipitated in other sediments.

Changes in hydrological conditions, due to climatic variation or erosion, can cause changes in sites of deposition. In some localities, mineralization may be actively forming, whereas elsewhere it may be actively dissolving—in some instances within the same drainage system. The hydrogeochemical status of a system with respect to carnotite mineralization is best described by the carnotite solubility index, S.I. (Mann and Deutscher, 1978):

$$\text{S.I.} = \log\left(\frac{[\text{K}^+][\text{H}_2\text{VO}_4^-][\text{UO}_2^{2+}]}{K_{\text{sp}}[\text{H}^+]^2}\right) \quad (2)$$

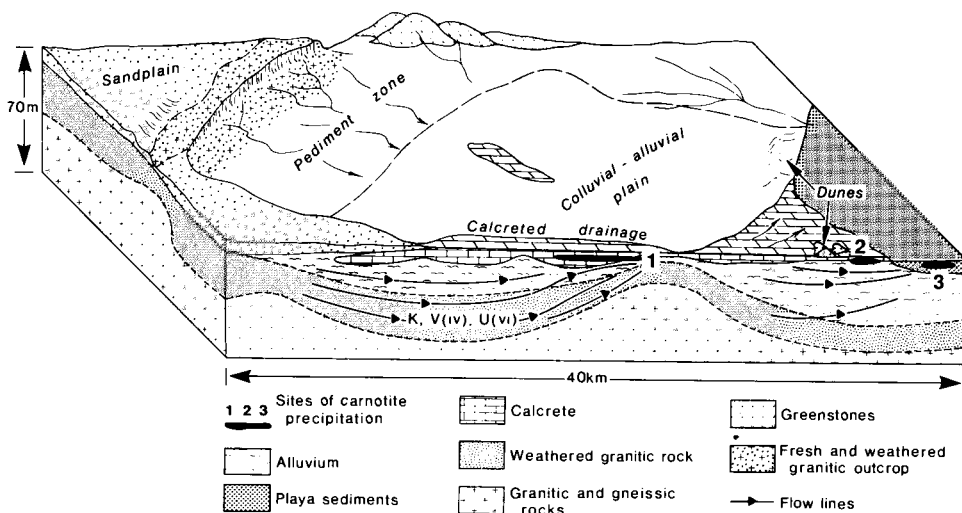


Fig. III.3-46. Block diagram illustrating geomorphological setting of carnotite mineralization in drainage sediments, Yilgarn Block, Western Australia. 1: valley calcrete; 2: calcrete platform; 3: playa. Modified after Deutscher et al. (1980). The setting is similar to that depicted in Figure I.1-3.

where K_{sp} , the carnotite solubility product, is written

$$K_{sp} = [K^+][UO_2^{2+}][H_2VO_4^-]/[H^+]^2 \quad (3)$$

For some Western Australian deposits, $K_{sp} = 10^{7.05}$ (Deutscher et al., 1980). A S.I. of zero indicates saturation with respect to carnotite, and hence precipitation, whereas negative values indicate undersaturation and dissolution of carnotite.

The S.I. can be used as an adjunct to U and V determinations in hydrogeochemical surveys. Uranium concentrations in groundwaters may delineate regions favourable for the weathering and release of U from granitoids, but high values (e.g. > 100 ppb U) do not necessarily indicate carnotite deposits. Since carnotite dissolves incongruently, releasing vanadium, V concentrations may provide a guide to mineralization, usually only being significant (20–50 ppb V) down-drainage from a (dissolving) carnotite-deposit. The S.I. may indicate proximity to sites of active precipitation, becoming less negative down-drainage towards such a site.

Pedogenic deposits

Pedogenic enrichment of U may occur in calcrete and underlying carbonated weathered bedrock in the upper 1 to 5 m of the profile. Such enrichments tend to overlie specific source rocks or occur a short distance downslope from them. They are formed by the capillary rise or evaporative pumping of groundwaters

above the water-table, so that activities of K^+ , V^{5+} and U^{6+} exceed the solubility product of carnotite. Total U contents exceeding 1000 ppm have been recorded (e.g. Minindi Creek; Butt, 1988) but, because the volume ratios of source to enrichment site are small, tonnages are low and the deposits are unlikely to be economic. Pedogenic concentration over source rocks having high abundances ($> 5\text{--}10$ ppm) of labile U may constitute false anomalies in exploration for concealed primary deposits, the surface expression of which may arise by analogous processes. However, anomalies derived from primary mineralization would be expected to contain elements additional to K and V.

SUMMARY AND CONCLUSION

The warm arid zone includes a wide range of climates, from semiarid on the margins of dry savanna and Mediterranean climatic regions, to the extreme aridity of the desert cores. Landscapes and regoliths show a similarly wide variation, ranging from terrains dominated by a widespread cover of lateritic cuirasse to those consisting of rocky outcrops and tracts of aeolian sand. Despite this diversity, however, there are numerous common features, for the differences in landscape and regolith are a continuum of response to alterations in the type of weathering and erosion brought about by climatic change. There is evidence that most, if not all, of the present arid zone once had a humid tropical climate similar to that of the wetter savannas and was mantled by a deep lateritic (*sensu lato*) regolith. The changes observed in a traverse from the wet savannas to the desert core, therefore, are essentially the same as the evolutionary trend to be experienced at a given site due to increasing aridity.

Recognition of the common history and evolution of the warm arid zone—and indeed of most tropically weathered regions—is one of the keys to understanding geochemical dispersion and the nature of the surface expression of mineralization. The geochemical characteristics of the regolith in these terrains are generally dominated by the effects of weathering under early humid climates (i.e. extreme surface leaching and a residual mineralogy of Al and Fe oxides and oxyhydroxides, kaolinite and resistant primary minerals including quartz). Weathering under arid conditions may have modified these characteristics, most commonly by further leaching and redistribution of elements deep in the profile (e.g. by saline groundwaters) and the addition of secondary minerals such as silica, gypsum, Ca and Mg carbonates and alkali salts. Erosion, instigated by uplift or climatic change, is also significant in determining the surface geochemical response of mineralization, for the depth of truncation of the original regolith profile determines which horizon will outcrop. Only in areas of complete erosion, most abundant in extremely arid climates, does the pre-existing profile have no significance.

Successful geochemical exploration in the arid zone, as in all environments, thus depends on the correct assessment of the origin of the regolith materials

used as sample media. For a given area or site, depending on the scale of the survey, this assessment can be achieved by:

(1) study of published and unpublished literature on the geomorphology, regolith and previous geochemical exploration of the region;

(2) geomorphological survey of the area to be explored, guided by appropriate remote sensing techniques, including aerial photography;

(3) on-site appraisal of the nature of the regolith represented by each landform unit. In many instances, it may be desirable to conduct drilling programmes to confirm the regolith stratigraphy and define parameters for sample identification;

(4) where possible, to conduct orientation surveys to optimize sampling and analytical procedures.

Each stage of this procedure should be guided by the concepts represented by the exploration and dispersion models described in this chapter, and the equivalent models in Chapters III.1, III.2 and IV.1. These indicate the most important features that need to be established to determine sampling and interpretational strategies. The models cannot take the place of orientation surveys, but they provide general guidelines as to the nature of the geochemical expression of mineralization that may be expected in each environment.

ACKNOWLEDGEMENTS

The data on the Transvaal gold mine, Western Australia are published by permission of Mawson Pacific Ltd. Data on Mount Gibson, Bardoc and Bounty have been released with the permission of Reynolds (Australia) Pty. Ltd., Aberfoyle Resources Ltd., and Aztec Mining Co. Ltd., respectively, and the Australian Mineral Industries Research Association Ltd. The text has benefitted greatly from comments by Dr. I.D.M. Robertson and Dr. R. Davy. The figures were drafted by Mr. A. Vartesi.

DISSECTED TERRAINS AND TROPICAL MOUNTAINS

C.R.M. BUTT and H. ZEEGERS

INTRODUCTION

Geochemical exploration procedures and responses in tropically weathered regions of high relief have many similarities irrespective of the geomorphological history or the past or present climates. At greater altitudes, the similarities increase and, indeed, more closely resemble those for hills and mountains in temperate and glaciated regions. The discussion in this chapter, therefore, is limited to hills and mountains at altitudes below that influenced by present or past (Pleistocene) cool climates, which in the seasonal tropics correspond to the forest limit at about 3500–4200 m.

With high relief, some of the distinctive geochemical and environmental attributes of tropical terrains, such as the predominance of weathering and chemical dispersion over erosion and mechanical dispersion, are lost. In all climates, the rate of chemical wasting is slow relative to that of physical denudation, hence neither development nor preservation of a deep weathering profile are possible and mechanical dispersion dominates. Thus, even in mountainous tropical rainforests, unaltered sulphide minerals may be present in stream sediments many kilometres from their source (Jones, 1973). Not only are geochemical procedures, such as stream sediment and footslope colluvium/talus sampling for regional surveys, common to most areas of high relief, but so too are some of the difficulties, such as those of access, communications and, in mountains, changeable weather.

Tropically weathered regions of strong relief do have some geochemical characteristics that differ from those of temperate regions and, to some extent, these vary according to the prevailing climate. The variations, however, are less pronounced as those described for regions of low relief in Part III. Certain features, such as the development of calcrete, remain characteristic of semiarid and arid regions (annual rainfall < 600 mm) but, in general, the geochemical expression of mineralization in dry savannas closely resembles that in semiarid regions. Similarly, there are few significant differences between wet savannas and rainforests. Accordingly, models and examples for regions of moderate to high relief are described under these two groups, namely

- wet savannas and rainforests, and
- dry savannas, semiarid and arid terrains.

DISTRIBUTION

High relief in tropically weathered terrains occurs as inselbergs, dissected plateaux and juvenile mountain ranges. Inselbergs (or bornhardts or monadnocks) are steep-sided hills having bare rock surfaces, commonly isolated but also in small groups and ranges. They are mostly found in shield areas and are commonly granitic, but may be formed of any massive, resistant rock. Inselbergs develop as residuals during deep weathering in savannas and may preserve their form during successive erosional events and climatic changes. In arid and other climatic zones, the presence of an inselberg–etchplain relief may be taken as evidence for past savanna climates. They present few exploration problems.

Dissected, and commonly uplifted, plateaux (raised etchplains) comprise mature landscapes of low relief bounded by strongly dissected margins. The integrity of the surface may be protected by a duricrust (laterite, bauxite, silcrete, calcrete) or by resistant, flat-lying sedimentary rocks. Such dissected plateaux are found principally in shield areas, where climatic change or uplift have resulted in instability, lowering of erosional base levels and rejuvenation of drainage. The strong relief of the marginal areas of dissection and scarp retreat may be localized when initiated only by climatic change (e.g. along “breakaway” escarpments in dry savannas and arid zones in West Africa and Australia), but is proportionately more extensive with increasing age and degree of uplift. Thus, in the Eastern and Western Ghats, India, bauxites are present on small remnants at altitudes of 1300–1550 m and 1980–2280 m, in ranges being dissected to a base level at 400 m.

Juvenile hills and mountain ranges are found in the tectonically active zones situated at lithospheric plate boundaries. In the tropics and adjacent areas, these include the mountains and islands of the Pacific “ring of fire”, and the mountains of Southeast Asia, northern India to Iran and the Mediterranean. These ranges generally have juvenile relief forms but mature surfaces may be preserved, even at quite high altitudes. Examples are the pediplains of the altiplano of the tropical Andes, cuirasse (at 3000 m) associated with Ni laterite in New Caledonia and red soils (at 1000 m) with Ni laterite in Oregon and California, USA.

Plateau remnants, and flat areas in present tropical ranges, have the geochemical characteristics of deeply weathered areas. The plateau surfaces themselves are described by the A models discussed in previous chapters. In higher levels of the dissected areas, parts of the old profile may be present (B models). Mostly, however, the profiles have been stripped or have not developed due to the aggressive erosion promoted by continued uplift; soils will therefore have developed on previously unweathered rocks, so that more direct geochemical responses can be expected (C models).

RAINFORESTS AND WET SAVANNAS

Rainforest and wet savanna environments of high relief are most common in tectonically active areas of central Africa, Central and South America and Southeast Asia. The deep, polygenetic weathering profiles described in Chapter III.1 require tectonic stability to form or be preserved. Accordingly, the weathering profiles developed in terrains of high relief are quite different from those found where the relief is lower. The pre-existing profiles are usually truncated and transported material is common on slopes (B * * [2,3] models). Remnants of the pre-existing lateritic profiles may be preserved on high plateaux and are the source of talus covering the residual profiles on upper slopes. Locally, stone-line profiles (B 3 0 [*] models) may form, even on steep slopes (see Ovala, p. 400). Conversely, elsewhere, erosion may have led to the complete stripping of the earlier profile so that fresh bedrock outcrops or is the immediate parent material of present soils (C models). These terrains are thus characterized by a wide variety of surface materials, including fresh rocks, saprolite, residual soils and thick transported overburden. The geochemical response in these environments depends strictly on which of these is present. Pronounced anomalies with strong contrasts are found to overlie many types of mineralization (e.g. porphyry Cu, Au, Sn, PGE) where soils are residual, or to be displaced downslope where mechanical transport or hydromorphic dispersion has occurred. However, there may be no geochemical expression where mineralization is overlain by entirely allochthonous material, for example as the result of landslips. The major problem facing the exploration geochemist, therefore, is to recognize the possible presence of such overburden, which may be quite difficult in remote and forested areas.

Pre-existing weathering profile partly truncated (B models)

Weathering profiles on steep slopes typically consist of variably truncated saprolite overlain by either a thin residual soil or a cover of semi-residual or transported overburden that is heterogeneous in grain size, composition and origin. Dispersion is mostly mechanical but anomalies may have some residual component in favourable situations. Hydromorphic dispersion may be important for some moderately mobile elements such as Cu and Au. As shown in Fig. IV.1-1, several dispersion models may be encountered on the same slope, ranging from B * * [2] to B * * [3] or C, complicating the interpretation of geochemical data. When the slopes are extremely steep, it may be almost impossible to collect near-surface samples that even approximately represent the underlying bedrock. Conversely, if anomalies are obtained in surface transported material, it may be quite difficult to locate their origin. Deep sampling, e.g. by hand auger, may be necessary, to avoid collecting transported material. Problems may also arise in the design of the sampling pattern. High relief and heavy forest may make it very difficult or impractical to cut lines on a regular grid. Sampling

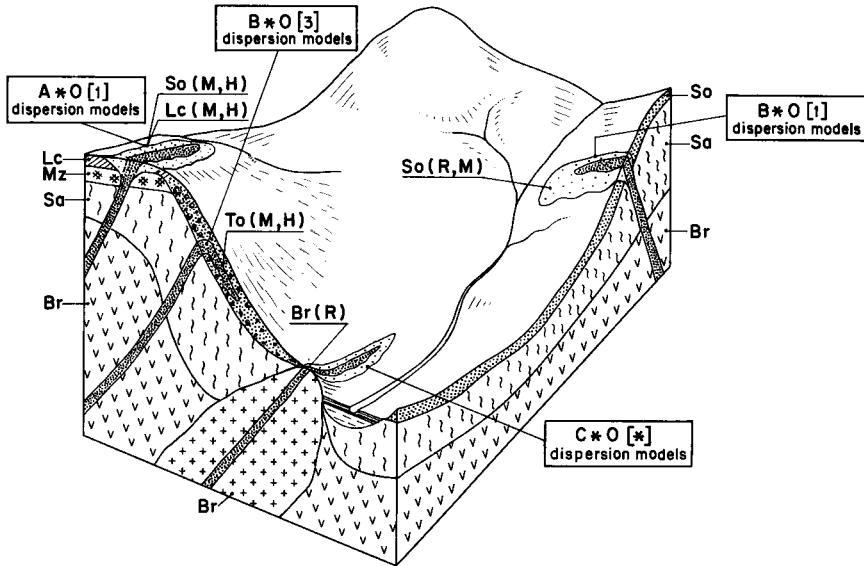


Fig. IV.1-1. Block diagram illustrating A-, B- and C-type dispersion models in terrain of high relief in rainforest environments. For abbreviations, see Fig. III.1-1.

along lines perpendicular to the slope is certainly more convenient, but may be unsuited to the geological situation. Similarly, sampling is easier on ridges and spurs and has been used successfully for regional surveys, but the coverage obtained may be biased towards particular geological units and is restricted to sites in which lateral dispersion is limited.

Variations in the conditions of dispersion and the problems arising at the anomaly interpretation stage are illustrated by the examples presented hereafter. Many of the case histories relate to exploration for porphyry Cu-Mo deposits, which typically occur in regions of tectonic and volcanic activity and hence high relief.

Exploration for porphyry Cu-Mo mineralization

In west Kalimantan, Indonesia, soil samples collected at 60 cm depth on a 100×100 m grid over an area of 25 km^2 gave anomalies in several elements (Viaene et al., 1981):

(1) Cu anomalies (200 to 1000 ppm) indicated mineralized, quartz-rich granodiorite. The anomalies did not correlate with either low pH values or with high Fe or Mn contents. Investigation of the anomalies by pitting showed there to be 2 types of profiles:

(a) shallow residual profiles with saprolite at about 1 m depth, locally with fresh disseminated chalcopyrite and molybdenite; models B 1 0 [1] and C 0 0 [1]. The Cu contents at depth are very similar to those in the soil samples.

(b) colluvial profiles with transported surface material (B 1 0 [2] model). The geochemical anomalies do not directly overlie the mineralization, but are displaced downslope.

(2) Au (0–4 ppm): the higher values have a scattered distribution, and only locally coincide with the Cu anomaly;

(3) Mo: the higher values (> 1.1 ppm) are clustered in the same area as those of Cu, with a similar, presumably mechanical, displacement downslope, relative to the mineralized source.

(4) Pb and Zn: higher values (> 52 ppm Pb and > 177 ppm Zn) are considered to be related to lithology or to scavenging by Fe oxyhydroxides.

These data demonstrate that even where colluviation and mass flow occur on steep slopes, porphyry-type Cu mineralization is reflected by the high Cu, Mo and, less accurately, Au contents of soils.

On Santo Nino, Philippines, a porphyry Cu deposit is indicated by cold extractable (100 ppm cxCu) and total (> 1000 ppm Cu) contents of soils. Geochemical techniques were found to delineate the mineralization, with the response being independent of the relief (Tupas et al., 1968).

On Viti Levu Island, Fiji, detailed soil and pit geochemistry were not always a reliable guide for the location of drill targets during reconnaissance surveys for porphyry Cu mineralization (Leggo, 1977). Elevations vary between 100 m and about 1200 m, and the annual rainfall exceeds 5000 mm. The depth of complete oxidation varies from nil to 30–80 m and partial oxidation may extend to 300 m in fractured rocks. Drilling suggests that the base of oxidation reflects an old, gently sloping, planar weathering surface that is little affected by the present topography. The soils are described locally as “steep-land soils”, formed under a humid, tropical (rainforest) climate. Depending on the nature of the bedrock, two main soil types are developed:

(1) humic latosols derived from rocks of intermediate composition;

(2) red-yellow podzolic soils on rocks of acidic composition.

Despite the heavy rainforest, many slopes are unstable. Accordingly, although in some areas the soil is essentially residual, in others, landslip deposits, mud avalanches and boulder terraces form a cover of transported overburden.

Soil samples were collected along ridge and spur lines or at various grid densities (e.g. 125 × 15 m; 30 × 15 m) at depth between 20 and 40 cm. The minus 0.2 mm fraction was analysed initially for Cu only, by AAS following HClO₄ digestion, and subsequently for Pb, Zn (HClO₄), Mo (HClO₄/HF) and Au (aqua regia). The ridge and spur soil sampling successfully outlined the mineralization, showing high contrast Cu anomalies except where there was transported overburden (B 1 0 [3] model). Detailed soil and pit geochemistry revealed that Cu has been leached from the surface, to a degree depending on the original sulphide content and on the nature of the weathering profile. Thus, several anomalous zones were defined in areas in residual soils by the 500 ppm Cu contour, with a maximum value of 2800 ppm. The soil anomalies in Au (threshold: 0.02 ppm, maximum: 0.5 ppm) and, to some extent, Mo (threshold: 8 ppm,

maximum 232 ppm) generally correlate with those of Cu. Pit sampling gave little additional information except where transported overburden was present (B 1 0 [2,3] models). Overall, Au was found to be a better pathfinder for Cu mineralization than either Mo or Zn.

In the Cu belt of west-central Puerto Rico, where the annual rainfall is about 2000 mm, Au proved to be a more reliable indicator of porphyry copper deposits than Cu itself (Learned and Boissen, 1973). In the prevailing freely drained, oxidizing environments, Au is more stable and relatively immobile compared to Cu, which has been leached and is depleted in the soil.

The geochemical expression of porphyry Cu mineralization in areas of high relief in humid tropical regions, based on examples from Philippines, Malaysia (Nungkok deposit, Sabah state) and Ecuador (Chaucha deposit), has been summarized by Saigusa (1975). A study of the relationships between the Cu content of soils, and of the underlying mineralization showed that the ratios of cold extractable to total Cu content of soils, and of the total Cu content of mineralization and soil, can be used to predict the potential of the target. Both ratios are largely dependant on the topographic situation. In average, the total Cu content of a given deposit is from 1.5 to 3 times that of the overlying soil.

Exploration for other styles of mineralization

Vein Sn mineralization, Tekka, Perak State, Malaysia (B,C 1 0 [1,2])

Dispersion from a subcropping mineralized vein system was studied by collecting soil samples every 16 m (50 feet) along 3 traverses, and at a closer interval (1.5 m or 5 feet) near Sn mineralization (Teh, 1979). The soil contents of Sn, Cu and Zn decrease sharply away from the veins so that the dispersion haloes have a width about ten times that of the vein itself. The mobile anion F^- , however, has a wider halo with a high contrast (several thousands of ppm) that may in part be related to primary dispersion. The less soluble elements (i.e. Sn and Pb) are affected by colluviation (soil creep) so that the dispersion haloes are slightly distorted downslope. Very clearly, in a situation such as this, where the saprolite and the mineralization subcrop, the dispersion halo is very restricted. Thus, although the mineralization has a distinct surface expression, the small magnitude and size of the anomaly suggest that soil geochemistry is not a favourable tool for rapid reconnaissance surveys.

Nickel laterite deposits, Philippines

Surface geochemistry was used in exploration for Ni-laterites in Palawan Island, Philippines (Ong and Sevillano, 1975). Three different geomorphological settings, ranging from steep slopes to quite gentle hills, were surveyed. Soils were sampled on a 300 × 300 m grid, and the Ni anomalies, commonly of high contrast, followed up by bedrock sampling by pitting. From a statistical study of the results obtained, the chance of finding Ni-rich lateritic ore in depth was assessed from the characteristics of the surface anomalies. The results (Table

TABLE IV.1-1

Palawan Island, Philippines: proportion (%) of prospecting pits, dug in different relief conditions as a follow-up to surface geochemical anomalies, that successfully demonstrated the presence of significant lateritic nickel mineralization (from Ong and Sevillano, 1975)

Anomaly contrast	Relief		
	Moderate	Middle	Rugged
High	96	70	70
Medium	86	65	59
Low	70	45	37

IV.1-1) clearly indicate that there are major problems in determining the relationship between a surface Ni anomaly and the presence of a lateritic Ni deposit at depth. The local conditions have to be taken very carefully into account, for the surface expression of the mineralization depends upon an estimate of the thickness and the nature of the residual soil or transported overburden, and upon the degree of preservation of the pre-existing lateritic profile within which the Ni enrichment has occurred.

Platinum mineralization, Sierra Leone (B 2 0 [1])

The geochemical dispersion of Pt and pathfinder elements (Cu, Pb, Zn, Cr, Ni) in a very mountainous and dissected area in the Freetown Igneous Complex was described by Davies and Bloxam (1979). The weathering profile is described as lateritic but, due to the high erosion rate, the residual profile is fairly shallow. The Complex is a layered series of troctolites, gabbros, anorthosites and some transitional lithologies. Mineralization consists of small Pt nuggets, dendrites and grains in stream gravels. Six hundred soil samples were collected at 30 m intervals along traverses across the main geological trend, at depths between 15 and 23 cm. For most of the elements analyzed, the median and threshold values in the minus 80-mesh (180 μm) fraction are quite low, given the geological environment and the possible occurrence of mineralization (Table IV.1-2). For example, median values of 80 ppm Ni and 43 ppm Zn are not compatible with the presence of mafic or ultramafic rocks. These low values probably reflect the incomplete digestion of the sample during analysis (aqua regia) rather than severe leaching due to the deep weathering. Although the anomalies do not appear to be displaced with respect to their source (lithology or mineralization), the dispersion haloes outlined by this weak acid digestion are probably mostly hydromorphic in origin.

Morobe goldfield, Papua New Guinea

The secondary dispersion of gold in the high relief rainforest environment of Papua New Guinea has been demonstrated by Webster and Mann (1984). Primary gold occurs as epithermal mineralization, with rich veins having a high Mn

TABLE IV.1-2

Freetown Igneous Complex, Sierra Leone: distribution parameters for Pt, Au and selected trace elements in lateritic soils (from Davies and Bloxam, 1979)

Element	N	Range	Median	Threshold
Pt ppb	10	5-100	10	76
Au ppb	17	10-220	30	152
Hg ppb	112	20-420	210	450
Cu ppm	95	1-61	19	46
Pb ppm	63	2-91	49	86
Zn ppm	92	13-103	43	88
Cr ppm	95	0-2340	350	1150
Co ppm	23	17-90	41	77
Ni ppm	134	20-287	80	208

content (as rhodochrosite). In the weathering zone, primary carbonates are replaced by Mn oxides ("wad") associated with prismatic quartz, forming the so-called "flatmakes", in which Au and Ag are both enriched. That the gold is secondary is proved by the presence of complex and delicate crystals (e.g. as dendrites) of gold and electrum, the latter also having increased grain size in the weathering zone. It is interesting to note that, in contrast to other morphoclimatic and geological environments, the Ag content of secondary gold may be high, with a fineness between 500 and 600. It is assumed that Au and Ag may be complexed by thiosulphate formed by the weathering of sulphides, buffered by carbonates, and precipitate together by reduction by precipitated manganese oxide. The mechanism is discussed more fully in Chapter V.3.

Gold mineralization, Ovala, Gabon (B 3 0 [1])

The lateral dispersion of gold in a stone-line profile developed in an area of high relief has been discussed by Edou-Minko (1988). The bedrock mineralization is an epigenetic deposit, possibly remobilized by metamorphism in a late Archaean or Proterozoic greenstone belt. The dispersion of Au was studied in several profiles along a traverse perpendicular to the mineralization, and parallel to the slope. The weathering profile is typically of the quartz stone-line type, as described elsewhere in Gabon (see Chapter III.2) with:

- (1) an upper, friable, yellow sandy horizon (about 1 m);
- (2) a thin stone line, with lithorelics, ferruginous nodules and quartz fragments embedded in a clay matrix (0.1-0.2 m);
- (3) saprolite.

The Au dispersion halo in whole samples is illustrated on Fig. IV.1-2. The dispersion halo extends downslope for at least 125 m from the subcropping mineralization, and the Au contents of the soils are > 1 ppm within some 50 m, and then 500-1000 ppb. The dispersion of Au in the fine (< 63 μ m) fraction was also studied, and was shown to be very similar to that of Au in the whole sample,

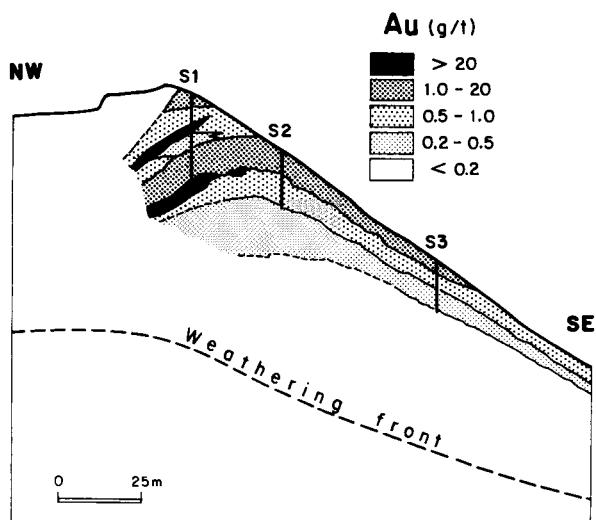


Fig. IV.1-2. Ovalla prospect, Gabon. Distribution of Au in whole samples in the upper part of the weathering profile (Edou Minko, 1988).

with contents ranging from 500–1000 ppb above mineralization, 200–500 ppb within 50 m and then less than 200 ppb. A morphological and geochemical study of free gold grains showed that most gold is primary near the mineralized zone. Secondary gold occurs as fine particles in the upper part of the profile and downslope in the dispersion halo, but only accounts for a small proportion of the total gold present. The supergene dispersion of Au at Ovalla is therefore controlled both by mechanical and chemical processes with a residual component over the subcrop of the bedrock mineralization.

Epithermal gold mineralization, Kelian, east Kalimantan, Indonesia (B20 [1,2])

Kelian is a Tertiary volcanic-hosted gold deposit having a resource potential of over 75 Mt at 1.8 g/t Au (Van Leeuwen et al., 1990). The prospect elevation is > 1000 m above sea level, but relief is quite gentle, the main mineralization corresponding to a hill not more than 200 m above the Kelian river. Climate is equatorial, with annual rainfall exceeding 3500 mm. Andesites and pyroclastics have been weathered to a depth ranging from 3 to 35 m.

Geochemical techniques were used from the early reconnaissance survey, which included: preliminary geological mapping, outcrop and float sampling, pan concentrate sampling, stream sediment sampling for Au, Ag, As and base metals. The mineralization was indicated by anomalous Au contents in some rock or float samples, cinnabar and gold in pan concentrate samples collected from the main stream up to 16 km downstream from the prospect, and anomalous concentrations of Au, Ag, As, Pb and Zn in stream sediment samples. During the initial

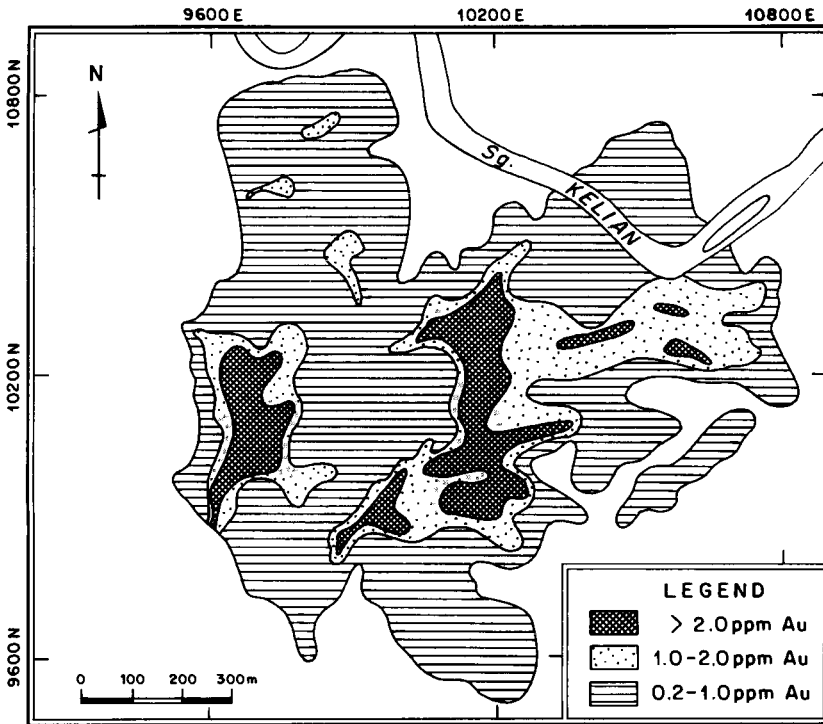


Fig. IV.1-3. Kelian deposit, Indonesia. Distribution of Au in soils. Redrawn from Van Leeuwen et al. (1990).

follow-up stage, soil geochemistry proved to be a very effective tool, allowing the delineation of most mineralized zones, even though these do not outcrop. Samples were collected by hand augering to less than 1 m depth, at a 50×20 m interval, and analyzed for Au, Ag, Cu, Pb and Zn. The distribution of gold in soils (Fig. IV.1-3) shows a wide anomalous halo with contents > 200 ppb and smaller anomalies sometimes exceeding 2 ppm Au. The distribution of Hg (Fig. IV.1-4) is very similar to that of Au, and the 100 ppb Hg contour line roughly outlines the limits of the hydrothermal alteration system. Silver and Pb anomalies (> 2 and > 300 ppm) are only present where Au contents exceed 2 ppm. Zinc anomalies are weak and, considering the topography, could have been displaced downslope. At more advanced stages of the exploration, intensive hand augering was used to assess the gold potential of the soil and underlying oxide mineralization.

The distributions of Au and Ag in the upper 50 m of the deposit indicate some enrichment of Au in the upper oxide zone, with average contents of 2.8 ppm compared with 1.2–1.8 ppm in the fresh or partly oxidized rocks. Conversely, Ag is relatively enriched in the lower part of the weathering profile. Thus, instead of being leached at the surface, Au is enriched, explaining the strength and high contrast of the soil geochemical anomaly.

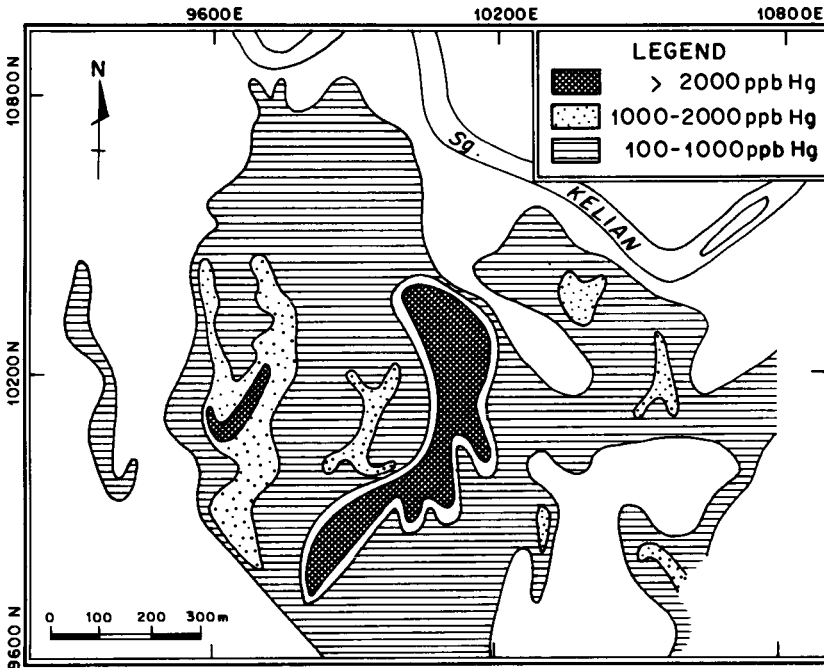


Fig. IV.1-4. Kelian deposit, Indonesia. Distribution of Hg in soils. Redrawn from Van Leeuwen et al. (1990).

At Kelian, the relief is not sufficiently pronounced for there to be significant displacement of the geochemical dispersion haloes. Similarly, mechanical erosion has not been strong enough to remove much weathered material, nor to deposit transported overburden on the residual profiles. Thus, the B 2 0 [1] model prevails over most of the prospect and conditions may be considered as very favourable for geochemical exploration.

DRY SAVANNAS, SEMIARID AND ARID TERRAINS

Stripping of the pre-existing weathered zone may be incomplete in uplifted plateaux and some ranges, particularly in dry savannas and semiarid regions, despite considerable dissection and the development of strong relief on a local or regional scale. More or less complete profiles may be present, especially on hill crests and in wide valleys, but here the relief is lower and more properly described by models given in Chapters III.2 and III.3. Rarely, full profiles are preserved on steep slopes (e.g. in the Darling Range, Western Australia), with a high physically-transported component in the duricrust. Commonly, however, only secondarily hardened saprolites and the lower and less weathered horizons

of the profile are preserved, since these are more resistant to erosion than the clay-rich upper saprolite and mottled zone. Since depths of weathering are lithologically controlled, some rocks may be essentially fresh at surface whereas others nearby are strongly altered. In places, possibly only the gossans date from earlier weathering episodes, the profiles on more resistant country rocks having been eroded. On the steep slopes of these terrains, especially in semiarid climates, outcrops of cemented saprolite and fresh rock contribute to the heterogeneous rubble layer that usually characterizes the surface; residual soils may only be patchily developed and occur as lithosols with little profile differentiation.

Stripping to deep levels in the profile exhumes zones that have been only partly leached or, alternatively, secondarily enriched. Many rock-forming minerals remain unweathered and gossans may have been eroded to expose secondary ore minerals and hence mobile elements such as Zn and Cd are retained. Supergene and lateritic enrichments of Cu-Mo and Ni-Co may be exposed over porphyry stocks and ultramafic rocks respectively and contribute to anomalies in outcrops and soils. Such Ni-Co anomalies can, of course, be very misleading during exploration for Ni sulphide mineralization. Soils reflect the compositions of these parent materials quite closely, with any lateral dispersion due mainly to mechanical processes. Anomaly strength depends on the degree of leaching or enrichment of the weathered mineralization but may be diluted by introduced aeolian or colluvial material or, in more arid regions, by the deposition of cements such as carbonates and silica. The principal dispersion characteristics are summarized by the model given in Fig. IV.1-5; the areas occupied by plateaux and slopes having complete lateritic profiles is small, so that examples of A dispersion models are very uncommon. Accordingly, B and C models, prevail, representing situations with more or less truncated profiles. In general, documented case histories suggest that there are few specific exploration problems except where colluvium or more exotic transported overburden displace or obscure the surface expression of mineralization.

*Pre-existing profile partly truncated, gossans and ironstones outcropping:
B * * [0,1] models*

For base metal sulphide exploration, gossan search and ironstone sampling are effective procedures (Chapter II.2). Gossans revealed the *Ilmars Cu-Zn-Pb deposit* (model B 1 0 [0,1]), situated in rugged terrain in the Kimberley region of northwest Australia, where weathering extends to 18–30 m (Halligan and Harris, 1980). Residual soils are only sparsely developed, but where present gave very strong anomalies (Fig. IV.1-6), with concentrations in the minus 175 μ m fraction being very similar to those of the gossan and primary mineralization. Anomaly width for Cu and Pb was 75–100 m but for Zn exceeded 200 m at over 1000 ppm, reflecting its greater dispersion.

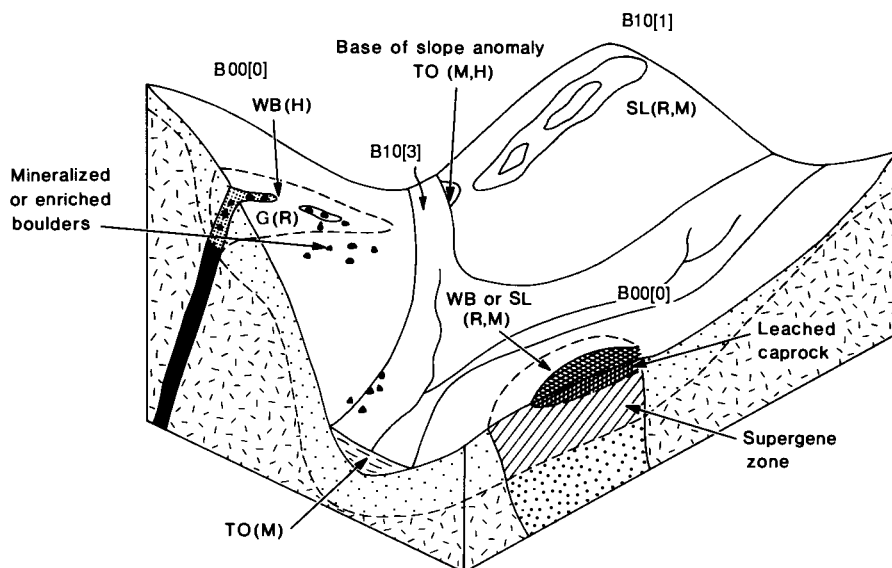


Fig. IV.1-5. Block diagram illustrating B-type dispersion models for partly stripped terrain of high relief in arid environments. For abbreviations, see Fig. III.1-1. Contours show general nature of anomaly; broken contours show subsurface anomaly. Derived in part from Butt and Smith (1980).

A number of case histories from northwestern and central India have demonstrated the usefulness of soil and gossan surveys in dissected lateritic and hilly terrain. For example, relict gossans and oxidation to depths > 30 m are present in the now arid *Khetri-Satkui-Saladipura Cu belt, Rajasthan* (model B 1 0 [0,1,2]). The prospective sequence forms prominent hills flanked by alluvial plains and dune fields. Except for localized areas of wind-blown sands, soils are residual, sometimes beneath surface scree. Soils surveys generally indicated mineralized shears by narrow, high contrast peaks (Dasgupta, 1963; Awasthi and Lal, 1981). Dispersion appeared to be minimal utilizing the minus $175 \mu\text{m}$ fraction (Fig. IV.1-7), but whether a coarser fraction would have been more effective was not reported. Similarly, in the more humid Chitradurga schist belt, Karnataka, base metal mineralization was successfully delineated by analysing the minus 80-mesh ($175 \mu\text{m}$) fraction of "C" horizon soils (Deshpande, 1982).

Broadly similar features are associated with the base metal sulphide deposits of southern Africa, where gossan development has been related to several older weathering surfaces (Andrew, 1984). Several deposits were discovered by gossan and soil surveys, typical examples being the Shangani Cu-Ni deposit, Zimbabwe (Philpott, 1975) and the Otjihase Cu-Zn deposit, Namibia (Scott, 1975; Garnett and Rea, 1985), described below.

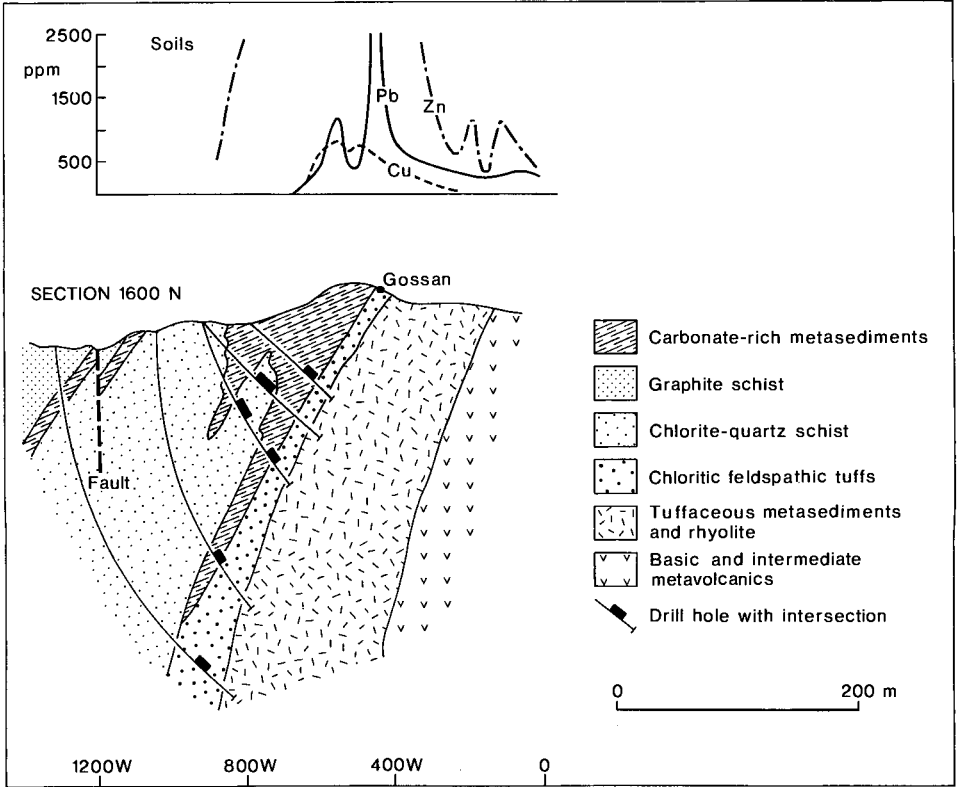


Fig. IV.1-6. Geological cross-section across the Ilmars Cu-Zn-Pb deposit, Kimberley region, Western Australia, illustrating soil geochemistry (minus 175 μm fraction) and main intersections of mineralization. From Halligan and Harris (1980).

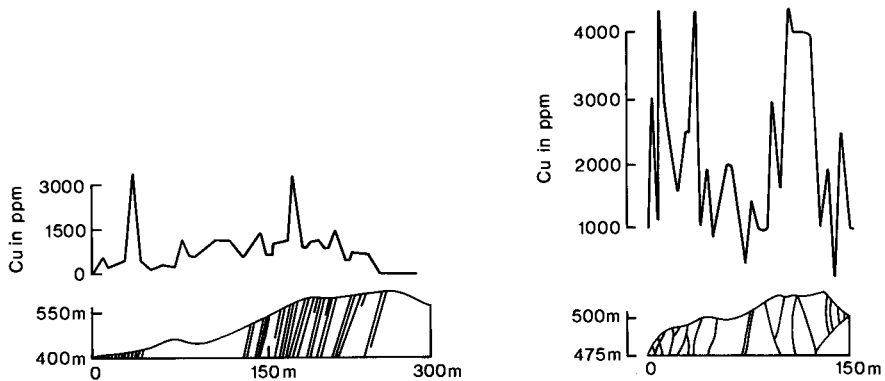


Fig. IV.1-7. Relationship between Cu mineralization and soil composition, Khetri copper belt, India. Modified after Das Gupta (1963).

Shangani Cu-Ni deposit, Zimbabwe (B 1 Si [0,1])

Shangani is situated in extrusive ultramafic rocks in a greenstone belt of the mid-Archaean Bulawayan series (Philpott, 1975). The weathered serpentinites hosting the mineralization have the highly silicified ("berberitic") horizons characteristic of lateritic profiles developed from dunitic ultramafic rocks, and the resistance of these horizons to erosion has resulted in locally high relief. The deposit was discovered during a two-stage exploration programme:

- (1) soil and rock sampling on a 300 × 60 m grid of a 500 km² area, with the discovery anomaly having up to 200 ppm Cu and 3200 ppm Ni;
- (2) detailed soil and rock sampling which outlined anomalies of 200–> 800 ppm Cu and 4000–> 6000 ppm Ni.

A small, scree-covered gossan (1 × 6.5 m) containing 2200 ppm Cu and 2310 ppm Ni discovered during the survey was found to be the surface expression of massive and disseminated Ni sulphides, grading 9.75% Ni, 1.20% Cu and 0.56% Ni, 0.08% Cu, respectively. No specific problems related to the relief were encountered and the interpretation of the surface geochemical data was complicated only by problems typical of Ni exploration in deeply weathered terrain, namely the differential behaviour of Cu and Ni. Thus, soils derived from weathered ultramafic rocks of all types were found to be lateritically enriched in Ni and Co, (> 2700 ppm Ni over serpentinites) and low in Cu, whereas soils over pyroxenites and gabbros had high Cu and low Ni contents. Copper has also been more strongly affected by surface leaching, the Ni/Cu ratio of anomalous soils (15–20) being significantly higher than that of sulphide ore (7–8). (N.B. These data are based on nitric-perchloric digestions of whole soil and rock samples; the effectiveness of this procedure compared to total digestion is discussed in Appendix 1.)

Otjihase Cu-Zn deposit, Namibia (B 0 Ca [0,1])

The deposit outcrops as a gossan on a ridge in the deeply dissected Khomas Highlands at an elevation linked to a supposed Cretaceous erosion surface and weathering may date from this period. Soils are shallow with little profile development, with pH 6.0–7.5 near the deposit, though lower (pH 5.5) over the gossan and higher (pH > 8.0) where calcretes are present. In the discovery surveys, the expected low mobility of Cu and Pb, and leaching of Zn, led to the use of sampling at 10 m intervals on lines 200–500 m apart. For cost reasons, sample pairs were composited to give an effective 20 m spacing. In the event, however, it was found that hydromorphic dispersion of Cu into the wallrocks, probably dating from an earlier weathering cycle, had resulted in an anomaly (ten times background) with a true width of 50–100 m at surface, and that downslope dispersion in soils extended up to 200 m from the gossan outcrop (Fig. IV.1-8). Scott (1975) reported that the fine fraction (minus 105 μm) gave the best response, a finding corroborated by Garnett and Rea (1985) for the minus 75 μm fraction. However, the latter authors found the anomaly smaller in all fractions, rarely exceeding 75 m downslope, with extremely low values within 10 m of the

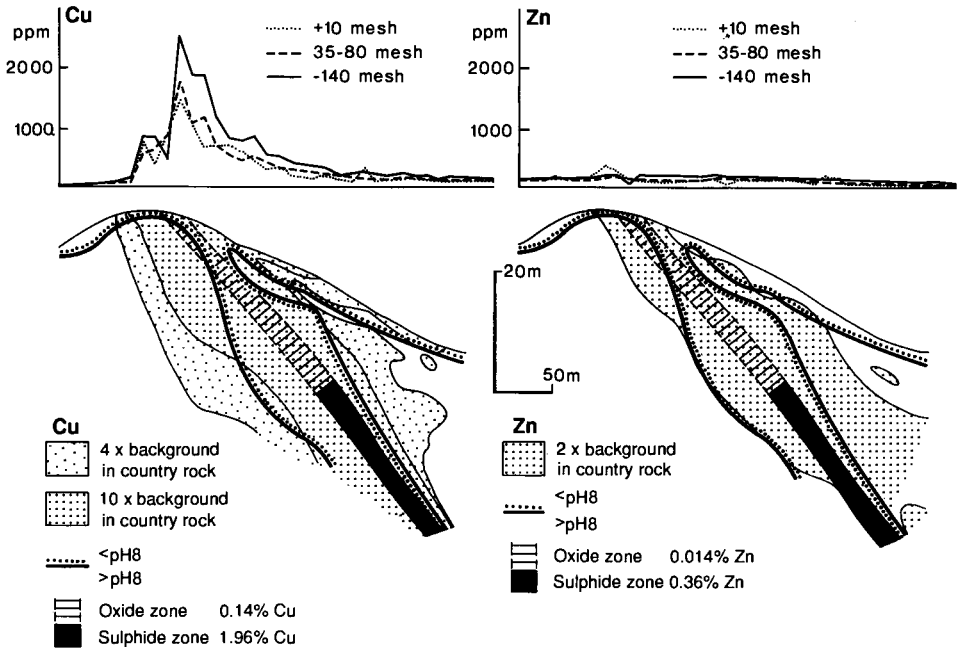


Fig. IV.1-8. Copper and Zn contents of soils and weathered bedrock, Otjihase, South Africa. Modified after Scott (1975). N.B. 10 mesh = 1.68 mm; 35 mesh = 420 μm ; 80 mesh = 177 μm ; 140 mesh = 105 μm .

source. Anomaly characteristics were not improved by using a coarse fraction, except when gossan fragments, individually handpicked from the samples, were analyzed. Zinc, Pb, Ag, Ba and Cr all gave similar responses to Cu using these fragments, but none was anomalous in other soil fractions except immediately over the gossan. (N.B. The composition of the gossan is given in Table II.2-24.) The greater effectiveness of Cu compared to other elements is because:

(1) only Cu has a hydromorphic anomaly in the weathered wallrocks which on further weathering contributes to the finer soil fractions;

(2) during soil formation, Zn, Ag and Cd are leached whereas Cu is retained.

This compares interestingly with the situation at the Cu-rich ironstone (pseudogossan) at Killara, Western Australia, where there is no wallrock enrichment (see p. 162). The Cu contents of the coarse fractions ($> 420 \mu\text{m}$) of the soils (0–15 cm) delineate the zone of the ironstone outcrop, due to the presence of physically dispersed ironstone fragments (Butt, 1979), but there is no anomaly in the fine fraction. The ironstones themselves contain up to 1850 ppm Cu (Table II.2-8), and the anomalous plus 2 mm fraction contains 140–640 ppm Cu, but none of the potential pathfinder elements is enriched in either ironstones or soils.

*Pre-existing profile partly truncated, no outcropping gossan or ironstones:
B* * [1,2] models*

When there are no gossans contributing clastic detritus to the soil, the geochemical expression of mineralization depends on the dispersion pattern within the pre-existing deep weathering profile. As is the case in regions of low relief, this in turn is reflected by the soils and will vary according to the degree of truncation of the profile. Because of continued erosion, present pedogenetic activity remains generally subordinate to inherited geochemical characteristics, irrespective of climate. For example, in Alabama, USA, which has a humid, warm temperate climate, red-brown soils are developed from an earlier lateritic weathering profile. A geochemical orientation survey over the *Hatchet Creek Cu prospect* (Clarke, 1971) showed differences in the expression of mineralization on the plateaux compared to the slopes. On the plateaux, where the pre-existing profile is almost complete (A 1 0 [1]), the effects of leaching during deep weathering are significant, with soils overlying mineralization having a mean Cu content of 550 ppm. On the slopes, however, where the profile has been truncated (B 1 0 [1]), the mean Cu content of soils over mineralization is 1200 ppm.

In more arid regions, soil compositions similarly reflect any zonation of the oxidation profile where this has been exhumed by dissection and can be a direct indication of supergene mineralization. This is well illustrated over Cu–Mo porphyries such as the *La Caridad deposit*, Mexico (models B,C 0 0 [0,1]). The ore (700 Mt averaging 0.72% Cu) is confined to a 90 m thick supergene zone of enrichment overlain by a leached capping 0–250 m thick (Coolbaugh, 1979). Mineralization was indicated by anomalous Cu, Mo and W contents in stream sediments 18 km down-drainage from the deposit. There is extensive talus and little soil development but nevertheless rock chip and soil surveys revealed the exact location of the deposit. For Cu, the survey showed anomalously low concentrations directly over the deposit, corresponding to the leached capping, surrounded by a halo of high values where the supergene enrichment has been exposed on the periphery (Fig. IV.1-9). In contrast, Mo was highest over the leached capping, reflecting its retention as molybdenite. Similarly, in the extreme aridity of the Atacama desert, Chile, Clark et al. (1967) noted that supergene enrichment of Cu, predominantly as chalcocite, was probably associated with the formation of pediplains or subsequent periods of aridity, uplift, declining water-tables and canyon-cutting. The later pediplains cross-cut enriched zones, hence any residual soils would be expected to be strongly anomalous.

Deep secondary alteration zones are also present over epithermal Ag-Pb-Zn mineralization in the Atacama desert. At *Caracoles*, for example, the veins, which are mostly 0.3 to 3 m wide in sets up to 3 km long, have an oxidation zone (0–80 m) overlying supergene enrichment at 80–150 m (Cabello, 1985). Soil samples were collected at a depth of 30 cm, beneath surface horizons of sands, gravels and salts (sodium sulphate and nitrate). Preliminary and detailed surveys

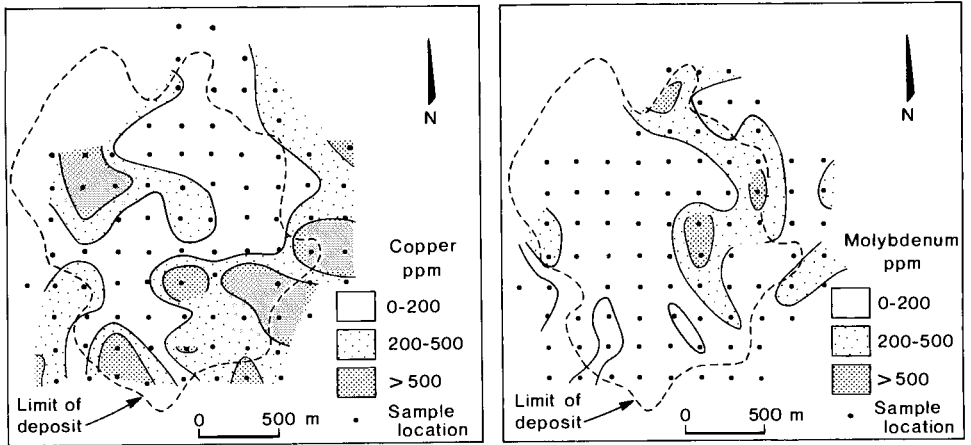


Fig. IV.1-9. Copper and Mo distribution in soils, La Caridad porphyry Cu deposit, Mexico. Modified after Coolbaugh (1979).

showed that the main mineralized structures were indicated by coincident Ag-Pb-Zn anomalies, with Cu having a less direct relationship. However, single element anomalies of any metal were generally of little significance. Concentrations of all elements were similar in soils and rocks (Table IV.1-3), and the results indicated that soil surveys are an effective exploration procedure.

Where soils are poorly developed, rock chip surveys of outcropping saprolite are possible and give similar responses to surveys utilizing fresh rocks (Govett, 1983). They are, of course, applicable to exploration for secondary deposits such as the willemite (Zn_2SiO_4) deposits at *Beltana and Aroona, South Australia* (model B 1 0 [0]). Here, weathering extends to 20–160 m and is considered to have led to the formation of the ores by replacement of limestone (Moeskops and

TABLE IV.1-3

Comparison of soil, rock and vein compositions, Caracoles, Chile (from Cabello, 1985)

		Ag ppm	Cu ppm	Pb ppm	Zn ppm
Soils	M	0.60	11.4	58	188
(N = 842)	S.D.	1.67	1.5	2.1	1.9
Rocks	M	0.57	18.5	58	209
(N = 48)	S.D.	1.40	2.2	2.5	3.5
Veins	M	48.9	72	975	2280
(N = 29)	S.D.	5.7	1.6	4.4	3.7

M = geometric mean; S.D. = standard deviation; N = number of samples.

TABLE IV.1-4
Compositions of outcrop samples around secondary willemite mineralization, Beltana, South Australia (from Moeskops and White, 1980a)

Rock type	Cu	Pb	Zn	V	As	
Beltana ore	M	320	> 35%	~ 300	> 1%	
	R	70-1500	-	60-1000	Sporadic lows to 500	
Lower Cambrian } Ajax Limestone	M	~ 100	> 1%	~ 100	~ 1000	
	R	30-200	0.04- > 1%	30-300	< 0.005- > 1%	
Willouran } Humanity Seat Formation	M	~ 130	> 1%	~ 60	~ 160	
	R	60-150	-	20-100	50-300	
Marinoan } Pound Quartzite	M	~ 40	~ 600	~ 40	< 50	
	R	3-70	300-1000	20-60	-	
Rock type	Cd	Ag	Ni	Ti	Ge	
Beltana ore	M	> 3	~ 0.1	~ 45	~ 450	~ 130
	R	Sporadic highs to 50	-	5-150	100-3000	< 3-300
Lower Cambrian } Ajax Limestone	M	~ 30	~ 0.2	~ 35	~ 1250	< 3
	R	< 3-200	0.1-0.4	5-300	0.001-1%	
Humanity Seat } Formation	M	~ 150	~ 0.2	~ 50	~ 250	< 3
	R	30-300	-	20-70	100-300	-
Marinoan } Pound Quartzite	M	< 3	~ 0.2	~ 50	~ 2000	< 3
	R	-	< 0.1-0.3	30-60	800-4000	-

M = mean (~ approximate); R = range. Data in ppm and percent.

White, 1980a). Rock chip surveys clearly indicated the outcropping orebodies and the enriched country rock (Table IV.1-4).

Because of profile truncation, relict hydromorphic haloes are likely to be small. Nevertheless, Filipek and Theobald (1981) found that fracture coatings on surface rock samples had high Cu, Zn and Pb contents that reflected supergene enrichment dating from earlier weathering cycles at the *North Silver Bell porphyry Cu deposit, Arizona*. High total or partial concentrations located the concealed supergene mineralization; however, because in the coatings these metals are concentrated in secondary Fe and Mn oxides which vary markedly in abundance, metal/Fe ratios would generally give a better response.

*Pre-existing profile partly truncated, with a cover of transported overburden: B * * [2,3] models*

Many slopes in areas of high relief have a cover of transported overburden that may displace or conceal geochemical anomalies. This was observed by Hunter (1980) at the *Esperanza Z2 Cu deposit* in the Mount Isa Belt, Queensland, Australia (model B 0 0 [2,3]). The relief conditions are strictly controlled by the geology, with steep ridges over quartzites and cherts and low rolling hills over dolomitic siltstones. Rocks are strongly weathered to 50 m, but the soil is mostly very thin (15–20 cm). The present climate is typically seasonal, with rainfall (mean 500 mm p.a.) mainly during the summer. Copper mineralization, intersected over a strike length of 450 m, has a mean thickness of 10 m at 1% Cu. Gossans, weathered rock chips and the minus 175 μm fraction of soils were sampled during exploration. The soil Cu anomaly was found to be displaced relative to the projected outcrop of the mineralization due to the downslope movement of scree and soil. The gossan composition is given in Table II.2-23.

In many arid regions, the close relationship between soil and bedrock contents may also be disturbed by the addition of aeolian components to the fine fraction. Hence, as described in Chapter III.3, the optimum response may be obtained by using the coarser size fractions. Thus, Moeskops and White (1980b) noted that the *Ediacara Mississippi Valley-type Pb-Zn-Cu deposit* in South Australia was shown best by the 500–1000 μm fraction of the thin (1–10 cm) soils, with mean concentrations diluted to 10–50% of those of the gossans (Table IV.1-5). In general, high concentrations of the main indicator metals (Mn, Cu, Pb, Zn, Ag) occurred sporadically over the Ediacara area, reflecting the occurrence of minor mineralization and a high background, despite homogenization of soil composition by introduced aeolian material. Ediacara is an example of model B 1 0 [0].

Pre-existing profile fully truncated (C models)

Complete removal of earlier deep weathering profiles is common in regions of high relief, particularly in very arid climates. Rock outcrops and surface rubble are abundant and any soils developed under the prevailing conditions are

TABLE IV.1-5
Comparison between rock, gossan and soil compositions, Ediacara, South Australia (from Moeskops and White, 1980b)

	Mn	Cu	Pb	Zn	Ag	Bi	Mo
<i>Fresh rocks</i>							
Mineralized	M 600 R 200-800	250 20-600	6000 0.02- > 2%	100 20-200	8 3-20	-	-
Unmineralized	M 600 R 200-800	15 5-30	300 200-400	30 20-50	0.3 0.1-6.0	-	-
<i>Fe-Mn Gossams</i>							
Northern area	M 1000 R 0.01- > 1%	250 70-3000	2000 0.08- > 1%	700 300-1500	10 1-30	to 6	to 30
<i>Soils (500-1000 μm fraction)</i>							
Mineralized area	M 400 R 100-700	100 50-150	500 50-750	300 50-750	0.1 0.05-1.0	-	-
Unmineralized area ^a	M 300	15	30	40	~ 0.05	-	-

^a Limited data only.

M = mean; R = range. Data in ppm and percent. As(50), Sb(30), Cd(3), Ga(1), Ge(3), In(10), Tl(1), Sn(1) and W(50) all below detection limit in gossans and soils, detection limit in brackets.

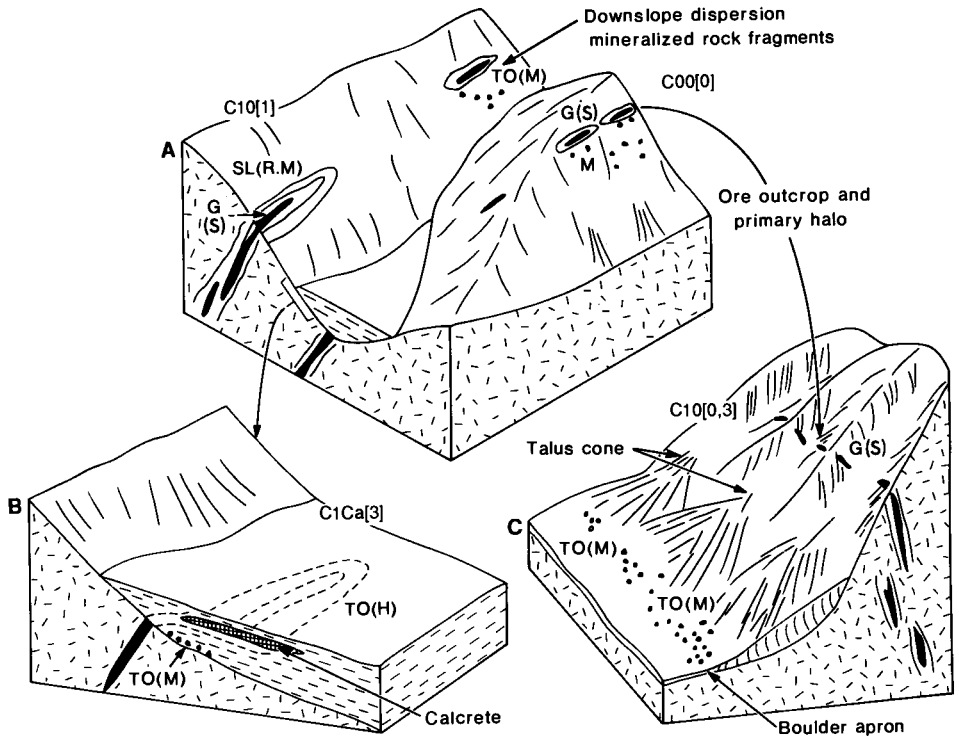


Fig. IV.1-10. Block diagrams illustrating C-type dispersion models in fully stripped terrain of high relief in arid environments. (A) Slopes with dominantly residual and semi-residual soils; (B) Valley floor with calcrete developed in alluvium; (C) Steep slopes with talus cones. Contours show general nature of anomaly; broken contours show subsurface anomaly; for abbreviations, see Fig. III.1-1.

generally shallow (5–20 cm) with little profile development but with a fine aeolian component. Deeper soils are formed in flatter areas and on transported overburden. Talus (scree) may have local importance as a detrital cover on the lower parts of rocky slopes, especially at high altitudes and in winter cold deserts. Geochemical dispersion characteristics are summarized by the model given in Fig. IV.1-10.

Soil responses in residual soils are similar to those described in the previous section, except that all dispersion is related to the present environment. Concentrations of mechanically dispersed elements may decay to background in 200–300 m, but even in very arid areas, some chemical dispersion may occur to give widespread anomalies—e.g. for Zn at near-neutral pH and for Mo, V or U in more alkaline environments. This is illustrated by the dispersion from a *Zn-Pb-Cu deposit, Namaqualand, Namibia* (Van Berkel, 1982) (model C 1 0 [1,2]), where Cu and Pb contents decline to background about 250 m downslope but Zn is still anomalous when truncated by a dry stream channel after 300 m (Fig. IV.1-11).

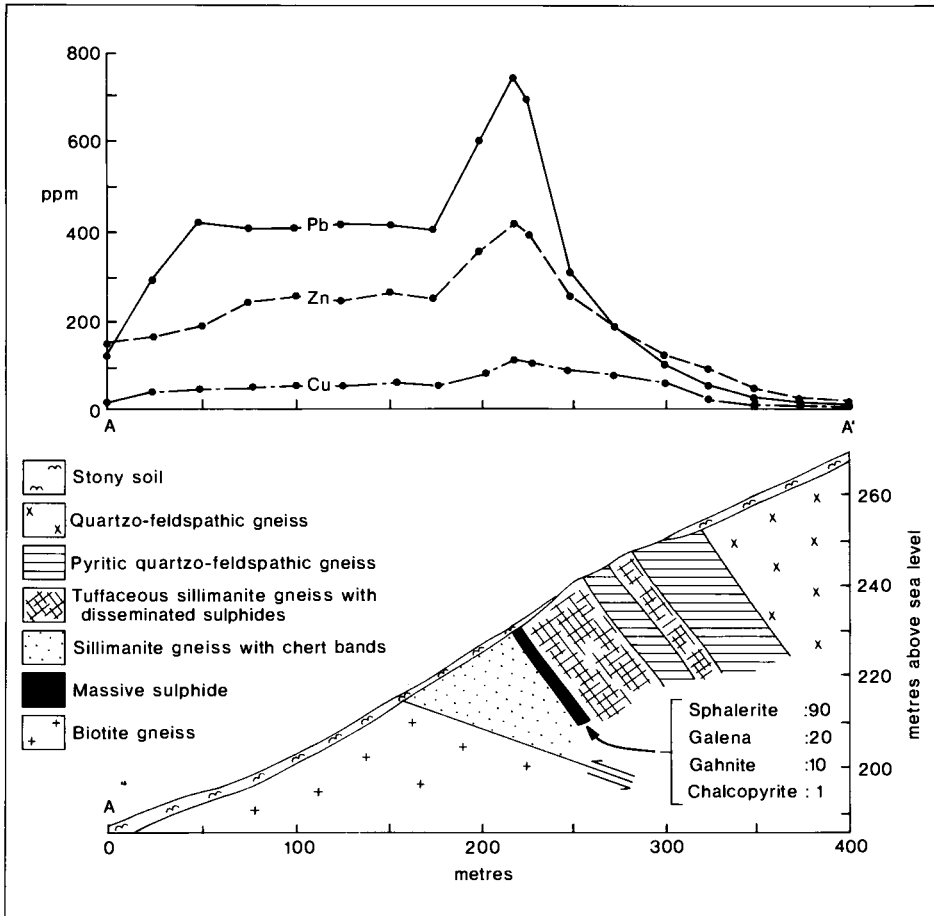


Fig. IV.1-11. Copper, Pb and Zn content of residual soil over massive sulphides, Namaqualand, Namibia. Modified after Van Berkel (1982).

Whereas Pb, Cu and some Zn (as gahnite) are dispersed mechanically, much Zn dispersion is hydromorphic, released in the weakly acid environment of the mineralization and precipitated in more alkaline conditions downslope. The change in Pb : Zn : Cu ratios from 20 : 100 : 1 in bedrock to 7 : 4 : 1 in soil implies relatively strong leaching of Zn, although the analyses of the soil (hot leach, minus $180 \mu\text{m}$ fraction) and rock (whole sample) were not strictly comparable. The relative mobilities of Zn and Cu in arid environments were also noted by Chaffee and Hessin (1971), where they complicate interpretation of the primary zonation of a porphyry Cu deposit in Arizona. Similarly, Snoep and Zeegers (1979) found that Cu was totally leached from some parts of the *Socos porphyry deposit, Peru*, whereas Mo was retained.

In general, where deep weathering is absent, residual soils yield an excellent response, as illustrated by relevant models and examples in the compilations by Lovering and McCarthy (1978) for the Basin and Range Province of the USA and Mexico and by Butt and Smith (1980) for Australia. A further example was given by El Din Khalil (1973) over gold-bearing veins at *Aberkateib* in the Red Sea Hills, Sudan. Using 50 g of the minus 150 μm fraction of thin (10 cm) residual soils, anomalies over 200 m wide, defined by the 0.1 g/t Au contour, were found over a vein system carrying over 10 g/t Au. The maximum concentration in the soil was 0.5 g/t Au, 30 ppb Hg over the vein. However, as in any old mining area, especially one of such antiquity, the possibility of contamination contributing to the anomaly must be considered.

Problems are, however, associated with transported overburden and commonly no response is obtained where it is present, unless hydromorphically dispersed metals have precipitated, for example as described in Chapter III.3 for Au, Cu and U in calcrete horizons (Figs. III.3-34 and III.3-45). If oxidation is active, gas or vapour geochemistry may have some application; biogenic near-surface enrichment of Au and other elements may occur, particularly in more vegetated, semiarid areas. Commonly, the overburden itself is of little value as a sample medium unless it is from a restricted source area. Windblown sand, loess and terrace alluvium are usually too exotic; conversely, colluvium and talus, accumulated at the base of slope, may contain debris from soils, gossans and oxidized or unoxidized mineralization upslope and hence be useful sample media for semi-regional surveys.

Talus samples have been used in very rugged terrain where soils are not developed and stream sediments are virtually absent. Compared to stream sediments, they represent smaller areas, so that a greater sampling density is required. However, the fine fractions (minus 180 μm) are produced mainly by mechanical processes and hence are equivalent to the clastic components of stream sediments, but they are more homogeneous. They may also contain hydromorphically dispersed metals precipitated from seepages at the base of slope. Composite samples are collected from several sites immediately above the boulder apron (Fig. IV.1-10) at intervals determined by the target size or width of the talus cone. The successful application of talus sampling was described by Maranzana (1972) at the *Los Pelambres porphyry Cu-Mo deposit* in the arid, glaciated Andes in Chile (model C 0 0 [2,3]). Talus cones cover about 80% of the area, hence it is a widespread sampling medium. Analyses of the fine fraction for Cu and Mo outlined areas coinciding with zones of potassic alteration associated with mineralization. Significant anomalies contained over 650 ppm Cu and/or 65 ppm Mo. Elsewhere, talus sampling has only been described for humid, glaciated terrain (British Columbia, Canada; Hoffman, 1977), but the technique should have application wherever talus is abundant.

CONCLUSIONS

Terrains of moderate to high relief in tropical and subtropical regions present relatively few geochemical exploration problems compared to those of moderate to low relief. The widespread, thick, strongly weathered regolith characteristic of regions of low relief is mostly absent or deeply truncated, either because it never developed or because it has been destroyed as a result of increased erosion following recent tectonism. Indeed, the geochemical expression of mineralization is very similar to that of equivalent temperate regions. Anomalies tend to be rather direct and of high contrast, with moderate downslope haloes due to physical and, in humid regions, hydromorphic dispersion. Massive sulphides weather to form gossans, although in some juvenile terrains, even in tropical rainforests, some sulphides may remain unweathered. Because of the strong erosion, gossans are rarely very strongly leached and retain high abundances of even the most mobile target and pathfinder metals. Eroded gossan particles enrich the coarse fractions of associated soils, and such leaching as does occur, particularly in humid regions, contributes to metal enrichment of finer fractions of the soils. Disseminated sulphide mineralization, such as Cu-Mo porphyries and epithermal Au deposits, also give strong geochemical responses, although supergene depletion and enrichment processes may have resulted in zoned anomalies. Some problems may be encountered in Ni sulphide exploration in dissected lateritic terrain, where enriched zones formed deep in the saprolite may now outcrop. However, such "false" Ni anomalies can readily be identified from an appraisal of the geomorphological setting and from the element association, i.e. high Ni, Cr \pm Mn, Co; low Cu, PGE. Similar appraisal is necessary in attempting preliminary assessments of reserves in lateritic and supergene enrichments of Ni and Cu, respectively, from near-surface sampling.

In humid regions, active leaching may give rise to anomalies in discharge sites such as seepages, springs and drainage channels. In some circumstances, the source of such anomalies may be difficult to trace, since nearby soils and the sediments in tributary drainages may be derived largely from transported material. Again, an assessment of the geomorphology, together with that of the hydrology and hydrogeochemistry of the site, may be necessary to trace the origin of the anomaly.

Transported overburden (e.g. talus, colluvium, landslip, aeolian sand, alluvium) on slopes and valley floors may give rise to problems, particularly if its presence is not recognized. Talus and colluvium can be used as sample media, particularly at a semi-regional scale; more rarely, vegetation or termite mounds (see p. 105) may provide a means of sampling "through" surficial transported cover and, in arid areas, sieving may be adequate to reduce the effects of dilution by aeolian material. Commonly, however, the overburden prevents the acquisition of adequate samples and it is necessary to sample beneath it, by hand auger or power drilling. The uppermost residual material is generally suitable, and may

be recognized by features such as a colour, texture or mineralogical change, or the presence of a sedimentary stone line.

In many terrains of high relief, particularly those that are thickly forested, logistic problems, such as those of access and communications, are more significant than technical problems of geology and geochemistry. The logistic problems may, however, contribute to the technical problems by preventing the selection of optimum sample sites, the collection of the most appropriate samples and an adequate assessment of the geological and geomorphological environment.

DIAMOND EXPLORATION IN TROPICAL TERRAINS

G.P. GREGORY and A.J.A. JANSE

INTRODUCTION

Economic primary deposits of diamond, about 1 part in 10 million, have only been found in kimberlite and olivine lamproite. Exploration for diamonds is based on exploration for these host rocks and, when found, they are tested for diamonds by bulk sampling. For convenience, and because these two rock types have a similar geochemistry, they are collectively referred to as *kimberlitic rocks*.

Most exploration methods for kimberlitic rocks are based on the detection of characteristic indicator minerals, including microdiamonds, in drainage or soil samples. When found, these minerals are backtracked to their source. In some areas, geophysical techniques, principally magnetics and Input EM, have proved successful. There is no doubt that these methods, either singly or in combination, are both efficient and successful at locating kimberlitic bodies. Consequently, geochemical soil and drainage surveys have not been widely or routinely used, although they have a role in local surveys.

For diamond exploration in tropical terrain, geochemical prospecting has been utilized in two main ways:

- (1) through analysis of soil or rock samples to detect or confirm the presence of nearby or underlying kimberlitic rocks, and
- (2) to differentiate significant from non-significant indicator minerals and to determine the "diamond potential" of kimberlite rocks.

Data relevant to the tropical weathering of kimberlite are derived mainly from Sierra Leone and northwest Australia and this account is biased towards these regions.

PETROLOGY AND GEOCHEMISTRY OF KIMBERLITIC ROCKS

Kimberlites are inequigranular rocks composed of megacrysts of olivine (or serpentine), "picroilmenite" (magnesian ilmenite), phlogopite, pyroxene and garnet, within a matrix of serpentine-group minerals and carbonate that contains microphenocrysts of mica, spinel, perovskite and rare diopside and monticellite, in varying proportions (Dawson, 1980). There are two textural types, diatreme facies and hypabyssal facies. The *diatreme* facies are fragmental rocks consist-

ing of kimberlite, country rock xenoliths, deep seated xenoliths and single crystals or cleavage fragments cemented by low temperature hydrothermal minerals. Tuffaceous phases and crater sediments may be preserved in little-eroded occurrences, whereas magmatic kimberlite may be present in deeply eroded pipes. The *hypabyssal* facies includes massive kimberlite, which contains few, if any, xenoliths of country rock, and kimberlite breccia, which contains various types of xenoliths set in a matrix of massive kimberlite.

Olivine lamproite differs from typical kimberlite in that amphibole (potassian richterite) may be locally abundant and the matrix may contain devitrified glass. It exhibits similar textural types to kimberlite. However, some important kimberlite indicator minerals are rare or absent in olivine lamproites (Table V.1-8).

Kimberlite and olivine lamproites have broadly similar chemical compositions because both are ultrabasic rocks with high Mg, Ni and Cr contents. However, they can be distinguished from other ultrabasic rocks because they are enriched, sometimes by one or two orders of magnitude, in elements typical of alkalic rocks, namely Nb, Sr, Rb, Cs, P and K. Olivine lamproites differ from kimberlite in that they have higher K_2O , SiO_2 , TiO_2 and P contents and lower CaO , Al_2O_3 and Fe contents (Table V.1-1).

THE TROPICAL WEATHERING OF KIMBERLITIC ROCKS

Humid tropics (rainforests)

The chemical weathering of kimberlite is remarkably similar in most humid tropical regions, being characterized by the profile:

fresh rock → blue ground → yellow ground → soil

A summary of the mineralogical and chemical changes that accompany the transition from fresh rock to yellow ground in the Yengema area of Sierra Leone is given in Fig. V.1-1 and Tables V.1-2 and V.1-3. These data show the weathering progression:

olivine → serpentine + brucite → Fe saponite + vermiculite
 → smectite + goethite.

Phlogopite alters to a mixture of smectite and chlorite, and perovskite alters to anatase; carbonates disappear, but resistant minerals such as ilmenite and (probably) chromite persist. The influx of Al and Fe^{3+} near to the surface forms halloysite and goethite and may mark the onset of laterite formation. These mineralogical changes are accompanied by the progressive depletion of MgO , CaO and Fe^{2+} and progressive enrichment of MnO_2 and Fe^{3+} from the fresh

TABLE V.1-1

Mean compositions of unweathered kimberlite and olivine lamproite

Element	Kimberlite		Olivine lamproite	
	(1)	(2)	(3)	(4)
SiO ₂ %	35.20	31.10	40.10-42.80	41.69
TiO ₂ %	2.32	2.03	2.64-5.77	3.38
Al ₂ O ₃ %	4.40	4.90	3.30-4.52	3.95
Fe ₂ O ₃ %			3.80-4.94	4.55
FeO%	9.80 ^a	10.50 ^a	2.37-4.98	3.89
MnO%	0.11	0.10	0.11-0.14	0.13
MgO%	27.90	23.90	19.04-26.90	23.58
CaO%	7.60	10.60	4.06-5.37	4.82
Na ₂ O%	0.32	0.31	0.37-0.63	0.46
K ₂ O%	0.98	2.10	3.46-5.11	4.24
P ₂ O ₅ %	0.70	0.70	0.60-1.48	0.91
H ₂ O ⁺ %	7.40	5.90	3.55-4.93	4.26
H ₂ O ⁻ %			0.95-2.32	1.71
CO ₂ %	3.30	7.10	0.10-0.70	0.24
S ppm	2000	8800	100-700	250 ^b
F ppm	68	7590	200-5400	3675 ^b
Ba ppm	137	1970	3875-18280	9175
Li ppm	2	56	5-12	7
Rb ppm		350	300-555	450
Sr ppm	40	1900	960-1245	1100
Pb ppm	0.9	50	20-50	32
Th ppm	4	54	18-70	43
U ppm	0.6	18.3	2-9	3.5
Zr ppm	84	700	565-1215	1100
Nb ppm	32	450	115-245	175
Y ppm	4	75	10-19	16
La ppm	26	200	160-410	260
Ce ppm	45	520	210-675	360
Sc ppm	7	30	9-22	17 ^b
V ppm	21	250	19-140	70 ^b
Cr ppm	550	2900	530-1705	1125
Co ppm	35	130	57-80	73 ^b
Ni ppm	710	1600	675-1500	1025
Cu ppm	10	300	46-95	58
Zn ppm	15	285	61-90	75
Sn ppm	1	30	2-19	8 ^b
Ga ppm		30	3-7	5
As ppm			1-2	1 ^b
Cl ppm	30	9800	50-140	80

^a: Iron as total FeO.^b: 5 analyses for Sc, Co; 4 analyses for Sn, As, Cl, S, F.

(1) Average basaltic kimberlite (Dawson, 1967) in Jaques et al. (1984a).

(2) Average micaceous kimberlite (Dawson, 1967) in Jaques et al. (1984a).

(3) Range of 6 olivine lamproites (Jaques et al. 1984a).

(4) Arithmetic mean of 6 olivine lamproites, calculated from Jaques et al., (1984a).

rock towards the surface. Silica is enriched to just below the water-table, above which it becomes depleted.

Seasonal tropics (savannas)

A typical profile over olivine lamproite from the West Kimberley area of Western Australia, which has a seasonally humid climate (1000 mm p.a. rainfall and an 8 month winter dry season), is illustrated in Fig. V.1-2. Weathering persists to a depth of at least 60 m and olivine phenocrysts and matrix olivine have been decomposed to a bluish-green mineral, possibly serpentine. Yellow ground occurs between 8 and 40 m, where serpentine and phlogopite have been decomposed and clay minerals, including montmorillonite, nontronite, possible saponite, and hydrophlogopite-vermiculite become dominant. Red clay is developed above the yellow ground and this is in turn overlain by varying amounts of colluvial overburden derived from the surrounding rocks. Nickel and, to a lesser extent, Cr are enriched in the blue and yellow ground compared to fresh rock, whereas the near-surface residual red clay soils are neither enriched nor depleted (Australian Selection Pty. Ltd., unpublished internal report)

Under similar conditions of chemical weathering, Kresten and Paul (1976) found fresh kimberlite in southern India (Andhra Pradesh) to contain olivine, phlogopite, serpentine, chlorite, calcite, apatite and palygorskite, whereas the equivalent rock in central India (Madhya Pradesh) consists of vermiculite, phlogopite, serpentine and smectite. They attributed this difference in mineralogy to be due to alteration during the last stages of emplacement and concluded that there was no systematic variation due to weathering, although vermiculite, serpentine and smectites generally decrease in abundance with increasing depth.

Semiarid and arid tropics

Clay formation is rare or absent during weathering of kimberlitic rocks in Namibia and Tanzania, and changes in mineralogy generally progress as shown for zones 2 and 3 at Yengema, Sierra Leone (Table V.1-2). Outcrops of silicified blue ground are common in flat-lying terrain in Namibia, whereas silcrete cap rocks, possibly developed during an earlier arid climate, are common over kimberlites in flat terrain in Tanzania. In slightly dissected areas of Namibia, fresh olivine is present at depths of only 1–2 m. Thus, in these areas, virtually all kimberlite indicator minerals are present over and near outcrops of kimberlitic rocks. However, as physical weathering greatly dominates over chemical weathering, soft and easily cleaved minerals disintegrate quickly, but hard, refractory minerals (e.g. garnet, ilmenite, chromite, zircon) persist.

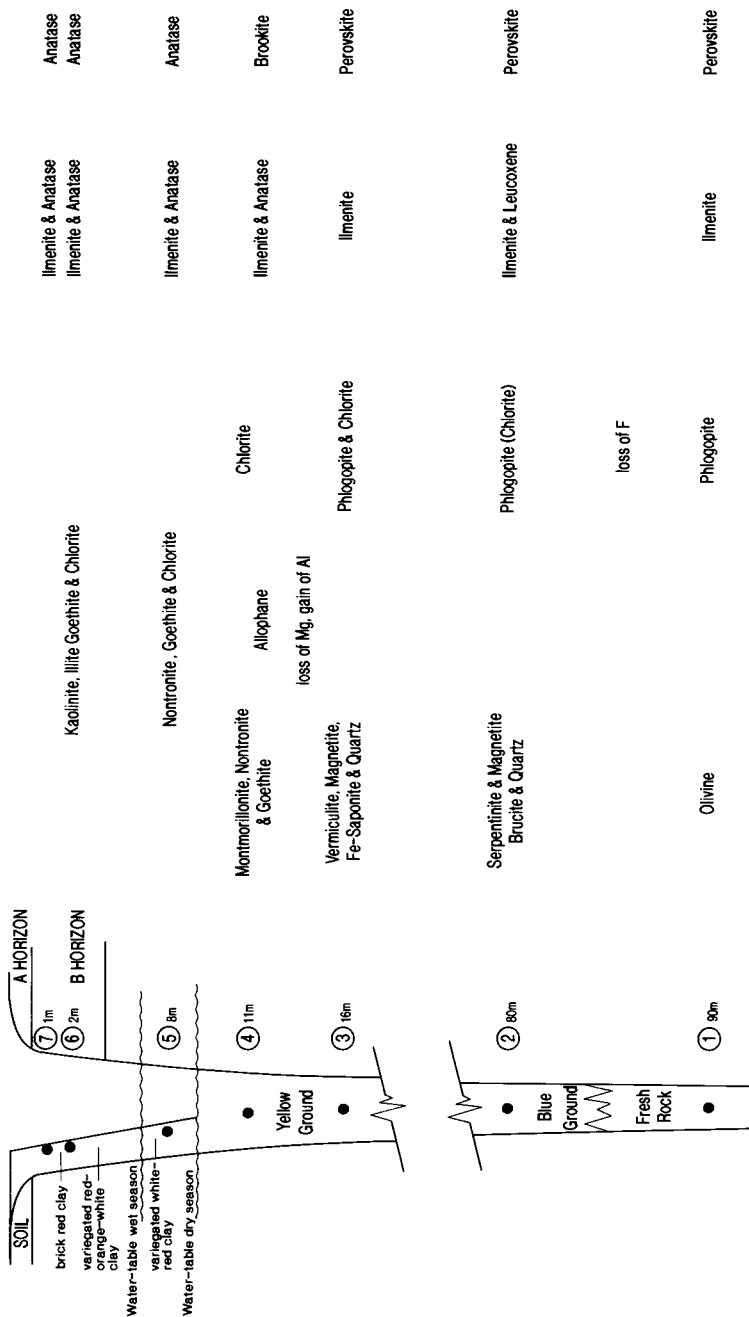


Fig. V.1-1. Mineralogy of the weathering profile over a kimberlite dyke, Sierra Leone. Adapted from Fairbairn and Robertson (1966). See also Tables V.1-2 and V.1-3.

DISTRIBUTION OF SELECTED ELEMENTS IN NEAR-SURFACE SAMPLES OVER AND NEAR KIMBERLITIC ROCKS

*Humid tropics**Yengema area, Sierra Leone*

In the Yengema area of Sierra Leone, kimberlites occur as a series of dykes, three small pipes and a ring structure. They intrude Archaean gneisses, migmatites and greenstone remnants. Topographically, the area is characterized by broad alluvial valleys, flanked by rolling and occasionally steep-sided hills, with a relief typically of 50 to 200 m. These hills were once covered with rainforest, but this has been felled and the hills are now cultivated.

The main lateritic surface is 200–300 m above the present elevation of the kimberlites and the weathering profile over these rocks is probably of Quaternary age. Residual soils developed in freely drained areas over kimberlite and base-

TABLE V.1-2

Calculated mineral distribution in a weathering profile over a kimberlite dyke, Sierra Leone (adapted from Fairbairn and Robertson, 1966)

	1 wt%	2 wt%	3 wt%	4 wt%	5 wt%	6 wt%	7 wt%
Olivine	32.55						
Serpentine	17.97	39.57					
Brucite	0.21	9.00					
Free silica		6.37	6.94	14.64	4.07		3.64
Phlogopite	16.90	14.70	17.14				
Chlorite		9.5		9.14	11.43	3.11	4.83
Vermiculite			8.00				
Fe-saponite			47.84				
Nontronite				25.00	62.50	6.25	3.13
Montmorillonite				15.00			
Allophane				20.28			
Kaolinite						46.53	40.85
Illite						3.29	7.43
Magnetite	6.24	7.49	4.00				
Goethite				8.66	6.54	29.10	29.39
Ilmenite	0.46	1.29			5.45	3.42	3.00
Perovskite	2.40	2.40	1.92				
Anatase				4.33	1.63	1.03	0.83

1. Hard rock, 90 m below water-table.
2. Blue ground, 80 m below water-table.
3. Blue ground, well below water-table.
4. Yellow ground, below water-table.
5. Yellow ground, in zone of water-table fluctuation.
6. Gleyed saprolite, 2 m above the water-table.
7. Red clay horizon, 6 m above the water-table.

TABLE V.1-3

Vertical distribution of selected elements in weathered kimberlite, Sierra Leone (modified from Fairbairn and Robertson, 1966)

Site	SiO ₂ %	Al ₂ O ₃ %	Fe ₂ O ₃ %	FeO%	MgO%	CaO%	Na ₂ O%	K ₂ O%
7	29.60	20.85	27.38	2.01	0.79	0.11	0.07	0.48
6	26.77	23.38	28.10	2.01	1.08	0.00	0.06	0.21
5	34.35	6.69	25.33	2.58	3.98	2.49	0.09	0.00
4	43.06	15.29	13.69	1.58	2.46	0.90	0.06	0.00
3	43.50	6.80	2.90	3.78	20.00	5.70	1.71	1.86
2	33.25	1.75	7.99	2.95	31.40	5.22	0.10	0.88
1	28.30	2.00	4.40	5.68	31.10	10.50	0.02	1.85

1. Hard rock, 90 m below water-table.
2. Blue ground, 80 m below water-table.
3. Blue ground well below water-table.
4. Yellow ground below water-table.
5. Yellow ground in zone of water-table fluctuation.
6. Gleyed saprolite, 2 m above the water-table.
7. Red clay horizon, 6 m above the water-table.

ment rocks are mature, though the profile is commonly truncated. The surface horizons typically consist of humic sandy soil, 0.0–0.3 m thick, overlying a prominent brick red to orange clay-rich horizon (0.6–1.0 m thick) that contains Fe oxide concretions in variable amounts. This irregularly overlies a zone of mottled clays, with saprolite present at 2–4 m depth. In the upper part of the profile, it is commonly difficult to distinguish visually between kimberlite, granite and granitic-derived alluvium, although the presence of microilmenite (magnesian ilmenite) and a clay-rich matrix is diagnostic of kimberlite. Profiles in swamps and broad valleys are characterised by a transported layer, 0.5–7 m thick, consisting of organic debris and ooze, clay, silt, sand and gravel, that directly overlies saprolite. The following data have been compiled from unpublished internal reports of the National Diamond Mining Company (SL) Ltd.

The Ni, Cr, Nb and Ce contents of samples collected from the C horizon of well-drained soils developed on kimberlite and of samples taken from the same horizon below the water-table in poorly drained areas are compared for two size fractions on Table V.1-4. There are some marked differences in metal contents between the two environments; for example, Ni and, to a lesser extent, Ce are much depleted in the well-drained profiles compared with the parent rock, whereas Cr and Nb are not. This distribution is interpreted as reflecting the different mobilities of the elements. There are no significant differences between the two size fractions. Because Ni and Nb are concentrated in kimberlite relative to the country rocks and represent “mobile” and “semi-mobile” elements, they were studied further as potential kimberlite indicator elements.

The vertical distributions of Ni and Nb in freely drained profiles over three kimberlite dykes and a poorly drained profile over Pipe 3, together with a limited

TABLE V.1-4
The Ni, Cr, Nb and Ce contents of weathered kimberlite and background rocks, Yengema, Sierra Leone

Rock	Size μm	Ni		Cr		Nb		Ce		ND
		Range ppm	Mean ppm	Range ppm	Mean ppm	Range ppm	Mean ppm	Range ppm	Mean ppm	
PDK	+175	260-1770	1055	1390-2530	2325	130-305	232	1-2555	1295	5
	-175	210-1465	1065	860-4840	2330	125-340	223	185-3885	1470	4
WDK	+175	44-255	85	1100-3410	2165	105-365	214	190-1665	550	5
	-175	54-205	95	300-3390	2080	123-360	237	160-2955	870	7
GSD	+175	37-60	44	19-270 ^a	70	2-31	12	120-435	140	8
	-175	36-160	69	33-200 ^a	70	8-47	16	38-385	250	8
TS	-3 mm	1010-2095	1605	960-2510	1730	6-13	9	8-16	11	3

XRF determinations.

PDK: Poorly drained kimberlite; WDK: Well drained kimberlite;

GSD: Granite, syenite, dolerite; TS: Talc Schist.

ND: Number of determinations.

^a excludes data for dolerite.

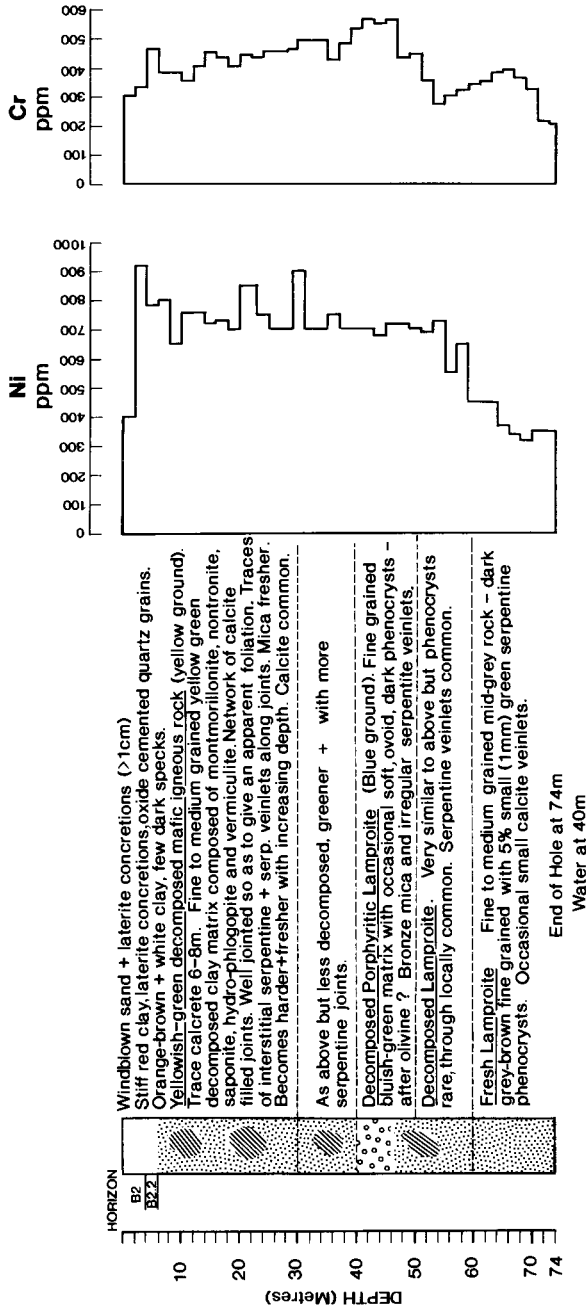


Fig. V.1-2. Distribution of Ni and Cr in a profile over olivine lamproite, Western Australia.

TABLE V.1-5

Variation in Nb and Ni contents with depth in profiles over kimberlite and background rocks, Yengema lease area, Sierra Leone. A: Upper Sinji; B: Manjamaqu

PROFILE OVER WELL DRAINED KIMBERLITE DYKE 0.3m WIDE, UPPER SINJIE

DEPTH (Metres)	MORPHOLOGY	NI OBIUM ppm		NICKEL ppm	
		+1.6 +0.175	-0.175 -0.175	+1.6 +0.175	-1.6 -0.175
0-0.3	Lateritic soil. Traces of fresh limonite. Blocky texture	58	41	110	74
0.3-0.6	Fe nodules and quartz loam	81	50	141	86
0.6-0.9	Less baselite iron nodules and mottles in yellow brown clay matrix	85	304	65	137
0.9-1.2	Baselite iron nodules in yellow brown clay matrix	116	109	52	114
1.2-1.5	Mainly yellow brown clay. Fe nodules	122	151	138	116
1.5-1.8	Baselite iron nodules in yellow brown clay matrix	27	24	30	113
1.8-2.1	Baselite iron nodules in yellow brown clay matrix	236	243	256	131
2.1-2.4	Baselite iron nodules in yellow brown clay matrix	269	226	237	133
2.4-2.7	Similar; blocky texture	331	410	339	131

PROFILE OVER POORLY DRAINED KIMBERLITE AT No.3 PIPE

DEPTH (Metres)	MORPHOLOGY	NI OBIUM ppm		NICKEL ppm	
		+1.6 +0.175	-0.175 -0.175	+1.6 +0.175	-1.6 -0.175
0-0.3	Blue-grey clay and quartz pebbles	80	67	90	306
0.3-0.6	Blue-grey clay	97	97	124	479
0.6-0.9	Blue-grey clay	88	81	117	491
0.9-1.2	Blue-grey clay and traces of kimberlite	91	81	101	414
1.2-1.5	Blue-grey clay	87	86	101	435
1.5-1.8	Blue-green clay decomposed. Fe nodules and palimpsest grains after olive press	76	71	100	321
1.8-2.1	Blue-green clay decomposed. Fe nodules and palimpsest grains after olive press	133	128	162	1170
2.1-2.4	Blue-green clay decomposed. Fe nodules and palimpsest grains after olive press	145	151	149	975
2.4-2.7	Blue-green clay decomposed. Fe nodules and palimpsest grains after olive press	166	146	146	1042
2.7-3.0	Blue-green clay decomposed. Fe nodules and palimpsest grains after olive press	138	134	129	980

PROFILE OVER WELL DRAINED KIMBERLITE DYKE 1m WIDE, UPPER SINJIE

DEPTH (Metres)	MORPHOLOGY	NI OBIUM ppm		NICKEL ppm	
		+1.6 +0.175	-0.175 -0.175	+1.6 +0.175	-1.6 -0.175
0-0.2	Dark grey silt	15	22	21	17
0.2-0.6	Fe nodules and quartz loam in light grey silt-silt loam	20	18	23	31
0.6-0.9	Fe nodules in a brown clay matrix	19	18	21	33
0.9-1.2	Fe nodules in a brown clay matrix	26	20	20	29
1.2-1.5	Fe nodules in a brown clay matrix	34	11	14	36
1.5-1.8	Fe nodules in a brown clay matrix	32	24	27	37
1.8-2.1	Brown-yellow brown clay. Blocky texture	67	27	31	45
2.1-2.4	Brown-yellow brown clay. Blocky texture	79	78	79	68
2.4-2.7	Traces of limonite	56	37	41	37

PROFILE OVER WELL DRAINED KIMBERLITE DYKE 0.3m WIDE, MANJAMAQU

DEPTH (Metres)	MORPHOLOGY	NI OBIUM ppm		NICKEL ppm	
		+1.6 +0.175	-0.175 -0.175	+1.6 +0.175	-1.6 -0.175
0.1-0.2	50% Fe nodules in grey clay matrix	73	17	15	72
0.2-0.7	Orange brown clay with embryonic nodules and palimpsest grains after olive press	57	17	21	76
1.1-1.3	Orange brown clay with embryonic nodules and palimpsest grains after olive press	83	39	32	80
2.0-2.3	Decomposed bottle granite	150	87	100	94
3.0-3.1	Decomposed bottle granite	224	190	163	104
3.8-3.9	Decomposed bottle granite	223	208	107	105

BACKGROUND PROFILE OVER LATERITIZED 'GRANITE' UPPER SINJI

DEPTH (Metres)	MORPHOLOGY	NI OBIUM ppm		NICKEL ppm	
		+1.6 +0.175	-0.175 -0.175	+1.6 +0.175	-1.6 -0.175
0-0.2	Dark grey humic loam	205	14	19	36
0.2-0.3	Quartz pebbles in orange grey clay matrix	17	15	18	72
0.3-0.6	Quartz pebbles in orange grey clay matrix	12	11	12	89
0.6-0.9	Lateritized granite	16	16	21	106
0.9-1.2	Lateritized granite	19	27	27	98
1.2-1.5	Lateritized granite	221	22	25	103
1.5-1.8	Lateritized granite	24	21	21	101
1.8-2.1	Lateritized granite	21	23	112	97
2.1-2.4	Decomposed granite with embryonic nodules	201	179	179	128
2.4-2.7	Decomposed granite with embryonic nodules	16	16	19	119
2.7-3.0	Decomposed granite with embryonic nodules	25	13	21	148

BACKGROUND PROFILE OVER RECRYSTALLIZED SYENITIC ROCKS, MANJAMAQU

DEPTH (Metres)	MORPHOLOGY	NI OBIUM ppm		NICKEL ppm	
		+1.6 +0.175	-0.175 -0.175	+1.6 +0.175	-1.6 -0.175
0-0.1	Dark grey loam	14	14	16	25
0.1-0.3	Orange clay with 20% orange mottles	11	22	16	39
0.3-0.6	Orange clay with 20% orange mottles	6	17	14	45
0.6-0.9	Orange clay with 20% orange mottles	34	16	22	55
0.9-1.6	Decomposed recrystallized syenite	27	16	19	44
1.6-2.4	Decomposed recrystallized syenite	10	12	12	39
2.4-3.0	Decomposed recrystallized syenite	33	19	18	50

number of profiles over background rocks, are given for three size fractions in Table V.1-5. These data show that the concentrations of Ni and Nb decrease progressively upwards from the top of the saprolite to the surface. This is especially marked in the freely drained profiles, in which the concentration of neither element is barely anomalous in the sandy soil and red clay horizons. In the poorly drained profile, however, Ni and Nb are markedly anomalous at the surface but neither is concentrated in the red clay horizon. Apart from elevated Nb concentrations at both depth and surface in the plus 1.6 mm fraction over one of the dykes, and a general tendency for the minus 175 μm fraction to contain higher metal contents in soils over the pipe, no significant difference is apparent between the size fractions.

Several profiles were sampled on a two degree slope close to the dykes at Sinjie and Manjamadu. Anomalous Ni concentrations were found to be confined to the dykes but anomalous Nb contents could be detected in the upper saprolite and red clay horizon for a few metres downslope from the dyke (Fig. V.1-3).

These data are consistent with earlier findings (I. Nichol, unpublished data, 1963) for the same area. However, Nichol also found that Cr contents decreased from the saprolite to the surface and that Fe was concentrated in the red clay horizon.

Subsequent regional surveys established threshold values of 60 ppm Ni and 50 ppm Nb for the minus 175 μm fraction of the upper saprolite in freely drained profiles, and 95 ppm Ni and 50 ppm Nb in poorly drained saprolites. These values indicate that there is some lateral dispersion of Ni from the upper saprolite and lower red clay horizons of freely drained soils over the kimberlite dyke at Manjamadu, but none is apparent in the poorly drained soils downslope from Pipe 3. The high Ni contents of the 0.9–2.0 mm fraction at Sinjie are attributed to an amphibolite remnant in the basement gneisses and are not considered significant.

Based on these data, a geochemical survey was carried out in 1976 to prospect for kimberlite pipes in three sub-areas in the Yengema district. The known deposits of kimberlite had been located by heavy mineral sampling between 1949 and 1962, but no new kimberlite pipes had been found subsequently despite extensive prospecting using heavy mineral sampling and resistivity and aeromagnetic surveys. Geochemical techniques were then selected to explore for deposits in case any pipes deficient in indicator minerals had been missed during earlier surveys.

A total of 14,000 soil samples were collected from the upper saprolite on a 30×120 m grid and the minus 0.0175 mm fraction analyzed by XRF for Nb and Ni. The results for one sub-area (6000 samples), which is typical of the whole, gave three populations of Nb and Ni, with the class limits shown in Table V.1-6. Niobium concentrations of 0–22 ppm reflect the abundance in the basement rocks, those of 23–40 ppm are typical of amphibolite or gabbro, and those greater than 40 ppm are derived from kimberlite or acid pegmatite; all kimberlite-derived Nb values exceed 70 ppm. For Ni, the threshold for freely drained

TABLE V.1-6

Class limits for 3 populations of Ni and Nb in soil samples, Yengema, Sierra Leone (data based on 6000 XRF determinations)

	Ni ppm	% of data	Nb ppm	% of data
Population 1	0-22	97.96	0-65	81.49
Population 2	23-40	2.01	65-265	17.61
Population 3	> 40	0.03	> 265	0.90

profiles over basement gneisses and migmatites is 65 ppm, whereas for poorly drained environments it is 95 ppm. Nickel contents of 95-265 ppm are due to basic rocks and kimberlite, and concentrations above 265 ppm Ni are indicative of talc schists or kimberlite.

A total of 5 new kimberlite dykes were found by this survey. One, the Manjamadu dyke (Fig. V.1-3), is unlike other dykes in the area, because indicator minerals are rare, abundant carbonate is present in fresh rock and diamonds recovered from the dyke are small and dirty.

Zaire

Anomalous Ni concentrations in the range 120-240 ppm, compared to a threshold of 40 ppm, occur in sandy soil over lateritized alluvium at 2 to 7.5 m depth over a kimberlite pipe in Zaire (Meneghal, 1982).

Seasonal tropics

Northwest Australia

In the West Kimberley region of northwest Australia, sub-economic concentrations of diamonds are found in olivine lamproites, whereas associated leucite lamproites are barren. Both lithologies are of Miocene age (Jaques et al., 1984b) and occur on the Lennard Shelf, a plain underlain by flat-lying Permian and Triassic arenaceous and argillaceous sediments that is flanked to the east by cliffs of Devonian reef limestones and dolomites. The leucite lamproites form plug-like hills that punctuate the plain, whereas the olivine lamproite intrusions form topographic lows, commonly rimmed by upstanding hills of sandstone (Gregory, 1984). Pisolitic lateritic duricrust of presumed Tertiary age occurs approximately 10 m above the present surface of the plain and xenoliths of the duricrust occur within the lamproites. The main period of lateritization must therefore predate intrusion of the lamproites and the weathering of the lamproites must be post-Miocene.

Fig. V.1-3. The distribution of Nb in three size fractions above a kimberlite dyke at Manjamadu, Sierra Leone. Data from internal reports of the National Diamond Company (SL) Ltd. Analyses by XRF.

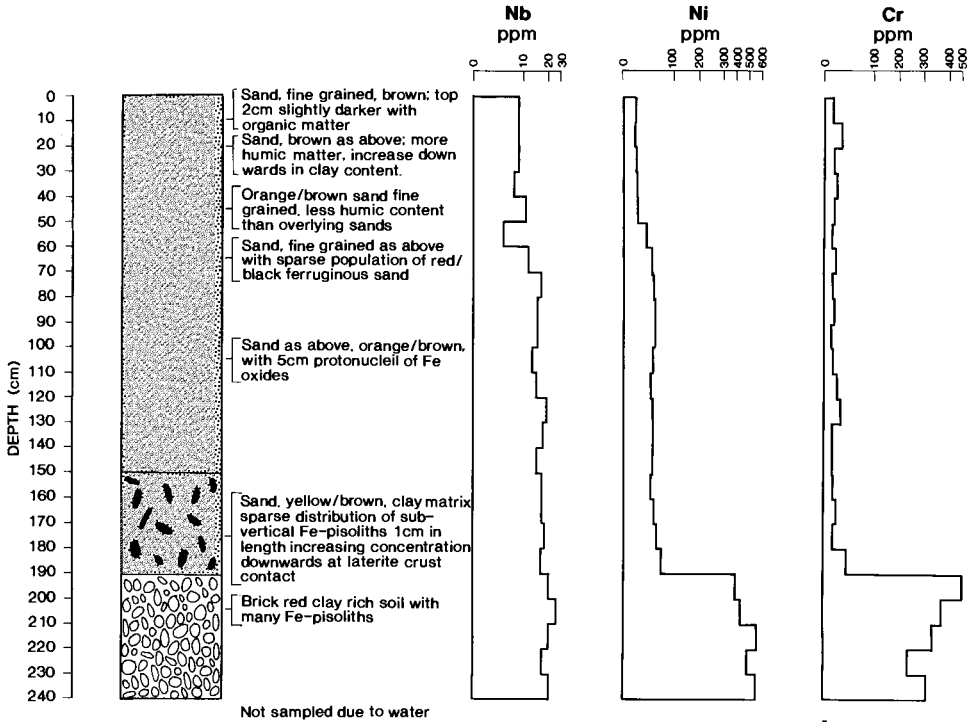


Fig. V.1-4. Near-surface distribution of Ni, Cr and Nb in the minus 2 mm fraction of soils over the Water Reserve olivine lamproite pipe, Ellendale area, Western Australia. Data provided by Century Metals and Mining Ltd.

The distribution of Ni, Cr and Nb in near-surface horizons of the regolith developed over olivine lamproite is illustrated on Fig. V.1-4. This profile, 5 m east of the profile shown in Fig. V.1-2, indicates that the concentrations of these elements in the ferruginous (B_2) horizon of the soil reflect those in the underlying olivine lamproite, although both Cr and Ni appear to be slightly depleted compared to the saprolite. The surface horizon consists of wind-blown sand and this contains anomalous concentrations of Ni, but not Cr, below 0.5 m depth. This indicates that some upward movement of Ni has occurred, possibly during present-day weathering and is consistent with data obtained by Haebig and Jackson (1986), who found anomalous Cr, Ni and Co contents in wind blown sand 7 m deep over an underlying olivine lamproite. These observations have obvious importance in geochemical prospecting in the area.

Haebig and Jackson (1986) also found that in areas where the ground is flat, or where there is a topographic depression over an olivine lamproite, there is little lateral dispersion of metal about the pipe. However, on sloping ground, an

TABLE V.1-7

Variations in Ni and Cr contents with depth over the Hinota diatreme, Madhya Pradesh, India (modified from Mathur and Alexander, 1983)

Depth m	Nickel ppm	Chromium ppm
0.3-0.9	45-65	100-150
1.8	130	130
2.4	120	180
Rock	285-750	

anomalous aureole may occur downslope for a distance equivalent to the diameter of the pipe.

Other examples

In central India, Mathur and Alexander (1983) showed Ni to be much depleted in the upper 2.4 m of soils over kimberlite. Data for Cr were inconsistent (Table V.1-7). In comparison, Aicard (1959) found Ni and Cr concentrations to increase with depth in soils over a kimberlite pipe in Mali, becoming constant below 3 m. Anomalous Cr values cover an area 5 times that of Ni, which is confined to the area of the pipe. This vertical distribution of metal is very similar to that described for Sierra Leone.

Arid tropics

In Botswana, some kimberlite pipes are overlain by 70-100 m of transported Kalahari Sand. Studies by Lock (1985 and written communication) have shown that none of the elements examined (Nb, Ni, Cr, SiO₂, MgO, TiO₂) were anomalous at the surface, although some (e.g. Cr) may be concentrated in present and palaeo-deflation zones. Lock concluded that geochemical prospecting is inappropriate in this environment, although heavy mineral sampling gives valuable results, as discussed below.

PATHFINDER MINERAL SAMPLING

Characteristics of pathfinder minerals

Heavy mineral sampling for pathfinder minerals in soil and drainage samples is one of the most widely used methods for exploring for kimberlitic rocks in all climatic regions. The compositions and abundances of the principal indicator minerals are given in Table V.1-8. There have been some significant recent developments in the use of the compositions of indicator minerals to predict the

TABLE V.1-8

Chemical characteristics of the principal kimberlite pathfinder minerals

		Garnet	Chromian diopside	Ilmenite	Chromite
SiO ₂ %		40-42	52-55	Nil	Nil
TiO ₂ %		< 0.5	< 0.5	50-60	< 1.0
Al ₂ O ₃ %		12-17	1-3	Nil	3-9
Cr ₂ O ₃ %	G9	2-4	1-3	0.5-3	60-65
	G10	> 4			
FeO ^a %		7-11	2-6	25-30	18-22
MgO %		18-20	18-22	10-15	10-15
CaO %	G9	3-8	16-20	Nil	Nil
	G10	1-4			
Na ₂ O %	G9	Nil	1-2	Nil	Nil
Kim		Common to abundant	Common	Common to abundant	Common to abundant
OL		Rare	Rare	Very rare	Abundant

Kim = occurrence in kimberlite.

OL = occurrence in olivine lamproite.

^a Total Fe as FeO.

G9, G10: types of pyrope garnet (Dawson and Stephens, 1975).

economic potential of a kimberlite pipe. Much of the data is unpublished, but some guides can be given.

(1) The Cr-rich Ca-poor pyrope garnets [the G10 group of Dawson and Stephens (1975)] are particularly important. These are garnets containing > 4 wt% Cr₂O₃ and < 3 wt% CaO. Such garnets indicate a pipe that originated in the diamond stability field and therefore may contain diamonds. However, in general, fewer than 5% of pyropes are G10 garnets, even in economic pipes, so that 50 or more grains have to be analyzed to obtain a statistically meaningful result.

(2) Kimberlitic ilmenites that contain > 10 wt% MgO and > 1 wt% Cr₂O₃ and in which the Cr content increases with increasing Mg content are commonly accepted as positive indicators of diamond-bearing kimberlite.

(3) Chromites that contain > 62 wt% Cr₂O₃, 10-15 wt% MgO, < 10 wt% Al₂O₃ and < 1 wt% TiO₂ are considered indicative of diamondiferous kimberlite.

Whereas a skilled observer can distinguish G10 garnets by their magenta colour, Mg-rich ilmenite and Cr-rich chromite are difficult to recognize visually and it may be necessary to analyze at least 50 mineral grains to determine whether they are present.

Dispersion of indicator minerals in the humid tropics

Sierra Leone

In a limited heavy mineral orientation study around the Manjamadu kimberlite dyke, Sierra Leone, samples (14 litres) were taken from each soil horizon

developed over the dyke and from the same depth and same horizons in soils over gneissic wall rocks for 3 m upslope and 16 m downslope (2°) from the dyke. The results showed that the picroilmenite (magnesian ilmenite) content of soils over kimberlite decreases upwards from the saprolite to the sandy soil horizon. The larger grains progressively disintegrate and some are coated by Fe oxides. Anomalous concentrations of picroilmenite are present upslope and over 16 m downslope, with grain size increasing towards the dyke. Grains were also found in the saprolite of the wall rocks. This dispersion of mineral grains from the dyke is attributed to mechanical eluviation of picroilmenite in the soil profile, particularly down root channels and joints (National Diamond Mining Company (SL) Ltd., unpublished internal reports). In contrast, although pyrope garnet is relatively more abundant than picroilmenite in the fresh kimberlite, very little pyrope was recovered during this orientation survey. This is attributed to decomposition of pyrope during chemical weathering and is consistent with empirical data that suggest picroilmenite to be more resistant than pyrope garnet in humid tropical environments. In comparison, in arid environments, pyrope is more resistant than picroilmenite.

Dispersion of indicator minerals in the arid tropics

Jwaneng, Botswana

Surface sampling for heavy minerals can be an effective exploration technique in arid regions, even in areas of transported overburden. For example, in the Jwaneng area, samples of the surface deflation layer may indicate the presence of kimberlite pipes deeply buried beneath Kalahari Sand (Lock, 1985 and written communication). The heavy minerals seem to have been brought to the surface by burrowing termites and concentrated by winnowing. Lock suggests that the grains have been transported by a multi-stage process and are being added continually to the surface deflation layer. This hypothesis is supported by the discovery of present-day termite activity at 70 m depth in the Jwaneng pipe and the coincidence of the surface heavy mineral anomaly with the subcrop of the pipe beneath the Kalahari Sand. Diffuse heavy mineral anomalies are also present over other kimberlites, concealed beneath 70–150 m of the Sand, so that whatever the mechanism of upward movement of mineral grains, the process is widespread and efficient.

Reconnaissance surveys in the Jwaneng area have been based on sampling the plus 420 μm fraction of the surface deflation layer at 10–15 m intervals along traverse lines. Heavy mineral anomalies, in which subdued indicator mineral counts (< 5) occur sporadically over an area of 750 km^2 , are dominated by picroilmenite (magnesian ilmenite). More detailed sampling reduced this “regional” anomaly to several discrete target areas. Pyrope is rarely found, either because of its scarcity in the parent kimberlite or, because of its lower density than picroilmenite, it has not been concentrated by winnowing.

DISCUSSION AND CONCLUSIONS

Kimberlite and olivine lamproite, the only primary host rocks of economic diamond deposits known to date, are ultrabasic rocks that also contain high concentrations of trace elements normally associated in alkalic rocks. Olivine lamproite, in particular, is ultrapotassic. This contrasting geochemistry has been exploited during prospecting by analysis for Ni and Cr (reflecting the ultrabasic character) and Nb (reflecting the alkalic character). However, with the advent of inexpensive multielement analytical techniques and computerized manipulation of data, a far greater number of elements can be now analyzed routinely and will enhance the value of the method. For example, P, Sr, Ce and Ba might supplement Nb data and Mg may provide substantial hydromorphic haloes, such as that in alluvium downstream from the Prairie Creek diatreme in Arkansas, USA (Gregory, 1969).

During chemical weathering in the humid tropics, Ni, Cr and Nb are strongly depleted in soil over kimberlitic rocks, but in the seasonal climate of northwest Australia, weathering is less severe and depletion is much less marked. In both environments, a red clay-rich horizon has developed. In summary:

(1) Nickel in kimberlitic rocks occurs dominantly in olivine (Gregory 1969) and is released at an early stage during weathering. The depletion of Ni in the soil and upper saprolite over kimberlite in deeply weathered areas is presumably due to leaching of Ni by downward percolating waters. Below the water-table, Ni contents are only slightly lower than those found in fresh rock. Thus in interpreting Ni results, the position of the sample with respect to the water-table is important. Anomalous concentrations of Ni were found in the upper saprolite over kimberlites in each study area.

(2) Niobium is contained dominantly in perovskite and ilmenite in kimberlite, and possibly in other minerals, e.g. priderite, in olivine lamproite. Depletion of Nb in the soil over kimberlite during chemical weathering is presumably due to decomposition of perovskite and removal of Nb as either simple or complex anions such as alkali niobates, soluble organo-metallic compounds or colloidal hydrolyzates. Niobium is present in the saprolite in concentrations comparable to those in the fresh rock. It is expected that in areas of less severe chemical weathering, near-surface samples will have anomalous Nb contents, as found in northwest Australia.

(3) Chromium in kimberlite occurs mainly in chromite, magnetite, ilmenite and, to a lesser degree, substituting for Fe^{3+} in ferromagnesian minerals. The three heavy minerals are resistant to weathering, but the depletion of Cr in the soil is evidence that they too break down in humid tropical environments.

Distinctive and unequivocal anomalies occur in the upper saprolite in all the areas studied and, where practical, this is considered the best horizon to sample in deeply weathered terrain. In areas where chemical weathering is less severe, or where erosion has truncated former profiles, such as in northwest Australia, anomalies may occur in near-surface samples. The anomalies are generally

confined to the area immediately overlying the kimberlitic rocks, although significant lateral dispersion of one or more elements may occur.

In both humid and arid deeply weathered areas, where heavy mineral grains are concentrated in the surface horizon, exploration "loam" sampling typically has a detection limit of 1 ppb (approximately one grain in 20 kg). Chemical analysis of kimberlite indicator minerals allows ranking of heavy mineral anomalies in terms of economic priority. Thus, not only is indicator mineral sampling more sensitive than geochemical sampling, but it is more target selective. In addition, heavy mineral haloes tend to be much broader than geochemical haloes, thereby providing a larger target.

The main use of geochemical sampling in diamond exploration is as a complementary technique to other methods. It is of particular value for identifying kimberlitic rocks where visual or mineralogical methods are hindered by deep weathering. It is also of considerable value in ranking the priority of indicator mineral anomalies. It may be of use as a "stand alone" method when prospecting for olivine lamproites in which typical kimberlite pathfinder minerals are rare or absent. Geochemistry is especially useful in areas of high geophysical contrast, except where alkalic and ultrabasic rocks occur together.

URANIUM EXPLORATION IN TROPICAL TERRAINS

F. BIANCONI and K. KÖGLER

INTRODUCTION

Exploration for uranium faces particular problems in lateritic terrain due to the mobility of U and its daughter products and the consequent development of numerous geochemical and radiometric anomalies, most of which have no significance. As a result, U anomalies in laterites are probably discarded too quickly as being insignificant in the course of an exploration programme, yet in some cases they may represent dispersion from primary mineralization. Indeed, the mobility of U in this environment is such that it tends to be dispersed rather than concentrated, although supergene enrichments are known in the oxidized zones over some orebodies. No economic concentrations of U have been found that may be considered equivalent to the lateritic deposits of Ni, Co, Al and Au. Minor occurrences of lateritic U are, however, quite common but follow-up investigations invariably seem to lead to disappointing results.

The geochemistry of U in this environment and the exploration problems it poses have been poorly documented and the main aim of this chapter is to present a classification of U concentrations in laterite based on their mechanisms of formation and to discuss guidelines for their effective exploration and evaluation.

GEOCHEMICAL AND GENETIC CONSIDERATIONS

Uranium in the lateritic environment

The lateritic environment is characterized by strongly oxidizing and deeply leaching hydrous weathering. The main process is the incongruent dissolution of rock forming silicates, which results in an overall depletion of Ca, Mg, Na, K and Si and concurrent residual enrichment of Al and Fe in the upper, strongly oxidized zone of the weathering profile (limonitic or ferruginous zone). The latter elements form authigenic clay minerals and oxyhydroxides, some of which have high adsorption capacities for metallic trace elements (see Chapter I.5; Fig. I.5-8). Acidity and oxidation potential range from low pH (4-5) and strongly positive Eh in the ferruginous zone to neutral or basic (pH 7-8) and less oxidizing conditions in the underlying mottled zone and saprolite.

The behaviour of metallic trace elements in this environment is complex and moderately well known, particularly for those elements that form economic deposits as the result of lateritic weathering, notably Ni and Au (e.g. Golightly, 1981 (Ni); Chapter V.3 (Au)). In contrast, the behaviour of U is poorly known; although numerous anomalous U concentrations have been found in laterites of many countries (e.g. Samama, 1984, 1986), very few detailed geochemical and mineralogical investigations have been reported, with the exception of the deposits of the Alligator Rivers district of the Northern Territory of Australia. The complex behaviour of U is apparent from the review of the published case histories, as described below: U remobilization and redeposition can occur within a wide lateral range, from practically nil to several hundred metres (e.g. Kögler et al., 1983, 1987). On the other hand, primary U mineralization may either be oxidized in situ without significant remobilization or be completely leached and dispersed (e.g. Gritsaenko et al., 1958).

Among the elements of economic importance, uranium has the unique feature of naturally decaying into a series of daughter products, some of which have chemical and physical properties that are very different from the parent element. This often results in geochemical fractionation during the lateritic weathering (see Table V.2-1), e.g. of ^{234}U from ^{238}U (Ivanovich and Harmon, 1982). Although several of these daughter products are important pathfinders for U (e.g. ^{214}Bi in radiometric surveys), they can produce false radiometric or emanometric (gaseous Rn and He) anomalies after geochemical fractionation from the parent element: typical examples are ^{226}Ra anomalies in black soils (e.g. Dickson et al., 1985, 1987b) or in Fe and Mn oxyhydroxide-rich surficial sediments (Bland and Levinson, 1986), which are not supported by U mineralization. Therefore, detailed knowledge of the geochemical behaviour in the lateritic environment of U and its daughter products is essential in exploration.

The chemical mobility of U in aqueous solutions is largely controlled by redox reactions and the formation of soluble complexes. In most primary mineralization, U is in the tetravalent state, i.e. U(IV). Under the oxidizing conditions of lateritic weathering, U(IV) is oxidized to the more soluble hexavalent stage, U(VI) and may then be transported in significant amounts by weathering solutions and groundwater. Accordingly, the mobility of U becomes a function of the solubility of U(VI) complexes in aqueous solutions. As a result, any supergene enrichment must be the result of the fixation of U from such solutions by either (a) precipitation and coprecipitation as discrete U minerals, or (b) adsorption by inorganic substances (organic substances are usually not accumulated during lateritic weathering and are therefore negligible in the present context). Both mechanisms are largely controlled by the following factors: changes in the composition or concentration of the solutions, changes in pH, changes in Eh (causing reduction of U(VI) to U(IV)) and the abundance, capacity and effectiveness of adsorbents. The latter can be strongly affected by the pH or the presence of competing ions.

In principle, these considerations also apply to most of the U daughter

TABLE V.2-1

Simplified ^{238}U natural decay series; full rectangles: main (broken rectangles: minor) sites of geochemical fractionation resulting in radiometric disequilibrium with parent nuclide and/or ^{238}U (modified from Levinson and Coetzee, 1978; Rosholt, 1958)

Nuclide	Atomic number	Type of decay (radiation)	Half-life	Geochemical characteristics causing fractionation
^{238}U	92	α, γ	4.51×10^9 years	
^{234}Th	90	β	24.1 days	Less mobile than ^{238}U in oxidizing environment
^{234}Pa	91	β	1.175 minutes	
^{234}U	92	α, γ	2.48×10^5 years	α -recoil; more mobile than ^{238}U in oxidizing environment
^{230}Th	90	α, γ	7.52×10^4 years	Less mobile than U
^{226}Ra	88	α, γ	1622 years	Mobile in acid waters, relatively immobile in alkaline waters
^{222}Rn	86	α, γ	3.825 days	Inert gas, mobile
^{218}Po	84	α, β	3.05 minutes	
^{214}Pb	82	β, γ	26.8 minutes	
^{214}Bi	83	β, α, γ	19.7 minutes	
^{214}Po	84	α, γ	1.63×10^{-4} seconds	
^{210}Pb	82	β, α, γ	22 years	Less mobile than U
^{210}Bi	83	β, α	5.02 days	
^{210}Po	84	α, γ	138.4 days	
^{206}Pb	82	Stable		
$\alpha + \text{electron} \rightarrow {}^4\text{He}$ (i.e. one ^{238}U decay $\rightarrow 8 {}^4\text{He}$)				Inert gas, mobile

products, with the notable exception of the noble gases ^{222}Rn and He. Furthermore, U is accompanied by Th in a number of primary ore and accessory minerals. However, Th is not oxidized to a mobile hexavalent stage under surface conditions so the two elements will fractionate during oxidative remobilization.

Uranium source

There are two principal sources of uranium:

(1) *Background concentrations.* More or less easily leachable U is present in a variety of sedimentary, metamorphic and igneous rocks in, for example, accessory uraninite in some leucogranites. Several resistate accessory minerals

contain U in various proportions, e.g. zircon (up to 2.7% U), xenotime (up to 3.6% U), and uranothorianite (up to 44.6% U; Boyle, 1982); if these minerals are in the metamict state, much of the contained U becomes chemically mobile and the host-rock is a good U source. The U in some surficial deposits may be derived from such background sources—for example, deposits in calcretes (see p. 386). However, mobilization of background U can also result in the formation of anomalous concentrations of no significance in exploration, usually called “false” (or “spurious”) anomalies.

(2) *Uranium mineralization*. Anomalies and concentrations of U in lateritic profiles resulting from the weathering of primary U mineralization (including economic orebodies) are significant and may be termed “true” in contrast to the previous type.

Transport

Aqueous solutions

The behaviour of U in aqueous solutions has been discussed by Langmuir (1978), Levinson (1980) and Boyle (1982), but very little is known on the composition of such solutions in the lateritic environment nor the form in which U is being transported. In many cases, the concentrations of phosphate, derived from the weathering of apatite (Snelling, 1980), and V are probably of major importance. Continuous downward leaching, particularly in laterites high in the landscape, will most probably prevent U precipitation resulting from changes in the composition or concentrations of the solutions. Such mechanisms are effective in arid areas where mixing of groundwaters and/or evaporation lead to the formation of calcrete-type surficial U mineralization (e.g. Mann and Deutscher, 1978; IAEA, 1984; see p. 386). Evaporation probably also plays a role in the precipitation of hexavalent U minerals where the water-table has been lowered by post-lateritic uplift and erosion, for example in seepages at the edges of laterite mesas.

Migration of solutions

Uranium-bearing weathering solutions may migrate vertically or laterally. *Vertical migration* related to groundwater fluctuations and downward percolation of infiltrating rainwater leads to the in-situ weathering (and possibly enrichment) of U present in the bedrock. Uranium concentrations of this type involve small-scale remobilization of at most a few tens of metres and are, therefore, essentially residual. *Lateral migration* related to groundwaterflow down-drainage involves lateral dispersion of U from primary mineralization and its precipitation downslope, thus forming hydromorphic dispersion haloes. Uranium derived from background sources may precipitate as false secondary concentrations which.

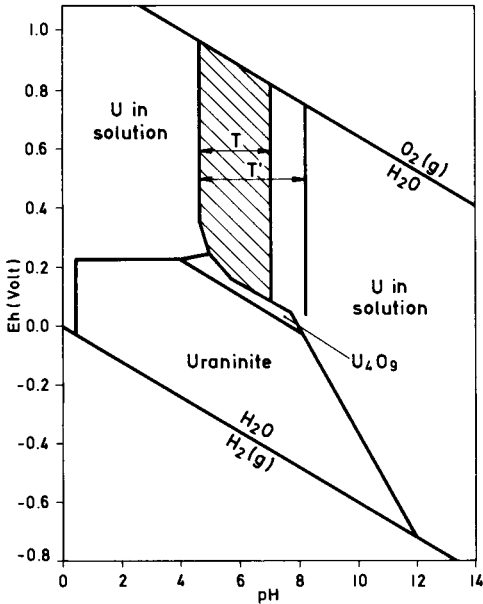


Fig. V.2-1. Eh-pH diagram showing the stability field of tyuyamunite at $p_{\text{CO}_2} = 10^{-2}$ atm. (T) and $10^{-3.5}$ atm. (T') and 25°C. Concentrations are: $K = 10^{-3}$ M (39 ppm), $U = 10^{-6}$ M (0.24 ppm), $V = 10^{-6}$ M (0.1 ppm VO_4). Modified after Langmuir (1978).

Precipitation

pH and Eh

Local changes in pH, from 4 in the surface horizons to weakly alkaline in the saprolite, are of major importance for the fixation of U by both adsorption and direct precipitation. The high sensitivity of hexavalent U minerals to changing pH is illustrated by the behaviour of tyuyamunite (for formulae of U minerals see Table V.2-3) which precipitates when the pH rises above 4.7 and redissolves at a pH over 7 (Fig. V.2-1), values well within the pH range found in laterite profiles.

The strongly oxidizing (high Eh) conditions prevailing in lateritic profiles largely exclude the fixation of U by reduction to U(IV). Exceptions are known from deep parts of the weathering profiles over U ores rich in reductants such as pyrite and organic matter. Reprecipitated sooty pitchblende is described from the USSR (Ashikhmin et al., 1983) and from Campo de Cercado, Brazil (Santos, 1981) and reprecipitated coffinite is described in the lower part of the weathering profile of the Oklo deposit, Gabon (Weber et al., 1975) and of the Bertholène deposit, France (Schmitt and Thiry, 1987).

Adsorbents

The abundance of materials with a wide range of adsorbing capacity is a major geochemical and mineralogical feature of laterite profiles and, therefore, adsorp-

TABLE V.2-2

Enrichment factors of U for natural adsorbents at pH 5 to 8.5; the enrichment factor is the ratio of U adsorbed by the mineral species to the U remaining in solution (modified from Samama, 1984)

Mineral adsorbent	Uranium enrichment factor
Amorphous Fe hydroxide	$1.1 \times 10^6 - 2.7 \times 10^6$
Fine-grained goethite	4×10^3
"Amorphous" Ti hydroxide	$8 \times 10^4 - 10^6$
Humic acids and peat	$10^3 - 10^4$
Phosphorites	15
Smectite (montmorillonite)	6
Kaolinite	$2 - 3.5 \times 10^4$

tion mechanisms are very important in the formation of U concentrations in laterites. The adsorption capacity of some common species, expressed by the geochemical enrichment factor (i.e. the ratio of the amount of U adsorbed by the mineral species to the U concentration in solution), is listed on Table V.2-2, from which it is apparent that Fe hydroxides have the highest values. The greatest adsorption capacity is to be expected in Al-goethite (Muller and Pagel, 1988).

Michel et al. (1983) have demonstrated that enrichment factors as high as 1.5×10^6 are attained in amorphous Fe oxyhydroxides, which have a very high surface area (Samama et al., 1989). As a result, local adsorptive enrichments of 600 ppm U may form from aqueous solutions containing 0.4 ppb U. The adsorption capacity is, in turn, controlled by (1) the pH, being greatest above 5 to 6 (Samama, 1984; Hsi and Langmuir, 1985; Moge et al., 1987; Samama, 1986) and (2) the crystallinity of the oxides. Minerals such as Fe hydroxide lose much of their adsorption capacity during aging and crystallization (e.g. Van der Weijden et al., 1976). In consequence, originally adsorbed U may be released (Moge et al., 1987) to form discrete minerals, as demonstrated by Barton (1956). Little attention has been given to the adsorption capacity of Mn oxides for U (Chao and Theobald, 1976; Watters and Sagala, 1979), although examples of U and ^{226}Ra concentrations in these species are known from lateritic and other environments (Boyle, 1982; Kögler et al., 1983; Bland and Levinson, 1986). Clay minerals appear to be less efficient U adsorbents than Fe hydroxides; however, Giblin (1980) demonstrated experimentally that kaolinite attains a U concentration factor of 3.5×10^4 at pH 6.5. Shirvington (1983) presented evidence to show that clay minerals have excellent long-term retention of U(VI), probably due in part to isomorphic substitution into the clay crystal lattice. Although organic matter is an important adsorbent in reducing environments, particularly in temperate regions, it is intrinsically rare in laterite profiles and adsorption of U onto organic substances is of little practical importance in this environment.

From the above considerations, it can be concluded that the understanding of adsorption mechanisms is the key for the correct evaluation of those U enrichments that do not contain discrete U minerals, whereas the recognition of pH

interfaces is essential for the understanding of U enrichments that precipitate as discrete U mineral phases.

Mineralogy

A great number of U minerals has been recorded from lateritic environments (Table V.2-3), but no systematic evaluation of the stability fields of the hexavalent U minerals is yet available. Empirically, it appears that the most common species are uranyl oxides, silicates, phosphates and vanadates; this order corresponds approximately to increasing lateral or vertical dispersion from the parent tetravalent species, uraninite/pitchblende. However, it should be noted that the occurrence of uranyl silicates, phosphates and vanadates is not restricted to the lateritic environment: this characteristic is shared with other near-surface environments, for example the calcrete-type U mineralization (Pagel, 1984). However, in the latter type, the vanadate carnotite is the most common species, whereas in laterites this mineral is rather the exception.

CLASSIFICATION AND EXAMPLES OF LATERITIC URANIUM CONCENTRATIONS

Lateritic uranium concentrations can be classified according to their genesis, as follows:

- (1) Residual U(-Th) concentrations.
- (2) Residual supergene enrichments.
- (3) Seepage concentrations.
- (4) Secondary seepage enrichments.

The four classes are not mutually exclusive and many gradations between them, or even superimposed types, probably exist. The four classes are briefly described below using examples taken from the literature. Their relative positions and spatial situation within the lateritic regolith are shown diagrammatically in Fig. V.2-2.

Uranium enrichments may also be distinguished on the basis of their U mineralogy:

- (a) Enrichments consisting of residual U(-Th) minerals;
- (b) Enrichments consisting of U adsorbed to non-uranium minerals;
- (c) Enrichments consisting of visible, supergene U minerals.

The first type is restricted to the class of residual U(-Th) concentrations by definition. The other two may occur in each of the four genetic classes. However, as clearly exemplified by the weathering of the Koongarra orebody in Australia (described below), more than one mineralogical type may occur in the same dispersion halo.

Residual U(-Th) concentrations

Concentrations of this type are formed by either in-situ fixation of U liberated from the weathering of accessory minerals, or by the physical accumulation of

TABLE V.2-3

Uranium mineralogy in the lateritic weathering profile; the sequence roughly corresponds to an increasing mobility with respect to lateral or vertical dispersion from the tetravalent primary mineralization

Mineral	Formula	Occurrence
1. U(IV)		
Sooty pitchblende ("U black")	UO_{2+x}	USSR, Campo de Cercado (Brazil)
Reprecipitated coffinite	$U(SiO_4)_{1-x}(OH)_{4x}$	Oklo (Gabon), Bertholène (France)
Ningyuite	$(U, Ca, REE)_2(PO_4)_2 \cdot 1-2H_2O$	USSR
2. U(VI)		
a) <i>Oxides</i>		
"Gummite"	Pb-uranyl-oxides	Ranger (north Australia), Oklo
Curite	$3PbO \cdot 8UO_3 \cdot 5H_2O$	Koongarra (north Australia)
Fourmarierite	$PbO \cdot 4UO_3 \cdot 5H_2O$	Koongarra, Amarinopolis (Brazil)
Vandendriesscheite	$PbO \cdot 7UO_3 \cdot 12H_2O$	Koongarra
Wölsendorfit	$(Pb, Ca)U_2O_7 \cdot 2H_2O$	Oklo
b) <i>Silicates</i>		
	(unspecified)	USSR
Kasolite	$Pb(UO_2)(SiO_3)(OH)_2$	Koongarra
Sklodowskite	$Mg(UO_2)_2(SiO_3)_2(OH)_2 \cdot 5H_2O$	Koongarra, Ranger, Amarinopolis
Uranophane	$Ca(UO_2)_2(SiO_3)_2(OH)_2 \cdot 5H_2O$	Koongarra, Tanzania, Zambia, Oklo, Amarinopolis
Beta-uranophane	$Ca(UO_2)_2(SiO_3)_2(OH)_2 \cdot 5H_2O$	USSR
Boltwoodite	$K_2(UO_2)_2(SiO_3)_2(OH)_2 \cdot 5H_2O$	Zambia
c) <i>Phosphates</i>		
Saléeite	$Mg(UO_2)_2(PO_4)_2 \cdot 8-10H_2O$	Koongarra, Ranger
Sabugalite	$HAl(UO_2)_4(PO_4)_4 \cdot 16H_2O$	Koongarra, Amarinopolis
Torbernite	$Cu(UO_2)_2(PO_4)_2 \cdot 12H_2O$	Koongarra, Oklo, Mounana (Gabon)
Metatorbernite	$Cu(UO_2)_2(PO_4)_2 \cdot 4-8H_2O$	Koongarra, Ranger
Renardite	$Pb(UO_2)_4(PO_4)_2(OH)_4 \cdot 7H_2O$	Koongarra, Mounana, Amarinopolis
Dewindtite	$Pb_3(UO_2)_5(PO_4)_4(OH)_4 \cdot 10H_2O$	Koongarra
Parsonsite	$Pb_2(UO_2)(PO_4)_2(OH)_4 \cdot 7H_2O$	Amarinopolis
Autunite	$Ca(UO_2)_2(PO_4)_2 \cdot 10-12H_2O$	USSR, Zambia, Mounana, Oklo, Amarinopolis, Burkina Faso
Meta-autunite	$Ca(UO_2)_2(PO_4)_2 \cdot 2-6H_2O$	USSR, Tanzania, Zambia, Amarinopolis
Phosphuranylite	$Ca(UO_2)_4(PO_4)_2(OH)_4 \cdot 7H_2O$	USSR, Tanzania, Zambia
Uranocircite	$Ba(UO_2)_2(PO_4)_2 \cdot 10H_2O$	Mounana
Meta-uranocircite	$Ba(UO_2)_2(PO_4)_2 \cdot 8H_2O$	Tanzania, Zambia, Amarinopolis
d) <i>Vanadates</i>		
Carnotite	$K_2(UO_2)_2(VO_4)_2 \cdot 3H_2O$	Koongarra, Tanzania, Madagascar
Tyuyamunit	$Ca(UO_2)_2(VO_4)_2 \cdot 5-8H_2O$	Koongarra, Tanzania
Meta-tyuyamunit	$Ca(UO_2)_2(VO_4)_2 \cdot 3-5H_2O$	Amarinopolis
Francevillite	$(Ba, Pb)(UO_2)_2(VO_4)_2 \cdot 5H_2O$	Tanzania, Madagascar
Sengierite	$Cu(UO_2)_2(VO_4)_2 \cdot 8-10H_2O$	Tanzania
Vanuralite	$(UO_2)_2Al(VO_4)_2(OH) \cdot 8H_2O$	Mounana
e) <i>Arsenates</i>		
Zeunerite	$Cu(UO_2)_2(AsO_4)_2 \cdot 10-12H_2O$	USSR
Abernathyite	$K_2(UO_2)_2(AsO_4)_2 \cdot 6H_2O$	Zambia

TABLE V.2-3 (continued)

Mineral	Formula	Occurrence
f) <i>Sulphates</i>		
Johannite	$\text{Cu}(\text{UO}_2)_2(\text{SO}_4)_2(\text{OH})_2 \cdot 6\text{H}_2\text{O}$	Koongarra
g) <i>Carbonates</i>		
Rutherfordine	$(\text{UO}_2)\text{CO}_3$	Oklo
h) <i>Adsorbed</i>		
	Onto clay minerals and Fe and Mn oxides/hydroxides.	Tanzania, Gabon, Mali, Central African Republic, Senegal, Morocco, Bihar (India), Campo de Cercado, Amorinopolis, Alligator River and Rum Junge (north Australia), USSR.

Data compiled from the following references:

Africa:

Gabon: Oklo and Mounana deposits (Geffroy, 1975; Lecoq et al., 1958; Pfiffelmann, 1975; Weber et al., 1975);

Tanzania: Madaba and Mkuju occurrences (Bianconi, 1987; Kögler et al., 1983 and 1987);

Zambia: occurrences in Karroo sandstones (Money and Prasad, 1979; Prasad et al., 1979);

Madagascar: Folakara occurrence (Premoli, 1979);

Central African Republic (Molina, 1983);

Burkina Faso, Mali, Morocco, Senegal (Samama, 1984).

South America:

Brazil: Amorinopolis (Barretto, 1985; Leonardos et al., 1987);

Campo de Cercado (Santos, 1981).

India: Bihar (Samama, 1984).

Australia:

Alligator River Uranium Field: Ranger orebodies (Eupene and Williams, 1980; Sherrington, 1983b); Koongarra orebody (Snelling, 1980); Rum Jungle area, Northern Territory, (Ruxton, 1963).

USSR: unspecified localities (Ashikhmin et al., 1983; Gritsaenko et al., 1958).

Europe:

France: Bertholène deposit (Schmitt and Thiry, 1987).

resistant uraniferous minerals. They are thus genetically autochthonous with respect to their U source. There are no known cases of economically significant concentrations of this type so that from an exploration point of view, they may therefore be classified as "autochthonous false anomalies" (case 1 in Fig. V.2-2). Since these minerals are usually also rich in Th, lateritic concentrations of this type are commonly characterized by high Th contents. Muller and Pagel (1988) have investigated a lateritic profile developed over gneissic basement carrying zircon and monazite as the main U and Th bearing accessory minerals. They have shown that both U and Th are mostly concentrated in indurated ferruginous nodules, with a slight U depletion at the top of the profile.

An example of this type of concentration is described by Molina (1983) from the Central African Republic. Follow-up ground work showed that airborne

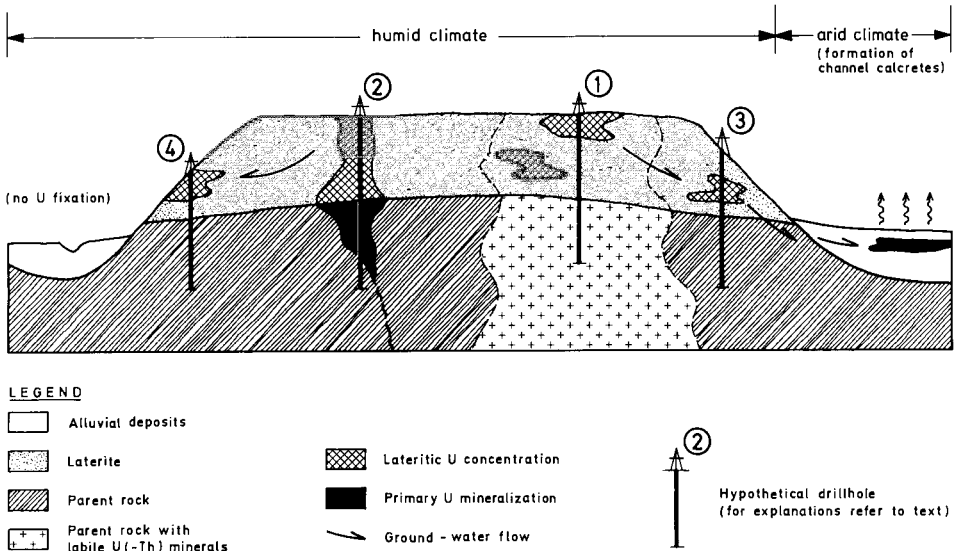


Fig. V.2-2. Diagrammatic cross-section of a lateritic regolith with examples of the four genetic classes of lateritic uranium enrichments and hypothetical drillholes.

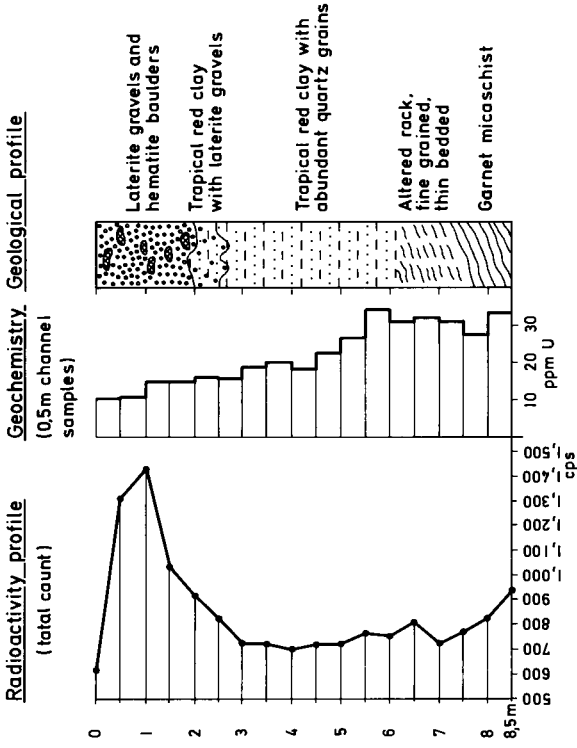
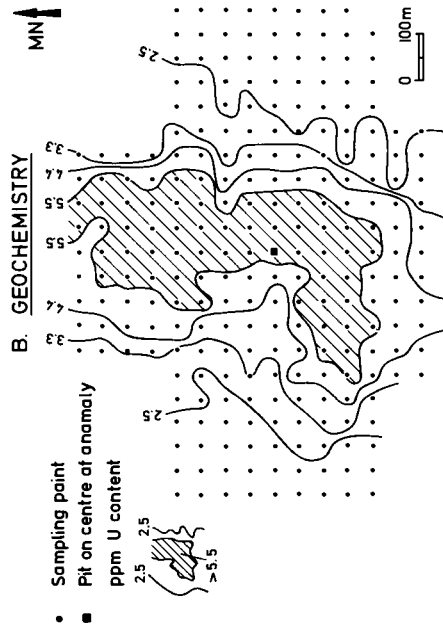
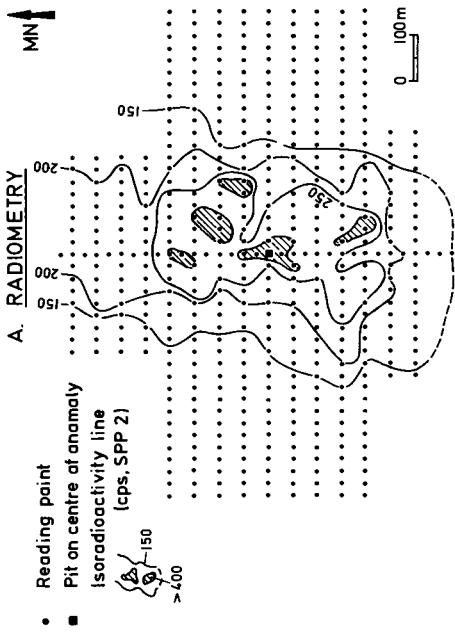
radiometric anomalies were confined to lateritic soil developed over Archaean metaquartzites and mica schists (model A 0 0 [0,1], see Table I.1-6). The strongest anomalies were evaluated in detail by grid-controlled (50×25 m) radiometry and soil sampling, followed by the excavation of pits through the lateritic cover to bedrock (Fig. V.2-3), which consists of gneisses containing abundant U- and Th-rich allanite. It is apparent from the pit section that the U content is poorly correlated with the radiometric profile. The reason for this is not given by Molina (1983), but two interpretations can be suggested:

(a) geochemical fractionation between Th and U, causing residual enrichment of the less mobile element Th in the ferruginous zone, producing the main component of the gamma anomaly;

(b) fractionation between ^{238}U and its daughter products resulting, for example, in a Ra-supported ^{214}Bi anomaly (the total count scintillometer used during this survey having essentially measured the gamma activity of ^{214}Bi). It should be noted that the lateritic weathering in this particular case resulted in a depletion of U in the profile compared to the underlying source rocks.

Similar anomalies of this type have been described by Lovering (1955), Gritsaenko et al. (1958), Ashikhmin et al. (1983) and Bokilo et al. (1988).

Fig. V.2-3. Uranium anomaly in laterite in the Central African Republic. (A) Grid-controlled ground radiometry; (B) Geochemistry; (C) Section through pit on centre of anomaly. Modified from Molina (1983); reproduced with permission of the I.A.E.A., Vienna.



C. PIT ON CENTRE OF ANOMALY

Residual supergene enrichments

This class encompasses enrichments that are formed during the lateritic weathering of primary U mineralization. Remobilization of U during this process is largely restricted to vertical displacement from the uppermost, oxidizing parts of the profile down to the lowest seasonal groundwater level. Secondary U enrichment is commonly significant in the lower levels where it can form in cementation zones. As in the previous class, enrichments of this type are autochthonous with respect to the U source (case 2 in Fig. V.2-2). Since they are related to primary U mineralization of possible economic interest, they can be termed "autochthonous true anomalies" for exploration purposes. Much of the literature on U in the lateritic environment is concerned with this type.

Examples from the USSR are described by Gritsaenko et al. (1958), who distinguished two levels in the weathering zone of sulphide bearing U veins. An upper level of complete oxidation (secondary hexavalent U minerals) occurs above the water-table. This is underlain by a zone of incomplete oxidation with hexavalent and (secondary) tetravalent U minerals (sooty pitchblende; the "produits noirs" of the French literature). The boundary of the two zones coincides with the zone of fluctuation of the water-table and may be completely depleted of U. Secondary U enrichment occurs in the zone of incomplete oxidation (cementation zone) below the water-table. The U mineralogy of the upper zone is dependent on the pH conditions: under strongly acidic conditions, such as in the presence of abundant weathering sulphides, no discrete hexavalent U minerals are stable and limonite may be the only uraniferous phase. In this case, U anomalies found at surface are not readily distinguished from anomalies caused by adsorption of laterally derived U.

The important role of reducing agents such as organic carbon and iron sulphides in the primary mineralization for the fixation of U during lateritic weathering has been pointed out by Ashikhmin et al. (1983). The authors describe a considerable (but presumably subeconomic) U enrichment in an unoxidized clay weathering zone above shales rich in reductants from an unspecified locality in the USSR.

The most thoroughly investigated deposits in the western world are the Ranger orebodies in northern Australia (Eupene and Williams, 1980; Sherrington et al., 1983a,b; Cruikshank and Pyke, 1986). The orebodies subcrop in an area of lateritic soil cover (model A 1 0 [0,1]; partly B 1 0 [0,1]). Their upward extension in the laterite profile enabled discovery by airborne radiometry and detection by ground methods such as radiometry, soil geochemistry, bedrock geochemistry, hydrogeochemistry and emanometry.

The depth of lateritic clays reaches 30 m, although minor surface oxidation along joints and foliations extends to 90 m below surface. Shallow flooding of the area is common in the rainy season, but the water-table drops to 4–15 m below surface in the dry season. The laterite is radioactive at surface, and limonitic pisoliths retain up to 1000 ppm U if developed above U ore; however, in the upper 2 m of the laterite profile U is slightly depleted. Hexavalent U

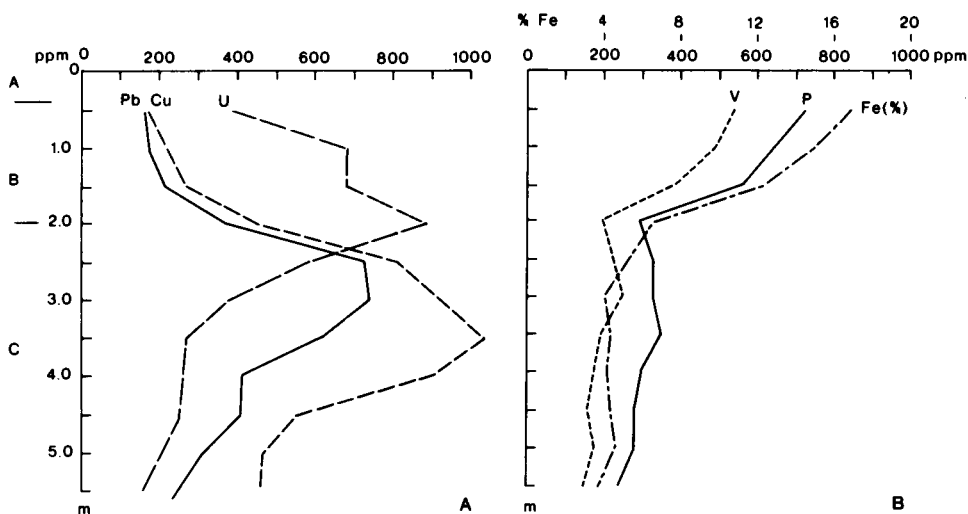


Fig. V.2-4. Element distributions in soil profiles over No. 3 orebody, Ranger One. (A) Pb, Cu and U; (B) V, P and Fe. Modified from Eupene and Williams (1980).

minerals, such as saléeite, sklodowskite, metatorbernite and “gummite”, appear only 0.4 m below surface. Since the primary ore contains less than 0.7% sulphides, weathering has not caused the development of extremely acidic conditions. Consequently, according to the model of Gritsaenko et al. (1958), the in-situ oxidation of the primary ore to hexavalent U minerals must predominate over dissolution and mobilization. This is confirmed by the low U content of surface waters downstream of the Ranger Three orebody, which decline from 3.8 to 5.5 ppb U adjacent to the orebody to 0.3 ppb U at a distance of 4 km. The vertical zonation of the weathering zone overlying the primary ore at Ranger One is shown in Fig. V.2-4 (Eupene and Williams, 1980). The U grades near the top of the profile are similar to those of the primary zone; however, a gradual depletion to 25% of the primary concentration occurs in the centre of the profile, but toward the base there is supergene enrichment to 1.5 times the primary grade. The depletion is strongest at about 5 m depth, which is within the zone of water-table fluctuation (0–15 m), i.e. corresponding to the zone of depletion described by Gritsaenko et al. (1958).

The U deposits in Gabon, Central Africa, are covered by a thick layer of lateritic clay (Lenoble and Gangloff, 1958). The oxidation of the U ore in the weathering profile is essentially in situ. Over the Mounana deposit (models B 2 0 [0,1] and B 3 0 [0,1]) the primary mineralization is oxidized to uranyl vanadates and phosphates (Pffiffelmann, 1975), and to adsorbed U, probably onto Fe hydroxides (Lecoq et al., 1958) in the ochreous lateritic clays at surface. The latter concentrations were located by a airborne radiometric survey and eventually led to the discovery of the primary orebody. Over the Oklo deposit, the

oxidation minerals are reprecipitated coffinite in the deeper horizons of the weathering profile, indicating an Eh interface (Weber et al., 1975) and “gummites”, uranyl silicate (alpha-uranophane) and uranyl phosphates (torbernite and autunite) in the higher levels (Geffroy, 1975).

A similar mineralogical zonation is reported by Schmitt and Thiry (1987) from the weathering profile over the Bertholène deposit in France. The surficial ferruginous zone carries uranyl phosphates and vanadates, and the underlying bleached zone (possibly saprolite, with high silica concentration) is mineralized with coffinite; below the water-table, primary pitchblende mineralization is preserved.

A further example of this type is Amornópolis, Goiás, Brazil, described by Barretto (1985) and Leonardos et al. (1987). Sandstone-hosted pitchblende-coffinite mineralization in the Devonian Ponta Grossa Formation occurs in elongated trends (possibly palaeochannels) within dissected laterite plateaux (models A 0 0 [0] and B 0 0 [0]). In-situ oxidized mineralization, consisting of various uranyl oxides, silicates, phosphates and vanadates, as pockets, impregnations and nodules within the laterite, outcrops where the mineralized trends are cross-cut by the margins of the mesas. Across the mesas, the trends are expressed as elongated radiometric anomalies in the lateritic cover.

From the examples described above, it is evident that the U concentrations in the shallow horizons tend to not correlate well with the grade of the underlying primary mineralization. Downward leaching and a resulting decrease in grade appear to be normal, with a zone of relative enrichment at depth. Lateritic weathering is therefore a destructive process and only an oxidized relic of the original mineralization remains near the surface.

Seepage concentrations

This class comprises U enrichments formed by the fixation of U that has been derived from primary background sources (e.g. uraniferous accessory minerals) and transported laterally in solution. These enrichments are allochthonous with respect to their U sources and, since they are not genetically related to economic primary U mineralization, they can be termed “allochthonous false anomalies” (case 3 in Fig. V.2-2).

Seepage concentrations of U are probably mostly of the adsorptive type and, unfortunately for the U explorationist, are very common in all types of lateritic terrains. A possible explanation for their abundance can be deduced from the results of work by Michel et al. (1983), namely that the U enrichment is mainly a function of the efficiency of available adsorbents, even if the absolute concentration of dissolved U is very low. In many surveys, attempts have been made to overcome this problem by normalizing the U content of a sample with respect to the corresponding Mn and Fe contents (e.g. Chao and Theobald, 1976; Filipek and Theobald, 1981; Watters, 1983). Michel et al. (1983) have suggested that the normalization should be between the concentrations of adsorbed U in a given sample and the available sorption surface. They found that the actual U content

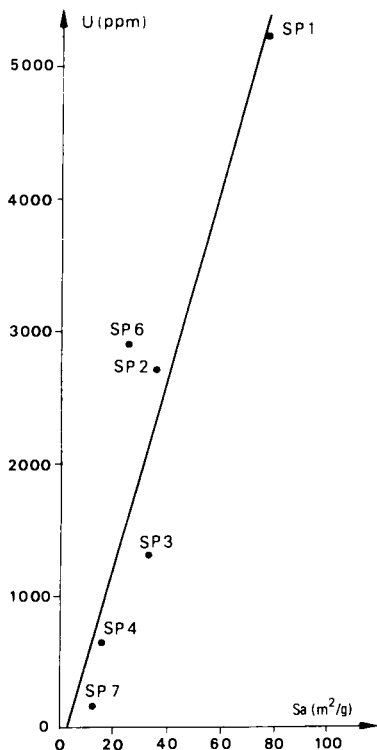


Fig. V.2-5. Uranium/surface area (Sa) correlation diagram for six bulk samples of ferruginous concretions (Saint Pierre de Cantal, France). The alignment indicates that the different adsorbent species are in equilibrium with waters of identical U content and result from modern leaching of the ore. Redrawn from Michel et al. (1983); reproduced with permission of the I.A.E.A., Vienna.

of samples which are in equilibrium with the same groundwater is a function of the global active surface of the respective samples (Fig. V.2-5). A corresponding normalization procedure may, therefore, represent a powerful tool for distinguishing between “false” and “true” anomalies: if an anomalous sample plots on the same line as the samples of the background population, the anomaly has probably been formed by the concentration of background U and can, therefore, be classified as “false” and thus discarded from follow-up investigations.

Examples of lateritic U anomalies which can be classified as adsorption-type anomalies without visible discrete U-minerals are common in the literature. Sherrington et al. (1983a,b) mention adsorption-type U anomalies (“hot laterites”), without known relation to mineralization, in the Ranger area of northern Australia. Similar cases have been described from the USSR by Gritsaenko et al. (1958).

It is, of course, possible that many adsorption-type U concentrations contain discrete U minerals of microscopic to submicroscopic dimensions: much re-

search remains to be done on this problem. A notable case in which the enrichment of background U has formed discrete U minerals is the Les Bondons U occurrence in the French Massif Central; here, U from a background granitic source has precipitated as sooty pitchblende. The occurrence is one of over 70 of the same type and is described in detail by Samama (1986). Irregular, tabular, low-grade U concentrations as sooty pitchblende in disseminations and veinlets are found in the saprolite of a supposedly Permian to Jurassic lateritic regolith derived from Palaeozoic schists rich in carbonaceous matter and pyrite. The schists are intruded by Hercynian granites containing up to 13.6 ppm U, partly in labile form. The U occurrences are usually found within 1000 m of the granite/schist contact. Samama (1986) proposed the following genetic model: U was leached from the weathering crust of the granites and was transported in groundwater (probably as uranyl carbonate complexes) along the regional slopes. Where the groundwater entered the alkaline and reducing environment of the pyritic saprolite, U precipitated by redox processes, mainly as sooty pitchblende. Although U has been concentrated by a factor of 150, the occurrences are not economic. This is a rare example of U derived from background sources precipitating as discrete minerals in a lateritic environment.

The apparent lack of economic U concentrations from background sources in lateritic profiles is probably mainly due to the absence of suitable traps. In the normal case, U in solution will be transported beyond the lateritic profile and precipitate in other environments, for example, into channel calcretes or fluvial sandstones. One example is the Yeelirrie calcrete-type deposit in Western Australia, where the primary sources of U are Archaean granites overlain by a lateritic regolith. Uranium liberated by post-lateritic weathering is transported by groundwater into the calcrete environment (Fig. V.2-2; see also p. 386).

Secondary seepage enrichments

Secondary seepage enrichments, like seepage concentrations, are U enrichments that are laterally displaced from their source. However, in this case, the source is primary U mineralization. In the exploration context, enrichments of this type can be termed "allochthonous true anomalies" (case 4 in Fig. V.2-2). The correct recognition of such enrichments is clearly very important in U exploration in lateritic environments, since they might lead to the discovery of economic primary U mineralization.

An example of U concentrations of this type is described by Kögler et al. (1983) from the Madaba area, southern Tanzania. The area consists of erosional remnants of Tertiary laterite peneplains that have been dissected by deeply incised valleys (models A 0 0 [0-3] and B 0 0 [0-3]). The laterite is developed on shallow dipping Palaeozoic to Mesozoic Karroo sandstones and siltstones which are host to peneconcordant sandstone-type U mineralization in a well-defined stratigraphic interval. Secondary U accumulations are found in the mottled zone and saprolite (pallid zone) of the laterite more than 60 m stratigraphically above the mineralization and more than 1 km laterally from its projected intersection

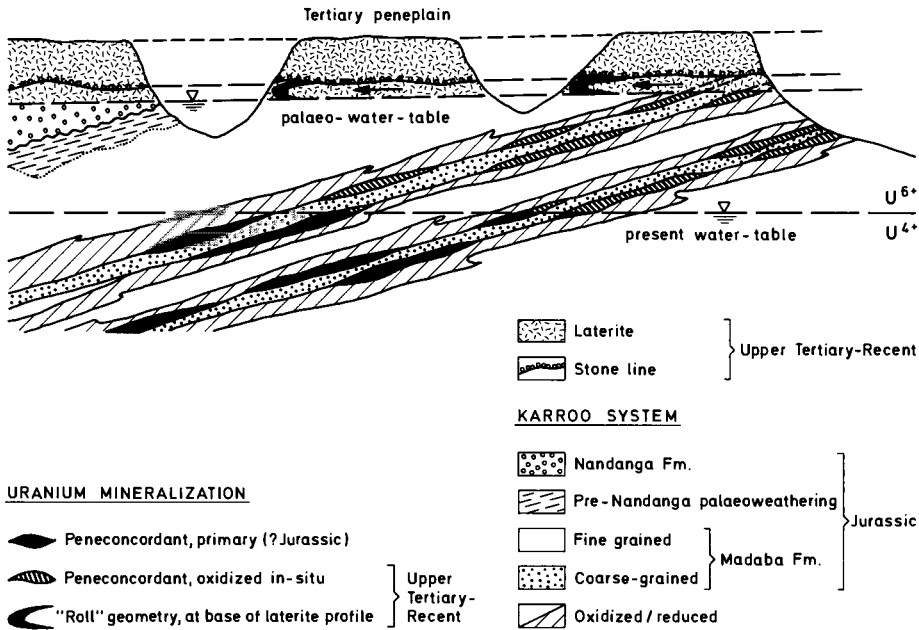


Fig. V.2-6. Diagrammatic cross-section (not to scale) of the Madaba area, Tanzania, showing the model for the formation of uranium mineralization in the laterite profile. Modified from Kögler et al. (1983); reproduced with permission of the I.A.E.A., Vienna.

with the original laterite peneplain (Fig. V.2-6). The secondary U concentrations are of various types and comprise uraniferous Mn oxide without discrete U minerals, discrete uranyl vanadates associated with Mn-Fe oxide/hydroxide impregnated sandstone, and uranyl vanadate mineralization having rollfront geometry. They are interpreted as the result of U from the primary peneconcordant sandstone-type mineralization being mobilized and transported laterally by groundwater over several hundred metres and finally adsorbed or precipitated at the palaeo-water-table in the laterite.

A further example is the dispersion halo of the Nabarlek orebody in northern Australia (model B 2 0 [1,2]). The top of the steeply dipping orebody is truncated by the recent lateritic weathering surface. The water-table fluctuates between 0 and 15 m below surface during the year. Shirvington (1980) investigated a continuous secondary dispersion halo in lateritic red clays downslope from the suboutcropping orebody by alpha-spectrometric determinations of ²³⁸U and the daughter isotope ²³⁴U. The results indicate that the remote parts of this halo formed within the last few 0.1 Ma, whereas the apex directly above the orebody is 4 to 7 times older. Beyond the continuous dispersion halo, which is approximately 700 m long, subrecent accumulations of U derived from the leaching of the main orebody occur at distances of up to 1200 m. Strong fractionation of the

two U isotopes was found and Shirvington (1980) suggested that the technique distinguished between (a) U dispersed by weathering processes from the zone of primary mineralization giving a hydromorphic halo, with relative ^{234}U enrichment, and (b) near-surface traces of primary mineralization oxidized in situ and having relative ^{238}U enrichment. This technique may, therefore, represent a powerful tool for the evaluation and follow-up of seepage (i.e. laterally displaced, hydromorphic) U enrichments.

Dispersion in the weathered zone of the Koongarra deposit, also in northern Australia, has been particularly well studied (Snelling, 1980, 1984). The primary orebody is covered by 25–30 m of limonitic residual soil and kaolinized schist, in turn overlain by thin surficial sands (model B 2 0 [1,2]). A pit over the peak of an airborne radiometric anomaly exposed hexavalent U minerals at 3.4 m depth and led to the discovery of the steeply dipping primary orebody. The water-table fluctuates between surface and a depth of 8–9 m during the year.

The near-surface expression of the mineralization is a combination of in-situ oxidation and lateral dispersion (Fig. V.2-7). The following zones are distinguished:

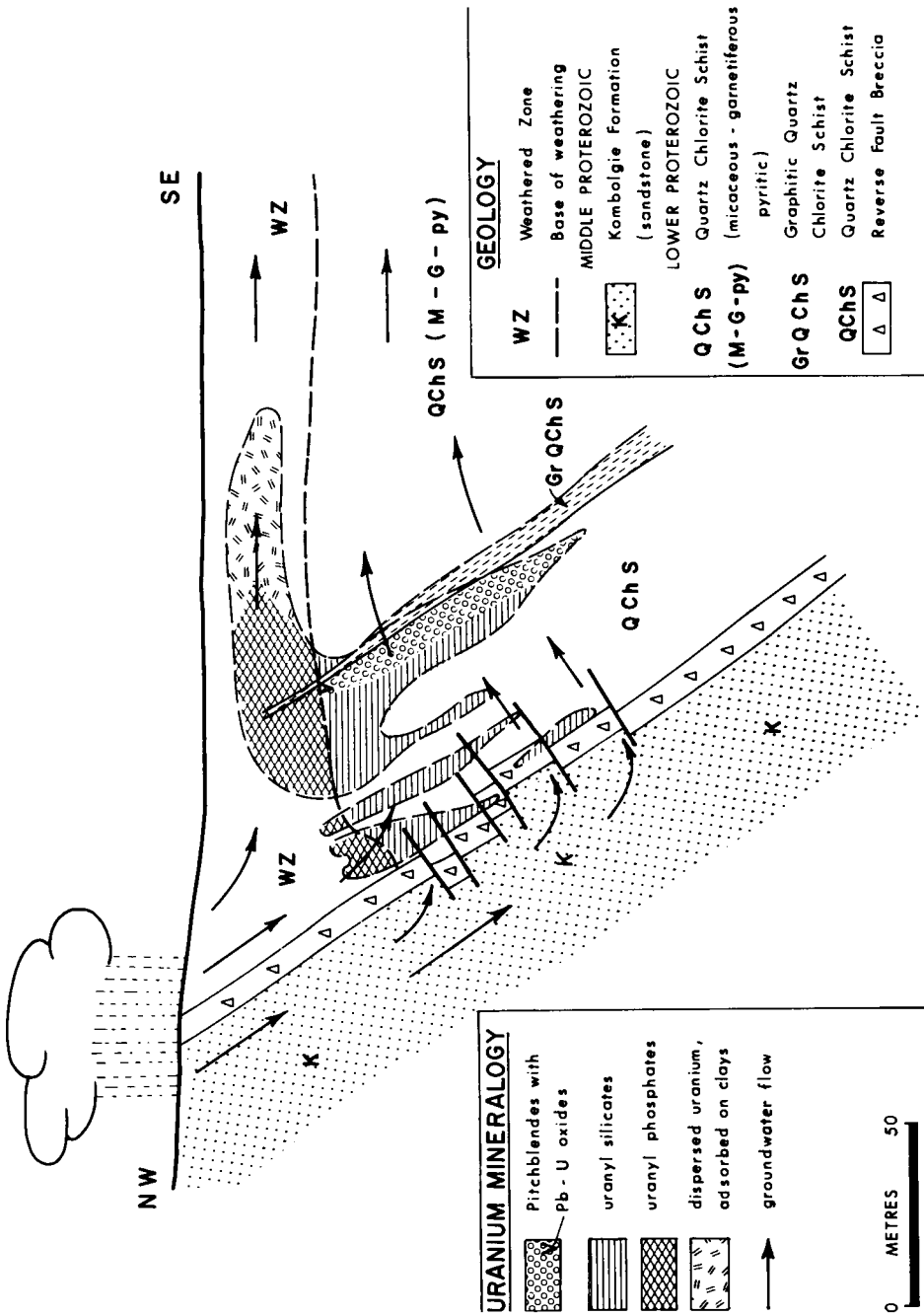
(1) a zone of in-situ alteration of uraninite veins to U-Pb oxides (“gummite”, comprising curite, fourmarierite, vandendriesscheite) and uranyl silicates (kasolite, uranophane, sklodowskite) below the water-table;

(2) a zone of oxidation within the lateritic weathering profile, with a dispersion fan of ore grade material that extends downslope for about 80 m and consists of uranyl phosphates, sulphate and vanadates. In this zone, oxidation is stronger and the solubility of U is governed by the phosphate concentration, derived from the weathering of apatite;

(3) a hydromorphic dispersion zone consisting of U adsorbed onto clays or, possibly, goethite. In this zone, U is still accompanied by anomalous Cu but not by Pb, which is only present in zones 1 and 2.

Downslope U dispersion within the lateritic weathered zone has also been described from the Rum Jungle area, northern Australia (Ruxton, 1963). The Rum Jungle Creek South U orebody was “blind”, being covered by a lateritic weathering profile and ferruginous soil that had no surface U concentrations immediately above the orebody (model B 2 Fe [2,3]). The nearest surface anomaly was of the adsorptive type, about 130 m downslope from the orebody in a creek bench cut in the ferruginous soil. Follow-up of this hydromorphic anomaly by pattern diamond drilling led to the discovery of the orebody.

Fig. V.2-7. Simplified cross-section through the Koongarra No. 1 orebody. The distribution of the various uranium minerals and the paths of present-day groundwater circulation are shown schematically. Redrawn from Snelling (1984).



EXPLORATION AND EVALUATION OF LATERITIC U CONCENTRATIONS

From the review of the available literature, it is apparent that there are no techniques or strategies specific to the lateritic environment during the early (reconnaissance and prospecting) stages of exploration. The remoteness and limited infrastructure usually typical of this environment dictate the application of fast and inexpensive techniques for covering large areas, such as airborne and ground radiometric surveys and geochemical stream sediment surveys.

In an orientation survey carried out after the discovery of the Mounana U deposit, Gabon, Grimbert (1963) noted a U dispersion of only 1 km in water but of 3 km in stream sediments. Accordingly, he recommended the use of stream sediments, collected at a density of 1 sample/km, in the reconnaissance ("strategic") stage. More recently, Samama et al. (1989) described a further orientation drainage survey in Gabon, in the Franceville district, and showed that the definition of significant U anomalies can be optimized by using the surface area of the stream sediments to correct the raw data, as this takes the adsorption capacity of the sample into account. Watters and Sagala (1979) and Watters (1983), on the other hand, recommend the use of heavy mineral concentrates of stream sediments, since the results of their work in tropical and subtropical environments have indicated an enhancement of anomaly contrast relative to the corresponding and more commonly used minus 80-mesh (180 μm) fraction; as a result, a much lower sample density may be used in the reconnaissance stage. It is only after the detection of an anomaly that the specific character of the lateritic environment determines the exploration strategy.

Anomalies are investigated in detail by using the standard techniques of U exploration, i.e. grid-controlled geological mapping and radiometric and soil surveys. Soil samples are analyzed for U and possible pathfinder or accompanying elements, such as Pb, Cu, Zn, Co, Ni, V, Mo, As, Se and Au. The most useful of these depend on the type of U deposit and corresponding geological environment and will have to be determined by an orientation survey. Sherrington and Gatehouse (1980) established the usefulness of the surficial ferruginous pisoliths ("pea gravel") as a sampling medium suitable for U and other metals over the Ranger One orebodies, Northern Territory, Australia. Although U concentrations are only a fraction of the underlying primary concentrations, they are sufficiently high to give a strong anomaly contrast. However, in the laterite profile overlying the Mounana U deposit, Gabon, Grimbert (1963) found that although Pb and V are concentrated in the horizon containing Mn and Fe concretions, U is not. (The use of pisolith sampling in exploration is discussed in Chapter III.3.) Where orebodies are blind, gases may give surface expression to mineralization. For example, the presence of the Jabiluka Two U (-Au) deposit is indicated by the anomalous Hg content in soil-gas, derived from the associated base metal mineralization (Carr et al., 1986).

Once an anomaly has been fully delineated at surface, the investigations are directed at depth. At this stage, it is imperative to penetrate and sample the

complete lateritic profile down to the unweathered bedrock. The principal techniques are trenching, pitting and/or drilling: in less developed countries, hand-dug trenches and pits are the most cost-effective means. However, if the lateritic profile is deeper than about 10 m, drilling has to be employed. A particularly suitable technique is the rotary airblast (RAB) drilling developed in Australia. This can penetrate the weathering profile very quickly to obtain chip samples, which also yield useful information on bedrock geology (e.g. Pagel et al., 1984).

At this point, the crucial evaluation takes place, i.e. the correct determination of the type of radiometric anomaly or U concentration. From the preceding paragraphs, it is evident that supergene residual enrichments are the easiest to recognize because the follow-up trenching or drilling will eventually reach the underlying primary mineralization (case 2 in Fig. V.2-2). The Mounana and Ranger One orebodies are good examples of this type.

The evaluation of an anomaly is much more difficult if no in-situ oxidized and/or primary mineralization is found. In some situations, follow-up areas can be selected by pinpointing the approximate location of the projected outcrop or subcrop of potentially uraniferous lithologies and/or structural elements beneath the lateritic cover by detailed geological mapping. If the anomaly is of the adsorptive type and associated with enhanced Th contents, it is most probably a residual U(-Th) type concentration, and is thus not significant (case 1 in Fig. V.2-2). Confirmation of this interpretation requires the use of more sophisticated and expensive techniques, such as alpha spectrometry and the determination of the hypothetical U concentration factor. Microscopy may be used as a further evaluation tool: the identification of discrete minerals at the microscopic scale may indicate that the U anomaly is significant (G.H. Sherrington, written communication, 1987). If a secondary seepage enrichment can be suspected (cases 3 and 4 in Fig. V.2-2), the anomaly has to be followed-up laterally and upflow (which is not necessarily upslope!) along the assumed (palaeo-)water-table, which might lead to the localization of the primary U source. The follow-up investigations must therefore be guided by geomorphological and hydrological considerations in order to reconstruct the hydrogeological setting at the time of formation of the anomaly. A possible pitfall in the case of older anomalies is the later inversion of the flow-pattern as a result of young tectonic movements such as block tilting. The investigation of the geometric shape of the anomaly and of possible geochemical and mineralogical zonations might be useful in determining the (palaeo-)groundwaterflow. The alpha-spectrometric determination of younger U migration could also yield important information, as shown by the case histories from the Nabarlek orebody and from Tanzania.

Detailed discussions of most techniques and of the appropriate sequence of application are given elsewhere (e.g. Boyle, 1982; I.A.E.A., 1983, 1988) and are not repeated here. However, the following complementary observations may be made. A number of techniques based on the determination of natural decay products are not specific for U but may also detect Th. The presence of

disequilibrium due to geochemical fractionation processes, which are common in the surficial environment, often limits their usefulness (e.g. Dickson and Snelling, 1980). This proviso also applies to radiometric surveys, for the total gamma radioactivity measured by conventional scintillometers is derived mainly from the daughter product ^{214}Bi and hence is subject to mobility of ^{226}Ra . Under favourable conditions, ^{222}Rn , He and the stable Pb isotopes at the end of the decay chains can be helpful in the detection of blind U mineralization in lateritic terrains. Apparent successes, all from the Koongarra area, are reported by Pedersen et al. (1980) (Rn), Butt and Gole (1986), and Gole et al. (1986) (He), and Dickson et al. (1985, 1987b) (Pb isotopes). Dickson et al. (1987a) have shown that Ra isotopic measurements coupled with hydrogeochemistry can be applied for evaluating the likely source of surface ^{226}Ra anomalies that have accumulated from groundwaters; this procedure may help in the selection of only those anomalies with the highest potential for further exploration by more expensive techniques. Biogeochemistry has been tested over the Ranger One orebody (Eupene and Williams, 1980; Sherrington et al., 1983b; Cruikshank and Pyke, 1986): the best response was found in the U and Mg contents in the ash of leaves of some *Eucalyptus* species. Geophysical techniques other than radiometry might be employed as indirect tools: at Ranger One, magnetometry (airborne and ground) and gravity surveys were found to be useful in assisting in semi-regional geological mapping (Sherrington et al., 1983b). A common problem is that magnetic minerals such as maghemite and residual magnetite in the near-surface laterite can make the interpretation of electromagnetic and magnetic responses difficult, if not impossible.

The general rule in mineral exploration, i.e. that only the correct combination of several techniques leads to success, is of course valid also in the U exploration in lateritic terrains. The basic tools remain geological–geomorphological mapping, radiometry, trenching, drilling and chemical U analysis. Which complementary elements and techniques are useful in a specific area can only be determined by orientation surveys. The main point to be kept in mind when planning U exploration in lateritic terrain is that bedrock is covered by deep and extensive weathering products: this dictates the use of expensive subsurface techniques at a very early stage. Therefore, a careful selection of the location and size of working areas is crucial for cost-effective and efficient exploration programmes.

ACKNOWLEDGEMENTS

The present chapter has been greatly improved by the constructive criticism of C.R.M. Butt and G.H. Sherrington, who also provided unpublished literature: their co-operation is gratefully acknowledged. Mrs. E. Gruno and Mr. G. Möller drafted Figs. V.2-1, 2, 3, 6, and 7. Mrs. M. Abu Salah typed several versions of the manuscript.

THE GEOCHEMISTRY OF GOLD IN LATERITIC TERRAINS

D.J. GRAY, C.R.M. BUTT and L.M. LAWRANCE

INTRODUCTION

Metallic gold is almost inert under the physico-chemical conditions prevailing in most weathering environments. Accordingly, it generally behaves as an immobile element and secondary dispersion is predominantly by physical mechanisms. This resistance to weathering is largely responsible for the economic concentration of Au as placer deposits in alluvial systems and as residual deposits in lateritic terrains. Similarly, chemical resistance, coupled with the high specific gravity, is the property exploited by panning, historically the most important exploration technique. Nevertheless, there are many situations in which the chemical mobility of Au during weathering can either be demonstrated or inferred. These are mostly, but not exclusively, environments both humid and arid that have been tropically weathered. This evidence includes:

- (a) the presence of euhedral crystals, dendrites and other delicate forms of Au in weathering profiles and sediments deposited in high energy environments;
- (b) the etching of Au grains and crystals, both primary and those inferred to be secondary;
- (c) the commonly smaller size of Au grains in the weathered zone compared to those of the underlying primary deposit;
- (d) the higher fineness (lower Ag content) of Au in the weathered zone, especially the upper horizons of lateritic profiles, and the similar loss of Cu and other metals;
- (e) the presence, in many weathering environments, of Ag-depleted rims on Au grains in placers and residual profiles;
- (f) changes in the total mass of Au in saprolite compared to equivalent unweathered rock, calculated on an isovolumetric basis;
- (g) the chemical regeneration of placers in the humid tropics, especially, within a few decades;
- (h) the wider lateral dispersion of Au in saprolite, in arid regions, compared to the primary zone;
- (i) the presence of very finely divided Au enriching recently precipitated calcretes in soils on both residual and transported overburden;
- (j) the presence of Au in living plants and in organic litter.

This evidence points to Au having at least limited mobility during weathering, which becomes significant in some environments. This mobility has long been

recognized; for example, Liversidge (1893a,b) cited examples from many gold-fields in the USA, South Africa, Russia and Australia and reported experimental results that indicated the possible involvement of organic matter, halide and sulphur complexes in the process. This chapter reviews the most probable dissolution, transport and precipitation mechanisms responsible for the observed distribution and characteristics of Au in the regolith and relates them to particular weathering environments. An understanding of these mechanisms and the role played by the parent material, pedological reactions, topography and climate is critical in expanding the potential for geochemical prospecting for Au concealed within or by the regolith.

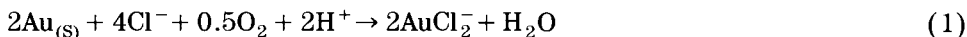
GOLD IN THE WEATHERING ENVIRONMENT

The aqueous chemistry of gold

Gold only becomes geochemically mobile where complexing anions are present in groundwater. The chemical species that could play such a role are listed in Table V.3-1. They become important under different chemical conditions, so that knowledge of the controls on the solubility of their complexes will aid interpretation of the geochemistry of Au in various environments.

Halide complexes

Chloride has long been suspected of being an important ligand for complexing Au (Liversidge, 1893a,b; Krauskopf, 1951; Cloke and Kelly, 1964). Highly acid, saline and oxidizing conditions are required for dissolution of Au chloride (AuCl_2^-):



In solutions containing one mole/litre chloride (1 M Cl = 35,000 mg/L, i.e. about twice the concentration in sea water), that are acid (pH 3) and highly oxidizing (Eh > 800 mV), Au concentrations may reach 10^{-6} M (200 $\mu\text{g/L}$). Under slightly less oxidizing conditions (Eh > 680 mV), concentrations of 10^{-8} M Au (2 $\mu\text{g/L}$) are possible (Fig. V.3-1A). Such highly oxidizing conditions have been produced in laboratory simulations of weathering in the presence of MnO_2 (Cloke and Kelly, 1964; Miller and Fisher, 1973; Lakin et al., 1974). In this chemical environment, the oxidation potential is controlled by the Mn^{2+}/Mn oxide redox couple:



Groundwaters sampled by the authors at a Au deposit close to Kalgoorlie, Western Australia were highly saline ([Cl] = 21,000–107,000 mg/L) and had

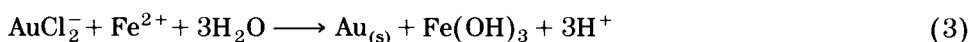
TABLE V.3-1

Potentially important aqueous gold species

Species	Possible origin	Solubility conditions	Product
$\text{AuCl}_2^- / \text{AuCl}_4^-$	Oxidative dissolution of gold under acid saline conditions. $\text{Au} + 2\text{Cl}^- \xrightarrow{[\text{O}]/[\text{H}^+]} \text{AuCl}_2^-$	Oxidized/saline/acidic; pH < 4.0, Cl > 35000 mg/L	High fineness gold
AuI_2^-	Dissolution of gold under moderately oxidative conditions $\text{Au} + 2\text{I}^- \xrightarrow{[\text{O}]/[\text{H}^+]} \text{AuI}_2^-$	Enhanced where I^- is released by decomposition of organic matter	High fineness gold
$\text{Au}(\text{HS})_2^-$	Dissolution of gold by reduced waters during early supergene alteration, or by biologically generated reducing solutions $\text{Au} + 2\text{SH}^- \xrightarrow{[\text{O}]} \text{Au}(\text{SH})_2^-$	Reduced/neutral	Medium-high fineness gold
$\text{Au}(\text{S}_2\text{O}_3)_2^{3-}$	Weathering of gold/pyrite in neutral to alkaline solution. $\text{Au} + 2\text{S}_2\text{O}_3^{2-} \xrightarrow{[\text{O}]} \text{Au}(\text{S}_2\text{O}_3)_2^{3-}$	Alkaline to weakly acid (meta-stable)	Medium fineness gold
$\text{Au}(\text{CN})_2^-$	Interaction of cyanide with gold $\text{Au} + 2\text{CN}^- \xrightarrow{[\text{O}]} \text{Au}(\text{CN})_2^-$	Cyanide present	Low fineness gold
Au-organic matter	Interaction of organic matter with gold under oxidizing conditions. $\text{Au} + \text{OM} \xrightarrow{[\text{O}]} \text{Au}^+ - \text{OM}?$	Not certain, may depend on source of material	High fineness gold fine grained
Colloidal gold	May be formed during reduction of gold by organic matter $\text{Au}^+ + \text{OM}^- \longrightarrow \text{Au}^0$	Not confirmed for natural waters	High fineness gold fine grained

high concentrations of soluble Mn (0.1–18 mg/L), and 5 of the 41 samples were found to have an Eh > 800 mV. These 5 samples, in particular, have a theoretical solubility of greater than 200 $\mu\text{g/L}$ Au chloride. The actual Au solubility was lower, although concentrations up to 3.7 $\mu\text{g/L}$ Au, which is highly anomalous, were observed.

Gold chloride complexes are important for Au mobility in specific environments, as described above. The complexes could be precipitated by reducing conditions and, in particular, by the presence of ferrous iron, which readily reduces Au:



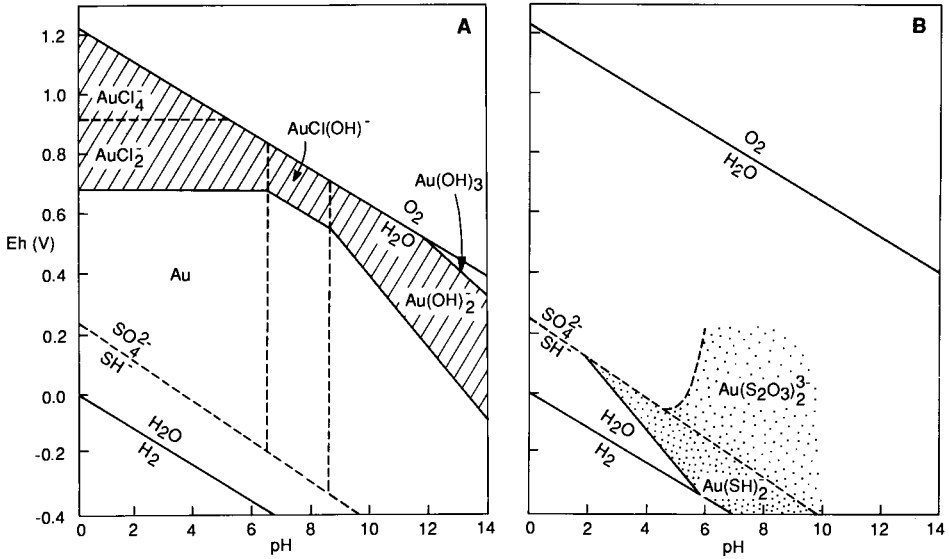


Fig. V.3-1. Eh-pH diagram for Au ($10^{-8}M$) in: (A) a 0.01 M (320 mg/L) S solution. (B) a 1 M (35000 mg/L) Cl solution.

In the groundwaters discussed above, soluble Au and soluble Fe had an antagonistic character: Au was only soluble where there was less than 0.1 mg/L total Fe. This effect is presumably due to Fe^{2+} (if present) reducing and precipitating Au chloride.

The other halides, particularly iodide, form stronger complexes than chloride. Iodide generally has a low concentration in groundwater, though enhanced levels may result from the decomposition of organic matter. Under such conditions, iodide complexes may be important for Au mobilization in surface horizons.

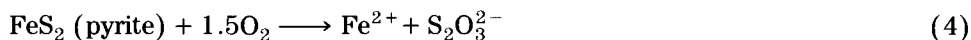
Thio-complexes

Sulphur forms a number of species with varying oxidation states from -2 to $+6$ (see Fig. II.1-1). Among the most common are (from lowest to highest oxidation state) hydrogen sulphide (SH^-), solid S, thiosulphate ($S_2O_3^{2-}$), sulphite (SO_3^{2-}), and sulphate (SO_4^{2-}). Solid S obviously will not mobilize Au and sulphate, the most stable form of S in oxygen-containing solutions, does not complex with Au. The most important sulphur species for Au mobilization are considered to be hydrogen sulphide and thiosulphate, under conditions as described below.

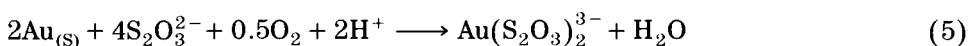
Gold bisulphide complex $[Au(SH)_2]^-$ is mobile only under highly reducing conditions. It is of particular importance for the hydrothermal transport of Au (e.g. Seward, 1973, 1982; Boyle, 1979; Baranova and Ryzhenko, 1981) but has only a restricted occurrence in the supergene zone. Sulphide may exist in solution at 10–1000 mg/L in the vicinity of pyrite deposits (Subzhiyeva and Volkov, 1982). $Au(SH)_2^-$ solubility is greatest in neutral reducing conditions;

assuming a total dissolved S content of $2 \times 10^{-2} M$ (700 mg/L), under optimum conditions, total dissolved Au will equal $6 \times 10^{-6} M$ (1200 $\mu\text{g/L}$).

In the presence of oxygen, sulphide will be oxidized to sulphate. However, under neutral to alkaline weathering conditions, appreciable amounts of the intermediate product, thiosulphate, may be formed (Listova et al., 1968; Granger and Warren, 1969; Goldhaber, 1983; Webster, 1984) during pyrite oxidation:



The thiosulphate ion is meta-stable (i.e. it is unstable on thermodynamic grounds but may exist in solution for long periods due to its kinetic inertness; Rolla and Chakrabarti, 1982; Subzhiyeva and Volkov, 1982). It can dissolve Au even under weakly oxidizing conditions (Listova et al., 1968; Goleva et al., 1970; Lakin et al., 1974; Pitul'ko, 1976; Plyusnin et al., 1981; Webster and Mann, 1984; Webster, 1984, 1986):



The Au-thiosulphate complex is soluble under alkaline, neutral and slightly acid conditions. Appreciable thiosulphate production will only occur if the weathering pyrite is buffered by alkaline species. Mann (1984b) calculated that 400–800 g of CaCO_3 are required for every 240 g of FeS_2 to maintain alkaline conditions for thiosulphate production, and therefore significant Au thiosulphate mobilization. Other factors which could influence the stability of the thiosulphate anion, and therefore of the Au complex, include organisms or metals having variable oxidation states, such as Fe or Mn. The solubility behaviour of Au in S-rich solutions is summarized in Fig. V.3-1B.

Cyanide complexes

Gold forms the very strong $\text{Au}(\text{CN})_2^-$ complex, which is stable over a wide range of pH/Eh conditions. The limiting factor to Au cyanide solubility is the concentration of available cyanide. Certain plants and microorganisms are known to release cyanide (Sneath, 1972; Lakin et al., 1974) and can accumulate appreciable Au (Warren, 1982). Bacteria such as the cyanogenic species *Chromobacterium violaceum* produce up to 200 mg/L cyanide in vivo (Rodgers and Knowles, 1978), and can solubilize up to 215 mg/L ($10^{-3} M$) Au from the pure metal (Smith and Hunt, 1985). Cyanogenic bacteria are frequently associated with plants, soil and organic matter (Corpe, 1951; Saupe et al., 1982) and zones such as a highly organic horizon or the immediate surroundings of an active root of a cyanogenic plant could contain elevated levels of cyanide and cause Au mobility. The $\text{Au}(\text{CN})_2^-$ complex is inert in moderately acid, neutral and alkaline conditions (Boyle, 1979). However, as with the Au thiosulphate complex, decomposition of the cyanide and precipitation of the Au may occur as the result of specific chemical or biological factors.

Organic complexes

Numerous studies (e.g. Freise, 1931; Fetzer, 1934, 1946; Ong and Swanson, 1969; Baker, 1973; Boyle et al., 1975; Baker, 1978; Roslyakov, 1984; Grégoire, 1985; Fedoseyeva et al., 1986; Gatellier and Disnar, 1988) have indicated highly varying interactions between Au and organic matter. Whereas solid organic matter and some soluble organic phases have been shown to remove Au from solution, other soluble organic phases have been found to solubilize Au under moderately oxidizing conditions. In general, Au-organic interactions are highly dependent on the chemical nature of the organic material, the concentrations of the phases, and the composition of the groundwater.

Gold readily forms colloids or sols (i.e. molecular aggregations up to 5 μm in size) and such chemical species have been known for centuries (Boyle, 1979). Colloidal Au, stabilized by organic matter, has been observed in the laboratory (Goni et al., 1967; Ong and Swanson, 1969; Ong et al., 1969; Fedoseyeva et al., 1987) and has been postulated as an important mechanism for the mobilization of Au. These colloids are negatively charged and therefore could be mobile in negatively charged soils, precipitating where they contact a soil horizon containing positively charged minerals such as Fe oxides. However, attempts to demonstrate the natural occurrence of colloidal Au have been unsuccessful (Boyle, 1979; Kolotov et al., 1980), possibly due to experimental difficulties at low concentrations of dissolved Au. Thus, on this basis, it appears that colloidal Au will only be important for Au mobility, if at all, in the presence of dissolved organic matter.

Many of the chemical species that may cause Au mobility (e.g. iodide, sulphide, thiosulphate, cyanide, organic matter) are partly or extensively influenced by biological factors. Thus, soil organisms such as bacteria, fungi or plants may have major effects on Au mobility. Many plants can accumulate or adsorb Au (Razin and Rozhkov, 1966; Shacklette et al., 1970; Kaspar et al., 1972; Girling et al., 1979; Warren, 1982; Smith and Keele, 1984; Erdman and Olson, 1985), and represent a useful exploration sample medium. Some plants not only accumulate Au but may be important in its redistribution, taking up Au at depth and releasing it at the surface as litter (Erdman and Olson, 1985). This hypothesis may explain some zones of depletion and concentration in surface horizons of the regolith.

In addition to plants and plant products, bacteria and other microorganisms may have a significant influence on Au solubility and even have value in Au exploration (Watterson, 1985). Bacteria commonly alter the surrounding chemistry by catalyzing reactions; for example, sulphur bacteria may cause Au to dissolve, by initiating pyrite oxidation, or to precipitate by catalyzing the oxidation of thiosulphate ligands (Postgate, 1951). Certain species of bacteria may release or decompose cyanide (Knowles, 1976; Rodgers and Knowles, 1978; Smith and Hunt, 1985), potentially affecting Au solubility, whereas other bacteria could cause significant Au solubility by releasing amino acid ligands (Korobushkina et al., 1974).

TABLE V.3-2

Equilibrium electrum composition for various ligands

Ion	Final electrum composition	
	Mole% Ag	Fineness
Cl ⁻	5×10^{-9}	1000
I ⁻	2×10^{-8}	1000
SH ⁻	0.3	998
S ₂ O ₃ ²⁻	2.6	985
SO ₃ ²⁻	35	770
CN ⁻	99.7	5

Composition of secondary gold in the supergene zone

Secondary Au is commonly of higher purity (fineness) than its primary source (Boyle, 1979; Wilson, 1984), with a tendency during weathering to alter from an Au/Ag alloy (electrum) towards pure Au metal (Mann 1984a,b; Webster 1984, 1986). This may be achieved either by dissolution of the electrum, followed by Au metal precipitation, or via selective leaching of Ag. The equilibrium fineness of Au is dependent on the ligand controlling Au solubility (Table V.3-2). The trend towards pure Au during weathering is most marked for the halide and sulphide complexes, weaker for thiosulphate complexes and reversed for cyanide complexes.

Electrum is more readily dissolved in chloride-rich waters than Au metal (Mann, 1984b). However, the soluble Au chloride complex is unstable relative to Au metal, so that ions such as Fe²⁺ in solution will reduce the Au and a separate phase of high fineness Au metal may precipitate. Silver, in contrast, will remain in solution and be leached from the system. When thiosulphate is present, Au and Ag reprecipitate together, forming secondary Au of medium fineness (Webster and Mann, 1984; Webster 1984, 1986). This precipitation may be caused by Mn oxides, which are abundant at the site at Wau, Papua New Guinea investigated by Webster.

Alteration of primary metallic gold

Gold grains are commonly observed to be etched or partially dissolved (Mann 1984a; Freyssinet and Butt, 1988a,b,c; Freyssinet et al., 1989b; Colin et al., 1989; Lawrance, 1991; see Figs. III.1-13, III.2-35 and III.3-9). Etched surfaces may also show secondary precipitation, suggesting several generations of dissolution and precipitation over a scale of a few micrometres (Lawrance, 1988b). Iron oxides are sometimes observed to be associated with etched surfaces and may appear partially to replace the Au (Mann, 1984a). Small particles of high fineness Au may occur within Fe oxides, presumably having reprecipitated from the solubilized primary Au.

Where primary Au grains survive into the upper part of the regolith, they are commonly of higher fineness than Au in the unweathered rock (Hallbauer and Utter, 1977; Freyssinet and Butt, 1988a,b; Freyssinet et al., 1990). This is consistent with the expected composition of Au metal equilibrated with weathering solutions, as described above. Possible mechanisms for this effect, which might act together or separately, are:

(a) selective dissolution of Ag-rich Au grains, leaving a residuum of Ag-poor grains;

(b) precipitation of Au derived from elsewhere in the profile or regolith toposequence;

(c) selective depletion of Ag from electrum, resulting in the grains having reduced Ag contents.

The relative importance of these mechanisms is not known, but some inferences may be made from the common presence of Ag-poor rims on primary Au grains in weathered profiles and placer deposits (Desborough et al., 1970; Koshman and Yugay, 1972; Nefedov et al., 1982; Mann, 1984a; Giusti and Smith, 1984; Michel, 1987; Freyssinet et al., 1987; Bowles, 1988; Clough and Craw, 1989; Freyssinet et al., 1989b). The rims are solid and are thus distinguished from "lacy" rims that possibly result from direct precipitation of Au from solution (Giusti, 1986). The Ag-poor rims consistently have the following properties:

(1) they generally contain \ll 1% Ag, compared to grain interiors having $>$ 5% Ag;

(2) they are commonly irregular and up to 50 μm thick;

(3) the interface between the Ag-poor rim and the interior is very sharp, beyond the resolution of an electron microprobe beam (1 μm);

(4) the composition of the rim is not influenced by variations in the Ag content of the primary grain;

(5) Cu is depleted in the same manner as Ag;

(6) morphological characteristics, such as the presence of rims flanking cracks that penetrate deep into the grains, suggest that the phenomenon is due to Ag depletion rather than Au deposition.

Although points (1)–(5) are consistent with the deposition of Au derived from an exotic source, point (6) is consistent with an overall depletion of Ag. A possible explanation is that the rims are the consequence of galvanic reactions on the electrum surface involving the simultaneous solution of Ag^+ and Au^+ ions, the immediate replating of Au onto the electrum surface and the Ag leached as solution species such as Ag^+ or AgCl_2^- . The macro-analogue of such an electrum/Au cell was indicated by Mann and Webster (Mann, 1984a; Webster, 1984, 1986) who demonstrated that significant voltages could be generated between electrum and Au metal under a variety of solution conditions. Such a galvanic reaction is essentially a plating mechanism at the microscopic level, but has the net effect of depleting an electrum grain of Ag.

This mechanism is preferred kinetically to reactions that involve the dissolu-

tion of Au from electrum, and transport to a precipitation site distant from the source. These reactions are highly dependent on rate-limiting steps such as the diffusion of oxidizing agents such as H_2O_2 or Fe^{3+} to the electrum surface and diffusion of a reducing agent to the point of precipitation. The favourability of a localized, galvanic, reaction is demonstrated by the ubiquitous nature of grains with Ag-poor rims of this type.

Silver-poor rims can cover part or all of the primary Au grain (Giusti, 1986). Mann (1984a) described grains in which dissolution of Au is occurring or has occurred on one side at a contact with Fe oxide, whereas on the other side there is a Ag-poor rim. It is conceivable that for small grains (i.e. less than $100\ \mu\text{m}$ diameter) the Ag-poor "rims" could replace the whole electrum grain. Conversely, where Ag-poor rims surround grains, they may assist in preserving them from further chemical attack (Giusti and Smith, 1984).

Particles of weathered primary Au with Ag-poor rims but with both Ag-poor and Ag-rich (to 50% Ag) zones on internal grain boundaries are reported from colluvial lateritic soils in the semiarid Gentio do Ouro area, northeast Brazil (Grimm and Friedrich, 1989, 1990). The Ag-rich zones are similar to Ag-poor rims in having very sharp boundaries with the primary Au-Ag alloy. In addition, they only occur in conjunction with Ag-poor rims and some at least appear to be lamellar (Figs. 3b and 3c in Grimm and Friedrich (1990)). Such observations have not been previously documented. Grimm and Friedrich ascribe the formation of the Ag-rich rims to an earlier phase of mobilization by thiosulphate complexation, with rapid precipitation as the Ag-rich zones on a surface of the primary grain. The Ag-poor rims are considered to be due to more recent Ag-depletion by chloride complexation by saline soil waters. A difficulty with this mechanism is that Au-thiosulphate complexes are stable to reduction so that precipitation tends to occur via adsorption or decomposition of the thiosulphate group. Such precipitation reactions would be expected to occur onto the surfaces of oxides of Fe or Mn, rather than onto a Au grain. It is also difficult to conceptualize a reaction whereby major quantities of Au and Ag are dissolved from a primary Au grain and then *rapidly* reprecipitated onto the same, or another, grain. In addition, the close association between the Ag-poor and Ag-rich zones suggests there to be a genetic link between them. It is not clear what this may be, but it may have a bearing on the origin of all Ag-poor rims.

THE FORMATION OF SUPERGENE GOLD DEPOSITS IN LATERITIC TERRAIN

The distribution of Au in lateritic profiles

Economic or near-economic supergene concentrations of Au occur in deeply weathered regoliths in most climatic zones. They are mostly small ($< 1.5\ \text{Mt}$), low grade (1.5–5.0 g/t) relative or absolute accumulations characterized by predominantly secondary Au, with some residual primary Au and occasional

nuggets (Mann, 1984b; Butt, 1989a,b; Lawrance, 1991). There are two principal types of deposit:

(1) *Lateritic supergene deposits*. These are more or less flat-lying enrichment zones contiguous with the ferruginous and mottled zones of the lateritic profile. In highly leached rainforest environments, such enrichments are associated with lateritic stone lines (e.g. Ity, Ivory Coast, see p. 288). They are characterized by fine-grained Au of high fineness ($Ag < 0.5\%$) and some residual primary grains (Michel, 1987; Freyssinet and Butt, 1988b; Freyssinet et al., 1989a; Davies et al., 1989). Particles of coarse Au may be present, however, as small primary nuggets enclosed within pisoliths and as euhedral secondary crystals developed with Fe oxide segregations. Many accumulations of this type are known, but mining has been largely restricted to regions in Australia having Mediterranean and arid climates (e.g. Boddington: Davy and El-Ansary, 1986; Callion: Glasson et al., 1988 and p. 319; Mount Gibson: 313); in West Africa, lateritic ore is mined at Syama, Mali (Ellison and Blaylock, 1990), which has a savanna climate, and development is planned at Ity, Ivory Coast (Fig. III.2-36), a lateritic stone-line deposit in a rainforest environment.

(2) *Saprolitic supergene deposits*. These occur deeper in the profile, either confined to the source unit or laterally dispersed into the weathered wall rocks, commonly as one or more subhorizontal zones. The Au is dominantly secondary and of high fineness, but residual primary grains become more abundant deeper in the profile (Freyssinet and Butt, 1988b). Saprolitic enrichments are known and mined only from arid (or once arid) environments, again principally in Australia (e.g. Transvaal mine, p. 351; Hannan South: Ivey, 1987, and Lawrance, 1988b, 1991) but also in Africa (Um Nabardi, Sudan: Fletcher, 1985; p. 343).

In arid areas, lateritic and saprolitic deposits may both be present where profiles are complete, separated by a zone 5–20 m thick that is barren of Au, though not necessarily of other ore-related elements. Within the weathered lode or other source, this is commonly referred to as the “depleted zone”. The depleted zone may be present even where the laterite has been eroded, either at the present surface or beneath transported overburden; as such, it presents a considerable hindrance to exploration for concealed supergene and primary mineralization. Neither saprolitic enrichment nor a depleted zone have been reported in more humid climates; Au appears to be slightly leached throughout the saprolite, but there is no dispersion into wall rocks and little or no secondary Au is present (e.g. Espérance, French Guiana, see p. 253; Dondo Mobei, Gabon, see p. 288).

The similarities and differences in Au distributions in lateritic regoliths between humid and arid areas are due to the similarity of the initial deep weathering and differences in the modifications imposed by later events. They are the result of the reactions listed in Table V.3-1 taking place selectively under the varied environments imposed by geomorphological and climatic changes; as such, they typify the importance of interpreting geochemical data in terms of the weathering history, the underlying theme to this volume.

Gold mobility during lateritization

During lateritization in seasonally humid, tropical climates, oxidation at the weathering front deep below the water-table produces neutral to acid conditions, with lower pH favoured by felsic rocks and high sulphide contents. Gold associated with tellurides or held in the lattice of the sulphides and other minerals may be released, but the free metal remains largely immobile due to the absence of suitable complexing ligands. Thiosulphate ions are formed only by sulphide oxidation in neutral to alkaline conditions and concentrations of chloride ions and organic matter are very low. Accordingly, although some corrosion and reduction of size occurs, primary Ag-rich grains persist through the saprolite and into the ferruginous zone (Freyssinet et al., 1987; Freyssinet et al., 1989b; Colin et al., 1989), lateral dispersion into saprolitic wall-rocks is minimal. Free Au (and Ag) may be mobilized, however, if high concentrations of carbonate are present in the primary mineralization, because the oxidation of pyrite in such an alkaline environment produces thiosulphate (equation (4)). This mechanism has been invoked to explain the solution and reprecipitation of electrum in the rainforest of the Papua New Guinea Highlands (Webster and Mann, 1984), although the high relief and freely draining, relatively thin regolith differ from lateritic conditions. It may also account for Au mobility below the redox front in the saturated, highly saline saprolite at the Hannan South mine, Western Australia (Lawrance, 1991).

Lateral dispersion of Au is evident towards the top of the lateritic profile, particularly in the ferruginous and mottled horizons (Michel, 1987; Freyssinet et al., 1989b). This is due to a combination of (a) residual concentration and surface wash during landsurface reduction, (b) chemical mobility, as complexes formed with humic acids produced by rapid degradation of organic matter in the soil, and (c) illuviation of colloidal organic complexes and very fine grains of free metal. Some Au may also be contributed directly to the soil in organic litter after uptake by plants. Reduction of the complexes results in the incorporation of fine-grained Au with low Ag contents in Fe oxides, particularly in the lower part of the ferruginous horizon and in the mottled zone. Such mechanisms can account for the formation of lateritic Au deposits and Au anomalies, with their mixture of high and low fineness gold, that form widespread blankets over relatively narrow mineralized sources.

The relative contribution of the physical and chemical mechanisms is uncertain, during both this and subsequent climatic episodes. The presence of Ag-poor rims on residual primary grains (see above) suggests that it is possible that Ag may be completely removed from small grains whereas the Au reprecipitates immediately, yielding a product of high fineness. Downward mechanical illuviation of Au particles and colloids is also possible and could be responsible for some of the observed distributions.

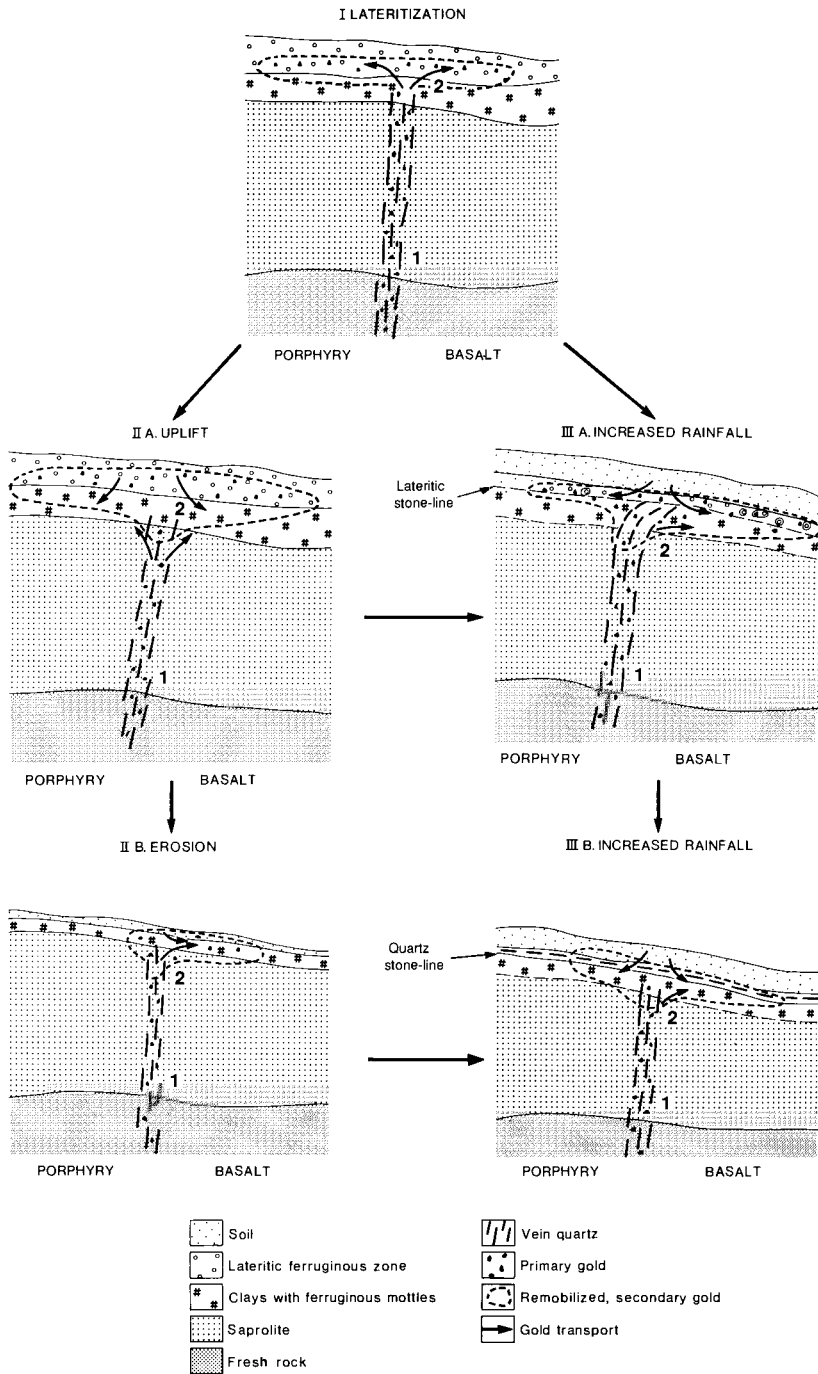


Fig. V.3-2. Model illustrating Au dispersion during lateritization and modifications due to uplift and a change to a more humid climate. Ligands probably responsible for Au mobilization: 1: thiosulphate; 2: organic; 3: chloride. Modified after Butt (1989a).

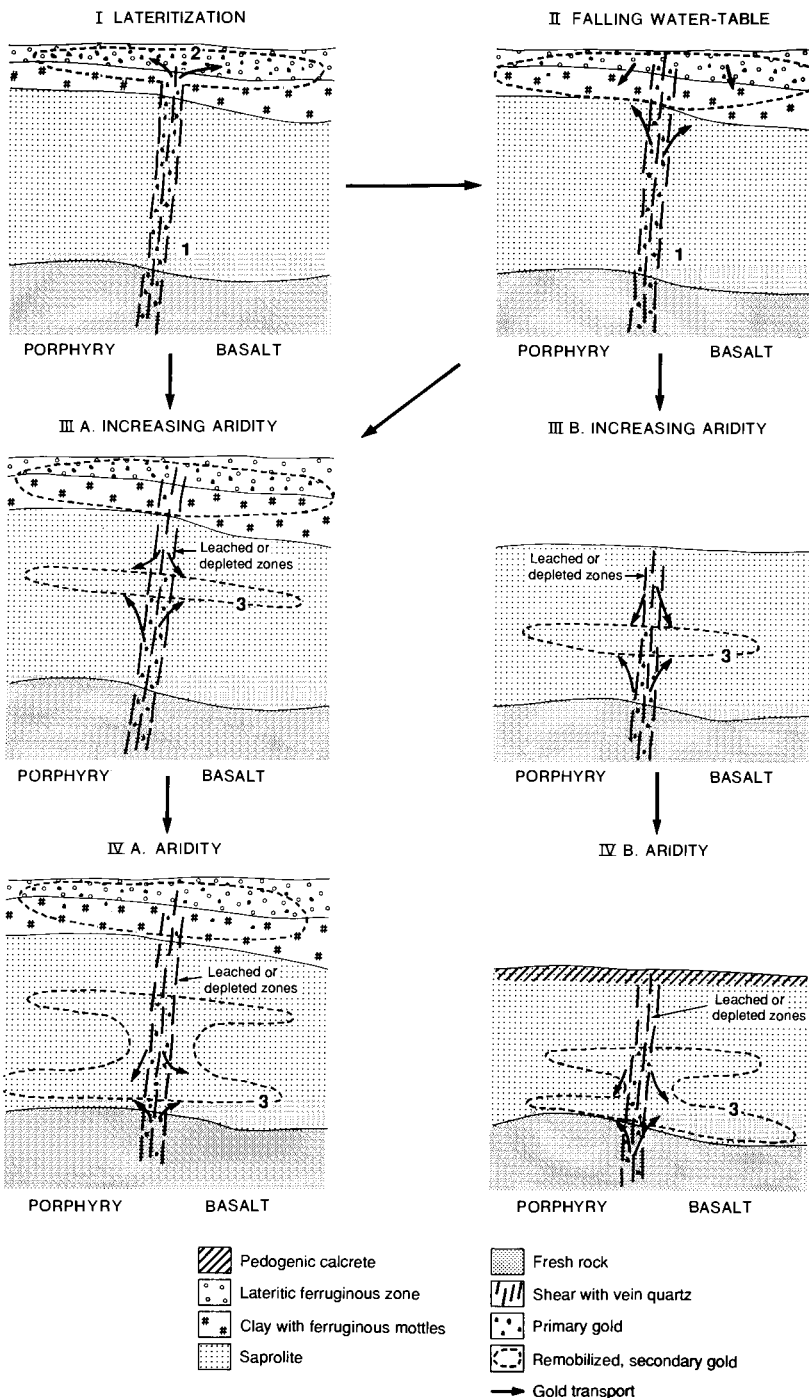


Fig. V.3-3. Model illustrating Au dispersion during lateritization and modifications due to uplift and a change to an arid climate. Ligands probably responsible for Au mobilization: 1: thiosulphate; 2: organic; 3: chloride. Modified after Butt (1989a).

Gold mobility in rainforest environments

The effects of a change to more humid rainforest climate and some epeirogenic uplift are indicated in Fig. V.3-2. Reactions at the weathering front are similar to those occurring during lateritization. However, upper horizons of the pre-existing profile are subject to increased leaching, ultimately forming stone-line profiles (e.g. Fig. III.2-25). Where there has been little erosion, previously formed lateritic enrichments of Au are retained in resistant cuirasse in the stone line. Instead they have been leached from the overlying friable soil, possibly as Au-humate complexes. These either precipitate near the stone line with neo-formed Fe oxides, augmenting the enrichment due to the degraded laterite (e.g. Ity, Ivory Coast; Fig. III.2-36), or are removed entirely, perhaps to precipitate as placers in drainages. Similar leaching may affect lower horizons of the profile; the result is an absolute loss of Au and some other elements, with no appreciable lateral dispersion halo being formed in the saprolite. At Dondo Mobi, Gabon (Fig. III.2-34), Au is concentrated in these upper horizons by a factor of 3.5 compared to the saprolite. The "mushroom-shaped" surface enrichment halo extends at low concentrations for over 500 m to link with placers in adjacent drainages. The Au particles are smaller in the soil anomaly than the saprolite (Fig. III.2-35), due to the etching of primary Au grains and precipitation of secondary grains (Colin et al., 1989).

If the original profile is truncated by erosion, any lateritic enrichment is destroyed. Strong leaching and dispersion of Au again occur in the soil but there is no enrichment in the saprolite (e.g. Espérance, French Guiana, Fig. III.2-10).

Gold mobility in arid environments

The effects of epeirogenic uplift and a more arid climate are shown in Fig. V.3-3. Lowering of the water-table results in the progressive dehydration of the upper horizons, and lower rainfall leads to generally decreased leaching. Alkalis and alkaline earths derived from rainfall and continued slow weathering are retained in the regolith. These changes cause the mechanisms of Au mobilization to change also. The decrease in vegetation greatly reduces the availability of humic complexes for Au mobility. More prevalent alkaline conditions increase the possibility of thiosulphate formation during sulphide oxidation (equation (4)), but the rate of weathering is mostly very slow. More significant, however, is the development of salinity, for this permits the formation of soluble Au chloride complexes (equation (1)).

In the present warm arid zones, the change from a wet savanna climate has taken place since the mid-Tertiary or earlier. During this long period, several reversals to humid climates have occurred, temporarily restoring conditions conducive to deep weathering. Accordingly, the lowering of the water-table has been punctuated by still-stands or temporary rises. Such events have great significance, for under these circumstances, the increased rainfall leaches precip-

itated salts and recreates redox conditions suitable for ferrolysis, thus producing acid and saline groundwaters (Mann, 1983, 1984a). As these waters become more strongly oxidizing, possibly controlled by the Mn redox couple (equation (2)), they can become capable of dissolving Au. In the near-coastal Darling Range of Western Australia, for example, recent humidity has resulted in active ferrolysis and leaching by saline waters. Elsewhere in the region, the rise in water-table caused by clearing for agriculture has mimicked this climatic change. During these humid periods, therefore, Au may be dissolved and mobilized. Gold precipitation will take place in response to a rise in pH or dilution of the chloride concentration, both of which may occur when solutions percolating through the unsaturated zone reach the water-table. Precipitation is also caused by the reduction of the Au chloride by ferrous iron (equation (3)). This reaction may also occur at the water-table, if the groundwaters contain ferrous iron. Probably more important as a site for precipitation, however, is the interface between an upper oxidized aquifer and a lower reduced aquifer. Such double aquifer systems have been commonly observed in the Yilgarn Block of Western Australia, and precipitation at their interfaces could result in enrichments parallel to but below the water-table (Figs. III.3-3 and III.3-4).

Successive humid periods during the general lowering of the water-table account for the supergene enrichments within the weathered mineralization and in saprolitic wall rocks. Typical examples are Hannan South, Western Australia (Ivey, 1987; Lawrance, 1991), now beneath a playa (Fig. V.3-4), and Um Nabardi, Sudan, where enrichment occurs at the water-table at 50 m (Fletcher, 1985; see Fig. III.3-19). Because electrum may be more soluble than pure Au, primary Au could be preferentially dissolved during this process, thus assisting the preservation of pre-existing lateritic secondary enrichments. Additionally, the repeated strong leaching of the upper saprolite leads to the formation of the depletion zone between the lateritic and saprolitic deposits. Where the profile is truncated, any lateritic enrichment will have been destroyed. Nevertheless, leaching of the upper horizons can still occur (Fig. V.3-3), so the near-surface expression of mineralization is minimal.

GOLD DISPERSION AND THE SURFACE EXPRESSION OF MINERALIZATION

The nature of the surface expression of Au mineralization in lateritically weathered terrains depends very strongly upon the climatic and erosional history. The most critical factors are the degree of truncation of any lateritic profile, the effects of post-lateritic weathering, including that occurring at present, and the type of overburden. The relevant features, exemplified by the case histories presented in Parts III and IV, can best be summarized with reference to the model classification described in Chapter I.1.

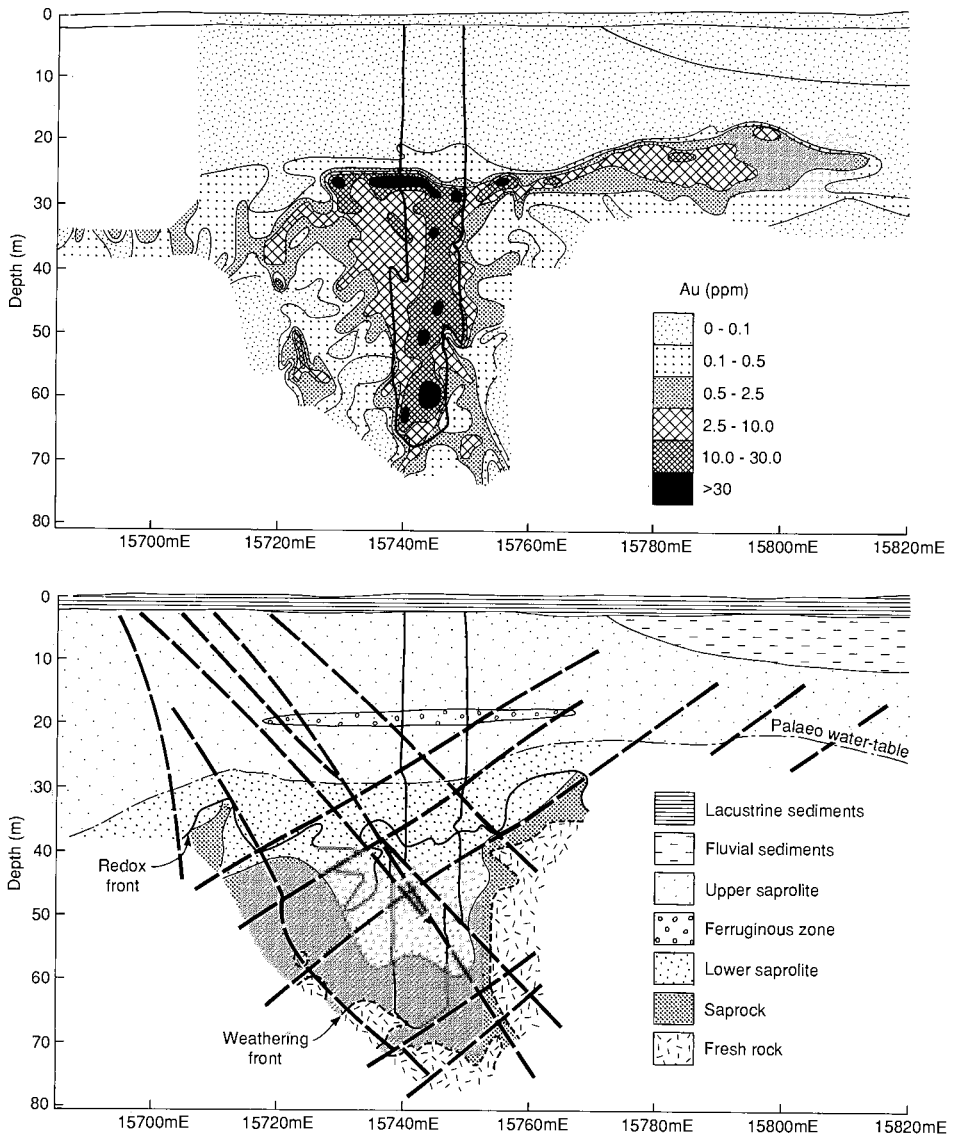


Fig. V.3-4. Cross-section through the Hannan South Au deposit, Western Australia, illustrating leaching of Au from the upper saprolite and lateral dispersion at a redox front. The deposit is now situated beneath a playa and saturated by hypersaline groundwater. From Lawrance (1991); published by permission of Croesus Mining Ltd.

Pre-existing lateritic profile mostly preserved: A-type models

Where the lateritic profile is complete, the surface expression of mineralization in all morphoclimatic zones reflects the concentration and dispersion of Au

in the ferruginous horizons. Anomalies in the mottled zone, cuirasse, nodular horizon and residual soil tend to be laterally extensive relative to the size of the primary mineralization. Where there is no soil present, the enriched lateritic material itself outcrops, although the uppermost horizons are generally of lower grade. Similarly, the Au contents of residual soils are greatly reduced relative to those of the immediately underlying horizons, even when these represent a significant resource. Nevertheless, they remain anomalous and represent a satisfactory sample.

The low Au contents of the soils and upper lateritic horizons are considered to be due to leaching during lateritization and, after uplift or climatic change, by the formation of soils from lateritic material. Gold has probably been mobilized as organic complexes. In highly leached rainforest environments (e.g. Mébaga, Gabon, see p. 284), dispersion during lateritization and subsequently during the formation of the lateritic stone line has resulted in the vertical and lateral homogenization of Au contents over a wide area. There is no focus to the anomalies and hence no benefit in sampling at an interval closer than 100 m. Follow-up is best by saprolite sampling by drilling. In some arid regions, there is evidence that Au dispersion is affected by the precipitation of pedogenic calcrete and that surface leaching may be partly offset by the concentration of Au in carbonates (e.g. Callion, see p. 319). The mechanisms of enrichment are uncertain but the Au may be derived from decaying vegetation or from the replacement of Au-bearing minerals by the carbonates. A more complex situation may exist at sites such as Boddington, Western Australia (Davy and El Ansary, 1986; Symons, 1988), where the present Mediterranean climate has succeeded earlier arid and humid climates. Here, post-lateritic mobilization of Au has probably also been as chloride complexes. The soil and upper nodular horizon are strongly leached and Au has concentrated in the cemented horizon (cuirasse) and the mottled zone. Indeed, leaching has been so severe that these materials are bauxitic and have maximum Cu contents of 70–100 ppm overlying primary and supergene mineralization containing over 1% Cu.

Deeper in the profile, there are significant differences between areas that have remained relatively humid and those that have been subjected to aridity (Figs. V.3-2 and V.3-3). In humid environments, there has been some rounding and etching of Au grains and some overall loss of Au (e.g. about 20% of the mass at Espérance, French Guiana, Table III.2–5) and despite some homogenization, there has been little or no dispersion into the wall rocks. The residual Au retains its primary (Ag-rich) composition and is present throughout the saprolite. In contrast, in arid areas, Au is severely leached from the upper part of the saprolite (depleted zone) but may be concentrated at depth. It is predominantly secondary (Ag-poor) and may show some dispersion into wall rocks, though the lateral extent is far less than in the ferruginous horizons. These contrasting characteristics are due to differences in the dominant mechanisms of Au mobilization. In humid areas, organic complexation is the principal mechanism and its effectiveness must diminish with increasing depth; in arid areas, lowering of the water-ta-

ble and the accumulation of alkali metal halides permits chloride complexation in oxidizing, acid environments deep in the profile. These differing characteristics are also of considerable exploration significance, implying that:

(1) in all areas, targets sought in the saprolite and primary zone are narrow relative to anomalies in soils and lateritic horizons;

(2) in humid tropical regions, there is reduced potential for significant supergene enrichment in the saprolite;

(3) in arid regions, deep sampling, preferably by angle drilling, is necessary to follow-up surface anomalies, due to the leaching (depletion) of the upper saprolite and the uncertainty as to whether there will be significant lateral dispersion at depth.

Pre-existing lateritic profile partly truncated: B-type models

Where the profile is partly truncated, anomalies in all environments tend to be small in size. Lateral dispersion in the surface horizons is restricted to the soil and is commonly the result of physical processes such as mass flow (colluviation) and sheetwash (Chapter I.6). There are, however, significant differences in dispersion characteristics depending on the weathering history and present climate.

In humid tropical regions, soils develop from Au-rich saprolite and hence anomalies tend to be of high contrast. Except in strongly leached rainforest environments (e.g. Dorlin, French Guiana, see p. 271), maximum Au contents in soil may be as much as 50% of those in the saprolite and primary zone. As in areas where the profile has been fully preserved, Au in the saprolite appears to have been little affected by weathering. Gold grains are etched and rounded but of primary (Ag-rich) composition and there is no significant lateral dispersion. By comparison, in areas that have experienced a post-lateritic arid phase, redistribution of Au has given rise to some important features:

(1) Leaching has caused depletion of Au from the upper saprolite (Fig. V.3-3), in places to 20 m or more from surface. However, enrichment and, in some situations, lateral dispersion may have occurred deep in the saprolite. Much of the Au is secondary and may show evidence of several episodes of solution and redeposition (Lawrance, 1988b). In most instances, this may be assumed to be the result of chloride complexation.

(2) Residual soils developed from leached saprolite have very low Au contents and give restricted anomalies of low contrast. However, some surface enrichment is possible, associated with, for example, pedogenic carbonates, and may give surface expression to mineralization even where there is transported overburden (e.g. Bounty, Western Australia, Fig. III.3-25).

(3) Widespread anomalies may be detected by sampling the ferruginous fragments that are commonly present as a surface "lag" in dry savannas and semiarid regions (Carver et al., 1987; see p. 346). The lag may include nodular or cemented lateritic materials and hence contain the remnants of an eroded

lateritic Au enrichment, or be derived from the erosion of outcropping weathered mineralization. Sheetwash is responsible for even greater dispersion of lag fragments, hence anomalies are commonly of very low contrast.

These dispersion characteristics suggest that very close sampling intervals are necessary for the detection of Au anomalies in soils, although widespread, low contrast anomalies may be determined by lag sampling or the bulk leach extraction of gold (BLEG) from soils and drainage sediments. As in regions where the profile is preserved, follow-up sampling of the saprolite must account for the lack of secondary dispersion and, in arid regions, for the probable near-surface depletion of Au.

Pre-existing lateritic profile absent: C-type models

The surface expression of Au mineralization is generally very localized in the absence of any lateritic profile, except in areas of moderate to high relief where physical processes have caused the erosion and downslope dispersion of particulate Au. Nevertheless, evidence for recent secondary mobilization of Au may be found in a wide range of weathering environments and in a few instances gives rise to significant anomalies. Thus, the dissolution and reprecipitation of Au by short-lived chloride solutions is suspected to be responsible for the presence of coarse Au particles on outcropping mineralization in Saudi Arabia (Salpeteur and Sabir, 1989), although such dispersion is thought to be by wind (Fig. III.3-38). More important is the surface enrichment of Au through up to 5 m of transported overburden giving expression to the Mount Pleasant deposit in semiarid Western Australia (Fig. III.3-34). This is thought to be the result of the transport of Au-bearing solutions by evaporation or evapotranspiration and entrapment of Au in calcareous soils (Lawrance, 1988a; 1991). In climatic contrast, the precipitation of secondary electrum in stream channels in the Highland rainforests of Wau, Papua New Guinea is considered to be due to Au and Ag mobilization as thiosulphate complexes (equation (5)) and their oxidative precipitation with Mn oxides (Webster and Mann, 1984).

SUMMARY: RECOMMENDATIONS FOR GOLD EXPLORATION

The intensive exploration activity for Au in the past decade has demonstrated that an appreciation of the influence of weathering on dispersion, combined with careful sampling and analysis, can result in the successful discovery of significant new deposits. The advent of highly sensitive analytical procedures such as graphite furnace atomic absorption spectroscopy, ICP-MS and instrumental neutron activation to complement conventional fire assay fusion has enabled routine determination of Au with detection limits of 1 ppb and, with bulk leach techniques, to 0.01 ppb (see Table A.2-6). Accordingly, much exploration has continued to rely solely on analysis for Au, depending upon its low background

abundance and the ability to detect widespread dispersion haloes due to the general stability of the element in the weathering environment. Such reliance on Au alone has reinforced the requirement for the use of large sample weights; initial samples more than 1 kg are essential, to be crushed and split so that preferably at least 250 g are pulverized and 30–50 g used for analysis. Bulk leaching of 2–5 kg samples improves the sampling statistics, but this is offset by the uncertainties inherent in such a partial extraction procedure.

Valuable additional information can be obtained by multielement analysis, either for a “Au pathfinder” suite (e.g. As, Sb, B, Bi, Hg, Mo, W) or for a wide range of elements useful in exploration for other commodities and in lithological and regolith mapping. Pathfinder elements may be valuable in giving larger anomalies than for Au (e.g. As), hence requiring lower sampling densities, or for confirming anomalies and localizing their source in regions where Au has been chemically dispersed (e.g. B, Bi, W). Several examples are given in Parts III and IV. However, not all Au mineralization has a reliable suite of pathfinder elements and some elements, e.g. As, may yield numerous false anomalies, so Au alone may be preferred. A number of sampling strategies are possible and these are outlined below; recommendations for sampling procedures and sample preparation are given in Appendices 1 and 2.

Bulk leach extraction of gold (BLEG)

The widest dispersion haloes have resulted from the mass flow and sheetwash of fine materials enriched in Au into colluvial and drainage sediments. This dispersion can be detected by the static leaching of large samples (2–5 kg) in sodium cyanide solution. BLEG surveys have been extensively and successfully used in exploration in semiarid Australia and, to a lesser extent, in humid northern Australia and the islands of Southeast Asia, detecting anomalies mostly in the range 0.5–5.0 ppb compared to a background of 0.2 ppb or less. The sensitivity of BLEG can be used to analyse composite samples and hence reduce the total analytical load (Smith, 1987a). Thus, only one fifth of the samples from an 800 × 50 m grid need to be analysed by compositing to a 800 × 200 m grid, analyzing the individual samples only when the composite is anomalous. The apparent advantage is partly offset by uncertainties of the extraction efficiency when applied to unprepared samples, or by the costs involved in grinding to increase that efficiency.

Pisolith / lateritic nodule and lag sampling

These have been successfully used for regional surveys of areas having complete or partly truncated lateritic regoliths, particularly in semiarid regions and dry savannas. They have application where conventional stream sediment surveys are inappropriate or instead of such surveys. Sampling as widely as 3 km on triangular grids can reveal regional trends (Smith et al., 1989) closing to

100 m during follow-up (see p. 307–309). Regional surveys of this type are most effective when multielement analyses are performed, thereby taking advantage of the wider primary and secondary dispersion haloes of pathfinder elements.

Soil sampling

Regional to semi-regional soil surveys have been widely used for “first pass” exploration or to follow-up to stream sediment, BLEG, pisolith or lag surveys. The most appropriate sample interval varies according to the geomorphological environment and the purpose of the survey. Thus, wide spacings (1500×500 m) may be suitable in deeply weathered areas for multielement reconnaissance surveys, particularly where complete profiles are preserved. In comparison, closer intervals of 200×50 m or less may be necessary for Au surveys of tenement areas of a few square kilometres where profiles are partly or completely truncated and there is only limited dispersion. Soil surveys essentially duplicate pisolith surveys where there is extensive outcrop of cuirasse or nodular laterite and replace them where these materials are covered (e.g. in stone-line profiles, see Chapter III.2), or have been eroded. Sample depths are best selected on the basis of local orientation surveys, or by comparing with relevant case histories such as those in Parts III and IV. In general, given the association of Au with both fine fractions and nodular or cementing materials (e.g. Fe oxides, carbonates), whole samples are preferred for analysis, unless dilution by particular fractions can be recognized.

Drilling

Power drilling can be the most efficient method of soil sampling where cemented horizons are present or if composite samples of whole soil profiles 1–2 m deep are required (e.g. Bounty and Transvaal, see p. 351). Although superjacent anomalies have been recorded in soils developed from transported overburden, such anomalies cannot be relied upon, so drilling to sample buried residuum (nodular laterite, saprolite) is recommended.

Deep drilling may be used as a direct follow up to relatively widely spaced (200×50 m) soil sampling or after more detailed surveys are used. Auger, vacuum and rotary air blast (RAB) drilling are suitable above the water-table, and open-hole or reverse-circulation percussion below the water-table. Care must be taken to ensure that the procedure does not entail the preferential loss or concentration of particular size fractions; for example, the air-return during RAB drilling must be adequate to ensure return of dense particles, including Au, and cyclones or dust-traps used to prevent loss of fine material. Vertical drilling is suitable for following-up anomalies in the ferruginous horizons or evaluating lateritic deposits. However, in environments where there is little secondary dispersion in the saprolite, it is commonly essential to drill overlapping angle holes to ensure that supergene mineralization is intersected. In semiarid areas,

where such mineralization may occur beneath a depleted zone, as much as 15–20 m deep, such drilling must be at very close intervals and preferably reach nearly fresh rock (e.g. Transvaal mine, see p. 351). Samples should be collected at 1 or 2 m intervals, but analytical costs can be reduced by compositing samples over 4 or 5 m.

HEAVY MINERAL SURVEYS IN EXPLORATION OF LATERITIC TERRAIN

G. FRIEDRICH, A. MARKER and M. KANIG

INTRODUCTION

Geochemical techniques aim to recognize, in deeply weathered environments, the signature of mineralization concealed beneath or within the regolith. Some components of that signature are carried by resistate minerals, which in favourable situations can be recovered by gravimetric separation of bulk samples, prior to mineralogical determination or to chemical analysis. If the whole of the geochemical signature is not required, specific components associated with one or several heavy mineral phases may be used instead of more conventional geochemical approaches. This has long been the case for gold, for which panning has been widely used in exploration and development stages. Panning of soils ("loaming") has been well established as a technique for exploration of deeply weathered terrain in Australia for over a century (Cash, 1959) and is still very popular for exploration in many countries (e.g. "pintas" technique in Brazil) and can be efficient in some situations. However, for some types of bedrock mineralization, for example, gold included in the crystal lattice of minerals such as arsenopyrite, or as free but very fine grains ($< 50 \mu\text{m}$) panning may not always be suitable (Zeegers, 1987).

Numerous geochemical exploration programmes have been carried out in tropically weathered terrain during the last decade, but only a few appear to have used heavy minerals (HM) surveys. Preference has generally been given to the total analysis of geochemical samples, whether for use in exploration, mapping or bedrock identification. This is because such analyses may yield useful information, irrespective of the dispersion mechanisms of the various elements. Thus, hydromorphic dispersion from mineralization may be detected, perhaps even where the overburden is transported (Butt, 1981; Smith, 1983). However, HM surveys may be an effective procedure in lateritic and deeply weathered regions and, in this chapter, their use in determining the origin of the regolith (i.e. whether residual or transported), lithological mapping and mineral exploration are discussed.

HEAVY MINERALS IN LATERITIC ENVIRONMENTS

Tropical weathering results in the structural and textural disintegration of the rock as a result of the chemical transformation of the rock-forming minerals. The

less mobile elements and the resistant, mainly heavy (i.e. dense) minerals become residually enriched by a factor up to 10 depending on rock type and intensity of weathering (Schellmann, 1986; Friedrich et al., 1987). Whereas the secondary phases (e.g. clay minerals and the hydroxides and oxides of Fe, Al and Mn) represent the product of significant transformation of primary silicates, these heavy minerals are little affected by weathering and thus constitute part of the residual skeleton of the original parent material. The concentration of stable heavy minerals generally increases from the least weathered saprolite horizons at the bottom of the profile to the most evolved horizons at the top as a result of progressive residual enrichment (Van Andel and Weyl, 1952; Friedrich et al., 1981). The heavy minerals vary in their resistance to weathering and, in consequence, the proportion of the less stable minerals decreases towards the top of the profile. In general, the ratios of the most resistant heavy minerals remain constant throughout the in-situ profile except where illuviation affects fine-grained material (Schellmann, 1987). Size fraction analysis indicates that most heavy minerals in rocks and weathered materials have grain sizes between 50 and 400 μm (Friedrich et al., 1980; Boenigk, 1983; Friedrich et al., 1987). Weathering commonly causes minerals to disintegrate and hence the grain size decreases; however, coarser grains may be found as the result of authigenic growth, as has been described for zircon, anatase, maghemite and rutile (Carroll, 1953; Valetton, 1955; Kubiena, 1962; Saxena, 1966; Taylor and Schwertmann, 1978; Schwertmann, 1983). Such authigenic minerals may be characterized by low trace element contents (Marker and Martin, 1985).

METHODS OF SAMPLE PREPARATION

Heavy minerals in hard lateritic duricrusts have to be liberated by selective crushing and grinding, whereas those in friable materials such as soils and saprolites require little treatment prior to mineral concentration. The fine-grained limonitic phase can be removed by desliming in a hydrocyclone or simple hand-bucket in the field (Schellmann, 1981; Friedrich et al., 1984) and the resultant coarse-grained residual and aggregated phases screened to leave a raw concentrate that can be further processed by gravity concentration methods such as jigging, panning or by use of shaking tables or heavy liquids (Fig. V.4-1). Magnetite (and maghemite) can be readily separated by hand-magnet and minerals of lower susceptibility using a Frantz magnetic separator. The HM fraction can then be examined in detail by optical and electron-optical techniques, chemical analysis (e.g. XRF: Thijssen et al., 1979), partial extraction and subsequent AAS analysis (Farrell, 1984) and microanalytical methods.

IDENTIFICATION OF TRANSPORTED WEATHERING MATERIAL

Although chemical processes dominate the formation of the deep regolith of tropically weathered terrains, physical erosion and redeposition are also of great

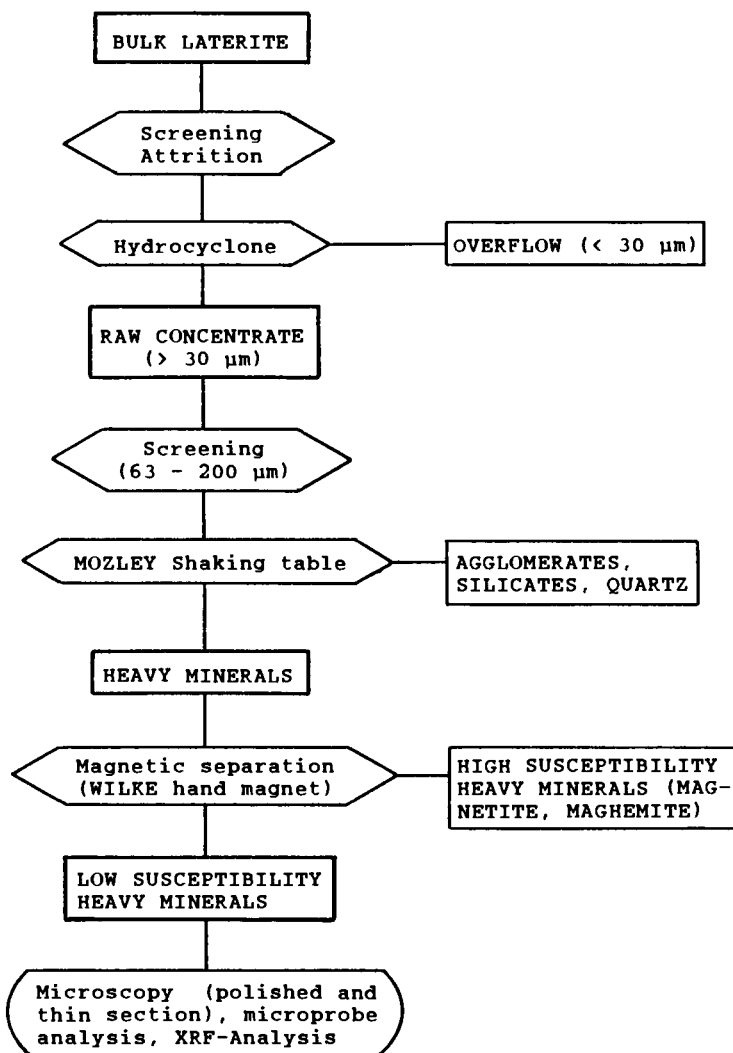


Fig. V.4-1. Flow sheet for the separation, concentration and analysis of the heavy minerals from lateritic materials (Friedrich et al., 1987).

importance. This is especially true in now more arid areas which may have an extensive cover of transported weathering material (Tricart, 1972; Thomas, 1974). The uppermost horizons in particular may range in composition and derivation from fully residual (in situ, autochthonous) to entirely transported (allochthonous), exhibiting numerous transitional types. Recognition of the possible transported origin of lateritic material is of major importance, since the expression of primary bedrock features, including lithology and mineralization,

may be dispersed, diluted or dislocated. However, identification of transported or reworked material from macroscopic evidence is very difficult. Homogeneous texture, friable sandy consistency, occurrence of exotic and/or poorly weathered rock material, broken pisoliths, bedding structures and certain types of stone line may serve as indications. However, these features are not necessarily unequivocal and, moreover, can only be observed in good profile exposures, which are usually scarce.

Geochemical analysis can give evidence for transport and intermixing of weathered material derived from different lithologies. For example, the partly transported nature of lateritic horizons above ultramafic rocks may be indicated by unusually high Zr and Ti concentrations (Golightly, 1981; Schellmann, 1987; Marker, 1988; Schellmann, 1989). Similarly, Valetton et al. (1987) demonstrated the contribution of "sialic" weathering material to transported horizons above ultramafics in Greece by the increased concentrations and positive correlation of Ti and Al. In general, the association of residually enriched "mafic" elements such as Cr, Ni and Fe together with "sialic" elements such as Ti, Zr, Ga and Al in near-surface horizons may indicate intermixing of weathering material derived from mafics-ultramafics and acidic rocks. Another example is described by Butt and Nickel (1981) from Mount Keith, Western Australia. Here, the ferruginous

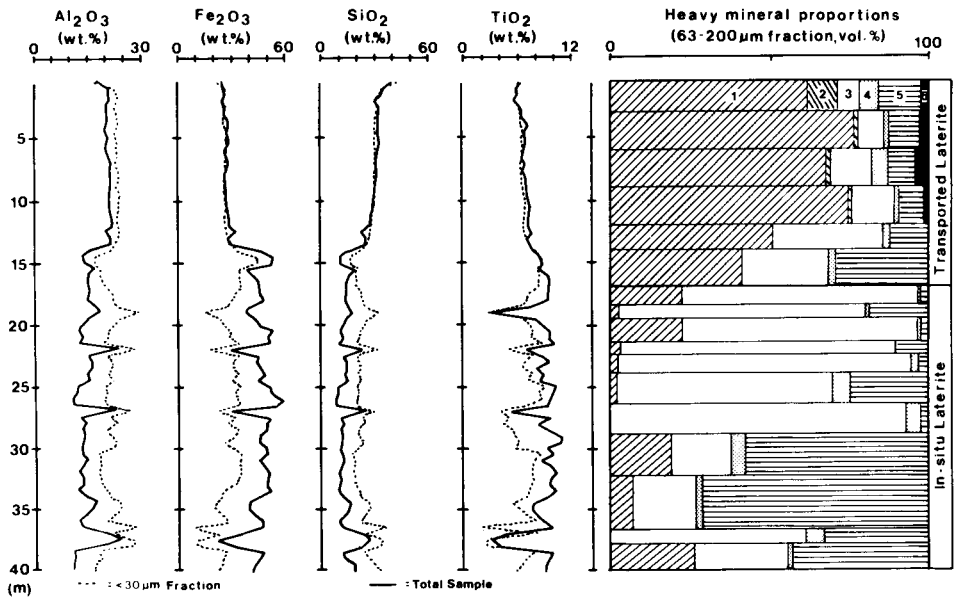


Fig. V.4-2. Distribution of Al_2O_3 , Fe_2O_3 , SiO_2 , and TiO_2 and the proportions of 1: ilmenite + Ti-magnetite, 2: ilmeno-rutile, 3: martite, 4: leucoxene, 5: limonite-leucoxene, 6: chrome-spinel + zircon in heavy mineral concentrates from weathering profile JAC2 above jacupirangite, Jacupiranga Alkaline Complex Brazil. The contact between transported and in-situ laterite is shown by increasing proportions of ilmenite + Ti-magnetite and introduced Cr-spinel + zircon.

horizon of a lateritized dunite is enriched in Zr, Ti and Al derived by the illuviation of zircon, anatase and kaolinite from overlying sediments of acidic and mafic/ultramafic origin. The contribution of weathered ultramafic rocks to this overburden is indicated by chromite, which is absent from the underlying serpentinized dunite (see p. 100 and Fig. I.6-1).

Since the degree of weathering of heavy minerals generally increases from the bottom to the top of in-situ weathering profiles, the intermixing of strongly weathered and less weathered grains of one mineral species may also indicate reworking and transport. Those derived from a distant source may even be characterized by considering rounding and abrasion due to transport (Friedrich et al., 1987).

The identification of semi-residual and transported weathering horizons can best be achieved by investigation of complete weathering profiles, in boreholes, pits or exposures. The hiatus between in-situ and transported horizons can be unequivocally proven by investigation of the HM association, as shown in Fig. V.4-2. The origin of these materials should preferably be established before they are used as geochemical sample media, since this information may be crucial to the interpretation of the results, particularly where there is a thick cover of semi-residual and transported overburden. Heavy mineral studies may be useful in establishing a model for the geomorphological evolution of the target area and delineate proximal or distal source areas of weathered material, thus giving a dimension for the dislocation of primary bedrock features.

THE USE OF HEAVY MINERAL SURVEYS IN GEOLOGICAL MAPPING

Bedrock recognition

Residual concentrations of lithospecific elements are commonly related to the accumulation of resistant heavy minerals, thus emphasizing the importance of these minerals, especially in more detailed surveys (Matheis, 1981). The suitability of Ti, Zr and Cr as discriminator elements in weathering products (Hallberg, 1984) is due to their occurrence in resistant heavy minerals such as zircon, baddeleyite, ilmenite, Ti-magnetite, rutile, anatase and Cr-spinel. The use of the Zr/Ti ratio for discriminating between the weathering products of different source rocks must, however, be restricted to residual profiles. As shown in Fig. V.4-3, transported and semi-residual weathering products show clustering at an average Zr/Ti ratio similar to that of intermediate rocks. The clustering is a function of the mixing due to reworking of lateritic and transported material derived from different sources.

The association of lithospecific elements to resistant heavy minerals is commonly evident from the total analysis of weathered material. For example, a comparison of the total and $< 30 \mu\text{m}$ (hydrocyclone processing) fractions of samples from a lateritized dunite profile reveals that the total sample has higher

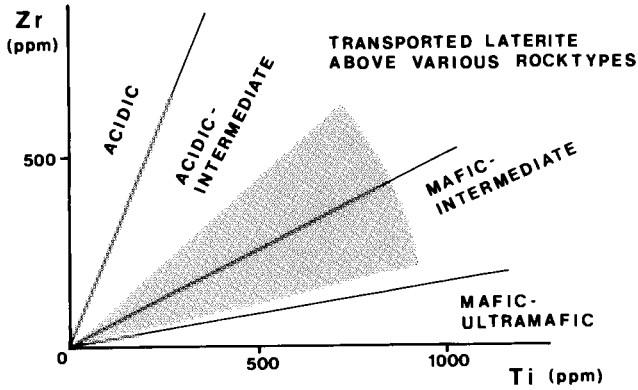


Fig. V.4-3. Range of Zr/Ti-ratios found in transported laterites above various lithologies in Brazil and the Philippines (Friedrich et al., 1987 and Marker, 1988). The fields of acidic to mafic-ultramafic rocks and their weathering products are given by Hallberg (1984). Compare with Fig. I.6-1.

concentrations of Ti, Zr and Cr (Fig. V.4-4). The results are in accordance with the distribution of Cr-spinel, zircon and ilmenite or Ti-magnetite contents in the HM concentrate in which the abundances of zircon and Ti oxide increase towards

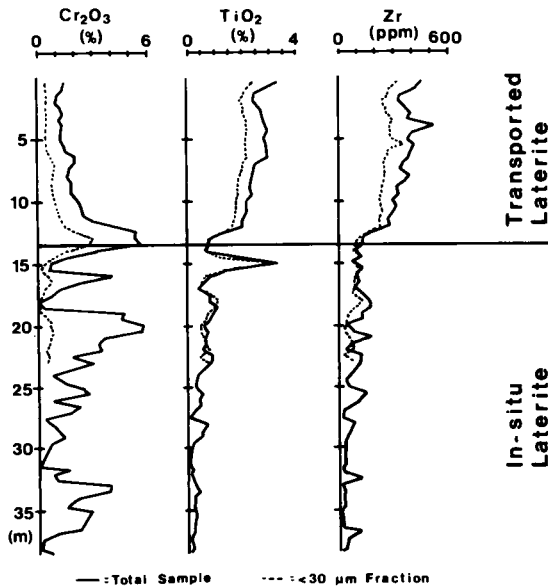


Fig. V.4-4. Distribution of Cr, TiO₂ and Zr in total sample and the < 30 μm fraction from weathering profile DUN1 (Jacupiranga Alkaline Complex Brazil), consisting of in-situ laterite above dunitic bedrock and transported laterite. Data from Friedrich et al. (1987).

TABLE V.4-1

Heavy minerals occurring as residual constituents in tropical weathering products: physical properties, main primary occurrences and their suitability for bedrock identification

Mineral	Refractive index (n)	Density	Weathering stability	Mechanical stability	Magnetic properties	Main primary occurrence	Bedrock identification
Topaz		3.5-3.6	s	m	-	Margins of plutons; greisens	m
Andalusite		3.1-3.2	s	s	-	Metamorphic rocks	w
Tourmaline		3.0-3.3	vs	vs	m	Pegmatitic/pneumatolytic stage of acid magmatic rocks	s
Epidote		3.3-4.2	s	s	w	Metamorphic rocks;	w
Kyanite	1.6-1.9	3.6-3.7	s	m	-	High pressure mineral of mesozonal regional metamorphic rocks	w
Xenotime		4.4-4.7	m	m	m	Acidic and intermediate magmatic rocks (granites, pegmatites)	m
Monazite		4.9-5.3	s	s	w	Acidic magmatic rocks	w
Sphene		5.0-5.5	m	w	w	Acidic and intermediate magmatic schists	w
Zircon		4.5-4.8	vs	vs	-	Acidic rocks	w
Cassiterite		6.8-7.1	vs	vs	-	Pegmatitic/pneumatolytic stage of granitic rocks	s
Baddeleyite	1.9-2.9	5.4-6.0	vs	vs	-	Nepheline-syenites, carbonatites	m
Perovskite		4.0-4.3	s	s	-	Alkaline rocks	m
Anatase		3.8-3.9	vs	s	-	Low temperature neogenetic phase in sediments and weathering products	w
Brookite		3.9-4.1	vs	s	-	Similar to anatase	vs
Rutile		4.2-4.5	vs	vs	-	Various rocks	s
Pyrochlore		4.3-6.5	s	m	m	Alkaline rocks; carbonatites	s
Chromite		4.5-5.0	s	s	m	Ultramafic rocks	vs
Ilmenite	opaque	4.5-5.0	s	s	m/s	Various rocks; very common	s
Magnetite		5.1-5.2	w	s	vs	Various rocks; very common	w

(w = weak; m = medium; s = strong; vs = very strong)

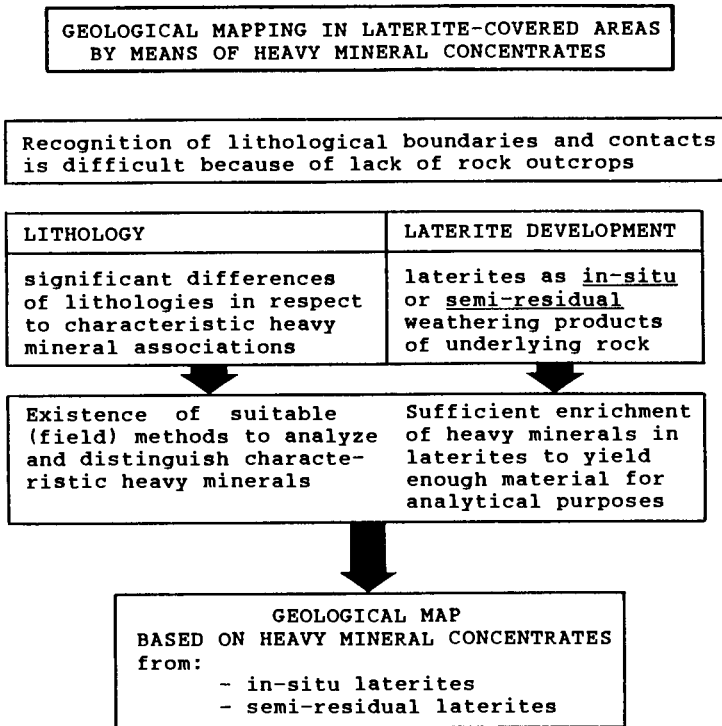


Fig. V.4-5. Criteria for the suitability of heavy minerals in geological mapping of laterite-covered terrain.

the top of the transported laterite horizon, whereas the abundance of Cr-spinel increases towards the bottom. Lithospecific elements can also be bound to secondary minerals and accumulations, such as iron oxyhydroxides in pisoliths.

The heavy minerals that are considered most suitable for mapping and bedrock recognition in tropically weathered areas are listed in Table V.4-1. These minerals are sufficiently abundant and stable during weathering or mechanical transport to permit recognition of their source from the geochemical and mineralogical properties (Friedrich et al., 1987). This is particularly true for Cr-spinels, the composition of which can be related to different types of ultramafic rocks (Irvine, 1967; Coleman, 1977; Leblanc et al., 1980; Rammelmair et al., 1987; Marker, 1988). Tourmaline composition may also be a very good indicator of bulk rock geochemistry, even when it has been remobilized during tectonism (Plimer, 1986). Some criteria indicating the appropriateness of HM surveys for geological mapping in lateritic terrain are given in Fig. V.4-5.

Niobium contents in soils, being controlled by the occurrence of pyrochlore, can be used for the recognition of alkaline and kimberlitic rocks (see Chapter V.1). Barron (1982) reported concentrations of up to 1.6 wt% Nb₂O₅ in soils of

the Muri Mountains Alkaline Complex, Guyana. Similarly, in Brazil, Von Maravic et al. (1983) found characteristic concentrations of 1.2 wt% Nb_2O_5 in soils over the Catalão Alkaline Complex, 3 wt% Nb_2O_5 in soils over the Araxá Complex (both in Brazil) and an average of 2.5 wt% Nb_2O_5 in laterites over carbonatitic syenites of the Lueshe carbonatite, Zaire. In addition to pyrochlore, soils above

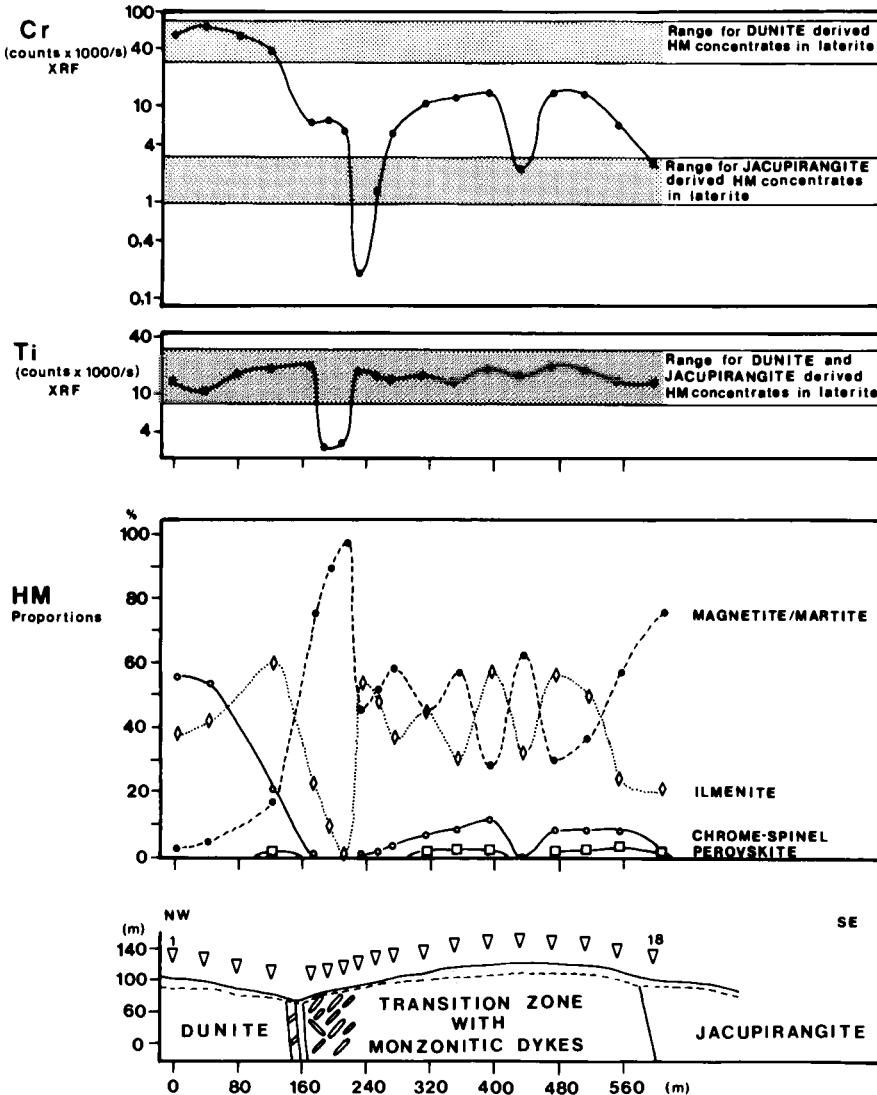


Fig. V.4-6. Chromium and Ti count-rates (XRF) and quantitative proportions of different heavy minerals from concentrates (63–200 μm), separated from surficial lateritic weathering material in the transition zone between dunites and jacupirangites, Jacupiranga Alkaline Complex Brazil. From Friedrich et al. (1987).

alkaline rocks are generally characterized by high abundances of zircon, baddeleyite, apatite, Nb-rutile, Nb-rich ilmenite, columbite, monazite and florencite (Barron, 1982; Von Maravic et al., 1983; Reedman, 1984; Friedrich et al., 1987).

The association of lithospecific heavy minerals may serve as a bedrock indicator, even in partly reworked laterites. At the Jacupiranga Alkaline Complex, São Paulo State, Brazil, Cr-spinels are characteristic of dunites but absent from jacupirangite (nepheline-bearing pyroxenite). This difference enabled the contact between the two lithologies to be traced in laterite-covered areas by using the Cr-spinel/Ti-Fe-oxide ratio of HM concentrates from surface samples. This led to a new geological map and genetic interpretation of the complex (Friedrich et al., 1987). The thick laterite cover at Jacupiranga appears to be semi-residual, but long-distance transport of allochthonous material can be excluded. Weathering has resulted in the relative enrichment of up to 10 wt% residual heavy minerals in in-situ lateritic soils. The heavy mineral survey also revealed a "transition zone" between dunite and jacupirangite (Fig. V.4-6) having intermediate Cr concentrations and essentially stable Ti concentrations, except for a region where there are monzonitic dyke swarms. The heavy mineral survey showed that this zone is characterized by intermediate Cr-spinel, unusually high magnetite and very low ilmenite abundances, and the presence of perovskite which causes significantly elevated Ce concentrations in total samples of the laterite. This transition, which surrounds the dunite block, is considered to be a zone in which the dunite is partially assimilated by jacupirangitic melt (Germann et al., 1987).

The application of HM surveys for mapping and bedrock recognition is greatest where the weathering is mainly residual. The heavy minerals essentially retain their original mineralogical and compositional features and are thus highly indicative of the host rock. However, in areas where transported overburden is abundant, the use of heavy minerals surveys is restricted. Unlike aqueous geochemical processes, which can result in hydromorphic dispersion patterns of primary anomalies into transported overburden, stable minerals and the trace elements they contain are subject to mechanical transport and hence give no surface expression to mineralization in such areas. An exception, however, is the presence of diamond indicator minerals in soils where kimberlites are overlain by 70 m of Kalahari Sand in Botswana (Locke, 1985; see Chapter V.1). It is suspected that the minerals have been introduced into the soils by burrowing termites.

Chromian-spinel composition as indicator of different ultramafic rocks

The use of Cr-spinels as petrogenetic indicators has been emphasized by Irvine (1967), Coleman (1977), Leblanc et al. (1980) and Dick and Bullen (1984). These authors have demonstrated the good correlation between the chemical composition of chromitites and accessory Cr-spinels and their ultramafic host rocks.

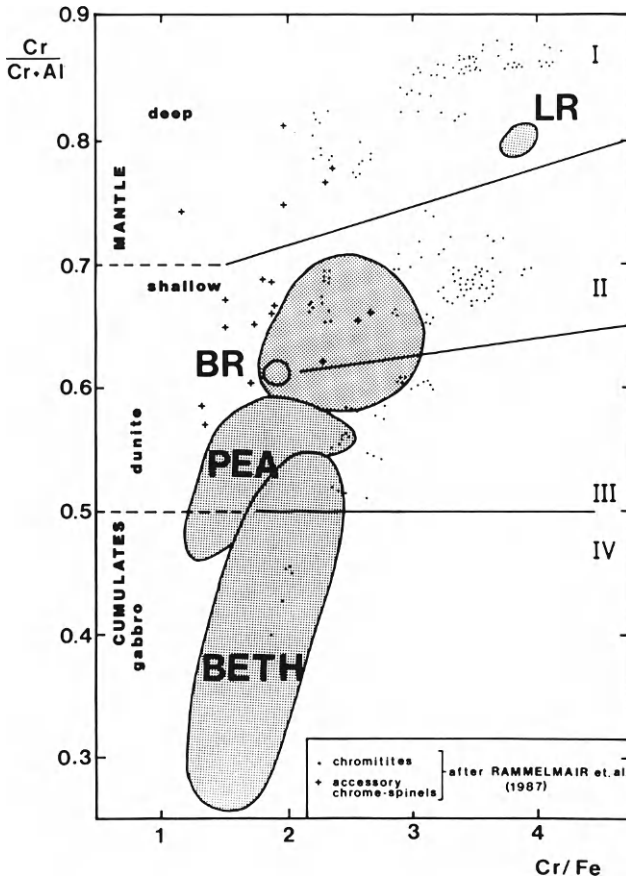


Fig. V.4-7. Plot of $\text{Cr}/\text{Cr}+\text{Al}$ and Cr/Fe , displaying the relationships between Cr-spinels from chromitites and accessory Cr-spinels in country rocks and lateritic weathering products, Central Palawan ophiolite, Philippines. The fields delineated TORO, LR, BR, PEA and BETH (see text) represent clusters of data for Cr-spinels from laterites (concentrates and single grains); sectors I–IV refer to groups of chromitites. From Rammelmair et al. (1987).

Accessory Cr-spinels have become considerably enriched in lateritic weathering products of ultramafic rocks in the Philippines (Friedrich et al., 1980). A study of their mineralogical and compositional features has led to an accurate characterization of the weathering products. The $\text{Cr}/\text{Cr} + \text{Al}$ ratios of accessory Cr-spinels from laterites overlying different intrusive levels of the ophiolite sequence correspond to the petrological composition of the sequence of units within the ophiolite. Accessory Cr-spinels from the tectonite complex are characterized by the highest $\text{Cr}/\text{Cr} + \text{Al}$ and Cr/Fe ratios; their composition matches with that of Cr-spinels from laterites of Leopard Ridge (LR) and Toronto (TORO) shown in Fig. V.4-7. The harzburgites of the tectonite unit host economically important occurrences of chromitites with high Cr/Fe and $\text{Cr}/\text{Cr} + \text{Al}$ ratios

TABLE V.4-2
Compositions of accessory chromian-spinels from ultramafic rocks in different geological settings

Geological setting	Host rock	Mean composition								Content in rock wt%
		wt%								
		Cr ₂ O ₃	Al ₂ O ₃	MgO	Fe ₂ O ₃	FeO	MnO	TiO ₂		
Ophiolites (Philippines)	Harzburgite	54	17	10	0	18	0.2	0.03	0.5	
	Harzb./dunite	46	23	11	1	18	0.2	0.05	> 3	
	Dunite/mafic	30	40	15	0	15	0.1	0.10	> 3	
	Cumulate									
Precambrian Alpine-type (Serro)	Lherzolitite	38	30	13	0	19	0.1	0.10	< 0.5	
	Talc schist	53	15	7	0	24	0.5	0.50	≪ 0.1	
Alkaline intrusion (Jacupiranga)	Dunite	33	7	9	-47		-0.7	5.0	> 0.5	
	Mean:				(0.2 ZnO)					
		Variation: Cr ₂ O ₃ : 14-48; Al ₂ O ₃ : 0.5-10; total FeO: 30-70; MgO: 3-10; TiO ₂ : 1-9; MnO: 0.3-2.8; ZnO: 0-1.2.								

TABLE V.4-3

Some characteristics of accessory Cr-spinels from ultramafic rocks in different geological settings

Geological setting	Host rock	Grain morphology; grain size	Degree of weathering	Associated HMs in rock
Ophiolites (Philippines)	Harzburgite	Xenomorphic-vermiform, < 100 μm	+	Magnetite
	Harzb./dunite	Euhedral-subhedral, > 100 μm	++	Magnetite
	Dunite/mafic	Euhedral, > 150 μm	+++	Magnetite
	Cumulate			
	Lherzolite	Xenomorphic-vermiform, < 100 μm	+++	Magnetite
Precambrian	Talc schist	Euhedral-subhedral, > 150 μm	++	Rutile, Ilmenite, Ti-magnetite
Alpine-type (Serro)			(martite)	
Alkaline intrusion (Jacupiranga)	Dunite	Euhedral-subhedral, > 100 μm	+++	Ti-magnetite, Ilmenite, Magnetite

(Sector I and II in Fig. V.4-7). Higher units in the ophiolite are characterized by the significantly lower Cr/Cr + Al ratios of the accessory Cr-spinels, which can also be traced in the laterites. Consequently, rocks of different areas (Blue Ridge (BR), Peacock (PEA) and Bethlehem (BETH)) can be classified as dunites of ultramafic cumulates (Sector III) and as dunites from the lower level of the mafic cumulates, including troctolites and picrites (Sector IV), by means of laterite-hosted accessory Cr-spinels. These findings are in accordance with the mapping results of Rammelmair et al. (1987) and, in addition, underline the relationship between composition of chromitite-derived Cr-spinels (Sector I–IV) and accessory Cr-spinels in the host rocks and their lateritic weathering products, both having nearly identical Cr/Cr + Al ratios.

The compositions, morphology and grain size of Cr-spinels, their concentration in rock and laterite, and the associated heavy mineral assemblages can give useful hints for mapping and bedrock identification (Tables V.4-2 and V.4-3). Hydrothermally-altered Cr-spinels from the Jacupiranga Alkaline Complex and from the metamorphosed Precambrian ultramafics at Serro, Minas Gerais, are characterized by unusually high Ti, Mn and Zn contents, due to a hydrothermal overprint. Similarly, Al-rich accessory Cr-spinels from lherzolites and cumulate ultramafic–mafic rocks of ophiolite sequences can be distinguished by grain size, morphology and concentration in rock and laterite.

THE USE OF HEAVY MINERALS IN MINERAL EXPLORATION

Heavy minerals can serve as a prospecting tool in lateritic environments if

(1) specific heavy minerals are indirectly related to the target, e.g. as alteration haloes or accessory minerals, or

(2) the target consists itself of those minerals, e.g. chromite in chromitites.

There are few examples of the use of residual heavy minerals in exploration of lateritic terrain, although as accessories (e.g. as native metals, cassiterite) they may indicate gossans or dispersed gossan fragments (Nickel, 1983; Smith and Perdrix, 1983; see also Chapters II.2 and III.3). Tourmaline seems to have potential as an indicator mineral because of its high stability (Levinson, 1980); thus, the Li, Cs and Rb contents of tourmaline may be characteristic of specific pegmatites or Sn deposits. Similarly, ferruginous tourmaline is associated with Au mineralization at Dorlin, French Guiana, and can be used locally as an indicator mineral (Zeegers, 1987; see p. 272).

Magnesian ilmenites and other high temperature minerals are associated with diamond-bearing kimberlites and may serve as an exploration tool (Pasteris, 1980; see Chapter V.1). The properties of natural rutiles in placer deposits can contribute to the discrimination of primary source rock (Goldsmith and Force, 1978; Martin, 1985).

Under lateritic conditions, many soluble pathfinder elements, including those mobilized from heavy minerals, are preferentially scavenged by limonitic concretionary phases. By concentrating these phases in "loam" concentrates, Farrell (1984) outlined Ni-Cu-Co sulphide mineralization in Western Australia. The best responses were found for Cu, Cr, Cu and Ni, which were extracted from the 840–1680 μm HM fraction. Nickel, Cu, Cr and Zn contents of magnetite and goethite-limonite from mineralization are high with respect to those from background samples. Watters (1983) also stressed the importance of HM concentrates for U exploration, since extractable U is fixed by secondary Fe and Mn oxides. Minor U mineralization in central Kalimantan (Indonesia) was found by analyzing leachates of these phases. Assuming that limonitic concretions and coatings also play an important role in U fixation in soils, similar procedures may have application in analysing soil samples.

Residual deposits of heavy minerals may develop where tropical weathering processes lead to an upgrading of primary concentrations and HM surveys have some application in exploration for such deposits. The HM concentrates are themselves of interest if they contain cassiterite, gold, platinum or diamonds. The enrichment of Nb-bearing pyrochlore during weathering has led to the formation of important residual ore deposits such as Araxá and Catalão in Brazil and Lueshe in northeast Zaire. The pyrochlore content of weathered material (up to 7 wt%) is a discriminating factor in outlining economically feasible areas in the Lueshe carbonatite (Von Maravic et al., 1983). Similarly, heavy mineral associations consisting of typically bipyramidal zircon, Nb-rutile, euhedral pyrochlore, magnetite, ilmenite and anatase were found indicative for exploration of the Muri Mountains Alkaline Complex in Guyana/Brazil (Barron, 1982).

Chromian spinels, contained in ultramafic rocks as accessory minerals or in the form of disseminated or massive ore bodies, are subject to high residual enrichment in regions of deep tropical weathering. Exploration for concealed orebodies by determining the distribution patterns and chemical composition of

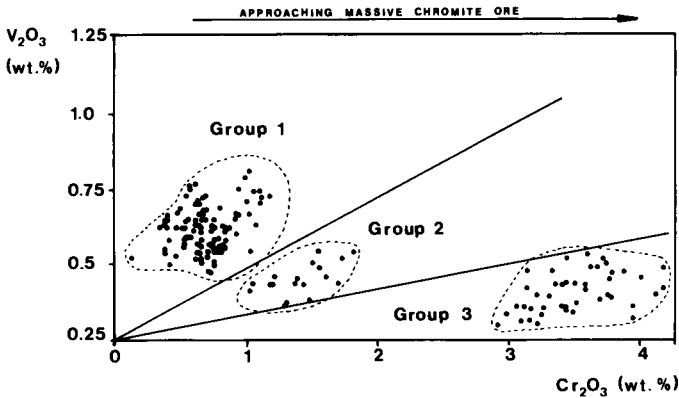


Fig. V.4-8. V_2O_3/Cr_2O_3 ratios of rutiles from lateritized ultramafic rocks (group 1), weathered disseminated chromite ore (group 2) and massive chromitites (group 3). From Marker and Martin (1985).

Cr-spinels in the lateritic soil in the Philippines was carried out by Friedrich et al. (1983) and Kater et al. (1984). Hidden chromite orebodies were traced by the high HM contents (per unit volume) in the overlying laterite and characteristic high Cr/Fe ratios of the total and non-magnetic HM fraction.

The relationship between trace element composition of rutiles and associated accessory Cr-spinels and massive chromitites in ultramafic rocks (talc-schists) of Serro, Brazil, is shown in Fig. V.4-8. Rutiles formed during metamorphism show gradually increasing Cr contents (1.3–4.0 wt% Cr_2O_3) and decreasing V contents (1.0–0.6 wt% V_2O_3) in approaching the massive chromitites (Marker and Martin, 1985).

CONCLUDING REMARKS

Geological mapping and mineral prospecting in tropical areas has always to aim at a multifaceted approach, because the processes leading to alteration of primary bedrock features are complex. Heavy mineral surveys represent a reconnaissance technique that, when used in combination with geochemical and geomorphological methods, are suitable for some applications in regolith and geological mapping, bedrock identification and in mineral exploration. Heavy minerals represent an excellent tool for identifying reworked and transported weathered horizons. They may indicate the proportion of the transported (allochthonous) component in semi-residual (semi-autochthonous) material and contribute to reconstruction of geomorphological development (Table V.4-4). Heavy mineral distributions may reflect several factors that contribute to the formation and composition of transported horizons, including geomorphological evolution, transport distances and directions, and source areas. Geological mapping and

TABLE V.4-4

Comparison of the characteristics of heavy minerals in tropical weathering products of semi-residual and transported origin, under contrasting climatic and geomorphological conditions

	Semi-residual	Transported
Climate	Tropical humid	Arid
Geomorphology	Moderate to high relief, vertical mass movement, chemical weathering, in-situ processes	Low relief, horizontal mass movement, erosion, hardpans
<i>Heavy Minerals</i>		
Distribution	Predominance of residual HM-components, increasing with regolith depth.	Depositionally controlled HM-associations. Distribution in profile commonly homogeneous.
Morphology	Slightly weathered grains, preservation of original angular shapes	Roundness due to abrasion during transport; commonly highly weathered.
Grain size distribution	Poorly sorted, predominance of colluvial transport	Well-sorted due to long-distance mechanical transport.
Geochemistry	Pattern interpretable in terms of litho-geochemistry	Erratic patterns
Abundance	Relatively high, due to predominance of residual enrichment processes (except quartz-rich rocks) Relatively high abundance of mechanically unstable minerals.	Relatively low, due to dilution by mechanically supplied quartz Relatively low abundance of mechanically unstable heavy minerals.
Bedrock identification	Possible after verification of geomorphological environment	Difficult because of distal source-areas of weathering material and polycyclic reworking.

bedrock identification by heavy mineral surveys are most promising in areas with a residual weathering cover. Characteristic heavy mineral patterns of the bedrock may be directly reflected in the overlying regolith. Lithological units as well as primary mineralization can be traced by heavy mineral assemblages and/or their chemical and mineralogical composition.

SUMMARY AND PROCEDURAL RECOMMENDATIONS

H. ZEEGERS and C.R.M. BUTT

INTRODUCTION

Tropically weathered terrains present a number of problems that affect the application of most mineral exploration techniques. The widespread occurrence of a regolith 20– > 100 m thick implies that outcrops are rare or of poor quality. This thus restricts the use of conventional geological mapping, and places increased reliance on the integrated use of the ancillary techniques of geophysics and geochemistry. Of these, geochemistry appears to have a predominant role, particularly for exploration at a sub-regional to local scale, but can only be effective if the characteristics of the terrain are understood and the most appropriate sampling and interpretational techniques are selected. These topics have been discussed in detail in this volume and the conclusions have been summarized in the form of a number of dispersion and exploration models. The purpose of this chapter is to outline the procedures needed to utilize this information and hence optimize the exploration programme. The necessary steps are to:

- (1) recognize the problems posed by the terrain and the limitations it places on exploration methods;
- (2) define the objective of the programme (e.g. mapping, reconnaissance, specific commodity or style of mineralization) and the scale;
- (3) determine the nature of the landscape (i.e. geomorphology, regolith);
- (4) estimate the probable dispersion models that apply in the area;
- (5) select the sampling and analytical techniques necessary to detect the expected expression of the target.

The chapter concludes with a brief evaluation of the effectiveness of geochemical procedures in exploration of these terrains, and a discussion of the relationship between geochemical exploration and environmental change.

EXPLORATION PROBLEMS IN TROPICALLY WEATHERED TERRAINS

In addition to common logistic difficulties of poor access, extreme climatic conditions and remoteness from adequate technical support, the complex morphoclimatic evolution of tropically weathered terrains give rise to several specific

exploration problems. These affect geophysical and geochemical procedures alike and apply a number of constraints on their use.

In general, geophysical exploration procedures appear to be most appropriate for regional appraisal and area selection. Remote sensing, gravity surveys and, in particular, airborne magnetic surveys indicate broad scale geological and structural features in all terrains, but in areas of deep weathering, their application at the prospect scale is hindered by specific properties of the regolith. Apart from the obvious effect of increasing the distance between the sensor and the target, these include:

(1) *Magnetic surveys.* The concentration of resistant magnetite and secondary maghemite in lateritic duricrusts and gravels mask magnetic and electromagnetic responses from bedrock sources.

(2) *Electrical methods.* The low resistivity of the overburden (10–50 ohm-metres) and resistivity contrasts within and at the base of the regolith screen the target from electromagnetic (especially frequency-domain) and induced polarization techniques and superimpose spurious signals.

(3) *Seismic and gravity surveys.* The complex zonation, transitional contacts and density contrasts of the regolith attenuate responses and/or give false anomalies in shallow seismic and gravity surveys.

(4) *Radiometric surveys.* Transported overburden may suppress or eliminate radiometric responses; in contrast, false anomalies may be produced by concentrations of U and Th in resistant minerals in surface horizons or by the separation of U and its daughter products by ongoing weathering (see Chapter V.2).

Geochemical procedures, utilizing soil and other regolith materials as sample media, are most valuable for exploration at sub-regional to local scales, although reconnaissance and regional stream sediment surveys have importance for general appraisal and area selection. However, the evolution of the terrain and the development of the regolith give rise to several problems that may hinder their effective application. These include:

(1) profound mineralogical, chemical and physical alteration of bedrock and associated mineralization, so that distinctions between even broad lithological classes are difficult;

(2) strong leaching of most ore-related elements, particularly from upper horizons of the regolith, resulting in only subtle surface expression of mineralization;

(3) the development of spurious secondary concentrations of target elements in weathered, unmineralized rocks;

(4) lateral changes in the nature of the regolith, due to variations in the depth of truncation of earlier, pre-existing profiles by the present erosional surface;

(5) the presence of a cover of transported overburden, which may itself have been weathered after deposition;

(6) the superimposition, in a single profile, of the effects of weathering under different environmental conditions.

Effective geochemical exploration can only be achieved by the recognition of

these problems and other properties of the terrain, and by the selection of techniques of sampling and data interpretation appropriate to the target being sought.

EXPLORATION OBJECTIVES

The objectives of any exploration programme must be clearly defined in order to determine the most appropriate operational procedures. The possible targets for the programme may be:

(1) all commodities, when an assessment (inventory) of the mineral potential of a region is required, or

(2) specific commodities and/or styles of mineralization, e.g.

(a) base metals (volcanogenic metal sulphides, Cu-Mo porphyries, sediment-hosted Pb-Zn deposits, vein-type deposits, skarns);

(b) precious metals (epithermal Au, Au in shear zones, Pt-Pd in layered intrusions);

(c) commodities requiring special procedures, such as diamonds and uranium (Chapters V.1 and V.2).

(d) supergene mineralization (Au and Ni in lateritic regoliths).

In exploration for specific commodities or types of mineralization, the nature of the expected geochemical anomaly, which is the initial target of the exploration programme, should be defined. In particular, it is important to estimate the dimensions of the anomaly with respect to the size of an economic deposit and its primary halo, and to predict mineral and element associations that may give a multielement signature. For example:

(1) Mineralization in structurally controlled Au deposits may be some n metres wide, whereas the alteration halo, commonly having high As contents, may be $10n$ or $100n$ metres wide. The regional exploration target, therefore, is not necessarily the mineralization itself, but the alteration halo. Furthermore, since As is widely dispersed in the upper horizons of lateritic profiles, the initial geochemical target may be more than $1000n$ metres wide.

(2) Some epithermal precious metal deposits are characterized by large sericitic alteration haloes. These may be reflected by high K_2O contents in soil samples, because sericite is resistant to weathering.

(3) Volcanogenic massive sulphide (VMS) mineralization is commonly expressed at the surface as gossans. These are generally smaller than the primary deposit but mechanical dispersion of gossan fragments may give widespread anomalies in soils, lateritic pisoliths and stream sediments. Gossans may be strongly leached of the principal ore elements but may be distinguished by anomalous concentrations of pathfinder elements, such as Sn, W and Bi, or platinum group elements. Some VMS deposits have extensive alteration haloes containing minerals such as Ba-rich sericite that give distinctive geochemical signatures.

There are, nevertheless, disadvantages to exploration programmes that are too closely focussed, because they may miss the unexpected—i.e. novel styles of mineralization, “conventional” deposits in unusual settings, economic deposits of other commodities. Wherever possible, and particularly at regional scales, a multielement, multicommodity approach is desirable; alternatively, reference samples should be retained for future use.

RECOGNITION OF THE WEATHERING AND GEOMORPHOLOGICAL ENVIRONMENT

The geomorphology and the regolith of a region are the product of its weathering history and hence of the past and present processes of weathering and geochemical dispersion. They are fundamental parameters in the definition of the dispersion models and therefore in deciding the most appropriate means for exploration of an area. The model relevant to an area can thus be established from the surficial characteristics of the terrain, at a level of detail commensurate with the scale of exploration and the nature of the target. Important features to be determined are:

(1) *Climatic history*. This determines the sequence and nature of the dominant processes of weathering and regolith formation. Throughout most of the middle to low latitudes, the earliest climatic episodes of significance are those that led to the widespread development of deep lateritic regoliths during the late Mesozoic to mid-Tertiary. Such regoliths are suspected to have formed under seasonally humid, tropical climates similar to those that prevail in the present humid savannas, although cooler conditions are suspected in some regions. Except in areas of high relief or extreme aridity, the lateritic regoliths have been largely preserved; they have, however, been modified by weathering under the changing climatic conditions that characterize the late Tertiary and Quaternary. The most significant changes are those in rainfall, i.e. to more humid (rainforest) or less humid (semiarid or arid) conditions—in most places, these correspond to the present climate.

(2) *Present climate*. The temperature, rainfall and seasonality determine the currently active processes of weathering and dispersion. These climatic factors generally only have to be considered at a regional scale, although local variations are important in some situations, e.g. rain shadow effects in areas of high relief. In regions in which the earlier lateritic regolith has been wholly or partially preserved, the active processes are modifying or over-printing existing dispersion patterns.

(3) *Geomorphology*. This is a guide to the weathering and erosional history of a region and provides information as to the nature, distribution and degree of preservation of the regolith. Geomorphological information is available at a regional scale for all countries from the general literature, but detailed information suitable for exploration at sub-regional to local scales will commonly have to be gathered as part of an exploration programme. This is best achieved by

interpretation of remote sensing images and aerial photography, followed up by checking in the field. The most suitable interpretation is one that subdivides the terrain into units that group landscape elements according to the nature of the regolith, such as the facet–landform–land system classification (Chapter I.1), because these give information about the nature and distribution of possible sample media. It is particularly important that an initial geomorphological appraisal of an area is able to indicate (i) whether landscape units are erosional or depositional and, (ii) the position of these units with respect to the horizon of the pre-existing profile that forms the surface (if erosional) or immediately underlies the sediment (if depositional). This information can be used to guide sampling programmes (e.g. for district-scale surveys using specific sample types, such as residual to semi-residual lateritic pisoliths and nodules) or to assist data interpretation by subdividing data sets according to the sample type. The initial appraisal should, of course, be updated and refined as exploration progresses and, if necessary, data obtained early in an exploration programme should be reassessed on the basis of an increased understanding of the terrain. In complex terrains, or those for which little information is available, it may well be appropriate to do some reconnaissance drilling of the regolith to determine its horizon development and stratigraphy, and to establish the nature of local modifications of the profile. For detailed exploration, data interpretation may require landform/regolith characteristics to be mapped at the facet scale (e.g. Mount Gibson, see Chapter III.3, p. 313) in order to determine the provenance of anomalous samples.

APPLICATION OF THE APPROPRIATE DISPERSION MODELS

Once the weathering and geomorphological environments have been satisfactorily identified, the relevant dispersion models can be anticipated. Dispersion models indicate the expected geochemical response for a given element (or suite of elements) in a particular environment. As described in Chapter I.2 and Part III, regoliths in tropically weathered terrains have a number of specific horizons, namely (from bottom to top), unweathered bedrock, saprolite, mottled zone, ferruginous zone (cuirasse, lateritic duricrust) and soil. These horizons have each developed under different physico-chemical conditions and therefore represent different situations in which geochemical dispersion may occur. In general, the *size* of the dispersion halo increases in the upper horizons, particularly where some mechanical (or palaeo-mechanical) component is added to the hydromorphic dispersion processes of chemical weathering. Conversely, however, the *abundance* of an element and the anomaly/background *contrast* tend to decrease higher in the profile and with distance from the source. The behaviour of each horizon is reflected by the overall funnel- or mushroom-shape of the dispersion haloes. In consequence, either the degree of truncation or the sampling depth are determinants for anticipating the geochemical response.

The geochemical response can be expressed in terms of the components of the model codes as defined in Chapter I.1:

$$\text{Sum (R, H, M)} = A > B > C$$

i.e. the size of the dispersion halo resulting from residual (R), hydromorphic (H) and mechanical (M) dispersion is larger where the pre-existing lateritic profile is preserved (A-type models). Conversely, it is smaller where the profile is truncated (B-type models) or completely eroded (C-type models), or if the samples are collected deeper in the profile, such as in the saprolite. This generalization may not hold for terrains in which the water-table has been lowered or in which there is redox stratification in the groundwaters, because dispersed ore elements may have accumulated at either the old or the present water-tables or redox fronts. Except for Au (Fig. V.3-4), dispersion haloes at these levels have generally only been recognized retrospectively, rather than used as exploration guides; examples of Pb dispersion in saprolite include Teutonic Bore in semiarid Western Australia (Fig. III.3-15) and Woodcutters in the savanna climate of the Northern Territory, Australia (Taube, 1978).

It is also generally true for humid terrains that:

$$\text{Sum (H, M) for models } * 3 * [0,1,2] > * 2 * [0,1,2] > * 1 * [0,1,2]$$

i.e. the extent of geochemical dispersion, in residual or semi-residual sample media, is proportional to the degree of leaching of the pre-existing profile under recent or current climatic conditions. The greatest dispersion is generally observed where recent leaching is strongest (* 3 * [0,1,2] models), although the resultant anomaly contrasts may be too weak for practical application. By comparison, in arid terrains with little active leaching, several elements, including Pb, Cu and Au are mobilized and dispersed by highly saline groundwaters. Gold mobility may be dramatically influenced by the increase in salinity and is responsible for the formation of the supergene enrichments in the saprolite (see Chapter V.3).

Where transported (allochthonous) overburden is present above the weathering profile, dispersion haloes are rarely found at the surface, i.e.

$$\text{Sum (R, H, M)} = 0 \text{ (or nearly so) for models } * * * [3]$$

There are some exceptions, especially where the overburden contains some residual material or where plants or termites have been active. Post-lateritic processes can also enhance the dispersion of several elements, including base metals, Au and U. Dispersion into overburden has been observed in Australia, in savanna (e.g. Thalanga, Queensland, see p. 236) and semiarid climates (e.g. see Figs. III.3-28, 29, 33 and 44) and is probably present in other regions.

The foregoing illustrates the importance of defining the model code(s) for each site or area. Such a coded description of the morphological and weathering

situations also make it possible to compare dispersion characteristics of sites from widely separated regions. Thus, if previous experience or orientation surveys are lacking in some areas, and hence no a priori dispersion model can be established, it is possible to extrapolate from areas with equivalent models codes. For example, the following terrains can readily be compared:

(1) *rainforest*: Gabon, French Guiana, Brazilian Amazonia, Indonesia, western Burma, Malaysia;

(2) *savanna*: West Africa, Brazil, India, northern Australia; New Caledonia, Madagascar;

(3) *semiarid*: Western Australia, northeast Brazil, Sahel.

Such comparisons, if based on the model codes, may help in anticipating the geochemical behaviour of various elements and predicting their dispersion characteristics, including consideration of the possible occurrence of supergene mineralization. Elements such as Ni, Al, Fe, Mn, Ti, P, REE, Nb and Au may be present as economic deposits in lateritic regoliths in specific environments that are described by the codes. The model codes also permit comparisons between areas even if they are in different climatic environments. Sites with similar degrees of preservation of the profile (i.e. A, B or C) and similar overburden (i.e. geomorphological setting) will have similar geochemical responses, except for any modifications (leaching or neo-formation and precipitation) induced by post-lateritic climatic or environmental changes. These similarities are expressed by the comparisons in Fig. I.1-6. Thus, much geochemical data from now semiarid deeply weathered terrains (e.g. Sahel, Australia) are best interpreted in terms of the weathering processes now observable in regions of humid savanna. Conversely, exploration experience and procedures developed in better explored areas such as Australia can be applied (with care) to equivalent terrains in more humid climates. The closer the climatic equivalence, the more appropriate is the comparison, but dispersion characteristics related to the common lateritic event persist. This is evident in comparisons of the mineralogy and geochemistry of gossans over similar mineralization (Chapter II.2), enrichments of Ni in saprolites of ultramafic rocks and the relative accumulation and lateral dispersion of Au in lateritic horizons (compare Mborguéné, Cameroun (Fig. III.2-8) with Callion, Western Australia (Fig. III.3-8)).

SELECTION OF EXPLORATION PROCEDURES

Sample media and scale of exploration

There are optimal sample densities and sample types applicable for each phase of exploration. At the regional scale, if large areas have to be covered, only a few samples per km² can be collected. The most suitable sample media will be those in which the geochemical dispersion halo is best developed, i.e. in which the sum of the residual (R), hydromorphic (H) and mechanical (M) components

give the broadest anomalies. Where “soils” rather than stream sediments are sampled, this can best be achieved by collecting lateritic gravels, “lag” samples or other surface materials that have undergone some transport. At more detailed phases of exploration, samples should be selected to provide a more accurate image of the underlying mineralization, i.e. corresponding to smaller dispersion haloes. This is normally achieved by collecting samples from a greater depth. Thus, the basal horizons of the lateritic ferruginous zone or of soils developed from saprolite may help in delineating the target if sampled on 100 m centres. If greater precision is required and where trenching is not possible or inappropriate, saprolite sampling by auger or RAB drilling at intervals as close as 5 or 10 m may be necessary. More detailed discussion of the various sample media and sampling procedures are discussed in Appendix 1.

The geomorphological setting, as expressed by the model codes, should be taken into account in optimizing the sampling procedure. For example, gossan search is an effective procedure in truncated or partly truncated terrains (B * * [0,1] and C * * [0,1] models), especially in arid to dry savanna environments where outcrops are more readily seen. However, as exploration of an area progresses over time, the potential for gossan discoveries diminishes and exploration has to focus on areas with a cover of soil or transported overburden. Similarly, in A * * [*] situations, the regolith may be covered by 1–5 m of ferruginous cuirasse (lateritic duricrust). In such circumstances, saprolite sampling by light auger or RAB drilling techniques may be impractical and it may be best to proceed to test anomalies directly by deeper percussion or diamond drilling. A reliable assessment of the setting and appropriate dispersion model thus allows exploration programmes to be better designed.

The foregoing are only very general principles; specific problems related to particular weathering environments or commodities are considered in earlier chapters of this volume, mostly through examples and case histories that illustrate and discuss the dispersion models and the exploration approach.

Sample preparation and analysis

Sampling and analytical procedures are discussed in Appendix 2. Selection of the most appropriate of these can be made by reference to the relevant dispersion models and case histories, which generally discuss the nature of the sample media, including size fraction where appropriate, and the suite of elements chosen for analysis.

The materials that comprise the surface horizons of the regolith in tropically weathered terrains commonly consist of size fractions having distinctly different mineralogical compositions. For example, soils overlying or derived from lateritic cuirasse have a fine fraction composed principally of quartz, kaolinite and other clay minerals, and a coarse fraction of pisoliths, nodules and lithorelics composed principally of secondary Fe oxides and oxyhydroxides. Most trace elements are specifically bound to one of these size fractions, i.e. the various

components of the geochemical signature are not evenly distributed between the various minerals. Accordingly, sieving to recover either fine or coarse material may result in enhancing or depressing the concentration (and anomaly contrast) of a given element. Elements such as As, Bi, Mo and Cu are commonly more abundant in the ferruginous fractions whereas Ni, Mn, Co and Zn tend to be concentrated in the clay fraction.

Different grain sizes have importance not only because of their effects on element concentrations and contrasts but also because they may give rise to different sizes of dispersion halo. In stone-line weathering profiles, for example, the coarse fractions of the stone-line horizon, which have normally undergone some mechanical transport, commonly exhibit wider dispersion haloes than the clay-rich fine fractions, which are mostly residual. Different size fractions should always be examined in case they retain particular pathfinder elements (e.g. B in coarse tourmaline, Au as fine grained particles).

Saprolite sampling is important in tropically weathered terrains. It has some similarities to lithochemical sampling, but with differences due to hydromorphic dispersion that may depress element concentrations but enlarge anomaly size. Saprolite is commonly friable, particularly in humid environments, and can therefore be sampled by digging small pits or by hand augering, methods that can be used even in remote locations. Saprolite sampling also has great value in providing lithological information and hence is a valuable mapping aid. Nevertheless, the potential for mapping should not overshadow the principal aim of the sampling programme, namely to detect mineralization via primary or secondary geochemical dispersion haloes. The latter is commonly best achieved by sampling high in the saprolite, where dispersion is greatest, whereas the best geological information is obtained from less weathered material deep in the profile. Such deep sampling, however, is costly and if over-emphasized may compromise the effectiveness of the exploration programme by reducing the area that can be explored within budget.

Gossans are the most direct sample medium for they are the weathered expression of the mineralization itself. They may be sampled in outcrop or drill intersection and their geochemical signature can indicate the nature of the underlying primary deposit.

Data interpretation

The interpretation of data from geochemical surveys in tropically weathered terrains has to take into account the dispersion model(s) appropriate to the region, the sample media and the specific characteristics of the elements concerned. Individual geochemical surveys, whether at regional or local scales, commonly use a range of different sample media that have different geochemical responses. For example, if a soil sampling grid covers both A-type (pre-existing profile preserved) and B-type (pre-existing profile partly truncated) situations, at least three sample media will be used: soil developed on ferruginous cuirasse,

ferruginous cuirasse itself, and soil developed on saprolite. The geochemical contrast will be greater in the soil derived from the saprolite, but the size of the dispersion halo will be far smaller. Similar considerations apply in most surveys; even when attempts are made to standardize the sample type, such as by choosing a specific size fraction or collecting ferruginous pisoliths, nodules or lags, the geochemical responses will vary. Interpretation of the data must account for these variations by relating them to the position of the sample in the regolith. Ideally, regolith landform maps should be prepared, at least at the sub-regional to prospect scale, noting the presence of erosional and depositional environments, the degree of truncation of the lateritic regolith and the nature and thickness of any overburden. If prepared before sampling, they can be used to guide the sampling programme; if prepared during and after sampling, they can be used to subdivide the samples into comparable groups.

EFFECTIVENESS OF GEOCHEMICAL EXPLORATION IN TROPICALLY WEATHERED TERRAINS

The present situation

The numerous examples from different climatic zones cited in this volume and the general literature demonstrate that geochemistry is an efficient tool for mineral exploration in tropically weathered terrains. Its importance is emphasized when it is considered that most geophysical techniques have limited application, particularly at the local scale. Geochemical responses are better in many tropical environments than in more temperate regions due to the presence of mushroom- or funnel-like haloes that represent significant enlargements of the target size near the surface. For example, gold mineralization or deposits of massive base metal sulphides that are only a few metres wide are commonly indicated by anomalies that can be detected by soil or laterite sampling on grids of 100×100 m or more. These large dispersion haloes are a product of the long periods during which the regoliths have evolved, resulting in a greater degree of residual accumulation and physical and hydromorphic (chemical) dispersion of ore-related elements. In comparison, regoliths in many temperate terrains have evolved over only a few tens of thousands of years so that dispersion, other than that due to glacial action, is of restricted extent.

Where regoliths are strongly evolved, e.g. older A-type situations (pre-existing profile fully preserved), exploration problems rival those in temperate regions, although additional opportunities exist in the form of supergene deposits. Element dispersion (and reconcentration) mechanisms are more complex and the weathered expression of mineralization is more difficult to detect. For example, mobile elements such as Zn and Cu can be strongly leached and significant mineralization may therefore only be revealed at the surface by subtle, low contrast anomalies or by pathfinder elements having very low abundances. Further complexities are caused by chemical and physical modifications brought

about by alterations in environmental conditions due to uplift or marked climatic change. Accordingly, increasing attention has to be paid to the processes of regolith evolution and landscape development and their effects on geochemical dispersion.

Quantitative interpretation of geochemical data tends to be of limited value in deeply weathered terrains. Such interpretation should ideally involve the definition of each sample site in terms of its geomorphological and weathering situation, and the geochemical data weighted accordingly. At present, this can only be achieved empirically, with samples sorted according to field information or to geochemical characteristics defined by multielement analysis. Indeed, such analysis can provide valuable additional information concerning the sample and the sampling site:

- high Fe contents may indicate the presence of ferruginous cuirasse;
- in humid regions, high contents of alkaline earth elements indicate a low degree of leaching, with the sample probably collected deep in the saprolite. In arid regions, high abundances of these elements may indicate the presence of calcrete;
- high Si contents may indicate the presence of transported material or secondary silicification;
- Ti/Zr ratios can be used to indicate bedrock lithology.

Outlook and future developments

Future exploration will increasingly have to address more complex, highly evolved terrains that have few outcrops and in which mineralization is concealed by thick regoliths of residual and/or transported material. For exploration to be effective and efficient, increased attention will have to be given to understanding dispersion mechanisms through holistic laboratory and field studies of weathering reactions, hydrogeochemistry and the role of biological agents, including microorganisms. This is important not only for designing procedures for locating primary mineralization but also to determine the processes responsible for the formation of economic supergene mineral deposits. Greater emphasis also needs to be paid to regolith landform mapping, for this is the key to optimizing sampling and interpretational procedures and the development of dispersion models. Such models must indicate the constraints on the geochemical signature imposed by the terrain, rather than be specific for particular genetic types of deposit, for this might preclude the identification of novel styles of mineralization. They must also encompass the whole regolith, rather than emphasize the surface expression, for anomalies in deeper horizons are important exploration targets; for some commodities (e.g. Au, Ni, REE), dispersion models may also be genetic models for supergene deposits.

More generally, the dispersion models summarize the long term effects of environmental, particularly climatic, change. Geochemists are thus well placed to evaluate some of the causes and effects of predicted future changes, such as

global warming, currently the subject of much debate, by analogy with relevant models. They also have a role in establishing “baseline” or background conditions, against which the effects of any future changes can be compared.

EXPLORATION GEOCHEMISTRY AND ANTHROPOGENIC ENVIRONMENTAL CHANGE

Introduction

The principal theme to this volume has been to investigate the effects of environmental change on geochemical dispersion. The changes are brought about by tectonic activity (principally uplift) and long term alterations of the climate, both of which may affect the mechanisms and rates of physical erosion and chemical weathering (Table I.1-5). Similar changes may be mimicked, at least in the short term, by human activity (e.g. deforestation). The objective of this section is to discuss the possible influence of such anthropogenic environmental changes on weathering and element dispersion, particularly as they may affect the geochemical expression of mineralization. In addition, exploration itself can have some, usually minor, environmental impact, much of which can readily be avoided if the causes and effects are understood.

Human activity, weathering and geochemical dispersion

Human activities that result in gross changes in vegetation and drainage have the greatest impact on the surface environment. The most profound and long-lasting effects are probably those due to deforestation and the development of agriculture. These have a direct influence on the soil environment and, more problematically, possible indirect influences as causes of changes in rainfall patterns (e.g. “desertification”) and as contributors to the so-called but unproven “greenhouse effect”. Irrigation, including terracing for paddy cultivation, drainage, urban development, land reclamation, major earth-works and mining are important on more local scales. Each of these may affect the processes of weathering and geochemical dispersion and hence have significance in exploration by altering the surface expression of mineralization as shown by the composition of sample media such as saprolites, soils, vegetation, stream sediments, groundwater and surface waters. Deforestation is the most widespread and is discussed below. In addition, many of these activities, particularly agriculture, urban and industrial development, and mining, may pollute and contaminate these media so that their further use in exploration is difficult or impossible. Conversely, there is potential for the use of geochemical methods in detecting such changes, but consideration of this topic is beyond the scope of this volume.

Deforestation

Deforestation by fire has long been practised by Man as a land management tool. It is used for releasing, if only temporarily, more fertile land in “slash and

burn" communities and for controlling vegetation distributions for hunting, grazing and, latterly, agricultural communities. It is probable that many grasslands in savanna and semiarid climates have been produced and maintained by this activity, preventing their reversion to a forested or shrub-dominated vegetation. Deforestation by fire and logging, together with overgrazing (especially in semiarid regions), has the following effects on weathering processes:

(1) The soil is both destabilized and exposed to the direct impact of precipitation and wind. The result is a greatly increased rate of erosion, particularly of unconsolidated surface horizons, including the organic, fertile topsoils, and the exposure of indurated lower horizons such as lateritic duricrusts, calcretes, silcretes and fresh rocks. Areas of high relief are subjected to very rapid erosion by gullyng and, in humid regions, mass-flow (including landslip), whereas areas of low relief are eroded more by sheetwash, some gullyng and, in arid regions, wind. These may influence exploration by diluting colluvial and drainage samples with barren material and increasing the sedimentary cover in depositional areas, but conversely, erosion may remove or incise through upper leached or transported horizons to expose underlying anomalous materials.

(2) The upper horizons of the soil become desiccated by exposure to the sun and wind. This is particularly significant in the dry season in savanna climates and may lead to the irreversible dehydration and induration of lateritic ferruginous horizons. Other effects include more pronounced shrink and swell of smectitic soils, increased runoff due to the development of soil hydrophobicity and the precipitation of dissolved matter at or near the surface. In savannas, there appears to be increased precipitation of Fe oxyhydroxides (the "pedogenic" laterites of McFarlane (1976)), and in more arid areas dissolved salts may precipitate due to evaporation. The implications for geochemical dispersion and exploration are not clear; induration changes the physical nature of sample media and it is possible that surficial precipitates may include components derived from underlying mineralization.

(3) Reduced evapotranspiration due to the vegetation change from deep-rooted trees and shrubs to shallow-rooted grasses and other species results in increased water retention and a rise in water-table. In valleys, the water-table may intersect the surface, causing gleying and waterlogging of the soil. This mechanism is responsible for increasing salinization in some dry savanna and semiarid regions (e.g. Thailand, southern Australia) and possibly for the headward advance of dambo swamps in East Africa. In arid, saline environments, ferrolisis reactions result in the generation of acid, oxidizing groundwaters capable of mobilizing metals including Pb, Cu, Zn, Mn, U, Ra, Au and Ag (Mann, 1983, 1984a, 1984b); the increased groundwater flux due to deforestation promotes these reactions and locally is capable of greatly increasing the mobilization and dispersion of these metals.

Geochemical dispersion patterns or anomalies related to changes in land use and hydrology have not been recognized in tropical and subtropical regions. However, in temperate Northern Ireland, Butt and Nichol (1979) noted that the

distribution of metal-rich seepages and soils containing hydromorphically dispersed Pb and Zn corresponded to cultivated and recently reforested areas rather than to adjacent mature forest. They attributed this to a change in the local hydrology after clearing. In the mature forest, soils are acid and freely drained, and water tends to flow downwards, leaching the ore metals, whereas in cleared areas, there is a rise in the water-table and soil pH, so that metals oxidize and precipitate in soils and ditches close to their source. The occurrence of hydromorphic anomalies in other environments may similarly have been induced or enhanced by changes in vegetation caused by recent or past human activity. It is also important to note that surveys conducted after such changes, whether due to logging, agriculture or fire, may give markedly different results to those completed beforehand.

Pollution and contamination

Pollution by agricultural chemicals, mining and smelting activity, and industrial waste, represents a continuing problem in exploration. It may give rise to clastic, hydromorphic or biogenic dispersion patterns that closely resemble natural ones. The most difficult to identify and circumvent are those due to past mining activity, for they are derived from equivalent mineralization as the exploration target and may mask a more subtle natural anomaly. The problems posed by pollution are discussed by Rose et al. (1979) and Levinson (1980); these authors conclude that although, locally, contamination may give rise to considerable difficulties in interpretation, these are not insuperable. Exploration may itself result in contamination; spoil left on the ground after trenching and drilling is soon washed into drainages. Such spoil is clearly visible in drainage channels in some intensively explored areas in Western Australia and is an obvious source of contamination when, for example, the area is re-examined for another commodity.

Environmental impact of exploration

Exploration activities themselves may have a detrimental environmental impact even in areas where no significant discoveries are made. In general, the impact, though unsightly, is minor and temporary. However, the disturbance caused by clearing for tracks, drill pads and cut lines may, in sensitive areas, locally cause severe erosion by developing into water courses or, in arid regions, becoming the focus for "blow-outs" by wind. In addition, unfilled trenches and uncapped drill holes may be dangerous and can also become traps for animals and birds. As discussed above, the spoil may become widely spread if left. Most of this damage is readily avoided, or at least minimized, by careful planning and rehabilitation, at little extra cost. In view of the increasing recognition of the significance of such damage, and for the trend for legislation to enforce restoration, the adoption of appropriate measures from the commencement of exploration is warranted.

APPENDIX 1 — SAMPLE MEDIA USED IN GEOCHEMICAL EXPLORATION IN TROPICALLY WEATHERED ENVIRONMENTS: DEFINITIONS AND USE

GOSSANS

(see Chapters II.1 and II.2)

Definition and description

A gossan is the weathered expression, commonly as an ironstone, of a rock containing a substantial proportion of sulphides. The term has no economic connotations in that it covers weathering of iron sulphides as well as base metal sulphide bodies. The terms barren or false gossans have been used to describe gossans derived from sulphide bodies that do not contain appreciable amounts of minerals of economic importance. As many gossans are the products of past climatic episodes, they are subject to truncation. Intermediate zones of the gossan profile may then be exposed, with secondary minerals such as carbonates outcropping at surface, possibly with partial destruction of primary gossan fabrics.

Distribution

Gossans have developed on sulphide mineralization in most tropical environments, but appear to be uncommon in wet savannas and rainforests. They are best developed in dry savannas and arid areas where there has been widespread preservation of complete or partly truncated lateritic regoliths. Immature gossans, containing secondary ore minerals or relict primary sulphides, are found in strongly truncated situations (B or C dispersion models).

Use as a sample medium

Many base-metal deposits in Australia, India, southern Africa, Sudan and the Arabian peninsular have been found by the discovery and recognition of outcropping gossans. The main exploration problems are:

- (1) to distinguish gossans from other ironstones, including laterites, and
- (2) amongst "true" gossans, to identify those that have been formed from economically significant sulphide mineralization.

A common approach has been to analyze samples for the main target elements, such as Cu–Pb–Zn or Ni–Cu, and to examine anomalous samples for boxwork textures (Blanchard, 1968) or some significant mineralogical parame-

ters. In practice, since concentration of target elements may be strongly depleted in the gossan, especially where stripping is not advanced, systematic multielement analysis for a wide range of pathfinder or target elements (including Au) may be more diagnostic (Wilhelm and Kosakevitch, 1979). The choice of pathfinder elements depends upon those expected to be in the target mineralization and on the mobilities of elements during weathering. At the surface, elements such as As, Bi, Hg, Mo, Sb, Se, Sn, Ba, Ge and Ag may be significant and, lower in the profile, Cd, In and Te may also occur. For interpretation, various graphical and statistical approaches have been used for evaluating gossans geochemical data, from simple statistical analysis to sophisticated multivariate processing.

Sampling procedures

Most gossans are extremely heterogeneous and it is therefore desirable to collect a substantial number of samples from each occurrence. Samples are usually taken from the surface, or from trenches, drill cuttings or core. Subsurface samples may differ markedly from surface gossans in chemical and mineralogical composition, so that sampling depth should be taken into account when interpreting the geochemical data.

IRONSTONES

(see Chapters II.1 and II.2)

Definition and description

The term ironstone is used to describe highly ferruginous, usually discrete, weathered outcrops. An ironstone may be essentially linear in outcrop pattern, following an underlying geological unit or structure, or form a horizon—commonly the uppermost—of a lateritic profile, and be essentially conformable with the weathering surface. Certain unweathered ferruginous rocks, such as jaspers, banded iron formation or some exhalites are sometimes referred to as ironstones but they are excluded from this definition. Ironstones formed from the weathering of sulphide bodies are gossans, and are discussed in the previous section. Ironstones enriched in target elements but not derived principally from weathering of sulphides have been termed false gossans or pseudogossans. They have been found most extensively in semiarid and savanna environments, particularly in Australia.

Distribution

Ironstones are commonly formed as largely residual accumulations on Fe-rich lithologies or as exotic accumulations of Fe oxides along channelways such as

faults, fractures, lithological contacts or bedding planes. In the latter situations, the Fe may have been derived by leakage from Fe-rich source rocks or by weathering of the country rocks, with precipitation occurring in a chemically favourable zone. Those ironstones formed as horizons of a lateritic profile (variously termed lateritic ironstones, ferricretes, plinthite, cuirasse, canga) tend to have a sheet-like form, and often occur as duricrusts on plateau residuals, or marking previous levels of water-tables in such profiles.

Most ironstones are found where the deep weathering mantle is preserved, at least in part. They are composed essentially of goethite and hematite, with variable amounts of quartz and minor phyllosilicates, feldspars and Mn-bearing minerals. Ironstones along faults may contain a high proportion of quartz breccia. In lateritic ironstones, original rock fabrics may be partly preserved or completely destroyed. Botryoidal, cellular and pisolitic fabrics, produced by weathering processes, are common.

Use as a sampling medium

Ironstones are routinely sampled during the search for gossans, and analyzed for a suitable range of target elements. However, anomalous concentrations of one or more such elements are diagnostic only of gossans in the simplest weathering situations (C models). Where weathering is more advanced (A and many B models), other ironstones anomalous in base metals (pseudogossans) can form from a variety of lithologies (in many cases from rocks lacking sulphides) of quite "normal" compositions. Exotically-derived Fe (and Mn) oxides precipitated along channelways such as faults and contacts can accumulate other metals (e.g. Co, Cu, Ni, Ba, Pb or Zn) leached from adjacent rocks. Techniques of distinguishing between gossans and other ironstones are discussed fully in Chapter II.2.

SAPROLITE

(see Chapters I.2, I.3, III.1, III.2 and III.3)

Definition and description

Saprolite represents the lower horizons of lateritic weathering profiles. It may be overlain by upper horizons (mottled zone, lateritic cuirasse) where most of the pre-existing profile is preserved (A dispersion models) or exposed or obscured by residual soils or transported overburden in truncated situations (B dispersion models). The chemical alteration responsible for the transformation of the bedrock includes:

- (1) Leaching of soluble constituents by groundwater, resulting in relative enrichment of insoluble constituents.
- (2) Precipitation of materials such as silica, Fe oxide and Ca–Mg carbonates as absolute enrichments.

These processes nevertheless preserve rock fabrics as relics by pseudomorphically replacing primary minerals and cementing the secondary product, respectively. The principal secondary minerals constituting the saprolite are Fe and Al oxides, kaolinite and smectites. Uncemented saprolites are mostly soft and have a wide range of colours: green, grey and yellow to brown, red and black. When bleached to pale grey or white, they are commonly referred to as “pallid zone”.

Distribution

Saprolites are abundant wherever there are lateritic regoliths, either preserved or partly truncated. They outcrop in truncated situations, commonly covered by a relatively thin soil. As they are rather soft, they are less well preserved in areas of high relief, due to removal by erosion.

Use as a sampling medium

Saprolite sampling is in common use in most tropically weathered terrains. It replaces both lithochemical sampling where fresh rocks are absent and soil sampling where soils are poorly developed or allochthonous. Geochemical anomalies in saprolite are mostly residual, but extensive hydromorphic dispersion haloes have been recorded for Au and Pb in some semiarid and dry savanna environments (e.g. Woodcutters (Taube, 1978); Teutonic Bore, see p. 336; Chapter V.3). Therefore, the target size expected for a given ore-type depends largely upon the chemical mobility of the elements present under the conditions of the original deep weathering and subsequent episodes. In general, the less mobile the element and the deeper (i.e. the nearer to fresh rock) the sample is taken, the smaller the anomaly size. Of the usual target elements, those immobilized in Fe oxides, clay minerals or stable secondary minerals (e.g. Cu, Mo, As, Sb and Pb) have strong anomalies in saprolites derived from mineralized rocks. Conversely, for mobile elements such as Zn, the effect of weathering can be such as to leach them almost entirely, especially from near-surface horizons (e.g. THR prospect, see p. 262), so that detectable anomaly is again restricted. Primary alteration haloes are preserved if the elements are held in resistant minerals such as sericite, tourmaline or barite (e.g. Dorlin, see p. 271).

Sampling procedures

Outcropping saprolite can be chip-sampled as an adjunct to gossan, ironstone or laterite sampling. However, as a survey technique, this is liable to bias, since only the most resistant or secondarily hardened rocks are exposed, and these may not be representative of the unexposed rocks. Trenching (costeaming), if logistically possible, is useful for localized investigations where the saprolite is rather soft. Elsewhere, various drilling techniques have to be employed. Auger drilling is intensively used in remote, poorly accessible areas such as the

rainforests of Africa or South America. Hand augering is adequate for shallow drilling in humid climates where the weathering profile does not include very hard horizons such as lateritic cuirasse or stone lines. Power augers are required where stone lines (rainforest A 3 * [*] or B 3 * [*]), very dense clays or secondary cementation, e.g. by silica or carbonate, are present.

Augering is generally not possible where lateritic cuirasse is present (A 0 * [*] or A 1 * [*]), or where profiles are strongly indurated (e.g. by silicification), and is unsuitable for collecting very wet or very deep samples. For these situations, more powerful systems, such as rotary air blast (RAB), open-hole or reverse-circulation blade, roller or percussion, or air-core drilling are necessary. A number of sampling strategies can be adopted; these include drilling:

- (1) to a set depth and/or until the drill cannot penetrate farther;
- (2) until "recognizable saprolite" is visible in the cuttings;
- (3) in areas of deep transported overburden, to base of the overburden and collecting the uppermost "in situ" material, whether having recognizable rock fabrics or not.

Samples obtained by these methods are usually composites of cuttings from 1- or 2-m intervals. It is best if the cuttings are passed through a cyclone, to minimize dust-loss, either directly into plastic bags or into spoil heaps on the ground. Wet samples may be collected directly into calico bags. Analyses are usually of "whole-rock" samples; any size fractionation in the cuttings is likely to be an artefact of the drilling procedure, rather than being representative of the original material. Analytical samples are generally collected by:

- (1) grab sampling from individual spoil heaps;
- (2) splitting the cuttings as they leave the cyclone;
- (3) "pipe-sampling" cuttings in plastic bags or calico (Barnes, 1987). The bag is laid on its side and a PVC pipe, 5–6 cm in diameter, inserted diagonally through the cuttings; one or more such pipe samples are taken from each bag.

Even if saprolite represents the target for sampling, samples should ideally be collected from throughout the profile to take advantage of the dispersion haloes of the target and pathfinder elements in different horizons of the regolith. For obvious reasons of economy, such full sampling is not normally practised except on few orientation holes. As a compromise, samples may be collected from each "recognizable horizon" or from several set depths. Alternatively, aliquots of several samples may be composited for analysis and the individual subsamples only analysed separately if anomalous concentrations are found.

Accurate logging of drill material is essential for the correct selection of analytical samples and for data interpretation. This important, usually complex, aspect of saprolite sampling is often neglected. The drill spacing is also critical, especially where little or no secondary dispersion into saprolite is expected. Where samples are collected deep in the saprolite, dispersion may be so restricted that the anomaly is much the same width as the primary mineralization itself. For narrow targets, such as massive sulphide shoots or Au mineralization in humid environments where there is little lateral dispersion, vertical drilling on

centres of 10 or even 5 m across strike is commonly used. Rather wider intervals may be adequate if overlapping angle drilling is used—but care must be taken to allow for the effects of zones of strong leaching.

LATERITIC CUIRASSE (DURICRUST), LATERITIC GRAVELS AND LAG

Definition and description

Lateritic cuirasse is composed of various structural forms of secondary segregations of Fe and Al oxides such as mottles, nodules, pisoliths and oololiths, cemented by a matrix of clays and Fe and Al oxides. The term “lateritic gravel” is used to refer to uncemented accumulations of the segregations. Lag is the residual accumulation of coarse, usually hard, fragments that form a thin pavement in semiarid terrains and some dry savannas. It is most useful as a sample medium when the fragments are ferruginous and lateritic in origin. Lateritic cuirasse and gravels are the products of Fe oxide accumulation towards the top of typical lateritic weathering profiles, as described in Chapter I.3. They represent the final stage of such weathering and are generally largely residual, although mechanical reworking is a common feature of the surface horizons. The primary mineral assemblage is almost totally replaced by hematite, goethite, gibbsite and kaolinite in varying proportions, with some quartz and other resistant minerals. Their chemical composition may differ considerably from that of underlying bedrock and strong enrichments (relative or absolute) may be observed for elements such as Fe, Al, Ti, Zr, Cr, V, Mo, As, REE, Th, W and, possibly, Au, commonly giving rise to considerable interpretational problems. Conversely, other elements may be severely leached, e.g. Ca, Mg, Zn, Ni, Ag, S, Cd, Co and U.

Distribution

Lateritic cuirasses and gravels are found wherever the pre-existing weathering profile has been neither truncated nor degraded during later climatic episodes. Such situations, corresponding to the A * * [0,1] dispersion models (e.g. see Fig. I.1-6), are found in all lateritically weathered regions. Preservation is best in areas of low to moderate relief in semiarid or seasonally humid climatic zones. Lags are present in similar areas where erosion and truncation of the profile has occurred but has not been very severe.

Use as a sampling medium

In poorly dissected areas, lateritic cuirasse and gravels are commonly the only readily accessible sampling medium. Target and pathfinder elements may have been widely dispersed by chemical or mechanical processes during the long

period of development. Thus, secondary dispersion haloes may considerably enlarge the size of the exploration target, making possible the use of quite wide sampling intervals. Accordingly, elements having some chemical characteristics similar to iron (e.g. As, Mo and, to some extent, Cu) may be particularly important. The geochemical signature of hydrothermal alteration haloes may be (at least partly) preserved in the lateritic cuirasse if a given element is held in a resistant mineral, such as K_2O in muscovite or B in tourmaline. Where the upper part of the lateritic cuirasse has been mechanically reworked, further enlargement of the dispersion halo is observed for most elements in the degradation products. Thus, lateritic gravels and lags have considerable value as a sampling medium and are extensively used in Australia (see Chapter III.3). At the regional scale, their greatest potential is realized by multielement analyses, in order to determine subtle trends and anomalies in somewhat 'spotty', low contrast data.

Sampling procedures

Where outcropping (i.e. A 0 0 [0] models), lateritic cuirasse may be chip sampled in the same manner as gossans, ironstones and outcropping saprolite. Preferably, the exposed surface should be discarded to avoid any possible contamination or leaching, and the nature of the material (e.g. pisolitic, massive, lamellar, tubular) documented. Where the cuirasse is covered by residual or semi-residual soil (i.e. A * * [1] and A * * [2] models), it is better to sample the cuirasse by drilling rather than collect surface soils, because higher element abundances and contrasts will be obtained. This procedure is essential if the cuirasse is overlain by transported overburden (e.g. A * * [3] models). Similarly, uncemented lateritic gravels are preferable to associated soils as sample media and if possible should be segregated from fine matrix material prior to analysis. It is recommended that a sample mass of at least 1 kg is collected over a radius of 5–10 m, using pisoliths and nodules no larger than 1–2 cm in diameter to avoid undue bias (Smith et al., 1989). Lag samples (1 kg) may be swept from the surface and are best sieved to reject both fine transported material and coarse fragments. Generally, finer materials (2–6 mm) are used than for lateritic gravel sampling but they tend to be less homogeneous so that data may need to be normalized for Fe content (Carver et al., 1987).

The broad dispersion haloes commonly permit very wide sample intervals to be used, as discussed in Chapter III.3. Sampling on 1–3 km centres may be adequate for the detection of regional patterns, closing to 50–100 m for detailed follow-up. If possible, sampling for regional surveys should be directed at the loose gravel horizon, to take advantage of the wide dispersion halo, whereas for prospect evaluation sampling should be directed at the deeper cuirasse horizon.

Definition, description and distribution

Soils may be defined as unconsolidated, surficial weathering products developed in situ from an underlying parent material. They are almost ubiquitous throughout tropically weathered terrains, being absent only on rock outcrops, including inselbergs, actively eroding slopes, some duricrust surfaces and active depositional areas including talus, sand dunes and playa surfaces. They may vary in character from thin, coarse grained, poorly differentiated lithosols in some deserts to thick, well-differentiated silt- and clay-rich soils in more humid regions.

Soils are formed by the interaction of climate, organisms (including vegetation) and groundwater with the parent substratum over varying periods of time. In areas of tropical weathering, the parent substratum is commonly residual weathered bedrock or some form of transported overburden. Usually, only those soils developed on residuum are of value as exploration sample media. The properties of the regolith material from which the soil is derived is generally more important than the classification of the soil within established systems of nomenclature. In situations having well-preserved pre-existing lateritic weathering profiles (A dispersion models), the soil has generally developed by the degradation of the upper horizons of the profile, e.g. from lateritic cuirasse. It therefore consists predominantly of Fe and Al oxides and clay minerals, with quartz present as a diluent. Geochemical responses obtained in such soils vary, depending on the element and on the relative proportion of the main mineral phases. As in the parent laterites, mobile elements such as Zn and Ni are strongly leached, whereas others may be concentrated in Fe oxides. Sample preparation is thus particularly important, permitting the selection and concentration of specific mineral phases; the fine fraction may be mostly composed of quartz and clay minerals whereas the coarse fraction contains most of the Fe and/or Al oxides. As stated in the previous section, it is commonly preferable to collect the lateritic material from which the soil is derived; where this is not possible, the coarse fraction may give a similar response.

Where the pre-existing profile is truncated (B models), residual soils have developed from saprolite, and accordingly contain abundant clay minerals such as kaolinite and smectite. Geochemical responses tend to be very similar to those in the saprolite; abundances and contrasts may be lower due to leaching (in humid climates) or dilution by calcrete (in arid climates), but anomalies are greater in area. Accordingly, residual and semi-residual soils may be preferred to shallow saprolite as sample media on the basis of the geochemical response and lower cost of sampling. Where the profile has been completely stripped (C models), residual soils have developed directly by the weathering of fresh bedrock. In addition to clay minerals and iron oxides, soils, particularly the deeper horizons, may contain appreciable quantities of primary minerals, espe-

cially in areas of high relief and in arid regions. The geochemical response of mineralization is accordingly very direct, yielding areally restricted anomalies of high contrast. Broader anomalies may be present in humid regions of moderate to high relief due to hydromorphic dispersion.

Use as a sampling medium

Soil anomalies tend to be greater in area than in the parent material due to mechanical and chemical dispersion during their formation. Accordingly, where possible, soil surveys are conducted prior to the more specific and costly saprolite and bedrock sampling. They have particular application in semi-regional to prospect scale exploration of areas of poor outcrop in which the soil is residual or semi-residual. Either before or during a survey, therefore, it is important to distinguish between those soils that are likely to reflect bedrock chemistry and those that have developed on or from transported overburden and which, with rare exceptions, will show no geochemical relationship with the underlying bedrock. Nevertheless, not all anomalies in residual soils reflect the presence of mineralization. Some may be due to secondary concentrations in ironstones or weathered bedrock that form the soil parent material and such possibilities must be considered in data interpretation. Soil sampling grids should be run across strike, using spacings appropriate to the expected target size. Provided that a consistent sample medium is used, the data can be contoured or presented as stacked profiles to highlight zones of interest.

Despite the increasing availability of high quality multielement analysis, the majority of soil surveys rely on the determination of only the target element(s). There is, however, considerable merit in analysing for a wider range of elements, whether to explore for unexpected commodities or to assist in data interpretation. For example, multielement analysis is of great value in determining the significance of base metal anomalies in areas where secondary concentration is a possibility or where hydromorphic dispersion is or has been active; the distributions of less mobile pathfinder elements (e.g. Sn, W, Pb, Pt) can indicate whether such anomalies are related to a mineralized source and, if so, whether they have been displaced downslope during weathering. Multielement surveys tend to emphasize target and pathfinder elements; major element soil geochemistry is comparatively little used but can be useful for:

- (1) defining lithological changes in soil-covered terrains;
- (2) recognizing geological marker horizons in monotonous sequences;
- (3) mapping alteration haloes associated with mineralization;
- (4) normalizing data when minor element abundances are partly controlled by the presence of specific minerals, e.g. Fe oxides, Ca and Mg carbonates;
- (5) determining the degree of surface leaching or evolution towards lateritization, e.g. by ratioing SiO_2 or Fe_2O_3 contents with those of the alkali or alkaline-earth elements.

Sampling procedures

Within any particular soil horizon, other than those developed from lateritic cuirasse and gravels, most elements tend to be fairly uniformly dispersed regardless of soil fraction. This effect can be more apparent than real, because dry sieving is commonly ineffective in separating fine fractions. Clay particles aggregate and can coat coarser particles so that clean separations are rarely possible and analytical results are accordingly modified. Nevertheless, fine soil fractions are commonly convenient because metal contents are enhanced by the removal of barren quartz and no further sample preparation is necessary prior to analysis. Where soils are strongly differentiated, care must be exercised to sample a consistent soil horizon. The use of a constant sample depth is not recommended, for profile conditions can change markedly along a slope. Where such consistency is not possible, the sample types collected must be documented for use in subsequent interpretation. The requirement to confirm optimum sampling horizons and sample fractions by orientation surveys cannot be overemphasized.

TRANSPORTED OVERBURDEN

Definition and distribution

Transported overburden is material of exotic or redistributed origin, in some cases partly cemented by iron oxides, silica or carbonates, that blankets weathered and fresh bedrock. It includes:

- colluvium, sheetwash deposits and alluvium;
- piedmont fan and outwash deposits of gravels, sand and clay characteristically forming extensive blankets shedding from dissected plateaux and zones of higher relief;
- talus and landslip deposits in areas of moderate to high relief;
- aeolian clay (loess) and sand in desert environments;
- evaporites.

Transported material is a dominant feature of many warm semiarid and arid regions, at least as a thin veneer, and its presence has a considerable bearing on geochemical exploration practice.

Use as a sampling medium

In regions where bedrock and mineralization are extensively weathered and leached, further dispersion is usually limited to mechanical smearing at the bedrock/overburden interface. Dispersion to the surface is generally precluded in arid regions and it is no coincidence that most mineral discoveries in such terrain have been made on hills, with outcrop and residual soil, that rise above the overburden-covered plains. However, there is some evidence that subtle

dispersion haloes may develop, either in specific soil horizons (e.g. carbonate horizons, see Mount Pleasant, p. 365) or deeper in the overburden (e.g. Redross and Dalgara, see p. 357, 358). However, the presence or identification of such haloes cannot be relied upon.

Sampling procedures

Generally, overburden sampling is avoided and systematic grid drilling to residuum is preferred, perhaps combined with geophysical techniques. Drill spacings should be selected according to the nature of the sample to be taken. Thus, if a complete profile has been preserved, wide-spaced sampling of the lateritic gravel or cuirasse horizon is appropriate, whereas if the profile is truncated, closely-spaced sampling of the saprolite will be necessary. Although costly, the latter approach does permit additional geological information to be obtained.

APPENDIX 2 — SAMPLE PREPARATION AND ANALYSIS

SAMPLE PREPARATION

Almost all samples require some preparation prior to chemical analysis. The few exceptions include samples to be analysed for gold by bulk cyanide leach (BLEG), for which 1–5 kg or more of unprocessed samples are steeped in sodium cyanide solution. All other samples need to be reduced in bulk (mass) and particle size by sieving, splitting, crushing and grinding. The latter processes inevitably introduce contamination and the selection of methods used should take this into account.

Sieving

The selection of a particular size fraction for analysis is generally only applicable for soil (and drainage) samples. It should not be usually attempted on drill cuttings from moderately consolidated weathered bedrock or transported overburden, since the comminution is largely an artefact of the drilling process. For soils, orientation surveys will indicate the most appropriate size fraction for analysis but, when reviewing the available case histories, it is evident that the fine (minus 80-mesh (177 μm) and minus 100-mesh (125 μm)) fractions recovered from sieving are the most routinely used. It should be remembered that if dry sieving is used, it may be difficult to separate clay aggregates from silt and sand fractions. Indeed, in some soils and unconsolidated materials, the clay fraction is largely in form of spherules which may not disaggregate even during wet sieving. The only situations which may require separation of the coarse

dispersion haloes may develop, either in specific soil horizons (e.g. carbonate horizons, see Mount Pleasant, p. 365) or deeper in the overburden (e.g. Redross and Dalgara, see p. 357, 358). However, the presence or identification of such haloes cannot be relied upon.

Sampling procedures

Generally, overburden sampling is avoided and systematic grid drilling to residuum is preferred, perhaps combined with geophysical techniques. Drill spacings should be selected according to the nature of the sample to be taken. Thus, if a complete profile has been preserved, wide-spaced sampling of the lateritic gravel or cuirasse horizon is appropriate, whereas if the profile is truncated, closely-spaced sampling of the saprolite will be necessary. Although costly, the latter approach does permit additional geological information to be obtained.

APPENDIX 2 — SAMPLE PREPARATION AND ANALYSIS

SAMPLE PREPARATION

Almost all samples require some preparation prior to chemical analysis. The few exceptions include samples to be analysed for gold by bulk cyanide leach (BLEG), for which 1–5 kg or more of unprocessed samples are steeped in sodium cyanide solution. All other samples need to be reduced in bulk (mass) and particle size by sieving, splitting, crushing and grinding. The latter processes inevitably introduce contamination and the selection of methods used should take this into account.

Sieving

The selection of a particular size fraction for analysis is generally only applicable for soil (and drainage) samples. It should not be usually attempted on drill cuttings from moderately consolidated weathered bedrock or transported overburden, since the comminution is largely an artefact of the drilling process. For soils, orientation surveys will indicate the most appropriate size fraction for analysis but, when reviewing the available case histories, it is evident that the fine (minus 80-mesh (177 μm) and minus 100-mesh (125 μm)) fractions recovered from sieving are the most routinely used. It should be remembered that if dry sieving is used, it may be difficult to separate clay aggregates from silt and sand fractions. Indeed, in some soils and unconsolidated materials, the clay fraction is largely in form of spherules which may not disaggregate even during wet sieving. The only situations which may require separation of the coarse

fraction are those in which the soil has developed on a fully preserved lateritic profile (A models). In these, the coarse fraction consists mainly of Fe and/or Al oxides which preferentially concentrate many target and pathfinder elements, as indicated by several case histories in Chapters III.1–III.3. In many instances, it is preferable to sample the lateritic gravels and cuirasse directly, rather than the soils. The use of coarse soil fractions has previously been recommended in very arid areas, to reduce the effects of dilution by fine aeolian dust (e.g. Bugrov, 1974; Barbier, 1987). However, the coarse fraction may be diluted by quartz sand and evaporites, and the minerals, both primary and secondary, that host the ore-related elements may be abraded to a fine grain size, so that the apparent advantage is lost. The use of either the whole sample or a fine fraction is now advocated for such environments (Salpeteur and Sabir, 1989; see p. 369).

During routine saprolite surveys, sieving prior to analysis may be sufficient for a fast and cheap selection of samples for later reprocessing (by crushing and grinding) and analysis. That possibility depends largely upon the style of the mineralization being sought, and should be investigated by orientation survey. The procedure is inappropriate if important pathfinder elements are associated with resistant minerals such as quartz, tourmaline or magnetite. A better procedure is to prepare composite samples and to crush, grind and analyze them properly.

Crushing

Samples need to be reduced to 1–5 mm in diameter before splitting and fine grinding. This is most effectively achieved using jaw-crushers or disc grinders. Tests have shown that a jaw crusher with tungsten carbide crushing surface introduces less than 1 ppm Bi, Cd, In, Mo or Sn, and less than 0.1 ppm Ag. However, on average 15 ppm W and 1–2 ppm Co may be introduced during the crushing of laterite samples. Three times this amount may be added to hard chert and up to 200 ppm W to very hard materials, such as quartz, silcrete and granitoids. Separate crushing using W- and Co-free hardened steel is therefore recommended where low thresholds for these elements are involved (Smith and Butt, 1983). A possible alternative, a jaw crusher faced with partially stabilized zirconia (PSZ), gave no detectable contamination for soft materials (e.g. serpentine, limestone) but was found to add 10 ppm Zr to lateritic pisoliths and up to 225 ppm Zr to quartz (I.D.M. Robertson, personal communication, 1989). The least trace element contamination is introduced by crushing small sample amounts to 20 mm between hydraulically-driven PSZ plates followed by alumina disc-grinding, but the procedure is very slow.

Grinding

A grain size of less than 100 μm (preferably 60–75 μm) is desirable for most analytical procedures. Such fine milling or grinding, particularly for sample

TABLE A.2-1

Contamination introduced by ring mill grinders made from different materials (from Smith and Butt, 1983); for quartz sand ground in agate, metallic contamination was below detection limit; analysis by semi-quantitative optical emission spectroscopy

Chromium steel	Manganese carbon steel	Tungsten carbide	Composition range
Fe, Cr	Fe	W, Co	10%–100%
–	–	–	1%–10%
Si, Mn	Si, Mn, Cr	–	0.1%–1%
Al, Mg, Ti, V, Cu, Ni, Co, Mo, W, Ba	Cu, Mo, W	Si, Al, Mg, Fe, Mn, Ti, Cu, As, Cr	100–1000 ppm
Zr, Bi,	Al, Mg, Bi, Co	Pb, Bi	10–100 ppm
<i>Contamination of quartz sand by grinding.</i>			
In chromium steel	In manganese carbon steel	In tungsten carbide	Composition range
Fe (approx. 1%)	Fe (approx. 1%)	–	0.1–1%
Cr	–	Fe, Cr, W	100–1000 ppm
Ni, Cu, Zr	Mn, Cr, Cu, W	Ni, Cr	10–100 ppm
Mn, V, Mo	Ni, Mo	Cu	1–10 ppm

masses of 100–500 g, is most conveniently achieved using ring-mills. By its very nature, the process is prone to introduce contamination from the grinding surfaces. Tests carried out on the milling of quartz sand blanks of 2 mm particle size to give a product of minus 100 μm using standard grinding times (from 45 to 90 seconds) for routine samples introduced levels of contaminants shown in Table A.2-1. For many purposes, tungsten carbide ring-mills may be adequate, but if highly abrasive (e.g. silicified) samples are ground, contamination can be severe, with Co and W introduced in the sample at concentration levels ranging between 100 and 1000 ppm; for example, up to 1250 ppm W and 120 ppm Co, are added to silcretes and quartzites on grinding. When low pathfinder element abundance are expected, e.g. in multielement surveys using laterite geochemistry, samples should ideally be ground in agate. However, the procedure is slow, particularly for large or hard samples, and costly, given the fragility of the grinding vessels. As an alternative, case-hardened Mn-carbon steel ring-mills provide a useful compromise of large capacity, short grinding time and low contamination. The contamination introduced into a highly abrasive, coarse (< 10 mm) quartz sample by such a mill is shown in Table A.2-2. The quartz was ground for 80 seconds to < 75 μm and as such represents a very severe test; finer, less abrasive material would give much lower contamination. (N.B. Steel mills are commonly made from Cr-steel, which may introduce unacceptably high amounts of Cr, Ni, Cu and other elements.) Laboratories carrying out trace element analysis should be able to furnish their customers with analyses of the impact materials of the mill and analyses of quartz blanks ground by it.

TABLE A.2-2

Trace metal composition (in ppm) of Mn-steel ring-grinder parts and the contamination (in ppb) introduced into highly abrasive coarse quartz (I.D.M. Robertson, written communication, 1989)

	Steel ppm	Contamination ppb		Steel ppm	Contamination ppb
Ag	< 10	< 70	Nb	220	1500
As	5	40	Ni	620	4500
Ba	< 20	< 150	Pb	20	150
Bi	< 10	< 70	Sb	25	200
Cd	< 2	< 15	Sn	80	600
Co	70	500	Ta	< 100	< 700
Cr	795	5500	Ti	45	300
Cu	850	6000	V	40	300
In	< 5	< 35	W	< 20	< 150
Mn	6590	45000	Zn	30	200
Mo	260	2000			

For much geochemical work, it is necessary to pay close attention to the prevention of cross-contamination between successive samples during sample preparation. Many Fe- and Mn-rich samples have the unfortunate characteristic of forming a smeared coating on the grinding surface. Similar carry-over contamination may occur with gold and other native metals. The problem may only be partly overcome by passing one or more quartz blanks through the apparatus so that additional treatment may be required (e.g. sand-blasting or ultrasonic wash), adding further cost to sample preparation stage. The outcome, however, is to increase greatly the reliability of the subsequent analysis.

ANALYSIS

A full discussion of analytical procedures is beyond the scope of this volume. However, the increasing demand for multielement analysis, commonly with low detection limits, requires some comment. The choice of the analytical procedure can be quite important due to the limitations of sample digestion procedures and the characteristics of different analytical instruments. It is also important to note that samples from tropically weathered terrain commonly have high Fe concentrations. These may be responsible for spectral interferences, requiring specific correction procedures. It is generally desirable to analyze for "total" rather than "partial" metal contents, for in such samples the dispersed metals tend to be immobilized within the lattices of fairly resistant minerals such as hematite, goethite or clay minerals, rather than simply adsorbed on clays and amorphous oxides. This statement is not always applicable, of course, for some chemical dispersion is active in all terrains and partial extraction techniques will have value in detecting it.

For techniques such as direct reading emission spectrometry (OES), X-ray fluorescence spectrometry (XRF), neutron activation (NAA) and fire assay fusion, the sample is processed directly. However, some of the most commonly used geochemical analytical techniques, namely colorimetry, atomic absorption spectroscopy (AAS), inductively coupled plasma torch (ICP) and ICP coupled with mass spectrometry (ICP/MS) require the sample to be presented in solution. Irrespective of the accuracy and precision with which the dissolved components can be determined, the efficiency of the dissolution is a crucial step. The suitability of some commonly used acid digestion procedures (hydrofluoric-perchloric acids, nitric-perchloric acids and perchloric acid) followed by AAS was examined by Gedeon et al. (1977), using XRF as an arbiter. The samples were derived from lateritized rocks and had a wide range of mineralogical and chemical compositions. Some results are shown Table A.2-3. The HF-HClO₄ digestion gave the most precise results over the widest ranges. Extractions, except for Cr and V, tend to be close to 100%. The HNO₃-HClO₄ digestion gave better extractions than HClO₄ alone, but both left many minerals only partly dissolved (Table A.2-4). In general, the weaker digestions gave moderately precise, if inaccurate, results for Co, Cu, Fe, Mn, Ni and Zn, especially from the weathered ultramafic rocks in which the concentrations were within the optimum range for AAS analysis. However, since the efficiency of digestion varied between batches, in some cases the precision was poor. All three digestions were clearly unsatisfactory for Cr and V. For both metals, the low solubility of the main host minerals (chromite, fuchsite, hematite and magnetite) is a problem and for V, instrument conditions are difficult. Even when acceptable precisions can be obtained from the weaker acids for certain elements, the results may nevertheless be unsatisfactory, since extractions are not only very poor but tend to vary with sample type (Table A.2-3). Thus, if varying sample types are compared, which is usual during exploration in lateritic terrain and inevitable in studies of whole profiles, the validity of conclusions based on the weaker attack is open to question. Since secondary minerals such as hematite and goethite are not being fully dissolved, secondarily dispersed metals such as Cu, Ni and Zn, held within these minerals, are not being released and the data obtained are incomplete and perhaps distorted. Where the amounts of metals released by the weaker attacks are used as criteria for interpretation, for example in distinguishing between base metal gossans and pseudogossans (Chapter II.2), then the conditions under which the analysis is performed must be controlled as rigorously as possible, so as to obtain truly comparable data.

The appearance of ICP, ICP/MS and NAA has had a major impact on geochemical exploration methods. They provide routine multielement analysis at low cost and also execute some of the specialized demands. As with AAS, ICP systems require dissolution of the sample. Consequently, the problem of residue after acid attack remains very relevant. In order to overcome this problem, fusion followed by acid digestion can be carried out. Nevertheless, no dissolution technique is appropriate for all elements. For example, specific procedures may

TABLE A.2-3

Accuracy of acid digestions. Mean extraction (percent) determined by comparing AAS results (with simultaneous background correction) with XRF results (from Gedeon et al., 1977)

	Cr			Cu			Fe			Ni			Zn		
	HF	NP	PE	HF	NP	PE	HF	NP	PE	HF	NP	PE	HF	NP	PE
Pisoliths in clays (u-m)	55	50	<10	>100	70	15	95	75	10	>100	60	25	>100	50	15
Ferruginous clays (u-m)	55	40	25	95	80	70	100	85	-	>100	95	55	>100	80	45
Silicified clays (u-m)	55	40	25	95	80	70	100	85	-	>100	95	55	>100	80	45
Silicified serpentinite	70	65	30	80	80	65	95	95	40	95	95	75	100	100	70
Saprolite serpentinite	55	55	35	80	75	75	95	90	50	100	100	95	100	90	65
Fresh serpentinite	60	55	45	75	80	80	90	90	45	>100	>100	>100	>100	120	90
Weathered talc-carbonate	55	30	<10	85	65	10	90	65	<10	95	45	<10	85	40	<10
Fresh talc-carbonate	60	60	40	90	85	75	90	70	50	>1100	40	35	90	60	35
Weathered diacite	>100	35	20	90	60	35	80	65	15	>100	35	15	>100	50	25
Saprolitic mica schist	90	25	<10	95	80	35	85	90	25	>100	85	45	>100	90	35
Saprolitic amphibolite	90	35	15	90	70	45	80	70	-	>100	60	45	>100	50	35

HF: hydrofluoric-perchloric acids; NP: nitric-perchloric acids; PE: perchloric acid.

u-m: derived from ultramafic rocks.

TABLE A.2-4

Stability of minerals in some weathered and fresh rocks during nitric-perchloric acid digestion (from Gedeon et al., 1977)

Fully dissolved

Smectites, carbonates, chlorite

Fully or partly dissolved

Serpentine, goethite, hematite

Partly or undissolved

Quartz, talc, muscovite,

Feldspars, amphiboles, kaolinite, chromite, magnetite

be needed to determine elements held in refractory minerals or for those requiring special techniques such as the generation of volatile hydrides (e.g. As, Sb, Bi). Routine analysis by ICP is gradually supplanting AAS except for some specific groups of elements best done by that technique, particularly those for which a graphite furnace provides very low detection limits. The latter include Au, Pt and Pd, routinely analysed by AAS graphite furnace following fire assay fusion. Anodic stripping voltammetry has potential in field analysis for Au and base metals (Lintern et al., 1988 and in press).

Instrumental techniques such as NAA, XRF and OES provide total analysis without dissolution. XRF is almost unrivalled for major element analysis for unweathered rocks but the cost is relatively high; for weathered rocks and soils, lower-cost ICP analyses are quite adequate. Trace element analysis by XRF using pressed powder pellets is particularly suitable for elements in refractory minerals, e.g. Bi, Nb, Sn, Th, U, V, Y, Zr, but only at concentrations exceeding about 5 ppm. NAA is valuable for rare earth elements and also for Au and a range of pathfinder elements such as As, Sb, Mo and W; as such, it may be preferred over more usual procedures such as fire assay and ICP or AAS for this suite of elements. Semi-quantitative OES is now less commonly used, although the detection limit of 1 ppm or less for Ag, Bi and Sn is still difficult to achieve by other methods.

A listing of detection limits for a wide range of elements by commercially available analytical methods is given in Table A.2-5. Specifically, techniques for Au, Pt and Pd analysis are summarized in Table A.2-6. Fire assay and INAA analyses give total contents, whereas Au analyses by aqua regia and alkali cyanide (including BLEG) are only partial. Although the cyanide procedure is closely related to the carbon-in-pulp extraction used in many mines, total analysis is usually considered essential for the evaluation of mineralization and is commonly preferred during exploration. However, the partial extractions are generally satisfactory for exploration in weathered environments unless it is suspected that the gold is shielded from the solutions by silicates or iron oxides. The BLEG procedure, which involves the static leaching of bulk, disaggregated

TABLE A.2-5

Commonly quoted lower limits of detection for a range of trace elements by different analytical procedures

	OES	ICP	ICP-MS	INAA	XRF	AAS
Sb	30		0.1	0.1	4 ^a	1 ^b
As	50			2	2	1 ^b
B		10				
Ba	1	5	10	100	10	
Be	1	1	0.1			
Bi	1		0.2		4 ^a	10
Cd	3		0.2		5 ^a	0.5
Ce		15	0.05	2	10	
Cr	5	10		5	5	
Cs			0.1	1	10	
Co	5	5	1	1	10	5
Cu	1	5			5	2
Ga	1				4	
Ge	3		2		4	
In	10		0.02		15 ^a	
La		5	0.05	0.5	10	
Pb	1		5		4	5
Li		2	0.05			
Mn		15		0.5		5
Hg						0.005 ^b
Mo	3	5	5	0.2	4 ^a	1
Ni		10			5	5
Nb	20	10		0.5	4	
Sc		1		0.1		
Se				5	2	0.1 ^b
Ag	0.1	5		5		0.1
Ta	100	10	0.1	0.5	10	
Te	20				10	0.1 ^b
Th		10	0.05	0.5	5	
Tl	1		0.05		10	10
Sn	1		0.5		4 ^a	
W	50		0.5	5	10	
U		200	0.05	2	3	
V		2			5	
Zn		5		100	5	5
Zr		5	0.01		5	

^a XRF: 2 by long count;

^b AAS: vapour generation.

AAS and ICP data based either on mixed acid digests incorporating HF or on fusions.

but uncrushed samples in cyanide, and concentrating the leachate by zinc precipitation, solvent extraction or adsorption on carbon, may not fully dissolve coarse gold. However, the procedure is very sensitive, permitting the detection of gold at sub-ppb levels, with the large sample giving good sampling statistics.

TABLE A.2-6

Methods in common use to determine Au, Pt and Pd in geological samples (modified after Hall and Bonham-Carter, 1988)

Decomposition	Analysis	Detection limits, ppb			Weight, g
		Au	Pt	Pd	
Pb-FA	F-AAS	5	400	40	30-50
	DCP- or ICP-ES	1	10	2	20
	INAA	1	10	10	30-50
	ICP-MS	1	2	2	10
	ICP-AFS	2	5	2	20
NiS-FA	INAA	1	5	5	25
	ICP-MS	1	1	1	25
AR or HBr-Br ₂	GF-AAS	1	-	-	10-30
NaCN	GF-AAS	1	-	-	10-100
NaCN (BLEG)	F- or GF-AAS	0.005	-	-	2-5 kg
	INAA	0.005	-	-	5 kg
None	INAA	5	-	-	10-30

-: inappropriate or no data.

Glossary:

Pb-FA: Lead fire assay; NiS-FA: Nickel sulphide fire assay;

AR: Aqua regia; BLEG: bulk leach extraction of gold;

F-AAS: Flame atomic absorption spectrometry;

GF-AAS: Graphite furnace atomic absorption spectrometry

ICP: Inductively coupled plasma; DCP: Direct current plasma;

ES: Emission spectrometry; MS: Mass spectrometry;

AFS: Atomic fluorescence spectrometry;

INAA: Instrumental neutron activation analysis

Numerous variations on these procedures have been developed, addressing different sample types and requirements, and having different sensitivity, precision and accuracy.

APPENDIX 3 — PROFILE TERMINOLOGY AND GLOSSARY OF TERMS

PROFILE TERMINOLOGY

There is no universally agreed system for the terminology of deeply weathered regoliths, whether for whole profiles, individual horizons or for many distinctive secondary structures, despite being a subject of discussion for many years. There is a wide range of materials within the regolith, with great variations in mineralogical and chemical composition, fabric and origin, even within a single profile or toposequence. Many of the terms are poorly defined or misapplied, and used in different senses by different authors. Accordingly, comparisons of like situations in widely separated regions are greatly hindered by the inadequacy of the

TABLE A.2-6

Methods in common use to determine Au, Pt and Pd in geological samples (modified after Hall and Bonham-Carter, 1988)

Decomposition	Analysis	Detection limits, ppb			Weight, g
		Au	Pt	Pd	
Pb-FA	F-AAS	5	400	40	30-50
	DCP- or ICP-ES	1	10	2	20
	INAA	1	10	10	30-50
	ICP-MS	1	2	2	10
	ICP-AFS	2	5	2	20
NiS-FA	INAA	1	5	5	25
	ICP-MS	1	1	1	25
AR or HBr-Br ₂	GF-AAS	1	-	-	10-30
NaCN	GF-AAS	1	-	-	10-100
NaCN (BLEG)	F- or GF-AAS	0.005	-	-	2-5 kg
	INAA	0.005	-	-	5 kg
None	INAA	5	-	-	10-30

-: inappropriate or no data.

Glossary:

Pb-FA: Lead fire assay; NiS-FA: Nickel sulphide fire assay;
 AR: Aqua regia; BLEG: bulk leach extraction of gold;
 F-AAS: Flame atomic absorption spectrometry;
 GF-AAS: Graphite furnace atomic absorption spectrometry
 ICP: Inductively coupled plasma; DCP: Direct current plasma;
 ES: Emission spectrometry; MS: Mass spectrometry;
 AFS: Atomic fluorescence spectrometry;
 INAA: Instrumental neutron activation analysis

Numerous variations on these procedures have been developed, addressing different sample types and requirements, and having different sensitivity, precision and accuracy.

APPENDIX 3 — PROFILE TERMINOLOGY AND GLOSSARY OF TERMS

PROFILE TERMINOLOGY

There is no universally agreed system for the terminology of deeply weathered regoliths, whether for whole profiles, individual horizons or for many distinctive secondary structures, despite being a subject of discussion for many years. There is a wide range of materials within the regolith, with great variations in mineralogical and chemical composition, fabric and origin, even within a single profile or toposequence. Many of the terms are poorly defined or misapplied, and used in different senses by different authors. Accordingly, comparisons of like situations in widely separated regions are greatly hindered by the inadequacy of the

TABLE A.3-1
Terminology applied to deeply weathered regoliths having essentially complete, residual (lateritic) profiles

Broad subdivisions	General terms	Preferred terms (This volume)	Alternative Terminologies (Nahon and Tardy, Chapter II.1)	(French: e.g. Leprun, 1981)	(Anand et al., 1989)
Pedolith	Ferruginous zone [Laterite]	Lateritic gravel	Pebbly ferruginous layer		Lateritic gravel
			Pisolitic iron crust		
	[Lateritic ironstone]	Cuirasse (pisolitic, nodular, massive)	Indurated conglomeratic iron crust	Cuirasse [Ferricrete]	Lateritic duricrust (pisolitic, nodular, vermiciform, massive, fragmental)
	[Plinthite]		Soft nodular crust	Carapace nodulaire	
Mottled zone		Mottled (clay) zone	Mottled (clay) zone	Argiles tachetées	Mottled zone
		Plasmic/arenose horizon			
Saprolite (Saprolith)	Saprolite [Pallid zone]	Saprolite	Fine saprolite	Lithomarge Argiles bariolées	Saprolite
			Coarse saprolite	Altération pistache Arène/grus	Saprock
Protolith	Bedrock	Unweathered/fresh bedrock	Bedrock	Roche mere	Fresh rock
	Unweathered rock				

Alternate or descriptive terms in round brackets (...).
Informal or equivocal terms in square brackets [...].

existing terminology and lack of consensus in its use. This is exemplified by the continuing debate on the use of the terms “laterite” and “lateritic profile” (see McFarlane, 1976). It represented a considerable problem in the compilation of this volume and is evident in the numerous general and specific descriptions of weathering profiles given in different chapters. Wherever possible, the same terminology has been applied in an attempt to emphasize the similarities between regolith profiles in widely separated and contrasting environments. However, it has not been practicable or indeed desirable to apply a single system of nomenclature, since neither authors nor editors could have been able to verify its constant application, and incorrect usage may impose an apparent similarity greater than in fact exists.

Some of the principal systems of nomenclature used to describe lateritic regoliths are compared in Table A.3-1, to demonstrate the equivalence between different terminologies adopted in this volume and related literature. Definitions of the principal terms used in this volume are given in the *Glossary of Terms*. A few new, or newly-defined, terms have been used. *Saprock* is introduced by Trescases (Chapter I.2) for the horizon representing the earliest stage of weathering; a maximum of 20% of the weatherable minerals being altered has been suggested as an arbitrary upper limit for this horizon (Anand and Butt, 1988). *Saprock* may be absent or only very thin in some profiles. *Saprolite* may then be considered to be material with more than 20% of weatherable minerals altered, and *saprolith* to include all weathered materials having a lithic fabric, i.e. *saprock* and *saprolite*. *Pedolith* is suggested to describe the (upper) parts of the regolith, above the pedoplasmation front, in which the original lithic fabric, preserved in the *saprolite*, has been destroyed by soil formation and other processes, and a new fabric has been developed. *Plasmic* and *arenose* can be applied to clay- and sand-rich zones, respectively, in which the lithic fabric has been destroyed by settling, compaction and consolidation (Chapter I.6).

The colours of a regolith unit or component are commonly the most readily described attributes, particularly in material obtained by auger, rotary air blast or percussion drilling. Colours are mass properties caused by the combinations of the colours of particles, coatings and cements. Colour may be diagnostic of particular compositions, minerals or weathering environments. However, dramatic variations in colour may be due to quite small changes in the abundance or oxidation state of some components, particularly iron, greatly reducing its usefulness. The description of colours is highly subjective, so that where possible, they should be named using the standard terms employed in the Munsell System, and specified with the Munsell notation when used diagnostically.

GLOSSARY OF TERMS

Alluvium

A general term for clay, silt sand and gravel deposited as a sorted or semi-sorted sediment during comparatively recent geological time on the bed or flood plain of a river or stream. *Adjective*: alluvial.

Accretion

A mass/body produced by overgrowth upon a pre-existing nucleus. Tending to increase by external additions or accumulations. Weathering of a nucleus can also produce skins that have different mineralogical and chemical composition from that of the nucleus.

Altération pistache

French term referring to a green coloured, lower horizon of the saprolite, particularly over basic rock. Characterized by the presence of smectites, especially nontronites.

Altérite

French term, usually synonymous with saprolite. However, for some authors, "altérite" refers less specifically to residual weathered material and "isaltérite" refers to saprolite.

Arène

French term; see *grus*.

Arenose horizon

A sandy horizon, found above the pedoplasmation front, which consists of a grain-supported (or nearly so) fabric. The loss of lithic fabric appears to be caused by solution of weatherable primary and secondary minerals and settling of resistant minerals, dominantly quartz (cf. *plasmic horizon*).

Argiles bariolées

French term, "variegated clay" zone. Refers to typical thick, soft clay-rich saprolites consisting of more or less sandy and pale clays, with fine violet and red spots and flecks derived from the weathering of ferromagnesian minerals.

Argiles tachetées

French term, "mottled clay" zone; see *mottled zone*.

Bauxite

Economic term; an ore of aluminium. Lateritic bauxites are highly aluminous facies of the upper horizons of lateritic regoliths. Bauxites may form on any source rock, but most typically on basalts, syenites, marls and shales, in freely drained, strongly leached environments. They contain abundant Al hydroxides (gibbsite, less commonly boehmite, diaspore) and Al-rich Fe oxides and hydroxides and may have similar pisolitic and nodular fabrics to equivalent ferruginous zones of less strongly leached regoliths.

Calcrete

An generally indurated material formed by the in situ cementation or replacement, or both, of pre-existing regolith by calcite and/or dolomite precipitated

from soil water or groundwater. They vary widely in carbonate content and properties, from friable, fine grained soils to coarse nodular horizons to limestone rock. There are two principal genetic types, namely (1) pedogenic or vadose calcretes and (2) groundwater or phreatic calcretes.

Caliche

Spanish–North American term used synonymously for calcrete.

Cap rock

The weathered product of disseminated sulphide mineralization, (particularly porphyry Cu–Au–Mo deposits) which may be ferruginous (i.e. an ironstone) or siliceous (i.e. silcrete).

Carapace nodulaire

French term referring to the lower, poorly indurated horizon of the ferruginous zone of a laterite profile. Consists of ferruginous nodules and pisoliths in a weakly cemented matrix of kaolinite and Fe oxides and oxyhydroxides.

Cellular

Fabric consisting of irregular to rounded bladder, cell or bubble shaped voids, especially in lateritic duricrust.

Cementation front

A transformation front resulting in cementation by introduced components such as oxides and oxyhydroxides of Al, Fe and Mn, silica and Ca or Mg carbonates.

Cobbles

Fragments with a high sphericity, ranging in diameter from 60 to 200 mm.

Colluvium

A general term for deposits on slopes or at the base of slopes that have been transported chiefly by mass flow. May be extended to include material that has been transported across surfaces by sheetwash, i.e. flowing water not confined to specific channels. *Adjective*: colluvial.

Concretion

A hard, compact mass/aggregate of mineral matter, round or irregular in shape and usually different in composition from the substrate on which it occurs. In this sense, “concretion” is a general term which includes both pisoliths and nodules. Concretions are thought to be formed by precipitation from solution about a nucleus or centre.

Cortex

An outer layer or skin; applied to the outer layers of concretions.

Cuirasse

French term, "ironcrust". Highly indurated facies or horizon of the ferruginous zone of a lateritic regolith, with a massive, pisolitic, nodular or vesicular fabric. Synonymous with lateritic duricrust.

Cutan

A modification of the texture, structure or fabric of a soil material at a natural surface due to the concentration of particular constituents; e.g. argillan-clay cutan or clay skin.

Duricrust

Indurated materials at or just below the surface. The material may be ferruginous, aluminous, siliceous or calcareous, or a combination of these. Siliceous and calcareous materials are normally referred to as silcrete and calcrete respectively.

Eluviation

Movement of soil material from a soil horizon. Refers particularly to solids, especially colloidal particles. *Adjective*: eluvial; cf. Illuviation.

Fabric

The physical nature of a regolith unit or component according to the spatial arrangement, orientation (or lack of it) and mutual relationships of the discrete elements such as particles, crystals, cements and voids of which it is composed. Fabric refers to the smaller (microscopic and mesoscopic) features; the term structure is used for larger features. Used in preference to "texture".

Facet

An homogeneous element of a landscape, defined in terms of the slope, material and drainage conditions in which it is developed. The facet is the smallest unit of an ad hoc hierarchical system of landsurface classification, in which combinations of facets are termed landforms and combinations of landforms are termed land systems.

Ferralsol, ferrallitic soil, sol ferrallitique

Humid tropical soil characterized by a high Fe oxide content, formed by the leaching of silica and bases. Commonly used synonymously for laterite, latosol, oxisol.

Ferricrete

A conglomerate of surficial sands and gravels cemented by Fe "salts" (Lampugh, 1902); more generally, indurated material formed by the in-situ cementa-

tion or replacement, or both, of pre-existing regolith by Fe oxides and oxyhydroxides precipitated from soil water or groundwater. The fabric, mineralogy and composition of ferricretes may reflect those of the parent (regolith) material and hence, if residual, the underlying lithology. Some authors restrict the term to the ferruginous horizon of lateritic regoliths (synonymous with cuirasse, lateritic duricrust) but the more general definition is preferred.

Gossan

The weathered expression of rocks that contained substantial matrix or massive sulphide mineralization. Because these are commonly Fe sulphides, the resultant gossans are rich in Fe oxides and oxyhydroxides and are therefore a form of ironstone. Those gossans formed by weathering of Fe-poor sulphides (e.g. carbonate-hosted Pb–Zn deposits) will give Fe-poor gossans; such gossans may be siliceous or have a high Mn-content. The term *gossan* has no economic connotation, nor does it describe the mode of occurrence.

Barren gossans: formed by the weathering of Fe sulphides containing no elements of economic significance (commonly refers to base metals).

Direct gossan: formed in situ (synonym: indigenous).

False gossan: a discrete ferruginous outcrop (ironstone) with a fabric and/or composition suggestive of a gossan, but not developed over sulphides (synonym: pseudogossan).

Fertile gossans: formed by weathering of sulphides (commonly of base metals) of potential economic significance.

Fossil gossan: formed during an earlier weathering episode; particularly applies to gossans buried by later sedimentary or volcanic events.

Pseudogossan: see false gossan.

Solution-deposited gossan: an accumulation of hydromorphically transported Fe oxides derived from a sulphide source. It may occur within a gossan profile or some distance away (synonym: leakage gossan).

Translocated gossan: gossan that has been mechanically moved. It may subsequently have been recemented.

Gravel

Fragments ranging in dimensions from 2 mm to 60 mm in diameter. “Gravel” is a size fraction, commonly used colloquially in Australia to refer to pisoliths, nodules and hardened mottles, and includes fragments that are of irregular shape. Recommended use only with qualifier, e.g. lateritic gravels, lithic gravels.

Grus

Fragmental disintegration product of largely unweathered granitic rocks. Commonly applied to surface products, but also present as a porous horizon ranging from a few centimetres to 10 m or more thick at the base of saprolite. In the French literature, *grus* or “arène” are used to designate such horizons over any lithology. *Grus* differs from saprock in that it is friable rather than compact.

Hardpan

A subsurface indurated horizon. Red-brown hardpans in Australia are characterized by the presence of a porous matrix, commonly red-brown in colour, cemented by silica (commonly hyalite), in a variety of transported or residual host materials.

Horizon

A layer within the regolith approximately parallel to the landsurface and differing from adjacent, genetically related, layers in physical, chemical and/or biological properties, or in characteristics such as colour, pH, structure, fabric, texture, consistency, and types and number of organisms. Common soil horizons include:

O: Upper horizon containing fibrous (peaty) or massive organic matter.

A: Near-surface mineral horizon containing humified organic matter.

E (formerly A2): pale, commonly sandy, eluvial horizon with little organic matter, with sesquioxides and clays leached or translocated to lower horizons.

B: illuvial horizons enriched in clay, and/or sesquioxides and/or organic matter derived from overlying horizons. (N.B. the term "B horizon" should not be used to refer to the ferruginous zone of the lateritic profile.)

C: mineral horizon from which the solum is presumed to have been derived but that has been little affected by active pedogenic processes.

Illuviation

The process of deposition of soil material moved from one horizon to another within the soil; usually from an upper to a lower horizon within a profile, but also laterally within a toposequence. Refers particularly to solids, especially colloidal particles. *Adjective*: illuvial; cf. Eluviation.

Ironstone

Highly ferruginous weathered material consisting mainly of Fe oxides and oxyhydroxides, with variable amounts of Al hydroxides, silica and phyllosilicates:

(1) forming an horizon of a laterite profile and essentially conformable with the land surface, i.e. lateritic ironstone or duricrust;

(2) essentially linear in outcrop pattern, following an underlying geological unit or structure. Ironstones formed over weathering sulphide mineralization are gossans. Ironstones enriched in target elements but not derived principally from weathering sulphides have been termed false gossans or pseudogossans.

Lateritic ironstone: see cuirasse, duricrust.

Leakage ironstones—contact, fault and drainage ironstones: ironstones that form where dissolved Fe, commonly as the reduced ferrous (Fe^{2+}) ion, is oxidized as the solutions encounter an O_2 -rich environment and the resultant Fe^{3+} is hydrolyzed and precipitates. The Fe, originally derived from the weathering of Fe-bearing minerals, is precipitated at depth along joints, lithological contacts and faults, and at the surface in seepage areas and in drainage ironstones.

Stratigraphic ironstones: in-situ weathering products of Fe-rich lithologies.

Isaltérite

French term, synonymous with saprolite; cf. Altérite.

Lag

A veneer or pavement of fragments of diverse origins or composition on the land surface. Commonly applied to highly ferruginous concretions. Fragments may be faceted, rounded or varnished.

Landform

An landscape feature having a distinctive morphology, the development of which can be related to particular processes or structures. A specific combination of facets.

Land system

A repeated association or pattern of landforms characteristic of a terrain.

Laterite

(Latin *later* = brick, tile). A highly weathered material, depleted in alkalis and alkaline earths, composed primarily of secondary oxides and oxyhydroxides of Fe (goethite, hematite, maghemite), and hydroxides of aluminium (e.g. gibbsite). The oxides of Fe and Al may contain other minerals including clays and other secondary minerals (kaolinite, halloysite, anatase, rutile), resistant primary minerals (quartz, zircon, etc.) and weatherable primary minerals (ilmenite, muscovite). The laterite horizon is hard or subject to hardening upon exposure. The term "laterite" is used by some authors to refer to the whole lateritic weathering profile (ferruginous zone, mottled zone, saprolite) but the restricted usage, applying to the ferruginous/aluminous horizon only, is more common. It is, perhaps, best considered as an informal term. *Adjective*: lateritic.

Lithic

Pertaining to stone or rock. *Lithic fabric*: rock fabric; applied to fresh or weathered materials (e.g. saprolite, lithorelics) that retain the original fabric. Where weathered, most or all of the primary minerals are pseudomorphed by secondary minerals.

Lithomarge

Compact, massive, usually kaolinitic clay. Sometimes applied in the French and Indian literature to clay-rich zones of the regolith, particularly in the upper saprolite.

Lithorelic

A discrete, highly weathered fragment or entity having a primary, lithic fabric. Usually applied where the bulk of the material in which it occurs has a secondary

fabric (e.g. a lithorelic may form the core of a nodule). A *lithorelict* is an unweathered fragment in an assemblage of secondary minerals.

Litter

Freshly fallen plant (or animal) matter on the ground surface.

Massive

Homogenous, without visible internal fabric.

Microaggregation (front)

A transformation (front) resulting in the development of a microaggregated fabric in friable soil.

Mottles

Spots, blotches or streaks of subdominant colours different from the matrix colour and also different from the colours of nodules and pisoliths. Mottles commonly have diffuse boundaries and differ in mineralogical composition from nodules, pisoliths and matrix.

Mottled zone

An horizon, generally within the pedolith, characterized by localized spots, blotches and streaks of Fe oxides and oxyhydroxides that, with further mobilization and concentration, become reorganized into secondary structures. Nodule growth progressively destroys pre-existing fabrics, although microfabrics may be preserved in the nucleus.

Nodule

A small, irregularly shaped mass of mineral substance, usually rounded but may be re-entrant, and less than 60 mm in diameter, commonly, but not necessarily, with an outer skin or cortex. The majority of nodules observed in a lateritic profile are less than 40 mm in diameter. As sphericity increases, the terms "lateritic nodule" and "lateritic pisolith" merge. Lateritic nodules form by the precipitation of Fe oxides in pores. Where the process is initiated in the saprolite or saprolitic blocks, primary rock fabrics may be preserved as lithorelics in the core. Where initiated in material that has undergone consolidation or other reorganization, the secondary fabric may be preserved.

Oolith

Oolith is similar to pisolith but with a diameter of less than 2 mm.

Pallid zone

Descriptive term, generally referring to bleached kaolinitic zones of the pedolith and saprolith occurring below the ferruginous and mottled zones of

some lateritic profiles, usually over felsic rocks. Use of the term is not recommended.

Pedogenesis

Soil formation. *Adjective*: pedogenic.

Pedolith

Upper part of the regolith, above the pedoplasation front, that has been subjected to soil forming processes resulting in the loss of the fabric of the parent material and the development of new fabrics, including secondary structures such as pisoliths. The pedolith may develop from residuum, i.e. from saprolite, saprock or bedrock, or from transported overburden.

Pedoplasation front

Transformation front at which the lithic fabric is destroyed, although commonly with little chemical reworking (pedoplasation, Flach et al., 1968). It forms the boundary between the saprolite (or saprolith) and pedolith in deeply weathered profiles.

Pedoturbation

Mixing of soil components, other than caused by illuviation, e.g. that due to biological activity and to self-churning in vertisols.

Pisolith

A spherical or ellipsoidal concretionary or accretionary body resembling a *pea* in shape and limited in size to bodies of over 2 mm diameter. It can have a concentric internal structure but concentric lamination is not diagnostic; however, most pisoliths have an outer cortex or skin.

Plasmic horizon

The horizon in which the lithic fabric of the saprolite (or saprock) has been replaced by a new, mesoscopically homogeneous, *plasmic* fabric, above the pedoplasation front. The loss of lithic fabric is caused by solution and authigenesis of minerals and the mechanical processes such as shrink and swell of clays and settling of resistant primary and secondary minerals through instability induced by leaching. It consists of massive clays or silty clays over rocks poor in quartz; a sandy arenose horizon (qv) forms over quartz-rich rocks. Major structural features, such as quartz veins and lithological contacts, may be preserved, possibly with change in orientation (dip).

Plinthite

Iron-rich, humus-poor mixture of clay, commonly occurring as mottles, firm but uncemented when moist but hardening irreversibly into an ironstone hardpan

or irregular aggregates on repeated wetting and drying. Used synonymously for lateritic duricrust or cuirasse by some authors.

Protolith

General term for parent material from which the regolith has formed.

Reg

Desert pavement consisting of wind-polished angular gravel- to cobble-sized rock debris, commonly with coatings of desert varnish.

Regolith

The entire unconsolidated and secondarily recemented cover that overlies the more coherent bedrock and that has been formed by the weathering, erosion, transport and/or deposition of older material. The regolith thus includes fractured and weathered basement rocks, saprolites, soils, organic accumulations, glacial deposits, colluvium, alluvium, evaporitic sediments, loess and aeolian deposits. May be subdivided into a lower unit, the saprolith, and an upper unit, the pedolith.

Relic

A memorial. Commonly applied to original fabrics or textures that remain visible after the replacement of pre-existing minerals.

Relict

A survivor. A species (plant, animal, mineral) in a changed environment; e.g. a primary mineral, especially a weatherable one, present within a predominantly secondary mineral assemblage.

Saprock

Compact, slightly weathered rock with low porosity; less than 20% of weatherable minerals altered. Weathering effects are present mainly at the microsites of contacts between minerals and intramineral fissures, along shears and fractures through the rock as a whole or affecting only a few individual mineral grains or mineral species.

Saprolite

Weathered bedrock in which fine fabrics, originally expressed by the arrangement of the primary mineral constituents of the rock (e.g. crystal, grains), are retained. Compared to saprock (qv), material with more than 20% of weatherable minerals altered. Saprolite may be extended to include weathered rocks in which only larger structures such as bedding, schistosity, veining or lithological contacts are preserved. The presence of saprolite implies that weathering has been essentially isovolumetric. (*Coarse saprolite*: saprolite containing blocks or remnants of unweathered rock; *fine saprolite*: saprolite without blocks or remnants of unweathered rock.)

Saprolith

That part of the regolith with a lithic fabric and potentially subdivisible into horizons, e.g. saprock and saprolite. (cf. Pedolith).

Silcrete

Strongly silicified, indurated regolith components, generally of low permeability, commonly having a conchoidal fracture with a vitreous lustre. They appear to represent the complete or near-complete silicification of a precursor regolith horizon by the infilling of available voids, including fractures. They may be classified broadly into pedogenic or groundwater types. Most are dense and massive, but some may be cellular, with boxwork fabrics. The fabric, mineralogy and composition of silcretes may reflect those of the parent (regolith) material and hence, if residual, the underlying lithology. Thus, silcretes over granites and sandstones have a floating or terrazzo fabric and tend to be enriched in Ti and Zr; silcretes with lithic fabrics (e.g. on dunites) are silicified saprolites with initial constituents diluted or replaced by silica.

Soil

Upper part of the regolith, commonly defined as that which supports plant life. In particular, refers to those surface horizons reacting to the present environment; *palaeosols* are soils that formed under past environmental conditions.

Solum

The upper and most weathered part of the soil profile; the A and B horizons.

Surface degradation front

Transformation front in the topsoil resulting from dissolution and leaching due to the presence of biochemical compounds and a contrasting moisture regime.

Texture

The physical nature of a regolith unit or component according to the proportions of different size fractions (e.g. sand, silt, clay). For physical characteristics related to the spatial arrangement of the constituents at the microscopic and mesoscopic scale, the term "fabric" is preferred.

Transformation front

The advancing boundary of a change (or transformation) in the composition or other property of the regolith due to changes in physico-chemical conditions.

Transported overburden

General term referring to material of exotic or redistributed origin such as alluvium, colluvium, sheetwash, evaporitic sediments, aeolian clay (parna or loess), piedmont fan deposits and glacial debris that blanket fresh or weathered

bedrock. It may be friable or partially or wholly consolidated, cemented by iron oxide, silica, carbonates, gypsum or clays.

Ultra-desiccation front

A transformation front resulting from the imposition of very dry conditions which causes the dissociation of stable clay-oxyhydroxide bonds and the collapse of the soil microfabric.

Vermiform

A fabric consisting of tubes, pipes or worm-shaped voids.

Vesicle

A small cell- or bubble-shaped void. *Adjective*: vesicular.

Weathered bedrock

General term used to denote rock that has been chemically altered but which is still coherent, has some original structural elements preserved and is essentially in situ, with no lateral physical movement having taken place (cf. Saprolite, Saprock).

Weathering front

The transformation front marking the commencement of weathering at the base of the regolith. The rock-saprock interface.

REFERENCES

- Aicard, P., 1959. The application of geochemical methods (Cr and Ni) to prospecting for kimberlite pipes. *Ann. Mines*, 103–110.
- Aleva, G.J.J., 1983. On weathering and denudation of humid tropical valley interfluvial and their triple planation surfaces. *Geol. Mijnbouw*, 62: 383–388.
- Alexander, M.A., 1977. *Introduction to Soil Microbiology*. Wiley, New York, 467 pp.
- Ambrosi, J.P., 1984. *Pétrologie et Géochimie d'une Séquence de Profils Latéritiques Cuirassés Ferrugineux de la Région de Diouga, Burkina Faso*. Ph.D. Thesis, University of Poitiers (unpublished), 223 pp. (In French).
- Ambrosi, J.P. and Nahon, D., 1986. Petrological and geochemical differentiation of lateritic iron crust profiles. *Chem. Geol.*, 57: 371–393.
- Ambrosi, J.P., Nahon, D. and Herbillon, A.J., 1986. A study of the epigenetic replacement of kaolinite by hematite in laterite-petrographical evidences and a discussion on the mechanism involved. *Geoderma*, 37: 283–294.
- Anand, R.R. and Butt, C.R.M., 1988. *The Terminology and Classification of the Deeply Weathered Regolith*. Discussion paper, CSIRO Australia, Division of Exploration Geoscience, Floreat Park (unpublished), 29 pp.
- Anand, R.A. and Gilkes, R.J., 1987. The association of maghemite and corundum in Darling Range laterites, Western Australia. *Aust. J. Soil Res.*, 35: 303–311.
- Anand, R.R., Churchward, H.M. and Smith, R.E., 1991. *Regolith-landform Development and Siting and Bonding of Elements in Regolith Units, Mt. Gibson District, Western Australia*. Restricted Report 165R, CSIRO, Australia, Division of Exploration Geoscience, Perth, 95 pp. (Unpublished).
- Anand, R.R., Gilkes, R.J., Armitage, T.M. and Hillyer, J.W., 1985. Feldspar weathering in a lateritic saprolite. *Clays Clay Miner.*, 33: 31–43.
- Anand, R.R., Smith, R.E., Innes, J. and Churchward, H.M., 1989. *Exploration Geochemistry about the Mt. Gibson Gold Deposits, Western Australia*. Restricted Report, 20R, CSIRO Australia, Division of Exploration Geoscience, Perth, 93 pp.
- Andrew, R.L., 1980. Supergene alteration and gossan textures of base-metal ores in Southern Africa. *Miner. Sci. Eng.*, 12: 193–215.
- Andrew, R.L., 1984. The geochemistry of selected base-metal gossans, southern Africa. In: R. Davy and R.H. Mazzucchelli (Editors), *Geochemical Exploration in Arid and Deeply Weathered Terrains*. *J. Geochem. Explor.*, 22: 161–192.
- Ashikhmin, A.A., Kuznezov, S.V. and Shmariovich, E.M., 1983. *Preservation and Concentration of Uranium Ore Mineralization in Zones of Weathering*. Plenum, New York pp. 364–373. (Also *Litol. Polezn. Iskop.* (translated), 4: 58–68).
- Awasthi S.C. and Lal J.K., 1981. Geology and geochemistry of sulphide mineralization in Teejanwani Hill, Mahendragarh District, Haryana. *Geol. Surv. India, Rep.*, 112: 17–24.
- Aye, F., Cheze, Y. and Abbass, M., 1985. Discovery of a major massive sulphide province in northeastern Sudan. In: *Prospecting in Areas of Desert Terrain*. Institute of Mining and Metallurgy, London, pp. 43–48.
- Baes, C.F. and Mesmer, R.E., 1976. *The Hydrolysis of Cations*. Wiley, New York, 487 pp.
- Bailey, L.K. and Peters, E., 1976. Decomposition of pyrite in acids by pressure leaching and anodization: the case for an electrochemical mechanism. *Can. Metall. Q.*, 15: 333–344.
- Baker, W.E., 1973. The role of humic acids from Tasmanian podzolic soils in mineral degradation and metal mobilization. *Geochim. Cosmochim. Acta*, 37: 269–281.

- Baker, W.E., 1978. The role of humic acid in the transport of gold. *Geochim. Cosmochim. Acta*, 42: 645–649.
- Ball, L.C., 1908. Cloncurry copper mining district. *Geol. Surv. Queensl., Publ.*, 215: 242–255.
- Baranova, N.N. and Ryzhenko, B.N., 1981. Computer simulation of the Au-Cl-S-Na-H₂O system in relation to the transport and deposition of gold in hydrothermal processes. *Geochem. Int.*, 18(4): 46–60.
- Barbier, J., 1987. Arid environment geochemical exploration in Saudi Arabia. The problem of aeolian contamination. *J. Geochem. Explor.*, 27: 29–51.
- Bardossy, G., 1982. *Karst Bauxites*. Elsevier, Amsterdam, 441 pp.
- Bardossy, G., 1983. A comparison of the main lateritic bauxite regions of our globe. In: A.J. Melfi and A. Carvalho (Editors), *Lateritisation Processes*. University of Sao Paulo Press, Sao Paulo, pp. 15–51.
- Barnes, J.F.H., 1987. Practical methods of drill hole sampling. In: *Meaningful Sampling in Gold Exploration*. Bulletin, 7. Australian Institute of Geoscientists, Sydney, pp. 145–170.
- Barretto, P.M.C., 1985. Sedimentary and tectonic environments for uranium mineralization in the Parana Basin, Brazil. In: *Geological Environments of Sandstone-type Uranium Deposits*. International Atomic Energy Agency, Vienna, pp. 173–194.
- Barron, C.N., 1982. Exploration characteristics of the Muri Mountains alkaline complex, Guyana–Brazil border. In: D.J.C. Laming and A.K. Gibbs (Editors), *Hidden Wealth: Mineral Exploration Techniques in Tropical Forest Areas*. Report No. 7. Association of Geoscientists for International Development, Bangkok, pp. 196–201.
- Barron, E.J., 1983. A warm, equable Cretaceous: the nature of the problem. *Earth-Sci. Rev.*, 19: 305–308.
- Barton, P.B., 1956. Fixation of uranium in the oxidized base metal ores of Goodspring district. *Econ. Geol.*, 51: 178–191.
- Berner, R.A., 1981. Kinetics of weathering and diagenesis. In: A.C. Lasaga and R.J. Kirkpatrick (Editors), *Kinetics of Geochemical Processes*. Reviews in Mineralogy, 8. Mineralogical Society of America, pp. 111–134.
- Berner, R.A. and Holdren, G.R. Jr., 1979. Mechanism of feldspar weathering, II. Observations of feldspars from soils. *Geochim. Cosmochim. Acta*, 43: 1173–1186.
- Berner, R.A., Sjoberg, E.L., Velbel, M.A. and Krom, M.D., 1980. Dissolution of pyroxenes and amphiboles during weathering. *Science*, 207: 1205–1206.
- Berner, W., Lasaga, A. and Garrels, R.M., 1983. The carbonate-silicate geochemical cycle and its effect on atmospheric carbon dioxide over the past 100 million years. *Am. J. Sci.*, 283: 641–683.
- Bianconi, F., 1987. Uranium geology of Tanzania. In: G. Friedrich and R. Gatzweiler (Editors), *Uranium Mineralization*. Monograph Series on Mineral Deposits, 27. Borntraeger, Berlin, pp. 11–25.
- Birot, P., 1968. *The Cycle of Erosion in Different Climates*. (Trans: C.I. Jackson and K.M. Clayton). Batsford, London, 144 pp.
- Blain, C.F., 1981. *Geochemistry of the Gossans of Wadi Wassat, Kingdom of Saudi Arabia*. Miscellaneous Document, 25. U.S. Geological Survey, Saudi Arabia Mission.
- Blain, C.F. and Andrew, R.L., 1977. Sulphide weathering and the evaluation of gossans in mineral exploration. *Miner. Sci. Eng.*, 9: 119–150.
- Blake, D.H., 1987. *Geology of the Mount Isa Inlier and Environs, Queensland and Northern Territory*. Bulletin, 225. Bureau of Mineral Resources, Canberra, 83 pp.
- Blanchard, R., 1939. Interpretation of leached outcrops. *J. Chem. Soc. S. Africa*, 39: 344–372.
- Blanchard, R., 1944. Chemical and mineralogical composition of twenty typical limonites. *Am. Mineral.*, 29: 111–114.
- Blanchard, R., 1968. *Interpretation of Leached Outcrops*. Bulletin, 66. Nevada Bureau of Mines, University of Nevada, Reno, 196 pp.
- Bland, C.J. and Levinson, A.A., 1986. Non-significant anomalies in the search for uranium in Saskatchewan, Canada. *Appl. Geochem.*, 1: 249–253.

- Bloomfield, K., Reedman, J.H. and Tether, J.G.G., 1971. Geochemical exploration of carbonarite complexes in Uganda. In: R.W. Boyle and J.I. McGerrigle (Editors), *Geochemical Exploration*. Special Volume, II. Canadian Institute of Minerals and Metallurgy, pp. 85–102.
- Blot, A., Carn, M., Leprun, J.C. and Pion, J.C., 1976. Premier bilan des études géologiques et pédologiques d'un corps ultrabasique et de son contexte: Koussane au Sénégal oriental. *Cah. ORSTOM, Ser. Pedol.*, VIII: 113–145. (In French).
- Blot, A., Leprun, J.C. and Pion, J.C., 1978. Corrélations géochimiques entre les cuirasses ferrugineuses et les roches du socle cristallin au Sénégal et en Haute Volta. Lithodépendance et héritage géochimique. *C. R. Acad. Sci., Paris*, 286. (In French).
- Bocquier, G., 1971. *Génèse et Evolution de Deux Toposequences de Sols Tropicaux du Tchad. Interprétation Biogéodynamique*. Mémoire 62. ORSTOM, Paris, 350 pp. (In French).
- Bocquier, G., Boulangé, B., Ildefonse, P., Nahon, D. and Muller, D., 1983. Transfers, accumulation modes, mineralogical transformations and complexity of historical development in lateritic profiles. In: A.J. Melfi and A. Carvalho (Editors), *Lateritisation Processes*. University of Sao Paulo Press, Sao Paulo, pp. 331–343.
- Bocquier, G., Muller, J.P. and Boulangé, B., 1984. Les latérites. Connaissances et perspectives actuelles sur les mécanismes de leur différenciation. In: *Livre Jubilaire du Cinquantenaire*. Association Française pour l'Etude du Sol, Paris, pp. 123–138. (In French).
- Boenigk, W., 1983. *Schwermineralanalyse*. F. Enke, Stuttgart, 158 pp. (In German).
- Bokilo, J.F., Bernat, M. and Muller, J.P., 1988. Short living isotopes disequilibria in mineral phases of a laterite weathered profile. *Chem. Geol.*, 70: 124. (Abstract).
- Bolviken, B., 1979. The redox potential field of the earth. In: L.H. Ahrens (Editor), *Origin and Distribution of the Elements*. Pergamon Press, Oxford, pp. 649–665.
- Bose, S.S., 1982. Studies on some aspects of geochemical prospecting for sulphide mineralization in Kesarpur area, Mayurshanj District, Orissa. In: *Proceedings of the Symposium on Geochemical Prospecting and Techniques*. Special Publication, 8. Geological Survey of India, pp. 229–237.
- Bose, S.S., 1984. A geochemical approach to delineate target areas for copper mineralisation around Kesarpur in Northern Orissa, India. *J. Geol. Soc. India*, 25: 475–483.
- Boulangé, B., 1984. *Les Formations Bauxitiques Latéritiques de Côte d'Ivoire. Les Facies, Leur Transformation, Leur Distribution et l'Evolution du Modèle*. Travaux et Documents, 175. ORSTOM, Paris, 363 pp. (In French).
- Boulet, R., 1970. La géomorphologie et les principaux types de sols en Haute Volta septentrionale. *Cah. ORSTOM, Ser. Pedol.*, 8: 245–271. (In French).
- Boulet, R., 1974. *Toposéquences de Sols Tropicaux en Haute Volta. Equilibre et Déséquilibre Pédobioclimatique*. Mémoire, 85. ORSTOM, Paris, 272 pp. (In French).
- Boulet, R., 1978. Existence de systèmes à forte différenciation latérale en milieu ferrallitique guyanais: un nouvel exemple de couvertures ferrallitiques en déséquilibre. *Sci. Sol*, 2: 75–82. (In French).
- Boulet, R., Chauvel, A. and Lucas, Y., 1984. Les systèmes de transformation en pédologie. In: *Livre Jubilaire du Cinquantenaire*. Association Française pour l'Etude du Sol, Paris, pp. 167–179. (In French).
- Bowden, J.W., Posner, A.M. and Quirk, J.P., 1980. Adsorption and charging phenomena in variable charge soils. In: B.K.G. Theng (Editor), *Soils with Variable Charge*. Special Publication. New Zealand Society of Soil Science, pp. 147–166.
- Bowles, J.F.W., 1986. The development of platinum group metals in laterites. *Econ. Geol.*, 81: 1278–1285.
- Bowles, J.F.W., 1988. Mechanical and chemical modification of alluvial gold. *Australas. Inst. Min. Metall. Bull.*, 293: 9–11.
- Boyle, R.W., 1974. *Elemental Associations in Mineral Deposits and Indicator Elements of Interest in Geochemical Prospecting*. Paper 74–75. Geological Survey of Canada, Ottawa, 40 pp.
- Boyle, R.W., 1979. The geochemistry of gold and its deposits. *Geol. Surv. Can., Bull.*, 280: 584.

- Boyle, R.W., 1982. *Geochemical Prospecting for Thorium and Uranium Deposits*. Elsevier, Amsterdam, 498 pp.
- Boyle, R.W., Alexander, W.M. and Aslin, G.E.M., 1975. *Some Observations on the Solubility of Gold*. Paper 75-24. Geological Survey of Canada, 6 pp.
- Brabant, P. and Gavaud, M., 1985. *Atlas des Sols du Nord-Cameroun*. ORSTOM, Paris. (In French).
- Brabham, G.R., Coxhell, S., O'Shea, A. and Ross, A.F., 1990. Geological setting of primary gold-silver deposits, Mt Gibson, Western Australia. *Tenth Australian Geological Convention*, Hobart, Abstracts Volume 25. Geological Society of Australia, Sydney, pp. 150-151. (Abstract).
- Bradshaw, P.M.D., 1975. Conceptual models in exploration geochemistry—The Canadian Cordillera and Canadian Shield. *J. Geochem. Explor.*, 4: 1-213.
- Brimhall, G.H. and Dietrich, W.E., 1987. Constitutive mass balance relations between chemical composition, volume, density, porosity, and strain in metasomatic hydrochemical systems: results on weathering and pedogenesis. *Geochim. Cosmochim. Acta*, 51: 567-587.
- Brinkman, R., 1970. Ferrololysis, a hydromorphic soil forming process. *Geoderma*, 3: 199-206.
- Brock, P.W.G., 1973. Follow-up and interpretation of reconnaissance geochemical survey in North Karamoja, Uganda. *Overseas Geol. Miner. Resour.*, 41: 45-60.
- Brookins, D.G., 1988. *Eh-pH Diagrams for Geochemistry*. Springer, Berlin, 176 pp.
- Brown, A.G., 1970. *Dispersion of Copper and Associated Trace Elements in a Kalahari Sand Environment, Northwest Zambia*. Ph.D. Thesis, Imperial College, London University (unpublished), 283 pp.
- Buchanan, F., 1807. In: *A Journey from Mandras through the Countries of Mysore, Kanara and Malabar, Volume 2 and Volume 3*. East India Co., London, Volume 2: pp. 436-461, 559; Volume 3: 66, 89, 251, 258, 378.
- Budel, J., 1968. Geomorphology—principles. In: R.W. Fairbridge (Editor), *Encyclopaedia of Geomorphology*. Reinhold, New York, pp. 416-422.
- Budel, J., 1982. *Climatic Geomorphology*. (Trans: L. Fischer and D. Busch). Princeton University Press, Princeton, 443 pp.
- Bugg, S.F., 1982. Lead-zinc deposits of the Coast Province of Kenya, and some exploration guidelines. *Overseas Geol. Miner. Resour.*, 59., 20 pp.
- Bugrov, V., 1974. Geochemical sampling techniques in the eastern desert of Egypt. *J. Geochem. Explor.*, 3: 67-75.
- Bugrov, V.A. and Shalaby, I.M., 1975. Geochemical prospecting in the eastern deserts of Egypt. In: I.L. Elliott and W.K. Fletcher (Editors), *Geochemical Exploration 1974*. Developments in Economic Geology, 1. Elsevier, Amsterdam, pp. 523-530.
- Bull, A.J. and Mazzucchelli, R.H., 1975. Application of discriminant analysis to the geochemical evaluation of gossans. In: I.L. Elliott and W.L. Fletcher (Editors), *Geochemical Exploration 1974*. Developments in Economic Geology, 1. Elsevier, Amsterdam, pp. 219-226.
- Busche, D. and Erbe, W., 1987. Silicate karst landforms of southern Sahara (north-eastern Niger and southern Lybia). In: M.J. McFarlane (Editor), *Laterites: Some Aspects of Current Research*. *Z. Geomorphol., Suppl.*, 64: 55-72.
- Busemberg, E. and Clemency, C.V., 1976. The dissolution kinetics of feldspars at 25 degrees C and 1 atm CO₂ partial pressure. *Geochim. Cosmochim. Acta*, 40: 41-50.
- Butt, C.R.M., 1979. Geochemistry of a pseudogossan developed on a black shale-dolerite contact, Killara, Western Australia. *J. Geochem. Explor.*, 11: 131-156.
- Butt, C.R.M., 1981. Some aspects of geochemical exploration in lateritic terrains in Australia. In: *Lateritisation Processes*. Oxford and IBH Publishing Co., New Delhi, pp. 369-380.
- Butt, C.R.M., 1985. Granite weathering and silcrete formation on the Yilgarn Block, Western Australia. *Aust. J. Earth Sci.*, 32: 415-432.
- Butt, C.R.M., 1986. *Platinum Group Elements in Weathered Ultramafic Rocks at Mt. Keith*. Restricted Report, MG 3R. CSIRO Australia, Division of Minerals and Geochemistry, Perth, 17 pp.
- Butt, C.R.M., 1987. A basis for geochemical exploration models for tropical terrains. In: Y. Ogura (Editor), *Proceedings of an International Seminar on Laterite*, October 14-17, 1985, Tokyo, Japan. *Chem. Geol.*, 60: 5-16.

- Butt, C.R.M., 1988. Major uranium provinces: Yilgarn Block and Gascoyne Province. In: *Recognition of Uranium Provinces*. International Atomic Energy Agency, Vienna, pp. 273–304.
- Butt, C.R.M., 1989a. Geomorphology and climatic history—keys to understanding geochemical dispersion in deeply weathered terrain. In: G.D. Garland (Editor), *Proceedings of Exploration '87. Third Decennial International Conference on Geophysical and Geochemical Exploration for Minerals and Groundwater*. Special Volume 3. Ontario Geological Survey, Toronto, pp. 323–334.
- Butt, C.R.M., 1989b. Genesis of supergene gold deposits in the lateritic regolith of the Yilgarn Block, Western Australia. In: R.R. Keays, W.R.H. Ramsay and D.I. Groves (Editors), *The Geology of Gold Deposits: The Perspective in 1988*. Economic Geology Monograph, 6. Economic Geology, New Haven, pp. 460–470.
- Butt, C.R.M. and Gole, M.J., 1986. Groundwater helium surveys in mineral exploration in Australia. *J. Geochem. Explor.*, 25: 309–344.
- Butt, C.R.M. and Nickel, E.H., 1981. Mineralogy and geochemistry of the weathering of the disseminated nickel sulfide deposit at Mt Keith, Western Australia. *Econ. Geol.*, 76: 1736–1751.
- Butt, C.R.M. and Nichol, I., 1979. The identification of various types of stream sediment anomalies in Northern Ireland. *J. Geochem. Explor.*, 11: 13–32.
- Butt, C.R.M. and Sheppy, N.R., 1975. Geochemical exploration problems in Western Australia exemplified by the Mt. Keith area. In: I.L. Elliott and W.K. Fletcher (Editors), *Geochemical Exploration 1974*. Developments in Economic Geology, 1. Elsevier, Amsterdam, pp. 392–415.
- Butt, C.R.M. and Smith, R.E. (Editors), 1980. *Conceptual Models in Exploration Geochemistry, 4 Australia*. Developments in Economic Geology, 13. Elsevier, Amsterdam, 275 pp. (Also *J. Geochem. Explor.*, 12: 89–365).
- Butt, C.R.M. and Zeegers, H., 1989. Classification of geochemical exploration models for tropically weathered terrains. In: S.E. Jenness (Editor), *Geochemical Exploration 1987*. *J. Geochem. Explor.*, 32: 65–74.
- Cabello, J., 1985. Geochemical prospecting at the Caracoles silver district, Atacama desert, Antofasta Province, Chile. In: *Prospecting in Areas of Desert Terrain*. Institute of Mining and Metallurgy, London, pp. 21–30.
- Cameron, E., 1984. The Yeelirrie calcrete uranium deposit, Western Australia. In: *Surficial Uranium Deposits*. International Atomic Energy Agency, Vienna, pp. 157–164.
- Carlisle, D., 1983. Concentration of uranium and vanadium in calcretes and gypcretes. In: E.C.L. Wilson (Editor), *Residual Deposits: Surface Related Weathering Processes and Materials*. Geological Society of London,
- Carr, G.R., 1984. Primary geochemical and mineralogical dispersion in the vicinity of the Lady Loretta Zn–Pb–Ag deposit, northwest Queensland. *J. Geochem. Explor.*, 22: 217–238.
- Carr, G.R., Wilmshurst, J.R. and Ryall W.R., 1986. Evaluation of mercury pathfinder techniques: base metal and uranium deposits. *J. Geochem. Explor.*, 26: 1–117.
- Carroll, D., 1953. Weatherability of zircon. *J. Sediment. Petrol.*, 23: 106–116.
- Carver, R.N., Chenoweth, L.M., Mazzucchelli, R.H., Oates, C.J. and Robbins, T.W., 1987. “Lag”—A geochemical sampling medium for arid terrain. In: R.G. Garrett (Editor), *Geochemical Exploration 1985*. Part I. *J. Geochem. Explor.*, 28: 183–199.
- Cash, S.J., 1959. *Loaming for Gold*. 2nd ed. (1980), Hesperian Press, Perth, 75 pp.
- Chace, F.M., Cumberlidge, J.T., Cameron, W.L. and Van Nort, S.D., 1969. Applied geology at the Nickel Mountain mine, Riddle, Oregon. *Econ. Geol.*, 64: 1–16.
- Chaffee, M.A. and Hessin, T.D., 1971. Evaluation of geochemical sampling in the search for concealed ‘porphyry’ copper-molybdenum deposits on pediments in Southern Arizona. In: R.W. Boyle and J.I. McGerrigle (Editors), *Geochemical Exploration*. Special Volume 1. Canadian Institute of Mining and Metallurgy, Toronto, pp. 401–409.
- Chao, T.T. and Theobald, P.K. Jr., 1976. The significance of secondary iron and manganese oxides in geochemical exploration. *Econ. Geol.*, 71: 1560–1569.
- Chatelin, Y., 1968. Notes de pédologie gabonaise. Géomorphologie et pédologie dans le sud Gabon, des monts Birougou au littoral. *Cah. ORSTOM, Ser. Pedol.*, VI: 20. (In French).

- Chaussidon, J. and Pedro, G., 1979. Rôle de l'état hydrique du système poreux sur l'évolution du milieu. Réalité de l'altération dans les systèmes à faible teneur en eau. *Sci. Sol.*, 2 and 3: 223–237. (In French).
- Chauvel, A., 1977. *Recherches sur la Transformation des Sols Ferrallitiques dans la Zone Tropicale à Saisons Contrastées*. Travaux et Documents, 62. ORSTOM, Paris, 532 pp. (In French).
- Chauvel, A., Boulet, R., Join, P. and Bocquier, G., 1983. Aluminium and iron oxy-hydroxides segregation in nodules of latosols developed on a Tertiary sediment (Barreiras Group), near Manaus, Amazon Basin, Brazil. In: A.J. Melfi and A. Carvalho (Editors), *Lateritisation Processes*. University of Sao Paulo Press, Sao Paulo, pp. 508–526.
- Clark, A.H., Cooke, R.U., Mortimer, C. and Sillitoe, R.H., 1967. Relationship between supergene mineral alteration and geomorphology, southern Atacama desert, Chile—an interim report. *Trans. Inst. Min. Metall. Sect. B, Appl. Earth Sci.*, 76: 89–96.
- Clarke, E.T., Loeppert, R.H. and Ehrman, J.M., 1985. Crystallization of iron oxides on calcite surfaces in static systems. *Clays Clay Miner.*, 33: 152–158.
- Clarke, O.M., 1971. Geochemical prospecting in lateritic soils of Alabama. In: R.W. Boyle and J.I. McGerrigle (Editors), *Geochemical Exploration*. Special Volume 11. Canadian Institute of Mining and Metallurgy, Toronto, pp. 122–125.
- Clema, J.M. and Stevens-Hoare, N.P., 1973. A method of distinguishing Ni gossans from other ironstones on the Yilgarn Shield. *J. Geochem. Explor.*, 2: 393–402.
- Cline, G.R., Powell, P.E., Staniszlo, P.J. and Reid, C.P.P., 1983. Comparison of the abilities of hydroxamic and other natural organic acids to chelate iron and other ions in soil. *Soil Sci.*, 136: 145–157.
- Cloke, P.L. and Kelly, W.C., 1964. Solubility of gold under inorganic supergene conditions. *Econ. Geol.*, 59: 259–270.
- Cloud, P., Gustafson, L.B. and Watson, J.A.L., 1980. The works of living social insects as pseudofossils and the age of the oldest known Metazoa. *Science*, 210: 1013–1015.
- Clough, D.M. and Craw, D., 1989. Authigenic gold-marcasite association: evidence for nugget growth by chemical accretion in fluvial gravels, Southland, New Zealand. *Econ. Geol.*, 84: 953–958.
- Cochrane, R.H.A., 1973. *A Guide to the Geochemistry of Nickeliferous Gossans and Related Rocks from the Eastern Goldfields*. Report, Western Australian Department of Mines, Perth, pp. 115–121.
- Cole, M.M., 1977. Landsat and airborne multi-spectral and thermal imagery used for geological mapping and identification of ore horizons in Lady Annie–Lady Loretta and Dugald River areas, Queensland, Australia. *Trans. Inst. Min. Metall., Sect. B, Appl. Earth Sci.*, 86: 195–215.
- Cole, M.M., 1980. Geobotanical expression of orebodies. *Trans. Geol. Soc. S. Afr.*, 85: 13–28.
- Cole, M.M., 1985. Simple remote sensing in prospecting for gold, uranium and base metals in desert areas in Australia and South Africa: some case studies. In: *Prospecting in Desert Terrain*. Institute of Mining and Metallurgy, London, pp. 233–248.
- Coleman, R.G., 1977. *Ophiolites*. Springer, New York, 229 pp.
- Colin, F. and Lecomte, P., 1986. Gold behaviour in weathering profiles under humid tropics (Dondo Mabi, Gabon). In: R. Rodriguez-Clemente and Y. Tardy (Editors), *Geochemistry and Mineral Formation in the Earth Surface*. Proceedings of an International Meeting, Granada, Spain, 1986. Consejo Superior de Investigaciones Científicas (CSIC), Madrid. (Abstract).
- Colin, F. and Lecomte, P., 1988. Etude minéralogique et chimique du profil d'altération du prospect aurifère de Mébaga Mvomo (Gabon). *Chron. Mines Rech. Minière*, 491: 55–65. (In French).
- Colin, F., Lecomte, P. and Boulangé, B., 1989. Dissolution features of gold particles in a lateritic profile at Dondo Mabi Gabon. *Geoderma*, 45: 241–250.
- Colin, F., Noack, Y., Trecases, J.J. and Nahon, D., 1985. L'altération latéritique débutante des pyroxénites de Jacuba, Niquelandia, Brésil. *Clays Clay Miner.*, 20: 93–113. (In French).
- Collinet, J., 1969. Contribution à l'étude des "stone line" dans la région du Moyen Ogooué (Gabon). *Cah. ORSTOM, Ser. Pedol.*, VII: 42. (In French).

- Cooke, H.J., 1981. Landform evolution in the context of climatic change and neo-Tectonism in the middle Kalahari of north central Botswana. *Trans. Inst. Brit. Geogr.*, 5: 80–99.
- Cooke, R.U. and Warren, A., 1973. *Geomorphology in Deserts*. Batsford, London, 374 pp.
- Coolbaugh, D.F., 1979. Geophysics and geochemistry in the discovery and development of the La Caridad porphyry copper deposit, Sonora, Mexico. In: P.J. Hood (Editor), *Geophysics and Geochemistry in the Search for Metallic Ores*. Economic Geological Report, 31. Geological Survey of Canada, Ottawa, pp. 721–725.
- Coope, J.A., 1958. *Studies in Geochemical Prospecting for Nickel in Bechuanaland and Tanganyika*. Ph.D. Thesis, Imperial College, London University (unpublished).
- Coope, J.A., 1973. Geochemical prospecting for porphyry copper-type mineralization—a review. *J. Geochem. Explor.*, 2: 81–102.
- Corpe, W.A., 1951. A study of the wide spread distribution of Chromobacterium species in soil by a simple technique. *J. Bacteriol.*, 62: 515–517.
- Cowden, A., Donaldson, M.J., Naldrett, A.J. and Campbell, I.H., 1986. Platinum group elements and gold in the komatiite-hosted Fe-Ni-Cu sulphide deposits at Kambalda, Western Australia. *Econ. Geol.*, 81: 1226–1235.
- Cox, R., 1975. Geochemical soil surveys in exploration for nickel copper sulphides at Pioneer, near Norseman, Western Australia. In: I.L. Elliott and W.K. Fletcher (Editors), *Geochemical Exploration 1974*. Developments in Economic Geology, 1. Elsevier, Amsterdam, pp. 437–460.
- Cox, R. and Curtis, R., 1977. The discovery of the Lady Loretta zinc-lead-silver deposit, northwest Queensland, Australia—a geochemical exploration case history. In: C.R.M. Butt and I.G.P. Wilding (Editors), *Geochemical Exploration, 1976*. *J. Geochem. Explor.*, 8: 189–202.
- C.P.C.S., 1967. *Classification des Sols*. Commission de Pédologie et de Cartographie des sols. Ecole Nationale Supérieure Agronomique, Grignon, 87 pp. (In French).
- Cruikshank, B.I. and Pyke, J.G., 1986. Biochemistry and soil geochemistry of the Ranger One, Number 3 orebody, Australia. *Uranium*, 3: 1–26.
- Cumberlidge, J.T. and Chace, F.M., 1967. The geology of the Nickel Mountain mine, Riddle, Oregon. In: J.D. Ridge (Editor), *Ore Deposits of the United States, 1933–67*. Volume 2. American Institute of Mining and Metallurgical Engineers, New York, pp. 1650–1672.
- Dahlberg, E.H., 1982. Geochemical investigation of magnetic and electromagnetic anomalies in the upper Nickerie copper-rare earth mineralization area, Suriname. In: D.J.C. Laming and A.K. Gibbs (Editors), *Hidden Wealth: Mineral Exploration Techniques in Tropical Forest Areas*. Report No. 7. Association of Geoscientists for International Development, Bangkok, pp. 95–109.
- Danchin, R., 1972. In: *Aspects of the Geochemistry of Calcretes and Soils from Various Localities in the North-west Cape*. Anglo-American Research Laboratory, Johannesburg (unpublished report).
- Daniels, J.L., 1975. Palaeogeographic development of Western Australia-Precambrian. In: *Geology of Western Australia*. Memoir No. 2. Geological Survey of Western Australia, pp. 437–445.
- Dasgupta, S.P., 1963. Geochemical prospecting in the Khetri copper belt, Rajasthan, India. In: *Proceedings of Seminar on Geochemical Prospects, Methods and Techniques*. Mineral Research and Development, Series 21. United Nations, ECAFE, New York, pp. 111–116.
- Davies, T.C. and Bloxam, T.W., 1979. Heavy-metal distribution in laterites, southwest of Regent, Freetown Igneous Complex, Sierra Leone. *Econ. Geol.*, 74: 638–644.
- Davies, T.C., Friedrich, G. and Wiechowski, A., 1989. Geochemistry and mineralogy of laterites in the Sula Mountains greenstone belt, Lake Sonfon gold district, Sierra Leone. *J. Geochem. Explor.*, 32: 75–98. (Abstract).
- Davis, J.C., 1973. *Statistics and Data Analysis in Geology*. Wiley, New York, 550 pp.
- Davy, R. and El-Ansary, M., 1986. Geochemical patterns in the laterite profile at the Boddington gold deposit, Western Australia. *J. Geochem. Explor.*, 26: 119–144.
- Davy, R., Clarke, R., Sale, M. and Parker, M., 1988. The nature and origin of the gold-bearing laterites at Mount Gibson, Western Australia. In: *Second International Conference on Prospecting in*

- Arid Terrain*, Perth, Western Australia, Abstract Volume. Australasian Institute of Mining and Metallurgy, Melbourne, pp. 45–47. (Abstract).
- Davy, R., Clarke, R., Sale, M. and Parker, M., 1989. *Gold-bearing Laterite Profiles at Mount Gibson, Murchison Province, Western Australia*. Record, Geological Survey of Western Australia, Perth, 66 pp.
- Dawson, J.B., 1967. Geochemistry and origin of kimberlite. In: P.J. Wyllie (Editor), *Ultramafic and Related Rocks*. Wiley, New York, pp. 241–251.
- Dawson, J.B., 1980. *Kimberlites and Their Xenoliths*. Springer, Berlin, 252 pp.
- Dawson, J.B. and Stephens, W.E., 1975. Statistical classification of garnets from kimberlite and associated xenoliths. *J. Geol.*, 83: 589–607.
- De Oliveira, J.J., 1983. Lateritic soil profiles in semiarid environment: pedological, geochemical and mineralogical data. In: A.J. Melfi and A. Carvalho (Editors), *Lateritisation Processes*. University of Sao Paulo Press, Sao Paulo, pp. 499–506.
- De Vivo, B., Giunta, G., Lima, A., Ramaglia, V., Orsi, G., Perrone, V. and Zuppeta, A., 1981. An application of moving average analysis and R-mode factor analysis to a regional geochemical reconnaissance on residual soils of Southern Sudan. *Rend. Soc. Ital. Mineral. Petrol.* 37: 387–406.
- Debnam, A.H. and Webb, J.S., 1960. Some geochemical anomalies in soil and stream sediment related to beryl pegmatites in Rhodesia and Uganda. *Trans. Inst. Min. Metall., Sect. B, Appl. Earth Sci.*, 69: 329–344.
- Delmas, A.B., 1979. *Etude Expérimentale des Phénomènes de Dissolution des Sels et des Silicates. Approche Cinétique*. Ph.D. Thesis, Institut National de la Recherche Agronomique, Paris (unpublished), 256 pp. (In French).
- Delvigne, J., Bisdom, E.B.A., Sleeman, J. and Stoops, G., 1979. Olivines, their pseudomorphs and secondary products. *Pedologie*, XXIX, 3: 247–309.
- Desborough, G.A., Raymond, W.H. and Jagmin, P.J., 1970. Distribution of silver and copper in placer gold derived from the northeastern part of the Colorado mineral belt. *Econ. Geol.*, 65: 937–944.
- Deshpande, M.L., 1982. Regional geochemical soil survey in the area southeast of Medakeripura, Chitradurga Schist Belt, Karnataka (Mysore). In: *Proceedings of the Symposium on Geochemical Prospecting, Methods and Techniques*, Calcutta, 1975. Special Publication No. 8. Geological Survey of India, Calcutta, pp. 51–58.
- Deutscher, R.L., Mann, A.W. and Butt, C.R.M., 1980. Model for calcrete uranium mineralization. In: C.R.M. Butt and R.E. Smith (Editors), *Conceptual Models in Exploration Geochemistry—Australia*. *J. Geochem. Explor.*, 12: 158–161.
- Dick, H.J.B. and Bullen, T., 1984. Chromian spinel as a petrogenetic indicator in abyssal and alpine-type peridotites and spatially associated lavas. *Contrib. Mineral. Petrol.*, 86: 54–76.
- Dickson, B.L. and Snelling, A.A., 1980. Movements of uranium and daughter isotopes in the Koongarra uranium deposit. In: J. Ferguson and A.B. Goleby (Editors), *Uranium in the Pine Creek Geosyncline*. International Atomic Energy Agency, Vienna, pp. 499–507.
- Dickson, B.L., Giblin, A.M. and Snelling, A.A., 1987. The source of radium in anomalous accumulations near sandstone escarpments, Australia. *Appl. Geochem.*, 2: 385–398.
- Dickson, B.L., Gulson, B.L. and Snelling, A.A., 1985. Evaluation of lead isotopic methods for uranium exploration, Koongarra area, Northern Territory, Australia. *J. Geochem. Explor.*, 24: 81–102.
- Dickson, B.L., Gulson, B.L. and Snelling, A.A., 1987. Further assessment of stable lead isotope measurements for uranium exploration, Pine Creek Geosyncline, Northern Territory, Australia. *J. Geochem. Explor.*, 27: 63–75.
- Didier, P., Nahon, D., Fritz, B. and Tardy, Y., 1983. Activity of water as a geochemical controlling factor in ferricretes. A thermodynamic model in the system kaolinite Fe-Al oxihydroxides. *Sci. Geol.*, 71: 35–44.
- Didier, P., Perret, D., Tardy, Y. and Nahon, D., 1985. Equilibres entre kaolinites ferrifères, goethites alumineuses et hématites alumineuses dans les systèmes cuirasses. Rôle de l'activité de l'eau et de la taille des pores. *Sci. Géol., Bull.*, 38: 383–397. (In French).

- Dommanget, A., Diallo, M. and Guilloux, L., 1985. Un nouveau type de gisement d'or: Loula (Mali). *Chron. Mines Rech. Minière*, 481: 5–18. (In French).
- Dommergues, Y. and Mangenot, F., 1970. *Ecologie Microbienne du Sol*. Masson, Paris, 796 pp. (In French).
- d'Orey, F.L.C., 1975. Contribution of termite mounds to locating hidden copper deposits. *Trans. Inst. Min. Metall., Sect. B, Appl. Earth Sci.*, 84: 150–151.
- Duchaufour, P., 1982. *Pedology*. (Trans: T.R. Paton). George Allen and Unwin, London, 448 pp.
- Duncan, R.K., 1988. Discovery of the Mt Weld carbonatite. In: *Research and Development for the Minerals Industry*. Conference Proceedings. Western Australian School of Mines, Kalgoorlie, pp. 86–93.
- Dunlop, A.C., Atherden, P.R. and Govett, G.J.S., 1983. Lead distribution in drainage channels about the Elura zinc-lead-silver deposit, Cobar, New South Wales, Australia. *J. Geochem. Explor.*, 18: 195–204.
- Dury, G.H., 1971. Relict deep weathering and duricrusting in relation to the palaeoenvironment of middle latitudes. *Geogr. J.*, 137: 511–522.
- Dutrizac, J.E., Jamber, J.L. and O'Reilly, J.B., 1983. Man's first use of jarosite: the pre-Roman mining-metallurgical operations at Rio Tinto, Spain. *Can. Inst. Min. Metall., Bull.*, 76: 78–82.
- Edou-Minko, A., 1988. *Pétrologie et Géochimie des Latérites à "Stone-line" du Gîte d'or d'Ovala — Application à la Prospection en Zone Equatoriale Humide (Gabon)*. Ph.D. Thesis, University of Poitiers (unpublished), 147 pp. (In French).
- El Din Khalil, B., 1973. *Quantitative Interpretation of Secondary Dispersion Patterns of Gold Deposits in the Red Sea Hills, Sudan*. Bulletin 24. Geological and Mineral Resources Department, Ministry of Industry and Mining, Khartoum, 63 pp.
- Elias, M., Donaldson, M.J. and Giorgetta, N., 1981. Geology, mineralogy and chemistry of lateritic nickel-cobalt deposits near Kalgoorlie, Western Australia. *Econ. Geol.*, 76: 1775–1783.
- Ellison, D. and Blaylock, G., 1990. The Syama gold project, Mali. *Min. Mag.* (May): 346–349.
- Embrecht, J. and Stoops, G., 1982. Microscopical aspect of garnet weathering in a humid tropical environment. *J. Soil Sci.*, 33: 535–545.
- Emmons, S.F., 1900. The secondary enrichment of ore deposits. *Am. Inst. Min. Metall. Pet. Eng., Trans.*, 30: 177–217.
- Emmons, W.H., 1917. The enrichment of ore deposits. *U.S., Geol. Surv., Bull.*, 625.
- Erdman, J.A. and Olson, J.C., 1985. The use of plants in prospecting for gold: a brief overview with a selected bibliography and topic index. *J. Geochem. Explor.*, 24: 281–309.
- Erickson, R.L. and Marranzino, A.P., 1960. *Geochemical Prospecting for Copper in the Rocky Range, Beaver County, Utah*. Professional Paper 400-B. United States Geological Survey, pp. 98–101.
- Esson, J., 1983. Geochemistry of the nickeliferous laterite profile, Liberdade, Brazil. In: R.C.L. Wilson (Editor), *Residual Deposits: Surface Related Weathering Processes and Raw Materials*. Geological Society of London Special Publication, 11. Blackwell, London, pp. 91–99.
- Esson, J. and Surcan Dos Santos, B., 1978. Chemistry and mineralogy of section through lateritic nickel deposit at Liberdade, Brazil. *Trans. Inst. Min. Metall., Sect. B, Appl. Earth Sci.*, 87: 53–60.
- Eswaran, H., Lim, C.H., Sooryanarayanan, V. and Daud, N., 1977. Scanning electron microscopy of secondary minerals in Fe–Mn glauconites. In: *Proceedings of the Fifth International Meeting on Soil Micromorphology*. Grenada, pp. 851–855.
- Eugster, H.P. and Maglione, G., 1979. Brines and evaporites of the Lake Chad basin, Africa. *Geochim. Cosmochim. Acta*, 43: 973–981.
- Eupene, G.S. and Williams, B.T., 1980. Ranger One uranium deposits, Pine Creek Block, N.T. In: C.R.M. Butt and R.E. Smith (Editors), *Conceptual Models in Exploration Geochemistry, Australia*. *J. Geochem. Explor.*, 12: 230–233.
- Evans, D.L., 1981. Laterisation as a possible contributor to gold placers. *Eng. Min. J.*, 182: 86–89.

- Fairbairn, P.E. and Robertson, R.M.S., 1966. Stages in the tropical weathering of kimberlites. *Clays Clay Miner.*, 6: 351-370.
- FAO-UNESCO, 1974. *Soil Map of the World*. Rome, Paris.
- Farrah, H. and Pickering, W.F., 1979. pH effects in the adsorption of heavy metal ions by clays. *Chem. Geol.*, 25: 317-326.
- Farrell, B.L., 1984. The use of "loam" concentrates in geochemical exploration in deeply weathered arid terrains. *J. Geochem. Explor.*, 22: 101-118.
- Fedoseyeva, V.I., Fedoseyev, N.F. and Zvonareva, G.V., 1986. Interaction of some gold complexes with humic and fulvic acids. *Geochem. Int.*, 23(3): 106-110.
- Fetzer, W.G., 1934. Transportation of gold by organic solutions. *Econ. Geol.*, 29: 599-604.
- Fetzer, W.G., 1946. Humic acids and true organic acids as solvents of minerals. *Econ. Geol.*, 41: 47-56.
- Filipek, L.H. and Theobald, P.K., 1981. Sequential extraction techniques applied to a porphyry copper deposit in the Basin and Range Province. *J. Geochem. Explor.*, 14: 155-174.
- Flach, W., Cady, J.G. and Nettleton, W.D., 1968. Pedogenetic alteration of highly weathered parent material. In: *Transactions of the Ninth International Congress on Soil Science*, 4: 343-351.
- Fletcher, R.J., 1985. Geochemical exploration for gold in the Red Sea Hills, Sudan. In: *Prospecting in Areas of Desert Terrain*. Institute of Mining and Metallurgy, London, pp. 79-94.
- Fortescue, J.A.C., 1975. The use of landscape geochemistry to process exploration geochemical data. *J. Geochem. Explor.*, 4: 3-13.
- Fox, R.M., 1830. On the electromagnetic properties of metalliferous veins in the mines of Cornwall. *Philos. Trans. R. Soc. London*, p. 399.
- Frakes, L.A., 1979. *Climates Throughout Geologic Time*. Elsevier, Amsterdam, 310 pp.
- Freise, F.W., 1931. The transportation of gold by organic underground solutions. *Econ. Geol.*, 26: 421-431.
- Freyssinet, P. and Butt, C.R.M., 1988a. *Morphology and Geochemistry of Gold in a Lateritic Profile, Reedy Mine, Western Australia*. Restricted Report, MG 58R. CSIRO Australia, Division of Exploration Geoscience, Perth, 14 pp.
- Freyssinet, P. and Butt, C.R.M., 1988b. *Morphology and Geochemistry of Gold in a Lateritic Profile, Bardoc Mine, Western Australia*. Restricted Report, MG 59R. CSIRO Australia, Division of Exploration Geoscience, Perth, pp. 19.
- Freyssinet, P. and Butt, C.R.M., 1988c. *Morphology and Geochemistry of Gold in a Lateritic Profile, Beasley Creek, Laverton, Western Australia*. Restricted Report, MG 60R. CSIRO Australia, Division of Exploration Geoscience, Perth, 12 pp.
- Freyssinet, P., Lawrance, L.M. and Butt, C.R.M., 1990. Geochemistry and morphology of gold in lateritic profiles in savanna and semi-arid climates. In: Y. Noack and D. Nahon (Editors), *Geochemistry of the Earth's Surface and of Mineral Formation*. *Chem. Geol.*, 84: 61-63. (Abstract).
- Freyssinet, P., Lecomte, P. and Edimo, A., 1989a. Dispersion of gold and base metals in the Mborguéné lateritic profile, east Cameroun. In: S.E. Jenness (Editor), *Geochemical Exploration 1987*. *J. Geochem. Explor.*, 32: 99-116.
- Freyssinet, P., Zeegers, H. and Tardy, Y., 1987. Néof ormation d'or dans les cuirasses latéritiques: dissolution, migration, précipitation. *C. R. Acad. Sci., Paris*, 305: 867-874. (In French).
- Freyssinet, P., Zeegers, H. and Tardy, Y., 1989b. Morphology and geochemistry of gold grains in lateritic profiles of southern Mali. In: S.E. Jenness (Editor), *Geochemical Exploration 1987*. *J. Geochem. Explor.*, 32: 17-31.
- Frick, C., 1985. A study of the soil geochemistry of the Platreef in the Bushveld complex, South Africa. *J. Geochem. Explor.*, 24: 51-80.
- Frick, C., Strauss, S.W. and Dixon, R., 1989. The use of chlorine, bromine and fluorine in detecting a buried Cu-Zn orebody along the zinc-line in the Murchison range, South Africa. In: G.L. Coatzee (Editor), *Exploration Geochemistry in Southern Africa*. *J. Geochem. Explor.*, 34: 83-102.
- Friedrich, G.H.W. and Christensen, S.M., 1977. Geochemical dispersion patterns associated with the Lake Yindarlgooda sulphide mineralization, Western Australia. In: C.R.M. Butt and I.G.P. Wilding (Editors), *Geochemical Exploration 1976*. *J. Geochem. Explor.*, 8: 219-234.

- Friedrich, G., Brunemann, H.-G., Thijssen, T. and Wallner, P., 1980. Chromite in lateritic soils as potential ore reserves in the Philippines. *Z. Erzbergbau Metallhuettenwes.*, 33: 414–420.
- Friedrich, G., Brunemann, H.-G., Wilcke, J. and Stumpf, E.F., 1981. Chrome-spinels in lateritic soils and ultramafic source rocks, Acoje Mine, Zambales, Philippines. In: *Symposium on Metallogeny of Mafic and Ultramafic Complexes*, Athens. 1. UNESCO, Paris, pp. 257–278.
- Friedrich, G., Marker, A., Kanig, M. and Germann, A., 1987. Mineral prospecting and geological mapping in laterite covered areas of Brazil. In: *Final Report BMFT Research Project RG 8301 5*. Institute für Mineralogie und Lagerstättenlehre, RWTH Aachen (unpublished), 373 pp.
- Friedrich, G., Wallner, P., Kater, G. and Brunemann, H.-G., 1983. Concealed chromite ore bodies indicated by the distribution patterns and chemical composition of chrome-spinels in the overlying residual lateritic soil, Eastern Visayas, Philippines. In: A.J. Melfi and A. Carvalho (Editors), *Lateritisation Processes*. University of Sao Paulo Press, Sao Paulo, pp. 177–184.
- Friedrich, G., Wilcke, J., Marker, A., Hock, M. and Oh, J.-S., 1984. Untersuchungen natürlicher Vorkommen von Chromitanreicherungen in lateritischen Boden und ultramafischen Ausgangsgesteinen. In: *Final Report, BMFT Research Project R 214*, Volumes I and II. Institute für Mineralogie und Lagerstättenlehre, RWTH Aachen (unpublished), 683 pp. (In German).
- Fritsch, E., 1984. *Les Transformations d'une Couverture Ferrallitique: Analyse Minéralogique et Structurale d'une Toposéquence sur Schistes en Guyane Française*. Ph.D. Thesis, University of Paris, 138 pp. (In French).
- Fritz, B., 1975. *Etude Thermodynamique et Simulation des Réactions entre Minéraux et Solutions. Application à la Géochimie des Altérations et des Eaux Continentales*. Sciences Géologiques, Mémoire, 41. Université Louis Pasteur, Strasbourg, 152 pp. 152. (In French).
- Fritz, B., 1980. *Etude Thermodynamique et Modélisation des Réactions Hydrothermales et Diagénetiques*. Sciences Géologiques, Mémoire, 65. Université Louis Pasteur, Strasbourg, 197 pp. (In French).
- Furlong, D.N., Yates, D.E. and Healey, T.W., 1981. Fundamental properties of the oxide/aqueous solution interface in electrodes of conductive metallic oxides. In: S. Trasatti (Editor), *Electrodes of Conductive Metallic Oxides*. Elsevier, Amsterdam, pp. 367–423.
- Gac, J.Y., 1979. *Géochimie du Bassin du Lac Tchad, Bilan d'Altération, de l'Erosion et de la Sédimentation*. Ph.D. Thesis, University of Strasbourg (unpublished), 248 pp.
- Gac, J.Y. and Pinta, M., 1973. Bilan de l'érosion et de l'altération en climat tropical humide. Estimation de la vitesse d'approfondissement des profils. Etude du bassin versant de l'Ouham (République Centrafricaine). *Cah. ORSTOM, Ser. Pedol.*, V, 1: 83–96. (In French).
- Garnett, D.L. and Rea, W.I., 1985. Geochemical prospecting in the area around the Otjihase copper deposit, Namibia. In: *Prospecting in Areas of Desert Terrain*. Institute of Mining and Metallurgy, London, pp. 191–208.
- Garnett, D.L., Rea, W.J. and Fuge, R., 1982. Geochemical exploration techniques applicable to calcrete-covered areas. In: H.W. Glenn (Editor), *Proceedings of the 12th Commonwealth Mining and Metallurgical Institute Congress*. Geological Society of South Africa, Johannesburg, pp. 945–955.
- Garrels, R.M. and Christ, C.L., 1965. *Solutions, Minerals and Equilibria*. Harpers, New York, 450 pp.
- Gatellier, J.-P. and Disnar, J.-R., 1988. Mécanismes et aspects cinétiques de la réduction de l'or (III) par la matière organique sédimentaire. Importance métallogénique. *C. R. Acad. Sci., Paris*, 306: 979–984. (In French).
- Gavaud, M., 1977. *Les Grands Traits de la Pédogénèse au Niger Méridional*. Travaux et Documents, 76. ORSTOM, Paris, 102 pp. (In French).
- Gedeon, A.Z., Butt, C.R.M., Gardner, K.A. and Hart, M.K., 1977. The applicability of some geochemical analytical techniques in determining "total" compositions of some lateritized rocks. In: C.R.M. Butt and I.G.P. Wilding (Editors), *Geochemical Exploration 1976*. *J. Geochem. Explor.*, 8: 283–303.

- Gee, R.D., 1989. The Gibson gold deposit. Monthly Notes, Western Australian Division, Geological Society of Australia, July: 2. (Abstract).
- Gee, R.D., 1990. *The Gibson Lateritic Gold Deposit. Geology of the Mineral Deposits of Australia and Papua New Guinea*. Australasian Institute of Mining and Metallurgy, Melbourne.
- Geffroy, J., 1975. Etude microscopique des minerais uranifères d'Oklo. In: *Le Phénomène d'Oklo*. International Atomic Energy Agency, Vienna, pp. 133–151. (In French).
- Gentili, J., 1958. *A Geography of Climate*. University of Western Australia Press, Nedlands, Western Australia, 172 pp.
- Germann, A., Marker, A. and Friedrich, G., 1987. The alkaline complex of Jacupiranga, Sao Paulo/Brazil—petrology and genetic considerations. *Zentralbl. Geol. Palaeontol., Teil 1, 7/8*: 807–818.
- Ghadiri, H. and Payne, D., 1988. The formation and characteristics of splash following raindrop impact on soil. *J. Soil Sci.*, 39: 563–575.
- Giblin, A.M., 1980. The role of clay adsorption in the genesis of uranium ores. In: J. Ferguson and A.B. Goleby (Editors), *Uranium in the Pine Creek Geosyncline*. International Atomic Energy Agency, Vienna, pp. 521–529.
- Gilbert, G.K., 1904. Domes and dome structure of the High Sierra. *Geol. Soc. Am., Bull.*, 15: 29–36.
- Giresse, P., 1978. Le contrôle climatique de la sédimentation marine et continentale en Afrique centrale atlantique à la fin du Quaternaire. Problèmes de corrélation. *Paleogeogr., Paleoclimatol., Paleocol.*, 23: 57–77. (In French).
- Girling, C.A., Peterson, P.J. and Warren, H.V., 1979. Plants as indicators of gold mineralization at Western Bar, British Columbia, Canada. *Econ. Geol.*, 74: 902–907.
- Giusti, L., 1986. The morphology, mineralogy, and behaviour of “fine grained” gold from placer deposits of Alberta: sampling and implications for mineral exploration. *Can. J. Earth Sci.*, 23: 1662–1672.
- Giusti, L. and Smith, D.G.W., 1984. An electron microprobe study of some Alberta placer gold. *Tschermaks Mineral. Petrogr. Mitt.*, 33: 187–202.
- Glasson, K.R., 1973. A study of anomalous copper-lead-zinc values in relation to rock types and weathering profiles in an area north of Mount Isa. In: *Proceedings of the Australasian Institute of Mining and Metallurgy, Western Australian Conference*. Australasian Institute of Mining and Metallurgy, Melbourne, pp. 27–40.
- Glasson, M.J., Lehne, R.W. and Wellmer, F.W., 1988. Gold exploration in the Callion area, Eastern Goldfields, Western Australia. *J. Geochem. Explor.*, 31: 1–19.
- Gleeson, C.F. and Poulin, R., 1989. Gold exploration in Niger using soils and termitaria. *J. Geochem. Explor.*, 31: 253–283.
- Goldhaber, M.B., 1983. Experimental study of metastable sulfur oxyanion formation during pyrite oxidation at pH 6–9 and 30 degrees C. *Am. J. Sci.*, 283: 193–217.
- Goldich, S.S., 1938. A study in rock weathering. *J. Geol.*, 46: 17–58.
- Goldsmith, R. and Force, E.R., 1978. Distribution of rutile in metamorphic rocks and implications for placer deposits. *Miner. Deposita*, 13: 329–343.
- Gole, M.J., Butt, C.R.M. and Snelling, A.A., 1986. A groundwater helium survey of the Koongarra uranium deposits, Pine Creek Geosyncline, Northern Territory. *Uranium*, 2: 343–360.
- Goleva, G.A., Krivenko, V.A. and Gutz, Z.G., 1970. Geochemical trends in the occurrence and migration forms of gold in natural waters. *Geochem. Int.*, 7(6): 518–529.
- Golightly, J.P., 1981. Nickeliferous laterite deposits. *Econ. Geol.*, 75th Anniversary Volume: 710–735.
- Goni, J., Guillemin, C. and Sarcia, C., 1967. Géochimie de l'or exogène. Etude expérimentale de la formation des dispersions colloïdales d'or et de leur stabilité. *Miner. Deposita*, 1: 259–268. (In French).
- Goossens, P.J., 1975. Geochemical behavior of galena under semi-arid climatic conditions: an example from Upper Volta, Western Africa. In: I.L. Elliott and W.K. Fletcher (Editors), *Geochemical Exploration, 1974*. Developments in Economic Geology, 1. Elsevier, Amsterdam, pp. 493–501.

- Goudie, A., 1972. The chemistry of world calcrete deposits. *J. Geol.*, 80: 449–463.
- Goudie, A., 1973. *Duricrusts in Tropical and Subtropical Landscapes*. Clarendon, Oxford, 174 pp.
- Govett, G.J.S., 1976. Detection of deeply buried and blind sulphide deposits by measurement of H^+ and conductivity of closely spaced surface soil samples. *J. Geochem. Explor.*, 6: 359–382.
- Govett, G.J.S., 1983. *Rock Geochemistry in Mineral Exploration*. Handbook of Exploration Geochemistry, 3. Elsevier, Amsterdam, 461 pp.
- Govett, G.J.S., 1987. Exploration geochemistry in some low-latitude areas—problems and techniques. *Trans. Inst. Min. Metall., Sect. B, Appl. Earth Sci.*, 96: 97–116.
- Govett, G.J.S. and Atherden, P.R., 1987. Electrogeochemical patterns in surface soils—detection of blind mineralization beneath exotic cover, Thalanga, Queensland. In: R.G. Garrett (Editor), *Geochemical Exploration 1985*. Part I. *J. Geochem. Explor.*, 28: 201–218.
- Grandin, G. and Thiry, M., 1983. Les grandes surfaces continentales tertiaires des régions chaudes—succession des types d'altération. *Cah. ORSTOM, Ser. Pedol.*, 13: 3–18. (In French).
- Granger, H.C. and Warren, C.G., 1969. Unstable sulfur compounds and the origin of roll-type uranium deposits. *Econ. Geol.*, 64: 160–171.
- Granier, C., Hartley, J., Michaud, J.C. and Troly, G., 1989. Contribution de la géochimie tridimensionnelle à la découverte, sous couverture allochtone, d'extensions du gisement polymétallique de Thalanga (Queensland, Australia). *J. Geochem. Explor.*, 32: 467–475. (In French).
- Granier, C., Lahoinie, J.P. and Vitali, C., 1963. Géochimie de l'or et du cuivre dans les formations latéritiques argileuses du Mont Flotou (Italy, Côte d'Ivoire). *Bull. Soc. Fr. Mineral. Cristallogr.*, 86: 252–258. (In French).
- Grégoire, D.C., 1985. Selective extraction of organically bound gold in soils, lake sediments and stream sediments. *J. Geochem. Explor.*, 23: 299–313.
- Gregory, G.P., 1969. *Geochemical Dispersion Patterns Related to Kimberlite Intrusives in North America*. Ph.D. Thesis, Imperial College, London.
- Gregory, G.P., 1984. Exploration for primary diamond deposits with special emphasis on the Lennard Shelf W.A. In: P.G. Purcell (Editor), *The Canning Basin, W.A. Proceedings of the Petroleum Exploration Society Symposium*, Perth. Geological Society of Australia, Melbourne, pp. 475–484.
- Greig, D.D., 1983. Primary and secondary dispersion at the Teutonic Bore deposit. In: B.H. Smith (Editor), *Geochemical Exploration in the Eastern Goldfields Region of Western Australia: Tour Guide*. Association of Exploration Geochemists, Perth, pp. 73–87.
- Grimbert, A., 1963. The application of geochemical prospecting for uranium in forested zones in the tropics. In: *Proceedings of the Seminar on Geochemical Prospecting, Methods and Techniques*. Mineral Resources Development Series, 21. United Nations, ECAFE, New York, pp. 81–94.
- Grimm, B. and Friedrich, G., 1989. Gold-bearing soils from Central Bahia, Brazil. *Zentralbl. Geol. Palaeontol., Teil 1*, 5/6: 1193–1203.
- Grimm, B. and Friedrich, G., 1990. Weathering effects on supergene gold in soils of a semi-arid environment, Gienio do Ouro, Brasil. In: Y. Noack and D. Nahon (Editors), *Geochemistry of the Earth's Surface and of Mineral Formation*. *Chem. Geol.*, 84: 70–73. (Abstract).
- Gritsaenko, G.S., Belova, L.N., Getseva, R.V. and Savelyeva, K.T., 1958. Mineralogical types of oxidation zones of hydrothermal uranium and sulfide uranium ores of the USSR. In: *Proceedings of the Second United Nations International Conference on Peaceful Uses of Atomic Energy*. 2. International Atomic Energy Agency, Vienna, pp. 469–471.
- Grove, A.T., 1969. Landforms and climatic change in the Kalahari and Ngamiland. *Geogr. J.*, 135: 191–212.
- Grubb, P.L.C., 1979. Genesis of bauxites deposits in the lower Amazon basin and Guiana coastal plain. *Econ. Geol.*, 74: 735–750.
- Guedria, A., Trichet, J. and Wilhelm, E., 1989. Behaviour of lead and zinc in calcrete-bearing soils around Bou Grine, Tunisia—its application to geochemical exploration. *J. Geochem. Explor.*, 32: 117–132.

- Guillemot, D., 1988. Le lever aérogéophysique du socle gabonais. *Chron. Mines Rech. Minière*, 491: 13–24. (In French).
- Gulson, B.L., 1986. *Lead Isotopes in Mineral Exploration*. Elsevier, Amsterdam, 245 pp.
- Gulson, B.L. and Mizon, K.J., 1979. Lead isotopes as a tool for gossan assessment in base metal exploration. *J. Geochem. Explor.*, 11: 299–320.
- Gulson, B.L. and Vaasjoki, M., 1983. Lead isotopes in geochemical exploration. In: R.E. Smith (Editor), *Geochemical Exploration in Deeply Weathered Terrain*. CSIRO Division of Mineralogy, Floreat Park, Western Australia, pp. 195–201.
- Haebig, E.A. and Jackson, D.G., 1986. Geochemical expression of some west Australian kimberlites and lamproites. In: *Proceedings of the Fourth International Kimberlite Conference*, Perth. Abstracts Volume, 466–468. (Abstract).
- Halitim, H., Robert, M. and Pedro, G., 1983. *Etude Expérimentale de l'Épigénie Calcaire des Silicates en Milieu Confiné: Caractérisation des Conditions de son Développement et des Modalités de sa Mise en Jeu*. Sciences Géologiques, Mémoire, 71. Université Louis Pasteur, Strasbourg, pp. 13–23. (In French).
- Hall, G.E.M. and Bonham-Carter, G.F., 1988. Review of methods to determine gold, platinum and palladium in production-oriented geochemical laboratories, with application of a statistical procedure to test for bias. *J. Geochem. Explor.*, 30: 255–286.
- Hallbauer, D.K. and Utter, T., 1977. Geochemical and morphological characteristics of gold particles from recent river deposits and the fossil placers of the Witwatersrand. *Miner. Deposita*, 12: 293–306.
- Hallberg, J.A., 1984. A geochemical arid to igneous rock identification in deeply weathered terrain. *J. Geochem. Explor.*, 20: 1–8.
- Halligan, R. and Harris, J.L., 1980. Ilmars Cu-Zn-Pb deposit, Halls Creek Province, W.A. In: C.R.M. Butt and R.E. Smith (Editors), *Conceptual Models in Exploration Geochemistry — Australia*. *J. Geochem. Explor.*, 12: 217–220.
- Hanssen, E. and Bourezg, M. (1990). Geology and geochemistry of gossans and ironstones in carbonate and aluminosilicate environments in northeast Algeria. *J. Geochem. Explor.*, 38: 323–349.
- Harrison, P.H., 1990. Platinum group elements. Review of exploration techniques and targets. In: *Mineral Exploration, Geology and Geophysics: Quo vadis?. Proceedings of 30th Annual Technical Meeting*. Australian Mineral Industries Research Association, Melbourne, pp. 1–15.
- Harvey, T.V., 1985. Recent experience with electrical geophysical exploration techniques in Saudi Arabia. In: *Prospecting in Areas of Desert Terrain*. Institute of Mining and Metallurgy, London, pp. 71–77.
- Heberlein, D.R., Fletcher, W.K. and Godwin, C.L., 1983. Litho-geochemistry of hypogene, supergene and leached cap samples, Berg porphyry copper deposit, British Columbia. *J. Geochem. Explor.*, 19: 595–609.
- Helgeson, H.C., 1968. Evaluation of irreversible reactions in geochemical processes involving minerals and aqueous solutions. I. Thermodynamic relations. *Geochim. Cosmochim. Acta*, 32: 853–877.
- Helgeson, H.C., 1971. Kinetics of mass transfer among silicates and aqueous solutions. *Geochim. Cosmochim. Acta*, 35: 421–469.
- Helgeson, H.C., Garrels, R.M. and MacKenzie, F.T., 1969. Evaluation of irreversible processes involving minerals and aqueous solutions. II. Application. *Geochim. Cosmochim. Acta*, 33: 455–481.
- Hervieu, J., 1968. *Contribution à l'Étude de l'Environnement en Milieu Tropical*. Mémoire, 24. ORSTOM, Paris, 465 pp. (In French).
- Hoffman, S.J., 1977. Talus fine sampling as a regional exploration technique in mountainous regions. *J. Geochem. Explor.*, 7: 349–360.
- Hore, M.K. and Harpavat, C.L., 1980. Pathfinder elements for geochemical exploration in Satkui area, Satkui-Dhanota-Raghnunathgarh shear zone, Khetri-Copper Belt District Jhunjhunu, Rajasthan. In:

- Proceedings of the Symposium on Chemical Analysis of Geological Materials*, Calcutta, 1979. Special Publication 1. Geological Survey of India, Calcutta, pp. 534–544.
- Howarth, R.J., (Editor), 1983. *Statistics and Data Analysis in Geochemical Prospecting*. Handbook of Exploration Geochemistry, 2. Elsevier, Amsterdam, 437 pp.
- Hsi, C.-K.D. and Langmuir, D., 1985. Adsorption of uranyl onto ferric oxyhydroxides: application of the surface complexation site-binding model. *Geochim. Cosmochim. Acta*, 49: 1931–1941.
- Huang, P.M. (Editor), 1986. *Interactions of Soil Minerals with Natural Organics and Microbes*. Special Publication, 17. Soil Science Society of America.
- Hudson, D.R., 1986. Platinum group minerals from the Kambalda nickel deposits, Western Australia. *Econ. Geol.*, 81: 1218–1225.
- Hume-Rothery, W. and Raynor, G.V., 1958. *The Structure of Metals and Alloys*. Monograph and Report Series, 1. The Institute of Metals, London.
- Hunter, M.J., 1980. Esperanza Z2 Cu deposit, Mt. Isa belt, Qld. In: C.R.M. Butt and R.E. Smith (Editors), *Conceptual Models in Exploration Geochemistry—Australia*. *J. Geochem. Explor.*, 12: 253–256.
- IAEA, 1983. *Uranium Exploration in Wet Tropical Environments*. International Atomic Energy Agency, Vienna, 162 pp.
- IAEA, 1984. *Surficial Uranium Deposits. Report of the Working Group on Uranium Geology*. TECDOC, 322. International Atomic Energy Agency, Vienna, 252 pp.
- IAEA, 1988. *Geochemical Exploration for Uranium*. International Atomic Energy Agency, Vienna, 96 pp.
- Ildefonse, P., Proust, D., Meunier, A. and Velde, B., 1979. Rôle de la structure dans l'altération des roches cristallines au sein des microsystemes. Mise en évidence de la succession des phénomènes de déstabilisation-recristallisation. *Sci. Sol*, 2/3: 239–257. (In French).
- Irvine, T.N., 1967. Chromian spinel as a petrogenetic indicator, Part II: Petrologic applications. *Can. J. Earth Sci.*, 4: 71–104.
- Ivanovich, M. and Harmon, R.S., 1982. *Uranium Series Disequilibrium: Application to Environmental Problems in the Earth Sciences*. Oxford University Press, Oxford, 571 pp.
- Ivey, M.E., 1987. The geology of the Hannan South gold mine, Kalgoorlie. In: *Second Eastern Goldfields Geological Field Conference, Abstracts and Excursion Guide*. Geological Society of Australia (WA Division), pp. 118–120. (Abstract).
- Jaques, A.L., Lewis, C.D., Smith, C.B., Gregory, G.P., Ferguson, J., Chappell, B.W. and McCulloch, M.T., 1984a. The diamond bearing ultrapotassic (lamproitic) rocks of the West Kimberley region, Western Australia. In: J. Kornprobst (Editor), *Kimberlites. Volume 1: Kimberlites and Related Rocks*. Developments in Petrology, 11A. Elsevier, Amsterdam, pp. 225–254.
- Jaques, A.L., Webb, A.W., Fanning, C.M., Black, C.P., Pidgeon, R.T., Ferguson, J., Smith, C.B. and Gregory, G.P., 1984b. The age of the diamond bearing pipes and associated leucite lamproites in the West Kimberley region, Western Australia. *Aust. Bur. Miner. Resour., Geol. Geophys., Bull.*, 9.
- Johnson, I.R. and Klingner, G.D., 1975. The Broken Hill ore deposit and its environment. In: C.L. Knight (Editor), *Economic Geology of Australia and Papua New Guinea. I: Metals*. Australasian Institute of Mining and Metallurgy, Melbourne.
- Jones, R.A., 1973. Geochemical prospecting in Papua New Guinea. In: *Proceedings of the Western Australian Conference*. Australasian Institute of Mining and Metallurgy, Melbourne, pp. 41–51.
- Joyce, A.S. and Clema, J.M., 1974. An application of statistics to the chemical recognition of Ni gossans in the Yilgarn Block, W.A. *Australas. Inst. Min. Metall., Proc.*, 252: 21–24.
- Jutson, J.T., 1950. *The Physiography of Western Australia*. Bulletin of the Geological Survey of Western Australia (3rd Ed.), 95. Geological Survey of Western Australia, Perth, pp. 366.
- Kalsotra, M.R. and Prasad, S., 1981. Geochemistry of trace elements in the laterites over Vindhyans. *Indian Miner.*, 35: 24–30.

- Kampf, N. and Schwertmann, U., 1983. Goethite and hematite in a climosequence in Southern Brazil and their application in classification of kaolinitic soils. *Geoderma*, 29: 27–39.
- Kaspar, J., Hudec, I., Schiller, P., Cook, G.B., Kitzinger, A. and Wolf, E., 1972. A contribution to the migration of gold in the biosphere of the humid mild zone. *Chem. Geol.*, 10: 299–305.
- Kater, G.N., Wallner, P.H. and Friedrich, G., 1984. A method of exploration for lateritic and bed-rock chromite mineralization used in the Philippines. *Econ. Geol.*, 79: 372–381.
- Kellogg, C.E., 1949. Preliminary suggestions for the classification and nomenclature of great soil groups in tropical and equatorial regions. *Commonw. Bur. Soil Sci. Tech. Commun.*, 46: 76–85.
- Kemp, E.M., 1981. Tertiary palaeogeography and the evolution of the Australian climate. In: A. Keast (Editor), *Ecological Biogeography of Australia*. Dr. W. Junk, The Hague, pp. 31–49.
- Kilpatrick, B.E., 1969. Nickel, chromium and cobalt in tropical soils over serpentinites, north west district, Guyana. In: F.C. Canney (Editor), *Proceedings of the 1st International Geochemical Exploration Symposium. Q. Colo. Sch. Mines*, 64: 323–332.
- King, L.C., 1957. The geomorphology of Africa. I: Erosion surfaces and their mode of origin. *Sci. Prog.*, 45: 672–681.
- Knowles, C.J., 1976. Microorganisms and cyanide. *Bacteriol. Rev.*, 40: 652–680.
- Kögler, K., Bianconi, F. and Buttner, W., 1983. Geochemical behaviour of uranium in lateritic profiles in southern Tanzania. In: *Uranium Exploration in Wet Tropical Environments*. International Atomic Energy Agency, Vienna, pp. 119–135.
- Kögler, K., Friedrich, G., Gatzweiler, R., Bianconi, F. and Theis, S., 1987. Alpha-spectrometric disequilibrium determinations on sandstone-type uranium mineralization in the lateritic environment of Tanzania. In: G. Friedrich and R. Gatzweiler (Editors), *Uranium Mineralization*. Monograph Series on Mineral Deposits, 27. Borntraeger, Berlin, pp. 161–174.
- Kolotov, B.A., Spasskaya, T.S., Vagner, B.B. and Minacheva, L.I., 1980. The relationship between colloidal and other forms of migration of gold in water in the supergene zones of ore deposits. *Geochem. Int.*, 17(4): 80–82.
- Köppen, W., 1936. *Das geographische System der Klimate*. Handbuch der Klimatologie, 1, Part C. Berlin. (In German).
- Korobushkina, E.D., Chernyak, A.S. and Mineev, G.G., 1974. Dissolution of gold by microorganisms and products of their metabolism. *Microbiology*, 43: 37–41.
- Kosakevitch, A., 1979. Chapeaux de fer: Problèmes de définition et de nomenclature pratique. *Bull. Bur. Rech. Geol. Minières*, II: 141–149. (In French).
- Koshman, P.N. and Yugay, T.A., 1972. The causes of variation in fineness levels of gold placers. *Geochem. Int.*, 9(6): 481–484.
- Krauskopf, K.B., 1951. The solubility of gold. *Econ. Geol.*, 45: 858–870.
- Kresten, P. and Paul, D.K., 1976. Mineralogy of Indian kimberlites: a thermal and X-ray study. *Can. Mineral.*, 14: 487–490.
- Kubiena, W., 1962. Die taxonomische Bedeutung der Art und Ausbildung von Eisenoxyhydratmineralien in Tropenboden. *Z. Pflanzenernähr. Düng., Bodenkd.*, 98: 205–213. (In German).
- Lacroix, A., 1914. Les latérites de la Guinée et les produits d'altération qui leur sont associés. *Nouv. Arch., Mus. Hist. Natur., Paris*, 5: 255–356.
- Lakin, H.W., Curtin, G.C. and Hubert, A.E., 1974. *Geochemistry of Gold in the Weathering Cycle*. Bulletin No. 1330. United States Geological Survey, 80 pp.
- Lamouroux, M., 1972. Etat et comportement du fer dans les sols formés sur roches carbonatées au Liban. *Sci. Sol.*, 1: 85–101. (In French).
- Lamplugh, G.W., 1902. Calcrete. *Geol. Mag.*, 9: 75.
- Langmuir, D., 1978. Uranium solution-mineral equilibrium at low temperatures with applications to sedimentary ore deposits. *Geochim. Cosmochim. Acta*, 42: 547–569.
- Langmuir, D., 1979. Techniques of estimating thermodynamic properties for some aqueous complexes of geochemical interest. In: E.A. Jenne (Editor), *Chemical Modelling in Aqueous Systems; Specification, Sorption, Solubility and Kinetics*. American Chemical Society Symposium Series, 93, pp. 353–387.

- Laporte, G., 1962. Reconnaissance pédologique le long de la voie ferrée Comilog (République du Congo). *Cah. ORSTOM, Ser. Pedol.*, 149. (In French).
- Laval, M., Johan, V. and Touliere, B., 1988. La carbonatite de Mabounié: exemple de formation d'un gîte résiduel à pyrochlore. *Chron. Mines Rech. Minière*, 491: 125–136. (In French).
- Laville-Timsit, L. and Wilhelm, E., 1982. Optimisation des méthodes de prospection géochimique régionale. *Bull. Bur. Rech. Geol. Minieres*, II: 45–56. (In French).
- Laville-Timsit, L., Leleu, M., Sarcia, C. and Zeegers, H., 1983. Geochemical dispersion of Pb and Zn in ferralitic environment: an example in French Guiana. In: A.J. Melfi and A. Carvalho (Editors), *Lateritisation Processes*. University of Sao Paulo Press, Sao Paulo, pp. 433–442.
- Lawrance, L.M., 1988a. Geochemical dispersion anomalies in transported overburden around the quartz vein system at the Mount Pleasant gold mine, Western Australia. In: *Second International Conference on Prospecting in Arid Terrain*, Perth, Western Australia (Abstract Volume). Australasian Institute of Mining and Metallurgy, Melbourne, pp. 87–93. (Abstract).
- Lawrance, L.M., 1988b. The morphology and geochemistry of supergene gold at Hannan South gold mine, Western Australia. In: A.D.T. Goode, E.L. Smyth, W.D. Birch and L.I. Bosma (Editors), *Bicentennial Gold 88*. Abstracts Series, 23, Volume 1. Geological Society of Australia, Melbourne, pp. 360–364. (Abstract).
- Lawrance, L.M., 1991. *Distribution of Gold and Associated Elements within Lateritic Weathering Profiles of the Yilgarn Block, Western Australia*. Ph.D. Thesis, University of Western Australia (unpublished). (In preparation).
- Learned, R.E. and Boissen, R., 1973. Gold—a useful pathfinder element in the search for porphyry copper deposits, Puerto Rico. In: M.J. Jones (Editor), *Geochemical Exploration 1972*. Institute of Mining and Metallurgy, London, pp. 93–103.
- Leblanc, M., Dupuy, C., Cassard, D., Moutte, J., Nicolas, A., Prinzhofer, A., Rabinovitch, M. and Rothier, P., 1980. Essai sur la genèse des corps podiformes de chromite dans les péridotites ophiolitiques: Etude des chromites de Nouvelle-Calédonie et comparaison avec celles de Méditerranée orientale. In: A. Panayotou (Editor), *Ophiolites. Proceedings of the International Ophiolite Symposium*, Cyprus, pp. 691–701. (In French).
- Lecomte, P., 1983. Profils d'altération à stone-lines au Gabon: premières hypothèses génétiques. In: *Principaux Résultats Scientifiques et Techniques du BRGM*. Bureau de Recherches Géologiques et Minières, Orléans, p. 211. (Résumé). (In French).
- Lecomte, P., 1988. Stone line profiles: importance in geochemical exploration. *J. Geochem. Explor.*, 30: 35–61.
- Lecomte, P., 1990. Metallic anomalies occurrence according to the nature of constituents in the weathering profile of the mineralized Mborguéné area (East Cameroun). *International Symposium on Geochemical Prospection*, Prague, Czechoslovakia. (Abstract).
- Lecomte, P. and Colin, F., 1989. Gold dispersion in a tropical rainforest weathering profile at Dondo Mubi, Gabon. *J. Geochem. Explor.*, 34: 285–301.
- Lecoq, J.J., Bigotte, G., Hinault, J. and Leconte, J.R., 1958. Prospecting for uranium and thorium minerals in the desert countries and in the equatorial forest regions of the French Union. In: *Proceedings of the Second United Nations International Conference on Peaceful Uses of Atomic Energy*. 2. International Atomic Energy Agency, Vienna, pp. 744–786.
- Leduc, C., 1986. Prospection géochimique de minéralisations de couverture en milieu carbonaté sous climat semi-aride: résultats d'une étude d'orientation de Zn-Pb de Bou Grine (Atlas tunisien). *Chron. Mines Rech. Minière*, 482: 33–37. (In French).
- Legge, P.J., Mill, J.H.A., Ringrose, C.R. and McDonald, I.R., 1990. Bottle Creek gold deposit. In: F.E. Hughes (Editor), *Geology of the Mineral Deposits of Australia and Papua New Guinea*. Australasian Institute of Mining and Metallurgy, Melbourne, pp. 357–361.
- Leggo, M.D., 1977. Contrasting geochemical expressions of copper mineralization at Namosi, Fiji. *J. Geochem. Explor.*, 8: 431–456.
- Leggo, M.J. and McKay, K.G., 1980. Forrestania nickel deposits, Yilgarn Block, W.A. In: C.R.M. Butt and R.E. Smith (Editors), *Conceptual Models in Exploration Geochemistry—Australia*. *J. Geochem. Explor.*, 12: 178–183.

- Lelong, F., Tardy, Y., Grandin, G., Trescases, J.J. and Boulangé, B., 1976. Pedogenesis, chemical weathering and processes of formation of some supergene ore deposits. In: K.H. Wolf (Editor), *Supergene and Surficial Ore Deposits; Textures and Fabrics*. Handbook of Stratabound and Stratiform Ore Deposits, 3. Elsevier, Amsterdam, pp. 93–173.
- Leueuf, N., 1959. *L'altération des Granites Calco-alcalins et des Granodiorites en Côte d'Ivoire Forestière et les Sols Qui en Sont Dérivés*. Ph.D. Thesis, University of Paris, 210 pp. (In French).
- Lenoble, A. and Gangloff, A., 1958. The present state of knowledge of thorium and uranium deposits in France and the French Union. In: *Proceedings of the Second United Nations International Conference on Peaceful Uses of Atomic Energy*. 2. International Atomic Energy Agency, Vienna, pp. 569–591.
- Leonardos, O.H., Fernandes, S.M., Fyfe, W.S. and Powell, M., 1987. The micro-chemistry of uraniumiferous laterites from Brazil: a natural example of inorganic chromatography. In: Y.Ogura (Editor), *Proceedings of an International Seminar on Laterite*, October 14–17, 1985, Tokyo, Japan. *Chem. Geol.*, 60: 111–119.
- Leprun, J.C., 1977. *Géochimie de la Surface et Formes du Relief. IV. La Dégradation des Cuirasses Ferrugineuses. Etude et Importance du Phénomène Pédologique en Afrique de l'Ouest*. Sciences Géologiques, Bulletin, 30: 265–273. (In French).
- Leprun, J.C., 1979. *Les Cuirasses Ferrugineuses des Pays Cristallins d'Afrique Occidentale Sèche. Génèse, Transformations, Dégradations*. Sciences Géologiques, Mémoire, 58. Université Louis Pasteur, Strasbourg, 224 pp. (In French).
- Leprun, J.C., 1981. Some features of iron crusts in dry Western Africa. In: *Lateritisation Processes*. Oxford and IBH Publishing Co., New Delhi, pp. 144–153.
- Lévêque, A., 1978. Les concentrations de fer dans les sols développés sur le socle granito-gneissique au Togo. *Cah. ORSTOM, Ser. Pedol.*, XVI: 3–22 (In French).
- Levinson, A.A., 1980. *Introduction to Exploration Geochemistry*. 2nd Ed. Applied Publishing, Wilmette, USA, 924 pp.
- Levinson, A.A. and Coetzee, G.L., 1978. Implications of disequilibrium in exploration for uranium ores in the surficial environment using radiometric techniques—a review. *Miner. Sci. Eng.*, 10: 19–27.
- Lintern, M.J., 1989. *Study of the Distribution of Gold in Soils at Mt. Hope, Western Australia*. Restricted Report, 24R. CSIRO Australia, Division of Exploration Geoscience, 17 pp.
- Lintern, M.J., Mann, A.W. and Longman, G.D., 1988. The determination of gold by anodic stripping voltammetry. *Anal. Chim. Acta*, 209: 193–203.
- Lintern, M.J., Mann, A.W. and Longman, G.D., in press. Field analysis of gold by cyanide digestion and anodic stripping voltammetry. *J. Geochem. Explor.*
- Listova, L.P., Vainshtein, A.Z. and Ryabinina, A.A., 1968. Dissolution of gold in media forming during oxidation of some sulphides. *Chem. Abstr.*, 68: 88967h. (Abstract).
- Liversidge, A., 1893a. On the origin of gold nuggets. *J. Proc. R. Soc. N. S. W.*, 27: 303–343.
- Liversidge, A., 1893b. On the crystallization of gold in hexagonal forms. *J. Proc. R. Soc. N. S. W.*, 27: 343–347.
- Locke, A., 1926. *Leached Outcrops as Guides to Copper Ores*. Bailliere, Tindall and Cox, London, 175 pp.
- Lock, N.P., 1985. Kimberlite exploration in the Kalahari region of southern Botswana with emphasis on the Jwaneng kimberlite province. In: *Prospecting in Areas of Desert Terrain*. Institute of Mining and Metallurgy, London, pp. 183–190.
- Lottermoser, B.G., 1988. Supergene, secondary malazite from the Mt Weld carbonatite laterite, Western Australia. *Neues Jahrb. Mineral., Monatsh.*, H.2: 67–70.
- Lovering, T., 1955. Progress in radioactive iron oxides investigation. *Econ. Geol.*, 50: 186–195.
- Lovering, T.G. and McCarthy, J.H., 1978. Conceptual models in exploration geochemistry—the Basin and Range Province of the Western United States and Northern Mexico. *J. Geochem. Explor.*, 9: 113–276.
- Lucas, Y., Boulet, R., Chauvel, A. and Veillon, L., 1987. Systèmes sols ferrallitiques-podzols en région amazonienne. In: D. Righi and A. Chauvel (Editors), *Podzols et Podzolisation*. Institut National de la Recherche Agronomique, Paris, pp. 53–65. (In French).

- Lucas, Y., Chauvel, A., Boulet, R., Ranzani, G. and Scatolini, F., 1984. Transicao latossolos-podzols sobre a formacao Barreiras na regio de Manaus, Amazonia. *Rev. Bras. Cienc. Solo*, 8: 325-335. (In Portuguese).
- Lucas, Y., Chauvel, A. and Ambrosi, J.P., 1986. Processes of aluminium and iron accumulation in latossols developed on quartz rich sediments from Central Amazonia (Manaus, Brazil). In: *Proceedings of the First International Symposium on Geochemistry of the Earth Surface*, March 1986. Granada, Spain,
- Lucas, Y., Kobilsek, B. and Chauvel, A., 1988. Structure, genesis and present evolution of amazonian bauxites developed on sediments. In: *Proceedings of the Sixth International Congress*. ICSOBA, Sao Paulo, Brazil.
- Mabbutt, J.A., 1977. *Desert Landforms*. Australian National University Press, Canberra, 340 pp.
- Mabbutt, J.A., 1980. Weathering history and landform development. In: C.R.M. Butt and R.E. Smith (Editors), *Conceptual Models in Exploration Geochemistry—Australia*. *J. Geochem. Explor.*, 12: 96-116.
- Mabbutt, J.A., Litchfield, W.H., Speck, N.H., Sofoulis, J., Wilcox, D.G., Arnold, J.M., Brookfield, M. and Wright, R.C., 1963. *General Report on the Lands of the Wiluna-Meekatharra Area, Western Australia, 1958*. Land Research Series, 7. CSIRO, Melbourne, 215 pp.
- Maglione, G., 1974. *Géochimie des Evaporites et Silicates Néoformés en Milieu Continental Confiné*. Ph.D. Thesis, University of Paris VI (unpublished). (In French).
- Maignien, R., 1958. *Le Cuirassement des Sols en Guinée, Afrique Occidentale*. Mémoire Service Carte Géologique, Alsace Lorraine, 16. Strasbourg, 223 pp.
- Maignien, R., 1966. *Review of Research on Laterites*. Natural Resources Research, IV. United Nations Educational Scientific and Cultural Organisation, Paris, 148 pp.
- Makumbi, M.N. and Jackson, M.L., 1977. Weathering of Karroo argillite under equatorial conditions. *Geoderma*, 19: 181-197.
- Mann, A.W., 1983. Hydrogeochemistry and weathering on the Yilgarn Block, Western Australia—ferrolysis and heavy metals in continental brines. *Geochim. Cosmochim. Acta*, 47: 181-190.
- Mann, A.W., 1984a. Mobility of gold and silver in lateritic weathering profiles: some observations from Western Australia. *Econ. Geol.*, 79: 38-49.
- Mann, A.W., 1984b. Redistribution of gold in the oxidized zone of some Western Australian deposits. In: *Gold-mining, Metallurgy and Geology. Proceedings of the Regional Conference on Mining and Metallurgy*, Perth and Kalgoorlie, October 1984. Australasian Institute of Mining and Metallurgy, Melbourne, pp. 1-12.
- Mann, A.W. and Deutscher, R.L., 1978. Genesis principles for the precipitation of carnotite in calcrete drainages in Western Australia. *Econ. Geol.*, 73: 1724-1737. (In French).
- Mann, A.W. and Horwitz, R.C., 1979. Groundwater calcrete deposits in Australia: some observations from Western Australia. *J. Geol. Soc. Aust.*, 26: 293-303.
- Maranzana, F., 1972. Application of talus sampling to geochemical exploration in arid areas. Los Pelambres alteration area, Chile. *Trans. Inst. Min. Metall., Sect. B, Appl. Earth Sci.*, 81: 26-33.
- Marker, A., 1988. *Lateritische Verwitterungsdecken über ultramafischen Gesteinskomplexen in Brasilien und den Philippinen*. Ph.D. Thesis, Institute für Mineralogie und Lagerstättenlehre, RWTH, Aachen (unpublished). (In German).
- Marker, A. and Martin, E.J., 1985. Relationship between chromite type and chemical composition of rutiles in the proterozoic ultramafic intrusion of Serro, Minas Gerais, Brazil. *Fortschr. Mineral.*, 63: p. 144.
- Martin, E.J., 1985. *Eigenschaften natürlicher Rutil als metallogenetische Kriterien*. Ph.D. Thesis, Institute für Mineralogie und Lagerstättenlehre, RWTH Aachen (unpublished), 213 pp. (In German).
- Massard, P., 1982. *Dissolution des Minéraux, Cinétique et Thermodynamique des Processus Irréversibles. Application à un Feldspath: l'Albite*. Ph.D. Thesis, University of Orsay, 128 pp. (In French).

- Matheis, G., 1981. Trace element patterns in lateritic soils applied to geochemical exploration. *J. Geochem. Explor.*, 15: 471–480.
- Matheis, G., 1983. Geochemical bedrock reflection in lateritic covers case histories from Nigeria, West Africa. In: A.J. Melfi and A. Carvalho (Editors), *Lateritisation Processes*. University of Sao Paulo Press, Sao Paulo, pp. 309–316.
- Matheis, G. and Pearson, M.J., 1982. Mineralogy and geochemical dispersion in lateritic soil profiles of Northern Nigeria. *Chem. Geol.*, 35: 129–145.
- Mathur, S.M. and Alexander, P.O., 1983. Preliminary pedo-geochemical and biogeochemical studies on the Hinota kimberlite, Panna District, MP. *Proc. Indian Acad. Sci., Earth Planet. Sci.*, 92: 81–88.
- Mazzucchelli, R.H., 1972. Secondary geochemical dispersion patterns associated with nickel sulphide deposits at Kambalda, Western Australia. *J. Geochem. Explor.*, 1: 103–116.
- Mazzucchelli, R.H., 1980. Warburton Range Cu prospects, Musgrave Block, W.A. In: C.R.M. Butt and R.E. Smith (Editors), *Conceptual Models in Exploration Geochemistry—Australia*. *J. Geochem. Explor.*, 12: 236–239.
- Mazzucchelli, R.H., 1987. Gold in stream sediments. In: *Meaningful Sampling in Gold Exploration*. Bulletin, 7. Australian Institute of Geoscientists, Sydney, pp. 85–103.
- Mazzucchelli, R.H. and James, C.H., 1966. Arsenic as a guide to gold mineralization in laterite-covered areas of Western Australia. *Trans. Inst. Min. Metall., Sect. B, Appl. Earth Sci.*, 75: 286–294.
- Mazzucchelli, R.H., Chapple, B.E.E. and Lynch, J.E., 1980. Northern Yorke Peninsular Cu, Gawler Block, S.A. In: C.R.M. Butt and R.E. Smith (Editors), *Conceptual Models in Exploration Geochemistry—Australia*. *J. Geochem. Explor.*, 12: 203–207.
- McFarlane, M.J., 1976. *Laterite and Landscape*. Academic Press, London, 151 pp.
- McFarlane, M.J. and Twidale, C.R., 1987. Karstic features associated with tropical weathering profiles. In: M.J. McFarlane (Editor), *Laterites: Some Aspects of Current Research*. *Z. Geomorphol., Suppl.*, 64: 73–95.
- Melfi, A.J. and Carvalho, A., 1983. *Bauxitization of Alkaline Rocks in Southern Brazil*. Sciences Géologiques, Mémoire, 73. Université Louis Pasteur, Strasbourg, pp. 161–172.
- Meneghal, L., 1982. Trial geochemical prospecting over kimberlite pipes of the Kundelungu Plateau, Shaba Province, Zaire. In: *Geochemistry in Zambia*. Report No. 9. Association of Geoscientists for International Development, Bangkok, pp. 77–91.
- Michard, G. and Fouillac, C., 1974. Evaluation des transferts d'éléments au cours des processus d'altération des minéraux par les fluides. *C. R. Acad. Sci., Paris*, 278D: 2727–2729. (In French).
- Michel, D., 1987. Concentration of gold in in situ laterites from Mato Grosso. *Miner. Deposita*, 22: 185–189.
- Michel, D., N'Ganzi, G. and Samama, J.C., 1983. Implications of adsorption for uranium geochemical prospecting in tropical conditions. In: *Uranium Exploration in Wet Tropical Environments*. International Atomic Energy Agency, Vienna, pp. 15–23.
- Michel, P., 1973. *Les Bassins des Fleuves Sénégal et Gambie. Etude Géomorphologique*. Mémoire, 63. ORSTOM, Paris, 752 pp.
- Michel, P., 1978. Cuirasses bauxitiques et ferrugineuses d'Afrique occidentale. Aperçu chronologique. In: *Géomorphologie des Reliefs Cuirassés dans les Pays Tropicaux, Chauds et Humides*. Travaux et Documents de Géographie, 33. Centre de Géographie et d'Etudes Tropicales, Bordeaux, pp. 11–32. (In French).
- Middleton, R.S. and Campbell, E.E., 1979. Geophysical and geochemical methods for mapping gold-bearing structures in Nicaragua. In: P.J. Hood (Editor), *Geophysics and Geochemistry in the Search for Metallic Ores*. Economic Geology, Report 31. Geological Survey of Canada, Ottawa, pp. 779–798.
- Miller, A.D. and Fisher, E.I., 1973. Dissolution of gold during oxidation by MnO₂. *Geochem. Int.*, 10(6): 656–663.
- Millot, G., 1964. *Géologie des Argiles*. Masson, Paris, 499 pp. (In French).
- Millot, G., 1980. *Les Grands Aplanissements des Socles Continentaux dans les Pays Sub-tropicaux et Désertiques*. H Séries, Mémoires de la Société Géologique de France, N10. (In French).

- Millot, G., 1983. Planation of continents by intertropical weathering and pedogenetic processes. In: A.J. Melfi and A. Carvalho (Editors), *Lateritisation Processes*. University of Sao Paulo Press, Sao Paulo, pp. 53–63.
- Millot, G. and Bonifas, M., 1955. *Transformations Isovolumétriques dans les Phénomènes de Latéritisation et de Bauxitization*. Bulletin Service Carte Géologique, Alsace Lorraine, 8: 3–10. (In French).
- Millot, G., Nahon, D., Paquet, H., Ruellan, A. and Tardy, Y., 1977. L'épigenie calcaire des roches silicatées dans les encroutements carbonatés en pays sub-aride, Anti-Atlas, Maroc. *Sci. Geol. Bull.*, 30: 129–152. (In French).
- Milnes, A.R. and Hutton, J.T., 1983. Calcretes in Australia. In: *Soils, An Australian Viewpoint*. CSIRO/Academic Press, Melbourne, pp. 119–162.
- Milnes, A.R. and Twidale, C.R., 1983. An overview of silicification in caenozoic landscapes of arid Central and Southern Australia. *Aust. J. Soil Res.*, 21: 387–410.
- Milnes, A.R., Bourman, R.P. and Northcote, K.M., 1985. Field relationships of ferricretes and weathered zones in southern South Australia: a contribution to "laterite" studies in Australia. *Aust. J. Soil Res.*, 23: 441–465.
- Moeskops, P.G., 1977. Yilgarn nickel gossan geochemistry—a review with new data. *J. Geochem. Explor.*, 8: 247–258.
- Moeskops, P.G. and White, A.H., 1980a. Beltana and Aroona Zn deposits, Adelaide Geosyncline, South Australia. In: C.R.M. Butt and R.E. Smith (Editors), *Conceptual Models in Exploration Geochemistry—Australia*. *J. Geochem. Explor.*, 12: 272–275.
- Moeskops, P.G. and White, A.H., 1980b. Ediacara Pb-(Zn)-(Cu) deposit, Adelaide Geosyncline, South Australia. In: C.R.M. Butt and R.E. Smith (Editors), *Conceptual Models in Exploration Geochemistry—Australia*. *J. Geochem. Explor.*, 12: 275–278.
- Moeyersons, J., 1978. The behaviour of stones and stone implements, buried in consolidating and creeping Kalahari sands. *Earth Surf.*, 3: 115–128.
- Moge, B., Samama, J.C. and Valence, G., 1987. Behaviour of uranium in ferrallitic environments—the case of the Kenieko occurrences (Mali). In: B. Poty and M. Pagel (Editors), *Concentration Mechanisms of Uranium in Geological Environments—A Conference Report*. *Uranium*, 3: 117–130.
- Molina, P., 1983. Exploration for uranium in tropical country. (A case history in the Central African Republic). In: *Uranium Exploration in Wet Tropical Environments*. International Atomic Energy Agency, Vienna, pp. 25–38.
- Money, N.J. and Prasad, R.S., 1979. Uranium mineralization in the Karroo System of Zambia. In: *Uranium Deposits in Africa: Geology and Exploration*. International Atomic Energy Agency, Vienna, pp. 21–39.
- Montgomery, R., 1971. *Secondary Dispersion of Molybdenum and Associated Elements in the Tropical Rainforest of Guyana*. Ph.D. Thesis, Imperial College, University of London (unpublished), 369 pp.
- Morris, R.C., 1980. A textural and mineralogical study of the relationship of iron ore to banded iron-formation in the Hamersley Iron Province of Western Australia. *Econ. Geol.*, 75: 184–209.
- Morris, R.C. and Fletcher, A.B., 1987. Increased solubility of quartz following ferrous-ferric iron reactions. *Nature*, 330: 558–561.
- Morrison, G.W., Teale, G.S. and Hodgkinson, I., 1987. Geology and gold mineralization at Mount Leyshon, North Queensland. In: *Proceedings of the Pacific Rim Congress*. Australasian Institute of Mining and Metallurgy, Melbourne, pp. 777–780.
- Mortland, M.M., 1968. Protonation of compounds at clay minerals surfaces. *Trans. Ninth Int. Congr. Soil Sci.*, 1: 691–698.
- Mösser, C. and Zeegers, H., 1988. The mineralogy and geochemistry of two copper-rich weathering profiles in Burkina Faso, West Africa. *J. Geochem. Explor.*, 30: 145–166.
- Mösser, C., Leprun, J.C. and Blot, A., 1985. Les éléments traces des fractions < 2 microns à kaolinite et smectite formées par alteration de roches silicatées acides en Afrique de l'Ouest (Sénégal et Haute Volta). *Chem. Geol.*, 48: 165–181. (In French).

- Mukherjee, K.K., 1979. Fluorine as a direct indicator in local soil geochemical survey in humid tropics—a case history. In: J.R. Watterson and P.K. Theobald (Editors), *Geochemical Exploration 1978*. Association of Exploration Geochemists, Toronto, pp. 139–144.
- Mulcahy, M.J., 1967. Landscapes, laterites and soils in southwestern Australia. In: J.N. Jennings and J.A. Mabbutt (Editors), *Landform Studies from Australia and New Guinea*. Cambridge University Press, Cambridge, pp. 211–230.
- Muller, D., Bocquier, G., Nahon, D. and Paquet, H., 1980. Analyse des différenciations minéralogiques et structurales d'un sol ferrallitique à horizons nodulaires du Congo. *Cah. ORSTOM, Ser. Pedol.*, XVIII: 87–110. (In French).
- Muller, J.P., 1978. La séquence verticale d'organisation des horizons meubles des sol ferrallitiques camerounais. Variation en latitude en fonction du pédoclimat et de l'âge des sols. *Cah. ORSTOM, Ser. Pedol.*, XVI: 73–82. (In French).
- Muller, J.P. and Pagel, M., 1988. Petrological controls of U-Th distribution in laterites. *Chem. Geol.*, 70: 189. (Abstract).
- Nahon, D., 1976. *Cuirasses Ferrugineuses et Encrôtements Calcaires au Sénégal Occidental et en Mauritanie. Systèmes Évolutifs. Structures, Relais et Coexistence*. Sciences Géologiques, Mémoire, 44. Université Louis Pasteur, Strasbourg, 232 pp. (In French).
- Nahon, D., 1986. Evolution of iron crusts in tropical landscapes. In: *Rates of Chemical Weathering of Rocks and Minerals*. Academic Press, London, pp. 169–191.
- Nahon, D., 1987. Microgeochemical environments in lateritic weathering. In: R. Rodriguez-Clemente and Y. Tardy (Editors), *Geochemistry and Mineral Formation in the Earth Surface*. Proceedings of an International Meeting, Granada, Spain, 1986. Consejo Superior de Investigaciones Científicas (CSIC), Madrid, pp. 141–156.
- Nahon, D. and Lappartient, J.R., 1977. Time factor and geochemistry of ironcrust genesis. *Catena*, 4: 249–254.
- Nahon, D. and Trompette, R., 1982. Origin of siltstones: glacial grinding versus weathering. *Sedimentology*, 29: 25–35.
- Nahon, D., Carozzi, A.V. and Parron, C., 1980. Lateritic weathering as a mechanism for the generation of ferruginous ooids. *J. Sediment. Petrol.*, 50: 1287–1298.
- Nahon, D., Colin, F. and Tardy, Y., 1982. Formation and distribution of Mg-Fe-Mn-smectites in the first stages of the lateritic weathering of forsterite and tephroite. *Clays Clay Miner.*, 17: 339–348.
- Nahon, D., Janot, C., Karpoff, A.M., Paquet, M. and Tardy, Y., 1977. Mineralogy, petrography and structure of iron crusts (ferricretes) developed on sandstones in the western part of Senegal. *Geoderma*, 19: 263–277.
- Nahon, D., Janot, C., Paquet, H., Parron, C. and Millot, G., 1979. Epigénie du quartz et de la kaolinite dans les accumulations et les cuirasses ferrugineuses superficielles. La signification des goethites et hématites alumineuses. *Sci. Geol., Bull.*, 32: 165–180. (In French).
- Nair, N.G.K., Santosh, M. and Mahadevan, R., 1985. Lateritisation as a possible contributor to gold placers in Nilambur valley, southeast India. *Chem. Geol.*, 60: 309–315.
- Nefedov, V.I., Zhavoronkov, M.M., Machavariani, G.V., Salyn, Ya.V., Makeev, V.A. and Zelenov, V.I., 1982. The variation of silver content in native gold particles as revealed by ESCA. *Phys. Chem. Miner.*, 8: 193–196.
- Nickel, E.H., 1982. The mineralogy and geochemistry of the Whim Creek gossan. *Australas. Inst. Min. Metall., Proc.*, 282: 33–45.
- Nickel, E.H., 1983. Weathering of sulphide bodies—generalized gossan profile-mineralogical and textural considerations. In: R.E. Smith (Editor), *Geochemical Exploration in Deeply Weathered Terrain*. CSIRO Division of Mineralogy, Floreat Park, Western Australia, pp. 73–87.
- Nickel, E.H., 1984. The mineralogy and geochemistry of the weathering profile of the Teutonic Bore Cu-Pb-Zn-Ag sulphide deposit. *J. Geochem. Explor.*, 22: 239–264.
- Nickel, E.H. and Daniels, J.L., 1985. Gossans. In: K.H. Wolf (Editor), *Regional Studies and Specific Deposits*. Handbook of Stratabound and Stratiform Ore Deposits, 13. Elsevier, Amsterdam, pp. 261–390.

- Nickel, E.H., Ross, J.R. and Thornber, M.R., 1974. The supergene alteration of pyrrhotite pentlandite ore at Kambalda, Western Australia. *Econ. Geol.*, 69: 93–107.
- Nisbet, B. and Joyce, P., 1980. Squirrel Hills Zn-mineralization, Mt. Isa belt, Qld. In: C.R.M. Butt and R.E. Smith (Editors), *Conceptual Models in Exploration Geochemistry—Australia*. *J. Geochem. Explor.*, 12: 259–264.
- Nissenbaum, A. and Serban, A., 1987. Enzymatic activity associated with humic substances in deep sediments from the Cariaco Trench and Walvis Ridge. *Geochim. Cosmochim. Acta*, 51: 373–378.
- Ollier, C.D., 1978. Early landform evolution. In: J.N. Jeans (Editor), *Australia, A Geography*. Sydney University Press, Sydney, pp. 85–98.
- Ollier, C.D., 1984. *Weathering*. Geomorphology Texts, 2. Longman, London, 270 pp.
- Ong, P.M. and Sevillano, A., 1975. Geochemistry in the exploration of nickeliferous laterite. In: I.L. Elliott and W.K. Fletcher (Editors), *Geochemical Exploration 1974*. Developments in Economic Geology, 1. Elsevier, Amsterdam, pp. 461–478.
- Ong, H.L. and Swanson, V.E., 1969. Natural organic acids in the transportation, deposition and concentration of gold. *Q. Colo. Sch. Mines*, 64: 395–425.
- Ong, H.L., Swanson, V.E. and Bisque, R.E., 1969. *Natural Organic Acids as Agents of Chemical Weathering*. Professional Paper 700C. U.S. Geological Survey, pp. 130–137.
- Ottmann, J. and Augustithis, S.S., 1967. Geochemistry and origin of “platinum-nuggets” in lateritic covers from ultrabasic rocks and birbirites of W. Ethiopia. *Miner. Deposita*, 1: 269–277.
- Overstreet, W.C., Stoesser, D.B., Overstreet, E.F. and Goudarzi, G.H., 1977. *Tertiary Laterite of the As Sarat Mountains Asir Province, Kingdom of Saudi Arabia*. Mineral Resources Bulletin, 21. Saudi Arabian Directorate General of Mineral Resources, Jeddah, 30 pp.
- Page, D.C. and Watson, M.D., 1976. The Pb-Zn deposit at Rosh Pinah mine, South West Africa. *Econ. Geol.*, 71: 306–327.
- Pagel, H.O., Borshoff, J. and Coles, R., 1984. Veinlike uranium deposits in the Rum Jungle area—geological setting and relevant exploration features. In: *Proceedings of the Australasian Institute of Mining and Metallurgy Conference*, Darwin, N.T., August 1984. Australasian Institute of Mining and Metallurgy, Melbourne, pp. 225–234.
- Pagel, M., 1984. Petrology, mineralogy and geochemistry of surficial uranium deposits. In: *Surficial Uranium Deposits*. International Atomic Energy Agency, Vienna, pp. 37–44.
- Paquet, H., Colin, F., Duplay, D. and Millot, G., 1987. Ni, Mn, Zn, Cr-smectites, early and effective traps for transition metals in supergene ore deposits. In: R. Rodriguez-Clemente and Y. Tardy (Editors), *Geochemistry and Mineral Formation in the Earth Surface*. Consejo Superior de Investigaciones Cientificas, Madrid, pp. 221–229.
- Parfitt, R.L., 1980. Chemical properties of variable charge soils. In: B.K.G. Theng (Editor), *Soils with Variable Charge*. Special Publication, New Zealand Society of Soil Science, pp. 167–194.
- Parks, G.A., 1967. Aqueous surface chemistry of oxides and complex oxide minerals. In: R.F. Gould (Editor), *Equilibrium Concepts in Natural Waters*. Advances in Chemistry, 67. pp. 121–159.
- Parks, G.A. and De Bruyn, P.J., 1962. The zero point charge of oxides. *J. Phys. Chem.*, 66: 967–973.
- Pasquali, J. and Lopez, C.J., 1982. Geochemical prospecting in humid tropical environments. In: D.J.C. Laming and A.K. Gibbs (Editors), *Hidden Wealth: Mineral Exploration Techniques in Tropical Forest Areas*. Report No. 7. Association of Geoscientists for International Development, pp. 75–79.
- Pasteris, J.D., 1980. The significance of groundmass ilmenite and megacryst ilmenite in kimberlites. *Contrib. Mineral. Petrol.*, 75: 315–325.
- Paton, T.R. and Williams, M.A.J., 1972. The concept of laterite. *Ann. Assoc. Am. Geograph.*, 62: 42–56.
- Pedersen, C.P., Dunbier, J. and Gingrich, J.E., 1980. Experience with the Track Etch method for uranium exploration in Northern Australia. In: J. Ferguson and A.B. Goleby (Editors), *Uranium in the Pine Creek Geosyncline*. International Atomic Energy Agency, Vienna, pp. 351–356.

- Pedro, G., 1964. *Contribution à l'Etude Expérimentale de l'Altération Géochimique des Roches Cristallines*. Ph.D. Thesis, University of Paris (also *Ann. Agron.*, 15: 85–191). (In French).
- Pedro, G., 1966. Essai sur la caractérisation géochimique des différents processus zonaux résultant de l'altération superficielle. *C. R. Acad. Sci., Paris*, 262D: 1828–1830. (In French).
- Pedro, G., 1983. Structuring of some basic pedological processes. *Geoderma*, 31: 289–299.
- Pedro, G., 1984. La genèse des argiles pédologiques, ses implications minéralogiques, physico-chimiques et hydriques. *Sci. Geol., Bull.*, 37 (4): 333–347.
- Pedro, G., 1985. Grandes tendances des sols mondiaux. *Cultivar*, 184: 78–81. (In French).
- Pedro, G. and Delmas, A.B., 1980–1981. Regards actuels sur les phénomènes d'altération hydrolytique, leur nature, leur diversité et leur place au cours de l'évolution géochimique superficielle. *Cah. ORSTOM, Ser. Pedol.*, 18: 57–74. (In French).
- Pedro, G. and Melfi, A.J., 1983. The superficial alteration in tropical region and the lateritisation phenomena. In: A.J. Melfi and A. Carvalho (Editors), *Lateritisation Processes*. University of Sao Paulo Press, Sao Paulo, pp. 3–13.
- Pedro, G. and Sieffermann, G., 1979. Weathering of rocks and formation of soils. In: F.R. Siegel (Editor), *Review of Research on Modern Problems in Geochemistry*. Earth Sciences, 16. UNESCO, Paris, pp. 39–55.
- Pedro, G., Chauvel, A. and Melfi, A.J., 1976. Recherche sur la constitution et la genèse des "Terra rossa estruturada" du Bresil. *Ann. Agron.*, 27: 265–294. (In French).
- Pedro, G., Jamagne, M. and Begon, J.C., 1969. Mineral interactions and transformations in relation to pedogenesis during the Quaternary. *Soil Sci.*, 107: 462–469.
- Pendleton, R.L., 1936. On the use of the term laterite. *Am. Soil Surv. Bull.*, 17: 102–108.
- Pfiffelmann, J.P., 1975. L'uranium dans le bassin de Franceville. In: *Le Phénomène d'Oklo*. International Atomic Energy Agency, Vienna, pp. 37–51. (In French).
- Philpott, D.E., 1975. Shangani—a geochemical discovery of a nickel-copper sulphide deposit. In: I.L. Elliott and W.K. Fletcher (Editors), *Geochemical Exploration 1974*. Developments in Economic Geology, 1. Elsevier, Amsterdam, pp. 503–510.
- Pion, J.C., 1979. *Altération des Massifs Cristallins Basiques en Zone Tropicale Sèche. Etude de Quelques Toposequences en Haute Volta*. Sciences Géologiques, Mémoire, 57. Université Louis Pasteur, Strasbourg, 220 pp. (In French).
- Pitul'ko, V.M., 1976. The behaviour of gold in the oxidation zones of deposits in the far north. *Geochem. Int.*, 13(2): 157–163.
- Plimer, I., 1986. Tourmalinites from the Golden Dyke Dome, Northern Australia. *Miner. Deposita*, 21: 263–270.
- Plyusnin, A.M., Pogrelnyak, Yu. F., Mironov, A.G. and Zhmodik, S.M., 1981. The behaviour of gold in the oxidation of gold bearing sulphides. *Geochem. Int.*, 18(3): 116–123.
- Pollack, H.R. and Zeegers, H., 1983. Influence de la granulométrie des prélèvements sur la réponse géochimique en milieu équatorial: un exemple au Surinam. *Chron. Mines Rech. Minière*, 472: 53–62. (In French).
- Postgate, J.R., 1951. The reduction of sulphur compounds by *Desulphovibrio desulphuricans*. *J. Gen. Microbiol.*, 5: 725–738.
- Pourbaix, M., 1963. *Atlas d'Equilibres Electrochimiques*. Gauthier-Villars, Paris, 644 pp. (In French).
- Prasad, E.A.V. and Vijaysaradhi, D., 1986. Chromium and vanadium in plant-soil-termite soil association. *Geobios*, 13: 134–136.
- Prasad E.A.V., Jayarama Gupta, M. and Dunn, C.E., 1987. Significance of termite mounds in gold exploration. *Curr. Sci. (India)*, 56: 1219–1222.
- Prasad, R.S., Money, N.J. and Thieme, J.G., 1979. Geology of the uranium occurrence in the Bungua area, Siavonga District, Zambia. In: *Uranium Deposits in Africa: Geology and Exploration*. International Atomic Energy Agency, Vienna, pp. 69–87.
- Premoli, C., 1979. Metallogeny of radioactive raw materials of Madagascar. In: *Uranium Deposits in Africa: Geology and Exploration*. International Atomic Energy Agency, Vienna, pp. 41–68.

- Prescott, J.A. and Pendleton, R.L., 1952. *Laterite and Lateritic soils*. Commonwealth Bureau of Soil Science Technical Communication, Report No. 47. Commonwealth Bureau of Soil Science, Farnham Royal Bucks, pp. 51.
- Pryce, W., 1778. *Mineralogia Cornubiensis*. Pitman Brothers, Bath.
- Raines, G.L. and Allen, M.S., 1975. Application of remote sensing and geochemistry to mineral exploration in Saudi Arabia: a case history. In: *Prospecting in Areas of Desert Terrain*. Institute of Mining and Metallurgy, London, pp. 1-10.
- Raines, G.L., McGee, L.G. and Sutley, S.J., 1985. Near-infrared spectra of West Shasta gossans compared with true and false gossans from Australian and Saudi Arabia. *Econ. Geol.*, 80: 2230-2239.
- Rammelmair, D., Raschka, H. and Steiner, L., 1987. Systematics of chromite occurrences in General Palawan, Philippines. *Miner. Deposita*, 22: 190-197.
- Rattigan, J.H., Gersteling, R.W. and Tonkin, D.G., 1977. Exploration geochemistry of the Stuart Shelf, South Australia. In: C.R.M. Butt and I.G.P. Wilding (Editors), *Geochemical Exploration 1976*. *J. Geochem. Explor.*, 8: 203-217.
- Razin, L.V. and Rozhkov, I.S., 1966. Geochemistry of gold in the crust of weathering and the biosphere of gold-ore deposits of the Kuranakh type. *Econ. Geol.*, 62: 437-438. (Review).
- Reedman, A.J., 1973. Prospection and evaluation of beryl pegmatites in south-west Uganda. *Overseas Geol. Miner. Resour.*, 41: 86-100.
- Reedman, J.H., 1974. Residual soil geochemistry in the discovery and evaluation of the Butiriku carbonatite, southeast Uganda. *Trans. Inst. Min. Metall., Sect. B, Appl. Earth Sci.*, 83: 1-12.
- Reedman, J.H., 1984. Resources of phosphate, niobium, iron and other elements in residual soils over the Sukulu carbonatite complex, southeastern Uganda. *Econ. Geol.*, 79: 716-724.
- Righi, D and Chauvel, A., 1987. *Podzols et Podzolisation*. Comptes Rendus Table Ronde Internationale, Poitiers, Association Française pour l'Etude du Sol, et Institut National de la Recherche Agronomique, 231 pp. (In French).
- Robbins, R.G., 1976. *Lands of the Ramu-Madang area, Papua New Guinea*. Land Research Series, 37. CSIRO, Melbourne, 134 pp.
- Robbins, T.E. and Chenoweth, L.M., 1984. Geochemical investigations associated with the Wilga and Currawong massive sulphide deposits, Benambra, Victoria. *J. Geochem. Explor.*, 22: 43-70.
- Robert, M., 1970. Etude expérimentale de la désagrégation du granite. *Ann. Agron.*, 21: 777-817. (In French).
- Robert, M., 1971. Etude expérimentale de l'évolution des micas (biotites): I. Les aspects du processus de vermiculitisation. *Ann. Agron.*, 22: 43-93. (In French).
- Robert, M., 1972. Etude expérimentale de l'évolution des micas. I. Les autres possibilités d'évolution des micas et leur place par rapport à la vermiculitisation. *Ann. Agron.*, 22: 155-181. (In French).
- Robert, M. and Pedro, G., 1972. An experimental evaluation of the effect of pH and concentration of salt solutions in altering trioctahedral micas. In: *Proceedings of the 12th International Clay Conference*, Madrid. II. pp. 103-120.
- Roberts, D.E. and Travis, G.A., 1985. Microtextural evaluation of nickel sulphide gossans in Western Australia. *Trans. R. Soc. Edinburgh, Earth Sci.*, 77: 81-98.
- Rodgers, P.B. and Knowles, C.J., 1978. Cyanide production and degradation during growth of *Chromobacterium violaceum*. *J. Gen. Microbiol.*, 108: 261-267.
- Rognon, P., 1976. Essai d'interprétation des variations climatiques au Sahara depuis 40.000 ans. *Rev. Geogr. Phys. Geol. Dyn.*, XVIII(2-3): 251-282. (In French).
- Rolla, E. and Chakrabarti, C.L., 1982. Kinetics of decomposition of tetrathionate, trithionate and thiosulphate in alkaline media. *Environ. Sci. Technol.*, 16: 852-857.
- Roquin, C., Dandjinou, T., Freyssinet, Ph. and Pion, J.C., 1989. The correlation between geochemical data and SPOT satellite imagery of lateritic terrain in southern Mali. In: S.E. Jenness (Editor), *Geochemical Exploration 1987*. *J. Geochem. Explor.*, 32: 149-168.
- Rose, A.W., Hawkes, H.E. and Webb, J.S., 1979. *Geochemistry in Mineral Exploration*. Academic Press, London, 637 pp.

- Rosholt, J.N., 1958. Radioactive disequilibrium studies as an aid in understanding the natural migration of uranium and its decay products. In: *Proceedings of the Second United Nations Conference on Peaceful Uses of Atomic Energy*. 2. International Atomic Energy Agency, Vienna, pp. 230–236.
- Roslyakov, N.A., 1984. Zonality of gold forms in the surficial environment as a criterion for buried gold deposits. *J. Geochem. Explor.*, 21: 333–340.
- Ruellan, A., Beaudet, G., Nahon, D., Paquet, H., Rognon, P. and Millot, G., 1979. Rôle des encroulements calcaires dans le façonnement des glaciers d'ablation des régions arides et semi-arides du Maroc. *C. R. Acad. Sci., Paris, Ser. D*, 289: 619–622.
- Ruhe, R.V., 1959. Stone lines in soils. *Soil Sci.*, 87: 223–231.
- Ruxton, B.P., 1958. Weathering and sub-surface erosion in granite at the piedmont angle, Balos, Sudan. *Geol. Mag.*, 95: 353–377.
- Ruxton, B.P., 1963. Some aspects of detailed geochemical testing at Rum Jungle, Northern Territory, Australia. In: *Proceedings of the Seminar on Geochemical Prospecting, Methods and Techniques*. Mineral Research and Development Series, 21. United Nations, ECAFE, New York, pp. 104–111.
- Ryall, W.R. and Taylor, G.F., 1981. In: *Gossan Evaluation Manual for Use in the Kingdom of Saudi Arabia*. Technical Record RF-TR-01-3. Ministry of Petroleum and Mineral Resources, Jiddah, 146 pp.
- Ryall, W.R., Scott, K.M., Taylor, G.F. and Moore, G.P., 1981. Mercury in stratabound copper mineralization in the Mammoth area, northwest Queensland. *J. Geochem. Explor.*, 16: 1–11.
- Saigusa, M., 1975. Relation between copper content in soils and copper grade in some porphyry copper deposits in humid tropical regions. In: I.L. Elliott and W.K. Fletcher (Editors), *Geochemical Exploration 1974*. Developments in Economic Geology, 1. Elsevier, Amsterdam, pp. 511–522.
- Salard-Cheboldaeff, M., 1981. Palynologie maestrichienne et tertiaire du Cameroun. Résultats botaniques. *Rev. Paleobot. Palynol.*, 32: 401–439. (In French).
- Salpateur, I., 1985. Geochemical dispersion from the Bir Tawilah wolfram-quartz veins in the pediplain area of Saudi Arabia. In: *Prospecting in Areas of Desert Terrain*. Institute of Mining and Metallurgy, London, pp. 141–154.
- Salpateur, I. and Sabir, H., 1989. Gold exploration in the central pediplain of the Saudi Arabian shield. *J. Geochem. Explor.*, 34: 189–215.
- Samama, J.C., 1984. Uranium in lateritic terrains. In: *Surficial Uranium Deposits*. International Atomic Energy Agency, Vienna, pp. 53–64.
- Samama, J.C., 1986. *Ore Fields and Continental Weathering*. Van Nostrand Reinhold, New York, 326 pp.
- Samama, J.-C., Royer, J.J. and N'Ganzi, C., 1989. Prise en compte de la surface spécifique des prélèvements en prospection géochimique: exemple de l'uranium dans les sédiments de ruisseau. In: S.E. Jenness (Editor), *Geochemical Exploration 1987*. *J. Geochem. Explor.*, 32: 453–466.
- Santos, R., 1981. Geology and mining development of the C-09 uranium deposit. In: *Uranium Deposits in Latin America: Geology and Exploration*. International Atomic Energy Agency, Vienna, pp. 533–553.
- Sato, M. and Mooney, H.M., 1960. The electrochemical mechanism of sulphide self potentials. *Geophysics*, 25: 226–249.
- Saupe, S.G., Seigler, D.S. and Escalante-Semerana, J.C., 1982. Bacterial contamination as a cause of spurious cyanide tests. *Phytochemistry*, 21: 2111–2112.
- Saxena, S.K., 1966. Evolution of zircons in sedimentary and metamorphic rocks. *Sedimentology*, 6: 1–33.
- Schellmann, W., 1981. Considerations on the definition and classification of laterites. In: *Lateritisation Processes*. Oxford and IBH Publishing Co., New Delhi, pp. 1–10.
- Schellmann, W., 1986. On the geochemistry of laterites. *Chem. Erde*, 45: 39–52.
- Schellmann, W., 1987. *Nickelexploration Tagaung Tavung, Birma*. Report, BGR Hannover (unpublished), 12 pp.

- Schellmann, W., 1989. Allochthonous surface alteration of Ni-laterites. *Chem. Geol.*, 74: 351–364.
- Schmitt, J.M and Thiry, M., 1987. Uranium behaviour in a gossan-type weathering system: example of the Bertholène deposit (Aveyron, France). *Bull. Soc. Fr. Mineral. Cristallogr.*, 110: 197–208.
- Schorin, H. and Puchelt, H., 1987. Geochemistry of a ferruginous bauxite profile from southeast Venezuela. *Chem. Geol.*, 64: 127–142.
- Schott, J., Berner, R.A. and Sjöberg, E.L., 1981. Mechanisms of pyroxene and amphibole weathering. I. Experimental studies of iron-free minerals. *Geochim. Cosmochim. Acta*, 45: 2123–2135.
- Schwertmann, U., 1983. The role of aluminium in iron oxide systems. In: A.J. Melfi and A. Carvalho (Editors), *Lateritisation Processes*. University of Sao Paulo Press, Sao Paulo, pp. 65–68.
- Scott, K.M., 1986. Sulfide geochemistry and wall rock alteration as a guide to mineralization, Mammoth area, NW Queensland. *J. Geochem. Explor.*, 25: 283–308.
- Scott, K.M., 1987. Solid solution in, and classification of, gossan-derived members of the alunite-jarosite family, northwest Queensland, Australia. *Am. Mineral.*, 72: 178–187.
- Scott, K.M. and Taylor, G.F., 1977. Geochemistry of the Mammoth copper deposit, northwest Queensland, Australia. *J. Geochem. Explor.*, 8: 153–168.
- Scott, K.M. and Taylor, G.F., 1982. Eastern Creek volcanics as the source of copper at the Mammoth mine, Northwest Queensland. *BMR J. Aust. Geol. Geophys.*, 7: 93–98.
- Scott, K.M. and Taylor, G.F., 1987. The oxidized profile of BIF-associated Pb–Zn mineralization: Pegmont, northwest Queensland, Australia. *J. Geochem. Explor.*, 27: 103–124.
- Scott, M.J., 1975. Case histories from a geochemical exploration programme—Windhoek district, South West Africa. In: I.L. Elliott and W.K. Fletcher (Editors), *Geochemical Exploration 1974*. Developments in Economic Geology, 1. Elsevier, Amsterdam, pp. 481–492.
- Segall, R.L., Smart R.St.C. and Turner, P.S., 1982. The dissolution of ionic and semiconducting oxides. *Chem. Aust.*, 49: 241–245.
- Segerstrom, K., 1963. Matureland of northern Chile and its relationship to ore deposits. *Geol. Soc. Am., Bull.*, 74: 513–518.
- Sen, A.K., 1981. *The Weathering Profile at Panchpatmali Plateau, Koraput District, Orissa*. Records of the Geological Survey of India, Calcutta, 112: 49–53.
- Seward, T.M., 1973. Thio complexes of gold and the transport of gold in hydrothermal ore solutions. *Geochim. Cosmochim. Acta*, 37: 379–399.
- Seward, T.M., 1982. The transport and deposition of gold in hydrothermal systems. In: R.P. Foster (Editor), *Gold '82: The Geology, Geochemistry and Genesis of Gold Deposits*. Geological Society of Zimbabwe, pp. 165–181.
- Shacklette, H.T., Lakin, H.W., Hubert, A.E. and Curtin, G.C., 1970. *Absorption of Gold by Plants*. Bulletin No. 1314-B. United States Geological Survey, 23 pp.
- Shannon, R.D., 1976. Revised effective ionic radii and systematic studies of interatomic distances in halides and chalcogenides. *Acta Crystallogr., Sect. A*, 32: p. 751.
- Sherrington, G.H. and Gatehouse, S.G., 1980. *Pea Gravels as a Guide to Mineralization*. Geopeko Ltd., Sydney (unpublished), pp. 11.
- Sherrington, G.H., Browne, A.L.L., Duffin, R.H. and Danielson, M.J., 1983a. Number three orebody, Ranger One, Australia—a case history. *J. Geochem. Explor.*, 19: 7–9. (Abstract).
- Sherrington, G.H., Browne, A.L.L., Duffin, R.H. and Danielson, M.J., 1983b. *The Number Three Orebody, Ranger One, Northern Territory, Australia. A Case History*. Geopeko Ltd, Sydney (unpublished), 21 pp.
- Shirvington, P.J., 1980. 234-U/238-U activity ratios in clay as a function of distance from primary ore. In: J. Ferguson and A.B. Goleby (Editors), *Uranium in the Pine Creek Geosyncline*. International Atomic Energy Agency, Vienna, pp. 509–519.
- Shirvington, P.J., 1983. Fixation of radionuclides in the ²³⁸U decay series in the vicinity of mineralized zones: 1. The Austatom uranium deposit, Northern Territory, Australia. *Geochimica Cosmochimica Acta*, 47: 403–412.
- Sillén, L.G. and Martell, A.E., 1964. *Stability Constants of Metal-ion Complexes*. Special Publication, 17. The Chemical Society, London, 754 pp.

- Sillén, L.G. and Martell, A.E., 1971. *Stability Constants of Metal-ion Complexes. Supplement No. 1*. Special Publication, 25. The Chemical Society, London, 865 pp.
- Sivarajasingham, S., Alexander, L.T., Cady, J.G. and Cline, M.G., 1962. Laterite. *Adv. Agron.*, 14: 1–60.
- Sivenas, P. and Beals, F.W., 1982. Natural geobatteries associated with sulphide ore deposits. 1. Theoretical studies. *J. Geochem. Explor.*, 17: 123–143.
- Smith, A.D. and Hunt, R.J., 1985. Solubilisation of gold by *Chromobacterium violaceum*. *J. Chem. Technol. Biotechnol.*, 35B: 110–116.
- Smith, B.H., 1987a. Dispersion of gold in soils. In: *Meaningful Sampling in Gold Exploration*. Bulletin, 7. Australian Institute of Geoscientists, Sydney, pp. 55–82.
- Smith, B.H. and Keele, R.A., 1984. Some observations on the geochemistry of gold mineralization in the weathered zone at Norseman, Western Australia. *J. Geochem. Explor.*, 22: 1–20.
- Smith, R.E., 1983. Generalized model for secondary dispersion haloes in transported overburden in weathered terrain. In: R.E. Smith (Editor), *Geochemical Exploration in Deeply Weathered Terrain*. CSIRO Division of Mineralogy, Floreat Park, Western Australia, pp. 153–154.
- Smith, R.E., 1987b. Some conceptual models for geochemistry in areas of preglacial deep weathering. In: R.G. Garrett (Editor), *Geochemical Exploration, 1985*. Part I. *J. Geochem. Explor.*, 28: 337–352.
- Smith, R.E., 1989. Using lateritic surfaces to advantage in exploration. In: G.D. Garland (Editor), *Proceedings of Exploration '87. Third Decennial International Conference on Geophysical and Geochemical Exploration for Minerals and Groundwater*. Special Volume 3. Ontario Geological Survey, Toronto, pp. 312–322.
- Smith, R.E. and Butt, C.R.M., 1983. Sample preparation. In: R.E. Smith (Editor), *Geochemical Exploration in Deeply Weathered Terrain*. CSIRO Australia, Division of Mineralogy, Floreat Park, Western Australia, pp. 23–25.
- Smith, R.E. and Perdrix, R.L., 1983. Pisolitic laterite geochemistry in the Golden Grove massive sulphide district, Western Australia. *J. Geochem. Explor.*, 18: 131–164.
- Smith, R.E., Birrell, R.D. and Brigden, J.F., 1989. The implications to exploration of chalcophile corridors in the Archaean Yilgarn Block, Western Australia, as revealed by laterite geochemistry. In: S.E. Jenness (Editor), *Geochemical Exploration 1987*. *J. Geochem. Explor.*, 32: 169–184.
- Smith, R.E., Campbell, N.A. and Litchfield, R., 1984. Multivariate statistical techniques applied to pisolite laterite geochemistry at Golden Grove, Western Australia. *J. Geochem. Explor.*, 22: 193–216.
- Smith, R.E., Campbell, N.A. and Perdrix, J.L., 1983. Identification of some Western Australian gossans by multi-element geochemistry. In: R.E. Smith (Editor), *Geochemical Exploration in Deeply Weathered Terrain*. CSIRO Australia, Division of Mineralogy, Floreat Park, Western Australia, pp. 75–90.
- Smith, R.E., Frater, K.M. and Moeskops, P.G., 1980. Golden Grove Cu–Zn deposit, Yilgarn Block, W.A. In: C.R.M. Butt and R.E. Smith (Editors), *Conceptual Models in Exploration Geochemistry—Australia*. *J. Geochem. Explor.*, 12: 195–199.
- Smith, R.E., Moeskops, P.G. and Nickel, E.H., 1979. Multi-element geochemistry at the Golden Grove Cu–Zn–Pb–Ag deposit. In: J.E. Glover, D.I. Groves and R.E. Smith (Editors), *Pathfinder and Multi-element Geochemistry in Mineral Exploration*. Publication No.4. Geology Department and Extension Service, University of Western Australia, Perth, pp. 30–41.
- Smith, R.E., O'Connell, A.M. and Edwards, R.G., 1976. Freddie Well Zn–Cu deposit. In: R.E. Smith, C.R.M. Butt and E. Bettenay (Editors), *Superficial Mineral Deposits and Exploration Geochemistry, Yilgarn Block, Western Australia*. Excursion Guide 41C. Twenty-fifth International Geological Congress, Sydney, pp. 45–48.
- Smith, R.E., Perdrix, J.L. and Davis, J.M., 1987. Dispersion into pisolitic laterite from the Greenbushes mineralised Sn–Ta pegmatite system, Western Australia. In: R.G. Garrett (Editor), *Geochemical Exploration 1985*. Part I. *J. Geochem. Explor.*, 28: 251–265.
- Smith, R.M. and Martell, A.E., 1976. *Inorganic Complexes. Critical Stability Constants*, 4. Plenum Press, New York, pp. 252.

- Smith, W.D., 1965. The broader aspects of secondary mineralization at Mount Isa, Queensland. *Australas. Inst. Min. Metall., Proc.*, 217: 33–38.
- Sneath, P.H.A., 1972. Identification methods applied to Chromobacterium. In: F.A. Skinner and D.W. Lovelock (Editors), *Identification Methods for Microbiologists*. Academic Press, London, pp. 15–20.
- Snelling, A.A., 1980. Uraninite and its alteration products, Koongarra uranium deposit. In: J. Ferguson and A.B. Goleby (Editors), *Uranium in the Pine Creek Geosyncline*. International Atomic Energy Agency, Vienna, pp. 487–498.
- Snelling, A.A., 1984. A soil geochemistry orientation survey for uranium at Koongarra, Northern Territory. *J. Geochem. Explor.*, 22: 83–99.
- Snoep, J. and Zeegers, H., 1979. Multi-metal soil geochemistry: a tool for identification and exploration of porphyry copper deposits. Two examples from Peru. *J. Geochem. Explor.*, 11: 103–130.
- Soil Survey Staff, 1975. Soil Taxonomy. Soil Conservation Service, United States Department of Agriculture, Washington, 754 pp.
- Stace, H.C.T., Hubble, G.D., Brewer, R., Northcote, K.H., Sleeman, J.R., Mulcahy, M.J. and Hallsworth, E.G., 1968. *A Handbook of Australian Soils*. Technical Publication, Classification, Cartographie, CSIRO and ISSS, Rellim, Glenside, Australia, 435 pp.
- Stoop, W.A., 1980. Ion adsorption mechanisms in oxidic soils; replication for zero point charge determinations. *Geoderma*, 23: 303–314.
- Stoops, G., 1967. Le profil d'altération au Bas-Congo (Kinshasa). *Pédologie*, 17: 60–105. (In French).
- Subzhiyeva, T.M. and Volkov, I.I., 1982. Thiosulphates and sulphites in thermal and hydrothermal waters. *Geochem. Int.*, 19(4): 94–98.
- Symons, P.M., 1988. The Boddington gold deposit. In: A.D.T. Goode and L.I. Bosma (Editors), *Bicentennial Gold 88*. Abstract Series, 22. Geological Society of Australia, Sydney, pp. 56–61. (Extended abstract).
- Talapatra, A.K., 1979. Gossan geochemistry as a guide to exploration of different types of sulfide mineralization in parts of Rajasthan, western India. In: J.R. Watterson and P.K. Theobald (Editors), *Geochemical Exploration 1978*. Association of Exploration Geochemists, Toronto, pp. 173–183.
- Tan, K.H., 1984. *Andosols. Benchmark Papers in Soil Science*, Van Nostrand Reinhold, New York, 418 pp.
- Tardy, Y., 1969. *Géochimie des Altérations. Etude des Arènes et des Eaux de Quelques Massifs Cristallins d'Europe et d'Afrique*. Ph.D. Thesis, University of Strasbourg, 199 pp. (also Mémoire Service Carte Géologique, Alsace Lorraine, 31: (In French).
- Tardy, Y., 1981. *Le Cycle de l'Eau. Climats, Paléoclimats et Géochimie Globale*. Masson, Paris, 338 pp. (In French).
- Tardy, Y., 1986. *Le Cycle de l'Eau. Climats, Paléoclimats et Géochimie Globale*. Masson, Paris, 338 pp. (In French).
- Tardy, Y. and Nahon, D., 1985. Geochemistry of laterites, stability of Al-goethite, Al-hematite and Fe³⁺-kaolinite in bauxites and ferricretes: an approach to the mechanism of concretion formation. *Am. J. Sci.*, 285: 865–903.
- Tardy, Y., Melfi, A.J. and Valetton, I., 1988. Climats et paléoclimats tropicaux périalantiques. Rôle des facteurs climatiques et thermodynamiques: température et activité de l'eau, sur la répartition et la composition minéralogique des bauxites et des cuirasses ferrugineuses au Brésil et en Afrique. *C. R. Acad. Sci., Paris*, 306: 289–295. (In French).
- Taube, A., 1978. Note on geochemical investigations in a deep lateritic weathering profile at Woodcutters L5 lead-zinc-silver prospect, N.T. *Australas. Inst. Min. Metall., Proc.*, 266: 47–50.
- Taufen, P.M. and Marchetto, C.M.L., 1989. Tropical weathering control of Ni, Cu, Co, and platinum group element distributions at the O'Toole Ni-Cu sulphide deposit, Minas Gerais, Brazil. *J. Geochem. Explor.*, 32: 185–197.

- Taylor, G., Coste, B., Lambert, A. and Zeegers, H., 1989. Geochemical signature (bedrock and saprolite) of gold mineralization and associated hydrothermal alteration at Dorlin, French Guyana. *J. Geochem. Explor.*, 32: 56–60. (Abstract).
- Taylor, G.F., 1973. The geochemistry of siderite in relation to ironstone in the Paradise Creek Formation, northwest Queensland. *J. Geochem. Explor.*, 2: 367–382.
- Taylor, G.F., 1987. Near-infrared spectra of West Shasta gossans compared with true and false gossans from Australia and Saudi Arabia and trace element content of gossans at four mines in the West Shasta massive sulfide district—a discussion. *Econ. Geol.*, 82: 230–232.
- Taylor, G.F. and Appleyard, E.C., 1983. Weathering of the zinc lead lode, Dugald River northwest Queensland. I. The gossan profile. *J. Geochem. Explor.*, 18: 87–110.
- Taylor, G.F. and Scott, K.M., 1982. Evaluation of gossans in relation to lead-zinc mineralization in the Mount Isa Inlier, Queensland. *Aust. Bur. Miner. Resour., Geol. Geophys., Bull.*, 7: 159–180.
- Taylor, G.F. and Scott, K.M., 1983. Weathering of the zinc-lead lode, Dugald River, northwest Queensland. II. Surface mineralogy and geochemistry. *J. Geochem. Explor.*, 18: 111–130.
- Taylor, G.F. and Sylvester, G.C., 1982. Analysis of a weathered profile on sulfide mineralization at Mugga Mugga, Western Australia. *J. Geochem. Explor.*, 16: 105–134.
- Taylor, G.F., Wilmshurst, J.R., Butt, C.R.M. and Smith, R.E., 1980. Ironstones and gossans. In: C.R.M. Butt and R.E. Smith (Editors), *Conceptual Models in Exploration Geochemistry—Australia*. *J. Geochem. Explor.*, 12: 118–122.
- Taylor, G.F., Wilmshurst, J.R., Togashi, Y. and Andrew, A.S., 1984. Geochemical and mineralogical haloes about the Elura Zn-Pb-Ag orebody, western New South Wales. *J. Geochem. Explor.*, 22: 265–290.
- Taylor, R.M. and Graley, A.M., 1967. The influence of ionic environments on the nature of iron oxides in soils. *J. Soil Sci.*, 18: 341–348.
- Taylor, R.M. and Schwertmann, U., 1978. The influence of aluminium on iron oxides—I. The influence of Al on Fe oxide formation from the Fe (II) system. *Clays Clay Miner.*, 26: 373–383.
- Teh, G.H., 1979. Geochemical studies around the Tekka area, Perak, peninsular Malaysia. *Bull. Geol. Soc. Malaysia*, 11: 353–373.
- Thijssen, T., Pluger, W. and Friedrich, G., 1979. Chrom- und Eisenbestimmungen an Chromiten aus Schwermineralkonzentraten mit einem tragbaren Isotop-rontgenfluoreszenzgerat. *Z. Erzbergbau Metallhuettenwes.*, 33: 497–499. (In German).
- Thomas, M.F., 1974. *Tropical Geomorphology—A Study of Weathering and Landform Developments in Warm Climates*. MacMillan, London, 332 pp.
- Thornber, M.R., 1975a. Supergene alteration of sulphides, I: A chemical model based on massive nickel sulphide deposits at Kambalda, Western Australia. *Chem. Geol.*, 15: 1–14.
- Thornber, M.R., 1975b. Supergene alteration of sulphides, II. A chemical study of the Kambalda nickel deposits. *Chem. Geol.*, 15: 117–144.
- Thornber, M.R., 1983. Mineralogical and electrochemical stability of the nickel-iron sulphides-pentlandite and violarite. *J. Appl. Electrochem.*, 13: 253–267.
- Thornber, M.R., 1985. Supergene alteration of sulphides. VII: Distribution of elements during the gossan-forming process. *Chem. Geol.*, 53: 279–301.
- Thornber, M.R. and Nickel, E.H., 1976. Supergene alteration of sulphides, III. The composition of associated carbonates. *Chem. Geol.*, 17: 45–72.
- Thornber, M.R. and Wildman, J.E., 1984. Supergene alteration of sulphides, VI. The binding of Cu, Ni, Zn, Co and Pb with gossan (iron bearing) minerals. *Chem. Geol.*, 44: 399–434.
- Thornber, M.R., Allchurch, P.D. and Nickel, E.H., 1981. Variations in gossan geochemistry at the Perseverance Nickel Sulphide Deposit, Western Australia: A descriptive and experimental study. *Econ. Geol.*, 76: 1764–1774.
- Tipping, E. and Cooke, D., 1982. The effect of adsorbed humic substances on the surface charge of goethite (alpha-FeOOH) in freshwaters. *Geochim. Cosmochim. Acta*, 46: 75–80.
- Toens, P.D. and Hambleton-Jones, B.B., 1984. Definition and classification of surficial uranium deposits. In: *Surficial Uranium Deposits*. International Atomic Energy Agency, Vienna, pp. 9–14.

- Tooms, J.S. and Jay, J.R., 1964. The role of the biochemical cycle in the development of copper-cobalt anomalies in the freely drained soils of the northern Rhodesian copperbelt. *Econ. Geol.*, 59: 826-834.
- Tooms, J.S. and Webb, J.S., 1961. Geochemical prospecting investigations in the Northern Rhodesian copper belt. *Econ. Geol.*, 56: 815-846.
- Tooms, J.S., Elliott, I. and Mather, A.L., 1965. Secondary dispersion of molybdenum from mineralisation, Sierra Leone. *Econ. Geol.*, 60: 1478-1496.
- Tordiffe, E.A.W., Vermaak, J.J., van der Westhuizen, W.A. and Beukes, G.J., 1989. The Jacomynspan copper-nickel prospect—a study of secondary dispersion in the calcretes of the Northern Cape Province, South Africa. In: G.L. Coatzee (Editor), *Exploration Geochemistry in Southern Africa. J. Geochem. Explor.*, 34: 31-45.
- Travis, G.A., Keays, R.R. and Davison, R.M., 1976. Palladium and iridium in the evaluation of nickel gossans in Western Australia. *Econ. Geol.*, 71: 1229-1243.
- Trescases, J-J., 1975. *L'évolution Géochimique Supergène des Roches Ultrabasiques en Zone Tropicale. Formation des Gisements Nickélicifères de Nouvelle-Calédonie*. Mémoire, 78. ORSTOM, Paris, 259 pp. (In French).
- Trescases, J-J., 1979. Remplacement progressif des silicates par les hydroxydes de fer et de nickel dans les profils d'altération tropicale des roches ultrabasiques. Accumulation résiduelle et épigénie. *Sci. Geol. Bull.*, 32: 181-188. (In French).
- Trescases, J-J., 1986. *Nickeliferous Laterites: a Review on the Contributions of the Last Ten Years*. Memoir, 120. Geological Survey of India, Calcutta, pp. 51-62.
- Trescases, J-J. and Melfi, A.J., 1985. Les gisements latéritiques du Brésil. *Pangea*, 5: 6-16. (In French).
- Trewartha, G.T., 1968. *An Introduction to Climate*. 4th ed. McGraw-Hill, New York, 408 pp.
- Tricart, J., 1972. *The Landforms of the Humid Tropics, Forests and Savannas*. (Trans: C.J.K. de Jonge). Longman and Co. Ltd, London, 306 pp.
- Trichet, J., 1969. *Contribution à l'Etude de l'Altération Expérimentale des Verres Volcaniques*. Ph.D. Thesis, Travaux Laboratoire E.N.S., 4. University of Paris, 152 pp. (In French).
- Trolard, F. and Tardy, Y., 1987. The stabilities of gibbsite, boehmite, aluminous goethites and aluminous hematites in bauxites, ferricretes and laterites as a function of water activity, temperature and particle size. *Geochim. Cosmochim. Acta*, 51: 945-957.
- Tupas M.H., Hale, W.E. and Govett, G.J.S. (Editors), 1968. *Exploration for Disseminated Copper Deposits in Humid, Mountainous, Tropical Terrain, Sto Nino, Mountain Province, Philippines*. Investigation Report, 66. Philippines Bureau of Mines, Manila, 115 pp.
- Turenne, J.F., 1977. *Mode d'Humification et Différenciation Podzolique dans deux Toposéquences Guyanaises*. Mémoire, 84. ORSTOM, Paris, 173 pp. (In French).
- Tyrwhitt, D.S., 1985. Exploration, development and geology of Telfer gold mine, Great Sandy Desert, Western Australia. In: *Prospecting in Areas of Desert Terrain*. Institute of Mining and Metallurgy, London, pp. 11-19.
- Valeton, I., 1955. Veränderungen an Zirkon und Turmalin in Buntsandstein und Keuper. *Heidelb. Beitr. Mineral. Petrogr.*, 3: 335-379. (In German).
- Valeton, I., 1972. *Bauxites*. Developments in Soil Science, 1. Elsevier, Amsterdam, 226 pp.
- Valeton, I., Biermann, M., Reche, R. and Rosenberg, F., 1987. Genesis of nickel laterites and bauxites in Greece during the Jurassic and Cretaceous, and their relation to ultrabasic parent rocks. *Ore Geol. Rev.*, 2: 359-404.
- Van Andel, T.H. and Weyl, R., 1952. Zur frage des Schwermineralverwitterung/In sedimenten. *Erdoel Kohle*, 5: 100-104. (In German).
- Van Berkel, F., 1982. *Geochemical Exploration in Arid and Semi-arid Environments*. Ph.D. Thesis, Rhodes University, South Africa (unpublished), 159 pp.
- Van der Weijden, C.H., Arthur, R.C. and Langmuir, D., 1976. Sorption of uranyl by hematite. Theoretical and geochemical implications. *Abstracts of the Annual Meeting*, Denver, Geological Society of America, pp. 1152.

- Van Leeuwen, T.M., Leach, T., Hawke, A.A. and Hawke, M.M., 1990. The Kelian disseminated gold deposit, East Kalimantan, Indonesia. In: J.W. Hedenquist, N.C. White and G. Siddeley (Editors), *Epithermal Gold Mineralization of the Circum-Pacific: Geology, Geochemistry, Origin and Exploration*, I. *J. Geochem. Explor.*, 35: 1–61.
- Van Moort, J.C. and Swenson, C.G., 1982. The oxidized zone of the Broken Hill lode, N.S.W. In: G.C. Amstutz (Editor), *Ore Genesis*. Springer, Berlin, pp. 251–267.
- Verheye, W., 1979. Le profil d'altération pédogéologique sur granodiorites en Côte d'Ivoire Centrale. *Rev. Geogr. Phys. Geol. Dyn.*, XXVIII: 49–60. (In French).
- Vermaak, J.J., 1984. *Aspects of the Secondary Dispersion of Ore-related Elements in Calcrete-environments of the Northern Cape Province*. M.Sc. Thesis, University of Orange Free State, Bloemfontein (unpublished), 136 pp.
- Viaene, W., Suhanda, T., Vandenberghe, N., Sunarya, Y. and Ottenburgs, R., 1981. Geochemical soil prospecting in northwest Kalimantan, Indonesia. In: A.W. Rose and H. Gundlach (Editors), *Geochemical Exploration 1980*. *J. Geochem. Explor.*, 15: 453–470.
- Vizier, J.F., 1983. *Etude des Phénomènes d'Hydromorphie dans les Sols des Régions Tropicales à Saisons Contrastées. Dynamique du Fer et Différenciation des Profils*. Travaux et Documents, 165. ORSTOM, Paris, 294 pp. (In French).
- Volkoff, B., 1985. Organisations régionales de la couverture pédologique du Brésil. Chronologie des différenciations. *Cah. ORSTOM, Ser. Pedol.*, XXI, 4: 225–236. (In French).
- Von Maravic, H., Morteani, G. and Roethe, G.A., 1983. Die niobreichen Verwitterungserze des Karbonatits von Lueshe, Zaire. *Z. Erzbergbau Metallhuettenwes.*, 36: 29–35. (In German).
- Warren, H.V., 1982. The significance of a discovery of gold crystals in overburden. In: *Precious Metals in the Northern Cordillera*. Association of Exploration Geochemists, Toronto, pp. 45–51.
- Watson, J.P., 1970. Contribution of termites to development of zinc anomaly in Kalahari sand. *Trans. Inst. Min. Metall., Sect. B, Appl. Earth Sci.*, 79: 53–59.
- Watson, J.P., 1972. The distribution of gold in termite mounds at a gold anomaly in the Kalahari sand. *Soil Sci.*, 113: 317–321.
- Watters, R.A., 1983. Geochemical exploration for uranium and other metals in tropical and subtropical environments using heavy mineral concentrates. *J. Geochem. Explor.*, 19: 103–124.
- Watters, R.A. and Sagala, F.P., 1979. Geochemical reconnaissance for uranium and base metals using heavy mineral separates in central and southern Sumatra. In: J.R. Watterson and P.K. Theobald (Editors), *Geochemical Exploration 1978*. Association of Exploration Geochemists, Toronto, pp. 317–327.
- Watterson, J.R., 1985. A procedure for estimating *Bacillus cereus* spores in soil and stream-sediment samples—a potential exploration technique. *J. Geochem. Explor.*, 23: 243–252.
- Watts, J.T., Tooms, J.S. and Webb, J.S., 1963. Geochemical dispersion of niobium from pyrochlore-bearing carbonatites in Northern Rhodesia. *Trans. Inst. Min. Metall.*, 72: 729–747.
- Webb, J.S., 1958. Observations on geochemical exploration in tropical terrains. In: *Proceedings of the XXth International Geological Congress, Mexico, 1956*. Symposium de Exploracion Geoquimica, 1. pp. 143–173.
- Webb, J.S. and Tooms, J.S., 1959. Geochemical drainage reconnaissance for copper in Northern Rhodesia. *Trans. Inst. Min. Metall., Sect. B, Appl. Earth Sci.*, 68: 125–144.
- Weber, F., Geffroy, J. and Le Mercier, M., 1975. Synthèse des études minéralogiques et pétrographiques des minerais d'Oklo, de leurs gangues et des roches encaissantes. In: *Le Phénomène d'Oklo*. International Atomic Energy Agency, Vienna, pp. 173–193. (In French).
- Webster, J.G., 1984. Thiosulphate complexing of gold and silver during the oxidation of a sulphide-bearing carbonate lode system, Upper Ridges Mine, Papua New Guinea. In: *Gold Mining, Metallurgy and Geology*. Regional Conference, Kalgoorlie, Australasian Institute of Mining and Metallurgy, Melbourne, 1–9.
- Webster, J.G., 1986. The solubility of gold and silver in the system Au-Ag-S-O₂-H₂O at 25 degrees C and 1 atm. *Geochim. Cosmochim. Acta*, 50: 1837–1845.

- Webster, J.G. and Mann, A.W., 1984. The influence of climate, geomorphology and primary geology on the supergene migration of gold and silver. *J. Geochem. Explor.*, 22: 21–42.
- Webster, R., 1965. A catena of soils on the northern Rhodesia plateau. *J. Soil Sci.*, 16: 31–43.
- Wilhelm, E. and Kosakevitch, A., 1979. Utilisation des chapeaux de fer comme guides de prospection. *Bull. Bur. Rech. Geol. Minières*, 2: 109–140. (In French).
- Wilhelm, E., Zeegers, H. and Ambrosi, J.P., 1985. Cuirasses latéritiques et prospection minière. In: J. Alexandre and J.J. Symoens (Editors), *Les Processus de Latéritisation; Journée d'Etude*. Académie Royale des Sciences d'Outre-Mer, Brussels, pp. 111–126. (In French).
- Williams, M.A.J., 1968. Termites and soil development near Brocks Creek, Northern Territory. *Aust. J. Sci.*, 31: 153–154.
- Williams, P.A., 1990. *Oxide Zone Geochemistry*. Ellis Horwood, London, 286 pp.
- Wilmshurst, J.R., 1975. The weathering products of nickeliferous sulphides and their associated rocks in Western Australia. In: I.L. Elliott and W.K. Fletcher (Editors), *Geochemical Exploration 1974*. Developments in Economic Geology, 1. Elsevier, Amsterdam, pp. 417–436.
- Wilmshurst, J.R. and Fisher, N.I., 1983. Classification scheme of gossans. In: R.E. Smith (Editor), *Geochemical Exploration in Deeply Weathered Terrain*. CSIRO Division of Mineralogy, Floreat Park, Western Australia, pp. 104–106.
- Wilson, A.F., 1984. Origin of quartz-free gold nuggets and supergene gold found in laterites and soils—A review and some new observations. *Aust. J. Earth Sci.*, 31: 303–316.
- Wollast, R., 1967. Kinetics of the alteration of K-feldspar in buffered solutions at low temperatures. *Geochim. Cosmochim. Acta*, 31: 635–648.
- Woods, R., 1976. Chemisorption at electrodes. In: A.J. Bard (Editor), *Electroanalytic Chemistry*, 9. Marcel Dekker, New York, pp. 1–162.
- Young, A., 1976. *Tropical Soils and Soil Survey*. Cambridge University Press, Cambridge, 468 pp.
- Zebrowski, C., 1975. Etude d'une climato-séquence dans l'île de la Réunion. *Cah. ORSTOM, Ser. Pedol.*, XIII(3/4): 255–278. (In French).
- Zeegers, H., 1979. Regional geochemical prospecting in equatorial areas. An example in French Guiana. In: J.R. Watterson and P.K. Theobald (Editors), *Geochemical Exploration 1978*. Association of Exploration Geochemists, Toronto, pp. 209–225.
- Zeegers, H., 1987. Remaniements de surface et prospection géochimique de l'or. *Chron. Mines Rech. Minière*, 488: 55–61. (In French).
- Zeegers, H. and Lepun, J.C., 1979. Evolution des concepts en altérologie tropicale et conséquences potentielles pour les prospections géochimiques en Afrique occidentale soudano-sahélienne. *Bull. Bur. Rech. Geol. Minières*, 2: 229–239. (In French).
- Zeegers, H., Al Shanfari, S.M., Al Muflehi, Y.A. and Lethlenet, J., 1985. Aspects of regional geochemical prospecting in desert conditions. In: *Prospecting in Areas of Desert Terrain*. Institute of Mining and Metallurgy, London, pp. 131–140.
- Zeegers, H., Goni, J. and Wilhelm, E., 1981. Geochemistry of lateritic profiles over a disseminated Cu–Mo mineralization in Upper Volta (West Africa)—Preliminary results. In: *Lateritisation Processes*. Oxford and IBH Publishing Co., New Delhi, pp. 359–368.
- Zeissink, H.E., 1969. The mineralogy and geochemistry of a nickeliferous laterite profile (Greenvale, Queensland, Australia). *Miner. Deposita*, 4: 132–152.
- Zimmerman, D.O., 1964. Gossans at northern leases, Mount Isa, as visible geochemical anomalies. In: J.T. Woodcock, R.T. Madigan and R.C. Thomas (Editors), *Proceedings of the Eighth Congress on Mining and Metallurgy*. Publication 6. Australasian Institute of Mining and Metallurgy, Melbourne, pp. 359–367.

AUTHOR INDEX

- Aicard, P., 433
Aleva, G.J.J., 11
Alexander, M.A., 64
Alexander, P.O., 433
Allen, M.S., 140
Ambrosi, J.P., 38, 44–46, 48, 207–209, 216,
217, 279
Anand, R.R., 12, 20, 55, 313, 316, 318, 532,
533
Andrew, A.S., 117
Andrew, R.L., 118, 126, 135, 136, 141, 142,
150, 152–154, 164, 169, 174, 180–182,
186–188, 405
Appleyard, E.C., 151, 172
Ashikhmin, A.A., 443, 447, 448, 450
Atherden, P.R., 237
Augustithis, S.S., 328
Awasthi, S.C., 405
Aye, F., 140, 156
- Baes, C.F., 80
Bailey, L.K., 122
Baker, W.E., 466
Ball, L.C., 185
Baranova, N.N., 464
Barbier, J., 99, 111, 360, 367, 369, 370, 372,
524
Bardossy, G., 38, 50, 55, 64
Barnes, J.F.H., 517
Barretto, P.M.C., 447, 452
Barron, C.N., 490, 492, 496
Barron, E.J., 11
Barton, P.B., 444
Beals, F.W., 129
Berner, R.A., 26, 36
Berner, W., 64
Bianconi, F., 439, 447
Biro, P., 98
Blain, C.F., 135, 141, 142, 150, 160
Blake, D.H., 197
Blanchard, R., 115, 142, 513
Bland, C.J., 440, 444
Blaylock, G., 470
Bloomfield, K., 222
Blot, A., 203, 205
- Bloxam, T.W., 399, 400
Bocquier, G., 60, 74, 206, 275, 281
Boenigk, W., 484
Boissen, R., 398
Bokilo, J.F., 448
Bonham-Carter, G.F., 531
Bonifas, M., 44
Bose, S.S., 268
Boulangé, D., 50, 60, 64
Boulet, R., 61, 64, 65, 67, 69, 71–73, 203–
205, 226, 275
Bourezg, M., 165, 182, 183
Bowden, J.W., 93
Bowles, J.F.W., 137, 222, 468
Boyle, R.W., 143, 188, 442, 444, 459, 464–
467
Brabant, P., 70, 74
Brabham, G.R., 316
Bradshaw, P.M.D., 17
Brimhall, G.H., 49
Brinkman, R., 61
Brock, P.W.G., 233
Brookins, D.G., 80
Brown, A.G., 224, 225, 298
Buchanan, F., 41
Budel, J., 1, 9, 10, 11, 13, 102, 103, 295,
297, 360
Bugg, S.F., 215, 216
Bugrov, V.A., 369–371, 524
Bull, A.S., 153, 193
Bullen, T., 492
Busche, D., 102
Busemberg, E., 36
Butt, C.R.M., 3, 18, 19, 21–23, 58, 63, 65,
97, 100, 102, 103, 117, 150, 162, 163,
295, 299, 304, 305, 321, 323–327, 330–
333, 335, 345, 351, 357, 361, 365, 390,
393, 405, 408, 416, 460, 461, 467, 468,
470, 472, 473, 483, 486, 499, 511, 524,
525, 533
- Cabello, J., 409, 410
Cameron, E., 99
Campbell, E.E., 216
Carlisle, D., 374, 375

- Carr, G.R., 117, 171, 458
 Carroll, D., 484
 Carvalho, A., 38
 Carver, R.N., 240, 308, 332, 336, 346–349, 478, 519
 Cash, S.J., 483
 Chace, F.M., 222
 Chaffee, M.A., 415
 Chakrabarti, C.L., 465
 Chao, T.T., 444, 452
 Chatelin, Y., 281
 Chaussidon, J., 61
 Chauvel, A., 35, 58, 60, 61, 74
 Chenoweth, L.M., 178, 179
 Christ, C.L., 26
 Christensen, S.M., 356
 Clark, A.H., 298, 409
 Clarke, E.T., 135
 Clarke, O.M., 409
 Clema, J.M., 153, 193
 Clemency, C.V., 36
 Cline, G.R., 94
 Cloke, P.L., 462
 Cloud, P., 104
 Clough, D.M., 468
 Cochrane, R.H.A., 193
 Coetzee, G.L., 441
 Cole, M.M., 140, 172
 Coleman, R.G., 490, 492
 Colin, F., 39, 276, 277, 285–287, 467, 471, 474
 Collinet, J., 276, 280
 Cooke, D., 93
 Cooke, H.J., 298
 Cooke, R.U., 98, 107
 Coolbaugh, D.F., 409, 410
 Coope, J.A., 108, 188
 Corpe, W.A., 465
 Cowden, A., 137
 Cox, R., 215, 351, 352, 378, 379
 CPCS, 76, 77
 Craw, D., 468
 Cruikshank, B.I., 450, 460
 Cumberlidge, J.T., 222
 Curtis, R., 215, 351, 352

 Dahlberg, E.H., 274
 Dalgarno, C.R., 356, 357
 Danchin, R., 379
 Daniels, J.L., 10, 116, 117, 135, 137, 141, 142, 188
 Dasgupta, S.P., 405, 406

 Davies, T.C., 252, 399, 400, 470
 Davis, J.C., 153
 Davy, R., 252, 316, 391, 470, 477
 Dawson, J.B., 419, 421, 434
 De Bruyn, P.L., 92
 De Oliveira, J.J., 298
 De Vivo, B., 214
 Debnam, A.H., 231
 Delmas, A.B., 26, 28, 36
 Delvigne, J., 60
 Desborough, G.A., 468
 Deshpande, M.L., 405
 Deutscher, R.L., 388, 389, 442
 Dick, H.J.B., 492
 Dickson, B.L., 440, 460
 Didier, P., 50, 60
 Dietrich, W.E., 49
 Disnar, J.R., 466
 Dommanget, A., 229
 Dommergues, Y., 64
 Duchaufour, P., 100, 102
 Duncan, R.K., 223, 329
 Dunlop, A.C., 332, 336, 340, 342
 Dury, G.H., 12
 Dutrizac, J.E., 115
 d'Orey, F.L.C., 105, 106, 109, 236

 Edou-Minko, A., 400, 401
 El Din Khalil, B., 416
 Elias, M., 328
 Ellison, D., 470
 El-Ansary, M., 252, 470
 Embrecht, J., 60
 Emmons, S.F., 115
 Emmons, W.H., 115
 Erbe, W., 102
 Erdman, J.A., 466
 Erickson, R.L., 386, 387
 Esson, J., 100, 203, 243
 Eswaran, H., 60
 Eugster, H.P., 35
 Eupene, G.S., 447, 450, 451, 460
 Evans, D.L., 222

 Fairbairn, P.E., 423–425
 FAO-UNESCO, 76, 77
 Farrah, H., 92
 Farrell, B.L., 484, 496
 Fedoseyeva, V.I., 466
 Fetzter, W.G., 466
 Filipek, L.H., 412, 452
 Fischer, N.I., 116, 462

- Flach, W., 60, 541
 Fletcher, R.J., 30, 297, 345, 346, 361, 470, 475
 Force, E.R., 496
 Fortescue, J.A.C., 17
 Fouillac, C., 26
 Frakes, L.A., 64
 Freise, F.W., 466
 Freyssinet, P., 219, 222, 249, 251, 252, 321, 323, 467, 468, 470, 471
 Frick, C., 348, 349, 350, 381, 384
 Friedrich, G.H.W., 356, 469, 483-485, 487, 488, 490-493, 497
 Fritsch, E., 69
 Fritz, B., 26, 46, 47
 Furlong, D.N., 93
- Gac, J.V., 50, 64
 Gangloff, A., 451
 Garnett, D.L., 379-381, 405, 407
 Garrels, R.M., 26
 Gatehouse, S.G., 458
 Gatellier, J.P., 466
 Gavaud, M., 63, 70, 74
 Gedeon, A.Z., 527-529
 Gee, R.D., 316
 Geffroy, J., 447, 452
 Gentili, J., 5
 Germann, A., 492
 Ghadiri, H., 107
 Giblin, A.M., 444
 Gilbert, G.K., 97
 Gilkes, R.J., 55
 Giresse, P., 241
 Girling, C.A., 466
 Giusti, L., 468, 469
 Glasson, M.J., 139, 319, 320, 470
 Gleeson, C.F., 105, 235, 304
 Goldhaber, M.B., 465
 Goldich, S.S., 35
 Goldsmith, R., 496
 Gole, M.J., 330, 331, 460
 Goleva, G.A., 465
 Golightly, J.P., 440, 486
 Goni, J., 466
 Goosens, P.J., 238, 239
 Goudie, A., 298, 374
 Govett, G.J.S., 234, 235, 237, 349, 410
 Graley, A.M., 75
 Grandin, G., 206
 Granger, H.C., 465
 Granier, C., 236, 288, 290, 334
- Gray, D.J., 461
 Grégoire, D.C., 466
 Gregory, G.P., 419, 431, 436
 Greig, D.D., 332, 337, 339
 Grimbert, A., 458
 Grimm, B., 469
 Gritsaenko, G.S., 440, 447, 448, 450, 451, 453
 Grove, A.T., 298
 Grubb, P.L.C., 70
 Guedria, A., 383, 384
 Guillemot, D., 267
 Gulson, B.L., 117, 156, 157, 159, 161
- Haebig, E.A., 432
 Hale, W.E., 362
 Halitim, H., 62
 Hall, G., 332
 Hall, G.E.M., 531
 Hallbauer, D.K., 468
 Hallberg, J.A., 100, 101, 487, 488
 Halligan, R., 404, 406
 Hambleton-Jones, B.B., 386
 Hanssen, E., 165, 182, 183
 Harmon, R.S., 440
 Harpavat, C.L., 297
 Harris, J.L., 404, 406
 Harrison, P.H., 384, 385
 Harvey, T.V., 297, 360
 Heberlein, D.R., 188
 Helgeson, H.C., 26, 36
 Hervieu, J., 64
 Hessin, T.D., 415
 Hoffman, S.J., 110
 Holdren, G.R., 26
 Hore, M.K., 297
 Horwitz, R.C., 99
 Howarth, R.J., 153
 Hsi, C.K.D., 444
 Huang, P.M., 64
 Hudson, D.R., 137
 Hume-Rothery, W., 82
 Hunt, R.J., 465, 466
 Hunter, M.J., 142, 185, 186
 Hutton, J.T., 62, 65
- IAEA, 386, 388, 442, 459
 Ildefonse, P., 27
 Irvine, T.N., 490, 492
 Ivanovich, M., 440
 Ivey, M.E., 470, 475

- Jackson, D.G., 432
 Jackson, M.L., 252, 254
 James, C.H., 209, 219, 309, 377
 Janse, A.J.A., 419
 Jaques, A.L., 421, 431
 Jay, J.R., 234
 Johnson, I.R., 174
 Jones, R.A., 109, 393
 Joyce, A.S., 153, 193, 197
 Joyce, P., 197
 Jutson, J.T., 111
- Kalsotra, M.R., 209
 Kampf, N., 75
 Kanig, M., 483
 Kaspar, J., 466
 Kater, G.N., 497
 Keele, R.A., 381, 382, 466
 Kellogg, C.E., 41
 Kelly, W.C., 462
 Kemp, E.M., 12
 Kilpatrick, B.E., 268
 King, L.C., 42
 Klingner, G.D., 174
 Knowles, A.R., 358, 359
 Knowles, C.J., 358, 465, 466
 Kögler, K., 439, 440, 444, 447, 454, 455
 Kolotov, B.A., 466
 Köppen, W., 4, 6, 7, 21, 59, 160, 161, 295
 Korobushkina, E.D., 466
 Kosakevitch, A., 116, 153, 514
 Koshman, P.N., 468
 Krauskopf, K.B., 462
 Kresten, P., 422
 Kubiena, W., 484
- Lacroix, A., 48
 Lakin, H.W., 462, 465
 Lal, J.K., 405
 Lamouroux, M., 75
 Lamplugh, G.W., 536
 Langmuir, D., 80, 87, 442-444
 Laporte, G., 275
 Lappartient, J.R., 64
 Laval, M., 222, 267, 329
 Laville-Timsit, L., 216, 229, 263
 Lawrence, L.M., 356, 365-367, 461, 467,
 470, 471, 475, 476, 478, 479
 Learned, R.E., 398
 Leblanc, M., 490, 492
 Lecomte, P., 103, 104, 203, 224, 241, 253,
 275-277, 279, 281, 285-287
- Lecoq, J.J., 447, 451
 Leduc, C., 383
 Legge, P.J., 190
 Leggo, M.D., 110, 334, 397
 Lelong, F., 39, 63
 Leneuf, N., 42, 50, 64
 Lenoble, A., 451
 Leonardos, O.H., 447, 452
 Leprun, J.C., 38, 63, 64, 74, 203, 207-209,
 532
 Lévêque, A., 275
 Levinson, A.A., 440-442, 444, 496, 512
 Lintern, M.J., 351, 353, 354, 529
 Listova, L.B., 465
 Liversidge, A., 462
 Lock, N.P., 104, 105, 362, 435, 492
 Locke, A., 115
 Lottermoser, B.G., 329
 Lovering, T.G., 416
 Lovering, T., 448
 Lucas, Y., 58, 60, 66, 70
- Mabbutt, J.A., 15, 296, 374
 Maglione, G., 35
 Maignien, R., 41
 Makumbi, M.N., 252, 254
 Mangenot, F., 64
 Mann, A.W., 87, 99, 117, 137, 222, 252, 301,
 388, 399, 442, 465, 467-471, 475, 479,
 511
 Maranzana, F., 110, 416
 Marchetto, C.M.L., 195
 Marker, A., 483, 484, 486, 488, 490, 497
 Marranzino, A.P., 386, 387
 Martell, A.E., 80
 Martin, E.J., 484, 496, 497
 Massard, P., 36
 Matheis, G., 205, 210, 273, 276, 487
 Mathur, S.M., 433
 Mazzucchelli, R.H., 153, 209, 219, 309, 336,
 347, 362, 363, 377, 385, 386
 McCarthy, J.H., 416
 McFarlane, M.J., 102, 511, 533
 McKay, K.G., 334
 Melfi, A.J., 37, 38, 61
 Meneghal, L., 431
 Mesmer, R.E., 80
 Michard, G., 26
 Michel, D., 222, 444, 452, 453, 468, 470,
 471
 Michel, P., 42, 206
 Middleton, R.S., 216

- Miller, A.D., 462
 Millot, G., 11, 33, 41, 44, 58, 62, 75, 206, 241
 Milnes A.R., 62, 63, 65
 Mizon, K.J., 156, 159, 161
 Moeskops, P.G., 153, 193–195, 410–413
 Moeyersons, J., 275
 Moge, B., 444
 Molina, P., 447, 448
 Money, N.J., 447
 Montgomery, R., 265–267
 Mooney, H.M., 119, 129
 Morris, R.C., 10, 30, 37
 Morrison, G.W., 188
 Mortland, M.M., 61
 Mosser, C., 209, 226–228, 238, 280
 Mukherjee, K.K., 274
 Mulcahy, M.J., 360
 Muller, D., 275, 276
 Muller, J.P., 45, 262, 444, 447
- Nahon, D., 41, 42, 44–49, 61–64, 74, 75, 99, 206–208, 243–246, 281, 374, 377, 532
 Nair, N.G.K., 222
 Nefedov, V.I., 468
 Nichol, I., 429, 511
 Nickel, E.H., 58, 63, 65, 93, 100, 116, 117, 123, 126, 135, 137, 141, 142, 176–178, 188, 325, 338, 486, 496
 Nisbet, B., 197
 Nissenbaum, A., 95
- Ollier, C.D., 98, 296
 Olson, J.C., 466
 Ong, H.L., 466
 Ong, P.M., 398, 399
 Ottemann, J., 328
 Overstreet, W.C., 297, 360
- Page, D.C., 182
 Pagel, H.O., 459
 Pagel, M., 444, 445, 447
 Paquet, H., 209
 Parfitt, R.L., 92, 93
 Parks, G.A., 92
 Pasquali, J., 245
 Pasteris, J.D., 496
 Paton, T.R., 12
 Paul, D.K., 422
 Payne, P., 107
 Pearson, M.J., 205, 210, 276
- Pedersen, C.P., 460
 Pedro, G., 10, 26, 27, 32–36, 60, 61, 242
 Pendleton, R.L., 41
 Perdrix, J.L., 108, 178, 209, 309, 313, 314, 318, 496
 Perring, R.J., 384
 Peters, E., 122
 Piffelmann, J.P., 447, 451
 Philpott, D.E., 405, 407
 Pickering, W.F., 92
 Pion, J.C., 226
 Pitul'ko, V.M., 465
 Plimer, I.R., 490
 Plyusnin, A.M., 465
 Pollack, H.R., 274
 Postgate, J.R., 466
 Poulin, P., 105, 235, 304
 Pourbaix, M., 80
 Prasad, E.A.V., 105
 Prasad, R.J., 209, 447
 Premoli, C., 447
 Prescott, J.A., 41
 Pryce, W., 115
 Puchelt, H., 203, 242
 Pyke, J.G., 450, 460
- Raines, G.L., 140
 Rammelmair, D., 490, 493, 495
 Rattigan, J.H., 356
 Raynor, G.V., 82
 Razin, L.V., 466
 Rea, W.J., 405, 407
 Reedman, J.H., 222, 223, 231, 492
 Righi, D., 35, 61
 Robbins, R.G., 16
 Robbins, T.E., 178, 179
 Robert, M., 26, 33
 Roberts, D.E., 193
 Robertson, I.D.M., 524, 526
 Robertson, R.M.S., 423–425
 Robertson, R.S., 104
 Rocquin, C., 219
 Rodgers, P.B., 465, 466
 Rognon, P., 64
 Rolla, E., 465
 Rose, A.W., 150, 234, 512
 Rosholt, J.N., 441
 Roslyakov, N.A., 466
 Rozhkov, I.S., 466
 Ruellan, A., 374
 Ruhe, R.V., 103
 Ruxton, B.P., 100, 447, 456

- Ryall, W.R., 117, 150, 151, 153, 168, 181, 186, 196, 361
 Ryzhenko, B.N., 464
- Sabir, H., 109–111, 336, 360, 369, 372, 373, 479, 524
 Sagala, F.P., 444, 458
 Saigusa, M., 398
 Salard-Cheboldaeff, M., 241
 Salpeteur, I., 109–111, 336, 360, 368–370, 372, 373, 479, 524
 Samama, J.C., 440, 444, 447, 454
 Santos, R., 443, 447
 Sato, M., 119, 129
 Saupe, S.G., 465
 Saxena, S.K., 484
 Schellmann, W., 484, 486
 Schmitt, J.M., 443, 447, 452
 Schorin, H., 203, 242
 Schott, J., 26
 Schwertmann, U., 75, 484
 Scott, K.M., 117, 133, 140, 142, 153, 154, 170, 172, 186, 189, 198
 Scott, M.J., 405, 407, 408
 Segall, R.L., 80
 Segerstrom, K., 298
 Serban, A., 95
 Sevillano, A., 398, 399
 Seward, T.M., 464
 Shacklette, H.T., 466
 Shalaby, I.M., 370, 371
 Shannon, R.D., 82
 Sheppy, N.R., 324, 325
 Sherrington, G.H., 447, 450, 453, 458–460
 Shirvington, P.J., 444, 455, 456
 Sieffermann, G., 10
 Sillén, L.G., 80
 Sivarajasingham, S., 41
 Sivenas, P., 129
 Smith, A.D., 465, 466
 Smith, B.H., 351, 381, 382, 466, 480
 Smith, D.G.W., 468, 469
 Smith, R.E., 18, 19, 21, 108, 117, 152–155, 166, 177, 178, 209, 219, 299, 304, 305, 308–310, 312–314, 318, 324, 333, 353, 361, 364, 405, 416, 480, 483, 496, 519, 524, 525
 Smith, R.M., 80
 Smith, W.D., 170
 Sneath, P.H.A., 465
 Snelling, A.A., 442, 447, 456, 460
 Snoep, J., 415
 Snowden, V., 355
- Soil Survey Staff, 77
 Stace, H.G.T., 63, 77
 Stephens, W.E., 434
 Stevens-Hoare, N.P., 153, 193
 Stoop, W.A., 92
 Stoops, G., 60, 103, 275
 Subzhiyeva, T.M., 464, 465
 Surcan Dos Santos, B., 243
 Swanson, V.E., 466
 Swensson, C.G., 171, 174
 Sylvester, G.C., 166–168
 Symons, P.M., 477
- Talapatra, A.K., 153
 Tan, K.H., 62
 Tardy, Y., 26, 34, 41, 42, 45–48, 50, 64, 209, 532
 Taube, A., 237, 334, 504, 516
 Taufen, P.M., 195
 Taylor, G., 100, 272
 Taylor, G.F., 115, 116, 119, 139, 140, 149, 150, 151, 153, 154, 162, 166–170, 172–174, 181, 186, 196, 198, 199, 340, 342, 343, 361
 Taylor, R.M., 75, 484
 Teh, G.H., 398
 Theobald, P.K., 412, 444, 452
 Thijssen, T., 484
 Thiry, M., 206, 443, 447, 452
 Thomas, M.F., 11, 14, 100, 102, 103, 107, 109, 297, 485
 Thornber, M.R., 79, 93, 115, 119, 123, 129, 130, 133, 135, 139
 Tipping, E., 93
 Toens, P.D., 386
 Tooms, J.S., 104–106, 108, 203, 205, 224, 225, 234
 Tordiffe, E.A.W., 379
 Travis, G.A., 137, 193, 194, 328
 Trescases, J.J., 25, 33, 37, 50, 64, 533
 Trewartha, G.T., 5, 7
 Tricart, J., 485
 Trichet, J., 26
 Trolard, F., 50
 Trompette, R., 206
 Tupas, M.H., 397
 Turenne, J.F., 69
 Twidale, C.R., 62, 102
 Tyrwhitt, D.S., 191
- Utter, T., 468
- Vaasjoki, M., 157, 158

- Valeton, I., 50, 484, 486
Van Andel, T.H., 484
Van Berkel, F., 414, 415
Van der Weijden, C.H., 444
Van Leeuwen, T.M., 401-403
Van Moort, J.C., 171, 174
Verheye, W., 268
Vermaak, J.J., 379, 381
Vijaysaradhi, D., 105
Vizier, J.F., 61
Volkoff, B., 75
Volkov, I.I., 464, 465
Von Maravic, H., 491, 492, 496
- Warren, A., 98, 107
Warren, C.G., 465
Warren, H.V., 465, 466
Watson, J.P., 104, 105
Watson, M.D., 182
Watters, R.A., 444, 452, 458, 496
Watterson, J.R., 466
Watts, J.T., 222
Webb, J.S., 104-106, 108, 203, 205, 224,
225, 231, 234
Weber, F., 443, 447, 452
- Webster, J.G., 87, 88, 137, 188, 399, 465,
467, 468, 471, 479
Webster, R., 103-105
Weyl, R., 484
White, A.H., 411-413
Wildman, J.E., 93, 117, 130
Wilhelm, E., 153, 205, 229, 514
Williams, B.T., 447, 450, 451, 460
Williams, M.A.J., 12, 105
Williams, P.A., 135
Wilmshurst, J.R., 116, 117, 191-193
Wilson, A.F., 252, 467
Wollast, R., 26
Woods, R., 129
- Young, A., 6, 7, 8, 100, 295
Yugay, T.A., 468
- Zebrowski, C., 62
Zeegers, H., 3, 18, 22, 23, 111, 150, 203,
208, 209, 211, 227, 228, 238, 241, 242,
252, 260, 261, 269, 274, 280, 393, 415,
483, 496, 499
Zeissink, H.E., 203
Zimmerman, D.O., 115

PLACE INDEX

1. GEOGRAPHICAL

- Algeria
Djebel Anini, 160, 182, 183
Djebel Debagh, 160, 164, 165, 182
Hoggar, 247
Kherzet Youcef, 160, 182, 183
Tadergound, 160, 164, 165
- Amazonia, 12, 66, 67, 70
- Arabian Desert, 18, 150, 295, 297, 359, 360
- Arabian Shield, 115, 168, 297, 360
- Australia
General 15, 65, 70, 100, 102, 104, 110,
140, 146, 151, 171, 201, 203, 205, 219,
240, 299, 304, 416, 419, 436, 462, 511
- Agnew, 33
- Alligator River district, 440, 447
- Aroona, 410
- Bardoc, 288, 321-323
- Beltana, 410, 411
- Benambra, 160, 178
- Blair, 347, 348
- Boddington, 310, 470, 477
- Bottle Creek, 151, 160, 189, 190
- Bounty, 335, 351-355, 377, 382, 478,
481
- Broken Hill, 143, 171, 172, 174
- Bulong, 328
- Callion, 308, 319, 320, 353, 378, 470,
477, 505
- Coober Pedy, 104
- Currawong, 178-180
- Dalgaranga, 236, 302, 357, 358, 516
- Darling Range, 20, 403, 475
- Dora Creek, 348, 349
- Dugald River, 140, 153, 172, 173, 176,
181
- Ediacara, 412, 413
- Ellendale, 432
- Elura, 148, 161, 198, 199, 302, 332, 334,
336, 340-342, 344
- Esperanza, 186, 412
- Fifield, 328
- Freddie Well, 160, 166, 168, 176-178,
364
- Gilgarna, 328
- Golden Grove, 108, 160, 166, 168, 176,
177, 302, 308-310, 312-314, 318, 357
- Great Australia, 160, 185
- Gunpowder, 160, 186
- Hamersley, 10
- Hannan South, 334, 356, 470, 471, 475,
476
- Ilmars, 404, 406
- Jabiluka Two, 458
- Johnson Creek, 160, 161, 163, 165
- Kadina, 356, 385, 386
- Kalgoorlie, 104, 151, 176, 189, 377, 462
- Kamarga, 160, 182, 184, 185
- Kambalda, 123, 124, 135, 193, 347, 358,
362-364, 378
- Kanmantoo, 201
- Killara, 160, 162, 163, 332, 335, 408
- Koongarra, 445, 446, 456, 457, 460
- Lady Loretta, 160, 170, 171, 181, 215,
265, 334, 351, 352
- Mammoth, 185, 186
- Mararoa Reef, 335, 381, 382
- Minindi Creek, 390
- Minyari, 346, 347
- Mount Gibson, 309, 310, 312, 313, 315-
318, 378, 470, 503
- Mount Isa, 115, 139, 143, 155, 157, 159-
162, 170-172, 181, 182, 185, 186, 412
- Mount Keith, 100, 101, 299, 324-327,
486
- Mount Leyshon, 160, 188, 189
- Mount Mulgine, 310
- Mount Pleasant, 335, 356, 365-367, 377,
382, 479, 523
- Mount Torrens, 161, 199, 200, 201
- Mount Weld carbonatite, 223, 268, 302,
329-331
- Mugga Mugga, 154, 160, 166, 167, 168
- Nabarlek, 455, 459
- Nairne, 201
- Namoonna, 160, 175, 176
- Norseman-Wiluna greenstone belt, 319,
321, 324, 336, 365

- Paradise Valley, 160, 162, 163, 171
 Pegmont, 140, 172, 174, 197
 Pernatty Lagoon, 356
 Pilbara Block, 176, 178
 Pine Creek geosyncline, 175, 348, 349
 Pioneer, 378, 379
 Queensland, 140, 153, 154, 159, 185
 Ranger, 446, 450, 451, 453, 458–460
 Redross, 356, 358, 359, 516
 Rum Jungle, 447, 456
 Squirrel Hills, 161, 197
 Tasmania, 12, 195
 Telfer, 160, 191, 192
 Teutonic Bore, 160, 176, 177, 236, 302,
 332, 334, 336–339, 343, 504, 516
 Thalanga, 236, 237, 334, 504, 516
 Transvaal, 334, 351–355, 470, 481
 West Kimberley, 422, 431
 Western Australia, 15, 20, 99, 150, 153–
 155, 299, 304, 376, 427, 496, 512
 Whim Creek, 160, 176–178
 Wilga, 178–180
 Windimurra Complex, 361, 383, 384
 Woodcutters, 334, 504
 Yeelirrie, 99, 454
 Yilgarn Block, 115, 151, 153, 161, 162,
 166, 167, 176, 178, 190, 191, 193–195,
 298, 309, 310, 313, 318, 329, 336, 345,
 351, 475
 Yindarigooda, 356
- Borneo, 150
 Botswana
 General, 108
 Jwaneng, 104, 435, 492
- Brazil
 General, 75
 Amorinópolis, 446, 452
 Araxá carbonatite, 329, 456, 496
 Campo de Cercado, 443, 446
 Catalão Alkaline Complex, 491
 Gentio do Ouro, 469
 Jacupiranga Alkaline Complex, 486, 488,
 491, 492, 495
 Liberdade, 100
 Muri Mountains Alkaline Complex, 491,
 496
 Niquelandia, 39
 O'Toole, 161, 195
 Poços de Caldas, 38
 Serro, 495, 497
- Brazilian Shield, 203
 Burkina Faso
 General, 64, 71, 73, 74
 Diouga, 216, 217
 Gan, 238, 239
 Goren, 211–214, 226
 Petite Suisse, 227, 228, 238
- Burma, 241, 505
- Cameroun
 Mborguénié, 249–251, 505
- Canada
 General, 139, 176
 Berg, 160, 188
 British Columbia, 416
 Howards Pass, 143, 171
 Kidd Creek, 146
 Sullivan, 171
 White Pine, 147
- Central African Republic, 50, 147–149
 Chad, 50, 100
 Chad (Lake), 35, 299
- Chile
 Atacama desert, 295, 298, 409
 Caracoles, 409, 410
 Los Pelambres, 416
- Congo Basin, 12, 241, 243
- Ecuador
 Chaucha, 398
- Egypt
 Gabbro Akaram, 370, 371
 Hamr Akarem, 370
- Ethiopia, 100, 328
- Fiji
 Viti Levu Island, 397
 Waivaka, 110
- France
 General, 50
 Bertholène, 443, 446, 452
 Les Bondons, 454
 Saint-Pierre-du-Cantal, 453
- French Guiana
 General, 64, 67–69, 71
 Cambrouze, 269–271
 Céline, 257–260
 Dorlin, 100, 109, 271, 272, 478, 496, 516
 D'Artagnan, 269
 Espérance, 253–257, 259, 260, 470, 474,
 477
 Saint-Pierre, 260, 261
 THR, 262–265, 269, 351, 516

- Gabon
 Dondo Mobi, 281, 286–289, 470, 474
 Mabounié Alkaline Complex, 267, 302, 329, 330
 Mavikou, 281–283
 Mébaga, 281, 284, 286, 293, 477
 Mikongo, 291, 293
 Mokékou, 291, 292
 Mounana, 446, 451, 458, 459
 Oklo, 443, 446, 451
 Ovale, 395, 400, 401
- Germany, 12
- Greece, 486
- Guinea
 Filon Bleu, 217, 218
- Guyana
 Mahdia, 265–267
 Muri Mountains Alkaline Complex, 268, 491, 496
 Guyana Shield, 241, 242
- India
 General, 42, 139, 203, 205
 Andhra Pradesh, 422
 Bihar, 447
 Chandidongri, 274
 Deccan, 100
 Eastern Ghats, 13, 394
 Khetri–Satkui–Saladipura Cu belt, 405, 406
 Khondapalli, 105
 Madhya Pradesh, 422
 Malabar, 41
 Orissa, 268
 Rajahstan, 185
 Thar Desert, 297, 299
 Western Ghats, 13, 394
- Indonesia
 Kalimantan, 396, 496
 Kelian, 401–403
- Iran, 394
- Ivory Coast
 General, 50, 60, 64
 Eboïnda region, 244
 Ity, 288, 290, 470, 474
 Toulepleu, 247–249
- Japan, 146
- Kalahari, 299
- Kalahari Desert, 295, 297, 298, 362
- Kenya
 Kinagoni Hill, 215, 216, 265
- Madagascar, 50
- Malaysia
 General, 241
 Nungkok, 398
 Tekka, 398
- Mali
 General, 433
 Banankoro, 219–221, 288
 Loulo, 229, 239
 Syama, 470
- Mauritania, 75, 99
- Mexico
 Basin and Range province, 416
 La Caridad, 409, 410
- Morocco, 447
- Mozambique
 Edmundian mine, 106, 236
- Namib Desert, 295, 297
- Namibia
 General, 422
 Gorob, 186, 187
 Kapok Graben, 182
 Matchless Amphibolite Belt, 160, 186, 187
 Matchless (deposit), 186, 187
 Namaqualand, 414, 415
 Ongeama, 186, 187
 Otjihase, 186, 187, 405, 407, 408
 Rosh Pinah, 160, 182, 183
- New Caledonia, 13, 50, 394
- Niger
 General, 63, 304
 Koma Bangou goldfield, 105, 236
 Liptako, 235
- Nigeria, 210, 273, 276
- Norway, 50
- Papua New Guinea
 General, 15, 16, 109, 151
 Morobe goldfield, 399
 Wau, 467, 471, 479
- Peru
 Socos, 415
- Philippines
 Palawan Island, 398, 399
 Santo Nino, 397
- Puerto Rico, 398
- Sahara, 12, 72, 150, 299
- Sahel, 12, 104, 297, 505
- Saudi Arabia
 General, 109, 110, 111, 140
 'Afif, 372
 Al Masane, 50, 151, 160, 180, 181

Ar Ridaniyah district, 161, 196
 Ash Sha'ib gossan, 150
 Bir Tawilah, 370, 372, 374, 479
 Jabal Sa'id, 372
 Nadj pediplain, 367, 369, 370
 Wadi Wassat, 160, 168, 169, 180

Senegal
 General, 75, 207
 Casamance, 74
 Sabodala, 230, 232, 233

Sierra Leone
 General, 150, 419
 Freetown Igneous Complex, 399
 Manjamandu, 428–431, 434
 Sinjie, 428, 429
 Yengema, 420, 422, 424–426, 428, 429, 431

Solomon Islands, 151

Somalia, 386

South Africa
 General, 462
 Aggeneys, 172, 174
 Berg River, 160, 164
 Bushveld Complex, 383
 Gamsberg, 143, 172, 174
 Jacomynspan, 379
 Letaba, 160, 180, 181
 Murchison belt, 180
 Plat Reef, 383, 384
 Putsberg, 379–381
 Uniondale, 160, 168, 169
 Vredendal, 160, 164

Spain
 Rio Tinto, 115

Sudan
 General, 100, 140, 156
 Aberkateib, 416
 Gebeit, 343, 345
 Red Sea Hills, 297, 343, 416
 Um Nabardi, 298, 334, 343, 345, 346, 470, 475
 Wan-Rumbeck, 214

Suriname
 Upper Nickerie region, 274

Tanzania
 General, 422
 Madaba, 446, 454, 455

Thailand, 511

Tunisia
 Bou Grine, 383, 384

Uganda
 Karamoga region, 232
 Sukulu, 222, 223, 268

USA
 General, 115, 139, 462
 Arizona, 415
 Basin and Range province, 416
 California, 222, 394
 Hatchet Creek, 409
 North Silver Bell, 412
 Oregon, 12, 222, 394
 Prairie Creek diatreme, 436
 Red Dog, 171
 Rocky Range, 386, 387
 Wisconsin, 12

USSR
 General, 139
 Kazakstan, 55
 Russia, 462

U.K.
 Cornwall, 115
 Northern Ireland, 12, 511

Zaire
 General, 431
 Lueshe carbonatite, 491, 496

Zambia
 General, 224
 Baluba, 106, 234
 Kasempa-Kitwe region, 235
 Zambian Copperbelt, 104, 108

Zimbabwe
 General, 104, 105, 224
 Shangani, 405, 407

2. DEPOSITS AND OCCURRENCES

Bauxite
 Amazonia, 64, 70
 Eastern Ghats (India), 13, 394
 Kazakstan (USSR), 55
 Poços de Caldas (Brazil), 38
 Saudi Arabia, 360
 Western Ghats (India), 13, 394

Copper, Cu-Mo porphyry
 Arizona (USA), 415
 Berg (Canada), 160, 188
 Chaucha (Ecuador), 398
 Kalimantan (Indonesia), 396
 La Caridad (Mexico), 409, 410
 Los Pelambres (Chile), 416
 Nungkok (Malaysia), 398
 North Silver Bell (USA), 412
 Philippines, 398

- Puerto Rico, 398
 Santo Nino (Philippines), 397
 Socos (Peru), 415
 Viti Levu Island (Fiji), 397
- Copper, undifferentiated**
 Céline (French Guiana), 257–260
 Dalgara (Australia), 236, 302, 357
 D'Artagnan (French Guiana), 269
 Esperanza Z 2 (Australia), 186, 412
 Goren (Burkina Faso), 211–214, 226
 Gorob (Namibia), 186, 187
 Great Australia (Australia), 160, 185
 Hatchet Creek (USA), 409
 Ilmars (Australia), 404, 406
 Jacomynspan (South Africa), 379
 Kadina (Australia), 356, 385, 386
 Kamarga (Australia), 162, 182, 185
 Kanmantoo (Australia), 201
 Los Pelambres (Chile), 416
 Mahdia (Guyana), 265–267
 Mammoth (Australia), 185, 186
 Matchless (Namibia), 186, 187
 Mavikou (Gabon), 281–283
 Mébaga (Gabon), 281, 284, 286, 293, 477
 Ongeama (Namibia), 186, 187
 Otjihase (Namibia), 186, 187, 405, 407, 408
 Petite Suisse (Burkina Faso), 227, 228, 238
 Putsberg (South Africa), 379–381
 Rocky Range (USA), 386, 387
 Teutonic Bore (Australia), 160, 176, 177, 236, 302, 332, 334, 336–339, 343, 504, 516
 Toulepleu (Ivory Coast), 247–249
 Upper Nickerie region (Suriname), 274
 Waivaka (Fiji), 110
- Diamonds, see Kimberlites**
- Gold, supergene**
 Bardoc (Australia), 288, 321–323
 Boddington (Australia), 310, 470, 477
 Bottle Creek (Australia), 151, 160, 189, 190
 Bounty (Australia), 335, 351–355, 377, 382, 478, 481
 Callion (Australia), 308, 319, 320, 470, 477, 505
 Hannan South (Australia), 334, 356, 470, 471, 475, 476
 Ity (Ivory Coast), 288, 290, 470, 474
- Mount Gibson (Australia), 309, 310, 313, 315–318, 378, 470, 503
 Syama (Mali), 470
 Transvaal (Australia), 334, 351–355, 470, 481
 Um Nabardi (Sudan), 298, 334, 343, 345, 346, 470, 475
- Gold, undifferentiated**
 Aberkateib (Sudan), 416
 Banankoro (Mali), 219–221, 288
 Bir Tawilah (Saudi Arabia), 370, 372, 374, 379
 Diouga (Burkina Faso), 216, 217
 Dondo Mobi (Gabon), 281, 286–289, 470, 474
 Dorlin (French Guiana), 100, 109, 271, 272, 478, 496, 516
 Espérance (French Guiana), 253–257, 259, 260, 470, 474, 477
 Filon Bleu (Guinea), 217, 218
 French Guiana, 496
 Gebeit (Sudan), 343, 345
 Kelian (Indonesia), 401–403
 Loulo (Mali), 229, 239
 Mararoa Reef (Australia), 335, 381, 382
 Mavikou (Gabon), 281–283
 Mborguéné (Cameroun), 249–251, 505
 Mébaga (Gabon), 281, 284, 286, 293, 477
 Mikongo (Gabon), 291, 293
 Minyari (Australia), 346, 347
 Morobe goldfield (Papua New Guinea), 399
 Mount Leyshon (Australia), 160, 188, 189
 Mount Pleasant (Australia), 335, 356, 365–367, 377, 382, 479
 Ovale (Gabon), 395, 400, 401
 Saint-Pierre (French Guiana), 260, 261
 Telfer (Australia), 160, 191, 192
 Toulepleu (Ivory Coast), 247–249
- Kimberlites and lamproites**
 Andra Pradesh (India), 422
 Australia, 419, 436
 Botswana, 433
 Ellendale (Australia), 432
 Jwaneng (Botswana), 435, 492
 Madhya Pradesh (India), 422, 433
 Mali, 433
 Manjamandu (Sierra Leone), 428–431, 434
 Namibia, 422
 Prairie Creek diatreme (USA), 436

- Sierra Leone, 419, 423, 425, 433
 Sinje (Sierra Leone), 428, 429
 Tanzania, 422
 West Kimberley (Australia), 422, 431
 Western Australia, 427
 Yengema (Sierra Leone), 419, 420, 422,
 424–426, 428, 429, 431
 Zaire, 431
- Lamproites, *see* Kimberlites
- Lead-zinc, carbonate-hosted
 General, 143, 157, 181, 537
 Baluba (Zambia), 234
 Djebel Anini (Algeria), 160, 182, 183
 Ediacara (Australia), 412
 Kamarga (Australia), 160, 182, 185
 Kherzet Youcef (Algeria), 160, 182, 183
 Rosh Pinah (Namibia), 160, 182, 183
- Lead-zinc, stratiform
 Aggeneys (South Africa), 172, 174
 Broken Hill (Australia), 143, 171, 172, 174
 Dugald River (Australia), 140, 153, 160,
 172, 173, 176, 181
 Gamsberg (South Africa), 143, 172, 174
 Howards Pass (Canada), 143, 171
 Namoonia (Australia), 160, 175, 176
 Pegmont (Australia), 140, 160, 172, 174
 Red Dog (USA), 171
 Sullivan (Canada), 171
- Lead-zinc, undifferentiated
 Aroona (Australia), 410
 Ar Ridaniyah district (Saudi Arabia), 161,
 196
 Beltana (Australia), 410, 411
 Bou Grine (Tunisia), 383, 384
 Dalgaringa (Australia), 236, 302, 357
 Dora Creek (Australia), 348, 349
 Elura (Australia), 148, 161, 198, 199, 302,
 332, 334, 336, 340–342, 344
 Gan (Burkina Faso), 238, 339
 Hilton (Australia), 181
 Kinagoni Hill (Kenya), 215, 216, 265
 Lady Loretta (Australia), 160, 170, 171,
 181, 215, 265, 334, 351, 352
 Mount Isa (Australia), 143, 157, 159–161,
 170, 171, 181, 185
 Namaqualand (Namibia), 414, 415
 THR (French Guiana), 262–265, 269, 351,
 516
- Molybdenum
 Goren (Burkina Faso), 211–214, 226
- Mahdia (Guyana), 265–267
 Mount Mulgine (Australia), 310
- Nickel, lateritic
 Bulong (Australia), 328
 California (USA), 394
 New Caledonia, 13, 394
 Oregon (USA), 394
 Palawan Island (Philippines), 398, 399
 Siberia (Australia), 328
- Nickel-copper sulphide
 Agnew (Australia), 133
 Blair (Australia), 347, 348
 Gabbro Akaram (Egypt), 370, 371
 Kambalda (Australia), 123, 124, 135, 193,
 347, 358, 362–364
 Mount Keith (Australia), 324–327
 O'Toole (Brazil), 161, 195
 Pioneer (Australia), 378, 379
 Redcross (Australia), 358, 359
 Shangani (Zimbabwe), 405, 407
 Western Australia, 150, 191, 496
- Platinum group elements (PGE)
 Freetown Igneous Complex (Sierra Leone),
 399
 Mount Keith (Australia), 324–327
 Plat Reef (South Africa), 383
 Windimurra Complex (Australia), 361,
 383, 384
- Rare earth elements (REE)
 Mabounié Alkaline Complex (Gabon), 267,
 302, 329, 330
 Mount Weld Carbonatite (Australia), 268,
 302, 329–331
 Sukulu (Uganda), 222, 223, 268
- Silver
 Caracoles (Chile), 409, 410
- Skarn
 Ar Ridaniyah district (Saudi Arabia), 161,
 196
 Squirrel Hills (Australia), 161, 197
 Tasmania (Australia), 195
- Uranium
 Alligator River district (Australia), 440,
 447
 Amarinopolis (Brazil), 446, 452
 Bertholène (France), 443, 446, 452
 Jabiluka Two (Australia), 458

- Koongarra (Australia), 445, 446, 456, 457, 460
 Les Boudons (France), 454
 Madaba (Tanzania), 446, 454, 455
 Minindi Creek (Australia), 390
 Mounana (Gabon), 446, 451, 458, 459
 Nabarlek (Australia), 455, 459
 Oklo (Gabon), 443, 446, 451
 Ranger (Australia), 446, 450, 451, 453, 458–460
 Rum Jungle (Australia), 447, 456
 Saint-Pierre-du-Cantal (France), 453
 Yeelirrie (Australia), 99, 454
- Volcanogenic massive sulphide**
 Al Masane (Saudi Arabia), 150, 151, 180
 Currawong (Australia), 178–180
- Freddie Well (Australia), 160, 166, 168, 176–178, 364
 Golden Grove (Australia), 108, 160, 166, 168, 176, 178, 302, 308–310, 312, 318, 357
 Kidd Creek (Canada), 146
 Letaba (South Africa), 160, 180, 181
 Mugga Mugga (Australia), 154, 160, 166, 167, 168
 Sudan, 140
 Teutonic Bore (Australia), 160, 176, 177, 236, 302, 332, 334, 336–339, 343, 504, 516
 Wadi Wassat (Saudi Arabia), 160, 168, 169, 180
 Whim Creek (Australia), 160, 176–178
 Wilga (Australia), 178–180

SUBJECT INDEX

- A-type models (pre-existing regolith complete)
 general, 19–22, 176, 203, 242, 275, 394
 arid, 304–332, 353, 377, 378, 404
 rainforest, 243–252, 262–268, 275–287,
 290–293
 savanna, 205–226, 234, 235, 304, 448,
 450, 452, 454, 476–478, 504, 515, 518,
 520, 524
- Acidolysis, 29, 35, 36
- Adsorbents, 440, 443, 444, 452
- Adsorption, 36, 80, 90–95, 130, 132, 135,
 142, 148, 180, 202, 229, 313, 328, 362,
 384, 439, 400, 466, 469, 526
 of uranium, 439, 440, 443–445, 447,
 450–456, 458, 459
- Aeolian
 deposits, 12, 20, 103, 105, 109, 111, 235,
 296–298, 307, 382, 336, 346, 360, 362,
 368–370, 375, 380, 386, 390, 405, 412,
 414–417, 432, 522, 542, 543
 dilution by, 99, 109, 111, 112, 336, 346,
 361, 365, 367–369, 381, 404, 412, 417,
 524
 dispersion, 62, 110, 111, 369, 372, 373,
 479
- Age, regoliths, 1, 7, 12, 41, 65, 103, 205,
 206, 296, 297, 329, 431
- Aerial photography
 gossan search, 139, 140, 361
 regolith mapping, 361, 391, 503
- Allitization, 20, 32, 36, 38, 40
- Alluvium
 anomalies in, 236, 243, 281, 356, 357,
 359, 365, 376, 386, 387, 431, 436
 general, 15, 20, 100, 105, 204, 522, 533,
 542, 543
 arid, 298, 303, 305, 307, 312, 316,
 319, 324, 330, 347, 356–360, 362,
 365, 370, 386–389, 405, 416, 417
 rainforest, 243, 252, 276, 281, 286,
 290, 296, 424, 425
 savanna, 235
 in dispersion models, 20, 22, 23, 324, 356,
 362, 386–389
- Alkalinolysis, 29, 33, 34, 36
- Altitude—effect on climate, 1, 2, 4, 7, 8, 98,
 110, 186, 393, 414
- Analytical methods, 526–531
- Anodic stripping voltammetry, 529
- Anodic reactions, 119, 122–130, 134
- Anions
 hydrolysis, 31–35, 91
 mobility, 79–81, 83–95
 sulphide oxidation, 119, 120, 122–126,
 132, 134, 135, 137, 148, 198, 202, 436,
 464–466
- Arenose horizon, 532–534
- Arid and semi-arid environments
 climate, 5–9
 climatic episodes, 12, 296, 300, 390
 diamond exploration, 422, 433, 435, 485
 dispersion models, 20, 21, 203, 219, 222,
 237, 304–390, 403–418, 442, 502, 504,
 506, 516
 distribution, 1, 6, 7, 11, 13, 295–299,
 303, 374, 390, 393, 403, 404, 505
 erosion in, 61, 98–101, 105–107, 109–
 113, 511
 landforms, 12–14, 18, 296, 297, 303–
 305, 331, 359, 394
 gold in, 252, 288, 319, 320, 336, 345,
 365, 366, 378, 416, 461, 469, 470, 474,
 477–481, 504
 gossans in, 135, 137, 142, 148–150, 168,
 178–180, 182, 186, 190, 197, 302, 334,
 349, 362, 405, 506, 513
 regoliths, 16, 42, 62, 63, 75–77, 142, 276,
 299–303, 335, 360, 367, 374, 393, 403,
 404, 409, 422, 502, 509
 weathering, 33, 40, 62, 95, 96, 132, 511,
 512
- Arsenic
 hydromorphic dispersion, 302
 in calcrete, 381–384
 in Fe oxides, 302, 342
 in gossans, 33, 168, 170, 178, 185, 186,
 189–191, 198, 313, 337, 340
 in ironstones, 163, 165
 pathfinder for Au, 272, 318, 319
 pathfinder for PGE, 383

Arsenic dispersion

- in laterites, 318
- in lateritic gravels, 377
- in lateritic regoliths, 217–219, 250, 251, 269, 271, 337, 339, 343, 344, 501
- in soil, 245, 269, 276, 346, 347, 371
- in transported overburden, 357, 365

Atomic absorption spectrometry, 218, 253, 260, 363, 397, 479, 484, 527–531

B-type models (pre-existing regolith truncated)

- general, 19–22, 176, 203, 242
- arid, 304, 331–359, 378–382, 385, 386, 403–412
- rainforest, 252–260, 265, 268–275, 287–292, 394–403
- savanna, 217, 224–240, 394–303, 451, 452, 454–456

Bacteria, 94, 465, 466, 507

Barium

- in gossans, 133, 150, 152, 171, 180, 186, 191, 198
- in ironstones, 162, 165

Barium dispersion

- in soil, 281–283
- in transported overburden, 365

Bauxite

- composition, 41, 50, 53–55, 447, 477
- distribution, 13, 360, 394, 534
- formation, 38, 50, 53, 64, 70

Bicarbonate, 62, 376

Biogenic dispersion, 104, 108, 324, 362, 366, 416, 512

Biogeochemistry, 460

Biomass, 8, 299, 300

Bioturbation, 104–105, 112, 275, 307, 362

Bisiallization, 32, 33, 36, 38

BLEG, 302, 308, 309, 332, 479–481, 523, 529

Boehmite, 50–55, 534

Boxworks, 136, 170, 175, 185, 191, 198, 202

Bulk leach extraction of gold—*see* BLEG

C-type models (pre-existing regolith absent)

- general, 19–22, 176, 203, 242, 394, 479, 480, 504, 506, 513, 515, 520
- arid, 304, 359–374, 378, 383, 384, 386, 403, 409, 412–416
- rainforest, 252, 395, 396
- savanna, 395, 396

Calcareous soils—*see* Calcrete

Calcrete

cementation, 20, 62, 75, 76, 99, 296, 298, 299, 353, 366, 374, 377, 394

classification, 375, 376, 534, 535

dilution by, 301, 363, 377–381, 383, 407, 520

dispersion models, 20, 377, 378, 385, 389

distribution, 7, 8, 298, 374, 393, 509

exploration in, 374–390

gold in, 301, 319, 335, 353, 354, 362, 365, 377, 378, 381, 416, 461, 477, 479

groundwater (valley, phreatic), 99, 301, 330, 376, 377, 386–389, 535

horizon, 99, 296, 298, 317, 319, 321, 332, 336, 353, 374, 383, 385, 511, 534–536

pedogenic (vadose), 374–377, 389, 390

precipitation, 34, 62, 374–376

uranium in, 99, 301, 376, 377, 386–390, 416, 442, 445, 454

Caliche—*see* Calcrete

Carbonatites, 222, 223, 302, 329–331

Cathodic reactions, 119–134

Cations

alkali, 61, 70, 141

hydrolysis, 31–35, 91, 126,

mobility, 79–83, 85–95, 388

sulphide oxidation, 122–126, 130–133, 202

Chelation, 93, 94, 148

Chloride

complexes, 82–89, 95, 135, 137, 148, 328, 337

in gold mobility, 87, 95, 137, 328, 462–464, 467, 469, 474–479

in groundwater, 135, 148, 337, 343, 403, 467, 469, 471, 474,

salts, 93, 144, 145, 343

Chromium

identifying overburden, 487, 488

in chromian spinels, 493–495

in Fe oxides, 496

in ironstones, 166, 169

in Ni gossans identification, 151–153, 166, 194

in rutiles, 497

in silcrete, 301, 326

pathfinder for PGE, 399

Chromium dispersion

in lateritic regoliths, 285, 286

in saprolite, 285, 286

Chromium in regoliths on ultramafic rocks

bedrock recognition, 492

- distribution in, 285, 286, 422, 425, 427–429, 432, 433, 436, 488
- Clastic dispersion—*see* Physical dispersion
- Clay minerals
- adsorption by, 36, 99, 105, 213, 234, 268, 335, 336, 357, 369, 373, 385, 429, 439, 444, 450, 455, 456, 507, 516, 522, 526
 - clay horizon, 28, 38, 41, 44, 46, 60–62, 312, 316, 321, 326, 359, 404, 425, 429, 533, 534, 541
 - in arid zones, 16, 72, 107, 204, 240, 319, 326–330, 351, 357, 378, 385, 436, 544
 - in rainforest, 66–70, 243, 245, 253, 254, 262–265, 268–269, 275–277, 281, 284, 287, 290, 291, 517
 - in lateritic profiles, 20, 44, 45, 60–62, 66, 104, 224, 316–319, 353, 404, 422, 450, 484, 506, 518, 520–523, 534
- Climate—*see* also Arid, Rainforest, Savanna, Temperate environments
- altitudinal variation, 7, 393
 - classification, 4–6
 - effect on dispersion, 1–3, 18–24, 112–114, 203–206, 240, 243, 252, 261, 292, 295, 366, 390, 462, 469, 502–505
 - effect on weathering
 - general, 1, 3, 7, 18–26, 33, 35, 41, 50, 58–65, 70–76, 95–97, 100, 101, 148–151, 160, 161, 393, 502–504, 520
 - arid, 75, 295–303, 309, 331, 345, 349, 360, 390
 - rainforest, 242, 243, 252, 261, 276, 280, 293
 - variation
 - general, 7, 11–13, 18–23, 38, 41, 42, 65, 71–76, 104, 113, 127, 422, 461, 474–478, 504, 505, 509–511, 513, 518
 - arid zones, 75, 295–303, 374, 388, 394
 - humid zones, 65, 71–74, 205–206, 241–243, 262
 - zones, 1, 7, 10, 11, 14, 18, 23, 38, 59, 77, 394
- Colloids, 99, 466, 471
- Colluvium
- general, 140, 198, 227, 236, 271, 276, 296, 298, 303, 306, 307, 312, 316, 319, 348, 349, 353, 356, 360, 362, 363, 365, 370, 381, 383, 386, 422
 - anomalies in, 105, 109, 110, 235, 236, 307, 335, 336, 349, 362, 367–370, 380, 393, 397, 398, 404, 416, 417, 469, 478, 480, 497, 503, 511, 520, 521
 - in dispersion models, 20, 21, 209, 226, 252, 269, 305–307, 309, 324, 332, 334, 395
- Complexes, complex ions
- general, 79, 80, 85, 88, 89, 95, 96
 - anionic, 87–89, 137, 188, 328, 388, 400, 436, 440, 454
 - in gold mobility, 87, 462–471, 474, 478
 - organic, 35, 58, 85, 88, 89, 94, 95, 148, 466, 467, 474, 477
- Contamination
- by mining activity, 111, 268, 372, 416, 510, 512, 519
 - in sample preparation, 141, 523–526
- Copper
- dispersion by sheetwash, 108
 - hydromorphic dispersion, 234, 274, 302, 359, 385–387, 407, 408
 - in calcrete, 378–380, 385–387
 - in dambos, 234
 - in Fe oxides, 302, 342, 496
 - in Fe–Mn oxides, 412
 - in gossans, 133, 150, 153, 154, 168, 170, 178, 180, 185–192, 194–199, 313, 340, 341, 343, 358, 364, 407, 412, 413
 - in ironstones, 139, 161–163, 165, 166, 194, 335, 408
 - in Mn oxides, 326
 - pathfinder for Au, 272
 - pathfinder for PGE, 383, 399
 - supergene enrichment, 409, 412
- Copper deposits and occurrences (undifferentiated)—*see* also Ni–Cu sulphide deposits, Porphyry Cu–Mo deposits
- arid, 182, 185, 186, 336–339, 343, 357, 379, 385, 386, 405, 407, 412, 416
 - rainforest, 110, 247, 257, 265, 269, 274, 281, 284
 - savanna, 221, 227, 238, 404
 - temperate, subtropical, 201, 409
- Copper dispersion
- in laterites, 313, 314
 - in lateritic regoliths, 212, 213, 227, 234, 238, 239, 259, 260, 343, 344, 385, 386, 408
 - in saprolite, 234, 247, 248, 274, 284, 285
 - in soil, 211–214, 233–235, 247, 248, 259, 274, 284, 285, 347–351, 364, 370, 371, 378–380, 397, 398, 404–410, 414, 415
 - in transported overburden, 235, 236, 357–359, 385–387

- Coprecipitation, 80, 93, 142, 148, 302, 326, 328, 329, 440
- Cuirasse—*see* Lateritic cuirasse
- Deforestation, 510, 511
- Diamond exploration
 general, 419–437, 501
 geochemical, 419–433
 indicator minerals, 105, 362, 419, 422, 424–426, 431–437, 492, 496
- Diaspore, 50–55, 534
- Diffusion, 126, 469
- Dissolution
 general, 28, 35, 44, 58, 60, 65, 80–83, 94, 102, 141, 306, 343, 543
 clay, 46, 61, 62, 70
 iron oxide, 47, 70, 150, 151, 206
 reactions, 29–31, 383, 388, 389, 443, 462
 silicate, 29–31, 37, 48, 62, 439
 sulphides, 119, 122–124, 130, 133, 136, 451
- Drilling
 auger, 481, 516, 517
 contamination, 512
 procedures, 151, 243, 297, 303, 307, 308, 324, 333, 334, 340, 356, 357, 362, 378, 385, 388, 391, 417, 459, 477, 478, 481, 482, 503, 516–519, 523
 rotary air blast (RAB) and percussion, 354–357, 459, 478, 481, 482, 506, 517
- Duricrust—*see* Calcrete, Cuirasse, Silcrete
- Eh, 81–84, 87, 95, 123, 125, 128, 136, 147, 148, 202, 262, 439–443, 452, 462, 463
- Eh–pH relationships
 general, 80–83, 88, 119, 123, 262, 504
 Au solubility, 462, 465, 471, 475, 504
 Fe solubility, 30, 31, 48, 81–83, 123, 125, 300, 475
 U solubility, 388, 439–443, 454
- Electrochemical
 dispersion, 237, 349
 weathering, 119–130, 135,
- Electrum
 primary, 190
 secondary, 199, 399, 400, 467, 471, 479
 weathering, 137, 467, 468, 475
- Element associations—*see* also Pathfinder elements
 general, 79, 156, 209, 240, 260, 308, 310, 371, 417, 436, 445–447, 486, 487, 501
 in gossan, 115, 137, 143, 146, 152, 156, 160, 161, 191–194, 202, 334, 400, 401
 primary, 143, 146, 147, 162, 215
- Eluvial–illuvial systems, 65, 70–73, 99, 538
- Eluviation, 58, 61–63, 65, 70, 73, 99–102, 112, 113, 272, 306, 435, 536, 538
- Eluvium, 229, 235
- Etchplains, 11–15, 110, 113, 296, 394
 –inselberg relief, 11, 13, 57, 359, 394
- Environmental change, effect
 on dispersion, 13, 113, 510–512
 of exploration, 512
- Evaporation, 4, 48, 50, 98, 299, 300, 350, 376, 388, 442, 479, 511
 –gradient, 150, 366, 375
- Evapotranspiration, 4, 62, 324, 366, 374, 376, 479, 511
- Facets, landform, 13–16, 18, 23, 306, 503, 536, 539
- False anomalies, 290, 302, 417, 440, 442, 447, 452, 453, 480, 500
- False gossans (*see* also Pseudogossans), 513, 514, 537, 538
- Feldspar weathering, 32–36, 39, 44, 46, 152, 162, 172, 281
- Ferricrete, 41, 42, 46, 74, 515, 536, 537
- Ferrollysis, 30, 475, 511
- Fire, 55, 98, 510–512
- Fire assay, 385, 479, 527, 529, 531
- Frost, 98, 110, 178
- Fulvic acid—*see* Humic acid
- Gas geochemistry, 331, 362, 416, 440, 441, 458
- Geophysical exploration
 general, 222, 267, 330, 356, 419, 437, 499, 523
 problems with, 330, 460, 500, 508
 procedures
 magnetic, 211, 324, 330, 340, 342, 419, 429, 460, 500
 radiometric, 99, 330, 388, 439, 448, 450–452, 458–460, 500
 various, 128, 129, 267, 330, 340, 419, 429, 500

- Gibbsite**
 formation, 12, 20, 32, 38, 39, 50, 51, 55, 60, 67, 245, 275
 in regoliths, 38, 54, 60–62, 64, 66, 70, 299, 518, 534, 535
- Glacial deposits**, 298, 542
- Goethite**
 adsorption by, 91–93, 132, 142, 148, 203, 240, 343, 444, 456, 496, 526, 527
 aluminous, 47–53, 299, 317, 444
 formation, 30, 32, 47–53, 55
 general, 12, 44–45, 62, 75, 132, 262, 420
 in profile, 28, 42–47, 54, 225, 275, 299, 317, 342, 420, 518, 539
 replacement by, 37, 60, 142, 245, 447
 replacement of, 37, 51–53, 75, 281
- Gold**
 aqueous geochemistry, 462–464
 complexes, 87, 95, 137, 464–467
 dispersion by termites, 235, 236
 hydromorphic dispersion, 252, 345, 346, 356, 357, 365, 479
 in calcrete, 308, 319, 335, 353, 354, 366, 367, 377, 378, 381, 382, 477, 478
 in gossans, 149, 151, 190, 191
 in Mn oxides, 400, 467, 479
 mobility, 95, 137, 188, 301, 471–475
 pathfinder for porphyry Cu deposits, 398
 placers, 222, 281, 286–289, 345, 474
- Gold deposits and occurrences**
 supergene
 general, 301, 303
 arid, 188, 190, 313, 315–323, 343, 345, 346, 351–355, 470, 477
 rainforest, 288, 290, 470
 savanna, 470
 undifferentiated
 arid, 191, 343, 346, 365, 370, 381, 416
 rainforest, 247, 249, 253, 260, 271, 281, 284, 286, 291, 399–401, 496
 savanna, 216, 217, 219, 229
 temperate, subtropical, 188
- Gold dispersion**
 in laterites, 315, 318
 in lateritic regoliths, 217–219, 250, 251, 255–257, 260, 261, 302, 320, 345, 346, 505
 in saprolite, 229, 231, 232, 247, 248, 284–286, 291, 292, 356
 in soil, 109, 219, 220, 229, 230, 247–249, 253, 255–257, 260, 261, 284–287, 291, 292, 345–347, 353, 354, 372, 402, 416
- in stone-line profiles, 287, 288, 290, 400, 401
 in transported overburden, 366, 367, 479
 in wadi sediments, 373
- Gold in lateritic regoliths**
 depletion zones, 320, 353, 355
 gossan, 188–192
 lateritic enrichment, 320, 470, 474
 saprolitic enrichment, 320, 370, 475, 476
 surface expression of Au mineralization, 477, 478
- Gold, particulate**
 composition, 221, 222, 320, 321, 323, 400, 467
 morphology, 219, 221, 287–289, 321, 322
 secondary, 400, 401, 467
 silver depletion, 222, 461, 468, 469, 471
- Gossan—see also False gossan, Pseudogossan and under deposit type**
 barren, 166–169, 351
 classification, 115, 116, 513, 514, 537
 composition, 115, 128, 130–135, 143, 146, 147, 202, 343, 351, 360, 417, 514
 detritus in soil, 109, 306, 333, 343, 346, 351, 361, 362, 365, 368, 372, 416, 417, 496, 501
 fabric, 115, 126, 127, 130, 135–137, 141–143,
 field relationships, 116, 138–151, 297, 334, 337, 351, 361, 407, 412
 formation, 2, 115–138, 148–151
 identification, 115, 126, 127, 139–161, 313, 334, 513, 514, 527
 mineralogy, 115, 123, 128–138, 140–145, 147, 404
 occurrence, 139, 149–151, 302, 360, 404, 505, 513
 profiles, 117, 124, 127, 128, 336, 340, 347, 513
 search, 2, 139, 140, 201, 202, 308, 334, 335, 361, 404, 405, 506, 507, 513–515
- Granite weathering**
 general, 63, 97, 111, 113, 386, 388, 389, 394, 454, 537
 profiles, 60, 63, 71, 73, 102, 225, 245, 265, 301, 425, 543
- Groundwater**
 as sample medium, 330, 388, 389, 460

- flow, 65, 100, 303, 442, 459
- in arid environments, 110, 113, 135, 148, 149, 150, 299, 300, 317, 323, 337, 403, 450, 457, 462–465, 475, 476, 485, 488, 490, 502, 504, 511
- in humid environments, 135, 148, 464, 465, 471
- redox conditions, 81, 123, 297, 504
- role in weathering, 29, 68, 79, 116, 162, 163, 172, 301, 323, 343, 356, 385, 440, 442, 454, 462, 464, 511, 515, 520, 537
- Gypcrete, 387
- Heavy minerals—*see also* Diamond
- identifying overburden, 67, 484–488, 498
- in exploration, 109, 111, 229, 284, 291, 345, 368, 369, 373, 458, 461, 483, 495–498, 516, 519,
- in gossans, 142–145, 176, 186, 335, 501
- relative concentration, 15, 44, 60, 63, 109, 133, 222, 302, 306, 329, 420, 435, 461, 483, 484, 487, 489, 496, 518
- rock identification, 111, 487–495
- sampling, 484, 485
- weathering of, 111, 368, 484, 487, 496
- Helium, 330, 331, 440, 441, 460
- Hematite
- general, 12, 62, 75, 262
- adsorption by, 91–93, 142, 148, 203, 240, 342, 496
- aluminous, 45, 47–53, 55, 206, 299, 317
- formation, 30, 47–53
- in regolith, 28, 42–47, 54, 66, 206, 225, 275, 299, 302, 317, 518, 539
- replacement by, 37, 45–50, 142, 207, 245
- replacement of, 47, 281
- Homogenization, profile, 60, 100–102, 112, 243, 262, 263, 541
- Horizons, regolith
- composition, 39, 47–53, 57–65, 69–70, 99–100, 105, 206, 209, 298–300
- geochemical significance
- general, 13, 18–20, 99, 436, 437, 485–487, 497, 517, 522, 523
- arid, 301–304, 306–307, 355, 376–378, 390
- rainforest, 245–247, 250–252, 262, 294
- savanna, 203–205, 209–210, 224, 240,
- lateritic, 28–30, 37–38, 41–47, 60, 63, 206–207, 210, 224, 226, 234, 243–245, 261–262, 268, 275, 296, 306, 531–533
- soil
- arid, 75, 99, 360
- general, 4, 12, 57, 59–62, 77, 538
- rainforest, 11, 35, 66–70, 104, 242, 243, 275–278, 291, 292
- savanna, 71–75, 101, 224
- Humic/fulvic matter—*see also* Organic matter
- in soil, 69, 76, 84, 92, 252, 253, 255, 257, 265, 276, 294, 383, 397, 425,
- mobilization, 84, 90, 93–96, 135, 137, 148, 474
- Hydration, 29, 51, 98
- Hydrogen ion concentration—*see* pH
- Hydrolysis, 29, 30–39, 79, 83, 95, 122–124, 126, 127, 129, 130, 133, 134, 136, 241, 281
- Hydromorphic anomalies
- general, 105, 109, 215, 436, 442, 456, 492, 504, 505, 512, 516, 521
- arid, 302, 306, 313, 335, 356, 359, 362, 365, 407, 408, 412,
- rainforest, 274, 395, 399
- savanna, 234, 235
- dispersion
- general, 96, 108, 147, 171, 483, 503, 507, 508
- arid, 300, 307, 318, 324, 336, 386, 415–417
- rainforest, 246, 247, 252, 257, 268, 280, 281
- savanna, 209, 212, 235, 237, 240
- Illuviation, 73, 99, 100, 104, 471, 484, 487, 536, 538, 541
- Indicator minerals—*see* Diamonds, Heavy minerals
- Inselbergs, 11, 71, 78, 98, 112, 394, 520
- Iodine/iodide, 82, 84–86, 145, 464, 466
- Ionic
- composition, groundwater, 199, 350
- conductivity, 126
- radius, 82
- strength, 87, 95
- Iron oxides
- adsorption by
- general, 36, 81, 91–93, 439, 440, 444, 451, 455, 490, 496, 516, 521, 524, 526
- arid, 302, 335, 342, 368, 369, 377, 379, 383, 384, 412
- in gossan, 130–132, 135, 136, 142, 143, 148, 150

- rainforest, 264, 274, 397
- savanna, 209, 212, 213, 228,
- formation, 32, 35, 60, 83, 119, 122, 123, 128–134
- gold with, 221, 252, 319–323, 384, 402, 466–471, 474, 481, 529
- hardening, 11, 41, 51
- in gossan, 119, 122, 123, 128–136, 140–143, 148, 149, 337, 351, 361, 514, 515, 537, 538
- in nodules, 41, 47, 60, 265, 267, 313, 298, 320
- in profiles
 - general, 15, 25, 38, 41–47, 60–64, 435, 484, 511, 516, 518, 534, 538, 540
 - savanna, 203, 207, 212, 223,
 - rainforest, 241, 245, 268, 272, 275, 277, 280, 290, 425
 - arid, 300, 306, 329, 390,
 - in soil, 60–64, 70, 290, 300, 316, 318
 - replacement by, 37, 38, 42, 135, 136, 368, 506
- Ironstones**
 - barren, 160–165, 332, 334, 335, 348, 521
 - classification, 116–118, 513–515, 537–541
 - identification, 115, 139–143, 147, 150–156, 158–161, 201, 202, 513–515
 - lateritic, 15, 99, 100, 102, 103, 141, 152, 166, 234, 294, 295, 299, 318
 - search, 139, 308, 377, 408, 409, 515
- Isotopes**
 - lead, 156–161, 441, 460
 - uranium, 441, 451, 455, 456, 460
- Isovolumetric weathering**, 28, 37, 44, 206, 322
- Kaolinite—see also Clay minerals**
 - adsorption by, 209, 213, 227, 228, 237, 444, 506
 - dispersion model, 203–205, 226–236, 252
 - Fe-rich, 39, 44, 50
 - formation, 12, 20, 32, 38, 39, 44, 45, 60, 72, 74, 280
 - in lateritic profile
 - general, 15, 35, 38, 41, 44, 60–64, 66–68, 77, 506, 516, 520, 535, 539, 540
 - savanna, 203, 206–213, 225, 456
 - rainforest, 66–68, 241, 242, 268, 277, 280
 - arid, 296, 299, 302, 312, 317, 319, 360, 487
 - replacement of, 45, 46, 48, 49, 447
 - weathering of, 20, 69, 102
- Kimberlites/lamproites**
 - general, 419–421
 - indicator minerals, 422, 433–437, 492, 496
 - weathering, 420, 422–428, 432, 436, 437, 490
- Lag**
 - occurrence, 334, 336, 346, 478, 518, 539
 - sample medium, 308, 332, 336, 442, 446–448, 478–481, 518, 519
- Lamproites—see Kimberlites**
- Landforms**
 - facets, 13–16, 18, 23, 306, 503, 536, 539
 - in arid terrain, 295, 296, 304, 305, 315, 374
 - in dispersion models, 1, 7, 10, 12–15, 18, 21, 23
 - in rainforest, 104, 241, 243, 262,
 - mapping, 316, 391, 499, 503, 508, 509
 - soils relationships, 62, 67–70, 74, 76, 77, 104
 - systems, 14, 18, 23, 503, 536, 539
- Landslides/landslips**, 13, 109, 110, 395, 397, 417, 511, 522
- Landsurface lowering**, 11, 319, 394
- Laterite**, 41, 42, 49–51, 53, 54, 61, 210, 307–309, 439, 440, 442–445, 452–455, 458, 490–493, 495, 533, 536, 539
- Lateritic cuirasse and duricrust**
 - general, 41, 42, 100, 103, 110, 162, 169, 203, 222, 242, 303, 306, 316, 346, 352, 353, 394, 431, 484, 500, 503, 506, 511, 515, 535–538, 542
 - anomalies in, 166, 211, 212, 215, 217–220, 318, 474, 477, 519
 - as sample media, 209, 218, 307, 309, 317, 324, 346, 508, 518, 519, 523, 524
- Lateritic pisoliths**
 - anomalies in, 108, 109, 139, 190, 308, 309, 314, 348, 378, 450, 501
 - as sample media, 108, 109, 139, 190, 219, 303–321, 324, 332, 336, 353, 458, 480, 481, 501, 503, 508, 508, 519
 - composition, 49, 54, 206–210
 - formation, 47, 49, 54, 302
 - gold in, 317–323, 378, 470, 480, 481
 - occurrence, 41, 42, 206, 213, 277, 280,

- 290, 300, 303, 312, 353, 357, 365, 431, 486, 518, 534–537, 541
 trace elements in, 100, 108, 109, 139, 219, 226, 303–321, 450, 458, 490
- Lateritic regoliths**
 complete—*see* A-type models
 definition, 41, 42, 206
 distribution, 12, 205, 243, 276, 296–298, 303, 304
 formation, 28, 37, 42, 47, 207
 gold in
 general, 210, 240, 290, 293, 300
 depletion zone, 477, 478
 lateritic enrichment, 19, 41, 302, 303, 469, 505, 518
 mobility, 252, 301, 335, 471–475, 504
 nickel in, 33, 37–39, 41, 152, 166, 209, 240, 301, 302, 326–328, 334, 335, 417, 436, 505, 518, 520
 on different lithologies, 37, 38, 63, 245, 299, 300, 397
 pre-existing, 18, 104, 150, 203, 205, 224–226, 242, 243, 252, 261, 262, 298, 360, 395, 409, 537
 profile nomenclature, 28, 42, 43, 206, 224, 225, 243, 244, 268, 276, 277, 300, 531–533
 residual, 28, 104, 215, 224, 235, 237, 240, 275, 279, 286, 303, 324–326, 328, 483, 487
 soils, 28, 57–77, 224, 225, 243, 244, 262, 276–279, 332, 334–336, 360, 362, 378, 394, 395, 409, 477, 478, 511, 520–522
 truncated—*see* B- and C-type models
- Leaching**, 4, 12, 20, 37, 65, 72, 241–243, 292, 293, 334, 474, 475, 477, 504
 in gossan formation, 123, 124, 130, 133–136, 141, 147–150, 170, 172, 302, 337, 343, 404
- Lead**
 hydromorphic dispersion, 236, 302, 512, 516
 in Fe oxides, 302, 342
 in Fe–Mn oxides, 412
 in gossans, 170–173, 175, 178, 180, 185, 186, 188–191, 194, 196–198, 337, 338, 340, 351, 364
 in ironstones, 194
 in calcrete, 380, 383, 384
 mobility, 135
 pathfinder for Au, 318, 319
 pathfinder for PGE, 399
- Lead dispersion**
 in lateritic regoliths, 250, 251, 260, 261, 337, 339, 343, 344
 in saprolite, 237, 334, 342, 343, 504
 in soil, 215, 216, 263, 264, 348, 349, 351, 352, 371, 380, 383, 404, 406, 414, 415
 in transported overburden, 236, 237, 357, 358, 365
- Lead isotopes**
 in gossan discrimination, 156–159, 161
 in uranium exploration, 460
- Lead–zinc deposits and occurrences—*see* also Volcanogenic massive sulphide deposits**
 carbonate-hosted
 general, 143, 157, 181, 537
 arid, 182, 183, 185
 savanna, 234
 stratiform
 arid, 171, 172, 181
 savanna, 175
 temperate, subtropical, 172
 undifferentiated
 arid, 143, 157, 159, 171, 181, 196, 332, 340, 348, 357, 383, 410
 rainforest, 262
 savanna, 215, 238
 gossans, 171–176, 198–201, 340–343
- Limonite—*see* Goethite, Hematite, Iron oxides**
- Lithology/rock type**
 regolith variation, 26, 37, 62, 63, 112, 113, 209, 242, 277, 279–281, 299, 300, 304, 331, 375, 404, 539, 543
 discrimination, 209, 215, 226, 273, 285, 294
 by heavy minerals, 484–495, 500, 507, 509, 521, 537
- Loess**, 111, 416, 522, 542, 543
- Mafic rocks**
 identification, 147, 379, 486
- Mass balance**, 39, 47–49, 100, 195, 256, 327, 328, 355, 383, 461
- Massive sulphide deposits**
 —*see* Volcanogenic massive sulphides (VMS)
 —*see* Ni–Cu sulphides
- Mechanical dispersion—*see* Physical dispersion**
- Mediterranean climate**, 7, 12, 20, 309, 360, 383, 477

- Microorganisms, 26, 58, 94, 96, 148, 464, 465, 507
- Minerals
 resistance to weathering, 15, 44, 109, 111–113, 122, 129, 286, 302, 306, 435, 487, 516, 519
- Mobility, general, 40, 79–81, 83, 87
- Mobility, effect of
 climate, 96, 247, 351, 366, 474, 475, 477
 complex formation, 89, 94, 95, 137, 463, 466
 microorganisms, 95
 redox conditions, 95, 471
- Models, exploration/dispersion
 general, 2, 17, 18–24, 104, 203, 242, 243, 261, 275, 303, 304, 374, 391, 393, 499, 502–510
 application, 23, 503–506
 classification, 18–23, 205
 codes, 24, 205
 for arid terrain, 302 et seq., 393, 403–416, 505
 for rainforests, 241 et seq., 393, 395–403, 505
 for savanna, 203 et seq., 393, 505
- Molybdenum
 in Fe oxides, 209
 in gossans, 170, 178, 185, 188, 189, 313
 mobility, 301
 oxidation states, 87
- Molybdenum deposits and occurrences (*see* also Porphyry Cu–Mo deposits), 211, 265, 310
- Molybdenum dispersion
 in lateritic regoliths, 212, 213, 250, 251, 260, 261
 in soil, 211, 212, 266, 267, 409, 410
 in transported overburden, 365, 366, 367
- Monosiallitization, 32, 36, 38, 60
- Montmorillonite—*see* Smectite
- Morphoclimatic zones, 9, 10, 14, 18, 295, 476
- Mountains, tropical, 12, 13, 393, 394
- Neutron activation analysis, 479, 527, 529–531
- Nickel
 hydromorphic dispersion, 359
 in calcrete, 378, 379
 in Fe oxides, 302, 342, 379, 496
 in Fe–Mn oxides, 163, 164
 in gossans, 133, 150, 170, 185, 186, 189, 193–195, 358, 407
 in ironstones, 166, 193, 194
 in Mn oxides, 180, 326, 328, 378
 in silcrete, 301, 326
 in weathering of ultramafic rocks, 33, 37–39
 pathfinder for PGE, 383, 399
- Nickel-copper sulphide deposits and occurrences
 in arid environments, 123, 133, 150, 324, 347, 358, 359, 362, 370, 371, 378, 379
 in savanna environments, 195, 405, 407
 geochemical exploration problems, 334, 363, 364, 370, 407, 417
 gossans, 191–195, 347, 358, 362, 363, 370, 378, 406, 407
 pathfinders for, 194, 195, 202, 334, 417
- Nickel dispersion
 in lateritic regoliths, 269, 271
 in saprolite, 285
 in soil, 270, 281, 282, 285, 347, 348, 363, 371, 378, 380
 in transported overburden, 358, 359
- Nickel in regoliths on ultramafic rocks
 distribution in, 285, 286, 422, 425, 427–429, 431–433, 436
- Nickel lateritic
 deposits and occurrences, 13, 328, 394, 398, 399
 related soil anomalies, 334, 335, 399, 404
- Nodules, lateritic, 46, 47, 49, 66, 70, 206, 224, 277, 307
 as sample media, 190, 219, 268, 308, 309, 480, 503, 508, 519
 definition, 535, 537, 540
 composition, 54, 55, 306
 formation, 28, 30, 37, 45, 47, 60, 61, 207
- Organic
 acids, 35, 58, 64
 complexes, 85, 88, 90, 93, 95, 323, 462, 466, 477
 matter, 29, 62, 64, 99, 150, 300, 443, 464, 465, 471, 538
 adsorption by, 36, 444
- Orientation surveys, 111, 151, 235, 309, 313, 363, 369, 372, 391, 409, 434, 435, 458, 460, 481, 505, 522–524
- Oxidation, 29, 30, 33, 63, 87, 94, 119, 122, 136, 142, 148–150, 450, 451, 456, 466, 471

Oxidation potential—*see* Eh

Pallid zone, 44, 206, 454, 516, 540

Pathfinder elements—*see* also Element associations

general, 137, 142–147, 151, 152, 160, 161, 202, 350, 368, 399, 408, 508

for gold, 100, 217, 277, 360, 480, 481

in gossan, 150–156, 160–162, 334, 337, 342, 343, 417, 501, 514

in laterite, 217, 308, 313, 360, 496, 518, 524

in soil/saprolite, 210, 240, 272, 313, 335, 371, 507, 521

leaching, 20, 149, 343, 508

negative, 151–153

Pedoplastic horizon—*see* Plasmic horizon

pH

general, 81, 101, 148, 149, 226, 538

contrast, 122, 136, 138, 145, 168, 512

high, 32, 33, 130, 133, 134, 198

indicators of, 133, 134, 142, 171, 175, 176, 182, 188, 196, 201, 202, 450

low, 32, 33, 83, 133, 134, 189, 471

pH, influence on

adsorption/coprecipitation, 91–93, 95, 130, 132, 180, 443

solubility, 29, 31, 32, 35, 83, 85, 88–90, 94–96, 101, 130–133, 138, 147–148, 165–166, 376, 396, 414, 443, 444

Phreatic calcrete—*see* Calcrete, Groundwater

Physical/clastic/mechanical anomalies

general, 504–508, 512, 518

in pisolitic laterite, 108, 109, 226, 306, 307, 313

in soil, 100, 234, 235, 247, 263, 269, 272, 275, 281, 360, 397, 414–417, 521

in transported overburden, 105, 236, 356, 492, 522

of gold, 105, 229, 318, 323, 401, 461, 471, 478, 479

of ironstone and gossan, 108, 109, 138, 151, 171, 215, 313, 332, 335, 342, 361–365, 408, 409, 501

Physical dispersion

general, 1, 2, 99–110, 393, 395

bioturbation, 104–105, 112, 275, 307, 362

by wind, 110, 112

churning, 61, 76, 100, 101, 112, 113, 332, 541,

consolidation, 102–104, 108, 112, 306, 533, 540

effect of lithology, 112, 113

eluviation, 58, 61–63, 65, 70, 73, 99–102, 112, 113, 272, 306, 435, 536, 538

homogenization, 44, 60, 61, 100–102, 112, 547

illuviation, 73, 99, 100, 104, 471, 484, 487, 536, 538, 541

landslip, 13, 110, 112, 395, 397, 417, 511, 522

mass flow, 62, 107, 109–113, 272, 276, 306, 307, 397, 478, 480, 511, 535

rainsplash, 107, 112

sheetwash, 107–109, 111–113, 303, 306, 307, 332, 365, 369, 377, 478–480, 511, 535

soil karst, 100, 102, 103, 112

solifluction, 13, 109, 112

Physical weathering

general, 97–99, 510

crystal growth, 98, 112

insolation, 98, 112

swelling, 40, 44, 46, 60, 61, 98, 112, 511

unloading, 97, 98, 112, 113

Pisoliths—*see* Lateritic pisoliths

Placers, 222, 281, 286, 299, 345, 461, 468, 474, 496

Plasmic horizon, 60, 61, 70, 532–534, 581

Platinum group elements (PGE)

in gossans, 194, 195

in ironstones, 194

in Mn oxides, 328

mobility, 301, 328

pathfinders for Ni–Cu sulfide deposits, 194, 417

Platinum group elements (PGE) deposits and occurrences, 324, 361, 383, 384, 399

Platinum group elements (PGE) dispersion

in soil, 384, 385

Platinum group elements (PGE) in lateritic regoliths

distribution in, 324

Podzolic soils, 35, 61, 62, 66–69, 99, 243, 397

Porphyry Cu–Mo deposits

deposits and occurrences

arid, 188, 409, 412, 415, 416

rainforest, 396–398

- exploration, 110, 146, 184, 188, 395–398, 404, 408, 409, 412, 415–417, 501, 535
- gossans, 188–191
- Potassium
- distribution in regoliths, 245, 254, 291, 292
 - in calcrete uranium deposits, 388–390
 - in gossans, 135, 136
 - in micas, 33
- Pseudogossans, 150, 154, 163, 164, 335, 408, 514, 515, 527, 537, 538
- Pyrite oxidation
- general, 129, 136, 147, 169, 170, 297, 443, 464, 466, 471
 - reactions, 30, 124, 129, 134
- Radioactive decay, 157, 439–441, 448, 460
- Radon, 330, 440, 441, 460
- Rainfall
- aerosols with, 58, 135
 - defining climate, 4–8, 59, 61–63
 - effective, 4, 6, 12, 26, 50
 - erosive power, 13, 106–111, 303
 - seasonality, 4, 6, 8, 12, 18, 20, 70–74, 107, 203, 241, 295
 - and weathering, 7, 59–63, 66, 75, 149, 150, 262, 275, 292, 300, 324, 474–476, 512
- Rainforest environments
- climate, 5, 6, 241
 - climatic episodes, 12, 242, 243, 262, 275, 276, 299, 502
 - diamonds, 424–431, 434, 435
 - distribution, 1, 7, 241, 393, 395, 405
 - dispersion models, 20, 21, 203, 209, 243–247, 252, 253, 261, 262, 268, 269, 275–281, 395, 396
 - erosion, 103, 107, 109, 112
 - gold, 247–252, 254–257, 260, 261, 269, 271–273, 281–289, 291–293, 399–403, 470, 471, 474, 477–479
 - gossans, 139, 293
 - landforms, 241, 243–245, 275, 276, 394, 395
 - regoliths, 28, 54, 66–71, 241–247, 252, 253, 262, 268, 275–280, 397, 420, 424–430
 - stone lines in, 20, 103, 104, 275–292, 517
 - vegetation, 8, 12, 13, 106, 241, 247
 - weathering in, 20, 66, 67, 241–245, 275–277, 280, 417
- Rainsplash, 107
- Rare earth elements (REE) partitioning, 329
- Rare earth elements (REE) deposits and occurrences, 222, 223, 267, 329
- Reconnaissance surveys
- gossan, 139, 140, 151, 336
 - laterite, 307–313, 318, 480, 481, 519
 - soil, 214, 219, 229, 272, 273, 319, 351, 354, 363, 367, 370, 372, 381, 388, 396, 397, 429, 435, 481, 521
 - stream sediment, 215, 219, 229, 230, 232, 247, 249, 253, 260, 262, 269, 272, 284, 290, 291, 345, 393, 401
- Redox—*see* Eh–pH relationships
- Regolith
- definition, 542
 - terminology, 28, 41–43, 204, 300, 531–533
- Regolith, effect of environmental change
- general, 1, 7, 10–13, 17, 20, 38, 63, 65–69, 113, 127, 205, 292–293
 - climatic
 - to arid, 12, 16, 17, 70–76, 149, 150, 237, 276, 295–301, 303, 309, 331, 343, 360, 403–404, 409, 473–475
 - to humid, 11, 17, 65–69, 241–243, 262, 268, 275, 276, 280, 281, 288, 472, 474
 - on dispersion models, 20, 21, 205, 502, 505, 599
 - on gold, 470, 472–475, 477
 - tectonic, 13, 17, 69–76, 151, 288, 394, 417, 442, 459, 472–475
- Relief
- effect on
 - dispersion, 1, 7, 18–20, 24, 116
 - erosion, 18, 62, 97, 106–107, 112, 113, 151, 331, 479
 - exploration in areas of
 - high, 12–14, 16; *see* Part IV
 - low, 14–16; *see* Part III
 - gossans, 140, 149, 151, 361
 - inherited, 1, 11, 296
- Remote sensing, 140, 391, 500, 503
- Resistant minerals—*see* Heavy minerals
- Resistivity, 121, 123, 124, 129, 429, 500
- Salinity
- effect on element mobility, 137, 301, 323, 343, 385, 474, 504
 - in arid areas, 110
 - origin, 511

- Sample media, 11, 17, 20, 57, 99, 210, 294, 503, 505–507, 510, 511, 513–515, 518, 521, 522
- Sample preparation, 141, 210, 336, 484, 485, 506, 507, 520, 522–526
- Sampling density, intervals
 in laterite surveys, 218, 219, 307, 309, 313, 318, 319, 324, 508, 519
 in saprolite surveys, 233, 260, 284, 294, 334, 429, 506, 518
 in soil surveys, 229, 239, 286, 319, 369, 407, 479, 481, 508
 in stream sediment surveys, 229, 458
- Sampling procedures
 by hand auger, 253, 258, 269, 402
 by percussion drilling, 319, 533
 by RAB drilling, 313, 353–355, 357, 459, 481, 506, 533
 gossans, 514
 laterite, cuirasse, 519
 saprolite, 516
 soils, 522
- Saprock, 28, 37, 43, 48, 75, 312, 533, 537, 541–545
- Saprolite
 as sample media, 253, 260, 294, 477, 479, 506, 507, 516, 517
 definition, 28, 37, 42, 44, 206, 515, 532–534, 539, 542
 dispersion in, 212, 217, 247–249, 258–261, 269–271, 284–287, 320, 334, 337, 339, 342, 356
 gold enrichment, 317, 319, 320, 470, 475, 476, 478
 mineralogy, 44, 45, 60, 61
 nickel enrichment, 334, 335, 417, 505
 silicification, 301, 326–328, 543
- Savanna environments
 climate, 3, 6, 38, 61
 dispersion models, 206–211, 226, 227, 237, 240
 distribution, 9, 10, 203, 395, 505
 dry, 61, 70
 vegetation, 107, 113, 511
 weathering processes, 36, 70, 422
 wet, humid, 61, 70, 395
- Seasonal climates—*see* Savanna
- Secondary enrichment
 copper, 188, 298, 404, 409
 gold, 302, 317, 320, 345, 346, 353, 400, 402
 in gossans, 149, 171, 195, 198, 340
 nickel, 152, 302, 326, 327, 334, 398, 399, 404, 407, 469–478
 silver, 400, 402
- Secondary minerals
 in gossans, 142, 143–148, 153, 160, 161, 165, 171, 172, 176, 178–182
 in regoliths, 15, 25, 35, 36, 240, 267, 321, 329, 446, 447, 467
- Selective extraction (partial extraction), 308, 309, 369, 383, 479, 480, 526, 529
- Self potentials, 128, 129
- Semi-arid environments—*see* Arid environments
- Sheetwash, 107–109, 111, 113, 303, 306, 307, 332, 365, 369, 377, 479, 480, 511, 535
- Silcrete
 definition, 536, 543
 pedogenic, 299, 301
 over ultramafic rocks, 301, 326–328, 407, 422
- Silver
 depletion of gold grains, 222, 461, 468, 469, 471
 in gossans, 115, 149, 168, 170, 171, 178, 186, 188, 189, 191, 197, 198, 313, 337, 342, 343, 351, 374
 in ironstones, 163
 in Mn oxides, 400, 479
 mobility, 87, 137, 471
- Silver deposits and occurrences, 409
- Silver dispersion
 in lateritic regoliths, 250, 251, 260, 261, 302
 in saprolites, 247, 248
 in soil, 351
 in transported overburden, 236, 365
- Size fractions, 99, 107–112, 210, 277–279, 281, 307–309, 335, 336, 362, 368, 369, 377, 416, 484, 506, 507, 522, 523
- Soil
 carbonates, 7, 62, 99, 295, 308, 353, 368, 369, 374–378, 381–383, 477
 classification, 1, 16, 77, 520
 climate, 1, 2, 4, 6–8, 26, 27, 58–62, 66–76
 composition, 225, 226, 277–280
 creep—*see* Solifluction
 formation, 26, 57–65, 105, 520
 horizons, 4, 28, 57–59, 99–103, 105, 206, 276–278, 538, 543
 profiles, 58, 59, 66–71, 224, 225, 252,

- 253, 265, 266, 268, 276, 277, 290, 291, 368, 383, 423, 425, 427, 432, 543
 sampling procedures, 368, 481, 483, 484, 522
- Soil types**
 arid environments, 7, 77, 100
 ferrallitic, 41, 77, 150, 243, 397, 536
 ferralsols, 77, 536
 latosols, 222, 273, 274, 397, 536
 lithosols, 13, 348, 351, 385, 404, 520
 podzols (podzolic), 66–69, 99, 243, 397
 vertisols, 61, 76, 100, 101, 112, 204, 332, 541
- Solifluction**, 3, 109, 112
- Solubility**
 by complexation, 88–90
 function of pH, 83, 89–91, 130–133
 index, 388
 product, 29, 53, 80, 85, 89, 389, 390
- Statistical data interpretation**, 152–156, 202, 335, 399
- Stability constants**, 85, 86, 88, 89, 93
- Stone lines**
 formation, 20, 60, 102–104, 109, 275, 277–280
 in rainforests, 67, 275–277, 280–292, 474
 in savannas, 205, 224–227, 234
- Stream sediments**, 109, 110, 139, 263, 309, 393, 416, 458
- Subtropics**, 6–9, 12, 13, 18, 40, 295, 511
- Sulphate**
 minerals, 29, 122, 130, 135, 144, 145, 149, 150, 239, 368
 ion, 30, 89, 464, 465
- Sulphide minerals**
 oxidation, 136, 142, 464, 465
 supergene, 135–137, 149, 185, 188
- Swelling**, 40, 44, 46, 60, 61, 98, 112, 511
- Talus**
 occurrence, 98, 110, 112, 169, 395, 414, 520, 522
 sample medium, 20, 393, 395, 414, 416, 417
- Temperate environments**
 high altitude, 7, 8, 13, 393
 climates, 5–8, 296
 gossans, 390, 418
 lateritic regoliths in, 7, 9–12, 295, 309, 409
 weathering, 26, 33, 417, 508, 511, 512
- Termitaria**
 as sample media, 105, 106, 109, 235, 236, 417
 rate of formation, 104–105
- Termites, bioturbation by**
 general, 104, 346, 504
 in stone lines, 104, 275
 of indicator minerals, 105, 106, 109, 225, 235, 236, 362, 435, 492
- Ti–Zr diagrams**, 100, 101, 497, 498, 509
- Topographic inversion**, 299, 304, 459
- Transformation reactions**, 33–35
- Transformation fronts**
 weathering, 11, 12, 59, 61, 64, 111, 296, 317, 329, 360, 471, 484, 544
 general, 11, 28, 47, 57–64, 80, 540, 543, 544
 pedoplasmatation, 28, 60, 61, 533, 534, 541
 cementation, 60–62, 535
- Transformation systems**, 65
 arid, 75, 76
 rainforest, 66–71
 savanna, 70–75
- Transported overburden—see also Aeolian deposits, Alluvium, Colluvium**
 dispersion in, 105, 234–237, 302, 309, 329, 330, 356–359, 362, 365–367, 382, 386–388, 395–398, 404, 412, 417, 435, 461, 478–481, 483
- exploration problems**
 general, 19, 140, 149, 190, 492, 500, 504, 520, 521
 arid, 303, 305, 324, 330, 332, 343, 349, 356–370, 403, 404, 412, 416, 433,
 rainforest, 252, 269, 276, 395–397
 savanna, 223, 235, 239, 240, 243
- identification**, 100, 102, 303, 324, 325, 483–488, 490, 497, 509
- in dispersion models**, 19–23, 226, 227, 233, 269, 305, 324–333, 343, 356–362, 365, 366, 395, 396, 405, 412, 503–506
- occurrence**, 14–16, 55, 210, 211, 243, 298, 360, 367, 381, 395, 396, 403, 522, 523, 543
- Truncated profiles—see B- and C-type models**
- Tungsten carbide, contamination**, 524, 525
- Ultrabasic/ultramafic rocks**
 identification, 324, 371, 420, 436, 490–496

- Ni enrichment, 39, 151, 152, 160, 285, 327, 334, 335, 359, 397, 398, 404, 417, 486–488, 505, 543
- Ni–Cu exploration, 147, 154, 191–195, 324, 347, 362–364, 370, 371, 378, 379, 407
- PGE in, 324–328, 399
- regoliths on, 37–39, 63, 100, 202, 245, 246, 300, 325, 327, 486, 487, 496
- weathering, 33, 49
- Uranium
- adsorption, 444, 452, 453
 - daughter products, 157, 158, 441, 460
 - geochemical fractionation, 440, 441, 456, 460
 - in calcrete, 99, 376, 386, 388–390, 454
 - mobility, 301, 388, 389, 439, 440, 442–445
 - oxidation states, 86, 87, 440
- Uranium deposits and occurrences
- arid, 99, 390, 454
 - rainforest, 443, 445, 446, 451, 458, 459
 - savanna, 440, 445–447, 450–460
 - temperate, subtropical, 443, 446, 452–454
- Uranium in lateritic regoliths
- exploration of lateritic U concentrations, 458, 459, 460, 496
 - in Fe–Mn oxides, 445, 455, 496
 - mineralogy, 443, 445–447
 - residual enrichments, 445–452
 - seepage concentrations, 453–457
- Vadose calcrete—*see* Pedogenic calcrete
- Vanadium
- in calcrete uranium deposits, 388–390
- Vertisols, 61, 76, 100, 101, 112, 204, 332, 541
- Volcanogenic massive sulphide (VMS) deposits and occurrences
- in arid environments, 167, 168, 176, 178–180, 308, 336, 337
 - in temperate, subtropical environments, 178
 - exploration, 146, 147, 152, 209, 215, 226, 239, 262, 275, 306–309, 332–334, 361, 367–369, 395, 404, 501, 508, 517
 - gossans, 152, 167–169, 176–181, 310–313, 336, 348–350, 357, 364, 365, 404, 406, 417, 501
 - during gossan formation, 123, 124, 127–130, 148, 149, 168, 169, 475, 511, 512
 - during weathering, 28, 45, 51, 54, 62, 69–71, 96, 124, 127–130, 206, 300, 301, 312, 326, 337, 362, 425, 436, 452
- element concentration at
- general, 149, 199, 237, 298, 326, 328, 334, 337, 340, 343, 409, 422, 450, 455, 459, 504
 - gold, 137, 320, 334, 345, 471–475, 478, 504
- fluctuations, 61, 62, 69, 73, 127, 148, 206, 450, 451, 455, 456
- lowering
- by uplift, 17, 64, 69, 151, 409
 - due to aridity, 17, 298–301, 409
 - effect on regolith, 11, 17, 128, 474
 - perched, 62, 69, 99, 326
 - reactions at, 123, 124, 127, 128, 130, 166, 436, 450
- Weathering
- effect of temperature, 3
 - of silicates, 29–35
 - of sulphides, 119–127, 133–137
 - rate, 3, 26, 36, 49, 50, 64, 65, 70, 94, 105, 123, 124, 127, 149, 274, 275, 299, 304, 393, 474, 511
 - resistance to, 304
 - physical, 97–99
 - profiles
 - gossan, 117, 128
 - lateritic
 - general, 37, 38, 42–47,
 - arid, 299–301, 331, 332, 359, 360, 422, 486
 - rainforest, 243–246, 252, 262, 268, 275–280, 289, 290, 420, 426
 - savanna, 204–209, 224–226, 422, 427
 - terminology, 531–533
- Wind—*see* also Aeolian
- dispersion by, 62, 110, 369, 372, 373, 479
 - erosion, 13, 62, 97, 106, 109, 307, 332, 359, 371, 511, 512, 542
- X-ray fluorescence analysis (XRF), 162, 163, 527–531
- Zero point of charge, 91, 92
- Zinc
- hydromorphic dispersion, 215, 302, 312, 356, 415
- Water-table

- in calcrete, 380, 381, 383, 384
 - in chromiam spinels, 495
 - in Fe oxides, 302, 342, 496
 - in Fe–Mn oxides, 163, 164, 412
 - in gossans, 133, 149, 150, 168, 170, 172, 175, 178–180, 185, 186, 188, 189, 191, 194–198, 315, 340, 342, 343, 364
 - in ironstones, 162, 164, 165
 - in Ni gossans identification, 194, 202
 - pathfinder for PGE, 399
- Zinc deposits and occurrences—*see* Lead–zinc deposits and occurrences
- Zinc dispersion
- in laterites, 313, 314
 - in lateritic regoliths, 337, 339, 343, 344, 408
 - in saprolite, 285, 334
 - in soil, 215, 263, 285, 348–352, 364, 380, 381, 383, 404, 406–408, 414, 425
 - in transported overburden, 236, 356–358, 365, 366
- Zirconium—*see* also Ti–Zr identifying overburden, 100, 101, 486–488
- in silcrete, 301, 543